AMOEBAE AS HOST MODELS TO STUDY THE INTERACTION WITH PATHOGENS

EDITED BY: Sascha Thewes, Thierry Soldati and Ludwig Eichinger

PUBLISHED IN: Frontiers in Cellular and Infection Microbiology

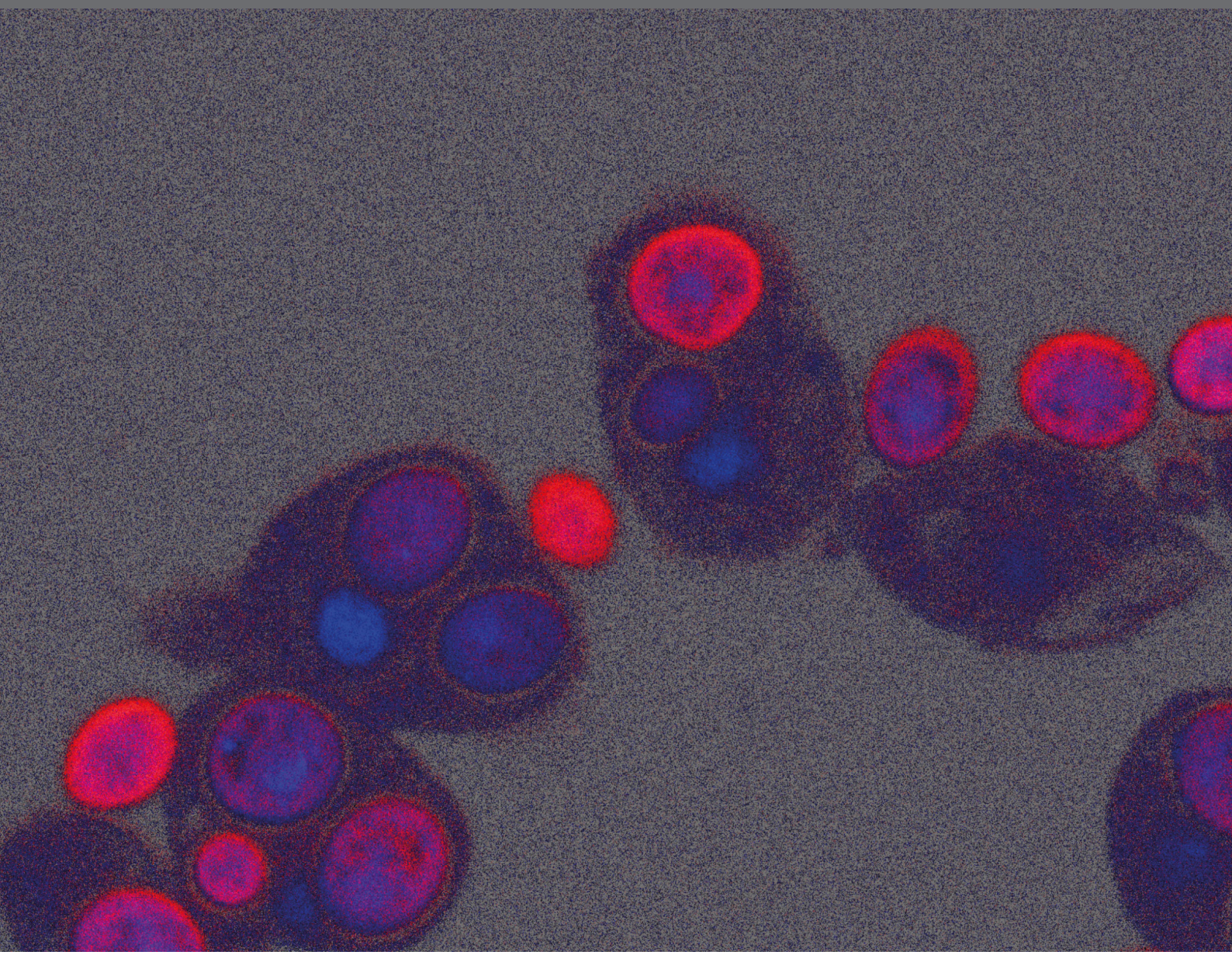

frontiers Research Topics

ISSN 1664-8714
ISBN 978-2-88945-935-3
DOI 10.3389/978-2-88945-935-3

About Frontiers

Frontiers is more than just an open-access publisher of scholarly articles: it is a pioneering approach to the world of academia, radically improving the way scholarly research is managed. The grand vision of Frontiers is a world where all people have an equal opportunity to seek, share and generate knowledge. Frontiers provides immediate and permanent online open access to all its publications, but this alone is not enough to realize our grand goals.

Frontiers Journal Series

The Frontiers Journal Series is a multi-tier and interdisciplinary set of open-access, online journals, promising a paradigm shift from the current review, selection and dissemination processes in academic publishing. All Frontiers journals are driven by researchers for researchers; therefore, they constitute a service to the scholarly community. At the same time, the Frontiers Journal Series operates on a revolutionary invention, the tiered publishing system, initially addressing specific communities of scholars, and gradually climbing up to broader public understanding, thus serving the interests of the lay society, too.

Dedication to Quality

Each Frontiers article is a landmark of the highest quality, thanks to genuinely collaborative interactions between authors and review editors, who include some of the world's best academicians. Research must be certified by peers before entering a stream of knowledge that may eventually reach the public - and shape society; therefore, Frontiers only applies the most rigorous and unbiased reviews.
Frontiers revolutionizes research publishing by freely delivering the most outstanding research, evaluated with no bias from both the academic and social point of view. By applying the most advanced information technologies, Frontiers is catapulting scholarly publishing into a new generation.

What are Frontiers Research Topics?

Frontiers Research Topics are very popular trademarks of the Frontiers Journals Series: they are collections of at least ten articles, all centered on a particular subject. With their unique mix of varied contributions from Original Research to Review Articles, Frontiers Research Topics unify the most influential researchers, the latest key findings and historical advances in a hot research area! Find out more on how to host your own Frontiers Research Topic or contribute to one as an author by contacting the Frontiers Editorial Office: researchtopics@frontiersin.org

AMOEBAE AS HOST MODELS TO STUDY THE INTERACTION WITH PATHOGENS

Topic Editors:
Sascha Thewes, Freie Universität Berlin, Germany
Thierry Soldati, University of Geneva, Switzerland
Ludwig Eichinger, University Hospital Cologne, Germany

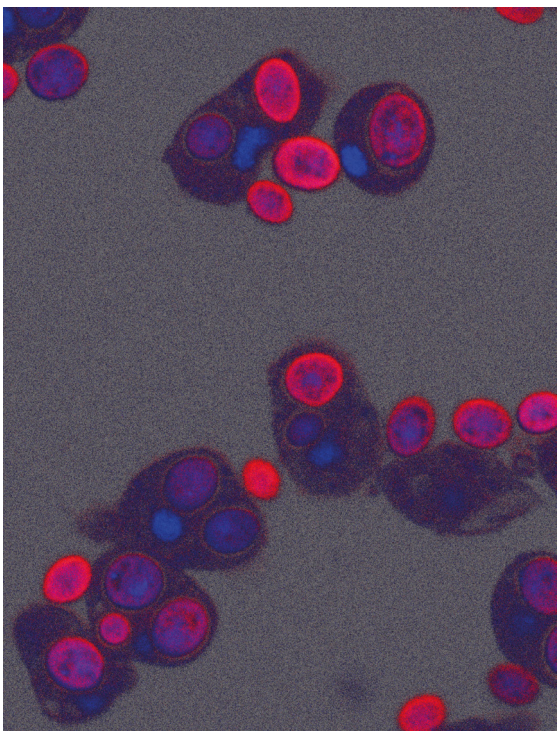

Dictyostelium discoideum cells phagocytosing TRITC-labelled yeast cells.
IImage: Maria Stumpf. Image processing: Ludwig Eichinger.

The human body is constantly faced with microorganisms. Most of these bacteria, fungi, and viruses are harmless, many of them are beneficial, and a small fraction is pathogenic. For humans, infection with pathogenic microorganisms can be very serious or even fatal, ranging from mild transient or chronic infections to death. The first line of defence against pathogens is our innate immune system. Beside chemical and physical defence mechanisms of the innate immune system, phagocytic cells such as macrophages play a crucial role in the fight against pathogenic microorganisms. However, phagocytic cells and pathogens are in a constant evolutionary arms race, inventing new strategies to successfully kill pathogens and learning how to resist phagocytosis and intracellular killing, respectively. If pathogens are not obligatory adapted to the human body or other animals, they also have to face environmental

phagocytes in the form of amoebae. Many aspects of phagocytosis and intracellular killing are surprisingly well conserved between amoebae and macrophages. Therefore, pathogens that have evolved with environmental amoebae as their "training grounds" can also be successful during infection of macrophages and other animal phagocytic cells.

In this Research Topic, we provide the latest knowledge about the potential of using amoebae as host models to study the interaction with pathogens. The Research Topic covers the interaction of amoebae with bacteria, fungi, and viruses and also illustrates the similarities and differences between amoebae and macrophages. Investigation of evolutionary conserved pathways of amoebae and macrophages furthers our understanding of the biology of host-pathogen interactions and helps to develop new anti-infection therapies.

Citation: Thewes, S., Soldati, T., Eichinger, L., eds. (2019). Amoebae as Host Models to Study the Interaction with Pathogens. Lausanne: Frontiers Media.
doi: 10.3389/978-2-88945-935-3

Table of Contents

frontiers in Cellular and Infection Microbiology

EDITORIAL
published: 19 March 2019
doi: 10.3389/fcimb.2019.00047

Editorial: Amoebae as Host Models to Study the Interaction With Pathogens

Sascha Thewes[1]*, *Thierry Soldati*[2]* and *Ludwig Eichinger*[3]*

[1] Department of Biology, Chemistry, Pharmacy, Institute for Biology – Microbiology, Freie Universität Berlin, Berlin, Germany, [2] Department of Biochemistry, Faculty of Science, University of Geneva, Sciences II, Geneva, Switzerland, [3] Medical Faculty, Center for Biochemistry, University Hospital Cologne, Cologne, Germany

Keywords: amoebae, host-pathogen-interaction, evolution, phagocytes, immune system

Editorial on the Research Topic

Amoebae as Host Models to Study the Interaction With Pathogens

Amoebae are eukaryotic microorganisms of great diversity. They do not form a single taxonomic group and are found among the protozoa, fungi, and algae. However, all amoebae are characterized by the amoeboid life style—the ability to change cell shape by extending and retracting pseudopods—and most amoebae can be considered as professional phagocytes, which feed on bacteria and other microorganisms by phagocytosis. But despite their impressive phagocytic activity, amoebae cannot degrade all microorganisms. Some resist the digestion and some even use amoebae as host cells for their own replication. Such microbial resistance is also observed in the complex relationship between phagocytes of the mammalian immune system and pathogenic bacteria. For example, *Legionella pneumophila* usually infects fresh-water amoebae, but can also use human alveolar macrophages to further its own replication. This similarity has led to the concept of "amoebae as training grounds for (intracellular) pathogenic bacteria," namely that pathogenic microorganisms can establish, select and "train" their virulence traits in free-living amoebae before being faced with phagocytic immune cells of animals (Molmeret et al., 2005). Recent studies using amoebae as host models for pathogens confirmed the broad plausibility of this concept. The amoebae used as host models predominantly belong to the phylum Amoebozoa, the closest phylum to fungi and animals, with their most prominent representatives from the genera *Acanthamoeba* and *Dictyostelium*. Both have been demonstrated to be useful host cells for the study of the complex interactions with bacterial pathogens such as *Legionella*, *Mycobacterium*, *Salmonella*, *Francisella*, and others (for reviews see Clarke, 2010; Bozzaro and Eichinger, 2011). Additionally, amoebae can also be used as model hosts for pathogenic fungi like *Cryptococcus*, *Aspergillus*, and *Candida* (Steenbergen et al., 2003; Chrisman et al., 2011; Hillmann et al., 2015; Mattern et al., 2015; Koller et al., 2016; Maisonneuve et al., 2016). These examples highlight the potential of amoebae as model hosts to study the interaction with a wide range of pathogenic microorganisms. In this Frontiers Research Topic a large range of aspects concerning amoebae as host cells for pathogens is covered.

WHICH AMOEBAE CAN BE USED AS HOSTS?

The currently most used and best-investigated amoebae hosts are *Acanthamoeba castellanii* and *Dictyostelium discoideum*. This is highlighted in a review by Swart et al. The authors summarize comprehensively the current knowledge on the interaction of *L. pneumophila* with its natural host *A. castellanii* and the versatile model host *D. discoideum*. The potential of *D. discoideum* as a host

OPEN ACCESS

Edited and reviewed by:
Thomas Rudel,
Universität Würzburg, Germany

***Correspondence:**
Sascha Thewes
sascha.thewes@fu-berlin.de
Thierry Soldati
thierry.soldati@unige.ch
Ludwig Eichinger
ludwig.eichinger@uni-koeln.de

Specialty section:
This article was submitted to Bacteria and Host, a section of the journal Frontiers in Cellular and Infection Microbiology

Received: *13 January 2019*
Accepted: *13 February 2019*
Published: *19 March 2019*

Citation:
Thewes S, Soldati T and Eichinger L (2019) Editorial: Amoebae as Host Models to Study the Interaction With Pathogens. Front. Cell. Infect. Microbiol. 9:47. doi: 10.3389/fcimb.2019.00047

model to study different cellular aspects of the interaction with (pathogenic) bacteria is also presented in a method-oriented article by Meena and Kimmel. The authors share a range of protocols using *D. discoideum* to study chemotaxis, phagocytosis, and macropinocytosis.

Further amoebae are used to study specific aspects of the interaction with various pathogens. Diesend et al. summarize the current knowledge about the infection of free-living amoebae with giant viruses. Here, the best-studied amoeba is *Acanthamoeba polyphaga*, which can be infected by a mimivirus. For the study of the interaction of amoebae with pathogenic fungi, the amoebal repertoire is currently the largest. In a review by Novohradská et al. the authors describe the amoebal species that have been used to study fungal interactions. Beside *A. castellanii* and *D. discoideum*, amoebae such as the common water contaminant *Vermamoeba vermiformis*, *Protostelium mycophagum*, and other mycophagous soil amoebae from the genera *Thecamoeba, Arachnula*, and *Vampyrella* have been used to study the interaction with human-, plant-, and entomopathogenic fungi.

WHICH PATHOGENS CAN BE STUDIED USING AMOEBAE?

The range of microorganisms, which can be studied using different amoebae, is not limited to a specific group. Amoebae are already well-established model systems to study the interaction with bacteria. The most prominent bacteria studied using *A. castellanii* and *D. discoideum* are currently from the genera *Legionella* and *Mycobacterium* (see above and reviews by Swart et al.; Cardenal-Muñoz et al.). Two original research articles also highlight this fact. Buracco et al. show that iron depletion or overload of *D. discoideum* cells impacts on the intracellular growth of *Legionella,* whereas changes in zinc and copper concentrations do not have any effect. Concerning mycobacteria, Samba-Louaka et al. show that free-living amoebae might serve as a reservoir for *Mycobacterium avium* subsp. *paratuberculosis*. The authors found that on farms, where cattle were infected with *M. avium* subsp. *paratuberculosis,* the bacteria were also found in environmental samples containing amoebae of the poorly described *Rosculus* genus. *Salmonella enterica* serovar Typhimurium is a further example of bacteria that can be studied using amoebae as hosts. Varas et al. show that inorganic polyphosphate (polyP) is crucial for the virulence of these bacteria. Mutation of the polyP kinase (*ppK*) gene in *S.* Typhimurium affects the ability of intracellular replication. Finally, the spectrum of pathogenic bacteria is constantly expanding. Recently, it has been shown that *Bordetella bronchiseptica* can use amoebae as an environmental niche and transmission vector (Taylor-Mulneix et al., 2017). In a perspective article Taylor-Mulneix et al. now ask whether amoebae are the missing link for the evolution of Bordetellae from environmental microbes to human respiratory pathogens. In this article the concept of amoebae as "training ground" for human pathogens is picked up again. Brock et al. underline this ecological relevance for amoebae as a reservoir for (pathogenic) bacteria in an original research article. The authors isolated environmental samples of *D. discoideum* and found that one third of the wild isolates carried one to six bacterial species per fruiting body. The majority of the isolated bacteria were from the genus Proteobacteria but also Actinobacteria, Bacteriodetes, and Firmicutes have been identified. Many of the bacterial genera isolated in this study include species that are implicated in causing diseases, such as *Brucella*, *Nocardia*, pathogenic *E. coli*, *Shigella*, and *Staphylococcus*, suggesting that free-living amoebae can serve as reservoirs for animal and human pathogenic bacteria.

In recent years the use of amoebae as host cells has been expanded to study interactions with different fungi. Novohradská et al. sum up the current knowledge regarding filamentous fungi (human-, plant-, and entomopathogenic). Watkins et al. show in their original research article that the environmental pathogenic yeast *Cryptococcus neoformans* escapes from *D. discoideum* cells after phagocytosis by two different pathways: canonical exocytosis and non-lytic release by vomocytosis, which are the same mechanisms for *C. neoformans* to escape from macrophages.

Last but not least, amoebae as host cells are not restricted to bacteria or fungi. They can also be used to study the interaction with viruses such as the giant mimivirus (Diesend et al.).

All these examples show that different amoebae can be used with a plethora of microorganisms to learn more about the relationship and interaction from an ecological, evolutionary, and medical point of view.

WHICH ASPECTS OF PHAGOCYTOSIS AND KILLING BY THE AMOEBAE ARE IN COMMON WITH MAMMALIAN PHAGOCYTES?

Although amoebae are used as host model systems to study interactions with pathogenic microorganisms, one major drawback is that most amoebae grow at environmental temperatures and are usually not able to grow at elevated temperatures such as the human body temperature. However, mammalian phagocytes and amoebae share many conserved cellular and molecular processes concerning phagocytosis and intracellular killing of pathogens. In a mini-review Mori et al. compare and discuss the roles for mammalian and *D. discoideum* coronins in the trafficking and survival of intracellular pathogens. Although many aspects of the regulation and function of coronins are still elusive, a conserved role for coronins in *D. discoideum* and mammals can be delineated. Similarly, mechanisms of host defense processes and intracellular virulence of *Legionella* and *Mycobacterium* are surprisingly highly evolutionarily conserved between animal macrophages and amoebae, as exhaustively reviewed by Swart et al. and Cardenal-Muñoz et al. Additionally, Watkins et al. show that vomocytosis of *Cryptococcus* cells is mechanistically conserved between amoebae and mammalian macrophages. Further, Novohradská et al. nicely compare the parallel events in the phagocytic processing of *Aspergillus* conidiae in mammalian

macrophages and amoebae, again supporting the concept of amoebae as training ground for pathogens.

Amoebae are also interesting models to study the early evolution of cell-autonomous, innate immunity (Leippe, 1999), which is reflected in an original research article by Dhakshinamoorthy et al. who investigated the pore-forming saposin-like proteins in the defense against bacterial infection. Such studies show that the limit of amoebae as host models systems is not reached yet.

CONCLUSIONS

It is undisputable that phagocytosis and intracellular processing of pathogenic microorganisms is not identical in every aspect in animal phagocytes and amoebae. However, this research topic and abundant recent publications have illustrated that numerous aspects of these processes are evolutionarily conserved between amoebae and animal phagocytes. Further, the advantages of amoebae as host cells are obvious. Amoebae can be cultivated easily in the lab and—especially in the case of *D. discoideum*—can be easily genetically manipulated. Additionally, many other tools for molecular and cell biology have been established for the use with amoebae.

Such powerful systems will allow to further our understanding of the biology and evolution of host-pathogen interactions. This will constitute the basis for the development of novel anti-infection therapies as it has been shown already for *Mycobacterium* and *Legionella* (Kicka et al., 2014; Harrison et al., 2015; Ouertatani-Sakouhi et al., 2017; Diop et al., 2018; Trofimov et al., 2018). In summary, the future for amoebae as model systems to unravel host-pathogen interactions has just begun.

AUTHOR CONTRIBUTIONS

All authors listed have made a substantial, direct and intellectual contribution to the work, and approved it for publication.

FUNDING

ST received funding from the Freie Universität Berlin. The TS lab is supported by grants from the Swiss National Science Foundation (310030_149390 and 310030_169386) and the SystemsX.ch initiative grant HostPathX. LE acknowledges support by the Deutsche Forschungsgemeinschaft (CRC670, TP01) and by Köln Fortune.

REFERENCES

Bozzaro, S., and Eichinger, L. (2011). The professional phagocyte *Dictyostelium discoideum* as a model host for bacterial pathogens. *Curr. Drug Targets* 12, 942–954. doi: 10.2174/138945011795677782

Chrisman, C. J., Albuquerque, P., Guimaraes, A. J., Nieves, E., and Casadevall, A. (2011). Phospholipids trigger *Cryptococcus neoformans* capsular enlargement during interactions with amoebae and macrophages. *PLoS Pathog.* 7:e1002047. doi: 10.1371/journal.ppat.1002047

Clarke, M. (2010). Recent insights into host-pathogen interactions from Dictyostelium. *Cell. Microbiol.* 12, 283–291. doi: 10.1111/j.1462-5822.2009.01413.x

Diop, E. A., Queiroz, E. F., Kicka, S., Rudaz, S., Diop, T., and Wolfender, J. L. (2018). Survey on medicinal plants traditionally used in Senegal for the treatment of tuberculosis (TB) and assessment of their antimycobacterial activity. *J. Ethnopharmacol.* 216, 71–78. doi: 10.1016/j.jep.2017.12.037

Harrison, C. F., Chiriano, G., Finsel, I., Manske, C., Hoffmann, C., Steiner, B., et al. (2015). Amoeba-based screening reveals a novel family of compounds restricting intracellular *Legionella pneumophila*. *ACS Infect. Dis.* 1, 327–338. doi: 10.1021/acsinfecdis.5b00002

Hillmann, F., Novohradska, S., Mattern, D. J., Forberger, T., Heinekamp, T., and Brakhage, A. A. (2015). Virulence determinants of the human pathogenic fungus *Aspergillus fumigatus* protect against soil amoeba predation. *Environ. Microbiol.* 17, 2858–2869. doi: 10.1111/1462-2920.12808

Kicka, S., Trofimov, V., Harrison, C., Ouertatani-Sakouhi, H., McKinney, J., Scapozza, L., et al. (2014). Establishment and validation of whole-cell based fluorescence assays to identify anti-mycobacterial compounds using the *Acanthamoeba castellanii-Mycobacterium marinum* host-pathogen system. *PLoS ONE* 9:e87834. doi: 10.1371/journal.pone.0087834

Koller, B., Schramm, C., Siebert, S., Triebel, J., Deland, E., Pfefferkorn, A. M., et al. (2016). *Dictyostelium discoideum* as a Novel Host System to Study the interaction between phagocytes and yeasts. *Front. Microbiol.* 7:1665. doi: 10.3389/fmicb.2016.01665

Leippe, M. (1999). Antimicrobial and cytolytic polypeptides of amoeboid protozoa–effector molecules of primitive phagocytes. *Dev. Comp. Immunol.* 23, 267–279. doi: 10.1016/S0145-305X(99)00010-5

Maisonneuve, E., Cateau, E., Kaaki, S., and Rodier, M. H. (2016). *Vermamoeba vermiformis-Aspergillus fumigatus* relationships and comparison with other phagocytic cells. *Parasitol. Res.* 115, 4097–4105. doi: 10.1007/s00436-016-5182-3

Mattern, D. J., Schoeler, H., Weber, J., Novohradska, S., Kraibooj, K., Dahse, H. M., et al. (2015). Identification of the antiphagocytic trypacidin gene cluster in the human-pathogenic fungus *Aspergillus fumigatus*. *Appl. Microbiol. Biotechnol.* 99, 10151–10161. doi: 10.1007/s00253-015-6898-1

Molmeret, M., Horn, M., Wagner, M., Santic, M., and Abu Kwaik, Y. (2005). Amoebae as training grounds for intracellular bacterial pathogens. *Appl. Environ. Microbiol.* 71, 20–28. doi: 10.1128/AEM.71.1.20-28.2005

Ouertatani-Sakouhi, H., Kicka, S., Chiriano, G., Harrison, C. F., Hilbi, H., and Cosson, P. (2017). Inhibitors of *Mycobacterium marinum* virulence identified in a *Dictyostelium discoideum* host model. *PLoS ONE* 12:e0181121. doi: 10.1371/journal.pone.0181121

Steenbergen, J. N., Nosanchuk, J. D., Malliaris, S. D., and Casadevall, A. (2003). *Cryptococcus neoformans* virulence is enhanced after growth in the genetically malleable host *Dictyostelium discoideum*. *Infect. Immun.* 71, 4862–4872. doi: 10.1128/IAI.71.9.4862-4872.2003

Taylor-Mulneix, D. L., Bendor, L., Linz, B., RiveraI, Ryman, V. E., Dewan, K. K. et al. (2017). *Bordetella bronchiseptica* exploits the complex life cycle of *Dictyostelium discoideum* as an amplifying transmission vector. *PLoS Biol.* 15:e2000420. doi: 10.1371/journal.pbio.2000420

Trofimov, V., Kicka, S., Mucaria, S., Hanna, N., Ramon-Olayo, F., Del Peral, L. V., et al. (2018). Antimycobacterial drug discovery using Mycobacteria-infected amoebae identifies anti-infectives and new molecular targets. *Sci. Rep.* 8:3939. doi: 10.1038/s41598-018-22228-6

Conflict of Interest Statement: The authors declare that the research was conducted in the absence of any commercial or financial relationships that could be construed as a potential conflict of interest.

frontiers in Cellular and Infection Microbiology

ORIGINAL RESEARCH
published: 23 November 2018
doi: 10.3389/fcimb.2018.00411

Diversity of Free-Living Environmental Bacteria and Their Interactions With a Bactivorous Amoeba

Debra A. Brock[1], Tamara S. Haselkorn[1], Justine R. Garcia[1], Usman Bashir[1], Tracy E. Douglas[1], Jesse Galloway[2], Fisher Brodie[2], David C. Queller[1] and Joan E. Strassmann[1]*

[1] Queller/Strassmann Laboratory, Washington University in St. Louis, Department of Biology, St. Louis, MO, United States, [2] Mountain Lake Biological Laboratory, University of Virginia, Mountain Lake, VA, United States

OPEN ACCESS

Edited by:
Sascha Thewes,
Freie Universität Berlin, Germany

Reviewed by:
Frank C. Gibson III,
University of Florida, United States
Eric D. Cambronne,
University of Texas at Austin, United States
Pauline Schaap,
University of Dundee, United Kingdom

***Correspondence:**
Debra A. Brock
dbrock@wustl.edu

Specialty section:
This article was submitted to Bacteria and Host, a section of the journal Frontiers in Cellular and Infection Microbiology

Received: 01 August 2018
Accepted: 05 November 2018
Published: 23 November 2018

Citation:
Brock DA, Haselkorn TS, Garcia JR, Bashir U, Douglas TE, Galloway J, Brodie F, Queller DC and Strassmann JE (2018) Diversity of Free-Living Environmental Bacteria and Their Interactions With a Bactivorous Amoeba. Front. Cell. Infect. Microbiol. 8:411. doi: 10.3389/fcimb.2018.00411

A small subset of bacteria in soil interact directly with eukaryotes. Which ones do so can reveal what is important to a eukaryote and how eukaryote defenses might be breached. Soil amoebae are simple eukaryotic organisms and as such could be particularly good for understanding how eukaryote microbiomes originate and are maintained. One such amoeba, *Dictyostelium discoideum,* has both permanent and temporary associations with bacteria. Here we focus on culturable bacterial associates in order to interrogate their relationship with *D. discoideum*. To do this, we isolated over 250 *D. discoideum* fruiting body samples from soil and deer feces at Mountain Lake Biological Station. In one-third of the wild *D. discoideum* we tested, one to six bacterial species were found per fruiting body sorus (spore mass) for a total of 174 bacterial isolates. The remaining two-thirds of *D. discoideum* fruiting body samples did not contain culturable bacteria, as is thought to be the norm. A majority (71.4%) of the unique bacterial haplotypes are in Proteobacteria. The rest are in either Actinobacteria, Bacteriodetes, or Firmicutes. The highest bacterial diversity was found in *D. discoideum* fruiting bodies originating from deer feces (27 OTUs), greater than either of those originating in shallow (11 OTUs) or in deep soil (4 OTUs). Rarefaction curves and the Chao1 estimator for species richness indicated the diversity in any substrate was not fully sampled, but for soil it came close. A majority of the *D. discoideum*-associated bacteria were edible by *D. discoideum* and supported its growth (75.2% for feces and 81.8% for soil habitats). However, we found several bacteria genera were able to evade phagocytosis and persist in *D. discoideum* cells through one or more social cycles. This study focuses not on the entire *D. discoideum* microbiome, but on the culturable subset of bacteria that have important eukaryote interactions as prey, symbionts, or pathogens. These eukaryote and bacteria interactions may provide fertile ground for investigations of bacteria using amoebas to gain an initial foothold in eukaryotes and of the origins of symbiosis and simple microbiomes.

Keywords: *Dictyostelium*, bacteria, microbiome, symbiosis, amoebae, sociality, persistence, predation

INTRODUCTION

Eukaryotes evolved in the context of a world already fully populated by bacteria and archaea (McFall-Ngai et al., 2013). Understanding the consequences and extent of this fairly recent realization is an enterprise still in its infancy. There are several different major approaches that include studies of the importance of gut microbiomes for food acquisition, plant root microbiomes for nutrient up-take, and the obligate symbioses of sap feeding insects and their bacteria (Moran et al., 2005; Alcock et al., 2014; Lareen et al., 2016). These studies and others are changing the way we view the place of eukaryotes in the living landscape. Important and paradigm changing as these studies are, they do not let us go back over two billion years to when eukaryotes were first adapting to the microbial world. Indeed, such a study would not be possible. However, we can make a closer approach to this goal by studying extant lineages from lineages more basal than animals and plants, though of course even their associations with bacteria still reflect modern adaptations and patterns.

Here, we use *Dictyostelium discoideum*, a single-celled bactivorous soil amoeba from a basal eukaryotic lineage, to investigate the range of interactions a micro-eukaryote has with bacteria in nature. The soil context is important because it is an environment where different organisms are in close contact with an abundance of potential bacterial prey. As such, our study organism exhibits a wide range of interactions with bacteria. First discovered as a predator of soil bacteria (Raper, 1937), *D. discoideum* has been employed as a model in many host-pathogen studies (Solomon et al., 2000; Alibaud et al., 2008; Hagedorn et al., 2009; Jia et al., 2009; Hasselbring et al., 2011), and has recently been found to engage in symbiotic associations with bacteria throughout their life history (Brock et al., 2011; DiSalvo et al., 2015). However, little is known about what bacteria *D. discoideum* associate with or prey upon in nature. The natural habitat of wild *D. discoideum* is deciduous forest soil and leaf litter and it is most commonly isolated from the acidic soils of eastern North America Appalachian forests (Cavender and Raper, 1965a,b; Raper, 1984; Landolt and Stephenson, 1986). Historically, Dictyostelids were first isolated from the dung of various herbivores (Raper, 1984) most notably from deer feces in North American forests (Stephenson and Landolt, 1992; Gilbert et al., 2007). Early work by Kenneth Raper indicated NC-4, the type-clone of *D. discoideum* isolated in the forests of North Carolina, could feed and develop on both gram-negative and gram positive non-pathogenic bacteria (Raper, 1937). In a later report, Raper and Smith also tested the growth of NC-4 against pathogenic bacteria species that may similarly occur in the soil, ascertaining that *D. discoideum* has a wide range of prey bacteria (Raper and Smith, 1939). More recently it has become clear that *D. discoideum* has different mechanisms for dealing with different prey species (Nasser et al., 2013).

D. discoideum can be thought of as a primitive macrophage capable of ingesting, killing and digesting at least one bacterium per minute as long as prey bacteria are available (Cosson and Soldati, 2008). Yet, upon depletion of available food, single-celled starving amoebae aggregate by the thousands using cAMP signals to form a multicellular organism (Kessin, 2001). During this transformation into a multicellular organism, *D. discoideum* slugs have some cells capable of immune-like functions (Chen et al., 2007; Brock et al., 2016a). These cells known as sentinel cells can remove bacterial pathogens as well as detoxify the slug to protect the presumptive spore population from harm. Slugs are motile and can migrate toward more favorable locations using light and heat as cues before terminally differentiating into a fruiting body. The fruiting body is composed a spherical sorus containing spores held aloft by a stalk to allow for spore dispersal. For decades, fruiting bodies containing the next generation of *Dictyostelium* spores were thought to be free from bacteria (Raper, 1937). However, some lineages of wild amoebae that we call farmers have stable interactions with different bacterial partners that are both food and weapons (Brock et al., 2011; Stallforth et al., 2013). Farmers have reduced sentinel cell numbers compared to *D. discoideum* clones without bacteria, suggesting a relaxation of innate immunity to allow carriage of bacterial associates (Brock et al., 2016a). We have reported two major clades of inedible *Burkholderia* as the most prominent bacterial partners of *D. discoideum* farmers (DiSalvo et al., 2015). These stable *Burkholderia* partners can colonize naïve *Dictyostelium* hosts and are the drivers of the proto-farming phenotype by allowing co-carriage of food bacteria through multiple social cycles.

To more completely explore the full nature and extent of the associations of a micro-eukaryote with bacteria in natural environments, we conducted a large-scale survey of soil and deer feces at Mountain Lake Biological Station in Virginia. We isolated wild *D. discoideum* to determine what, if any, culturable bacteria remain associated after *D. discoideum* amoebae differentiate into fruiting bodies. We focused on culturable bacteria in this survey to perform edibility and persistence assays to interrogate the type of interaction each bacterium had with wild *D. discoideum*. We found many different bacteria genera, which group into 32-species level OTUs (Operational Taxonomic Unit), transiently associated with the wild *D. discoideum* recovered from this survey. Here we detail the diversity of bacteria acquired by and maintained in *D. discoideum* throughout the social stage, and how bacterial diversity differs among different *D. discoideum* habitats. We show what these bacteria mean to their eukaryote host in the most ancient of relationships: predation and resistance of predation. The data presented here highlight the rich opportunities available to gain greater understanding of eukaryote-bacteria associations using a simple single-celled model organism.

MATERIALS AND METHODS

Deer Feces and Soil Collection

We collected samples of feces from white-tailed deer (*Odocoileus virginianus*) and of soil on 23 and 30 July 2014 from mixed deciduous forests at Mountain Lake Biological Station, Virginia (37.375654° −80.522140°) at Salt Pond Mountain on the eastern continental divide in the Appalachian Mountains (see **Figure 1** for collection locations and **Supplementary Table 1** for GPS coordinates and dates). On each collection date, we first identified and collected ten separate piles of fresh

deer feces. In addition to the feces, we collected two soil samples about 5 meters from each feces pile. One soil sample was shallow, just under the leaf litter about one to five centimeters deep. We collected the second soil sample about fifteen centimeters deep, adjacent to the shallow soil sample. We sterilized collection implements using ethanol wipes before and after each use to avoid cross contamination between sampling. This design gave us three samples at each location, one feces, one shallow soil, and one deep soil for a total of thirty samples for each date. From each location, we had four experimental plating categories: deep soil, shallow soil, feces slurry, and feces ball. We divided feces into slurry and ball to examine differences between the interior and surface of feces in regards to our survey method. See below for feces slurry preparation.

Culture of Dictyostelids From Soil and Feces

We plated all samples within two days of collection on hay agar plates. We prepared hay agar plates following Douglas et al. (2013). For food bacteria, we used overnight cultures of single colonies of *Klebsiella pneumoniae* grown in sterile Luria Broth (10 gm tryptone, 5 gm Oxoid yeast extract, and 10 gm NaCl per liter DDH_2O). *K. pneumoniae* was obtained from the *Dictyostelium* Stock Center (http://dictybase.org/StockCenter/StockCenter.html). To prepare the soil and feces for plating, we weighed five grams of soil or feces from each sample and placed it in a sterile 50 ml Falcon tube with sterile deionized water up to 50 ml. We dispersed the soil and feces in water by vortexing, then pipetted 300 μl of soil or feces slurry, per hay agar plate. We plated ten hay agar plates for each sample: five with 200 μl added overnight culture of food bacteria and five with no added food bacteria but with 200 μl Luria Broth added as control. Plating with and without added food bacteria allows us to germinate as many spores as possible present in the soil and feces samples in case suitable food bacteria for *D. discoideum* was not present or did not multiply under our growth conditions. After the liquid on each plate was absorbed (leaving the plates open in a biological safety cabinet for about 2–5 min), we added 6–12 activated charcoal pieces (Mars Fishcare Inc.) weighing about 100 milligrams. Activated charcoal can absorb a gaseous repellent released by culminating fruiting bodies aiding in their collection (Bonner and Dodd, 1962). Additionally, we placed one feces ball on each of five hay plates for each site. The feces ball was placed in a small indentation in the agar in the center of the hay plate with no additional bacteria added. We left the hay plates at room temperature (21°C) and checked them for growth of *D. discoideum* using a dissecting microscope for 6–10 days after plating. *D. discoideum* are readily and easily identifiable by their unique morphology compared to other Dictyostelids. We counted the number of distinct groups of fruiting bodies as areas positive for *D. discoideum* for each type of soil and feces (**Supplementary Table 2**). However, *D. discoideum* spores from the same soil sample could have come from the same fruiting body during the original collection process. Therefore, if more than one positive area is present on a test plate from the same soil sample, each area has the potential to be genetically different but may also be genetically the same.

Bacterial Presence or Absence in *D. discoideum* Fruiting Bodies

We found one to three distinct groupings of *D. discoideum* fruiting bodies on the positive hay plates, and we tested the sorus from a single fruiting body from each grouping to see if they contained bacteria. To do this, we used a sterile pipette tip to collect the sorus from a single fruiting body while viewing under a dissecting microscope. We placed the sorus in a 1.5 ml Eppendorf tube containing 50 μl of sterile non-nutrient buffer (2.25 g KH_2PO_4 and 0.67 g K_2HPO_4 per liter DDH_2O). Next, we vortexed the Eppendorf tube to disperse the fruiting body sorus contents. We then plated 10 μl of the sorus suspension on each of two SM/5 nutrient agar plates (2 g glucose, 2 g Oxoid bactopeptone, 2 g Oxoid yeast extract, 0.2 g $MgSO_4$, 1.9 g KH_2PO_4, 1 g K_2HPO_4, and 15.5 g agar per liter DDH_2O) either in association with *K. pneumonia* or in non-nutrient buffer at room temperature (21°C). This technique will reveal aerobic bacteria carried in *D. discoideum* sori that can be cultured, but not unculturable or anaerobic bacteria. We then sequenced 198 16S rRNA bacterial isolates from 95 fruiting body sori after streaking them to pick up a single clonal isolate (**Supplementary Table 3**). Twenty-four of the sequenced bacteria isolates had the same 16S rRNA identity as our food bacteria *K. pneumoniae*. We removed these bacteria sequences to eliminate any chance they were introduced during our isolation procedure and were not present in the soil or feces samples. We used the remaining 174 sequences in all subsequent calculations.

PCR Amplification, Bacterial Identification, and Diversity Analyses

We used the procedure outlined in "Identifying Unknown Bacteria using Biochemical and Molecular Methods" (www.nslc.wustl.edu/elgin/genomics/Bio3055/IdUnknBacteria06.pdf) to prepare template bacterial DNA for sequencing with one modification to the procedure. Instead of collecting bacteria grown in overnight liquid cultures, we collected a small amount of stationary phase bacteria clonally grown on a nutrient agar plate and prepared a suspension in water. The PCR amplification was done using a Gene Amp kit from Applied Biosystems (Roche). We used forward sequence 5′-CGG CCC AGA CTC CTA CGG GAG GCA GCA G-3′ and reverse sequence 5′-GCG TGG ACT ACC AGG GTA TCT AAT CC-3′ as primers to amplify about 460 bp of the 16S ribosomal RNA gene. The PCR fragments we generated were Sanger sequenced at GeneWiz (www.genewiz.com; South Plainfield New Jersey). Sequences were cleaned using Geneious 6.0 (http://www.geneious.com; Kearse et al., 2012), then aligned and clustered into OTUs (97% similarity) and identified with mothur (Schloss et al., 2009). We aligned sequences and taxonomically classified them using release 128 of the SILVA rRNA database (https://www.arb-silva.de/documentation/release-128/). We generated rarefaction curves and species richness estimates following the guidelines of Gotelli and Colwell (2011), and ran AMOVA (Analysis of

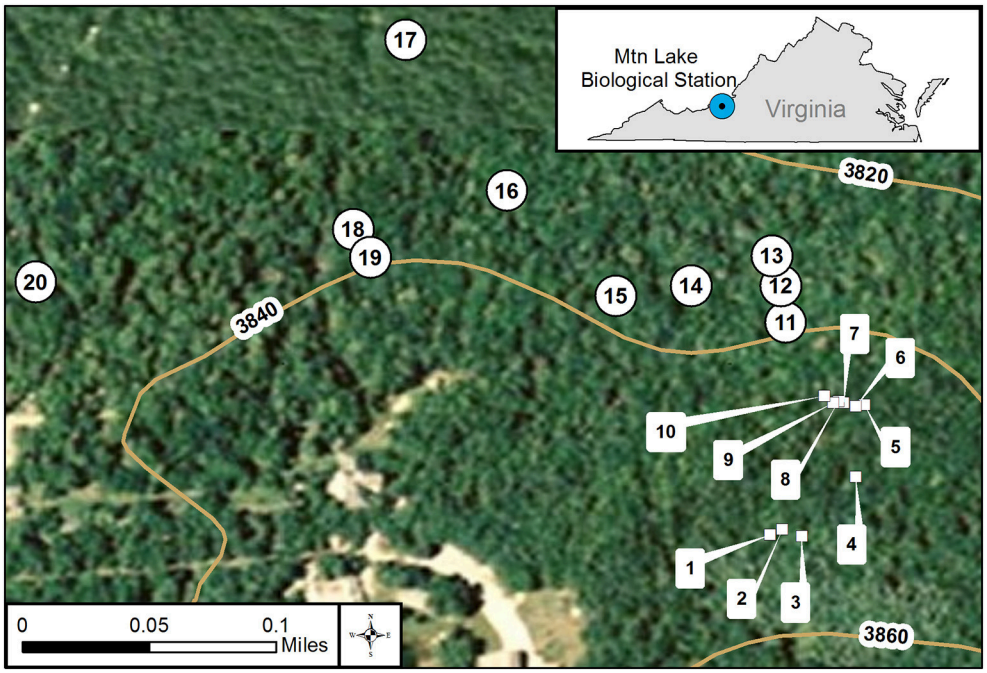

FIGURE 1 | GIS map of individual collection locations at Mt. Lake Biological Station, VA**.** We used GIS (geographical information system) to create a map of the collection locations. We did collections on two dates in July 2014 represented by square symbols numbered 1–10 and the round symbols numbered 11–20. The curved lines represent various elevations at our site. The small inset map details the location of Mt. Lake Biological Station in the state of Virginia, USA.

Molecular Variance) analysis in mothur. We pooled the deer feces slurry and ball samples for these analyses because very few bacteria associated with *D. discoideum* were isolated from the ball samples.

Phylogeny Construction

We aligned unique haplotypes of our cleaned sequences in Geneious 6.0, along with representative taxa of each major bacterial clade. We reconstructed the phylogeny using a maximum likelihood analysis in Mega 6 (Tamura et al., 2013). We used a general time-reversible model of sequence evolution and rooted the tree at the midpoint. Statistical support was generated using 1,000 bootstrap replicates. We display the phylogeny as a cladogram with edibility and sampling data mapped on using ITOL (Letunic and Bork, 2006). The full phylogeny with bootstrap values is included in the **Supplementary Materials**.

Edibility Assay

We tested bacterial isolates for edibility against four wild *D. discoideum* strains collected from this survey that were unassociated with bacteria. For this assay, we define edible bacteria as those bacteria with the capacity to support growth of *D. discoideum*. We used 159 bacteria isolates rather than all 174 bacteria species from our survey because fifteen grew too poorly on plates to assay. We chose two *D. discoideum* strains isolated from soil (4S 6.1 and 7S 4.1) and two *D. discoideum* strains isolated from feces (14P 2.2 and 18P 7.1). For the assay, we grew these four *D. discoideum* strains from spores on SM/5 nutrient agar plates supplemented with *K. pneumoniae* as our food bacteria at room temperature (21°C). We also grew each test bacterial isolate on SM/5 nutrient agar plates under the same conditions. Using a sterile inoculating loop, we first gathered a small amount of stationary phase test bacteria and then gathered spores from one of the test *D. discoideum* using the same loop. We streaked the bacteria/spore mixture densely across one quadrant of a subdivided SM/5 nutrient agar plate. We repeated the same procedure with different *D. discoideum* isolates across the other three quadrants. See **Supplementary Figure 1** for a cartoon schematic of the assay. After 1 week, we scored and tabulated the plates for edibility using the following qualitative categories: excellent (no bacteria present and abundant fruiting bodies), good (few bacteria present and many fruiting bodies), poor (many bacteria present and few fruiting bodies), inedible (abundant bacteria present and no fruiting bodies). See **Figure 7** for cartoon and representative images of edibility assay. We used Pearson's Chi-square goodness of fit to determine if our sample data are consistent with a hypothesized distribution of equal proportions as our null hypothesis, or of dissimilar distributions between feces and soil environments. We used software available from http://quantpsy.org/chisq/chisq.htm to calculate the chi-square test (Preacher, 2001).

Persistence Assay

We plated spores from one naïve clone unassociated with bacteria (QS9) individually with eighteen different bacteria genera to test for persistence through multiple *D. discoideum* social cycle rounds without additional bacteria. Seventeen

genera were isolated from this screen. The bacteria genera tested were *Achromobacter, Ancylobacter, Burkholderia, Comamonas, Escherichia, Flavobacterium, Oxalicibacterium, Paenibacillus, Pandoraea, Pseudomonas, Rahnella, Rhizobium, Serratia, Shinella, Staphylococcus, Stenotrophomonas, Variovorax.* We used the lab food bacteria *Klebsiella pneumoniae* as a negative (no persistence) control for a total of eighteen genera. We streaked the bacteria onto SM/5 plates from frozen stocks and grew to stationary phase at 21°C. We prepared bacterial suspensions in non-nutrient buffer at an OD_{600} of 1.5. To set up the assay, we collected spores from fruiting bodies under a dissecting scope by touching the top of a sorus using a sterile pipette tip. The spores were placed into sterile non-nutrient buffer. We determined spore density using a hemacytometer and a light microscope. We plated 2×10^5 spores and 200 µl of each of the eighteen test bacteria onto SM/5 nutrient agar plates. This is the initial plating. After the initial plating, all subsequent transfers were done bacteria-free meaning spores were collected from each test plate in non-nutrient buffer and plated onto nutrient agar as above without adding additional test bacteria. Bacteria growth and the eventual formation of fruiting bodies would only be able to occur in the test rounds if bacteria persisted in the spores from the initial plating with the test bacteria genera. We grew all rounds at room temperature (21°C) until fruiting bodies formed. Next, for each round we placed ten individual spore masses (sori) from randomly selected fruiting bodies onto SM/5 nutrient agar (spot test). We recorded bacterial growth and fruiting body formation in the individual test spots of spore masses after 5 days at room temperature (21°C).

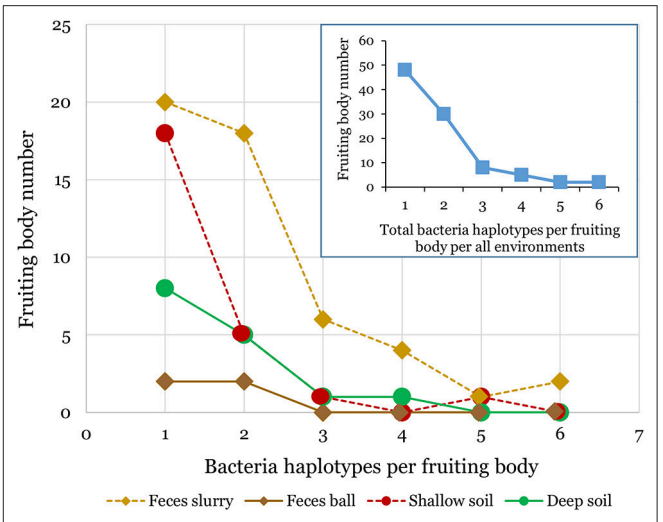

FIGURE 2 | Multiple bacteria isolates can transiently persist within individual *D. discoideum* fruiting bodies. We found bacteria associated with about one-third of the *D. discoideum* fruiting bodies isolated in this survey. Each individual fruiting body sorus positive for bacteria presence collected from either soil or feces environments contained from one to six bacteria isolates as shown in the above line graphs. The inset line graph quantifies the total number of bacteria isolates per fruiting body we isolated from all environments combined.

RESULTS

We found bacteria associated with 95 of the 254 *D. discoideum* sori isolated from this survey. The sorus is the spore-containing area located at the top of the fruiting body. The other 161 inspected sori contained no culturable bacteria. We isolated *D. discoideum* at all twenty locations from at least one type of soil or feces sample using either added or no added food bacteria (**Figure 1**; **Supplementary Table 2**). In total, we clonally isolated 174 culturable bacteria isolates (**Supplementary Table 3**). We found that one to six genetically distinct bacteria isolates can transiently persist through a social cycle in a single sorus isolated from wild *D. discoideum* (**Figure 2**). Although a fruiting body sorus may contain up to six bacteria isolates, we found the majority (82.1%) contain one or two bacteria isolates per fruiting body sorus.

We constructed a phylogeny of bacteria using unique haplotypes from 16S rRNA sequences (**Figure 3**). These haplotypes are located in four bacteria phyla: Actinobacteria, Bacteriodetes, Firmicutes, and Proteobacteria, the latter represented by three classes (Alpha, Beta, and Gamma). We found the majority (71.4%) of these unique bacterial haplotypes are Proteobacteria and these haplotypes are almost all edible (84.4%). Additionally, the bacteria haplotypes from Actinobacteria, Alphaproteobacteria, and Bacteriodetes were isolated only from *D. discoideum* originating from feces environments. There were about twice as many culturable bacteria genera associated with *D. discoideum* isolated from feces compared to soil environments. Seven genera overlap between the soil and feces environments (**Figure 4**), and these account for 63.8% of bacterial isolates from this survey.

When 16S rRNA sequences were clustered into OTUs at 97% similarity, we found the diversity of bacteria was highest in deer feces (27 OTUs), and lower in both the shallow (11 OTUs) and deep soil (4 OTUs) samples. Our experimental design included adding food bacteria (*K. pneumoniae*) to half of the selection plates. We found the addition of *K. pneumoniae* had no effect on the diversity of bacteria we collected from *D. discoideum* (AMOVA, $F_{(1,172)} = 1.04$, $p = 0.346$; with Kp = 25 OTUs, without Kp = 22 OTUs). Since each sample type varied in the number of bacteria we were able to culture, we used rarefaction curves and species richness estimates to compare the diversity between the sample types. None of the rarefaction curves reached saturation, indicating we did not fully sample the diversity in any sample type (**Figure 5A**). However, the Chao1 species richness estimates suggest that the total number of OTUs associated with *D. discoideum* at Mountain Lake is low and could be fully sampled with moderately more effort. The deer feces had a Chao1 estimated richness of 46.5 bacterial associates (95% CI of 32.2–99.9) while the shallow and deep soil were estimated to have 13.5 (11.3–28) and 5 (4.1–17.3) bacterial associates, respectively. We also assessed how well the number of sites we sampled captured the bacterial diversity since individual-based rarefaction can overestimate species richness when species distribution is patchy (Gotelli and Colwell, 2011), which is likely for *Dictyostelium* and its associated bacteria. Rarefaction curves at different taxonomic levels indicate we did not fully sample bacterial diversity except

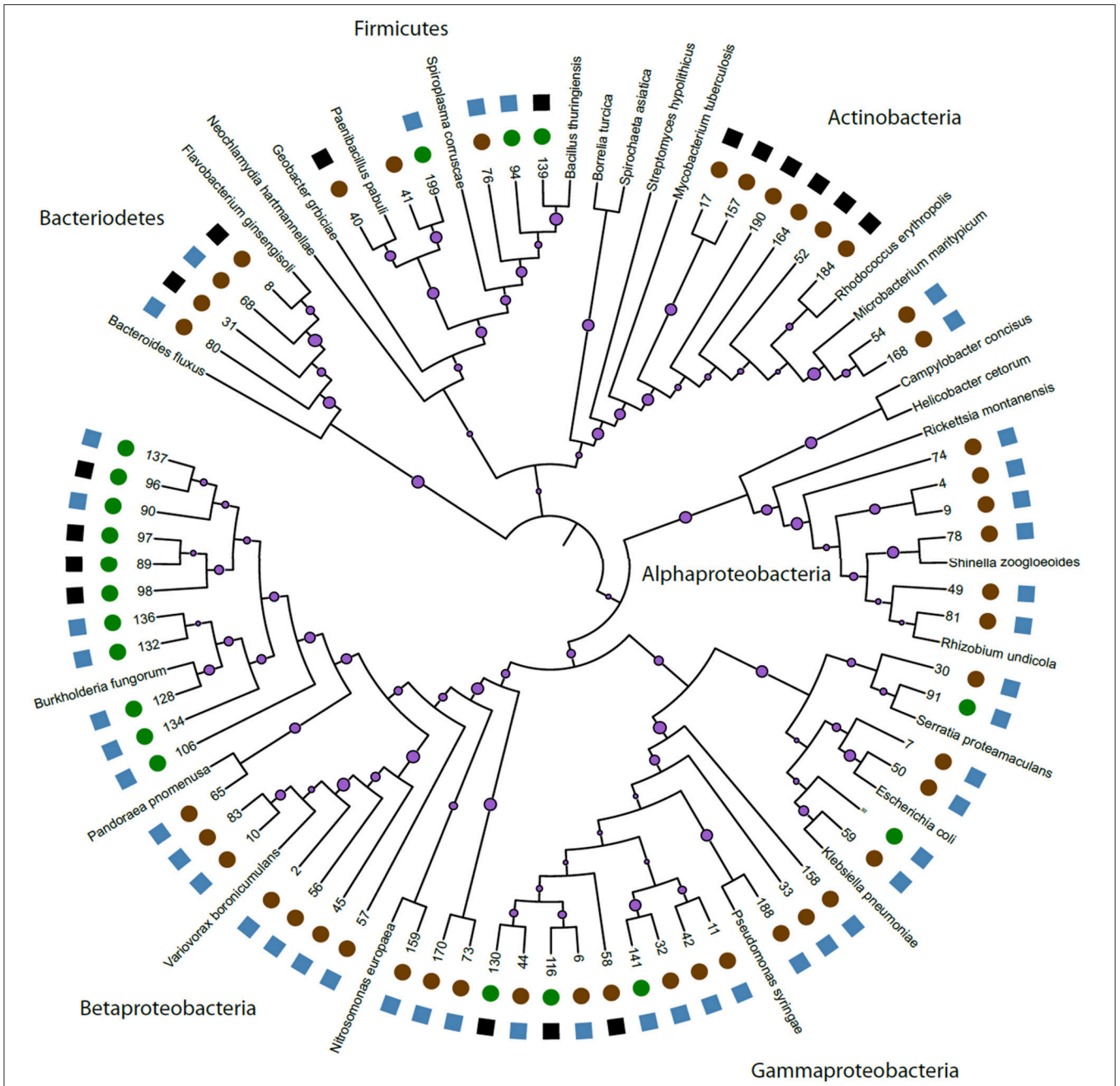

FIGURE 3 | Phylogeny of unique bacteria haplotypes. We created a phylogeny of unique bacteria haplotypes found in association with *D. discoideum*. We anchored this phylogeny with 26 named and sequenced bacteria. On the individual branches, we have purple circles representing bootstrap support from 1,000 bootstrap replicates with larger circle size indicating greater support. Bootstrap numbers for each branch length can be found in **Supplementary Figure 2**. The numbers at the end of the branches represent the bacteria we isolated during this survey. See **Supplementary Table 3** for further details. On the outside edge of the figure, we used circles to represent bacteria from our two environments: feces (brown) and soil (green). We used squares to represent edibility: edible (blue) and inedible (black) for each unique haplotype. Edibility for some bacteria genera had both inedible and edible bacteria and the blue or black edibility symbols square shown here represent a single unique bacterium in that genus.

at the phylum level (**Figure 5B**). As indicated by the sample type rarefaction, most of this undiscovered diversity is likely to be in deer feces.

We asked if the distribution of our four edibility types is the same in both feces and soil environments. *D. discoideum* amoebae generally lyse and digest phagocytized bacteria very quickly (Clarke and Maddera, 2006). Yet we found numerous bacteria persisting through the multicellular stage, which is triggered by starvation. Are these bacteria persisting because they were inedible and could not be broken down? We scored

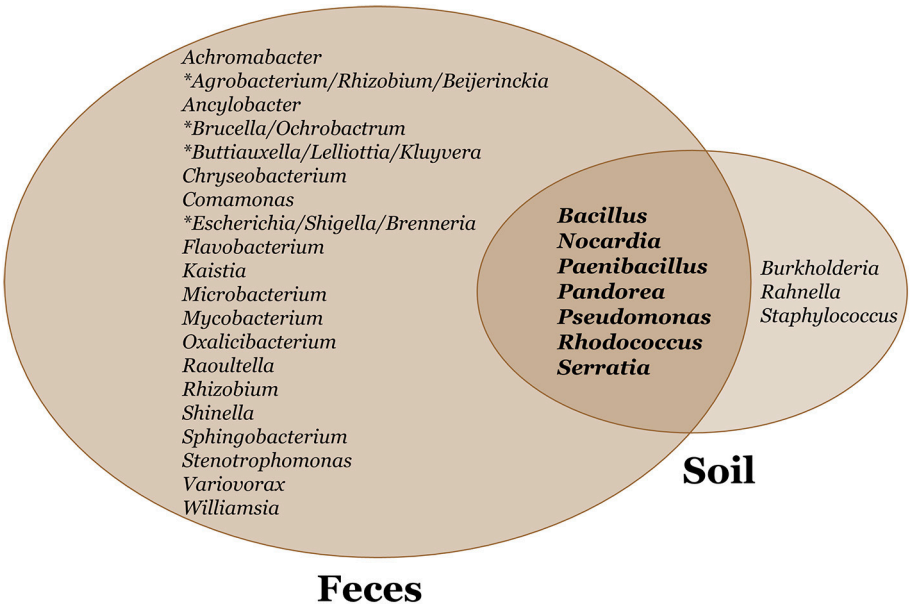

FIGURE 4 | Venn diagram of soil and feces bacteria genera associated with *D. discoideum*. We found seven bacteria genera overlap between soil and feces environments. We identified about twice as many culturable bacteria genera associated with *D. discoideum* isolated from feces compared to soil environments. A 460 bp PCR fragment generated from 16S rRNA primers was sequenced to identify these bacteria genera. The asterisk signifies bacteria genera of equal sequence identity.

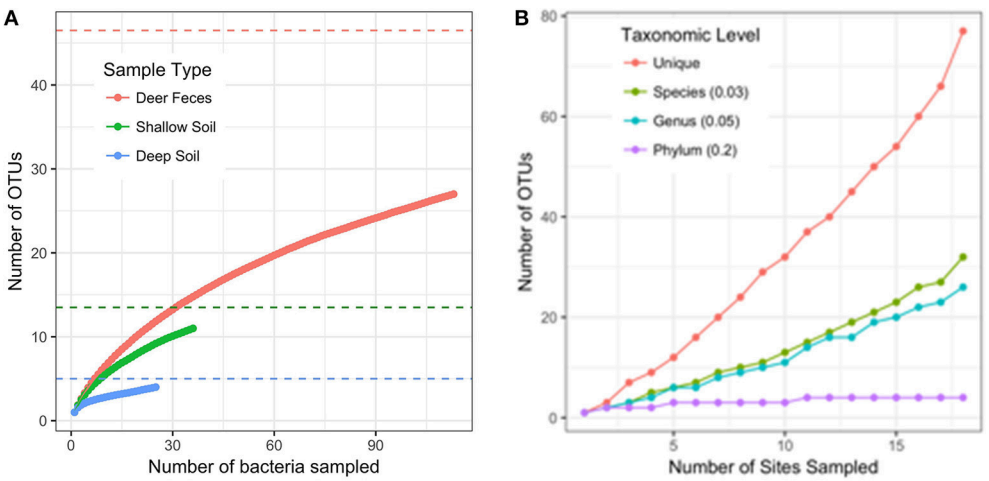

FIGURE 5 | Rarefaction curves**. (A)** Rarefaction curve for the number of bacterial isolates sampled separated by sample type (intact deer feces and feces slurry samples are combined into one category). OTUs are defined with a distance of 0.03. Dashed lines are the Chao1 estimates of species richness for the sample type with the corresponding color. **(B)** Rarefaction curve for the number of sites sampled. OTUs are defined at different taxonomic levels following the distance cutoffs recommend by Schloss and Handelsman, 2005. The "unique" category counts every non-identical sequence as a single OTU.

and tabulated edibility using four categories: excellent, good, poor, and inedible (**Figure 6A**). We found 75.2% and 81.8% of *D. discoideum*-associated bacteria from feces and soil habitats, respectively are edible with a range from excellent to poor. Additionally, we asked if there were any differences between soil-collected and feces-collected bacteria in the degree of edibility. Our null hypothesis is that no relationship exists between the distributions of edibility categorical types from the feces and soil sets in the population. We performed Pearson's chi-square test and rejected this hypothesis. The distributions of bacterial edibility types that associate with *D. discoideum* differ significantly from expected between soil and feces habitats though not strongly (chi-square = 9.1713; df = 3; $p = 0.027$; **Figure 6B**). The main driver is the larger proportions of excellent edible type and inedible type bacteria found in feces compared to soil.

A

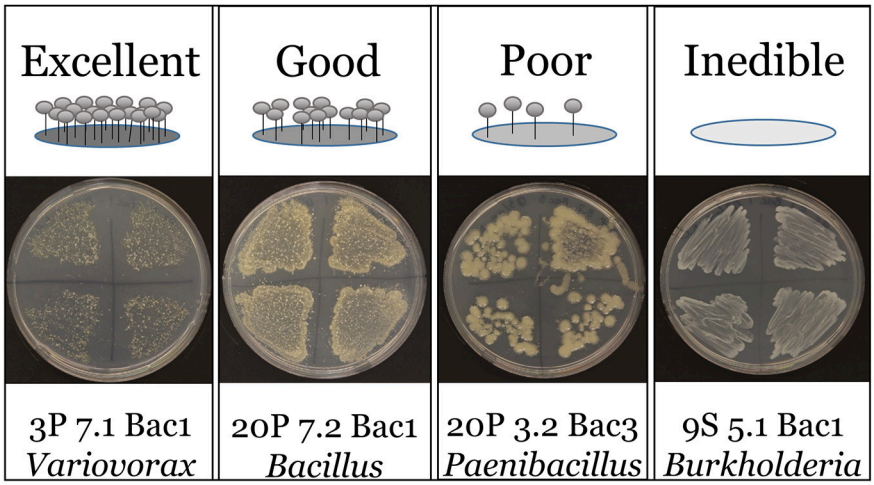

B

	Excellent	Good	Poor	Inedible
Feces	39 (32.70) [1.21]	23 (26.82) [0.54]	16 (20.93) [1.16]	26 (23.55) [0.26]
Soil	11 (17.30) [2.29]	18 (14.18) [1.03]	16 (11.07) [2.20]	10 (12.45) [0.48]

FIGURE 6 | Edibility assay rubric and Chi-square contingency table.**(A)** Top panel includes cartoon examples of our scoring rubric for bacteria edibility by wild *D. discoideum*: excellent (no bacteria present and abundant fruiting bodies), good (few bacteria present and many fruiting bodies), poor (many bacteria present and few fruiting bodies), inedible (abundant bacteria present and no fruiting bodies). Bottom panel includes representative images of bacteria and fruiting bodies on nutrient agar plates corresponding to each category from the assay. **(B)** Chi-square contingency table. The contingency table provides the following information for the edibility data: the top line is the observed total for each edibility type, the middle line in parentheses is the expected total for each edibility type, and the bottom line in brackets is the chi-square statistic for each edibility type.

Avoidance of digestion by bacteria after phagocytosis is thought to have first evolved as a method to resist predatory amoeba (Cosson and Soldati, 2008). We tested seventeen bacteria genera from our screen with the lab food bacteria *K. pneumoniae* as control to determine if these edible bacteria were able to persist through multiple social cycles (**Figure 7**). Each tested bacteria was the only food source for the *D. discoideum* amoebae so if persistence occurred the bacteria would be partially evading phagocytosis. We found nine out of 18 bacteria tested persisted through the first round and seven out of 18 through three social cycle rounds (**Figure 7**).

DISCUSSION

The extent of natural variation in *D. discoideum* relationships with soil bacteria has been largely unexplored. In this study, we investigated the range of culturable aerobic bacterial associations with *D. discoideum* fruiting bodies in a natural environment by conducting a survey of forest soil and deer feces at Mountain Lake Biological Station. *D. discoideum* are predators of bacteria and were previously thought to be bacteria-free during all life stages (Raper, 1937) until we reported some *D. discoideum* maintain a symbiotic relationship with a handful of *Burkholderia* species (Brock et al., 2011; DiSalvo et al., 2015). In this report, we demonstrate that newly isolated wild *D. discoideum* fruiting bodies are far from bacteria-free and are able to transiently carry a broad variety of bacteria throughout their life history. We also establish that many of the bacteria are able to evade phagocytosis and persist through multiple social cycle rounds lab conditions.

Overall, our collection strategy yielded similar numbers of *D. discoideum* clones from feces compared to soil environments. We isolated numerous bacteria from about one-third of these *D. discoideum* clones after terminal differentiation when fruiting bodies are formed. Edible bacteria make up the majority of the bacteria we collected (85% of feces and 81% of soil) and the high degree of edibility is in agreement with previous early reports that the type-clone of *D. discoideum* could feed on a wide range of bacterial species (Raper, 1937; Raper and Smith, 1939). The soil samples seem to be fairly poor sources of *D. discoideum*-associated bacteria based on the lower diversity of culturable bacteria in shallow soil (11 OTUs) and deep soil (4 OTUs) compared to deer feces (27 OTUs). Despite being extremely

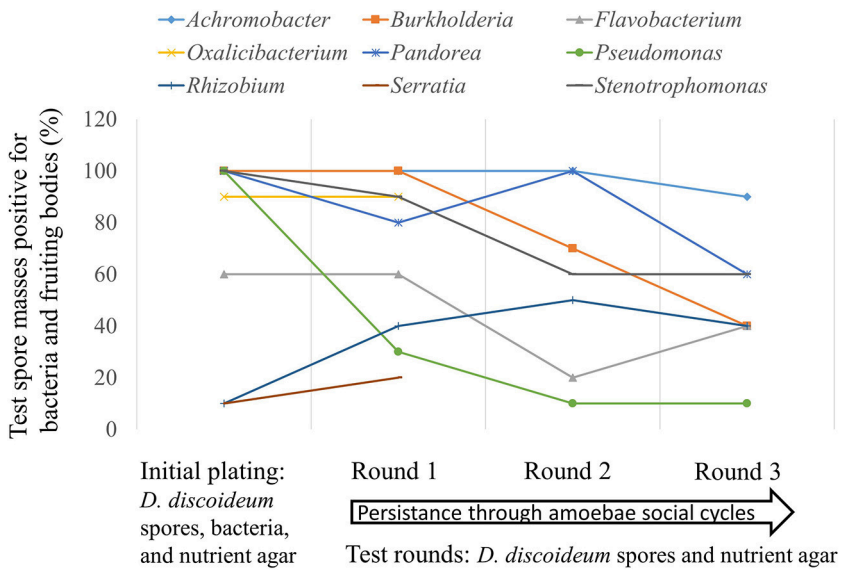

FIGURE 7 | Some bacteria genera are able to evade phagocytosis and persistently associate with *Dictyostelium* amoebae through multiple social cycles**.** We plated spores from one naïve non-farmer *D. discoideum* clone individually with 17 different bacteria genera isolated from this screen and the lab food bacteria *Klebsiella pneumoniae* as control (initial plating). After fruiting bodies formed, we serially passaged *D. discoideum* spores from each test bacteria for three rounds with no additional bacteria (test rounds). We tested ten random individual spore masses from fruiting bodies formed after completion of the social cycle for the presence of bacteria and fruiting bodies on nutrient agar. We did this after each round including the initial plating. Bacteria growth and the eventual formation of fruiting bodies would only be able to occur in the test rounds if bacteria persisted in the spores from the initial plating with the test bacteria genera. Nine of the eighteen bacteria genera evaded phagocytosis and were able to persist through one round of *D. discoideum* fruiting body formation on nutrient agar without additional food bacteria added; seven of the eighteen persisted through three social cycle rounds. The nine genera tested that did not persist are: *Ancylobacter, Comamonas, Escherichia, Klebsiella, Paenibacillus, Rahnella, Shinella, Staphylococcus,* and *Variovorax*.

bacteria-rich (Fierer, 2017), soil may have a scarcity of bacteria that serve as prey or are able to persist with *D. discoideum*. Deer feces, another environment densely colonized by bacteria, harbored more bacteria that could associate with *D. discoideum,* suggesting the type of habitat *D. discoideum* grows in likely affects which bacteria are available for uptake. In addition, the relatively few bacteria (Chao1 estimates of 5–47 culturable species) found within *D. discoideum* living in such bacteria-rich environments suggests that the association may be selective rather than being either promiscuous or haphazard. It is also important to note that we focused here on culturable aerobic bacteria in order to test the edibility and persistence of the bacteria collected. However, there are likely to be other bacteria associated with *D. discoideum* that cannot grow on the media we used, and a culture-free survey is necessary to get a complete picture of the *D. discoideum* microbiome.

The many bacteria we isolated associated with our wild *D. discoideum* isolates may or may not be residing inside the spores. These bacteria could be associating with *D. discoideum* in some other fashion. We have previously established that some wild *D. discoideum* known as farmers facultatively associate with certain bacteria, that these bacteria are located inside spores, and that they can be vertically transmitted to the next generation (Brock et al., 2011; DiSalvo et al., 2015). In this study we found several bacteria genera were able to persist through multiple social cycle rounds suggesting wherever these bacteria are located they are able to be transmitted to the next generation in some fashion. However, spot test percentages were lower in the persistence assay than we have previously shown with symbiotic *Burkholderia* sp. nov. in *D. discoideum* (DiSalvo et al., 2015), so carriage in the spores or fidelity of transmission of the tested bacteria genera may be less than we found for our symbiotic *Burkholderia*. Where bacteria from this survey are located within the *D. discoideum* fruiting bodies will need to be determined by future research, but it seems likely that at least a portion of them could be persisting inside the spores.

Non-digestion (persistence) of bacteria in hosts can be aided by manipulation of the host immune response, and bacteria have developed an arsenal of diverse mechanisms to do this (Sansonetti and Di Santo, 2007; Ribet and Cossart, 2015). Secretion systems are commonly used by bacteria to secrete effectors into a host cell after engulfment (Green and Mecsas, 2016). These secreted effectors facilitate escape of the bacteria from the phagosome or block phagosome fusion to the lysosome preventing bacterial cell death thereby creating a new niche in the host. Proteobacteria are particularly rich in secretion systems (T1SS, T2SS, T3SS, T4SS, T5aSS, T5bSS, T5cSS, and T6SS) having more different types of secretion systems than all other phyla (Abby et al., 2016). The majority of bacteria we isolated in total were in the Alpha, Beta, and Gamma classes of Proteobacteria and this was also true of the type bacteria that persisted through multiple social rounds of growth. A similar abundance of Proteobacteria classes was found among digestion-resistant bacteria in surveys of marine and fresh water ciliates,

another group of unicellular eukaryotes (Pucciarelli et al., 2015; Gong et al., 2016). Gong et al. (2016) suggested bacteria with type IV and VI secretion systems (T4SS and T6SS) as having a possible role in promoting these marine protist/bacteria associations. Both type IV and VI secretion systems transport proteins and effector molecules into eukaryotic cells and have been implicated in suppressing immunity and exporting virulence factors (Cascales and Christie, 2003; Bingle et al., 2008). Type VI secretion systems have also been shown to have non-pathogenic roles mediating symbiotic relationships between bacteria and eukaryotes as well (Parsons and Heffron, 2005; Chow and Mazmanian, 2010; Jani and Cotter, 2010). However, Proteobacteria are often abundant in forest soil (Janssen, 2006), so we are not certain how over-represented they might be in our samples.

Secretion systems are also one of the mechanisms bacteria use to secrete effectors that directly target components of the innate immune system such as Toll-like receptors and Nod-like receptors (Reddick and Alto, 2014). When multicellular, *D. discoideum* contain a cell type known as sentinel cells that provides immune-like and detoxification functions (Chen et al., 2007; Brock et al., 2016a). Additionally, Chen et al. (2007) found a Toll/Interleukin-1 Receptor (TIR) domain protein that is necessary for sentinel cells to effectively target bacteria to allow clearance of the bacteria from the slug. We have previously shown that wild *D. discoideum* farmers have fewer sentinel cells compared to *D. discoideum* with no associated bacteria suggesting a relaxed immune response promoting symbiotic interactions through a reduction in the clearance of carried bacteria (Brock et al., 2016a). The bacteria we found associated in the sori of wild *D. discoideum* fruiting bodies may be persisting through a similar mechanism.

Amoebae are proposed as reservoir hosts for pathogenic bacteria (Molmeret et al., 2005; Scheid, 2014; Strassmann and Shu, 2017). In support, Benavides-Montaño and Vadyvaloo recently reported *Yersinia pestis* can survive in *Acanthamoeba castellanii* amoebae for prolonged periods by using the type three secretion system to inhibit phagocytosis (Benavides-Montaño and Vadyvaloo, 2017). Bacteria can increase in virulence even after short associations with eukaryotes leading to environmental and health consequences. One example reports enhanced virulence of *Mycobacterium avium* in macrophage and mouse models after growth in *A. castellanii* (Cirillo et al., 1997). Another recent example describes increased dispersal ability and amplified virulence of *Bordetella bronchiseptica* after growth in *D. discoideum* along with macrophage and mouse models (Taylor-Mulneix et al., 2017). Many of the bacterial genera we isolated in this study are known to have members implicated in causing disease, such as *Brucella* (Brucellosis), *Escherichia/Shigella* (urinary tract infections/diarrhea), *Nocardia* (Nocardiosis), and *Staphylococcus* (urinary tract infections), suggesting similar possibilities for health consequences.

Digestion of bacteria by amoebae should occur quickly after engulfment (Clarke and Maddera, 2006). However, our ability to isolate culturable bacteria from wild fruiting body spore masses formed after starvation suggests the possibility of some level of persistence and host manipulation. Amoebae/bacteria relationships are important because they can inform us about the interdependent relationships of bacteria to all eukaryotes (Gilbert et al., 2012). The vast range of eukaryote-bacteria interactions can affect development, immunity, and evolution (Rosenberg and Zilber-Rosenberg, 2016). Based on the data presented here, we find a more multifaceted relationship between *D. discoideum* and bacteria than just that of predator/prey. *D. discoideum* has already been utilized extensively as a model system to study host/pathogen relationships as detailed in a recent review (Bozzaro and Eichinger, 2011), and more recently to study symbiotic relationships (Brock et al., 2011, 2013, 2016b; DiSalvo et al., 2015). This system will provide an excellent platform to discover if bacteria persistence in wild *D. discoideum* amoebae can initiate either increased infectivity in other hosts or, alternatively, symbiosis. Our study shows that the range of bacterial associates, whether pathogenic, symbiotic, or haphazard, is much larger than has been appreciated.

DATA ACCESSIBILITY

The bacterial 16S rRNA gene sequences from this study have been deposited in the Genbank numbers are MK177283–MK177456.

AUTHOR CONTRIBUTIONS

DB, DQ, and JS designed the experiments. FB and JG mapped and collected the samples. DB, UB, and TD performed the experiments. DB, JRG, TH, DQ, and JS analyzed the results and wrote the manuscript. All authors approved the final manuscript.

FUNDING

This material is based upon work supported by the National Science Foundation under Grants No. NSF IOS-1256416, NSF IOS-1656756, and the John Templeton Foundation grant 43667. The funders had no role in study design, data collection and interpretation, or the decision to submit the work for publication.

ACKNOWLEDGMENTS

We thank the Queller/Strassmann lab group for useful feedback and discussion, and especially Alicia Hubert for final touches on bacteria sequencing and figures. Many thanks to William E. Winston for creating the GIS location map of our experimental site.

SUPPLEMENTARY MATERIAL

The Supplementary Material for this article can be found online at: https://www.frontiersin.org/articles/10.3389/fcimb.2018.00411/full#supplementary-material

REFERENCES

Abby, S. S., Cury, J., Guglielmini, J., Néron, B., Touchon, M., and Rocha, E. P. (2016). Identification of protein secretion systems in bacterial genomes. *Sci. Rep.* 6:23080. doi: 10.1038/srep23080

Alcock, J., Maley, C. C., and Aktipis, C. (2014). Is eating behavior manipulated by the gastrointestinal microbiota? *evolutionary pressures and potential mechanisms. Bioessays* 36, 940–949. doi: 10.1002/bies.201400071

Alibaud, L., Köhler, T., Coudray, A., Prigent-Combaret, C., Bergeret, E., Perrin, J., et al. (2008). Pseudomonas aeruginosa virulence genes identified in a Dictyostelium host model. *Cell. Microbiol.* 10, 729–740. doi: 10.1111/j.1462-5822.2007.01080.x

Benavides-Montaño, J. A., and Vadyvaloo, V. (2017). Yersinia pestis resists predation by Acanthamoeba castellanii and exhibits prolonged intracellular survival. *Appl. Environ. Microbiol.* 83:e00593–17. doi: 10.1128/AEM.00593-17

Bingle, L. E., Bailey, C. M., and Pallen, M. J. (2008). Type VI secretion: a beginner's guide. *Curr. Opin. Microbiol.* 11, 3–8. doi: 10.1016/j.mib.2008.01.006

Bonner, J. T., and Dodd, M. R. (1962). Evidence for gas-induced orientation in the cellular slime molds. *Dev. Biol.* 5, 344–361. doi: 10.1016/0012-1606(62)90018-0

Bozzaro, S., and Eichinger, L. (2011). The professional phagocyte *Dictyostelium discoideum* as a model host for bacterial pathogens. *Curr. Drug Targets* 12, 942–954. doi: 10.2174/138945011795677782

Brock, D. A., Callison, W. É., Strassmann, J. E., and Queller, D. C. (2016a). Sentinel cells, symbiotic bacteria and toxin resistance in the social amoeba *Dictyostelium discoideum*. *Proc. Biol. Sci.* 283:20152727. doi: 10.1098/rspb.2015.2727

Brock, D. A., Douglas, T. E., Queller, D. C., and Strassmann, J. E. (2011). Primitive agriculture in a social amoeba. *Nature* 469, 393–396. doi: 10.1038/nature09668

Brock, D. A., Jones, K., Queller, D. C., and Strassmann, J. E. (2016b). Which phenotypic traits of *Dictyostelium discoideum* farmers are conferred by their bacterial symbionts? *Symbiosis* 68, 39–48. doi: 10.1007/s13199-015-0352-0

Brock, D. A., Read, S., Bozhchenko, A., Queller, D. C., and Strassmann, J. E. (2013). Social amoeba farmers carry defensive symbionts to protect and privatize their crops. *Nat. Commun.* 4:2385. doi: 10.1038/ncomms3385

Cascales, E., and Christie, P. J. (2003). The versatile bacterial type IV secretion systems. *Nat. Rev. Microbiol.* 1, 137–149. doi: 10.1038/nrmicro753

Cavender, J. C., and Raper, K. B. (1965a). The Acrasieae in nature. II. Forest soil as a primary habitat. *Am. J. Bot.* 52, 297–302. doi: 10.1002/j.1537-2197.1965.tb06789.x

Cavender, J. C., and Raper, K. B. (1965b). The Acrasieae in nature. III. occurrence and distribution in forests of eastern North America. *Am. J. Bot.* 52, 302–308. doi: 10.1002/j.1537-2197.1965.tb06790.x

Chen, G., Zhuchenko, O., and Kuspa, A. (2007). Immune-like phagocyte activity in the social amoeba. *Science* 317, 678–681. doi: 10.1126/science.1143991

Chow, J., and Mazmanian, S. K. (2010). A pathobiont of the microbiota balances host colonization and intestinal inflammation. *Cell Host Microbe* 7, 265–276. doi: 10.1016/j.chom.2010.03.004

Cirillo, J. D., Falkow, S., Tompkins, L. S., and Bermudez, L. E. (1997). Interaction of Mycobacterium avium with environmental amoebae enhances virulence. *Infect. Immun.* 65, 3759–3767.

Clarke, M., and Maddera, L. (2006). Phagocyte meets prey: uptake, internalization, and killing of bacteria by *Dictyostelium amoebae*. *Eur. J. Cell Biol.* 85, 1001–1010. doi: 10.1016/j.ejcb.2006.05.004

Cosson, P., and Soldati, T. (2008). Eat, kill or die: when amoeba meets bacteria. *Curr. Opin. Microbiol.* 11, 271–276. doi: 10.1016/j.mib.2008.05.005

DiSalvo, S., Haselkorn, T. S., Bashir, U., Jimenez, D., Brock, D. A., Queller, D. C., et al. (2015). Burkholderia bacteria infectiously induce the proto-farming symbiosis of *Dictyostelium amoebae* and food bacteria. *Proc. Natl. Acad. Sci. U.S.A.* 112:E5029–E5037. doi: 10.1073/pnas.1511878112

Douglas, T. E., Brock, D. A., Adu-Oppong, B., Queller, D. C., and Strassmann, J. E. (2013). Collection and cultivation of dictyostelids from the wild. *Methods. Mol. Biol.* 983, 113-124. doi: 10.1007/978-1-62703-302-2_6

Fierer, N. (2017). Embracing the unknown: disentangling the complexities of the soil microbiome. *Nat. Rev. Microbiol.* 15, 579–590. doi: 10.1038/nrmicro.2017.87

Gilbert, O. M., Foster, K. R., Mehdiabadi, N. J., Strassmann, J. E., and Queller, D. C. (2007). High relatedness maintains multicellular cooperation in a social amoeba by controlling cheater mutants. *Proc. Natl. Acad. Sci. U.S.A.* 104, 8913–8917. doi: 10.1073/pnas.0702723104

Gilbert, S. F., Sapp, J., and Tauber, A. I. (2012). A symbiotic view of life: we have never been individuals. *Q. Rev. Biol.* 87, 325–341. doi: 10.1086/668166

Gong, J., Qing, Y., Zou, S., Fu, R., Su, L., Zhang, X., et al. (2016). Protist-bacteria associations: Gammaproteobacteria and Alphaproteobacteria are prevalent as digestion-resistant bacteria in ciliated protozoa. *Front. Microbiol.* 7:498. doi: 10.3389/fmicb.2016.00498

Gotelli, N. J., and Colwell, R. K. (2011). "Estimating species richness," in *Biological Diversity: Frontiers in Measurement and Assessment* (Oxford, UK: Oxford University Press), 39–54.

Green, E. R., and Mecsas, J. (2016). Bacterial secretion systems–an overview. *Microbiol. Spectr.* 4. doi: 10.1128/microbiolspec

Hagedorn, M., Rohde, K. H., Russell, D. G., and Soldati, T. (2009). Infection by tubercular mycobacteria is spread by nonlytic ejection from their amoeba hosts. *Science* 323, 1729–1733. doi: 10.1126/science.1169381

Hasselbring, B. M., Patel, M. K., and Schell, M. A. (2011). *Dictyostelium discoideum* as a model system for identification of *Burkholderia pseudomallei* virulence factors. *Infect. Immun.* 79, 2079–2088. doi: 10.1128/IAI.01233-10

Jani, A. J., and Cotter, P. A. (2010). Type VI secretion: not just for pathogenesis anymore. *Cell Host Microbe* 8, 2–6. doi: 10.1016/j.chom.2010.06.012

Janssen, P. H. (2006). Identifying the dominant soil bacterial taxa in libraries of 16S rRNA and 16S rRNA genes. *Appl. Environ. Microbiol.* 72, 1719–1728. doi: 10.1128/AEM.72.3.1719-1728.2006

Jia, K., Thomas, C., Akbar, M., Sun, Q., Adams-Huet, B., Gilpin, C., et al. (2009). Autophagy genes protect against *Salmonella typhimurium* infection and mediate insulin signaling-regulated pathogen resistance. *Proc. Natl. Acad. Sci. U.S.A.* 106, 14564–14569. doi: 10.1073/pnas.0813319106

Kearse, M., Moir, R., Wilson, A., Stones-Havas, S., Cheung, M., Sturrock, S., et al. (2012). Geneious basic: an integrated and extendable desktop software platform for the organization and analysis of sequence data. *Bioinformatics* 28, 1647–1649. doi: 10.1093/bioinformatics/bts199

Kessin, R. H. (2001). *Dictyostelium - evolution, cell biology, and the development of multicellularity. Cambridge, UK: Cambridge Univ*ersity *Press*. doi: 10.1017/CBO9780511525315

Landolt, J. C., and Stephenson, S. L. (1986). Cellular slime molds in forest soils of southwestern Virginia. *Mycologia* 78, 500–502. doi: 10.1080/00275514.1986.12025279

Lareen, A., Burton, F., and Schäfer, P. (2016). Plant root-microbe communication in shaping root microbiomes. *Plant Mol. Biol.* 90, 575–587. doi: 10.1007/s11103-015-0417-8

Letunic, I., and Bork, P. (2006). Interactive Tree Of Life (iTOL): an online tool for phylogenetic tree display and annotation. *Bioinformatics* 23, 127–128. doi: 10.1093/bioinformatics/btl529

McFall-Ngai, M., Hadfield, M. G., Bosch, T. C., Carey, H. V., Domazet-Lošo, T., Douglas, A. E., et al. (2013). Animals in a bacterial world, a new imperative for the life sciences. *Proc. Nat. Acad. Sci. U.S.A.* 110, 3229–3236. doi: 10.1073/pnas.1218525110

Molmeret, M., Horn, M., Wagner, M., Santic, M., and Abu Kwaik, Y. (2005). Amoebae as training grounds for intracellular bacterial pathogens. *Appl. Environ. Microbiol.* 71, 20–28. doi: 10.1128/AEM.71.1.20-28.2005

Moran, N. A., Tran, P., and Gerardo, N. M. (2005). Symbiosis and insect diversification: an ancient symbiont of sap-feeding insects from the bacterial phylum *Bacteroidetes*. *Appl. Environ. Microbiol.* 71, 8802–8810. doi: 10.1128/AEM.71.12.8802-8810.2005

Nasser, W., Santhanam, B., Miranda, E. R., Parikh, A., Juneja, K., Rot, G., et al. (2013). Bacterial discrimination by dictyostelid amoebae reveals the complexity of ancient interspecies interactions. *Curr. Biol.* 23, 862–872. doi: 10.1016/j.cub.2013.04.034

Parsons, D. A., and Heffron, F. (2005). sciS, an icmF homolog in Salmonella enterica serovar Typhimurium, limits intracellular replication and decreases virulence. *Infect. Immun.* 73, 4338–4345. doi: 10.1128/IAI.73.7.4338-4345.2005

Preacher, K. J. (2001). *Calculation for the chi-square* test: *An Interactive Calculation Tool for Chi-Square Tests of Goodness of Fit and Independence [Computer software]*. Available online at: http://quantpsy.org

Pucciarelli, S., Devaraj, R. R., Mancini, A., Ballarini, P., Castelli, M., Schrallhammer, M., et al. (2015). Microbial consortium associated with the antarctic marine ciliate *Euplotes focardii*. *Microb. Ecol.* 70, 484–497. doi: 10.1007/s00248-015-0568-9

Raper, K. B. (1937). Growth and development of *Dictyostelium discoideum* with different bacterial associates. *J. Agr. Res.* 55, 289–316.

Raper, K. B. (1984). *The Dictyostelids. Princeton, NJ: Princeton Univ*ersity *Press.* doi: 10.1515/9781400856565

Raper, K. B., and Smith, N. R. (1939). The growth of *Dictyostelium discoideum* on pathogenic bacteria. *J. Bacteriol.* 38, 431–444.

Reddick, L. E., and Alto, N. M. (2014). Bacteria fighting back: how pathogens target and subvert the host innate immune system. *Mol. Cell* 54, 321–328. doi: 10.1016/j.molcel.2014.03.010

Ribet, D., and Cossart, P. (2015). How bacterial pathogens colonize their hosts and invade deeper tissues. *Microbes Infect.* 17, 173–183. doi: 10.1016/j.micinf.2015.01.004

Rosenberg, E., and Zilber-Rosenberg, I. (2016). Microbes drive evolution of animals and plants: the hologenome concept. *MBio* 7:e01395–e01315. doi: 10.1128/mBio.01395-15

Sansonetti, P. J., and Di Santo, J. P. (2007). Debugging how bacteria manipulate the immune response. *Immunity* 26, 149–161. doi: 10.1016/j.immuni.2007.02.004

Scheid, P. (2014). Relevance of free-living amoebae as hosts for phylogenetically diverse microorganisms. *Parasitol. Res.* 113, 2407–2414. doi: 10.1007/s00436-014-3932-7

Schloss, P. D., and Handelsman, J. (2005). Introducing DOTUR, a computer program for defining operational taxonomic units and estimating species richness. *Appl. Environ. Microbiol.* 71, 1501–1506. doi: 10.1128/AEM.71.3.1501-1506.2005

Schloss, P. D., Westcott, S. L., Ryabin, T., Hall, J. R., Hartmann, M., Hollister, E. B., et al. (2009). Introducing mothur: open-source, platform-independent, community-supported software for describing and comparing microbial communities. *Appl. Environ. Microbiol.* 75, 7537–7541. doi: 10.1128/AEM.01541-09

Solomon, J. M., Rupper, A., Cardelli, J. A., and Isberg, R. R. (2000). Intracellular growth of *Legionella* pneumophila in *Dictyostelium discoideum*, a system for genetic analysis of host-pathogen interactions. *Infect. Immun.* 68, 2939–2947. doi: 10.1128/IAI.68.5.2939-2947.2000

Stallforth, P., Brock, D. A., Cantley, A. M., Tian, X., Queller, D. C., Strassmann, J. E., et al. (2013). A bacterial symbiont is converted from an inedible producer of beneficial molecules into food by a single mutation in the gaca gene. *Proc. Natl. Acad. Sci. U.S.A.* 110, 14528–14533. doi: 10.1073/pnas.1308199110

Stephenson, S. L., and Landolt, J. C. (1992). Vertebrates as vectors of cellular slime molds in temperate forests. *Mycol. Res.* 96, 670–672. doi: 10.1016/S0953-7562(09)80495-4

Strassmann, J. E., and Shu, L. (2017). Ancient bacteria–amoeba relationships and pathogenic animal bacteria. *PLoS Biol.* 15:e2002460. doi: 10.1371/journal.pbio.2002460

Tamura, K., Stecher, G., Peterson, D., Filipski, A., and Kumar, S. (2013). MEGA6: molecular evolutionary genetics analysis version 6.0. *Mol. Biol. Evol.* 30, 2725–2729. doi: 10.1093/molbev/mst197

Taylor-Mulneix, D. L., Bendor, L., Linz, B., Rivera, I., Ryman, V. E., Dewan, K. K., et al. (2017). Bordetella bronchiseptica exploits the complex life cycle of *Dictyostelium discoideum* as an amplifying transmission vector. *PLoS Biol.* 15:e2000420. doi: 10.1371/journal.pbio.2000420

Conflict of Interest Statement: The authors declare that the research was conducted in the absence of any commercial or financial relationships that could be construed as a potential conflict of interest.

frontiers in Cellular and Infection Microbiology

ORIGINAL RESEARCH
published: 09 February 2018
doi: 10.3389/fcimb.2018.00028

Environmental *Mycobacterium avium* subsp. *paratuberculosis* Hosted by Free-Living Amoebae

Ascel Samba-Louaka[1], Etienne Robino[1], Thierry Cochard[2], Maxime Branger[2], Vincent Delafont[1], Willy Aucher[1], Wilfrid Wambeke[2], John P. Bannantine[3], Franck Biet[2] and Yann Héchard[1]**

[1] Université de Poitiers, Laboratoire Ecologie et Biologie des Interactions, UMR Centre National de la Recherche Scientifique 7267, Equipe Microbiologie de l'Eau, Poitiers, France, [2] Institut National de la Recherche Agronomique, Université de Tours, UMR1282, Infectiologie et Santé Publique, Nouzilly, France, [3] National Animal Disease Center, Agricultural Research Service, United States Department of Agriculture, Ames, IA, United States

Mycobacterium avium subsp. *paratuberculosis* is responsible for paratuberculosis in animals. This disease, leading to an inflammation of the gastrointestinal tract, has a high impact on animal health and an important economic burden. The environmental life cycle of *M. avium* subsp. *paratuberculosis* is poorly understood and several studies suggest that free-living amoebae (FLA) might be a potential environmental host. FLA are protozoa found in water and soil that are described as reservoirs of pathogenic and non-pathogenic bacteria in the environment. Indeed, bacteria able to survive within these amoebae would survive phagocytosis from immune cells. In this study, we assessed the *in vitro* interactions between several strains of *M. avium* subsp. *paratuberculosis* and *Acanthamoeba castellanii*. The results indicate that the bacteria were able to grow within the amoeba and that they can survive for several days within their host. To explore the presence of *M. avium* subsp. *paratuberculosis* in environmental amoebae, we sampled water from farms positive for paratuberculosis. A *M. avium* subsp. *paratuberculosis* strain was detected within an environmental amoeba identified as related to the poorly described *Rosculus* genus. The bacterial strain was genotyped, showing that it was similar to previous infectious strains isolated from cattle. In conclusion, we described that various *M. avium* subsp. *paratuberculosis* strains were able to grow within amoebae and that these bacteria could be found on farm within amoebae isolated from the cattle environment. It validates that infected amoebae might be a reservoir and vector for the transmission of *M. avium* subsp. *paratuberculosis*.

Keywords: paratuberculosis, amoebae, water, infection, *Mycobacterium*, *Rosculus*

OPEN ACCESS

Edited by:
Thierry Soldati,
Université de Genève, Switzerland

Reviewed by:
Marina Santic',
University of Rijeka, Croatia
Otmane Lamrabet,
Université de Genève, Switzerland
Fabienne Misguich,
Versailles Saint-Quentin-en-Yvelines University, France

****Correspondence:***
Franck Biet
franck.biet@inra.fr
Yann Héchard
yann.hechard@univ-poitiers.fr

Received: *31 October 2017*
Accepted: *23 January 2018*
Published: *09 February 2018*

Citation:
Samba-Louaka A, Robino E, Cochard T, Branger M, Delafont V, Aucher W, Wambeke W, Bannantine JP, Biet F and Héchard Y (2018) Environmental Mycobacterium avium subsp. paratuberculosis Hosted by Free-Living Amoebae. Front. Cell. Infect. Microbiol. 8:28. doi: 10.3389/fcimb.2018.00028

INTRODUCTION

Mycobacterium avium subsp. *paratuberculosis* (Map), the etiologic agent of paratuberculosis also called Johne's disease, induces extensive inflammation in the gastrointestinal tract of ruminants. This inflammation prevents absorption of nutrients, which leads to a chronic and progressive weight loss despite eating habits. The hallmark of advance stage disease in cattle is copious diarrhea, appearance of ribs and other skeletal bones. Paratuberculosis is responsible for economic losses up

to $1.5 billion annually to the dairy industries on the five continents (Ott et al., 1999; Sweeney et al., 2012). The management of this epidemic, is particularly difficult because efficient prophylactic tools are lacking. There is no treatment and the vaccine available is not very effective and not widely used because it compromises the diagnosis of bovine tuberculosis. Serological diagnostic tools lack specificity and are not adapted to early diagnosis of an infection, although this is beginning to change with the discovery of new antigens (Li et al., 2017). Another factor complicating the management of this epidemic involves the shedding of the bacteria in the environment where it is able to survive. Map is a genetically homogenous subspecies of *M. avium*, especially among bovine, human and wildlife isolates. However, two prominent lineages of Map have emerged following molecular strain typing and comparative genomic analysis—ovine (Map-S) and bovine (Map-C) strains (Biet et al., 2012). Initially, the Map-S and Map-C type strains were distinguished based on their molecular fingerprints using IS*1311* polymorphism, MLSSR typing and *hsp65* sequencing. However, beyond genetic typing, there are observed phenotypic differences including differences in their pigmentation, growth characteristics and lipopeptide structures in their cell walls (Bannantine et al., 2017). The environmental life cycle of Map is still poorly understood and at least one recent publication suggests that free-living amoebae (FLA) might be a potential environmental host (Salgado et al., 2015).

Free-living amoebae (FLA) are protozoa found in the same environmental niches as Map, including water and soil (Rodríguez-Zaragoza, 1994). FLA mainly feed on bacteria in the environment and digest them by phagocytosis. They thus play, along with other grazing protists, a key role in shaping the bacterial community composition in the environment (Jürgens and Matz, 2002). However, it has been repeatedly shown over the last decades that some bacteria may resist this digestion and persist or even grow within amoebae (Greub and Raoult, 2004). Importantly, these resistant bacteria are generally also more resistant to phagocytic immune cells, such as macrophages. This is well documented for *Legionella pneumophila* and for various *Mycobacterium* species in interaction with *Acanthamoeba castellanii*. The latter is the most common species in water and the best known FLA. As a consequence, FLA are considered as a training ground for pathogenic bacteria, including some *Mycobacterium* species (Molmeret et al., 2005; Salah et al., 2009). The fate of internalized mycobacteria can drastically vary according to the species, ranging from digestion (e.g., *M. bovis* BCG) and survival without replication (e.g., *M. tuberculosis*) to intra amoebal multiplication (e.g., *M. abscessus* or *M. chelonae*) (Drancourt, 2014). However, as described in this paper, most of the interactions were studied *in vitro* and only few studies have reported mycobacteria detected inside amoebae isolated from the environment (White et al., 2010; Amissah et al., 2014). Our group has previously described such interaction in drinking water (Delafont et al., 2014). Importantly, intra-amoebal growth of *Mycobacterium* would lead to improve its virulence (Cirillo et al., 1997).

The interaction between Map and amoebae has been poorly described. It was first reported in 2006 through a study showing *in vitro* that a strain of Map was ingested by *Acanthamoeba* and resisted digestion for at least 24 days (Whan et al., 2006). Four years later a short communication described the co-occurrence of Map and FLA in the soil (White et al., 2010). Amoebae and Map were found in the same soil samples and an amoeba strain was isolated harboring an intracellular acid-fast stained bacterium. Mura et al. (2006) described *in vitro* that Map persisted for up to four years in presence of *Acanthamoeba* (Mura et al., 2006). Recently, Map were found within amoebae isolated from soil after application of cattle slurry spiked with Map (Salgado et al., 2015). However, these studies used a very limited range of strains and no study has demonstrated clearly the presence of Map in environmental FLA.

Our study was aimed to assess the infectious potential of several Map strains including the two main genetic lineages of Map, C and S types toward *A. castellanii*. We also investigated whether Map-infected FLA might be found in the environment surrounding infected cattle.

MATERIALS AND METHODS

Cultivation of Microorganisms

Bacterial strains used in this study are listed in **Table 1**. Mycobacterial strains were grown at 37°C in Sauton medium or Middlebrook 7H9 broth (Difco Laboratories, Detroit, MI) with 0.2% glycerol and albumin-dextrose-catalase enrichment medium (ADC, Becton Dickinson, Le Pont de claix, France). *M. avium* subsp. *paratuberculosis* cultures were supplemented with 2 mg l^{-1} mycobactin J (Allied Monitor). Bacteria were harvested at mid-log phase and kept frozen (−80°C) in aliquots

TABLE 1 | Bacterial and amoebal strains.

Strains	Description, type, and genotype	References or source
BACTERIAL STRAINS		
K10–ATCCBAA-968	Bovine isolate, C type, [a]INMV 2	Li et al., 2005
205	Bovine isolate, C type, INMV 13	Biet et al., 2008
397	Ovine isolate, S type, INMV 70	Bannantine et al., 2012
453	Bovine isolate, C type, INMV 2	This study
6796	Ovine isolate, S type INMV 72	This study
7912	Bovine isolate, C type, INMV 9	Biet et al., 2008
GFPLux-Map K10	Green fluorescent protein (GFP)- and luciferase-expressing strains Map k10	Lefrançois et al., 2011
E. coli K12 MG1655		ATCC 47076
AMOEBA		
A. castellanii ATCC 30010		ATCC

[a] *Profiles described by Thibault et al. (2007) and available on http://mac-inmv.tours.inra.fr/*

until use. Recombinant *M. avium* subsp. *paratuberculosis*, strain K-10 expressing the Green fluorescent protein (GFP) - and luciferase described in Lefrançois et al. (2011) was grown in the Middlebrook 7H10 medium supplemented with ADC, 0.2 mg ml-1 mycobactin and 50 mg ml^{-1} of hygromycin. *Escherichia coli* strain K12 was grown in LB liquid medium (Lysogeny Broth: 10 g/L NaCl, 5 g/L yeast extract, 10 g/L tryptone), and incubated for 24 h at 37°C, under agitation (180 rpm).

The free-living amoeba *A. castellanii* ATCC 30010 was grown in PYG liquid medium (ATCC 712; 20 g/L proteose peptone, 1 g/L yeast extract, 1 g/L sodium citrate, 0.1 M D-glucose, 0.4 mM $CaCl_2$, 4 mM $MgSO_4$, 2.5 mM Na_2HPO_4, 2.5 mM KH_2PO_4, 50 μM $Fe(NH_4)_2(SO_4)_2$, pH 6.5) in 25 or 75 cm^2 flask. *A. castellanii* cultures were incubated at 30°C for 3–4 days, until a cell confluency of 80–90% was reached.

Isolation of Environmental Amoebae

Environmental water samples were collected in March 2016 from two farms located in "Indre et Loire" and reported to be contaminated with Map since more than 5 years. Two 1-L samples were taken for each herd from the drinking troughs. The samples were filtered through a 5 μm nitrocellulose membrane (N3771-100EA, Sigma-Aldrich). The membranes were placed onto NNA plates (Non Nutrient Agar, 15 g/L) seeded with *live E. coli* strain K12. The plates were incubated at 30°C and examined daily under phase-contrast microscopy. The presence of amoebal cells is characterized by the formation of a migration front, representing the amoebal movement upon agar plates, seeking for food. Amoebae were recovered by scrapping the agar plate at the migration front for collection or DNA extraction.

A. castellanii Infection by Different Genotypes of Map

A. castellanii cells from fully grown flasks were rinsed once using PAS buffer [Page's Amoeba Saline; 1 g/L sodium citrate, 0.4 mM $CaCl_2$, 4 mM $MgSO_4$, 2.5 mM Na_2HPO_4, 2.5 mM KH_2PO_4, 50 μM $Fe(NH_4)_2(SO_4)_2$, pH 6.5], and resuspended in a mixture of PAS/PYG (1:1) supplemented with 0.005% triton X-100, to avoid mycobacteria clumping in the medium. Trophozoites cells were harvested and detached by vigorously tapping the flask. The cell suspension was adjusted to a concentration of 1.25×10^5 cells/mL, and 2 mL of the suspension distributed in each well of a 12 well plates. Mycobacteria cells were dispersed by 3 passages through a 18 Gauge needle, followed by a centrifugation step at 200 g for 5 min. The suspensions were subsequently quantified by optical density (OD) at 600 nm, using an equivalence of 6×10^8 mycobacteria per mL for 1 OD unit. Mycobacteria suspensions were used to infect *A. castellanii* at an MOI (multiplicity of infection) of 10, i.e., 10 bacteria per amoeba cell. The infected cultures were then centrifuged at 500 g for 10 min to facilitate the infection, and incubated for 1 h at 30°C. The supernatant was then discarded and directly replaced with a fresh mixture of PAS/PYG (1:1), 0.005% triton X-100, supplemented with amikacin at 10 μM. Timepoints at 1, 24, 48, and 72 h post infection at 30°C were selected to estimate presence or growth of Mycobacteria by qPCR. To estimate the growth of *A. castellanii*, cells were harvested at different time points and counted using plastic counting slides FastRead 102 (Biosigma).

The localization of bacteria within amoeba was visualized using a recombinant rGFP-Map strain K-10 (**Table 1**) previously described (Lefrançois et al., 2011). Infected cultures were analyzed by fluorescence microscopy (BX41, Olympus).

Total Genomic DNA Extraction

Cells from infection experiments as well as from environmental amoebae isolated as described above, were used for DNA extraction. Amoeba cells (4×10^4 - 2×10^6) and associated mycobacteria were harvested and resuspended in 500 μL of PAS buffer. Cells were lysed by bead-beating in tubes containing 500 mg of small diameter glass beads (100 μm) and 4 glass beads of 2 mm diameter (Sigma) using Fastprep apparatus for 30 s (speed 5 m/s). The suspension was then processed for DNA extraction using NucleoSpin Microbial DNA (Macherey-Nagel), following manufacturer recommendations for bacterial DNA extraction.

Detection and Quantification of Mycobacteria by Quantitative PCR (qPCR)

The presence of bacterial genomic DNA was assessed by qPCR performed in a final volume of 10 μL, including 2 μL of extracted DNA, 2 μL of 5x Master Mix LightCycler® FastStart DNA Master^{plus} SYBR Green I (Roche), a set of primer pairs (**Table 2**), at a concentration of 0.5 μM each, and water in sufficient quantity for 10 μL. Experiments were carried out using a LightCycler 1.5 thermocycler (Roche), consisting in an initial denaturation step at 95°C for 10 min, 45 cycles of denaturation at 95°C for 10 s, annealing for 10 s at a temperature according to the primer pairs used, and elongation at 72°C for 20 s. Fusion curves were collected for each experiment. Quantification of DNA was performed by calculating fold changes using the $2^{-\Delta Ct}$ method. ΔCt corresponds to the difference in cycle threshold (Ct) between a specific time point and the condition at 1 h.

TABLE 2 | Oligonucleotide primers.

Name	Sequence	Melting temp. (°C)	References
atpE-F	5′-CGGYGCCGGTATCGGYGA-3′	58	Radomski et al., 2013
atpE-R	5′-CGAAGACGAACARSGCCAT-3′		
IS*900*-F	5′-GACGCGATGATCGAGGAG-3′	58	Pillai and Jayarao, 2002
IS*900*-R	5′-GGGCATGCTCAGGATGAT-3′		
F57-F	5′-TTGGACGATCCGAATATGT-3′	56	Tasara and Stephan, 2005
F57-R	5′-AGTGGGAGGCGTACCA-3′		

Multiple-Locus Variable Number Tandem Repeat Analysis (MLVA) Typing of Environmental Mycobacteria, Using MIRU-VNTR Markers

The method has been described previously (Thibault et al., 2007). The PCR mixture was composed as follows using the Go Taq Flexi DNA polymerase (Promega). Five microliters from DNA solution were added to a final volume of 25 μL containing 0.1 μL of Go Taq Flexi DNA polymerase (5 U/μL), 5 μl of betaine (Sigma), or 1 μl of dimethyl sulfoxide (Sigma); 0.2 mM (each) dATP, dCTP, dGTP, and dTTP (Promega); 5 μL of 5 × PCR buffer supplied by the manufacturer; 1 μM of primers see (Thibault et al., 2007); and 1.5 mM of $MgCl_2$. The reactions were carried out using a TC-520 thermal cycler (Techne). PCR conditions were as follows: 1 cycle of 5 min at 94°C; 30 cycles of 30 s at 94°C, 30 s at 55, 58, 60, 64°C according to MIRU-VNTR searched, and 30 s at 72°C; 1 cycle of 7 min at 72°C. To detect differences in repeat numbers, the PCR products were analyzed by electrophoresis using 1.5% agarose gels (agarose electrophoresis grade; Invitrogen).

Amoebal Identification

The identification of the amoeba isolated from the water troughs was performed through sequencing of a 18S rRNA gene amplicon. From the total genomic DNA extract, a PCR was performed using the universal F566 and R1200 eukaryotic primers, targeting the 18S rRNA gene (Hadziavdic et al., 2014). The amplicon was sequenced and the sequence compared to the nucleotide nr database using BLASTn.

Evaluation of Phagosomal Acidification

Mycobacteria suspension prepared as described previously were pre-labeled using pHrodo^{TM} Red succinimidyl ester (ThermoFischer Scientific) following manufacturer recommendations, but excluding the methanol washing step. Briefly, bacterial suspensions were incubated for 1 h in 0.1 M sodium bicarbonate buffer containing 20 μM pHrodo^{TM} Red succinimidyl ester, in the dark. Bacteria were then pelleted by centrifugation at 12,000 g for 5 min, and washed twice in PAS buffer supplemented with 0.005% triton X-100. *A. castellanii* monolayers were infected by labeled mycobacteria at a MOI of 10. After 4 h of incubation, trophozoites were detached, fixed with 2% paraformaldehyde for 10 min in the dark. Cells were pelleted by centrifugation at 800 g for 10 min, and resuspended in a 30 μL of SlowFade Diamonds antifade mountant (ThermoFischer Scientific) with Hoechst at a concentration of 400 ng/mL. Samples were examined using an epifluorescence microscope (BX41, Olympus).

Statistics

Results were statistically analyzed using GraphPad Prism software. Multiple comparison was performed using Kruskal–Wallis analysis followed by a Dunn's post-test. Differences with $p < 0.05$ were considered statistically significant.

RESULTS

Map Strains Grow within *A. castellanii*

In order to see whether Map strains would behave differently within amoeba, we investigated infection of *A. castellanii* by different genotype and genetic lineage of Map strains. *A. castellanii* were co-cultured with the reference strain (K10), two cattle strains (205, 7912), and two sheep strains (397, 6796). The fate of Map internalized by *A. castellanii* was determined by a qPCR based bacterial quantification assay, at 1, 24, 48, and 72 h post infection. We found that all Map persisted and even grew within *A. castellanii* (**Figure 1A**). There were no significant differences in growth rate between the strains ($p = 0.4441$) even though the K10 strain tended to be slightly slower. The fate of infected *A. castellanii* was also monitored throughout the infection, indicating that the host proliferation was not significantly modified ($p = 0.8939$) by the presence of Map in comparison with an uninfected *A. castellanii* culture (**Figure 1B**). Taken together, these results suggest that Map can successfully infect and grow within *A. castellanii* without any deleterious effect on its host.

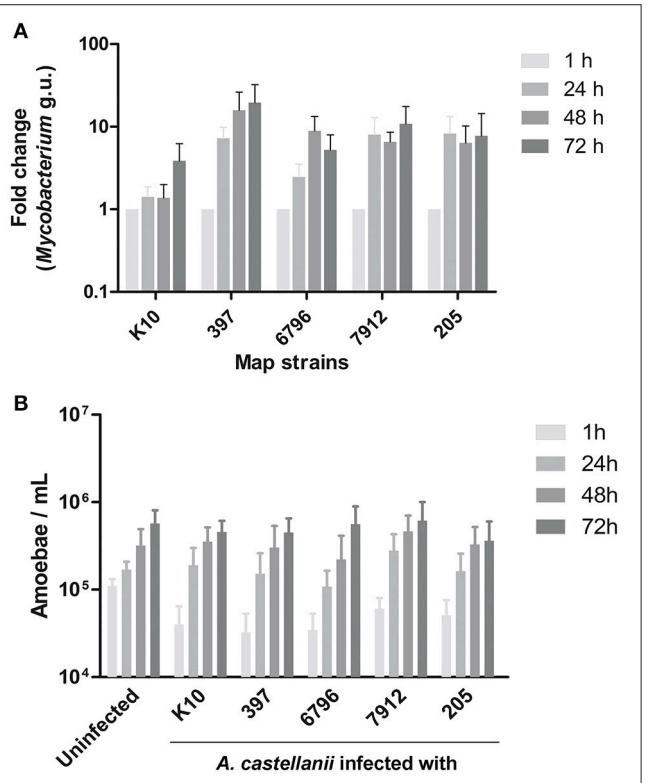

FIGURE 1 | *A. castellanii* is permissive to both ovine (S) and bovine (C) Map. **(A)** *A. castellanii* were infected with ovine (397, 6796) and bovine (K10, 7912, 205) strains of Map at a MOI of 10. Presence of *Mycobacterium* spp. was quantified (*Mycobacterium* genome unit) through qPCR amplification of the *atpE* gene, 1, 24, 48, and 72 h post-infection. Results represents the mean (±SEM) of four independent experiments ($p = 0.4441$). Results are normalized on the condition 1 h. **(B)** Uninfected and infected *A. castellanii* were counted 1, 24, 48, and 72 h post-infection. Results represents the mean (±SEM) of four independent experiments ($p = 0.8939$).

Map Resides within Phagosomal Compartments

To localize Map within *A. castellanii*, amoebae were infected with a Map K10 strain expressing a green fluorescent protein (GFP). Microscopy analysis of infected *A. castellanii* showed colocalization between the Map K10-GFP and *A. castellanii* 7 days after infection (**Figure 2A**). This figure also suggests that the bacteria were found inside *A. castellanii* vesicles. Later observations allowed to visualize *A. castellanii* cysts but no GFP signal from the K10-GFP strain was detected, suggesting that in our conditions Map K10 was not present within the cysts. We have also assessed the acidification of Map-containing intracellular compartments in the first hours of infection. Before infection, the Map K10-GFP strain was stained with the pHrodo dye, which fluoresces in a pH-dependent manner. The results show that a fraction of intracellular Map was labeled in red, indicating that they were found within acidified vacuoles, likely phagosomes, while other Map were not labeled (**Figure 2B**). These observations suggest that Map are phagocytised by *A. castellanii* and resides, at least transiently, within acidified vacuoles.

Map Is Found within an Environmental Amoeba in Infected Farm

As no study had isolated environmental FLA infected by Map so far, we investigated the potential Map-amoeba association in water from the drinking troughs in herds naturally infected by Map. From the two farms enrolled in this study, only one sample was positive for the presence of cultivable amoebae. Total genomic DNA extracted from the amoebal culture was used to

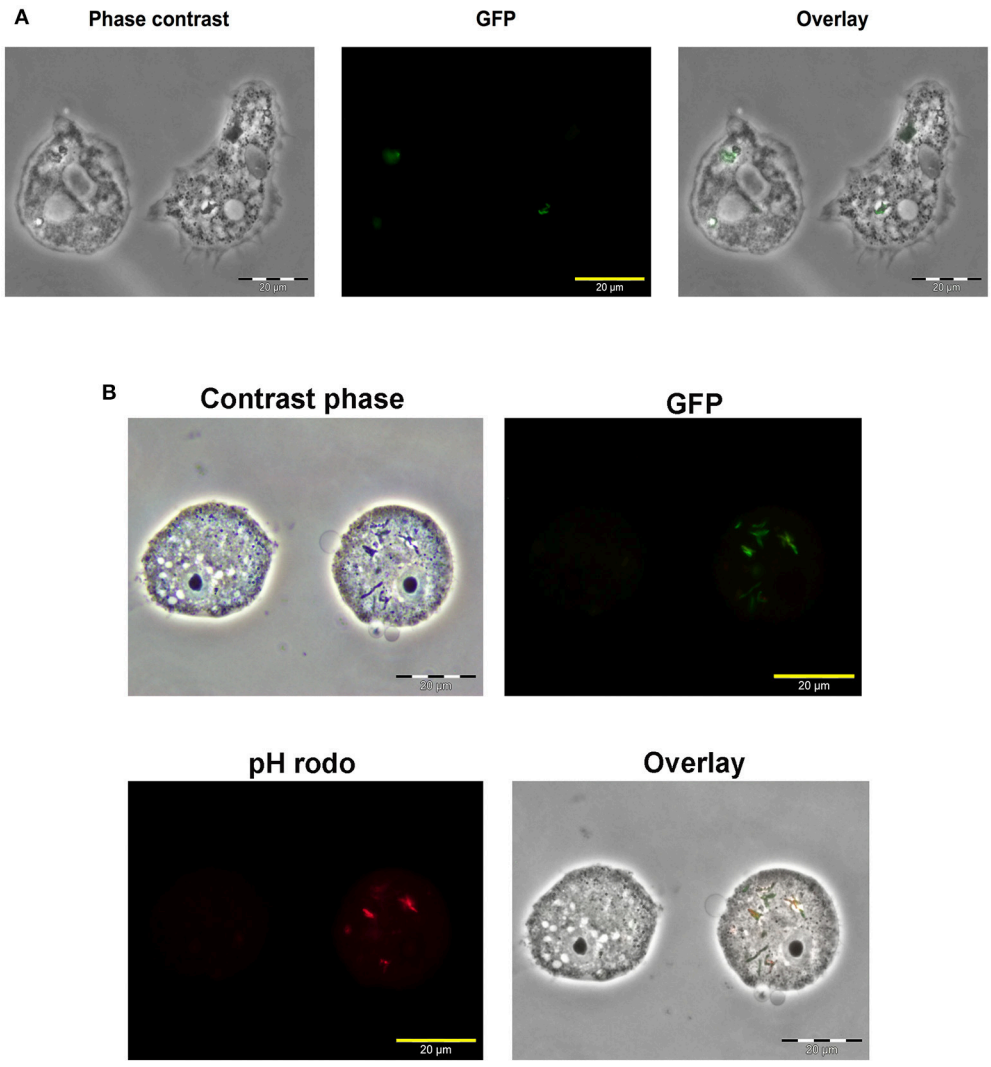

FIGURE 2 | Map K10 persists within *A. castellanii* for up to 7 days. **(A)** *A. castellanii* were co-cultured with a K10-GFP map strain at a MOI of 10. Mycobacteria localization within amoebae trophozoites was assessed by epifluorescence microscopy 7 days after the initial infection. **(B)** *A. castellanii* were infected with K10-GFP labeled with a pHrodo dye at a MOI of 10. At 4 h post-infection, infected cells were analyzed through epifluorescence microscopy to reveal the Map K10 strain and acidification of bacteria through GFP and red signals.

detect the presence of Map DNA using a Map-specific qPCR assay, targeting the IS*900* and F57 genes (**Table 3**). The successful amplification of the specific genomic target highlighted the presence of *Map* in association with the isolated amoebal culture. The Map strains K10, 397, and 7912 were used as positive control and *M. llatzerenze* as negative control for all PCR-based assays (**Table 3**). We have previously established a database containing isolated and genotyped Map strains from feces of infected cattle (Holbert et al., 2015). Therefore, we genotyped the Map-positive DNA from the amoeba culture, using MLVA genotyping and compare it to our database. The result of the MLVA genotyping based on the eight classical loci MIRU VNTR (Thibault et al., 2007) gave a profile INMV 2 identical to that of the 453 strain isolated from feces of cattle (**Table 4**).

Furthermore, in order to identify the amoeba isolate, we tried to subculture the strain but no subculture was observed. Thus, we performed a PCR targeting a portion of 18S rRNA coding gene. Sequencing of purified amplicon (1265 nucleotides, GenBank MG859939), indicated that the most closely related sequence to the isolate was *Rosculus ithacus*, a cercozoan amoeba, although the sequence identity was moderate (78%). Therefore, this amoebal isolate is likely to represent a newly described genus among the sainouroid clade.

DISCUSSION

A growing number of studies underlines the important role of amoebae in the carrying of pathogenic and non-pathogenic mycobacteria, as well as in providing an environmental source of mycobacterial infection. On a microbiological level, the question of on farm disease transmission is particularly relevant because of the characteristics of Map biology. Indeed the disease transmission happens through ingestion of Map then during the disease progression, animals excrete bacilli in their environment, ranging from a few and discontinuous bacterial excretions in asymptomatic phases to very high levels and continuously shedding at clinical stage of the disease (Magombedze et al., 2017). This means that even in the silent phases of the disease the animals can excrete Map in the environment and in particular in the water points of the herds. In this context, it was interesting to investigate whether Map can be hosted and survive in amoeba and if water points of infected herds could be a source of contamination of Map mediated by FLA. Some other pathogenic mycobacteria were able to survive in soil and this environment might be a source of infection (Ghodbane et al., 2014).

In this study, the five selected strains (C- and S-type) not only survived but also showed a growth trend within *A. castellanii* for at least 72 h. In previous studies the growth of Map was not so high in the first days post-infection. This difference could be due to the *Acanthamoeba* strains and the infection protocols that were used in each study (Mura et al., 2006; Whan et al., 2006). For example, the co-cultures were centrifuged to increase efficiency and better synchronize the infection process. These differences might also explain the higher levels of bacteria per amoeba we observed. Moreover, we demonstrated that Map can persist for at least 7 days within *A. castellanii*. Within Map there is little genetic variability nevertheless the evolutionary pattern deciphered by Turenne et al. (2006) and Alexander et al. (2009) showed that the Map sub-species evolved from a common ancestor *M. avium* subsp. *hominissuis* into two different genetic lineages associated with a host preference. We speak of a lineage of S-type for sheep and C-type for cattle. In this study the strains were selected for their difference in terms of genotype and to include representative S and C-type. Altogether these results suggest that amoeba may serve as a significant phagocytic model to further investigate comparable or distinct phenotypic traits obtained by each lineage S and C-type of Map.

We also observed that the growth of *A. castellanii* was not adversely affected by infection with any of the Map strains. This indicates that Map had no deleterious effects

TABLE 3 | Map-specific qPCR targeting the atpE, IS*900* and F57 genes.

Strains	PCR target		
	atpEF/atpER[a]	IS*900*F/IS*900*R[a]	F57F/F57R[a]
Map K10	+	+	+
Map 397	+	+	+
Map 7912	+	+	+
M. llatzerenze	+	–	–
Total DNAs from isolated amoeba	+	+	+

[a]*AtpE primer set is specific of Mycobacterium spp. IS900 and F57 primer sets are specific of Map.*

TABLE 4 | MLVA genotyping of Map strains.

	Number of repeats by MLVA loci[a]								Name
DNA	MIRU 292	MIRU X3	VNTR 25	VNTR 47	VNTR 3	VNTR 7	VNTR 10	VNTR 32	INMV
K10	3	2	3	3	2	2	2	8	2
397	7	1	3	3	1	1	1	8	70
205	2	2	3	3	2	2	2	8	13
6796	4	1	3	3	1	1	1	8	72
7912	2	1	3	3	2	2	2	8	9
453	3	2	3	3	2	2	2	8	2
Amoeba total DNA	3	2	3	3	2	2	2	8	2

[a]*MLVA analysis and profile identification according to web database application http://mac-inmv.tours.inra.fr/*

on amoebal viability. These results suggest that interactions between these two types of microorganisms could very likely happen in the environment. This stability could indeed favor Map resilience in the environment, providing a shelter against harsh conditions, as well as a potential substrate source for mycobacterial multiplication (Caire-Brändli et al., 2014; Barisch et al., 2015; Delafont et al., 2017).

Microscopy studies indicate that Map was localized within phagosomes and that some bacteria were found in acidified environment while others were not. This suggests that Map could block, to a certain extent, the normal acidification process of *A. castellanii* phagosomes. Inhibition of phagosomal acidification has been observed with other *Mycobacterium* species both in amoebae and macrophages (Kuehnel et al., 2001; Rohde et al., 2007; Delafont et al., 2017). Although much of the cell biology has been done on mycobacteria-macrophage interactions, further investigations would be required to better understand the fate of Map after its internalization in amoeba.

Amoeba-Map association in the environment has been poorly documented. To our knowledge, only one short communication has reported that amoeba isolated from soil were positive for Map-specific PCR but neither the Map nor the amoebae strains were characterized (White et al., 2010). In our study, two water troughs were selected for sampling, as those were providing the water source to distinct herds previously declared as infected by Map. We were able to recover cultivable FLA from one of the water troughs, confirming their presence in this environment. From the cultivated amoeba, the presence of Map DNA was detected using two specific primer sets by qPCR. This finding represents a strong argument in favor of interactions between amoebae and Map in environmental conditions. MLVA genotyping confirmed the identification of the species Map. The MLVA profile of the DNA was identical to that of an isolated strain from feces of a Map naturally infected cattle in the same farm (Holbert et al., 2015). These results not only confirm the presence of FLA harboring Map in the environment of animals on farm, but the identical genotypes recovered may also suggest a link between residence in amoeba and ability to infect cattle. Further investigations could be done to isolate the Map strains and improve the discrimination of genotype by combination of genotyping methods to ascertain the strains isolated from amoebae and animals are strictly identical. These results indicate that the strains might persist and circulate in the herd. They further suggest that fresh drinking water sources on farm may be important for healthy cows and that the problem of Johne's disease may be difficult to solve using herd management practices alone.

In addition, the identification of the amoebal isolate indicated that its closest sequence corresponds to *R. ithacus*. The latter is a coprophilic amoeba belonging to the sainouroid clade, as part of the Cercozoan radiation. Interestingly, protozoa from this clade were also identified in cow and sheep dung in a previous study (Bass et al., 2016). It is therefore not surprising to have identified such an amoeba from a drinking through providing cattle. However, we were not able to subculture this amoebal strain for some reason even after several try. It suggests that the culture method that was used is not fully efficient to subculture any FLA.

In conclusion, our study showed that various Map strains were able to persist and grow within *A. castellanii,* without observable deleterious effects on the host. A screening of environment surrounding Map-infected herds allowed to recover a free-living amoeba, representative of the sainouroid clade, from a drinking trough. This environmental amoeba harbored a Map strain that was genotyped. This study is bringing additional pieces of evidence reinforcing the role of amoebae in the persistence, and potential transmission, of pathogenic mycobacteria, including Map. This work should stimulate further studies focused on the characterization of environmental interactions between amoebae and pathogenic mycobacteria.

AUTHOR CONTRIBUTIONS

All the authors have substantial contributions to the conception or design of the work; or the acquisition, analysis, or interpretation of data for the work; drafting the work or revising it critically for important intellectual content and final approval of the version to be published.

ACKNOWLEDGMENTS

We would like to thank Manon Duforestel for her technical help and Laure Malherbe Duluc, GDS veterinarian responsible for the epidemiological surveillance of infected herds. YH laboratory is partly financed by the European Union and the region of Nouvelle Aquitaine through the "Habisan program" (CPER-FEDER).

REFERENCES

Alexander, D. C., Turenne, C. Y., and Behr, M. A. (2009). Insertion and deletion events that define the pathogen *Mycobacterium avium* subsp. *paratuberculosis*. *J. Bacteriol.* 191, 1018–1025. doi: 10.1128/JB.01340-08

Amissah, N. A., Gryseels, S., Tobias, N. J., Ravadgar, B., Suzuki, M., Vandelannoote, K., et al. (2014). Investigating the role of free-living amoebae as a reservoir for *Mycobacterium ulcerans*. *PLoS Negl. Trop. Dis.* 8:e3148. doi: 10.1371/journal.pntd.0003148

Bannantine, J. P., Etienne, G., Laval, F., Stabel, J. R., Lemassu, A., Daffé, M., et al. (2017). Cell wall peptidolipids of *Mycobacterium avium*: from genetic prediction to exact structure of a nonribosomal peptide. *Mol. Microbiol.* 105, 525–539. doi: 10.1111/mmi.13717

Bannantine, J. P., Wu, C. W., Hsu, C., Zhou, S., Schwartz, D. C., Bayles, D. O., et al. (2012). Genome sequencing of ovine isolates of *Mycobacterium avium* subspecies paratuberculosis offers insights into host association. *BMC Genomics* 13:89. doi: 10.1186/1471-2164-13-89

Barisch, C., Paschke, P., Hagedorn, M., Maniak, M., and Soldati, T. (2015). Lipid droplet dynamics at early stages of *Mycobacterium marinum* infection in Dictyostelium. *Cell. Microbiol.* 17, 1332–1349. doi: 10.1111/cmi.12437

Bass, D., Silberman, J. D., Brown, M. W., Pearce, R. A., Tice, A. K., Jousset, A., et al. (2016). Coprophilic amoebae and flagellates, including Guttulinopsis, *Rosculus* and Helkesimastix, characterise a divergent and diverse rhizarian radiation and

contribute to a large diversity of faecal-associated protists. *Environ. Microbiol.* 18, 1604–1619. doi: 10.1111/1462-2920.13235

Biet, F., Bay, S., Thibault, V. C., Euphrasie, D., Grayon, M., Ganneau, C., et al. (2008). Lipopentapeptide induces a strong host humoral response and distinguishes *Mycobacterium avium* subsp. paratuberculosis from *M. avium* subsp. avium. *Vaccine* 26, 257–268. doi: 10.1016/j.vaccine.2007.10.059

Biet, F., Sevilla, I. A., Cochard, T., Lefrançois, L. H., Garrido, J. M., Heron, I., et al. (2012). Inter- and intra-subtype genotypic differences that differentiate *Mycobacterium avium* subspecies paratuberculosis strains. *BMC Microbiol.* 12:264. doi: 10.1186/1471-2180-12-264

Caire-Brändli, I., Papadopoulos, A., Malaga, W., Marais, D., Canaan, S., Thilo, L., et al. (2014). Reversible lipid accumulation and associated division arrest of *Mycobacterium avium* in lipoprotein-induced foamy macrophages may resemble key events during latency and reactivation of tuberculosis. *Infect. Immun.* 82, 476–490. doi: 10.1128/IAI.01196-13

Cirillo, J. D., Falkow, S., Tompkins, L. S., and Bermudez, L. E. (1997). Interaction of *Mycobacterium avium* with environmental amoebae enhances virulence. *Infect. Immun.* 65, 3759–3767.

Delafont, V., Mougari, F., Cambau, E., Joyeux, M., Bouchon, D., Héchard, Y., et al. (2014). First evidence of amoebae-mycobacteria association in drinking water network. *Environ. Sci. Technol.* 48, 11872–11882. doi: 10.1021/es5036255

Delafont, V., Samba-Louaka, A., Cambau, E., Bouchon, D., Moulin, L., and Héchard, Y. (2017). Mycobacterium llatzerense, a waterborne *Mycobacterium*, that resists phagocytosis by *Acanthamoeba castellanii*. *Sci. Rep.* 7:46270. doi: 10.1038/srep46270

Drancourt, M. (2014). Looking in amoebae as a source of mycobacteria. *Microb. Pathog.* 77, 119–124. doi: 10.1016/j.micpath.2014.07.001

Ghodbane, R., Mba Medie, F., Lepidi, H., Nappez, C., and Drancourt, M. (2014). Long-term survival of tuberculosis complex mycobacteria in soil. *Microbiology* 160, 496–501. doi: 10.1099/mic.0.073379-0

Greub, G., and Raoult, D. (2004). Microorganisms resistant to free-living amoebae. *Clin. Microbiol. Rev.* 17, 413–433. doi: 10.1128/CMR.17.2.413-433.2004

Hadziavdic, K., Lekang, K., Lanzen, A., Jonassen, I., Thompson, E. M., and Troedsson, C. (2014). Characterization of the 18S rRNA gene for designing universal eukaryote specific primers. *PLoS ONE* 9:e87624. doi: 10.1371/journal.pone.0087624

Holbert, S., Branger, M., Souriau, A., Lamoureux, B., Ganneau, C., Richard, G., et al. (2015). Interferon gamma response to *Mycobacterium avium* subsp. paratuberculosis specific lipopentapeptide antigen L5P in cattle. *Res. Vet. Sci.* 102, 118–121. doi: 10.1016/j.rvsc.2015.07.017

Jürgens, K., and Matz, C. (2002). Predation as a shaping force for the phenotypic and genotypic composition of planktonic bacteria. *Antonie Van Leeuwenhoek* 81, 413–434. doi: 10.1023/A:1020505204959

Kuehnel, M. P., Goethe, R., Habermann, A., Mueller, E., Rohde, M., Griffiths, G., et al. (2001). Characterization of the intracellular survival of *Mycobacterium avium* ssp. paratuberculosis: phagosomal pH and fusogenicity in J774 macrophages compared with other mycobacteria. *Cell Microbiol.* 3, 551–566. doi: 10.1046/j.1462-5822.2001.00139.x

Lefrançois, L. H., Pujol, C., Bodier, C. C., Teixeira-Gomez, A. P., Drobecq, H., Rosso, M. L., et al. (2011). Characterization of the *Mycobacterium avium* subsp. paratuberculosis laminin-binding/histone-like protein (Lbp/Hlp) which reacts with sera from patients with Crohn's disease. *Microbes Infect* 13, 585–594. doi: 10.1016/j.micinf.2011.02.002

Li, L., Bannantine, J. P., Campo, J. J., Randall, A., Grohn, Y. T., Katani, R., et al. (2017). Identification of sero-reactive antigens for the early diagnosis of Johne's disease in cattle. *PLoS ONE* 12:e0184373. doi: 10.1371/journal.pone.0184373

Li, L., Bannantine, J. P., Zhang, Q., Amonsin, A., May, B. J., Alt, D., et al. (2005). The complete genome sequence of *Mycobacterium avium* subspecies paratuberculosis. *Proc. Natl. Acad. Sci. U.S.A.* 102, 12344–12349. doi: 10.1073/pnas.0505662102

Magombedze, G., Shiri, T., Eda, S., and Stabel, J. R. (2017). Inferring biomarkers for *Mycobacterium avium* subsp. paratuberculosis infection and disease progression in cattle using experimental data. *Sci. Rep.* 7:44765. doi: 10.1038/srep44765

Molmeret, M., Horn, M., Wagner, M., Santic, M., and Abu Kwaik, Y. (2005). Amoebae as training grounds for intracellular bacterial pathogens. *Appl. Environ. Microbiol.* 71, 20–28. doi: 10.1128/AEM.71.1.20-28.2005

Mura, M., Bull, T. J., Evans, H., Sidi-Boumedine, K., McMinn, L., Rhodes, G., et al. (2006). Replication and long-term persistence of bovine and human strains of *Mycobacterium avium* subsp. paratuberculosis within *Acanthamoeba* polyphaga. *Appl. Environ. Microbiol.* 72, 854–859. doi: 10.1128/AEM.72.1.854-859.2006

Ott, S. L., Wells, S. J., and Wagner, B. A. (1999). Herd-level economic losses associated with Johne's disease on US dairy operations. *Prev. Vet. Med.* 40, 179–192. doi: 10.1016/S0167-5877(99)00037-9

Pillai, S. R., and Jayarao, B. M. (2002). Application of IS900 PCR for detection of *Mycobacterium avium* subsp. paratuberculosis directly from raw milk. *J. Dairy Sci.* 85, 1052–1057. doi: 10.3168/jds.S0022-0302(02)74165-9

Radomski, N., Roguet, A., Lucas, F. S., Veyrier, F. J., Cambau, E., Accrombessi, H., et al. (2013). atpE gene as a new useful specific molecular target to quantify *Mycobacterium* in environmental samples. *BMC Microbiol.* 13:277. doi: 10.1186/1471-2180-13-277

Rodríguez-Zaragoza, S. (1994). Ecology of free-living amoebae. *Crit. Rev. Microbiol.* 20, 225–241. doi: 10.3109/10408419409114556

Rohde, K., Yates, R. M., Purdy, G. E., and Russell, D. G. (2007). *Mycobacterium tuberculosis* and the environment within the phagosome. *Immunol. Rev.* 219, 37–54. doi: 10.1111/j.1600-065X.2007.00547.x

Salah, I. B., Ghigo, E., and Drancourt, M. (2009). Free-living amoebae, a training field for macrophage resistance of mycobacteria. *Clin. Microbiol. Infect.* 15, 894–905. doi: 10.1111/j.1469-0691.2009.03011.x

Salgado, M., Alfaro, M., Salazar, F., Badilla, X., Troncoso, E., Zambrano, A., et al. (2015). Application of cattle slurry containing *Mycobacterium avium* subsp. paratuberculosis (MAP) to grassland soil and its effect on the relationship between MAP and free-living amoeba. *Vet. Microbiol.* 175, 26–34. doi: 10.1016/j.vetmic.2014.09.022

Sweeney, R. W., Collins, M. T., Koets, A. P., McGuirk, S. M., and Roussel, A. J. (2012). Paratuberculosis (Johne's disease) in cattle and other susceptible species. *J. Vet. Intern. Med.* 26, 1239–1250. doi: 10.1111/j.1939-1676.2012.01019.x

Tasara, T., and Stephan, R. (2005). Development of an F57 sequence-based real-time PCR assay for detection of *Mycobacterium avium* subsp. paratuberculosis in milk. *Appl. Environ. Microbiol.* 71, 5957–5968. doi: 10.1128/AEM.71.10.5957-5968.2005

Thibault, V. C., Grayon, M., Boschiroli, M. L., Hubbans, C., Overduin, P., Stevenson, K., et al. (2007). New variable-number tandem-repeat markers for typing *Mycobacterium avium* subsp. paratuberculosis and *M. avium* strains: comparison with IS900 and IS1245 restriction fragment length polymorphism typing. *J. Clin. Microbiol.* 45, 2404–2410. doi: 10.1128/JCM.00476-07

Turenne, C. Y., Semret, M., Cousins, D. V., Collins, D. M., and Behr, M. A. (2006). Sequencing of hsp65 distinguishes among subsets of the *Mycobacterium avium* complex. *J. Clin. Microbiol.* 44, 433–440. doi: 10.1128/JCM.44.2.433-440.2006

Whan, L., Grant, I. R., and Rowe, M. T. (2006). Interaction between *Mycobacterium avium* subsp. paratuberculosis and environmental protozoa. *BMC Microbiol.* 6:63. doi: 10.1186/1471-2180-6-63

White, C. I., Birtles, R. J., Wigley, P., and Jones, P. H. (2010). *Mycobacterium avium* subspecies paratuberculosis in free-living amoebae isolated from fields not used for grazing. *Vet. Rec.* 166, 401–402. doi: 10.1136/vr.b4797

Conflict of Interest Statement: The authors declare that the research was conducted in the absence of any commercial or financial relationships that could be construed as a potential conflict of interest.

frontiers in Cellular and Infection Microbiology

PERSPECTIVE
published: 11 December 2017
doi: 10.3389/fcimb.2017.00510

Evolution of Bordetellae from Environmental Microbes to Human Respiratory Pathogens: Amoebae as a Missing Link

Dawn L. Taylor-Mulneix†, Illiassou Hamidou Soumana†, Bodo Linz† and Eric T. Harvill*

Department of Infectious Diseases, Center for Vaccines and Immunology, College of Veterinary Medicine, University of Georgia, Athens, GA, United States

The genus *Bordetella* comprises several bacterial species that colonize the respiratory tract of mammals. It includes *B. pertussis*, a human-restricted pathogen that is the causative agent of Whooping Cough. In contrast, the closely related species *B. bronchiseptica* colonizes a broad range of animals as well as immunocompromised humans. Recent metagenomic studies have identified known and novel bordetellae isolated from different environmental sources, providing a new perspective on their natural history. Using phylogenetic analysis, we have shown that human and animal pathogenic bordetellae have most likely evolved from ancestors that originated from soil and water. Our recent study found that *B. bronchiseptica* can evade amoebic predation and utilize *Dictyostelium discoideum* as an expansion and transmission vector, which suggests that the evolutionary pressure to evade the amoebic predator enabled the rise of bordetellae as respiratory pathogens. Interactions with amoeba may represent the starting point for bacterial adaptation to eukaryotic cells. However, as bacteria evolve and adapt to a novel host, they can become specialized and restricted to a specific host. *B. pertussis* is known to colonize and cause infection only in humans, and this specialization to a closed human-to-human lifecycle has involved genome reduction and the loss of ability to utilize amoeba as an environmental reservoir. The discoveries from studying the interaction of *Bordetella* species with amoeba will elicit a better understanding of the evolutionary history of these and other important human pathogens.

Keywords: *Bordetella*, Amoeba, *Dictyostelium discoideum*, environmental microbes, respiratory pathogens

OPEN ACCESS

Edited by:
Thierry Soldati,
Université de Genève, Switzerland

Reviewed by:
Joan Strassmann,
Washington University in St. Louis, United States
Falk Hillmann,
Leibniz-Institut für Naturstoff-Forschung und Infektionsbiologie, Hans Knöll Institut, Germany

****Correspondence:***
Dawn L. Taylor-Mulneix
dlt4ylor@gmail.com

†These authors have contributed equally to this work.

Received: *13 October 2017*
Accepted: *27 November 2017*
Published: *11 December 2017*

Citation:
Taylor-Mulneix DL, Hamidou Soumana I, Linz B and Harvill ET (2017) Evolution of Bordetellae from Environmental Microbes to Human Respiratory Pathogens: Amoebae as a Missing Link. Front. Cell. Infect. Microbiol. 7:510. doi: 10.3389/fcimb.2017.00510

INTRODUCTION

The genus *Bordetella* comprises several bacterial species, which are pathogenic to animals and humans. The most clinically relevant species is *B. pertussis*, the causative agent of Pertussis disease, or Whooping Cough. This acute respiratory disease, known for the characteristic symptoms of paroxysmal cough, whooping, and post-tussive vomiting, is particularly serious and sometimes fatal in infants and elderly people. From a veterinary perspective *B. bronchiseptica* and *B. avium* are important. *B. bronchiseptica*, a respiratory pathogen of a wide range of mammals, causes a variety of pathologies ranging from chronic and often asymptomatic infection to more severe and acute

diseases, including bronchopneumonia and atrophic rhinitis in pigs, bronchitis in cats, snuffles in rabbits, and acute tracheobronchitis ("Kennel Cough") in dogs (Goodnow, 1980; Mattoo and Cherry, 2005). *B. avium* infects the respiratory tract of wild and domesticated birds, particularly turkeys, causing a respiratory disease with the symptoms known as bordetellosis or coryza in turkey chicks (Panigrahy et al., 1981; Kersters et al., 1984; Raffel et al., 2002). Recently, we identified that the bordetellae likely originated evolutionarily from soil and water environments and showed that the animal pathogen, *B. bronchiseptica,* can utilize amoeba, such as *Dictyostelium discoideum,* as environmental reservoirs and transmission vectors. We hypothesize that evolving the ability to evade amoebic predation and utilize amoebae as an environmental niche allowed bordetellae the transition from survival in soil and water to being respiratory pathogens.

ENVIRONMENTAL ORIGIN OF *BORDETELLA*

Bacteria of the genus *Bordetella* are known as colonizers of human and animal respiratory tracts. *B. pertussis*, *B. bronchiseptica,* and *B. parapertussis* form an evolutionary monophyletic group commonly referred to as "classical" bordetellae. Over the past decades, more distantly related *Bordetella* species, the "non-classical" species, have been described that colonize the respiratory tract and cause disease in birds (*B. avium* and *B. hinzii*), mice (*B. pseudohinzii*) and humans (*B. holmesii*, *B. bronchialis*, *B. flabilis,* and *B. sputigena*) (Kersters et al., 1984; Vandamme et al., 1995, 2015; Weyant et al., 1995; Ivanov et al., 2015, 2016), or were isolated from infected wounds of immunocompromised patients (*B. trematum* and *B. ansorpii*) (Vandamme et al., 1996; Ko et al., 2005). Although species associated with humans and animals have attracted the most attention, recent studies have revealed *Bordetella*-like bacteria in the environment. *B. petrii*, the first *Bordetella* species identified from a non-animal source, was initially isolated from an anaerobic bioreactor culture enriched by river sediment (von Wintzingerode et al., 2001), and has been subsequently found in marine sponges (Sfanos et al., 2005) and grass root consortia (Chowdhury et al., 2007). *B. petrii* has also been isolated from immunocompromised patients with ear infections and with pulmonary disease (Fry et al., 2005; Biederman et al., 2015; Nagata et al., 2015), suggesting that this species could also be an opportunistic pathogen in humans and animals, as has been observed for *Pseudomonas* spp. (de Bentzmann and Plesiat, 2011). In a recent study, three novel environmental *Bordetella* species were described, *B. muralis*, *B. tumulicola,* and *B. tumbae*, that have been isolated from a plaster wall surface of 1,300-year-old mural paintings in Japan (Tazato et al., 2015). With the vastly improved ability to study bacterial communities inhabiting diverse environmental niches, including soil, rocks, water, air, ice, plants, and animals (Schuster, 2008; Blottiere et al., 2013; Cowan et al., 2015; Anantharaman et al., 2016; Gionfriddo et al., 2016; Makhalanyane et al., 2016), and the ability to identify sequences from *Bordetella*-like bacteria in metagenomics datasets, we expect to see an increase in the number of described environmental *Bordetella* species.

We recently identified numerous 16S rRNA sequences of bacteria isolated from various environmental sources, including soil, water, plants and sediment, that displayed high sequence similarity with the 16S rRNA gene sequence of *Bordetella* (Hamidou Soumana et al., 2017). Based on 48 full-length 16S RNA sequences of strains recovered from these environments, we performed a phylogenetic analysis to determine the relatedness between human- and animal-associated *Bordetella* species and those isolated from environmental samples. The phylogenetic tree provided evidence for an environmental origin of bordetellae, as sequences from environmental samples possessed a significantly higher genetic diversity than those from human- and animal-associated samples. Sequences from environmental samples were present in all 10 sequence clades, including sequence clades at the root of the phylogenetic tree. In contrast, sequences from animal-associated species were found in only four sequence clades at the top of the tree. Together, the order of branching events within the phylogenetic tree suggested that *Bordetella* species, including human-restricted pathogens, arose from environmental ancestors (Hamidou Soumana et al., 2017). The evolution and adaptation to human and animal hosts most likely occurred after acquisition of virulence factors that enabled them to respond to new hosts.

The ability of micro-organisms to adapt to different environments and hosts requires a high genomic plasticity coupled with the capacity to sense and respond to environmental changes (Aujoulat et al., 2012). Under laboratory conditions, classical bordetellae such as *B. bronchiseptica* can respond to different environmental stimuli by switching between two distinct life styles. When cultured at 37°C, which mimics mammalian host temperatures, expression of genes associated with virulence and colonization in mammalian hosts is up-regulated. However, *B. bronchiseptica* adopts a second life style when cultured at 25°C or lower, during which expression of virulence-associated genes is down-regulated while expression of a large, alternative set of genes, such as those involved in motility and growth in dilute nutrients, is up-regulated. Expression of the latter genes has been hypothesized to be important under extra-host growth conditions or in an environmental niche (Taylor-Mulneix et al., 2017). This global gene regulation is under the control of the two-component system BvgAS, consisting of a sensor protein, BvgS, a transcriptional activator, BvgA, and a transcriptional repressor, BvgR (**Figure 1**). Upon phosphorylation by BvgS, BvgA binds to the promoter regions of the Bvg-activated genes and activates transcription. The last gene, *bvgR*, is responsible for the regulation of the Bvg-repressed genes (Merkel et al., 1998). Virulence-associated factors are expressed in the Bvg positive (Bvg^+) phase, and the alternative set of genes in the Bvg negative (Bvg^-) phase (**Figure 1**). The ability to switch between life styles seems to be conserved amongst bordetellae as *bvgA* and *bvgS* gene homologs have been found in the genomes of animal-associated species as well as the environmental *B. petrii* (Gerlach et al., 2004; Gross et al., 2010; Linz et al., 2016). In addition, *B. petrii*, *B. bronchiseptica,* and *B. hinzii*, all known to associate with mammalian hosts, were

shown to grow efficiently in soil at 25°C (Hamidou Soumana et al., 2017). These observations indicate that even though *B. bronchiseptica* has adapted to mammals, it has conserved the ability to survive under environment conditions, and respond to changes such as temperature fluctuations (Coote, 2001).

AMOEBA AS AN ENVIRONMENTAL RESERVOIR OF BORDETELLAE

Recently, we have reported the novel ability of *B. bronchiseptica* strain RB50 to utilize amoebae as an environmental niche and transmission vector (Taylor-Mulneix et al., 2017). *B. bronchiseptica* was chosen for this study because it is believed to resemble the progenitor of the classical bordetellae which are most highly associated with human disease (Diavatopoulos et al., 2005). While *B. pertussis* and *B. parapertussis* have undergone genome reduction in their adaption to human, *B. bronchiseptica* retains the largest genome, the widest range of animal hosts, and characteristics like motility and nutrient scavenging that are associated with the ability to survive in some environmental reservoir. Indeed, our data found that *B. bronchiseptica* establishes a commensal relationship with amoeba. While, as of yet, there is no data indicating whether *B. bronchiseptica* results in any benefit or harm to the amoeba, there is clear evidence that it benefits from its interactions with the amoeba *Dictyostelium discoideum* (Taylor-Mulneix et al., 2017).

Amoeba predation involves chemotaxis toward their bacterial food source, internalization, phagocytosis, killing, and metabolizing bacteria. *B. bronchiseptica* is amongst the few bacteria that can survive intracellularly within amoeba for extended periods of time (Hägele et al., 2000; Abd et al., 2003; Greub and Raoult, 2004). This intracellular survival was observed both in *D. discoideum* and in *Acanthamoeba castellanii* (Taylor-Mulneix et al., 2017). Furthermore, we showed that *B. bronchiseptica* can localize to the amoeba sori and associate with the amoeba through multiple passages while utilizing another bacterial food source. These data were quite striking as association with the amoeba was maintained through multiple passages despite the observation that *B. bronchiseptica* localized to the sori are not intracellular within the *D. discoideum* spores. However, *B. bronchiseptica* within the amoeba sori up-regulate expression of factors associated with cell adherence. These data suggest that bordetellae have evolved mechanisms that allow them to survive in long-term association with amoeba, including surviving intracellularly within these phagocytic cells. These mechanisms may also allow them to evade phagocytosis and killing by mammalian immune cells (Mattoo et al., 2000).

As the BvgAS two-component system appears to regulate genes associated with the different life styles of bordetellae (Bvg^+ in animal hosts and Bvg^- in a putative environmental niche), we hypothesized that the Bvg^- phase may be important during the bacterial interaction with amoebae. Indeed, *B. bronchiseptica* that were mutated to constantly express Bvg^+ associated virulence factors had a significantly lower recovery from the amoeba sori in comparison to wildtype or a Bvg^- mutant. These observations indicated an advantage for the Bvg^- phase and represents the

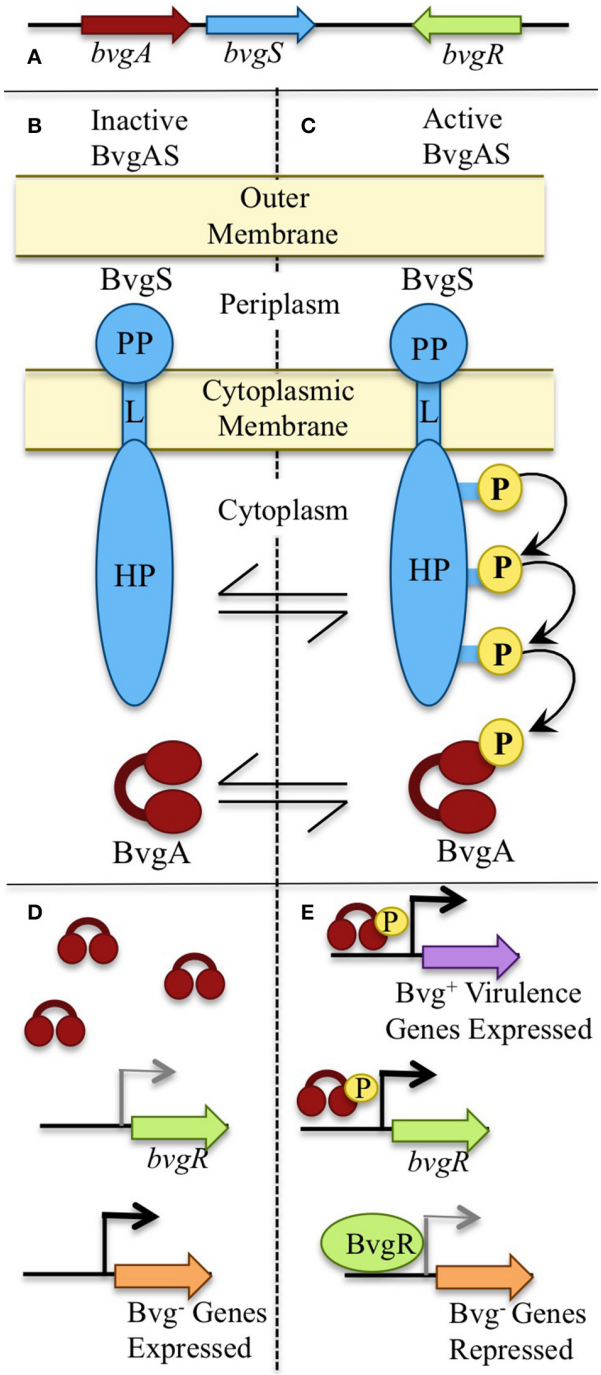

FIGURE 1 | The BvgAS phosphorelay. **(A)** The master regulatory system of bordetellae, Bordetella Virulence Genes (BVG), is expressed by *bvgS* and *bvgA*. **(B,C)** BvgS is a transmembrane sensor protein consisting of a periplasmid domain (PP) connected to the histidine phosphotransfer domains (HP) in the cytosol through a linker domain (L). **(B)** BvgS is inactive and un-phosphorylated when bacteria grow at temperatures below 25°C. **(D)** Bvg^- phase genes are transcribed when the BvgAS system is inactive. **(C)** Upon receiving inducing signals such as 37°C, BvgS autophosphorylates and initiates a phosphor-relay that leads to phosphorylation and activation of BvgA. **(E)** When the BvgAS system is active, Bvg^+ phase-associated genes are transcribed, including *bvgR*. BvgR represses expression of Bvg^- phase associated genes.

first report of a role for the Bvg^- phase in association with any host. Therefore, the presence of the Bvg^- phase across the *Bordetella* genus may be a clue to this genus' origin and evolution (Taylor-Mulneix et al., 2017).

AMOEBA AS A "TRAINING GROUND" FOR HUMAN PATHOGENS

The evolution of *Bordetella* species from environmental microbes to animal and human pathogens suggests the existence of an intermediate stage, or commensal host, that has facilitated the adaptation. Free-living amoeba such as *Acanthamoeba* spp. have been shown to serve as an environmental niche for several opportunistic bacterial pathogens such as *Burkholderia* spp., *Pseudomonas aeruginosa*, *Listeria monocytogenes*, *Legionella pneumophila,* and *Mycobacterium* (Cirillo et al., 1997; Hägele et al., 2000; Greub and Raoult, 2004; Drancourt, 2014; DiSalvo et al., 2015; Jose Maschio et al., 2015). *L. pneumophila* is an example of a bacterial pathogen that utilizes a similar strategy of invasion and life style inside both amoeba and macrophages (Hägele et al., 2000; Greub and Raoult, 2004). Our research has now added *B. bronchiseptica* to the list of bacteria that can survive amoebic predation and utilize amoeba as an environmental reservoir. Interestingly, the ability of *B. bronchiseptica* to survive internalization and resist digestion by eukaryotic cells is not limited to amoebae. Upon infection of a mammalian host, *B. bronchiseptica* and *B. pertussis* can survive inside macrophages, thereby enabling the bacteria to evade host immunity (Siciliano et al., 2006; Lamberti et al., 2010, 2013). The strategy to hide inside host immune cells such as macrophages provides a means of persistence in the host and facilitates the spread to other tissues and organs.

Single-celled amoeba and macrophages are fairly similar physiologically, therefore, these observations suggest that adaptation of environmental bacteria to amoeba may have served as an intermediate step to become animal- or human-associated pathogens (Molmeret et al., 2005). Similar to other species, the long-term bacteria-amoeba association may be the key that has allowed bordetellae to evolve the ability to associate with vertebrate hosts.

GENOME REDUCTION RESULTS IN FAILURE TO EMPLOY AMOEBA AS A HOST

B. pertussis and *B. parapertussis* evolved independently from a *B. bronchiseptica*-like ancestor (Parkhill et al., 2003; Diavatopoulos et al., 2005; Park et al., 2012; Linz et al., 2016). These species possess ≥98% nucleotide identity on the genome level and share many important virulence-associated factors, including toxins and adhesins, suggesting a relatively recent divergence. Indeed, a global phylogeny based on whole genome sequences of a worldwide collection of *B. pertussis* isolates showed two deep branches that coalesce to a last common ancestor about 2,300 (range 1,428–3,340) years ago. A subsequent expansion and diversification of one of the branches, that contains over 98% of all isolates, occurred about 500 years ago (Bart et al., 2014), which correlates with the first historic descriptions of Whooping Cough disease in Persia (Aslanabadi et al., 2015) and Europe (Bart et al., 2014). The extremely low sequence diversity in *B. pertussis* (Linz et al., 2016) indicates that the speciation and specialization to the human host was associated with a strong genetic bottleneck that drastically reduced the sequence diversity. It appears that this process was accompanied by the acquisition and massive expansion of insertion sequence elements (ISE), particularly of IS*481*. ISE's were inserted at hundreds of genomic locations, and homologous recombination between these identical DNA repeats resulted in a mosaic-like structure of the chromosome, in which short blocks of perfect collinearity are broken up by nearly 150 individual rearrangements, including chromosomal inversions. In fact, 88% of the genomic rearrangements in the genome of *B. pertussis* strain Tohama_I, in comparison to the genome of *B. bronchiseptica* strain RB50, are bordered by IS elements, mostly IS*481* (Parkhill et al., 2003). Recombination between ISE's also caused a large amount of deletion in the chromosome, which is reflected in the much smaller genome of *B. pertussis* (about 4.1 Mb with 3,816 CDS's) compared to that of *B. bronchiseptica* (about 5.3 Mb with 5,007 CDS's). *B. pertussis* lost over 1,000 genes during the evolution from a *B. bronchiseptica*-like ancestor, most of which encode transcriptional regulators, proteins involved in transport and metabolism of a wide range of compounds, as well as proteins of unknown function (Linz et al., 2016).

Similar to *B. pertussis*, *B. parapertussis* has also undergone host specialization; one lineage causes pertussis-like disease in humans (hereafter referred to as Bpp_{hu}), while the other causes pneumonia in sheep (Bpp_{ov}). Both *B. parapertussis* lineages have undergone genome reduction *via* ISE's, but much less drastic than *B. pertussis*, resulting in genome sizes of 4.7 Mb in Bpp_{hu} strain 12822 and of 4.8 Mb in Bpp_{ov} strain Bpp5 (Parkhill et al., 2003; Park et al., 2012). Genome comparisons of Bpp_{hu} strain 12822 and of Bpp_{ov} strain Bpp5 to *B. bronchiseptica* strain RB50 revealed a large degree of collinearity between the genomes, with a limited number of *IS1001*-flanked genomic breakpoints. However, the evolution of both *B. parapertussis* lineages proceeded independently as evidenced by different genomic rearrangements and different gene content (Parkhill et al., 2003; Park et al., 2012; Linz et al., 2016). As a result, 3,592 genes are shared between the *B. parapertussis* genomes while 829 genes are specific to the genome of Bpp_{hu} strain 12822 and 592 are specific to the genome of Bpp_{ov} strain Bpp5.

Another human-restricted pathogen, *B. holmesii*, which has been co-isolated with *B. pertussis* during outbreaks of Whooping Cough, also appears to have undergone substantial genome reduction. The genome of this emerging non-classical species (3.7 Mb) is about 1.2 Mb smaller than that of its closest relative *B. hinzii* (4.9 Mb). The *B. holmesii* genome contains multiple copies of three different ISE's (IS*407*, IS*481,* and IS*L3*). Similar to *B. pertussis*, many of the putative genomic breakpoints that disrupt the genome synteny are flanked by ISE's, suggesting genome reduction and rearrangements through homologous recombination between ISE's (Linz et al., 2016). Thus, specialization of several *Bordetella* species to an exclusively human host was associated with acquisition and expansion

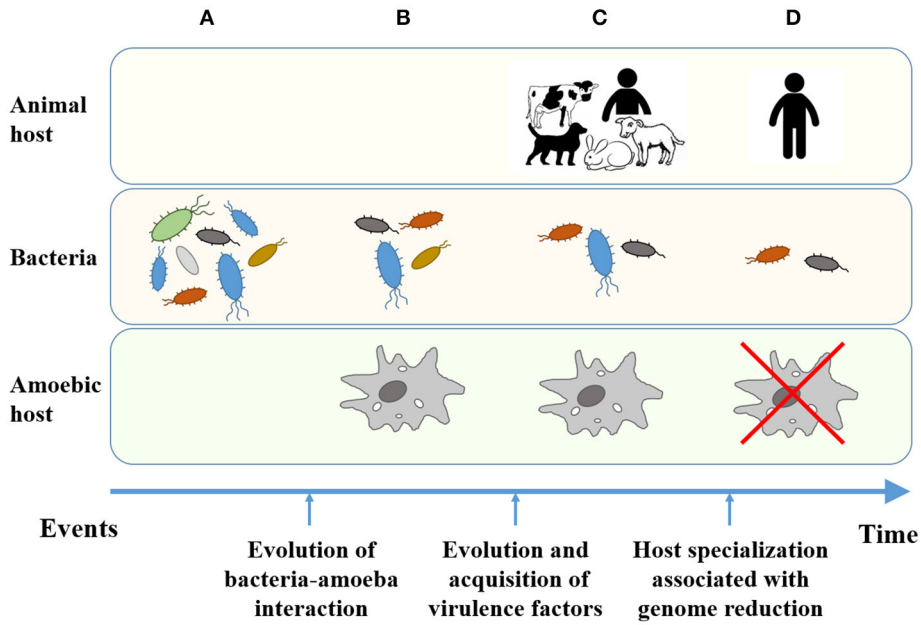

FIGURE 2 | Evolution of bacteria from environmental microbes to human-restricted pathogens. **(A)** Environmental bacteria as a food source for amoebae. **(B)** Bacteria developed resistance to digestion and the ability to interact with the new eukaryotic host. **(C)** Bacteria able to interact with and utilize amoebae evolved to animal pathogens. **(D)** Host-specialized bacterial pathogens lost the ability to resist predation and interact with lower eukaryotes.

of different classes of ISE's, and subsequent recombination between those perfect DNA repeats resulted in chromosomal rearrangements and extensive genome reduction in each of those lineages.

During the assessment of the ability of classical bordetellae to utilize *D. discoideum*, an interesting dichotomy has arisen. The ability to survive intracellularly and localize to the amoeba sori is conserved amongst *B. bronchiseptica*, but is absent in *B. pertussis* (manuscript in preparation). These data suggested that as *B. pertussis* adapted to the closed-cycle of using only humans as a host it underwent genome reduction and lost the ability to utilize *D. discoideum* as an environmental reservoir (**Figure 2**). In support of this theory, the Bpp_{ov} strain Bpp5 retained the ability to survive intracellularly and localize to the sori, while the human isolated Bpp_{hu} strain 12822 did not (manuscript in preparation). The observed difference between the two *B. parapertussis* lineages may be associated with a substantially different gene content in their genomes. All in all, the data suggest that while the ancestor-like *B. bronchiseptica* strains can utilize the amoeba as an environmental reservoir, genome reduction associated with host specialization has led to the inability of human-adapted bordetellae to evade amoebic predation (**Figure 2**). While the ability of the human-associated *B. holmesii* to employ the amoebic life cycle remains to be elucidated, we predict that its severe genome reduction likely involved loss of genes necessary for survival in and utilization of amoebae. Thus, during the evolution of bordetellae from soil microbes to human pathogens, the interaction with and role of amoeba is an important step that may be overlooked if one were to only compare *B. pertussis* with soil isolated bordetellae. All in all, it remains important to consider the whole bordetellae genus and the ability of each individual species to interact with amoeba. The association of genome data with the ecology of amoebic-bacterial interaction will provide important clues that will ultimately reveal key steps in the evolution of *Bordetella* from environmental microbes to human pathogens. Along this line, we have begun to investigate the interaction of multiple *Bordetella* species with the social amoeba *D. discoideum* to expand this fascinating field of research beyond the classical bordetellae.

CONCLUSION

The human immune system is so complex that it is able to efficiently resist invasion and/or resolve infection with little damage to the host. Yet, many human pathogens have arisen from progenitors found in soil and water environments. Therefore, it is important to understand the evolutionary pressures, which allow bacteria adapted to success in other environments to emerge as important human pathogens that cause major disease burden. Herein, we describe that the interaction of bordetellae with predatory amoeba in the environment may have favored the evolution of tools that prepared them for their interactions with mammalian phagocytes, contributing to their emergence as important human pathogens. As these bacteria established a chain of transmission in mammals and further adapted to these hosts, their specialization, and genome reduction, may come with a cost of losing the environmental reservoir. Further work in studying these and other human pathogens and their interaction with

amoebae will be important for understanding the mechanisms by which pathogens can evolve and develop mechanisms to evade host immune systems.

AUTHOR CONTRIBUTIONS

DT-M, IH, and BL contributed equally to this manuscript in regards to concept, writing, and editing. These authors should all be considered equally contributing first authors and we wish that the publication would reflect this. EH contributed to editing and obtaining funding.

FUNDING

NIH (grant numbers: AI116186, GM113681, AI107016) awarded to EH.

REFERENCES

Abd, H., Johansson, T., Golovliov, I., Sandstrom, G., and Forsman, M. (2003). Survival and growth of *Francisella tularensis* in *Acanthamoeba castellanii*. *Appl. Environ. Microbiol.* 69, 600–606. doi: 10.1128/AEM.69.1.600-606.2003

Anantharaman, K., Breier, J. A., and Dick, G. J. (2016). Metagenomic resolution of microbial functions in deep-sea hydrothermal plumes across the Eastern Lau Spreading Center. *ISME J.* 10, 225–239. doi: 10.1038/ismej.2015.81

Aslanabadi, A., Ghabili, K., Shad, K., Khalili, M., and Sajadi, M. M. (2015). Emergence of whooping cough: notes from three early epidemics in Persia. *Lancet Infect. Dis.* 15, 1480–1484. doi: 10.1016/S1473-3099(15)00292-3

Aujoulat, F., Roger, F., Bourdier, A., Lotthe, A., Lamy, B., Marchandin, H., et al. (2012). From environment to man: genome evolution and adaptation of human opportunistic bacterial pathogens. *Genes* 3, 191–232. doi: 10.3390/genes3020191

Bart, M. J., Harris, S. R., Advani, A., Arakawa, Y., Bottero, D., Bouchez, V., et al. (2014). Global population structure and evolution of *Bordetella pertussis* and their relationship with vaccination. *MBio* 5:e01074-14. doi: 10.1128/mBio.01074-14

Biederman, L., Rosen, M. R., Bobik, B. S., and Roberts, A. L. (2015). *Bordetella petrii* recovered from chronic pansinusitis in an adult with cystic fibrosis. *IDCases* 2, 97–98. doi: 10.1016/j.idcr.2015.09.004

Blottiere, H. M., de Vos, W. M., Ehrlich, S. D., and Dore, J. (2013). Human intestinal metagenomics: state of the art and future. *Curr. Opin. Microbiol.* 16, 232–239. doi: 10.1016/j.mib.2013.06.006

Chowdhury, S. P., Schmid, M., Hartmann, A., and Tripathi, A. K. (2007). Identification of diazotrophs in the culturable bacterial community associated with roots of *Lasiurus sindicus*, a perennial grass of thar desert, India. *Microb. Ecol.* 54, 82–90. doi: 10.1007/s00248-006-9174-1

Cirillo, J. D., Falkow, S., Tompkins, L. S., and Bermudez, L. E. (1997). Interaction of *Mycobacterium avium* with environmental amoebae enhances virulence. *Infect. Immun.* 65, 3759–3767.

Coote, J. G. (2001). Environmental sensing mechanisms in *Bordetella*. *Adv. Microb. Physiol.* 44, 141–181. doi: 10.1016/S0065-2911(01)44013-6

Cowan, D. A., Ramond, J. B., Makhalanyane, T. P., and De Maayer, P. (2015). Metagenomics of extreme environments. *Curr. Opin. Microbiol.* 25, 97–102. doi: 10.1016/j.mib.2015.05.005

de Bentzmann, S., and Plesiat, P. (2011). The *Pseudomonas aeruginosa* opportunistic pathogen and human infections. *Environ. Microbiol.* 13, 1655–1665. doi: 10.1111/j.1462-2920.2011.02469.x

Diavatopoulos, D. A., Cummings, C. A., Schouls, L. M., Brinig, M. M., Relman, D. A., and Mooi, F. R. (2005). *Bordetella pertussis*, the causative agent of whooping cough, evolved from a distinct, human-associated lineage of *B. bronchiseptica*. *PLoS Pathog.* 1:e45. doi: 10.1371/journal.ppat.0010045

DiSalvo, S., Haselkorn, T. S., Bashir, U., Jimenez, D., Brock, D. A., Queller, D. C., et al. (2015). *Burkholderia* bacteria infectiously induce the proto-farming symbiosis of *Dictyostelium* amoebae and food bacteria. *Proc. Natl. Acad. Sci. U.S.A.* 112, E5029–E5037. doi: 10.1073/pnas.1511878112

Drancourt, M. (2014). Looking in amoebae as a source of mycobacteria. *Microb. Pathog.* 77, 119–124. doi: 10.1016/j.micpath.2014.07.001

Fry, N. K., Duncan, J., Malnick, H., Warner, M., Smith, A. J., Jackson, M. S., et al. (2005). *Bordetella petrii* clinical isolate. *Emerg. Infect. Dis.* 11, 1131–1133. doi: 10.3201/eid1107.050046

Gerlach, G., Janzen, S., Beier, D., and Gross, R. (2004). Functional characterization of the BvgAS two-component system of *Bordetella holmesii*. *Microbiology* 150(Pt 11), 3715–3729. doi: 10.1099/mic.0.27432-0

Gionfriddo, C. M., Tate, M. T., Wick, R. R., Schultz, M. B., Zemla, A., Thelen, M. P., et al. (2016). Microbial mercury methylation in Antarctic sea ice. *Nat. Microbiol.* 1:16127. doi: 10.1038/nmicrobiol.2016.127

Goodnow, R. A. (1980). Biology of *Bordetella bronchiseptica*. *Microbiol. Rev.* 44, 722–738.

Greub, G., and Raoult, D. (2004). Microorganisms resistant to free-living amoebae. *Clin. Microbiol. Rev.* 17, 413–433. doi: 10.1128/CMR.17.2.413-433.2004

Gross, R., Keidel, K., and Schmitt, K. (2010). Resemblance and divergence: the "new" members of the genus *Bordetella*. *Med. Microbiol. Immunol.* 199, 155–163. doi: 10.1007/s00430-010-0148-z

Hägele, S., Kohler, R., Merkert, H., Schleicher, M., Hacker, J., and Steinert, M. (2000). *Dictyostelium discoideum*: a new host model system for intracellular pathogens of the genus *Legionella*. *Cell. Microbiol.* 2, 165–171. doi: 10.1046/j.1462-5822.2000.00044.x

Hamidou Soumana, I., Linz, B., and Harvill, E. T. (2017). Environmental origin of the genus *Bordetella*. *Front. Microbiol.* 8:28. doi: 10.3389/fmicb.2017.00028

Ivanov, Y. V., Linz, B., Register, K. B., Newman, J. D., Taylor, D. L., Boschert, K. R., et al. (2016). Identification and taxonomic characterization of *Bordetella pseudohinzii* sp. nov. isolated from laboratory-raised mice. *Int. J. Syst. Evol. Microbiol.* 66, 5452–5459. doi: 10.1099/ijsem.0.001540

Ivanov, Y. V., Shariat, N., Register, K. B., Linz, B., Rivera, I., Hu, K., et al. (2015). A newly discovered *Bordetella* species carries a transcriptionally active CRISPR-Cas with a small Cas9 endonuclease. *BMC Genomics* 16:863. doi: 10.1186/s12864-015-2028-9

Jose Maschio, V., Corcao, G., and Rott, M. B. (2015). Identification of *Pseudomonas* spp. as amoeba-resistant microorganisms in isolates of Acanthamoeba. *Rev. Inst. Med. Trop. Sao Paulo* 57, 81–83. doi: 10.1590/S0036-46652015000100012

Kersters, K., Hinz, K. H., Hertle, A., Segers, P., Lievens, A., Siegmann, O., et al. (1984). *Bordetella avium* sp. nov., isolated from the respiratory tracts of turkeys and other birds. *Int. J. Syst. Bacteriol.* 34, 56–70.

Ko, K. S., Peck, K. R., Oh, W. S., Lee, N. Y., Lee, J. H., and Song, J. H. (2005). New species of *Bordetella*, *Bordetella ansorpii* sp. nov., isolated from the purulent exudate of an epidermal cyst. *J. Clin. Microbiol.* 43, 2516–2519. doi: 10.1128/JCM.43.5.2516-2519.2005

Lamberti, Y., Gorgojo, J., Massillo, C., and Rodriguez, M. E. (2013). *Bordetella pertussis* entry into respiratory epithelial cells and intracellular survival. *Pathog. Dis.* 69, 194–204. doi: 10.1111/2049-632X.12072

Lamberti, Y. A., Hayes, J. A., Perez Vidakovics, M. L., Harvill, E. T., and Rodriguez, M. E. (2010). Intracellular trafficking of *Bordetella pertussis* in human macrophages. *Infect. Immun.* 78, 907–913. doi: 10.1128/IAI.01031-09

Linz, B., Ivanov, Y. V., Preston, A., Brinkac, L., Parkhill, J., Kim, M., et al. (2016). Acquisition and loss of virulence-associated factors during genome evolution and speciation in three clades of *Bordetella* species. *BMC Genomics* 17:767. doi: 10.1186/s12864-016-3112-5

Makhalanyane, T. P., Van Goethem, M. W., and Cowan, D. A. (2016). Microbial diversity and functional capacity in polar soils. *Curr. Opin. Biotechnol.* 38, 159–166. doi: 10.1016/j.copbio.2016.01.011

Mattoo, S., and Cherry, J. D. (2005). Molecular pathogenesis, epidemiology, and clinical manifestations of respiratory infections due to *Bordetella pertussis* and other *Bordetella* subspecies. *Clin. Microbiol. Rev.* 18, 326–382. doi: 10.1128/CMR.18.2.326-382.2005

Mattoo, S., Miller, J. F., and Cotter, P. A. (2000). Role of *Bordetella bronchiseptica* fimbriae in tracheal colonization and development of a humoral immune response. *Infect. Immun.* 68, 2024–2033. doi: 10.1128/IAI.68.4.2024-2033.2000

Merkel, T. J., Barros, C., and Stibitz, S. (1998). Characterization of the bvgR locus of *Bordetella pertussis*. *J. Bacteriol.* 180, 1682–1690.

Molmeret, M., Horn, M., Wagner, M., Santic, M., and Abu Kwaik, Y. (2005). Amoebae as training grounds for intracellular bacterial pathogens. *Appl. Environ. Microbiol.* 71, 20–28. doi: 10.1128/AEM.71.1.20-28.2005

Nagata, J. M., Charville, G. W., Klotz, J. M., Wickremasinghe, W. R., Kann, D. C., Schwenk, H. T., et al. (2015). *Bordetella petrii* sinusitis in an immunocompromised adolescent. *Pediatr. Infect. Dis. J.* 34, 458. doi: 10.1097/INF.0000000000000564

Panigrahy, B., Grumbles, L. C., Terry, R. J., Millar, D. L., and Hall, C. F. (1981). Bacterial coryza in turkeys in Texas. *Poult. Sci.* 60, 107–113. doi: 10.3382/ps.0600107

Park, J., Zhang, Y., Buboltz, A. M., Zhang, X. Q., Schuster, S. C., Ahuja, U., et al. (2012). Comparative genomics of the classical *Bordetella* subspecies: the evolution and exchange of virulence-associated diversity amongst closely related pathogens. *BMC Genomics* 13:545. doi: 10.1186/1471-2164-13-545

Parkhill, J., Sebaihia, M., Preston, A., Murphy, L. D., Thomson, N., Harris, D. E., et al. (2003). Comparative analysis of the genome sequences of *Bordetella pertussis*, *Bordetella parapertussis* and *Bordetella bronchiseptica*. *Nat. Genet.* 35, 32–40. doi: 10.1038/ng1227

Raffel, T. R., Register, K. B., Marks, S. A., and Temple, L. (2002). Prevalence of *Bordetella avium* infection in selected wild and domesticated birds in the eastern USA. *J. Wildl. Dis.* 38, 40–46. doi: 10.7589/0090-3558-38.1.40

Schuster, S. C. (2008). Next-generation sequencing transforms today's biology. *Nat. Methods* 5, 16–18. doi: 10.1038/nmeth1156

Sfanos, K., Harmody, D., Dang, P., Ledger, A., Pomponi, S., McCarthy, P., et al. (2005). A molecular systematic survey of cultured microbial associates of deep-water marine invertebrates. *Syst. Appl. Microbiol.* 28, 242–264. doi: 10.1016/j.syapm.2004.12.002

Siciliano, N. A., Skinner, J. A., and Yuk, M. H. (2006). *Bordetella bronchiseptica* modulates macrophage phenotype leading to the inhibition of $CD4^+$ T cell proliferation and the initiation of a Th17 immune response. *J. Immunol.* 177, 7131–7138. doi: 10.4049/jimmunol.177.10.7131

Taylor-Mulneix, D. L., Bendor, L., Linz, B., Rivera, I., Ryman, V. E., Dewan, K. K., et al. (2017). *Bordetella bronchiseptica* exploits the complex life cycle of *Dictyostelium discoideum* as an amplifying transmission vector. *PLoS Biol.* 15:e2000420. doi: 10.1371/journal.pbio.2000420

Tazato, N., Handa, Y., Nishijima, M., Kigawa, R., Sano, C., and Sugiyama, J. (2015). Novel environmental species isolated from the plaster wall surface of mural paintings in the Takamatsuzuka tumulus: *Bordetella muralis* sp. nov., *Bordetella tumulicola* sp. nov. and *Bordetella tumbae* sp. nov. *Int. J. Syst. Evol. Microbiol.* 65, 4830–4838. doi: 10.1099/ijsem.0.000655

Vandamme, P., Heyndrickx, M., Vancanneyt, M., Hoste, B., De Vos, P., Falsen, E., et al. (1996). *Bordetella trematum* sp. nov., isolated from wounds and ear infections in humans, and reassessment of Alcaligenes denitrificans Ruger and Tan 1983. *Int. J. Syst. Bacteriol.* 46, 849–858.

Vandamme, P., Hommez, J., Vancanneyt, M., Monsieurs, M., Hoste, B., Cookson, B., et al. (1995). *Bordetella hinzii* sp. nov., isolated from poultry and humans. *Int. J. Syst. Bacteriol.* 45, 37–45. doi: 10.1099/00207713-45-1-37

Vandamme, P. A., Peeters, C., Cnockaert, M., Inganas, E., Falsen, E., Moore, E. R., et al. (2015). *Bordetella bronchialis* sp. nov., *Bordetella flabilis* sp. nov. and *Bordetella sputigena* sp. nov., isolated from human respiratory specimens, and reclassification of *Achromobacter sediminum* Zhang et al. 2014 as *Verticia sediminum* gen. nov., comb. nov. *Int. J. Syst. Evol. Microbiol.* 65, 3674–3682. doi: 10.1099/ijsem.0.000473

von Wintzingerode, F., Schattke, A., Siddiqui, R. A., Rosick, U., Gobel, U. B., and Gross, R. (2001). *Bordetella petrii* sp. nov., isolated from an anaerobic bioreactor, and emended description of the genus *Bordetella*. *Int. J. Syst. Evol. Microbiol.* 51(Pt 4), 1257–1265. doi: 10.1099/00207713-51-4-1257

Weyant, R. S., Hollis, D. G., Weaver, R. E., Amin, M. F. M., Steigerwalt, A. G., Oconnor, S. P., et al. (1995). *Bordetella holmesii* sp, nov., a new Gram-negative species associated with septicemia. *J. Clin. Microbiol.* 33, 1–7.

Conflict of Interest Statement: The authors declare that the research was conducted in the absence of any commercial or financial relationships that could be construed as a potential conflict of interest.

frontiers in Cellular and Infection Microbiology

REVIEW
published: 02 March 2018
doi: 10.3389/fcimb.2018.00061

Acanthamoeba and *Dictyostelium* as Cellular Models for *Legionella* Infection

A. Leoni Swart[1], *Christopher F. Harrison*[2], *Ludwig Eichinger*[3]*, *Michael Steinert*[4]* and *Hubert Hilbi*[1]*

[1] Institute of Medical Microbiology, Medical Faculty, University of Zurich, Zurich, Switzerland, [2] Max von Pettenkofer Institute, Medical Faculty, Ludwig-Maximilians University Munich, Munich, Germany, [3] Institute for Biochemistry I, Medical Faculty, University Hospital Cologne, Cologne, Germany, [4] Department of Life Sciences, Institute of Microbiology, Technical University of Braunschweig, Braunschweig, Germany

OPEN ACCESS

Edited by:
Matthew S. Francis,
Umeå University, Sweden

Reviewed by:
Hayley J. Newton,
University of Melbourne, Australia
Eric D. Cambronne,
Oregon Health and Science University, United States
Jason King,
University of Sheffield, United Kingdom

***Correspondence:**
Ludwig Eichinger
ludwig.eichinger@uni-koeln.de
Michael Steinert
steinert@tu-bs.de
Hubert Hilbi
hilbi@imm.uzh.ch

Received: 23 November 2017
Accepted: 13 February 2018
Published: 02 March 2018

Citation:
Swart AL, Harrison CF, Eichinger L, Steinert M and Hilbi H (2018) Acanthamoeba and Dictyostelium as Cellular Models for Legionella Infection. Front. Cell. Infect. Microbiol. 8:61. doi: 10.3389/fcimb.2018.00061

Environmental bacteria of the genus *Legionella* naturally parasitize free-living amoebae. Upon inhalation of bacteria-laden aerosols, the opportunistic pathogens grow intracellularly in alveolar macrophages and can cause a life-threatening pneumonia termed Legionnaires' disease. Intracellular replication in amoebae and macrophages takes place in a unique membrane-bound compartment, the *Legionella*-containing vacuole (LCV). LCV formation requires the bacterial Icm/Dot type IV secretion system, which translocates literally hundreds of "effector" proteins into host cells, where they modulate crucial cellular processes for the pathogen's benefit. The mechanism of LCV formation appears to be evolutionarily conserved, and therefore, amoebae are not only ecologically significant niches for *Legionella* spp., but also useful cellular models for eukaryotic phagocytes. In particular, *Acanthamoeba castellanii* and *Dictyostelium discoideum* emerged over the last years as versatile and powerful models. Using genetic, biochemical and cell biological approaches, molecular interactions between amoebae and *Legionella pneumophila* have recently been investigated in detail with a focus on the role of phosphoinositide lipids, small and large GTPases, autophagy components and the retromer complex, as well as on bacterial effectors targeting these host factors.

Keywords: amoebae, effector protein, GTPase, host-pathogen interaction, pathogen vacuole, phosphoinositide lipid, retrograde transport, type IV secretion

LEGIONELLA SPP.—ENVIRONMENTAL BACTERIA AND OPPORTUNISTIC PATHOGENS

Legionella spp. are the causative agents of a potentially fatal pneumonia termed Legionnaires' disease. Overall, *Legionella pneumophila* is the clinically most relevant species, followed by *Legionella longbeachae*, which is associated with outbreaks of Legionnaires' disease particularly in Australia and New Zealand (Newton et al., 2010). The Gram-negative bacteria are ubiquitously

found in the environment, where they inhabit natural and man-made freshwater systems. Upon inhalation of *Legionella*-laden aerosols, the opportunistic pathogenic bacteria enter the human lung, where they infect alveolar macrophages and might cause a fulminant pneumonia (**Figure 1**). *Legionella* spp. are usually regarded to only accidentally infect humans after transmission by technical vectors such as cooling towers, fountains, or showers (Benin et al., 2002; Newton et al., 2010; Hilbi et al., 2011; Yamaguchi et al., 2017). However, recently the first probable transmission of a highly virulent *L. pneumophila* strain from person-to-person was reported (Correia et al., 2016).

L. pneumophila replicates intracellularly within a unique membrane compartment, which is called the *Legionella*-containing vacuole (LCV). This compartment avoids acidification and fusion with lysosomes, but extensively communicates with multiple vesicle trafficking pathways, including the endosomal, secretory and retrograde route, and after a series of maturation steps associates with the endoplasmic reticulum (ER) (Isberg et al., 2009; Asrat et al., 2014; Finsel and Hilbi, 2015; Personnic et al., 2016; Bärlocher et al., 2017b). LCV formation is mechanistically similar in amoebae and macrophages and requires the Icm/Dot (Intracellular multiplication/Defective organelle transport) type IV secretion system (T4SS) (Segal et al., 1998; Vogel et al., 1998; Segal and Shuman, 1999; Hägele et al., 2000; Solomon et al., 2000). This T4SS of *L. pneumophila* translocates ∼300 different "effector" proteins into host cells, wherein these virulence factors subvert pivotal processes such as signal transduction, cytoskeleton dynamics, and membrane trafficking (Isberg et al., 2009; Hubber and Roy, 2010; Hilbi and Haas, 2012; Haneburger and Hilbi, 2013; Sherwood and Roy, 2013; Finsel and Hilbi, 2015; Qiu and Luo, 2017). The Icm/Dot T4SS (but not the "effectorome") is conserved in the genus *Legionella*, including *L. longbeachae*, where it is also essential for virulence in amoebae and mice (Cazalet et al., 2004, 2010; Chien et al., 2004). Of note, the bioinformatics analysis of the *Legionella* genome sequences revealed a number of genes encoding eukaryotic-like proteins or motifs, which likely subvert host cell functions in order to allow the pathogen to survive and replicate intracellularly (Cazalet et al., 2004, 2010; Chien et al., 2004).

PROTOZOA AS ENVIRONMENTAL NICHES OF *LEGIONELLA* SPP.

Environmental microorganisms commonly colonize and form communities called biofilms, which comprise large numbers of prokaryotic and eukaryotic cells associating via adhesion molecules and secreted compounds. Biofilms are ubiquitously found in the environment and contain a plethora of bacterial species, many of which communicate via low molecular weight signaling molecules in a process termed quorum sensing (Hall-Stoodley et al., 2004; Hochstrasser and Hilbi, 2017). These biofilms are attacked ("grazed") by predatory amoebae and ciliates, resulting in a reduction in the bacterial population. In contrast to most other bacterial genera, *Legionella* spp. resist degradation by amoebae and other protozoa (Newton et al., 2010; Hilbi et al., 2011).

In its aquatic habitats *L. pneumophila* replicates intracellularly in various free-living protozoa, including amoebae such as *Acanthamoeba*, *Vermamoeba* (formerly *Hartmannella*), *Naegleria*, *Echinamoeba,* and *Vahlkampfia*, as well as in ciliates like *Tetrahymena* (Fields, 1996; Greub and Raoult, 2004; Hilbi et al., 2011; Hsu et al., 2015). From an evolutionary point of view, interactions of *L. pneumophila* with protozoa shaped the relationship and likely led to adaptive responses, which enable the pathogen to also infect mammalian phagocytes such as human alveolar macrophages (Greub and Raoult, 2004; Molmeret et al., 2005; Jäger et al., 2014). In addition to their role as natural reservoir and selection niche of virulence traits, protozoa can also enhance the transmission of *L. pneumophila* either as intact host cell or as expelled vesicles filled with bacteria (Rowbotham, 1986; Brieland et al., 1997; Amaro et al., 2015).

A number of studies indicated that *L. pneumophila* is highly adapted and manages to infect a wide range of protozoan and metazoan hosts (Hilbi et al., 2011; Bergmann and Steinert, 2015; Hsu et al., 2015). This suggests that many protozoan host species and other interaction partners of *L. pneumophila* in the environment remain to be discovered. Recently, we reported that *L. pneumophila,* protozoa and aquatic nematodes thrive in close association within biofilms (Rasch et al., 2016). Microscopic inspection of biofilms and inoculation experiments with mCherry-labeled *L. pneumophila* identified the ciliates *Oxytricha bifaria*, *Stylonychia mytilus,* and *Ciliophrya* sp. as potential new protozoan hosts of *L. pneumophila*. While several metazoan organisms were identified in the biofilm (Copepoda, Nauplius larvae, Rotifera, and nematodes), only the nematodes accumulated *L. pneumophila* within their intestines. This correlates with the finding that the nematode *Caenorhabditis elegans* can be infected with *L. pneumophila* under laboratory conditions (Brassinga et al., 2010; Komura et al., 2010).

To study the *Legionella*-protozoa-nematode interactions, we infected axenically grown *Acanthamoeba castellanii* and *C. elegans* with *L. pneumophila*. This model system indicated that nematode larvae rupture the infected amoebae cells and thus are exposed to *L. pneumophila* (Rasch et al., 2016). The interaction may be different for *Legionella*-filled amoebae cysts and spores. *D. discoideum* spores resist destruction by the pharyngeal grinders of nematodes such as *C. elegans* and seem to be disseminated by the nematode (Kessin et al., 1996). Thus, if infected with *Legionella*, cysts and spores might disseminate the pathogen along this route.

L. pneumophila grown in amoebae shows distinct features compared to bacteria grown in broth (**Figure 1**). Accordingly, upon growth in *Acanthamoeba polyphaga* the bacteria are more tolerant to antibiotics (Barker et al., 1995), while grown in *A. castellanii* the bacteria are more virulent compared to growth on agar plates (Cirillo et al., 1994). Furthermore, the amoeba species within which replication occurs seems to also play a role,

Abbreviations: Icm/Dot, intracellular multiplication/defective organelle trafficking; LCV, *Legionella*-containing vacuole; OCRL, oculocerebrorenal syndrome of Lowe; PI, phosphoinositide; T4SS, type IV secretion system; TGN, *trans*-Golgi network.

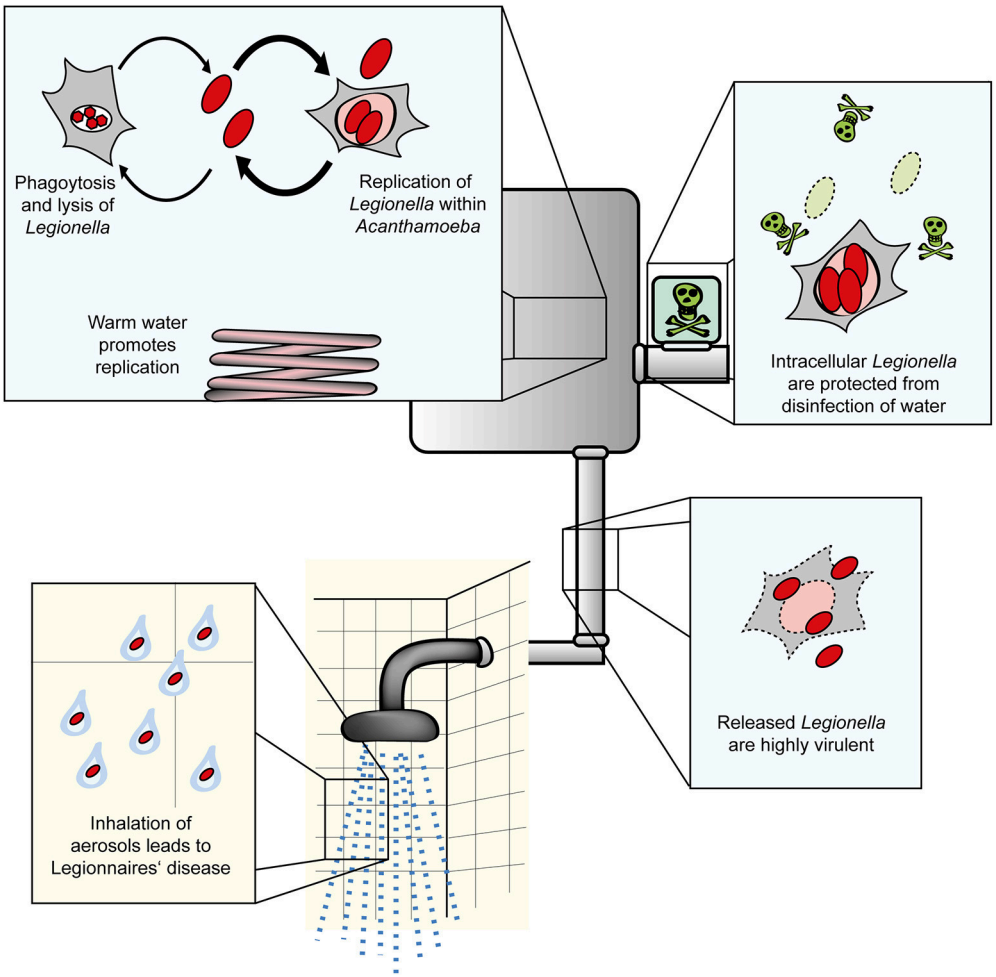

FIGURE 1 | Amoebae as natural reservoir for *Legionella* in water systems. *L. pneumophila* and amoebae are commonly isolated from natural and technical water systems. At cooler temperatures (below ca. 20–25°C), *L. pneumophila* resists *A. castellanii*, but does not or only slowly replicate in the amoebae. At elevated temperatures occurring in technical water systems, *L. pneumophila* efficiently replicates in the amoebae. Internalized *Legionella* bacteria are less susceptible to routine disinfection and released from the amoebae in a highly virulent form. Virulent bacteria present in aerosols are inhaled, infect alveolar macrophages and cause Legionnaires' disease.

such that resistance to chlorination is higher in bacteria released from *Hartmanella vermiformis* than from *A. castellanii* (Chang et al., 2009).

EVOLUTION AND GENE REGULATION OF *LEGIONELLA* IN AMOEBAE

Legionella spp. are known to undergo horizontal gene transfer (Miyamoto et al., 2003). Gene transfer between bacteria has been shown to be significantly enhanced within the digestive vacuole of protozoa, presenting the possibility that they may act as a "trading post" to allow the acquisition of virulence genes (Schlimme et al., 1997). Perhaps reflecting this process, *L. pneumophila* contains a number of genes believed to be derived from eukaryotic, bacterial, or even viral sources (Lurie-Weinberger et al., 2010). These findings suggest that amoebae can be considered as an evolutionary niche, wherein the selective pressure and the potential for *Legionella* to acquire new virulence-related genes is higher than in the extracellular environment (Greub and Raoult, 2004; Molmeret et al., 2005).

An analysis of the *L. pneumophila* transcriptome under different growth conditions revealed that expression of almost half the genome is altered upon shifting from replicative to transmissive phase (Brüggemann et al., 2006). This was observed for bacteria grown in either broth cultures or in *A. castellanii*. The transmissive phase, which occurs following completion of intracellular replication, is characterized by upregulation of virulence and invasion genes, including substrates of the Icm/Dot T4SS and motility genes (Brüggemann et al., 2006). The gene regulation of *L. pneumophila* is further complicated by the existence of non-coding (nc) RNAs, which have been shown to play a role in regulation of virulence traits (Romby et al., 2006). *L. pneumophila* contains a number of these regulatory ncRNAs,

which likely are implicated in virulence, since their expression changes during the bacterial biphasic life cycle or upon infection of *A. castellanii* (Weissenmayer et al., 2011).

ACANTHAMOEBA AS A NATURAL AND MODEL HOST OF *LEGIONELLA*

The distinct features of the protozoan genera *Acanthamoeba* and *Dictyostelium* have been particularly useful in examining the ecology and cellular host-interactions of *L. pneumophila*. Given the similarity of the infection process in amoebae and macrophages, the amoebae are powerful models to study bacteria-macrophage interactions (Hilbi et al., 2007; Escoll et al., 2013; Hoffmann et al., 2013; Bergmann and Steinert, 2015). *Acanthamoeba* has often been found in *Legionella*-positive habitats and has an extremely wide distribution. The amoebae have been isolated from diverse aquatic environments, including soil (Sawyer, 1989), roadside puddles (Sakamoto et al., 2009), fresh water lakes and rivers (John and Howard, 1995), frozen lakes (Brown and Cursons, 1977), the atmosphere (Rodriguez-Zaragoza et al., 1993), and even the Antarctic (Brown et al., 1982).

The majority of *Acanthamoeba* isolates from these aquatic environments harbor endosymbionts, such as viruses, bacteria, yeast, and protists (Greub and Raoult, 2004). However, for laboratory studies of host-pathogen interactions *Acanthamoeba* strains adapted to axenic growth are mostly used (Shevchuk et al., 2014; Eisenreich and Heuner, 2016). Like many other free-living amoebae, *Acanthamoeba* adopts a bi-phasic life cycle, comprising a vegetative trophozoite stage and a dormant cyst stage, which at least in part might explain the wide environmental range of these protozoa (Chávez-Munguía et al., 2005). *L. pneumophila* utilizes the trophozoites for replication and the double-walled cysts as shelter to escape harsh environmental conditions (Fields, 1996).

Acanthamoeba replicates by binary fission and, under culturing conditions, has a doubling time reported to range from 8 to 18 h (Berk and Garduño, 2013). The amoebae are highly motile and follow a random walk pattern with a movement speed of 0.1–0.2 μm/s. In the presence of chemical signals produced by bacteria, *Acanthamoeba* will use chemotaxis to "hunt," actively moving toward the source of these signals (Preston and King, 1984; Schuster and Levandowsky, 1996). Moreover, *Acanthamoeba* spp. are characterized by contractile vacuoles, which expel water for osmotic regulation (Bowers and Korn, 1973), and they contain glycogen storage vacuoles, lysosomes and digestive vacuoles, wherein *L. pneumophila* seems to replicate (Ulsamer et al., 1971; Bowers and Korn, 1973; Eisenreich and Heuner, 2016). Actin microfilaments adjacent to the plasma membrane of *A. castellanii* are responsible for forming protrusions (Pollard et al., 1970), and trophozoites produce short, spine-like projections at the edge of the cell, known as acanthapodia. As the amoebae are very motile, these projections are short-lived but constantly replaced, normally collapsing after less than a minute during active movement (Preston and King, 1984). *A. castellanii* also employs a diverse repertoire of putative pattern recognition receptors (PRRs), many of which with postulated orthologous functions in the innate immune systems of higher organisms (Clarke et al., 2013).

The genome of *A. castellanii* is polyploid and harbors ∼15,500 compact intron-rich genes, a number of which are predicted to have been acquired through inter-kingdom lateral gene transfer (Clarke et al., 2013). The genomic complexity of *A. castellanii* remains one of the barriers to its broad utilization as a model organism. Transfection has been predominantly unsuccessful, with only one report of success (Peng et al., 2005). Furthermore, the polyploid genome organization prevents simple knockout of genes of interest, although approaches using RNA interference to knock down gene expression have been successfully used (Lorenzo-Morales et al., 2005). Overall, however, the known sequence of the *A. castellanii* genome and the increasing number of available molecular tools will strongly augment ecological and cellular research with this authentic host of *L. pneumophila*.

DICTYOSTELIUM DISCOIDEUM: A VERSATILE CELLULAR MODEL FOR *LEGIONELLA* INFECTION

In contrast to *Acanthamoeba* spp., *Dictyostelium discoideum* is not a prevalent natural host for *L. pneumophila* in the environment. This social amoeba, which naturally lives in forest soil and has a narrow temperature tolerance of 20–25°C, undergoes a complex developmental program from a single cell to become a multicellular organism (Taylor et al., 2009; Bretschneider et al., 2016). *D. discoideum* replicates by mitotic division of single amoebae. These amoeba cells live of bacteria, which are taken up by phagocytosis. Laboratory strains, e.g., Ax2, can also thrive in liquid medium through macropinocytosis. Exhaustion of the nutrient supply triggers an intricate multicellular cooperativity. In response to cAMP signals, solitary cells aggregate by chemotaxis, and ∼100,000 cells form a migrating slug, which responds thermo-tactically and photo-tactically. At the final stage of morphogenesis a fruiting body is formed, consisting of a basal disc, a stalk, and spores. Accordingly, the genome of *D. discoideum* encodes morphogenetic traits such as cell-type determination, spatial patterning, cell death, and other features that are essential in multicellular but not unicellular organisms (Steinert and Heuner, 2005; Steinert, 2011; Schilde et al., 2016). The genome of *D. discoideum* is about 34 Mb and comprises six chromosomes, which range from 3.5 to 8.6 Mb in size. Most genes contain introns with conserved splice junctions. About 100 times smaller than the human genome, the *D. discoideum* genome encodes ∼12,500 predicted proteins, including a large number of mammalian orthologs (Eichinger et al., 2005). In addition, *D. discoideum* is increasingly used as a model for the study of genes that in mutant form cause disease in humans (Müller-Taubenberger et al., 2013).

The completed genome sequence of *D. discoideum*, a remarkable repertoire of molecular genetic tools, and the intrinsic biological features of the amoebae allow to study many fundamental cellular processes (Bergmann and Steinert, 2015; Bretschneider et al., 2016; Hochstrasser and Hilbi,

2017). In the haploid amoeba *D. discoideum* non-essential genes can be easily disrupted or replaced by homologous recombination. Further genetic manipulation strategies include random insertion mutagenesis (restriction-enzyme-mediated integration, REMI), multiple gene deletions, Cre/LoxP-mediated recombination, RNA interference techniques, and ectopic expression of endogenous or foreign genes (Kuspa and Loomis, 1992; Chen et al., 1994; Faix et al., 2004; Kuhlmann et al., 2006; Al-Quadan and Kwaik, 2011). The large mutant collection of the *Dictyostelium* stock center (http://www.dictybase.org) (Gaudet et al., 2011), easy cultivation, amenability to diverse biochemical and biological approaches, such as *in vivo* expression of fluorescence-tagged proteins, also contributed to the present strength and versatility of the *D. discoideum* model. Recent highlights resulting from using this model host of *L. pneumophila* will be discussed below.

INTRACELLULAR REPLICATION AND COMPETITION OF *L. PNEUMOPHILA* IN AMOEBAE

The amoeba plate test is a relatively simple assay to determine the ability of *L. pneumophila* mutants to form colonies in the presence of *A. castellanii* (Albers et al., 2005) (**Figure 2A**). A suspension of *A. castellanii* or media alone is spread onto charcoal yeast extract (CYE) agar plates, and allowed to dry. Serial dilutions of *L. pneumophila* are spotted onto the plates and incubated at 30 or 37°C for 3 days. This method allows comparing the growth of multiple strains on a single plate, in both the presence and absence of amoebae. In this manner, *L. pneumophila* mutants defective for amoebae resistance and intracellular replication can be determined in a semi-quantitative manner, alongside bacterial strains capable of suppressing these phenotypes (Albers et al., 2005). A variant of this method has been employed to screen clonal libraries of >20,000 *L. pneumophila* mutants for virulence defects (Aurass et al., 2009). In this approach, mutagenized bacteria are used to infect *A. castellanii* prior to plating.

While the amoeba plate test allows screening of strong replication phenotypes, the resulting output is not easily quantified. A more detailed analysis can be performed by measuring the number of bacteria present within or released by amoebae at given time points by determining bacterial colony forming units (CFU). *A. castellanii* or *D. discoideum* is infected with *L. pneumophila* in Ac medium or MB medium, respectively. In these media *L. pneumophila* is unable to replicate, which allows detection of intracellular replication exclusively. The host cells are then lysed by shear forces or mild detergent treatment, followed by plating on CYE agar to determine CFU. This assay has been used to assess the infection and replication of *L. pneumophila*, *L. dumoffii,* and *L. feelii* in *A. castellanii* (Moffat and Tompkins, 1992). Upon uptake of *L. pneumophila*, bacterial CFU drop significantly in the first few hours. Thereafter, the pathogen replicates intracellularly, leading to a 100–1,000 fold increase in bacterial numbers, and at the end of the cycle, the bacteria escape and disseminate. Bacterial amoebae resistance and intracellular replication can also be applied to screening of water samples. In this approach, samples negative for *Legionella* by normal culture techniques are incubated with amoebae, allowing intracellular growth of the bacteria to easily detectable numbers (Sanden et al., 1992).

Faster and more sensitive methods to determine intracellular replication of *L. pneumophila* in amoebae utilize an automated microtiter plate reader. This approach allows to measure the increase in optical density at 600 nm (Coil et al., 2008) or bacteria-produced fluorescence, e.g., GFP (Harrison et al., 2013, 2015a,b) (**Figure 2B**). To monitor intracellular growth by fluorescence increase over time, *A. castellanii* or *D. discoideum* is infected at 30/37°C or maximum at 25°C, respectively, with either GFP- or mCherry-producing *L. pneumophila* strains. To this end, we preferentially use LoFlo medium, a commercially available, complex *D. discoideum* medium that exhibits low auto-fluorescence and does not allow extracellular growth of *L. pneumophila*. The fluorescent signal for each sample is measured by microtiter plate reader at various time points post infection (p.i.). Since the fluorescence intensity is proportional to the number of bacteria present in a sample, the quantification of fluorescence increase reflects the rate of intracellular bacterial replication. Using the CFU or fluorescence assays, a number of *L. pneumophila* regulators or effector proteins, including LqsR (Tiaden et al., 2007), RidL (Finsel et al., 2013b), LppA (Weber et al., 2014a), and LegG1 (Rothmeier et al., 2013), have been found to promote intracellular replication in amoebae.

In contrast, the deletion of some other regulators (LqsA), effectors (SidC, SidM), or unknown proteins (HdeD) did not result in an intracellular growth defect of *L. pneumophila*. This might be due to robust intracellular replication of *L. pneumophila* involving redundant effectors, or simply because a gene is not required under the conditions tested. To discover weaker phenotypes of *L. pneumophila* mutant strains, we established the more sensitive amoebae competition test (Kessler et al., 2013). In this assay, *A. castellanii* is co-infected with the *L. pneumophila* parental and deletion mutant strain at a 1:1 ratio (multiplicity of infection of 0.01 each) and grown at 37°C for 15–21 days. Every third day the supernatant and lysed amoebae are diluted 1:1000, fresh amoebae are infected, and CFU are determined on agar plates containing kanamycin (to select for presence of the resistance cassette in the mutant strains) or not. Using this approach, *L. pneumophila* mutant strains lacking individual Lqs components (Kessler et al., 2013) or single effectors (LegG1, RidL, LppA, SidC) were outcompeted by the parental strain (Finsel et al., 2013b; Rothmeier et al., 2013; Dolinsky et al., 2014; Weber et al., 2014a). Thus, in the course of successive rounds of infection the fitter strain (usually the parental strain) will come to dominate the bacterial pool.

Using these assays, in addition to *L. pneumophila* mutant strains, the effect of host proteins on intracellular bacterial replication can also be assessed. Upon pharmacological inhibition of phosphoinositide (PI) 3-kinases (PI3Ks) by wortmannin or LY294002, or deletion of the kinases in *D. discoideum*, *L. pneumophila* replicated more efficiently, and therefore the PI3Ks restrict intracellular growth (Weber et al., 2006). In contrast, overproduction of the atlastin (Atl) homolog

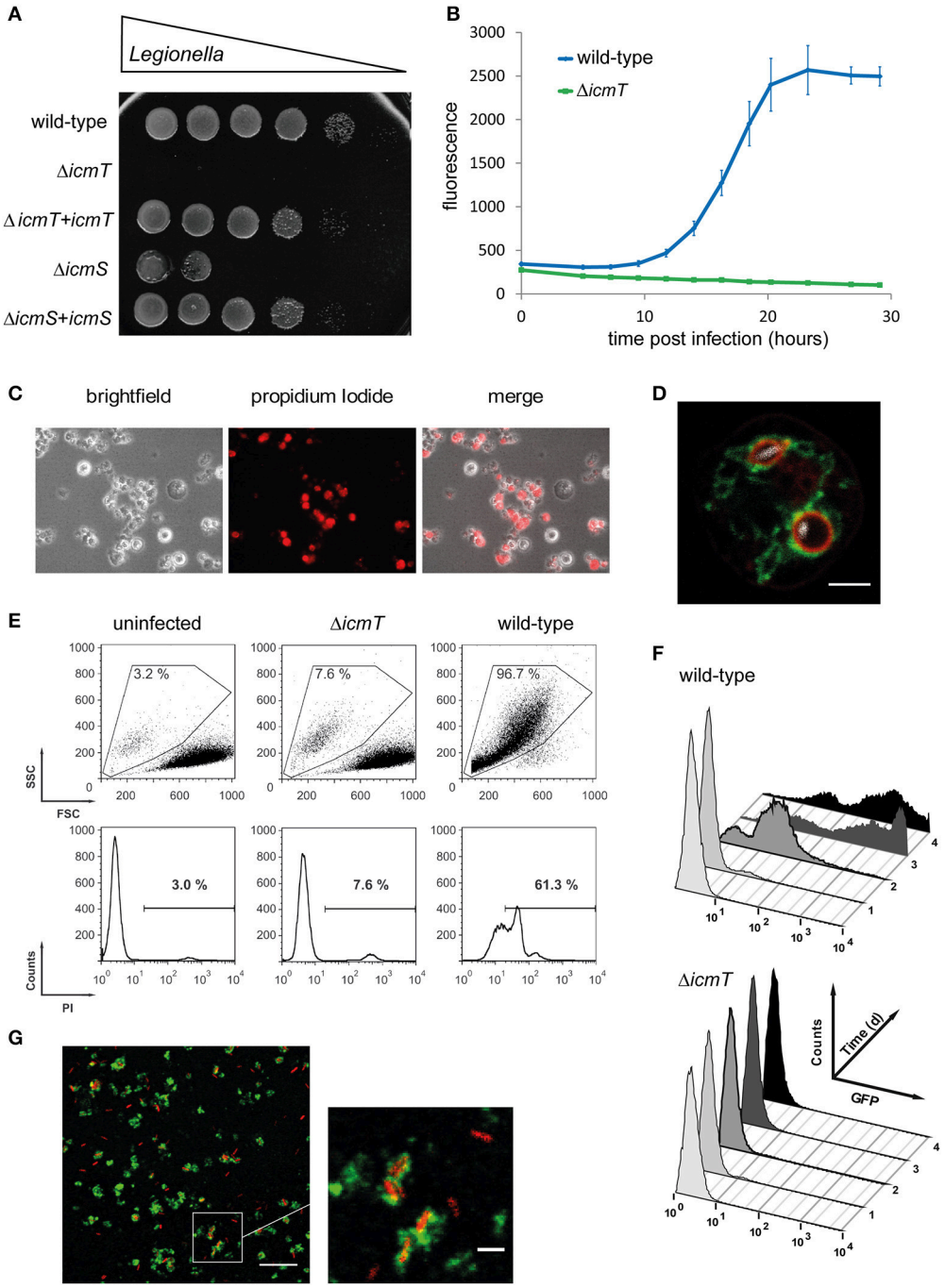

FIGURE 2 | Experimental approaches to study *Legionella* infection of amoebae. **(A)** Amoeba plate test showing serial dilutions of bacterial cultures spotted on a lawn of *A. castellanii*. Virulent *L. pneumophila* is amoeba-resistant and grows in high dilutions, while mutant strains lacking a functional Icm/Dot T4SS do not (Δ*icmT*) or barely (Δ*icmS*) grow. Growth defect of the mutants is complemented by plasmid-borne expression of the corresponding genes (Δ*icmT*+*icmT*, Δ*icmS*+*icmS*). **(B)** Intracellular replication quantified by fluorescence from GFP-producing *L. pneumophila*. Virulent bacteria show an increase in fluorescence over time, while Δ*icmT* mutant bacteria do not grow. **(C)** Fluorescence microscopy images of *L. pneumophila*-infected, dying amoebae that round up, losing the characteristic spiky morphology, and take up the fluorescent dye propidium iodide. **(D)** Live-cell confocal fluorescence microscopy of *D. discoideum* strain Ax3 producing P4C-mCherry (red) and GFP-Sey1 (green), infected (MOI 10, 2 h) with mCerulean-producing *L. pneumophila* JR32 (white). Scale bar: 2 μm. **(E)** Flow cytometry of *A. castellanii* infected with *L. pneumophila* wild-type or Δ*icmT* and stained with propidium iodide. Dye uptake and changes in morphology are quantified by fluorescence and light scattering, respectively. **(F)** Flow cytometry gating on infected *A. castellanii* reveals replication of GFP-producing intracellular *L. pneumophila* wild-type but not Δ*icmT* mutant bacteria. **(G)** LCV isolation by immuno-magnetic separation and density gradient centrifugation from lysates of *D. discoideum* Ax3, infected (MOI 10, 2 h) with DsRed-producing *L. pneumophila* JR32 (red). The preparation was immuno-stained with an anti-calnexin antibody, followed by a FITC-coupled secondary antibody (green). Scale bar: 10 μm, zoom: 2 μm. Image **(A)** was reproduced with permission from Albers et al. (2005) and images **(C,E,F)** from Tiaden et al. (2007).

Sey1 in *D. discoideum* promoted intracellular growth, while production of the catalytically inactive, dominant negative mutant protein Sey1_K154A or depletion by RNAi of Atl3 in mammalian cells inhibited intracellular replication of *L. pneumophila* (Steiner et al., 2017a).

THE TRANSCRIPTIONAL RESPONSE OF *D. DISCOIDEUM* UPON INFECTION WITH *L. PNEUMOPHILA*

In several infection models, including *D. discoideum* and human macrophages, it has been shown that the quantitative and qualitative modulation of diverse host cell functions is crucial for efficient intracellular replication of *L. pneumophila* (Bozzaro and Eichinger, 2011; Hochstrasser and Hilbi, 2017). Accordingly, the analysis of the transcriptional changes that occur in *D. discoideum* upon infection with *L. pneumophila* revealed important aspects of the complex host-pathogen cross-talk (Farbrother et al., 2006). The experiment was performed with cDNA-microarrays, covering approximately half of the *Dictyostelium* genome, and led to the identification of 731 differentially regulated host genes in a 48 h infection with the virulent *L. pneumophila* Philadelphia-1 strain JR32. In addition, a detailed analysis of the 24 h time point p.i. of *L. pneumophila* JR32, an avirulent *L. pneumophila* Δ*dotA* mutant, or *Legionella hackeliae* (reduced virulence), uncovered 131 differentially expressed genes common to all three strains compared with uninfected amoebae. The corresponding gene products are either involved in host-specific defense mechanisms or required for successful infection and proliferation of *L. pneumophila* (Farbrother et al., 2006).

Functional annotation of the differentially regulated genes of the 48 h and 24 h time points revealed that in addition to triggering a stress response, *L. pneumophila* not only interferes with intracellular vesicle trafficking, but also subverts and exploits the host metabolism. A considerable enrichment of differentially regulated genes involved in translation, proteolysis, nucleotide metabolism, and lipid modification was observed. Moreover, *L. pneumophila* induces the expression of multiple amino-acyl t-RNA synthetases (aaRSs). Interestingly, besides the canonical coupling of correct amino acids to t-RNA molecules, aaRSs were described to play an unexpected role in splicing, apoptosis, and regulation of transcription and translation (Hausmann and Ibba, 2008; Yannay-Cohen et al., 2009). Thus, the upregulation of *D. discoideum* aaRSs upon *L. pneumophila* infection may serve a similar function in different signaling pathways. The transcriptome results also showed that infection with *L. pneumophila* results in differential expression of host genes that are involved in bacterial degradation and autophagy. Additionally, genes encoding cytoskeleton proteins were enriched ∼7-fold during the early stage of infection. These findings likely reflect the uptake of bacteria and transport of the nascent phagosome inside the host cell (Farbrother et al., 2006).

In a different study it was found that infection of *D. discoideum* by *L. pneumophila* caused a decrease in mitochondrial messenger RNAs and a cleavage of the mitochondrial large subunit ribosomal RNA (LSU rRNA). The specific cleavage of the LSU rRNA in *D. discoideum* required functional *L. pneumophila* type II and type IV secretion systems. LSU rRNA cleavage was, however, not observed upon infection of *A. castellanii* or human U937 macrophages, suggesting that *L. pneumophila* might use distinct mechanisms to interrupt the mitochondrial metabolism in different hosts (Zhang and Kuspa, 2009).

In summary, the transcriptional changes in *L. pneumophila*-infected *D. discoideum* suggest complex and still poorly understood regulatory interactions between pathogen and host. In the course of establishing its replicative niche, *L. pneumophila* not only interferes with signaling processes, mitochondrial function, and intracellular vesicle trafficking, but also profoundly influences the metabolism of its host.

ANALYSIS OF *LEGIONELLA* INFECTION IN DEFINED *D. DISCOIDEUM* MUTANT STRAINS

Investigations of *D. discoideum* mutant strains have significantly contributed to our understanding of *Legionella* infection. Host cell factors implicated in host-pathogen interactions are either involved in the cellular defense or exploited by the pathogen in the course of infection. Consequently, the inactivation of distinct host factors may either favor or impede *Legionella* infection. To identify host genes crucial for *Legionella* infection, candidate gene approaches as well as untargeted mutational screens have been carried out in *D. discoideum* (Bozzaro et al., 2008; Li et al., 2009). In the candidate gene approach, either available *D. discoideum* mutants are used, which in many cases can be ordered from the *Dictyostelium* stock center (Fey et al., 2013), or novel genes of interest are disrupted, silenced, or the corresponding proteins overproduced as fluorescently tagged fusions (Bozzaro et al., 2008; Steinert, 2011; Steiner et al., 2017b). In order to dissect the complex cross-talk between *D. discoideum* and *L. pneumophila*, classical infection assays were performed, and a versatile methodology has been developed based on fluorescently tagged marker proteins, heterologously produced bacterial effectors and different visualization techniques (Eichinger and Rivero, 2006; Steinert, 2011; Steiner et al., 2017b). As select examples, we will discuss the role of the host cytoskeleton, autophagy machinery, and phospholipid metabolism in the infection process.

Most *D. discoideum* knock-out mutants of cytoskeletal proteins caused a decrease in the uptake and in the proliferation of *L. pneumophila*, indicating that an intact cytoskeleton is important (Bozzaro et al., 2013). Exceptions to this rule were the coronin A and B genes. Coronins comprise a large family of proteins that function mainly in actin cytoskeleton-associated processes. The proteins harbor a WD (Trp-Asp)-repeat domain containing seven repeats that form a seven-bladed β-propeller, adjacent to a unique region, and a C-terminal coiled coil region which mediates trimerization (Shina and Noegel, 2008). We studied uptake and replication of *L. pneumophila* in *D. discoideum* mutants where *corA* (encoding the conventional coronin), *corB* (encoding coronin 7 (CRN7)), or

vilA (encoding villidin a member of the coronin 4 family) were disrupted. Absence of conventional coronin reduced the uptake of *L. pneumophila* and enhanced intracellular growth. Villidin-deficient cells showed an even higher reduction in uptake, and intracellular growth was strongly reduced (Fajardo et al., 2004). In contrast, uptake of *L. pneumophila* was enhanced in CRN7-deficient cells but intracellular replication was not affected. Overexpression of CRN7 on the other hand caused reduced internalization and an increased replication of *L. pneumophila*, suggesting that CRN7 negatively regulates the internalization of the bacteria. A double mutant wherein the *corA* and *corB* genes were inactivated behaved like the *corA* deletion strain (Shina et al., 2010, 2011) (**Table 1**). CRN7 harbors a Cdc42- and Rac-interactive binding (CRIB) domain in each of its two β-propeller domains with a preference for GDP-loaded Rac. Thus, CRN7 might keep Rac GTPases in their GDP-bound form and locally prevent the activation of the downstream targets SCAR and WASP. Loss of CRN7 hyper-activates WASP, which promotes F-actin assembly leading to increased phagocytosis (Swaminathan et al., 2015).

In recent years, autophagy has been identified as an ancient and important cellular defense mechanism that targets intracellular pathogens for destruction (Sherwood and Roy, 2016). A number of pathogens are able to subvert this cellular defense, and also *L. pneumophila* interferes with the autophagy process of the host. In early studies with *D. discoideum* mutants deficient for either one of five different core autophagy genes autophagy appeared to be dispensable for intracellular replication of *L. pneumophila* at later stages of infection (Otto et al., 2004). However, infection assays with *atg9, atg16,* and *atg9/16* deletion mutants revealed a reduced uptake of *L. pneumophila* in these strains in comparison to Ax2 wild-type cells (Tung et al., 2010; Xiong et al., 2015). For the *atg9* deletion mutant it was further shown that those bacteria that entered the host were initially cleared less efficiently and at later stages of the infection multiplied more efficiently compared to the parental amoebae (Tung et al., 2010) (**Table 1**). It must be kept in mind that apart from its role in autophagy ATG9 likely has additional roles in trafficking, as it is localized to a number of cytoplasmic vesicular structures (Noda, 2017). Noteworthy, *atg9* and *atg16* were oppositely regulated in parental *D. discoideum* in response to infection (Farbrother et al., 2006; Tung et al., 2010).

The *L. pneumophila* Icm/Dot substrate RavZ is a cysteine protease that irreversibly cleaves lipid-conjugated Atg8 proteins on the membranes of nascent autophagic structures (Choy et al., 2012). Furthermore, the *L. pneumophila* sphingosine-1 phosphate lyase (LpSpl) targets host sphingolipid metabolism and inhibits autophagy in mouse macrophages (Rolando et al., 2016). These findings suggest that both, the host cell and the pathogen, modulate autophagy for their own benefit.

Another cellular process that is part of the defense reaction of the host and exploited by *L. pneumophila* is the PI lipid metabolism (Weber et al., 2009b; Haneburger and Hilbi, 2013). PI lipids are important for vesicle trafficking and organelle identity, since the cellular compartments are defined in part by their PI composition. The lipid head group can be phosphorylated or dephosphorylated at the 3′, 4′, and/or 5′ positions by specific PI kinases and PI phosphatases, resulting in an array of seven specific PIs (Di Paolo and De Camilli, 2006). Deletion or pharmacological inhibition of PI3Ks class I promotes intracellular replication of *L. pneumophila* and impairs the transition from tight to spacious LCVs (Weber et al., 2006). Disruption of *D. discoideum* PTEN (phosphatase and tensin homolog), a PI phosphatase antagonizing PI3Ks, reduces the uptake but does not affect proliferation of *L. pneumophila* (Peracino et al., 2010). *D. discoideum* PLC (phospholipase C) is involved in the PI metabolism through hydrolysis of PI(4,5)P_2 to diacylglycerol (DAG) and inositol 1,4,5-triphosphate (IP_3). Its inhibition dramatically reduced the engulfment of *L. pneumophila*, but had no effect on bacterial replication (Peracino et al., 2010).

Furthermore, in *D. discoideum* cells lacking the PI 5-phosphatase Dd5P4, a homolog of human OCRL (oculocerebrorenal syndrome of Lowe), bacterial replication and LCV formation occurred more efficiently. Dd5P4 localizes to LCVs via its N-terminus and might interact with the *L. pneumophila* PI(3)*P*-binding virulence factor LpnE (Weber et al., 2009a). The PI 5-phosphatase is catalytically active on the LCV, thereby increasing the PI(4)*P* available for binding of the *L. pneumophila* effector proteins SidC or SidM. An additional host protein, which plays a role in the PI metabolism is RpkA, an unusual seven-helix trans-membrane receptor with a predicted intracellular PI(4)*P* 5-kinase activity. RpkA is specific for lower eukaryotes and is recruited to nascent LCVs in *D. discoideum*. It disturbs the PI balance and thereby plays a role in the defense against *L. pneumophila*. RpkA interacts with the V-ATPase complex, but whether it can actively recruit the V-ATPase to the LCV is not known (Riyahi et al., 2011) (**Table 1**).

These examples illustrate the power of the *D. discoideum* system for the investigation of the host side during infection. The biological properties of this amoeba in combination with the straight-forward generation and analysis of mutant strains will continue to provide a potent and versatile model for the dissection of the complex cross-talk with *L. pneumophila*.

FLUORESCENCE MICROSCOPY OF *LEGIONELLA*-INFECTED LABELED *D. DISCOIDEUM*

The difficulty of performing genetic manipulations in *A. castellanii* implies that modifications of host cell factors, for example the production of GFP-labeled proteins, are not feasible. One of the few fluorescence assays that can be performed is the determination of *Legionella*-triggered cytotoxicity. To this end, the number of infected *A. castellanii* cells permeable to fluorescent dyes such as propidium iodide is counted, as has been done to assess the cytotoxicity of *L. pneumophila* deletion mutants (Albers et al., 2007) (**Figure 2C**). Given these constraints, genetically tractable amoebae such as *D. discoideum*, are more useful for cell biology and pathogen-host interaction studies, which examine the localization of specific markers to the LCV.

A plethora of genetic tools is available to study host-pathogen interactions using *D. discoideum*. In addition to DNA microarrays and targeted deletions or random mutations of

TABLE 1 | Selected *D. discoideum* mutants implicated in *L. pneumophila* interactions.

Host cell factor	Manipulation	Effects on infection:		References
		Uptake	Growth	
ATG 9	Knockout	Down	Up	Tung et al., 2010
ATG 16	Knockout	Down	n.t.	Xiong et al., 2015
ATG 9/ATG 16	Double knockout	Down	n.t.	Xiong et al., 2015
Coronin	Knockout	Down	Up	Solomon et al., 2000; Fajardo et al., 2004
		n.t.	Up	
Coronin 7	Knockout	Up	Normal	Shina et al., 2010
	Overexpression	Down	Normal	
Coronin/coronin 7	Double knockout	Down	Up	Shina et al., 2011
Dd5P4 (OCRL)	Knockout	Down	Up	Weber et al., 2009a
PLC	Inhibitors	Down	Normal	Peracino et al., 2010
PI3K 1/2	Double knockout	Normal	Up	Weber et al., 2006
PI3K 1/2/3/4/5/6	Sextuple knockout	Down	Up	Peracino et al., 2010
PI3K 1/2/3/4/5/6/PTEN	Septuple knockout	Down	Up	Peracino et al., 2010
PTEN	Knockout	Down	Normal	Peracino et al., 2010
RpkA	Knockout	Normal	Up	Riyahi et al., 2011
Sey1	Overexpression (WT)	n.t.	Up	Steiner et al., 2017a
	Overexpression (DN)	n.t.	Down	
TBC1D5	Knockout	n.t.	Down	Bärlocher et al., 2017a
Villidin	Knockout	Down	Down	Fajardo et al., 2004

L. pneumophila uptake and intracellular growth in D. discoideum mutants was assessed by different methods. Effects ("up" or "down") on bacterial uptake or intracellular growth are indicated relative to the parental amoeba strain or untreated amoebae, respectively. ATG, autophagy; PLC, phospholipase C; PI3K, phosphoinositide 3-kinase class I; PTEN, phosphatase and tensin homolog; Dd5P4, D. discoideum inositol 5-phosphatase 4; OCRL, oculocerebrorenal syndrome of Lowe; RpkA, receptor phosphatidylinositol kinase A; DN, dominant negative; WT, wild-type; n.t.: not tested.

genes, an extensive library of plasmids is available allowing constitutive or inducible production of fluorescently labeled probes in *D. discoideum* (http://wiki.dictybase.org/dictywiki/index.php/Vectors). Specifically, various expression vectors for N- or C-terminal fusions with green- or red-fluorescent proteins are available. These include extrachromosomal (Levi et al., 2000), extrachromosomal inducible expression (Veltman and van Haastert, 2013), or integrating plasmids (Manstein et al., 1995), as well as vectors for efficient generation of gene knockouts using one-step cloning (Wiegand et al., 2011). For the production of fluorescent probes, *D. discoideum* is transformed with one or multiple plasmids by electroporation (Weber et al., 2014b). Transformants are isolated by antibiotic selection and form microcolonies within 7–12 days after transformation.

A GFP-fusion protein commonly used in *D. discoideum* is calnexin-GFP, an ER-specific type I transmembrane protein and well-established LCV marker (Fajardo et al., 2004; Weber et al., 2006; Ragaz et al., 2008; Dolinsky et al., 2014). Within 2 h after uptake, calnexin accumulates on the membrane of LCVs containing virulent *L. pneumophila*, but not avirulent Δ*icmT* mutant bacteria, and to a significantly smaller extent on vacuoles harboring Δ*sidC* mutants (Ragaz et al., 2008; Dolinsky et al., 2014; Weber et al., 2014b). Using *D. discoideum* cells producing fluorescently labeled proteins, numerous other host proteins were found to localize to the LCV. These include small GTPases of the Rab family (Urwyler et al., 2009; Hoffmann et al., 2014), Rap1 (Schmölders et al., 2017), and Ran (Rothmeier et al., 2013), the ER tubule-resident large GTPase Atl3/Sey1 (Steiner et al., 2017a) (**Figure 2D**), as well as components implicated in the retrograde vesicle trafficking pathway, such as the *D. discoideum* OCRL homolog Dd5P4 (Weber et al., 2009a) and subunits of the retromer complex (Finsel et al., 2013a).

A caveat of microscopy methods using fixed samples is that the fixation techniques might alter the morphology of cellular structures such as membranes, vesicles, or microtubules. Time-lapse imaging of living cells on the other hand is optimal to follow cellular dynamics over time. A well-studied process is the PI conversion on the LCV membrane during infection (Weber and Hilbi, 2014; Weber et al., 2014b). *L. pneumophila*-infected *D. discoideum* producing various PI probes, including PH_{CRAC}-GFP for PI(3,4,5)P_3 and PI(3,4)P_2, 2×FYVE-GFP for PI(3)*P* or GFP-P4C_{SidC} for PI(4)*P*, were imaged live for time-lapse analysis (Weber et al., 2014b). Immediately upon bacterial uptake, the phagosome containing *L. pneumophila* transiently accumulates PI(3,4,5)P_3 for up to 1 min, and within that time-span, PI(3)*P* is acquired in a Icm/Dot independent manner. During the following 2 h, LCVs containing virulent *L. pneumophila* gradually replace PI(3)*P* with PI(4)*P*, whereas Δ*icmT* vacuoles remain PI(3)*P* positive (Weber et al., 2014b). Using dually labeled *D. discoideum*, the P4C-mRFPmars signal was spatially separated from calnexin-GFP-positive membranes and maintained for at least 8 h. Manipulation of the LCV PI pattern is of great importance for the bacterium. The PI 5-phosphatase Dd5P4 as well as PI3Ks and PI4KIIIβ have been

implicated in this process (Brombacher et al., 2009; Weber et al., 2009a,b).

Live-cell imaging was also employed to assess the LCV and microtubule dynamics in infected *D. discoideum* producing calnexin-GFP (Rothmeier et al., 2013) or GFP-α-tubulin (Simon et al., 2014). The *D. discoideum* strains were infected with DsRed-producing *L. pneumophila*, wild-type, Δ*legG1,* or the complemented mutant. LegG1 is an Icm/Dot-translocated RCC1-like-repeat effector protein, which activates the small GTPase Ran and increases cellular RanGTP levels (Rothmeier et al., 2013). Ran is a member of the Ras superfamily of small GTPases and controls various cellular processes, including nucleo-cytoplasmic transport (Stewart, 2007), assembly of the mitotic spindle apparatus (Goodman and Zheng, 2006; Clarke and Zhang, 2008), and the dynamics of non-centrosomal microtubules (Yudin and Fainzilber, 2009). LCV motility as well as microtubule stability was significantly reduced in *D. discoideum* infected with Δ*legG1* mutant bacteria.

QUANTITATIVE ASSESSMENT OF *LEGIONELLA* INFECTION BY (IMAGING) FLOW CYTOMETRY

Flow cytometry is a high-throughput technique that allows a simultaneous multi-parameter analysis of single cells. Large data sets, high resolution, accuracy, reproducibility, and sensitivity are major advantages of this approach to study uptake, cytotoxicity, and intracellular replication of *L. pneumophila* (Tiaden et al., 2013). The physiological status and integrity of a cell is reflected in the forward scatter/sideward scatter pattern (corresponding to cell size and "granularity," respectively), and membrane integrity can be tested by staining cellular DNA with the fluorescent dye propidium iodide, which is recorded as "cell-associated fluorescence."

Flow cytometry can be used to study in a quantitative manner *Acanthamoeba* phagocytosis. To this end, the rate and degree of uptake of fluorescent beads are assessed, i.e., the ratio of fluorescent vs. non-fluorescent amoebae (Avery et al., 1995), or, analogously, the infection by fluorescently labeled *L. pneumophila* is determined (Tiaden et al., 2013). Uptake of *L. pneumophila* is scored immediately after infection by determining an "uptake index," which is calculated from the signal-strength and percentage of amoebae infected with GFP-producing bacteria (Harf et al., 1997; Tiaden et al., 2013). Hence, cytotoxicity of *L. pneumophila* can be assessed as a change in size and shape of *A. castellanii*, measured by forward/sideward light scattering, as well as by loss of membrane integrity, as determined by the increase in permeability to propidium iodide (Tiaden et al., 2007, 2008) (**Figure 2E**).

Moreover, using flow cytometry and GFP-producing bacteria, not only the uptake efficiency can be determined, but also intracellular replication in *A. castellanii* or *D. discoideum* can be followed over several days. This approach has been utilized to examine the uptake and replication defects of *L. pneumophila* deletion mutants lacking components of the *Legionella* quorum sensing (Lqs) system: LqsR (Tiaden et al., 2007), LqsA or LqsS (Tiaden et al., 2010), LqsT or LqsS-LqsT (Kessler et al., 2013), as well as the entire *lqs* gene cluster (Tiaden et al., 2008) (**Figure 2F**). Analogously, flow cytometry can be employed to assess uptake and replication phenotypes of *D. discoideum* deletion mutant strains lacking PI3Ks (Weber et al., 2006) or Dd5P4 (Weber et al., 2009a). Finally, in addition to its use as a research tool, flow cytometry has also been developed as a diagnostic method to rapidly screen for *Legionella* contamination of bathing facilities and other water sources (Taguri et al., 2011).

In a technique termed imaging flow cytometry (IFC), flow cytometry is combined with fluorescence microscopy, enabling fast quantification of microscopic images. Using this approach, the high-throughput capacity and information about cell size, volume, and shape provided by the flow cytometer is combined with high-resolution spatial localization of fluorescent proteins of interest provided by a microscopic image, resulting in non-biased and quantitative, large datasets (Barteneva et al., 2012; Johansson et al., 2015). By means of specialized software, the acquired cellular images can be analyzed using bi-variant plots and histograms, in parallel with a sequential gating strategy.

Recently, we employed IFC and *D. discoideum* ectopically producing GFP- and mCherry-labeled fusion proteins to assess the accumulation of specific host proteins on LCVs in whole cells (Schmölders et al., 2017; Steiner et al., 2017a) or homogenates (Bärlocher et al., 2017a). Thus, active small GTPase Rap1 was found to localize to a higher extent to LCVs containing the parental *L. pneumophila* strain Lp02 as compared to LCVs harboring the "pentuple" mutant strain (Schmölders et al., 2017), which lacks five gene clusters encoding 31% of the effector proteins (O'Connor et al., 2011). The method was also utilized to quantify the recruitment of calnexin-GFP or GFP-Sey1 to PI(4)*P*-positive LCVs labeled with P4C-mCherry. Dually labeled *D. discoideum* amoebae producing P4C-mCherry and GFP-Sey1 or GFP-Sey1_K154A were infected, and co-localization of PI(4)*P* with *L. pneumophila* was analyzed for 10,000 events per time point p.i. IFC confirmed and quantified the fluorescence microscopy finding that PI(4)*P* accumulates at the LCV in a Sey1-independent manner. Finally, the Rab7 GAP TBC1D5 was scored on LCVs. However, in this case lysates of infected *D. discoideum* had to be prepared to reduce background and increase sensitivity (Bärlocher et al., 2017a). To this end, *D. discoideum* amoebae producing in tandem GFP-TBC1D5 and the endosomal marker AmtA-mCherry were infected with mPlum-producing *L. pneumophila*, and the localization of TBC1D5 was analyzed by IFC in cell homogenates. For each condition, over 3,000 cells were analyzed, and TBC1D5 was found to localize to wild-type-, but not Δ*icmT*-containing LCVs.

CHEMOTACTIC MIGRATION OF *LEGIONELLA*-INFECTED *D. DISCOIDEUM*

In a process termed chemotaxis, phagocytes migrate in a directed manner toward an attractant. Thus, *D. discoideum*,

macrophages or neutrophils sense and respond to cAMP, the chemokines CCL5, and tumor necrosis factor (TNF)-α, or the formyl-methionyl-leucyl-phenylalanine (fMLP) peptide, respectively. The migration of eukaryotic cells critically depends on microtubule polarization and dynamics (Etienne-Manneville, 2013), which in turn is controlled by the small GTPase Ran.

Given the impact of the Icm/Dot substrate LegG1 on Ran GTPase activation and microtubule dynamics (Rothmeier et al., 2013), we analyzed the role of the *L. pneumophila* T4SS and LegG1 on host cell motility (Simon et al., 2014). Using *D. discoideum* amoebae or mammalian immune cells in under-agarose or Boyden chamber migration assays, *L. pneumophila* was found to inhibit cell migration in an Icm/Dot-dependent manner. *D. discoideum* infected with virulent *L. pneumophila* showed a substantially reduced migration when compared to amoebae infected with Δ*icmT* mutant bacteria. The migration inhibition observed was not due to an uptake defect or cytotoxicity. Interestingly, *D. discoideum* infected with the Δ*legG1* mutant strain was hyper-inhibited for directed migration in the under-agarose assay, which was reverted upon overproduction of LegG1 to an extent comparable to amoebae infected with wild-type bacteria. Single cell tracking indicated that the directionality as well as the velocity of *D. discoideum* infected with the parental strain or Δ*legG1* is impaired. Thus, the Ran activator LegG1 promotes cell motility by stabilizing microtubules and thereby might antagonize the possibly deleterious impact of other *L. pneumophila* Icm/Dot substrates on the host cytoskeleton.

Recently, the effect of the small signaling molecule LAI-1 (*Legionella* autoinducer-1, 3-hydroxypentadecane-4-one) on chemotactic migration of *D. discoideum* was analyzed (Simon et al., 2015). This study was based on the observations that *L. pneumophila* lacking the autoinducer synthase LqsA no longer impaired the migration of infected amoebae, and a Δ*icmT* mutant strain overproducing LqsA inhibited cell migration, obviously in an Icm/Dot-independent manner. Synthetic LAI-1 dose-dependently inhibited the migration of *D. discoideum* in the micromolar range. RNA interference with epithelial cells subjected to a scratch ("wound closure") assay revealed that LAI-1 signaling requires the scaffold protein IQGAP1, the small GTPase Cdc42 as well as the Cdc42-specific guanine nucleotide exchange factor ARHGEF9, but not other modulators of Cdc42, or RhoA, Rac1 or Ran GTPase. Thus, the *L. pneumophila* signaling molecule LAI-1 produced either in the LCV or added exogenously promotes inter-kingdom signaling.

In summary, *L. pneumophila* modulates the motility of eukaryotic cells not only by means of Icm/Dot substrates, but also through the Lqs system and the small signaling molecule LAI-1 (Personnic et al., 2017). At present, it is unclear what the benefit of host cell migration inhibition for *L. pneumophila* might be. The phenomenon might simply be an indirect effect of perturbation of trafficking pathways and cytoskeletal dynamics. More intriguingly, however, it might also reflect the fact that macropinocytosis competes with migration of *D. discoideum*, two processes balanced by PI(3,4,5)P_3 (Veltman, 2015). Hence, by inhibiting cell migration, *L. pneumophila* might promote its macropinocytic uptake by the amoebae.

CELL BIOLOGICAL, BIOCHEMICAL, AND PROTEOMICS ANALYSIS OF PURIFIED INTACT LCVS

Intact LCVs from *D. discoideum* can be purified by a straight-forward two-step protocol involving immuno-affinity enrichment using an antibody against the Icm/Dot substrate SidC, which selectively decorates the pathogen vacuole, and a secondary antibody coupled to magnetic beads. This first step is followed by conventional Histodenz gradient density centrifugation, yielding intact LCVs in high purity and yield (Urwyler et al., 2010; Hoffmann et al., 2012, 2013) (**Figure 2G**). Using *D. discoideum* producing the LCV marker calnexin-GFP, infected with red fluorescent *L. pneumophila*, the LCV purification procedure can be easily followed by fluorescence microscopy.

Proteomics analysis of these purified LCVs revealed the presence of 560–1150 host proteins (Urwyler et al., 2009; Hoffmann et al., 2014; Schmölders et al., 2017). Amoebae proteins identified include small Rab GTPases, Rap1, Ran, and its effector Ran binding protein 1 (RanBP1). Moreover, large GTPases, components of the endosomal and late secretory trafficking pathways, as well as protein or lipid kinases and phosphatases were identified, many of which had not been implicated in LCV formation before. The accumulation of several of these host proteins on the LCV was confirmed by fluorescence microscopy using *D. discoideum* strains producing the corresponding GFP-fusion proteins (Urwyler et al., 2009; Finsel et al., 2013a; Rothmeier et al., 2013; Hoffmann et al., 2014; Schmölders et al., 2017; Steiner et al., 2017a). While some of these host factors accumulate on LCVs in an Icm/Dot-dependent manner (e.g., Rab1,−7,−8,−14, Rap1, Ran, RanBP1, Sey1), others localize to the pathogen vacuole Icm/Dot-independently (e.g., retromer subunits).

Preparations of intact LCVs can also be utilized for biochemical experiments (Steiner et al., 2017a). To this end, *D. discoideum* producing calnexin-GFP, GFP-Sey1, or catalytically inactive GFP-Sey1_K154A were infected with mCherry-producing virulent *L. pneumophila*. LCVs were purified according to the two-step protocol described above, and subsequently, the effect of GTP, GDP or the non-hydrolysable GTP analog Gpp(NH)p was analyzed by fluorescence microscopy. Interestingly, the purified LCVs aggregated and expanded their size about 2-fold in a Sey1- and GTP-dependent manner. This experiment revealed in a reductionist system the importance of Sey1 activity for LCV aggregation and circumferential ER remodeling.

SCREEN FOR ANTIVIRULENCE COMPOUNDS IN *LEGIONELLA*-INFECTED AMOEBAE

Antibiotic resistance of human pathogens is an ever-rising and global problem. The approach to develop new bactericidal or bacteriostatic antibiotics is compromised by a high selection pressure on pathogens to become resistant against these

compounds. A more efficient method is to target the virulence and the ability of bacteria to infect the host, rather than targeting directly the capacity to multiply. Such an "anti-virulence" strategy aims at specific mechanisms that promote bacterial pathogenicity, including metabolic pathways, binding to and uptake by host cells, signaling, and vesicle trafficking pathways, or the secretion and mode of action of toxins. There is the hope that anti-virulence compounds reduce the evolutionary pressure to develop drug resistance, and by selectively targeting virulent bacteria, spare the normal host microbiota.

Another major obstacle in developing novel antibiotic or anti-virulence compounds is the limited compound accessibility of intracellular bacteria, reflected in compromised bioavailability of a compound. To efficiently address these problems, and given the similarities between amoebae and human immune phagocytes such as macrophages or neutrophils (Hilbi et al., 2007; Escoll et al., 2013; Hoffmann et al., 2013), we established *A. castellanii* as a robust and high-throughput compatible model system to screen for anti-virulence compounds. To this end, the amoebae were seeded into 96-well plates and infected with GFP-producing *L. pneumophila*. The progress of intracellular growth correlates with an increase in fluorescence (Harrison et al., 2013, 2015b). The medium chosen minimizes auto-fluorescence and growth of the amoebae, as well as extracellular growth of the bacteria. Under these conditions, bacterial replication typically comprised a lag and a replicative phase, after which all amoebae were dead and bacterial fluorescence remained constant. Upon addition of low molecular weight compounds to infected amoebae, we identified palmostatin M—a β-lactone inhibitor of eukaryotic Ras depalmitoylases and Ras signaling (Hedberg et al., 2011; Rusch et al., 2011)—as an inhibitor of intracellular growth of *L. pneumophila* as well as of *Mycobacterium marinum* and *Mycobacterium tuberculosis* (Harrison et al., 2013; Kicka et al., 2014).

Moreover, using this *A. castellanii—L. pneumophila* infection assay, we screened a highly diverse, pathway-based chemical library, referred to as the Sinergia library (Harrison et al., 2015a). Structure-activity relationship (SAR) studies using variants of a hit compound thus identified revealed essential structural features, namely a triple-ring scaffold with a central triazine moiety, substituted by two piperidine or pyrrolidine rings in positions 3 and 5, and by an amine group bearing a single aliphatic chain moiety in position 1. The most effective compound, ZINC00615682, inhibited intracellular growth of *L. pneumophila* with an IC_{50} of ∼20 nM in *A. castellanii* and somewhat less efficiently in *D. discoideum* or macrophages (Harrison et al., 2015a). These results validate the amoebae-based screen and demonstrate that a corresponding SAR analysis allows the identification of novel inhibitors of intracellularly growing *L. pneumophila* and other bacteria.

CONCLUSIONS AND OUTLOOK

Intense research over the last years revealed that amoebae not only represent an important ecological niche of the environmental bacterium *L. pneumophila*, but are also versatile and powerful models for the molecular and cellular analysis of host-pathogen interactions. The natural host *A. castellanii* is permissive for *L. pneumophila* over a range of different temperatures, and this robust system is useful to assess bacterial mutant phenotypes, as well as to screen for anti-virulence compounds. The social amoeba *D. discoideum* is genetically tractable and allows analysis of host mutant strains. Dually labeled *D. discoideum* strains are ideally suited for (live-cell) fluorescence microscopy, imaging flow cytometry, cell migration assays, or LCV isolation. Purified intact LCVs can be further analyzed by proteomics and cell biological or biochemical tests. Obvious limitations of the amoebae models are the apparent lack of key components of cell-autonomous innate immunity pathways, such as caspase family proteases and the transcription factor NF-kB (Eichinger et al., 2005; Clarke et al., 2013). On the other hand, amoebae models are useful for the analysis of host-pathogen interactions beyond *Legionella* infection. Accordingly, *Acanthamoeba* spp. and *D. discoideum* can serve to assess various aspects of cellular virulence for a large number of pathogenic bacteria including *Mycobacterium* spp., *Burkholderia* spp., and *Vibrio cholerae* (Hilbi et al., 2007; Cosson and Soldati, 2008). Hence, amoebae and other protozoa will continue to provide valuable insights into important aspects of the ecology and virulence of amoeba-resistant environmental bacterial pathogens.

AUTHOR CONTRIBUTIONS

ALS, CFH, LE, MS, and HH wrote the manuscript.

ACKNOWLEDGMENTS

We would like to thank Stephen Weber for providing **Figure 2D**. Research in the laboratory of HH was supported by the Swiss National Science Foundation (SNF; 31003A_153200), the University of Zürich, the Novartis Foundation for Medical-Biological Research, the OPO foundation, and the German Ministry of Education and Research (BMBF) in the context of the EU Infect-ERA initiative (project EUGENPATH; 031A410A). LE acknowledges support of this work by the German Research Foundation (Deutsche Forschungsgemeinschaft, DFG: CRC670, TP01) and by Köln Fortune. Research in the laboratory of MS was supported by DFG STE 838/8-1. The funders had no role in study design, data collection and analysis, decision to publish, or preparation of the manuscript.

REFERENCES

Albers, U., Reus, K., Shuman, H. A., and Hilbi, H. (2005). The amoebae plate test implicates a paralogue of *lpxB* in the interaction of *Legionella pneumophila* with *Acanthamoeba castellanii*. *Microbiology* 151, 167–182. doi: 10.1099/mic.0.27563-0

Albers, U., Tiaden, A., Spirig, T., Al Alam, D., Goyert, S. M., Gangloff, S. C., et al. (2007). Expression of *Legionella pneumophila* paralogous lipid

A biosynthesis genes under different growth conditions. *Microbiology* 153, 3817–3829. doi: 10.1099/mic.0.2007/009829-0

Al-Quadan, T., and Kwaik, Y. A. (2011). Molecular characterization of exploitation of the polyubiquitination and farnesylation machineries of *Dictyostelium discoideum* by the AnkB F-Box effector of *Legionella pneumophila*. *Front. Microbiol.* 2:23. doi: 10.3389/fmicb.2011.00023

Amaro, F., Wang, W., Gilbert, J. A., Anderson, O. R., and Shuman, H. A. (2015). Diverse protist grazers select for virulence-related traits in *Legionella*. *ISME J.* 9, 1607–1618. doi: 10.1038/ismej.2014.248

Asrat, S., de Jesús, D. A., Hempstead, A. D., Ramabhadran, V., and Isberg, R. R. (2014). Bacterial pathogen manipulation of host membrane trafficking. *Annu. Rev. Cell Dev. Biol.* 30, 79–109. doi: 10.1146/annurev-cellbio-100913-013439

Aurass, P., Pless, B., Rydzewski, K., Holland, G., Bannert, N., and Flieger, A. (2009). *BdhA-patD* operon as a virulence determinant, revealed by a novel large-scale approach for identification of *Legionella pneumophila* mutants defective for amoeba infection. *Appl. Environ. Microbiol.* 75, 4506–4515. doi: 10.1128/AEM.00187-09

Avery, S. V., Harwood, J. L., and Lloyd, D. (1995). Quantification and characterization of phagocytosis in the soil amoeba *Acanthamoeba castellanii* by flow cytometry. *Appl. Environ. Microbiol.* 61, 1124–1132.

Barker, J., Scaife, H., and Brown, M. R. (1995). Intraphagocytic growth induces an antibiotic-resistant phenotype of *Legionella pneumophila*. *Antimicrob. Agents Chemother.* 39, 2684–2688. doi: 10.1128/AAC.39.12.2684

Bärlocher, K., Hutter, C. A. J., Swart, A. L., Steiner, B., Welin, A., Hohl, M., et al. (2017a). Structural insights into *Legionella* RidL-Vps29 retromer subunit interaction reveal displacement of the regulator TBC1D5. *Nat. Commun.* 8:1543. doi: 10.1038/s41467-017-01512-5

Bärlocher, K., Welin, A., and Hilbi, H. (2017b). Formation of the *Legionella* replicative compartment at the crossroads of retrograde trafficking. *Front. Cell. Infect. Microbiol.* 7:482. doi: 10.3389/fcimb.2017.00482.

Barteneva, N. S., Fasler-Kan, E., and Vorobjev, I. A. (2012). Imaging flow cytometry: coping with heterogeneity in biological systems. *J. Histochem. Cytochem.* 60, 723–733. doi: 10.1369/0022155412453052

Benin, A. L., Benson, R. F., and Besser, R. E. (2002). Trends in Legionnaires' disease, 1980-1998: declining mortality and new patterns of diagnosis. *Clin. Infect. Dis.* 35, 1039–1046. doi: 10.1086/342903

Bergmann, S., and Steinert, M. (2015). From single cells to engineered and explanted tissues: new perspectives in bacterial infection biology. *Int. Rev. Cell Mol. Biol.* 319, 1–44. doi: 10.1016/bs.ircmb.2015.06.003

Berk, S. G., and Garduño, R. A. (2013). The *Tetrahymena* and *Acanthamoeba* model systems. *Methods Mol. Biol.* 954, 393–416. doi: 10.1007/978-1-62703-161-5_25

Bowers, B., and Korn, E. D. (1973). Cytochemical identification of phosphatase activity in the contractile vacuole of *Acanthamoeba castellanii*. *J. Cell Biol.* 59, 784–791. doi: 10.1083/jcb.59.3.784

Bozzaro, S., Bucci, C., and Steinert, M. (2008). Phagocytosis and host-pathogen interactions in *Dictyostelium* with a look at macrophages. *Int. Rev. Cell Mol. Biol.* 271, 253–300. doi: 10.1016/S1937-6448(08)01206-9

Bozzaro, S., and Eichinger, L. (2011). The professional phagocyte *Dictyostelium discoideum* as a model host for bacterial pathogens. *Curr. Drug Targets* 12, 942–954. doi: 10.2174/138945011795677782

Bozzaro, S., Peracino, B., and Eichinger, L. (2013). *Dictyostelium* host response to *Legionella* infection: strategies and assays. *Methods Mol. Biol.* 954, 417–438. doi: 10.1007/978-1-62703-161-5_26

Brassinga, A. K., Kinchen, J. M., Cupp, M. E., Day, S. R., Hoffman, P. S., and Sifri, C. D. (2010). *Caenorhabditis* is a metazoan host for *Legionella*. *Cell. Microbiol.* 12, 343–361. doi: 10.1111/j.1462-5822.2009.01398.x

Bretschneider, T., Othmer, H. G., and Weijer, C. J. (2016). Progress and perspectives in signal transduction, actin dynamics, and movement at the cell and tissue level: lessons from *Dictyostelium*. *Interface Focus* 6:20160047. doi: 10.1098/rsfs.2016.0047

Brieland, J., McClain, M., LeGendre, M., and Engleberg, C. (1997). Intrapulmonary *Hartmannella vermiformis*: a potential niche for *Legionella pneumophila* replication in a murine model of legionellosis. *Infect. Immun.* 65, 4892–4896.

Brombacher, E., Urwyler, S., Ragaz, C., Weber, S. S., Kami, K., Overduin, M., et al. (2009). Rab1 guanine nucleotide exchange factor SidM is a major phosphatidylinositol 4-phosphate-binding effector protein of *Legionella pneumophila*. *J. Biol. Chem.* 284, 4846–4856. doi: 10.1074/jbc.M807505200

Brown, T. J., and Cursons, R. T. (1977). Pathogenic free-living amebae (PFLA) from frozen swimming areas in Oslo, Norway. *Scand. J. Infect. Dis.* 9, 237–240. doi: 10.3109/inf.1977.9.issue-3.16

Brown, T. J., Cursons, R. T., and Keys, E. A. (1982). Amoebae from antarctic soil and water. *Appl. Environ. Microbiol.* 44, 491–493.

Brüggemann, H., Hagman, A., Jules, M., Sismeiro, O., Dillies, M. A., Gouyette, C., et al. (2006). Virulence strategies for infecting phagocytes deduced from the *in vivo* transcriptional program of *Legionella pneumophila*. *Cell. Microbiol.* 8, 1228–1240. doi: 10.1111/j.1462-5822.2006.00703.x

Cazalet, C., Gomez-Valero, L., Rusniok, C., Lomma, M., Dervins-Ravault, D., Newton, H. J., et al. (2010). Analysis of the *Legionella longbeachae* genome and transcriptome uncovers unique strategies to cause Legionnaires' disease. *PLoS Genet.* 6:e1000851. doi: 10.1371/journal.pgen.1000851

Cazalet, C., Rusniok, C., Brüggemann, H., Zidane, N., Magnier, A., Ma, L., et al. (2004). Evidence in the *Legionella pneumophila* genome for exploitation of host cell functions and high genome plasticity. *Nat. Genet.* 36, 1165–1173. doi: 10.1038/ng1447

Chang, C. W., Kao, C. H., and Liu, Y. F. (2009). Heterogeneity in chlorine susceptibility for *Legionella pneumophila* released from *Acanthamoeba* and *Hartmannella*. *J. Appl. Microbiol.* 106, 97–105. doi: 10.1111/j.1365-2672.2008.03980.x

Chávez-Munguía, B., Omaña-Molina, M., González-Robles, M., Gonzalez-Robles, A., Bonilla, P., and Martínez-Palomo, A. (2005). Ultrastructural study of encystation and excystation in *Acanthamoeba castellanii*. *J. Eukaryot. Microbiol.* 52, 153–158. doi: 10.1111/j.1550-7408.2005.04-3273.x

Chen, P., Ostrow, B. D., Tafuri, S. R., and Chisholm, R. L. (1994). Targeted disruption of the *Dictyostelium* RMLC gene produces cells defective in cytokinesis and development. *J. Cell Biol.* 127, 1933–1944. doi: 10.1083/jcb.127.6.1933

Chien, M., Morozova, I., Shi, S., Sheng, H., Chen, J., Gomez, S. M., et al. (2004). The genomic sequence of the accidental pathogen *Legionella pneumophila*. *Science* 305, 1966–1968. doi: 10.1126/science.1099776

Choy, A., Dancourt, J., Mugo, B., O'connor, T. J., Isberg, R. R., Melia, T. J., et al. (2012). The *Legionella* effector RavZ inhibits host autophagy through irreversible Atg8 deconjugation. *Science* 338, 1072–1076. doi: 10.1126/science.1227026

Cirillo, J. D., Falkow, S., and Tompkins, L. S. (1994). Growth of *Legionella pneumophila* in *Acanthamoeba castellanii* enhances invasion. *Infect. Immun.* 62, 3254–3261.

Clarke, M., Lohan, A. J., Liu, B., Lagkouvardos, I., Roy, S., Zafar, N., et al. (2013). Genome of *Acanthamoeba castellanii* highlights extensive lateral gene transfer and early evolution of tyrosine kinase signaling. *Genome Biol.* 14:R11. doi: 10.1186/gb-2013-14-2-r11

Clarke, P. R., and Zhang, C. (2008). Spatial and temporal coordination of mitosis by Ran GTPase. *Nat. Rev. Mol. Cell Biol.* 9, 464–477. doi: 10.1038/nrm2410

Coil, D. A., Anné, J., and Lammertyn, E. (2008). A faster and more accurate assay for intracellular replication of *Legionella pneumophila* in amoebae hosts. *J. Microbiol. Methods* 72, 214–216. doi: 10.1016/j.mimet.2007.11.009

Correia, A. M., Ferreira, J. S., Borges, V., Nunes, A., Gomes, B., Capucho, R., et al. (2016). Probable person-to-person transmission of Legionnaires' disease. *N. Engl. J. Med.* 374, 497–498. doi: 10.1056/NEJMc1505356

Cosson, P., and Soldati, T. (2008). Eat, kill or die: when amoeba meets bacteria. *Curr. Opin. Microbiol.* 11, 271–276. doi: 10.1016/j.mib.2008.05.005

Di Paolo, G., and De Camilli, P. (2006). Phosphoinositides in cell regulation and membrane dynamics. *Nature* 443, 651–657. doi: 10.1038/nature05185

Dolinsky, S., Haneburger, I., Cichy, A., Hannemann, M., Itzen, A., and Hilbi, H. (2014). The *Legionella longbeachae* Icm/Dot substrate SidC selectively binds phosphatidylinositol 4-phosphate with nanomolar affinity and promotes pathogen vacuole-endoplasmic reticulum interactions. *Infect. Immun.* 82, 4021–4033. doi: 10.1128/IAI.01685-14

Eichinger, L., Pachebat, J. A., Glöckner, G., Rajandream, M. A., Sucgang, R., Berriman, M., et al. (2005). The genome of the social amoeba *Dictyostelium discoideum*. *Nature* 435, 43–57. doi: 10.1038/nature03481

Eichinger, L., and Rivero, F. (2006). *Methods in Molecular Biology - Dictyostelium discoideum protocols*. Totowa, NJ: Humana Press.

Eisenreich, W., and Heuner, K. (2016). The life stage-specific pathometabolism of *Legionella pneumophila*. *FEBS Lett.* 590, 3868–3886. doi: 10.1002/1873-3468.12326

Escoll, P., Rolando, M., Gomez-Valero, L., and Buchrieser, C. (2013). From amoeba to macrophages: exploring the molecular mechanisms of *Legionella pneumophila* infection in both hosts. *Curr. Top. Microbiol. Immunol.* 376, 1–34. doi: 10.1007/82_2013_351

Etienne-Manneville, S. (2013). Microtubules in cell migration. *Annu. Rev. Cell Dev. Biol.* 29, 471–499. doi: 10.1146/annurev-cellbio-101011-155711

Faix, J., Kreppel, L., Shaulsky, G., Schleicher, M., and Kimmel, A. R. (2004). A rapid and efficient method to generate multiple gene disruptions in *Dictyostelium discoideum* using a single selectable marker and the Cre-*loxP* system. *Nucleic Acids Res.* 32:e143. doi: 10.1093/nar/gnh136

Fajardo, M., Schleicher, M., Noegel, A., Bozzaro, S., Killinger, S., Heuner, K., et al. (2004). Calnexin, calreticulin and cytoskeleton-associated proteins modulate uptake and growth of *Legionella pneumophila* in *Dictyostelium discoideum*. *Microbiology* 150, 2825–2835. doi: 10.1099/mic.0.27111-0

Farbrother, P., Wagner, C., Na, J., Tunggal, B., Morio, T., Urushihara, H., et al. (2006). *Dictyostelium* transcriptional host cell response upon infection with *Legionella*. *Cell. Microbiol.* 8, 438–456. doi: 10.1111/j.1462-5822.2005.00633.x

Fey, P., Dodson, R. J., Basu, S., and Chisholm, R. L. (2013). One stop shop for everything *Dictyostelium*: dictyBase and the Dicty Stock Center in 2012. *Methods Mol. Biol.* 983, 59–92. doi: 10.1007/978-1-62703-302-2_4

Fields, B. S. (1996). The molecular ecology of legionellae. *Trends Microbiol.* 4, 286–290. doi: 10.1016/0966-842X(96)10041-X

Finsel, I., and Hilbi, H. (2015). Formation of a pathogen vacuole according to *Legionella pneumophila*: how to kill one bird with many stones. *Cell. Microbiol.* 17, 935–950. doi: 10.1111/cmi.12450

Finsel, I., Hoffmann, C., and Hilbi, H. (2013a). Immunomagnetic purification of fluorescent *Legionella*-containing vacuoles. *Methods Mol. Biol.* 983, 431–443. doi: 10.1007/978-1-62703-302-2_24

Finsel, I., Ragaz, C., Hoffmann, C., Harrison, C. F., Weber, S., Van Rahden, V. A., et al. (2013b). The *Legionella* effector RidL inhibits retrograde trafficking to promote intracellular replication. *Cell Host Microbe* 14, 38–50. doi: 10.1016/j.chom.2013.06.001

Gaudet, P., Fey, P., Basu, S., Bushmanova, Y. A., Dodson, R., Sheppard, K. A., et al. (2011). DictyBase update 2011: web 2.0 functionality and the initial steps towards a genome portal for the Amoebozoa. *Nucleic Acids Res.* 39, D620–D624. doi: 10.1093/nar/gkq1103

Goodman, B., and Zheng, Y. (2006). Mitotic spindle morphogenesis: Ran on the microtubule cytoskeleton and beyond. *Biochem. Soc. Trans.* 34, 716–721. doi: 10.1042/BST0340716

Greub, G., and Raoult, D. (2004). Microorganisms resistant to free-living amoebae. *Clin. Microbiol. Rev.* 17, 413–433. doi: 10.1128/CMR.17.2.413-433.2004

Hägele, S., Köhler, R., Merkert, H., Schleicher, M., Hacker, J., and Steinert, M. (2000). *Dictyostelium discoideum*: a new host model system for intracellular pathogens of the genus *Legionella*. *Cell. Microbiol.* 2, 165–171. doi: 10.1046/j.1462-5822.2000.00044.x

Hall-Stoodley, L., Costerton, J. W., and Stoodley, P. (2004). Bacterial biofilms: from the natural environment to infectious diseases. *Nat. Rev. Microbiol.* 2, 95–108. doi: 10.1038/nrmicro821

Haneburger, I., and Hilbi, H. (2013). Phosphoinositide lipids and the *Legionella* pathogen vacuole. *Curr. Top. Microbiol. Immunol.* 376, 155–173. doi: 10.1007/82_2013_341

Harf, C., Goffinet, S., Meunier, O., Monteil, H., and Colin, D. A. (1997). Flow cytometric determination of endocytosis of viable labelled *Legionella pneumophila* by *Acanthamoeba palestinensis*. *Cytometry* 27, 269–274. doi: 10.1002/(SICI)1097-0320(19970301)27:3<269::AID-CYTO9>3.0.CO;2-9

Harrison, C. F., Chiriano, G., Finsel, I., Manske, C., Hoffmann, C., Steiner, B., et al. (2015a). Amoebae-based screening reveals a novel family of compounds restricting intracellular *Legionella pneumophila*. *ACS Inf. Dis.* 1, 327–338. doi: 10.1021/acsinfecdis.5b00002

Harrison, C. F., Kicka, S., Kranjc, A., Finsel, I., Chiriano, G., Ouertatani-Sakouhi, H., et al. (2015b). Adrenergic antagonists restrict replication of *Legionella*. *Microbiology* 161, 1392–1406. doi: 10.1099/mic.0.000094

Harrison, C. F., Kicka, S., Trofimov, V., Berschl, K., Ouertatani-Sakouhi, H., Ackermann, N., et al. (2013). Exploring anti-bacterial compounds against intracellular *Legionella*. *PLoS ONE* 8:e74813. doi: 10.1371/journal.pone.0074813

Hausmann, C. D., and Ibba, M. (2008). Aminoacyl-tRNA synthetase complexes: molecular multitasking revealed. *FEMS Microbiol. Rev.* 32, 705–721. doi: 10.1111/j.1574-6976.2008.00119.x

Hedberg, C., Dekker, F. J., Rusch, M., Renner, S., Wetzel, S., Vartak, N., et al. (2011). Development of highly potent inhibitors of the Ras-targeting human acyl protein thioesterases based on substrate similarity design. *Angew. Chem. Int. Ed Engl.* 50, 9832–9837. doi: 10.1002/anie.201102965

Hilbi, H., and Haas, A. (2012). Secretive bacterial pathogens and the secretory pathway. *Traffic* 13, 1187–1197. doi: 10.1111/j.1600-0854.2012.01344.x

Hilbi, H., Hoffmann, C., and Harrison, C. F. (2011). *Legionella* spp. outdoors: colonization, communication and persistence. *Environ. Microbiol. Rep.* 3, 286–296. doi: 10.1111/j.1758-2229.2011.00247.x

Hilbi, H., Weber, S. S., Ragaz, C., Nyfeler, Y., and Urwyler, S. (2007). Environmental predators as models for bacterial pathogenesis. *Environ. Microbiol.* 9, 563–575. doi: 10.1111/j.1462-2920.2007.01238.x

Hochstrasser, R., and Hilbi, H. (2017). Intra-species and inter-kingdom signaling of *Legionella pneumophila*. *Front. Microbiol.* 8:79. doi: 10.3389/fmicb.2017.00079

Hoffmann, C., Finsel, I., and Hilbi, H. (2012). Purification of pathogen vacuoles from *Legionella*-infected phagocytes. *J. Vis. Exp.* e4118. doi: 10.3791/4118

Hoffmann, C., Finsel, I., and Hilbi, H. (2013). Pathogen vacuole purification from *Legionella*-infected amoeba and macrophages. *Methods Mol. Biol.* 954, 309–321. doi: 10.1007/978-1-62703-161-5_18

Hoffmann, C., Finsel, I., Otto, A., Pfaffinger, G., Rothmeier, E., Hecker, M., et al. (2014). Functional analysis of novel Rab GTPases identified in the proteome of purified *Legionella*-containing vacuoles from macrophages. *Cell. Microbiol.* 16, 1034–1052. doi: 10.1111/cmi.12256

Hsu, T. K., Wu, S. F., Hsu, B. M., Kao, P. M., Tao, C. W., Shen, S. M., et al. (2015). Surveillance of parasitic *Legionella* in surface waters by using immunomagnetic separation and amoebae enrichment. *Pathog. Glob. Health* 109, 328–335. doi: 10.1179/2047773215Y.0000000034

Hubber, A., and Roy, C. R. (2010). Modulation of host cell function by *Legionella pneumophila* type IV effectors. *Annu. Rev. Cell Dev. Biol.* 26, 261–283. doi: 10.1146/annurev-cellbio-100109-104034

Isberg, R. R., O'connor, T. J., and Heidtman, M. (2009). The *Legionella pneumophila* replication vacuole: making a cosy niche inside host cells. *Nat. Rev. Microbiol.* 7, 13–24. doi: 10.1038/nrmicro1967

Jäger, J., Marwitz, S., Tiefenau, J., Rasch, J., Shevchuk, O., Kugler, C., et al. (2014). Human lung tissue explants reveal novel interactions during *Legionella pneumophila* infections. *Infect. Immun.* 82, 275–285. doi: 10.1128/IAI.00703-13

Johansson, J., Karlsson, A., Bylund, J., and Welin, A. (2015). Phagocyte interactions with *Mycobacterium tuberculosis*–Simultaneous analysis of phagocytosis, phagosome maturation and intracellular replication by imaging flow cytometry. *J. Immunol. Methods* 427, 73–84. doi: 10.1016/j.jim.2015.10.003

John, D. T., and Howard, M. J. (1995). Seasonal distribution of pathogenic free-living amebae in Oklahoma waters. *Parasitol. Res.* 81, 193–201.

Kessin, R. H., Gundersen, G. G., Zaydfudim, V., and Grimson, M. (1996). How cellular slime molds evade nematodes. *Proc. Natl. Acad. Sci. U.S.A.* 93, 4857–4861. doi: 10.1073/pnas.93.10.4857

Kessler, A., Schell, U., Sahr, T., Tiaden, A., Harrison, C., Buchrieser, C., et al. (2013). The *Legionella pneumophila* orphan sensor kinase LqsT regulates competence and pathogen-host interactions as a component of the LAI-1 circuit. *Environ. Microbiol.* 15, 646–662. doi: 10.1111/j.1462-2920.2012.02889.x

Kicka, S., Trofimov, V., Harrison, C., Ouertatani-Sakouhi, H., McKinney, J., Scapozza, L., et al. (2014). Establishment and validation of whole-cell based fluorescence assays to identify anti-mycobacterial compounds using the *Acanthamoeba castellanii-Mycobacterium marinum* host-pathogen system. *PLoS ONE* 9:e87834. doi: 10.1371/journal.pone.0087834

Komura, T., Yasui, C., Miyamoto, H., and Nishikawa, Y. (2010). *Caenorhabditis elegans* as an alternative model host for *Legionella pneumophila*, and protective effects of *Bifidobacterium infantis*. *Appl. Environ. Microbiol.* 76, 4105–4108. doi: 10.1128/AEM.03021-09

Kuhlmann, M., Popova, B., and Nellen, W. (2006). RNA interference and antisense-mediated gene silencing in *Dictyostelium*. *Methods Mol. Biol.* 346, 211–226. doi: 10.1385/1-59745-144-4:211

Kuspa, A., and Loomis, W. F. (1992). Tagging developmental genes in *Dictyostelium* by restriction enzyme-mediated integration of plasmid DNA. *Proc. Natl. Acad. Sci. U.S.A.* 89, 8803–8807. doi: 10.1073/pnas.89.18.8803

Levi, S., Polyakov, M., and Egelhoff, T. T. (2000). Green fluorescent protein and epitope tag fusion vectors for *Dictyostelium discoideum*. *Plasmid* 44, 231–238. doi: 10.1006/plas.2000.1487

Li, Z., Dugan, A. S., Bloomfield, G., Skelton, J., Ivens, A., Losick, V., et al. (2009). The amoebal MAP kinase response to *Legionella pneumophila* is regulated by DupA. *Cell Host Microbe* 6, 253–267. doi: 10.1016/j.chom.2009.08.005

Lorenzo-Morales, J., Ortega-Rivas, A., Foronda, P., Abreu-Acosta, N., Ballart, D., Martinez, E., et al. (2005). RNA interference (RNAi) for the silencing of extracellular serine proteases genes in *Acanthamoeba*: molecular analysis and effect on pathogenicity. *Mol. Biochem. Parasitol.* 144, 10–15. doi: 10.1016/j.molbiopara.2005.07.001

Lurie-Weinberger, M. N., Gomez-Valero, L., Merault, N., Glöckner, G., Buchrieser, C., and Gophna, U. (2010). The origins of eukaryotic-like proteins in *Legionella pneumophila*. *Int. J. Med. Microbiol.* 300, 470–481. doi: 10.1016/j.ijmm.2010.04.016

Manstein, D. J., Schuster, H. P., Morandini, P., and Hunt, D. M. (1995). Cloning vectors for the production of proteins in *Dictyostelium discoideum*. *Gene* 162, 129–134. doi: 10.1016/0378-1119(95)00351-6

Miyamoto, H., Yoshida, S., Taniguchi, H., and Shuman, H. A. (2003). Virulence conversion of *Legionella pneumophila* by conjugal transfer of chromosomal DNA. *J. Bacteriol.* 185, 6712–6718. doi: 10.1128/JB.185.22.6712-6718.2003

Moffat, J. F., and Tompkins, L. S. (1992). A quantitative model of intracellular growth of *Legionella pneumophila* in *Acanthamoeba castellanii*. *Infect. Immun.* 60, 296–301.

Molmeret, M., Horn, M., Wagner, M., Santic, M., and Abu Kwaik, Y. (2005). Amoebae as training grounds for intracellular bacterial pathogens. *Appl. Environ. Microbiol.* 71, 20–28. doi: 10.1128/AEM.71.1.20-28.2005

Müller-Taubenberger, A., Kortholt, A., and Eichinger, L. (2013). Simple system–substantial share: the use of *Dictyostelium* in cell biology and molecular medicine. *Eur. J. Cell Biol.* 92, 45–53. doi: 10.1016/j.ejcb.2012.10.003

. Newton, H. J., Ang, D. K., Van Driel, I. R., and Hartland, E. L. (2010). Molecular pathogenesis of infections caused by *Legionella pneumophila*. *Clin. Microbiol. Rev.* 23, 274–298. doi: 10.1128/CMR.00052-09

Noda, T. (2017). Autophagy in the context of the cellular membrane-trafficking system: the enigma of Atg9 vesicles. *Biochem. Soc. Trans.* 45, 1323–1331. doi: 10.1042/BST20170128

O'Connor, T. J., Adepoju, Y., Boyd, D., and Isberg, R. R. (2011). Minimization of the *Legionella pneumophila* genome reveals chromosomal regions involved in host range expansion. *Proc. Natl. Acad. Sci. U.S.A.* 108, 14733–14740. doi: 10.1073/pnas.1111678108

Otto, G. P., Wu, M. Y., Clarke, M., Lu, H., Anderson, O. R., Hilbi, H., et al. (2004). Macroautophagy is dispensable for intracellular replication of *Legionella pneumophila* in *Dictyostelium discoideum*. *Mol. Microbiol.* 51, 63–72. doi: 10.1046/j.1365-2958.2003.03826.x

Peng, Z., Omaruddin, R., and Bateman, E. (2005). Stable transfection of *Acanthamoeba castellanii*. *Biochim. Biophys. Acta* 1743, 93–100. doi: 10.1016/j.bbamcr.2004.08.014

Peracino, B., Balest, A., and Bozzaro, S. (2010). Phosphoinositides differentially regulate bacterial uptake and Nramp1-induced resistance to *Legionella* infection in *Dictyostelium*. *J. Cell Sci.* 123, 4039–4051. doi: 10.1242/jcs.072124

Personnic, N., Bärlocher, K., Finsel, I., and Hilbi, H. (2016). Subversion of retrograde trafficking by translocated pathogen effectors. *Trends Microbiol.* 24, 450–462. doi: 10.1016/j.tim.2016.02.003

Personnic, N., Striednig, B., and Hilbi, H. (2017). *Legionella* quorum sensing and its role in pathogen-host interactions. *Curr. Opin. Microbiol.* 41, 29–35. doi: 10.1016/j.mib.2017.11.010

Pollard, T. D., Shelton, E., Weihing, R. R., and Korn, E. D. (1970). Ultrastructural characterization of F-actin isolated from *Acanthamoeba castellanii* and identification of cytoplasmic filaments as F-actin by reaction with rabbit heavy meromyosin. *J. Mol. Biol.* 50, 91–97. doi: 10.1016/0022-2836(70)90106-3

Preston, T. M., and King, C. A. (1984). Amoeboid locomotion of *Acanthamoeba castellanii* with special reference to cell-substratum interactions. *J. Gen. Microbiol.* 130, 2317–2323. doi: 10.1099/00221287-130-9-2317

Qiu, J., and Luo, Z. Q. (2017). *Legionella* and *Coxiella* effectors: strength in diversity and activity. *Nat. Rev. Microbiol.* 15, 591–605. doi: 10.1038/nrmicro.2017.67

Ragaz, C., Pietsch, H., Urwyler, S., Tiaden, A., Weber, S. S., and Hilbi, H. (2008). The *Legionella pneumophila* phosphatidylinositol-4 phosphate-binding type IV substrate SidC recruits endoplasmic reticulum vesicles to a replication-permissive vacuole. *Cell. Microbiol.* 10, 2416–2433. doi: 10.1111/j.1462-5822.2008.01219.x

Rasch, J., Krüger, S., Fontvieille, D., Ünal, C. M., Michel, R., Labrosse, A., et al. (2016). *Legionella*-protozoa-nematode interactions in aquatic biofilms and influence of Mip on *Caenorhabditis elegans* colonization. *Int. J. Med. Microbiol.* 306, 443–451. doi: 10.1016/j.ijmm.2016.05.012

Riyahi, T. Y., Frese, F., Steinert, M., Omosigho, N. N., Glöckner, G., Eichinger, L., et al. (2011). RpkA, a highly conserved GPCR with a lipid kinase domain, has a role in phagocytosis and anti-bacterial defense. *PLoS ONE* 6:e27311. doi: 10.1371/journal.pone.0027311

Rodriguez-Zaragoza, S., Rivera, F., Bonilla, P., Ramirez, E., Gallegos, E., Calderon, A., et al. (1993). Amoebological study of the atmosphere of San Luis Potosi, SLP, Mexico. *J. Exp. Anal. Environ. Epidemiol.* 3(Suppl. 1.), 229–241.

Rolando, M., Escoll, P., Nora, T., Botti, J., Boitez, V., Bedia, C., et al. (2016). *Legionella pneumophila* S1P-lyase targets host sphingolipid metabolism and restrains autophagy. *Proc. Natl. Acad. Sci. U.S.A.* 113, 1901–1906. doi: 10.1073/pnas.1522067113

Romby, P., Vandenesch, F., and Wagner, E. G. (2006). The role of RNAs in the regulation of virulence-gene expression. *Curr. Opin. Microbiol.* 9, 229–236. doi: 10.1016/j.mib.2006.02.005

Rothmeier, E., Pfaffinger, G., Hoffmann, C., Harrison, C. F., Grabmayr, H., Repnik, U., et al. (2013). Activation of Ran GTPase by a *Legionella* effector promotes microtubule polymerization, pathogen vacuole motility and infection. *PLoS Pathog.* 9:e1003598. doi: 10.1371/journal.ppat.1003598

Rowbotham, T. J. (1986). Current views on the relationships between amoebae, legionellae and man. *Isr. J. Med. Sci.* 22, 678–689.

Rusch, M., Zimmermann, T. J., Bürger, M., Dekker, F. J., Görmer, K., Triola, G., et al. (2011). Identification of acyl protein thioesterases 1 and 2 as the cellular targets of the Ras-signaling modulators palmostatin B and M. *Angew. Chem. Int. Ed Engl.* 50, 9838–9842. doi: 10.1002/anie.201102967

Sakamoto, R., Ohno, A., Nakahara, T., Satomura, K., Iwanaga, S., Kouyama, Y., et al. (2009). *Legionella pneumophila* in rainwater on roads. *Emerging Infect. Dis.* 15, 1295–1297. doi: 10.3201/eid1508.090317

Sanden, G. N., Morrill, W. E., Fields, B. S., Breiman, R. F., and Barbaree, J. M. (1992). Incubation of water samples containing amoebae improves detection of legionellae by the culture method. *Appl. Environ. Microbiol.* 58, 2001–2004.

Sawyer, T. K. (1989). Free-living pathogenic and nonpathogenic amoebae in Maryland soils. *Appl. Environ. Microbiol.* 55, 1074–1077.

Schilde, C., Lawal, H. M., Noegel, A. A., Eichinger, L., Schaap, P., and Glöckner, G. (2016). A set of genes conserved in sequence and expression traces back the establishment of multicellularity in social amoebae. *BMC Genomics* 17:871. doi: 10.1186/s12864-016-3223-z

Schlimme, W., M., Marchiani, M., Hanselmann, K., and Jenni, B. (1997). Gene transfer between bacteria within digestive vacuoles of protozoa. *FEMS Microbiol. Ecol.* 23, 239–247. doi: 10.1111/j.1574-6941.1997.tb00406.x

Schmölders, J., Manske, C., Otto, A., Hoffmann, C., Steiner, B., Welin, A., et al. (2017). Comparative proteomics of purified pathogen vacuoles correlates intracellular replication of *Legionella pneumophila* with the small GTPase Ras-related protein 1 (Rap1). *Mol. Cell. Proteomics* 16, 622–641. doi: 10.1074/mcp.M116.063453

Schuster, F. L., and Levandowsky, M. (1996). Chemosensory responses of *Acanthamoeba castellanii*: visual analysis of random movement and responses to chemical signals. *J. Eukaryot. Microbiol.* 43, 150–158. doi: 10.1111/j.1550-7408.1996.tb04496.x

Segal, G., Purcell, M., and Shuman, H. A. (1998). Host cell killing and bacterial conjugation require overlapping sets of genes within a 22-kb region of the *Legionella pneumophila* genome. *Proc. Natl. Acad. Sci. U.S.A.* 95, 1669–1674. doi: 10.1073/pnas.95.4.1669

Segal, G., and Shuman, H. A. (1999). *Legionella pneumophila* utilizes the same genes to multiply within *Acanthamoeba castellanii* and human macrophages. *Infect. Immun.* 67, 2117–2124.

Sherwood, R. K., and Roy, C. R. (2013). A Rab-centric perspective of bacterial pathogen-occupied vacuoles. *Cell Host Microbe* 14, 256–268. doi: 10.1016/j.chom.2013.08.010

Sherwood, R. K., and Roy, C. R. (2016). Autophagy evasion and endoplasmic reticulum subversion: the yin and yang of *Legionella* intracellular infection. *Annu. Rev. Microbiol.* 70, 413–433. doi: 10.1146/annurev-micro-102215-095557

Shevchuk, O., Pägelow, D., Rasch, J., Döhrmann, S., Günther, G., Hoppe, J., et al. (2014). Polyketide synthase (PKS) reduces fusion of *Legionella pneumophila*-containing vacuoles with lysosomes and contributes to bacterial competitiveness during infection. *Int. J. Med. Microbiol.* 304, 1169–1181. doi: 10.1016/j.ijmm.2014.08.010

Shina, M. C., Müller-Taubenberger, A., Unal, C., Schleicher, M., Steinert, M., Eichinger, L., et al. (2011). Redundant and unique roles of coronin proteins in *Dictyostelium*. *Cell. Mol. Life Sci.* 68, 303–313. doi: 10.1007/s00018-010-0455-y

Shina, M. C., and Noegel, A. A. (2008). Invertebrate coronins. *Subcell. Biochem.* 48, 88–97. doi: 10.1007/978-0-387-09595-0_8

Shina, M. C., Unal, C., Eichinger, L., Müller-Taubenberger, A., Schleicher, M., Steinert, M., et al. (2010). A coronin7 homolog with functions in actin-driven processes. *J. Biol. Chem.* 285, 9249–9261. doi: 10.1074/jbc.M109.083725

Simon, S., Schell, U., Heuer, N., Hager, D., Albers, M. F., Matthias, J., et al. (2015). Inter-kingdom signaling by the *Legionella* quorum sensing molecule LAI-1 modulates cell migration through an IQGAP1-Cdc42-ARHGEF9-dependent pathway. *PLoS Pathog.* 11:e1005307. doi: 10.1371/journal.ppat.1005307

Simon, S., Wagner, M. A., Rothmeier, E., Müller-Taubenberger, A., and Hilbi, H. (2014). Icm/Dot-dependent inhibition of phagocyte migration by *Legionella* is antagonized by a translocated Ran GTPase activator. *Cell. Microbiol.* 16, 977–992. doi: 10.1111/cmi.12258.

Solomon, J. M., Rupper, A., Cardelli, J. A., and Isberg, R. R. (2000). Intracellular growth of *Legionella pneumophila* in *Dictyostelium discoideum*, a system for genetic analysis of host-pathogen interactions. *Infect. Immun.* 68, 2939–2947. doi: 10.1128/IAI.68.5.2939-2947.2000

Steiner, B., Swart, A. L., Welin, A., Weber, S., Personnic, N., Kaech, A., et al. (2017a). ER remodeling by the large GTPase atlastin promotes vacuolar growth of *Legionella pneumophila*. *EMBO Rep.* 18, 1817–1836. doi: 10.15252/embr.201743903

Steiner, B., Weber, S., and Hilbi, H. (2017b). Formation of the *Legionella*-containing vacuole: phosphoinositide conversion, GTPase modulation and ER dynamics. *Int. J. Med. Microbiol.* 308, 49–57. doi: 10.1016/j.ijmm.2017.08.004

Steinert, M. (2011). Pathogen-host interactions in *Dictyostelium*, *Legionella*, *Mycobacterium* and other pathogens. *Semin. Cell Dev. Biol.* 22, 70–76. doi: 10.1016/j.semcdb.2010.11.003

Steinert, M., and Heuner, K. (2005). *Dictyostelium* as host model for pathogenesis. *Cell. Microbiol.* 7, 307–314. doi: 10.1111/j.1462-5822.2005.00493.x

Stewart, M. (2007). Molecular mechanism of the nuclear protein import cycle. *Nat. Rev. Mol. Cell Biol.* 8, 195–208. doi: 10.1038/nrm2114

Swaminathan, K., Stumpf, M., Müller, R., Horn, A. C., Schmidbauer, J., Eichinger, L., et al. (2015). Coronin7 regulates WASP and SCAR through CRIB mediated interaction with Rac proteins. *Sci. Rep.* 5:14437. doi: 10.1038/srep14437

Taguri, T., Oda, Y., Sugiyama, K., Nishikawa, T., Endo, T., Izumiyama, S., et al. (2011). A rapid detection method using flow cytometry to monitor the risk of *Legionella* in bath water. *J. Microbiol. Methods* 86, 25–32. doi: 10.1016/j.mimet.2011.03.012

Taylor, M., Ross, K., and Bentham, R. (2009). *Legionella*, protozoa, and biofilms: interactions within complex microbial systems. *Microb. Ecol.* 58, 538–547. doi: 10.1007/s00248-009-9514-z

Tiaden, A. N., Kessler, A., and Hilbi, H. (2013). Analysis of *Legionella* infection by flow cytometry. *Methods Mol. Biol.* 954, 233–249. doi: 10.1007/978-1-62703-161-5_14

Tiaden, A., Spirig, T., Carranza, P., Brüggemann, H., Riedel, K., Eberl, L., et al. (2008). Synergistic contribution of the *Legionella pneumophila lqs* genes to pathogen-host interactions. *J. Bacteriol.* 190, 7532–7547. doi: 10.1128/JB.01002-08

Tiaden, A., Spirig, T., Sahr, T., Wälti, M. A., Boucke, K., Buchrieser, C., et al. (2010). The autoinducer synthase LqsA and putative sensor kinase LqsS regulate phagocyte interactions, extracellular filaments and a genomic island of *Legionella pneumophila*. *Environ. Microbiol.* 12, 1243–1259. doi: 10.1111/j.1462-2920.2010.02167.x

Tiaden, A., Spirig, T., Weber, S. S., Brüggemann, H., Bosshard, R., Buchrieser, C., et al. (2007). The *Legionella pneumophila* response regulator LqsR promotes host cell interactions as an element of the virulence regulatory network controlled by RpoS and LetA. *Cell. Microbiol.* 9, 2903–2920. doi: 10.1111/j.1462-5822.2007.01005.x

Tung, S. M., Unal, C., Ley, A., Peña, C., Tunggal, B., Noegel, A. A., et al. (2010). Loss of *Dictyostelium* Atg9 results in a pleiotropic phenotype affecting growth, development, phagocytosis and clearance and replication of *Legionella pneumophila*. *Cell. Microbiol.* 12, 765–780. doi: 10.1111/j.1462-5822.2010.01432.x

Ulsamer, A. G., Wright, P. L., Wetzel, M. G., and Korn, E. D. (1971). Plasma and phagosome membranes of *Acanthamoeba castellanii*. *J. Cell Biol.* 51, 193–215. doi: 10.1083/jcb.51.1.193

Urwyler, S., Finsel, I., Ragaz, C., and Hilbi, H. (2010). Isolation of *Legionella*-containing vacuoles by immuno-magnetic separation. *Curr. Protoc. Cell Biol. Chapter 3, Unit* 3 34. doi: 10.1002/0471143030.cb0334s46

Urwyler, S., Nyfeler, Y., Ragaz, C., Lee, H., Mueller, L. N., Aebersold, R., et al. (2009). Proteome analysis of *Legionella* vacuoles purified by magnetic immunoseparation reveals secretory and endosomal GTPases. *Traffic* 10, 76–87. doi: 10.1111/j.1600-0854.2008.00851.x

Veltman, D. M. (2015). Drink or drive: competition between macropinocytosis and cell migration. *Biochem. Soc. Trans.* 43, 129–132. doi: 10.1042/BST20140251

Veltman, D. M., and van Haastert, P. J. (2013). Extrachromosomal inducible expression. *Methods Mol. Biol.* 983, 269–281. doi: 10.1007/978-1-62703-302-2_14

Vogel, J. P., Andrews, H. L., Wong, S. K., and Isberg, R. R. (1998). Conjugative transfer by the virulence system of *Legionella pneumophila*. *Science* 279, 873–876. doi: 10.1126/science.279.5352.873

Weber, S., and Hilbi, H. (2014). Live-cell imaging of phosphoinositide dynamics during *Legionella* infection. *Methods Mol. Biol.* 1197, 153–167. doi: 10.1007/978-1-4939-1261-2_9

Weber, S. S., Ragaz, C., and Hilbi, H. (2009a). The inositol polyphosphate 5-phosphatase OCRL1 restricts intracellular growth of *Legionella*, localizes to the replicative vacuole and binds to the bacterial effector LpnE. *Cell. Microbiol.* 11, 442–460. doi: 10.1111/j.1462-5822.2008.01266.x

Weber, S. S., Ragaz, C., and Hilbi, H. (2009b). Pathogen trafficking pathways and host phosphoinositide metabolism. *Mol. Microbiol.* 71, 1341–1352. doi: 10.1111/j.1365-2958.2009.06608.x

Weber, S. S., Ragaz, C., Reus, K., Nyfeler, Y., and Hilbi, H. (2006). *Legionella pneumophila* exploits PI(4)P to anchor secreted effector proteins to the replicative vacuole. *PLoS Pathog.* 2:e46. doi: 10.1371/journal.ppat.0020046

Weber, S., Stirnimann, C. U., Wieser, M., Frey, D., Meier, R., Engelhardt, S., et al. (2014a). A type IV-translocated *Legionella* cysteine phytase counteracts intracellular growth restriction by phytate. *J. Biol. Chem.* 289, 34175–34188. doi: 10.1074/jbc.M114.592568

Weber, S., Wagner, M., and Hilbi, H. (2014b). Live-cell imaging of phosphoinositide dynamics and membrane architecture during *Legionella* infection. *MBio* 5, e00839–e00813. doi: 10.1128/mBio.00839-13

Weissenmayer, B. A., Prendergast, J. G., Lohan, A. J., and Loftus, B. J. (2011). Sequencing illustrates the transcriptional response of *Legionella pneumophila* during infection and identifies seventy novel small non-coding RNAs. *PLoS ONE* 6:e17570. doi: 10.1371/journal.pone.0017570

Wiegand, S., Kruse, J., Gronemann, S., and Hammann, C. (2011). Efficient generation of gene knockout plasmids for *Dictyostelium discoideum* using one-step cloning. *Genomics* 97, 321–325. doi: 10.1016/j.ygeno.2011.02.001

Xiong, Q., Ünal, C., Matthias, J., Steinert, M., and Eichinger, L. (2015). The phenotypes of Atg9, Atg16 and Atg9/16 knock-out mutants imply autophagy-dependent and -independent functions. *Open Biol.* 5:150008. doi: 10.1098/rsob.150008

Yamaguchi, N., Tokunaga, Y., Goto, S., Fujii, Y., Banno, F., and Edagawa, A. (2017). Rapid on-site monitoring of *Legionella pneumophila* in cooling

tower water using a portable microfluidic system. *Sci. Rep.* 7:3092. doi: 10.1038/s41598-017-03293-9

Yannay-Cohen, N., Carmi-Levy, I., Kay, G., Yang, C. M., Han, J. M., Kemeny, D. M., et al. (2009). LysRS serves as a key signaling molecule in the immune response by regulating gene expression. *Mol. Cell* 34, 603–611. doi: 10.1016/j.molcel.2009.05.019

Yudin, D., and Fainzilber, M. (2009). Ran on tracks–cytoplasmic roles for a nuclear regulator. *J. Cell Sci.* 122, 587–593. doi: 10.1242/jcs.015289

Zhang, C., and Kuspa, A. (2009). Transcriptional down-regulation and rRNA cleavage in *Dictyostelium discoideum* mitochondria during *Legionella pneumophila* infection. *PLoS ONE* 4:e5706. doi: 10.1371/journal.pone.0005706

Conflict of Interest Statement: The authors declare that the research was conducted in the absence of any commercial or financial relationships that could be construed as a potential conflict of interest.

frontiers in Cellular and Infection Microbiology

REVIEW
published: 09 January 2018
doi: 10.3389/fcimb.2017.00529

When Dicty Met Myco, a (Not So) Romantic Story about One Amoeba and Its Intracellular Pathogen

Elena Cardenal-Muñoz, Caroline Barisch, Louise H. Lefrançois, Ana T. López-Jiménez and Thierry Soldati*

Department of Biochemistry, Sciences II, Faculty of Sciences, University of Geneva, Geneva, Switzerland

In recent years, *Dictyostelium discoideum* has become an important model organism to study the cell biology of professional phagocytes. This amoeba not only shares many molecular features with mammalian macrophages, but most of its fundamental signal transduction pathways are conserved in humans. The broad range of existing genetic and biochemical tools, together with its suitability for cell culture and live microscopy, make *D. discoideum* an ideal and versatile laboratory organism. In this review, we focus on the use of *D. discoideum* as a phagocyte model for the study of mycobacterial infections, in particular *Mycobacterium marinum*. We look in detail at the intracellular cycle of *M. marinum*, from its uptake by *D. discoideum* to its active or passive egress into the extracellular medium. In addition, we describe the molecular mechanisms that both the mycobacterial invader and the amoeboid host have developed to fight against each other, and compare and contrast with those developed by mammalian phagocytes. Finally, we introduce the methods and specific tools that have been used so far to monitor the *D. discoideum—M. marinum* interaction.

Keywords: *Dictyostelium discoideum*, *Mycobacterium marinum*, host-pathogen interactions, model organisms, phagocytosis, infection, methods

OPEN ACCESS

Edited by:
Ludwig Eichinger, University of Cologne, Germany

Reviewed by:
Salvatore Bozzaro, Università degli Studi di Torino, Italy
Hubert Hilbi, University of Zurich, Switzerland

****Correspondence:***
Elena Cardenal-Muñoz
elena.cardenal@unige.ch

Received: *03 November 2017*
Accepted: *18 December 2017*
Published: *09 January 2018*

Citation:
Cardenal-Muñoz E, Barisch C, Lefrançois LH, López-Jiménez AT and Soldati T (2018) When Dicty Met Myco, a (Not So) Romantic Story about One Amoeba and Its Intracellular Pathogen. Front. Cell. Infect. Microbiol. 7:529. doi: 10.3389/fcimb.2017.00529

INTRODUCTION

The Amoeba *Dictyostelium discoideum*

Dictyostelium discoideum is a soil amoeba that feeds on bacteria by phagocytosis. The Amoebozoa branch split from the common lineage leading to fungi and animals, shortly after these crown organisms split from the Plant lineage (Eichinger et al., 2005). *D. discoideum* has a very AT-rich (77.75%) haploid genome, organized into 6 chromosomes, which has been sequenced and annotated (dictyBase, 2004; Eichinger et al., 2005). The isolation in the 70's of axenic strains that could feed on liquid medium by pinocytosis (Watts and Ashworth, 1970) enabled the easy laboratory culture of *D. discoideum*. In addition, this amoeba is genetically tractable, being relatively easy to transform for gene expression from extrachromosomal plasmids, generation of knockins, and knockouts by homologous recombination (Veltman et al., 2009a,b; Wiegand et al., 2011; Mukai et al., 2016), and mutagenesis by Restriction Enzyme-Mediated Integration (REMI) (Kuspa, 2006). Moreover, *D. discoideum* can be used in multiple cell biology, biochemistry, and imaging assays, as well as for high-throughput screens and RNAseq analysis (Eichinger and Rivero, 2013; Kicka et al., 2014; Rosengarten et al., 2015). For these reasons, *D. discoideum* has been extensively used as a model system to study very diverse biological processes such as motility, chemotaxis, vesicular

trafficking, gene expression, facultative multicellularity, and host-pathogen interactions (Barry and Bretscher, 2010; Maniak, 2011; Stevense et al., 2011; Loomis, 2014; Tosetti et al., 2014; Nichols et al., 2015).

Central Role of Autophagy in Development and Host-Microbe Interaction

In conditions of nutrient repletion, *D. discoideum* lives as a vegetative unicellular organism. However, when resources become scarce, the amoeba triggers a developmental program for the aggregation of hundreds of thousands of cells into a true multicellular organism (Raper, 1935; Dormann et al., 2000; Williams, 2006). This process is known as the "developmental cycle" of *D. discoideum* and has been extensively studied as one of the evolutionary origins of multicellularity. Aggregation and morphogenesis during development require a high level of cellular activity. To undertake this metabolic demand in the absence of nutrients, *D. discoideum* relays on macroautophagy (hereafter referred as autophagy), a major catabolic pathway in eukaryotes (Otto et al., 2004). Non-selective autophagy consists of the engulfment of bulk cytosolic material in a double-membrane compartment called the autophagosome. Upon fusion with lysosomes, autolysosomes degrade, and recycle their content, enabling cell survival under starvation. One of the major regulators of autophagy is the target of rapamycin complex 1 (TORC1). Under nutrient repletion, TORC1 downregulates autophagy by repressing the expression of autophagy genes and/or by phosphorylation and inhibition of proteins involved in autophagosome formation (reviewed in Nakatogawa, 2015). In *D. discoideum*, the TORC1 complex consists of the TOR serine/threonine kinase and two TOR activators, Lst8, and Raptor (Wullschleger et al., 2006; Rosel et al., 2012). Like in mammals, starvation decreases TORC1 activity, leading to induction of autophagy (King et al., 2011; Rosel et al., 2012).

Since many of the well-studied proteins known to participate in mammalian autophagy are conserved in this amoeba, autophagy can be easily monitored in *D. discoideum*. For instance, like in mammals, the activity of *D. discoideum* TORC1 can be analyzed by monitoring the phosphorylation state of Raptor and the TORC1 effector protein 4E-BP1 by immunoblotting (Rosel et al., 2012; Cardenal-Muñoz et al., 2017). In addition, in *D. discoideum* also the changes in autophagosome formation can be distinguished from changes in autophagic degradation by the differential response of Atg18 [WD-repeat protein interacting with phosphoinositides (WIPI) in mammals] and Atg8a (LC3/GABARAP family proteins in mammals) (Calvo-Garrido et al., 2010). Accordingly, during induction of autophagosome formation Atg8 and Atg18 translocate from the cytosol to membranes of nascent and elongating phagophores (the yet unclosed autophagic double membrane compartment). Immediately after closure of the autophagosome, Atg8 stays in both inner and outer membranes, while Atg18 dissociates. Upon fusion of the autophagosome with lysosomes, the hydrolytic enzymes delivered from the lysosome not only degrade the autophagic cargo but also the inner membrane of the autolysosome and its associated Atg8, while the Atg8 on the outside is recycled to the cytosol (reviewed in Dominguez-Martin et al., 2017).

In recent years, *D. discoideum* has also become an interesting model to study the molecular mechanisms regulating xenophagy (reviewed in Mesquita et al., 2016). Xenophagy is a selective autophagy pathway specifically recognizing and digesting intracellular pathogens. It relies on selective receptors that recruit the cargo to be degraded [i.e., bacteria or remnants of their phagosome decorated with "eat-me" signals such as ubiquitin (Ub) or galectins in mammals] to autophagic membranes (Thurston et al., 2009, 2016; Boyle and Randow, 2013; Noad et al., 2017). Several xenophagy receptors have been described in mammalian cells, but only one, p62, has been identified or studied so far in *D. discoideum* (Calvo-Garrido and Escalante, 2010; Gerstenmaier et al., 2015; Lampe et al., 2015; Cardenal-Muñoz et al., 2017). In addition, although *D. discoideum* lacks galectins, which recognize bacterial or host membrane glycans, another family of cytosolic lectins in this amoeba, the discoidins (Dsc), share many molecular and biological characteristics with galectins. Dsc are highly expressed upon starvation (Rosen et al., 1973), bind to self-glycans during development (Cooper and Barondes, 1984; Eitle et al., 1993) and can be secreted to the extracellular medium (Barondes et al., 1984). Interestingly, Dsc bind to sonicated extracts of *Escherichia coli* and *Klebsiella aerogenes* (Cooper et al., 1983), as well as to glutaraldehyde-fixed *K. aerogenes* bacteria (Madley and Hames, 1981). Recent studies have revealed that Dsc are enriched on compartments containing virulent *Legionella pneumophila* strains (i.e., Corby and JR32) but not the less virulent *L. hackelieae*, suggesting a role in innate immunity (Shevchuk et al., 2009; Urwyler et al., 2009). Moreover, one ortholog of the human TRIM37, a member of the Tripartite Motif protein superfamily (TRIMs) of autophagy receptors and regulators that often interact with galectins (Mandell et al., 2014; Kimura et al., 2015; Chauhan et al., 2016), has been identified in *D. discoideum* (Dunn et al., 2018). It will be interesting to uncover whether or not Dsc, TRIM-like protein and p62 cooperate in the immunity of *D. discoideum* against pathogenic bacteria.

The Bacterial Pathogen *Mycobacterium marinum*

Mycobacterium is the only genus of the *Mycobacteriaceae* family. It comprises more than 150 different species, among them two of the most important human pathogens, *M. leprae* and *M. tuberculosis* (Mtb), causing leprosy and tuberculosis, respectively. The latter represents the most severe bacterial diseases, responsible for 1.8 million deaths worldwide in 2015 (World Health Organization, 2015, http://www.who.int/tb/publications/global_report). One of the important features of Mtb is its capacity to persist inside its host in a non-replicating state with low metabolic activity. This phenomenon is called dormancy (or latency) and affects 2–3 billion people (i.e., one third of the world population). Latent tuberculosis is non-transmissible and presents no clinical manifestation. However, the disease reactivates in 5–10% of the cases usually as a consequence of immunosuppression, becoming contagious. Therefore, providing treatments to prevent the reactivation of

latent tuberculosis is an important concern in the control of this disease (World Health Organization, 2015).

Mtb belongs to the group of genetically related mycobacteria, the Mtb complex, that cause tuberculosis in human or other animals. However, another group of human pathogens emerging as a major public health problem is the Non-Tuberculous Mycobacteria (NTM) or Mycobacteria Other Than Tubercle bacilli (MOTT), which includes among others the species *M. ulcerans*, *M. abscessus*, *M. avium-intracellulare* complex (MAC) and *M. marinum* (Ryu et al., 2016). In contrast to Mtb, with no environmental reservoir demonstrated so far, *M. marinum* is an intracellular pathogenic mycobacterium with ubiquitous distribution. It can be found in aquatic environments, and it affects a wide range of freshwater and marine vertebrates including fish, amphibians, and turtles (Decostere et al., 2004). During infection of these animals, *M. marinum* forms granulomatous lesions highly similar to the ones produced by Mtb in humans. In addition, *M. marinum* also develops a latent disease in the zebrafish model (Parikka et al., 2012). Very importantly, and reflecting their genetic proximity, *M. marinum* is also an opportunistic pathogen of humans, but due to its optimal growth at 30°C, *M. marinum* infections are mostly localized and restricted to the skin and extremities. These lesions are usually painless and can be treated with anti-Mtb antibiotics when healing is not spontaneous (Aubry et al., 2017). At the cellular level, the infection course of *M. marinum* is also very similar to that of Mtb (reviewed in Ramakrishnan, 2004; Tobin and Ramakrishnan, 2008). Both bacteria avoid degradation within the host cells by arresting the maturation of their phagosomes and, contrary to the non-tuberculous *M. avium*, they escape to the host cytosol prior to dissemination (Stamm et al., 2003; Hagedorn et al., 2009; Simeone et al., 2015; Jamwal et al., 2016).

The genome of the *M. marinum* strain M was sequenced and annotated in 2008 by Stinear et al. (2008). Whole genome comparisons revealed that *M. marinum* is the ancestor of *M. ulcerans* and that both species are the closest relatives of the Mtb complex (Stinear et al., 2000, 2008). Among these species, *M. marinum* has the largest genome with 6.6 Mb, while the genome size of *M. ulcerans* and Mtb is 5.8 and 4.4 Mb, respectively. The genome of *M. marinum* shares 85% nucleotide identity with Mtb and 97% with *M. ulcerans*. Although phylogenetically and genetically close, Mtb and *M. marinum* present some differences such as the cell wall composition (Daffe et al., 1991; Tonjum et al., 1998), the abundance of proline-glutamic acid polymorphic guanine-cytosine-rich sequence (PE-PGRS) and proline-proline-glutamic acid (PPE) proteins (Cole et al., 1998; Bottai et al., 2012; Ates et al., 2015), and the synthesis of carotenoid pigments, which only occurs in *M. marinum* (Stinear et al., 2008).

Nevertheless, and more importantly, many virulence factors are conserved between *M. marinum* and Mtb. One example are the genes involved in dormancy (Dos-regulon) (Gerasimova et al., 2011). In addition, *M. marinum* and Mtb secrete virulence effector proteins through their complex cell walls thanks to very sophisticated secretion systems. In this context, the two mycobacteria possess five type VII secretion systems (T7SS) called ESX1-5 (reviewed in Groschel et al., 2016), in reference to the first secreted factor identified ESAT6 (Sorensen et al., 1995). The T7SS are not exclusive to mycobacteria and have been found in other bacterial genera such as *Streptomyces* and *Bacillus* (Gey Van Pittius et al., 2001; Pallen, 2002; Unnikrishnan et al., 2017). Despite their diversity, the T7SS share two common characteristics: the presence of FtsK/SpoIIIE transmembrane proteins and the secretion of small peptides of around 100 amino acids with the conserved motif Trp-X-Gly (WXG) (Pallen, 2002). The WXG motif is involved in the generation of a helix-turn-helix structure and is present in two of the most studied T7SS secreted peptides, the 6 kDa early secretory antigenic target ESAT6 and the 10 kDa culture filtrate protein CFP10 (Renshaw et al., 2005). Each ESX system is encoded in its respective ESX cluster or locus, which also contains the genes for secreted peptides and other accessory proteins (Bitter et al., 2009). The ESX loci do not complement each other (reviewed in Abdallah et al., 2007), which suggests that they are involved in different functions. Only three of them have been shown to play a role in pathogenesis: ESX-1, 3, and 5. Whereas ESX-3 is required for iron and zinc acquisition (Serafini et al., 2009, 2013; Siegrist et al., 2009, 2014), ESX-5 is involved in nutrient intake (Ates et al., 2015), cell wall integrity and secretion of PE and PPE proteins. The ESX-1 locus is the most studied, since it was shown to be very important for mycobacterial virulence (Pym et al., 2002). The attenuated *M. microti* and *M. bovis* BCG bacille Calmette–Guérin (BCG), used for vaccines, lack a partially overlapping region of the ESX-1 locus, which was called Region of Difference 1 (RD1). This region comprises two genes that encode the above mentioned secreted peptides ESAT6 and CFP10. Early studies using transposon libraries and purified proteins identified ESX-1, and in particular ESAT6 and CFP10, as membranolytic factors in both Mtb and *M. marinum* (Hsu et al., 2003; Gao et al., 2004). Importantly, the deletion of *M. marinum* RD1 can be complemented with homologous genes from Mtb, thus confirming the functional similarity of the RD1 regions in both species (Gao et al., 2004). Even though a 3.7 kb portion of *M. marinum* RD1 is partially duplicated within its genome (Stinear et al., 2008), deletion of RD1 prevents *M. marinum* escape from its phagosome as occurs with Mtb, suggesting that the duplicated fragment of *M. marinum* is not functional (Simeone et al., 2015; Cardenal-Muñoz et al., 2017).

These pathologic, phylogenetic, and genomic aspects make of *M. marinum* an interesting model to study mycobacterial infections. Importantly, *M. marinum* also has advantages for laboratory work. Despite the fact that this species is considered a slow growing mycobacterium, *M. marinum* grows faster than Mtb, with a doubling time of 6–8 h vs. the 20–24 h of Mtb. Furthermore, *M marinum* is a level 2 biosafety organism, and numerous molecular tools are available and transposable from Mtb to *M. marinum*, and *vice versa*.

The *D. discoideum*—*M. marinum* Infection Model

D. discoideum has been used to study conserved mechanisms of bacterial pathogenicity and host defenses involved in many

human diseases induced by diverse bacteria genera such as *Francisella*, *Legionella*, *Salmonella,* or *Mycobacterium* (Bozzaro and Eichinger, 2011; Weber and Hilbi, 2014; Brenz et al., 2017; Cardenal-Muñoz et al., 2017; Steiner et al., 2017). In both *D. discoideum* and human phagocytes, the main cell-autonomous defenses rely on the highly conserved microbicidal machinery that arms the phagosome (Boulais et al., 2010). This includes a number of genes and pathways involved in bacteria recognition, phagocytic uptake, actin dynamics, phagosome identity, acidification and maturation, lysosomal degradation, production of Reactive Oxygen Species (ROS), metal poisoning and nutrition immunity (recently reviewed in Dunn et al., 2018).

The ability of *M. marinum* to replicate within *D. discoideum* was first described in 2003 (Solomon et al., 2003). Solomon and collaborators monitored monolayers of *D. discoideum* infected with GFP-producing *M. marinum* at 25.5°C, a temperature optimal for the joint growth of host and bacterium. For these long-term infection assays, and to avoid rapid host cell death, *D. discoideum* needs to be infected at low multiplicity of infection (MOI $\leq$1–10). After an initial incubation without antibiotics, to allow the phagocytosis of *M. marinum*, streptomycin was added to the infection sample to impede the growth of extracellular bacteria. In this first approach, the increased growth of *M. marinum* was assessed by direct observation, but other quantitative methods such as luminescence recording, fluorescence-activated cell sorting (FACS) and colony-forming units (CFUs) counting have confirmed the intracellular proliferation of this bacterium within *D. discoideum*, both in static and shaking cultures (Solomon et al., 2003; Hagedorn and Soldati, 2007; Arafah et al., 2013). Other antibiotics such as amikacin or a mix of penicillin and streptomycin can be used to kill the extracellular *M. marinum* when performing infection assays in *D. discoideum* (Arafah et al., 2013). The presence of extracellular bacteria in the infection sample can be tested by incubating live cells with an anti-*M. marinum* serum (anti-mar) and performing immunofluorescence assays (Supplementary Table 1); Only the extracellular bacteria, and not those inside the amoeba, are accessible to the serum (Hagedorn et al., 2009).

M. MARINUM INFECTION COURSE IN *D. DISCOIDEUM*

The infection cycle of *M. marinum* in *D. discoideum* starts with the phagocytosis of the bacterium by the amoeba, and finishes with the bacterial egress from the cell (**Figure 1** and **Table 1**). Three different growth stages of *M. marinum* can be distinguished during the infection cycle: (i) an initial phase during the first 12 h post-infection (hpi), when *M. marinum* actively manipulates the *D. discoideum* phagocytic pathway to convert the phagosome where it resides into a replication-permissive niche [mycobacteria-containing vacuole (MCV)], (ii) an enhanced proliferation phase between 12 and 37 hpi, and (iii) a phase of arrested proliferation and/or decreased bacterial load due to bacterial death or release after 37 hpi (Hagedorn and Soldati, 2007). This infection cycle might be impacted by the number of bacteria initially taken up. When a single amoeba internalizes a clump of bacteria, the *M. marinum* clump either cannot initiate its intracellular growth, remaining in a dormant or undigested state as occurs in zebrafish, or causes cytotoxicity to *D. discoideum* (Solomon et al., 2003; Parikka et al., 2012).

Early *M. marinum* Infection Phase (~0–12 hpi)

During uptake, *M. marinum* is surrounded by a circular ruffle and ingested into a newly produced phagosome (**Figure 2**). The engulfment of the bacterium by the tight phagocytic cup has been observed by microscopy of live and fixed cells, using markers of the actin cytoskeleton of *D. discoideum* (Hagedorn et al., 2009). In addition, phagocytosis of GFP-producing or Alexa 488 hydrazide-labeled *M. marinum* has been quantitatively monitored by flow cytometry (Sattler et al., 2013). It is important to notice that the labeling of surface amines with Alexa Fluor 488-tetrafluorophenyl ester (Alexa Fluor 488-TFP), normally used for other bacteria such as *Klebsiella pneumoniae* or *Salmonella enterica*, is not suitable for *M. marinum*, presumably due to its extremely hydrophobic and poor-in-proteins cell wall (Sattler et al., 2013).

Ten minutes after phagocytosis, the early endosomal marker Rab5a is withdrawn from the *M. marinum* phagosome, compared to 3 min for the non-pathogenic *M. smegmatis* (Barisch et al., 2015a). Subsequently, the late endosome and lysosome marker Rab7a is detected at the early MCV (Cardenal-Muñoz et al., 2017), as occurs in macrophages (Lerena and Colombo, 2011). However, *M. marinum* rapidly bypasses the phagocytic pathway and blocks the maturation of its compartment. Thus, late maturation markers such as vacuolin and cathepsin D are absent from the MCV from 0.3 to 6 hpi, and the vacuolar H^+-ATPase (vATPase) is almost undetectable on the MCV at the end of this infection phase (12 hpi, **Figure 2**) (Hagedorn and Soldati, 2007). In this context, and contrary to *M. smegmatis*, only a small percentage of the phagocytosed *M. marinum* are killed by *D. discoideum* within the first hours (Hagedorn and Soldati, 2007), even in conditions of mild starvation that stimulate autophagy (i.e., phosphate buffer supplemented with 5% nutrient-rich medium) (Delince et al., 2016).

It has been shown that actin polymerization is required for the efficient maturation arrest of the *M. marinum* MCV during early infection of *D. discoideum* (Kolonko et al., 2014). Thus, Arp2/3 and WASH (Wiskott-Aldrich syndrome protein and Scar Homolog), two complexes involved in actin nucleation and polymerization on endosomal membranes (Duleh and Welch, 2010), can be observed in increasing association with the MCV from 0 to 6 hpi (**Figure 2**). This is concomitant with the presence of a patchy F-actin coat covering the MCV and with the absence of VatA, a peripheral subunit of the vATPase, on the same MCV at 6 hpi (Kolonko et al., 2014). On the contrary, amoebae either treated with the inhibitor of actin polymerization latrunculin A (LatA), producing a fusion construct between VacA and the actin-depolymerizing factor cofilin (VMC), or lacking the WASH complex (*wshA*-) harbor actin-negative

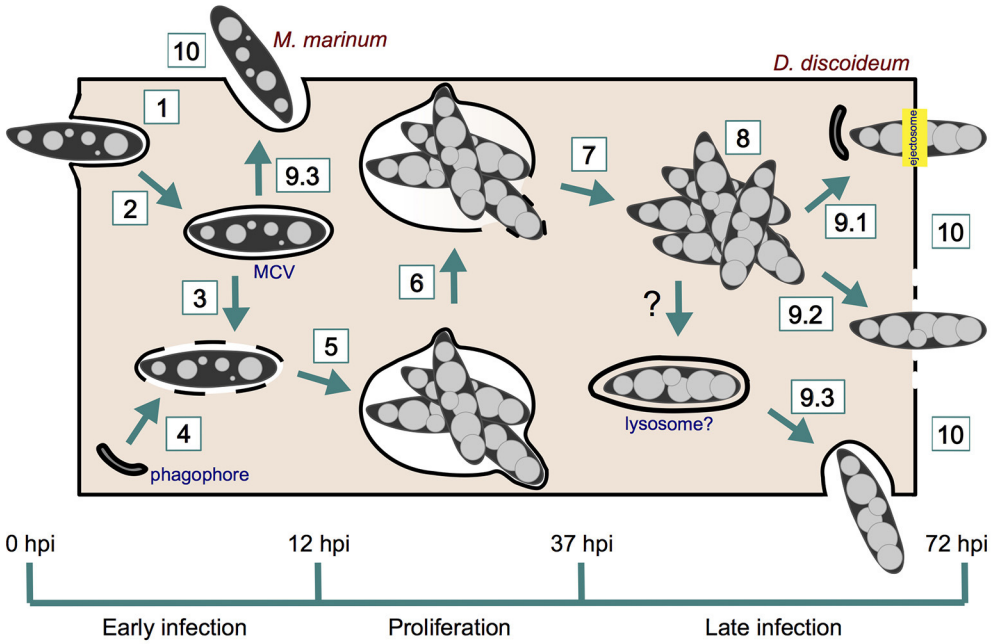

FIGURE 1 | *M. marinum* infection course in *D. discoideum*. *M. marinum* is phagocytosed by *D. discoideum* (1) and rapidly manipulates its phagocytic pathway to reside within a replicative niche (2). The ESX-1 secretion system of *M. marinum* perforates the MCV (3), which induces the recruitment of phagophores for membrane repair (4). *M. marinum* proliferates within its MCV (5), which finally breaks (6) and release mycobacteria to *D. discoideum* cytosol (7). Bacteria continue growing in the host cytosol (8) prior to egress by ejection (9.1), lytic death (9.2), or exocytosis (9.3). Phagophores are also recruited to the site of ejection for plasma membrane repair. Recapture into lysosome-like compartments may precede late exocytosis. However, this has not been shown yet in *D. discoideum*. Early exocytosis (9.3) can be induced upon starvation. Intercellular dissemination occurs after *M. marinum* release from the amoeba (10).

MCVs which accumulate VatA and VatM (a transmembrane subunit of the vATPase), while losing the endocytic marker p80. Interestingly, p80 is not lost from the phagosome containing *M. smegmatis* and the avirulent mutant *M. marinum* L1D (Kolonko et al., 2014) (Supplementary Table 2). In agreement with the LatA-dependent accumulation of the vATPase on MCVs, LatA treatment also leads to acidification of the bacterial compartment, resulting in decreased bacteria viability (Kolonko et al., 2014). Interestingly, actin polymerization also prevents the acidification of the *M. marinum* and Mtb phagosomes in murine phagocytes (Kolonko et al., 2014). In addition to Arp2/3 and WASH, the *D. discoideum* homolog of mammalian flotillin, vacuolin B (VacB), is also essential for the establishment of the MCV, assisting *M. marinum* in the retrieval of the vATPase from its niche. On the contrary, the small GTPase RacH of *D. discoideum* contributes to the maturation of the MCV into phagolysosomes, reducing the intracellular bacterial load (Hagedorn and Soldati, 2007) (Supplementary Table 3).

It has to be noticed that *M. marinum* does not interfere with the contractile vacuole of *D. discoideum* (Kolonko et al., 2014). This osmoregulatory organelle consists of interconnected vesicles, cisternae and tubules that fuse with the plasma membrane to expel the excess of water ingested during macropinocytosis and maintain cell volume (Patterson, 1980). The contractile vacuole accumulates Rab11 GTPase, vATPase, and calmodulin (Du et al., 2008), but the latter does not localize to the MCV (Kolonko et al., 2014; Cardenal-Muñoz et al., 2017). In addition, tetramethylrhodamine isothiocyanate (TRITC)-dextran, which labels the endolysosomal system but not the contractile vacuole (Clarke et al., 2002), can be found inside the MCV (Gerstenmaier et al., 2015).

M. marinum Proliferation Phase (~12–37 hpi)

After establishment as a replication-permissive niche, the MCV becomes more spacious (**Figures 1**, **2** and **Table 1**). It still harbors Rab7a and, as occurs in human monocytes, it accumulates the post-lysosomal marker vacuolin/flotillin (Hagedorn and Soldati, 2007; Barisch et al., 2015b). On the contrary, VatA association with MCVs significantly decreases (Kolonko et al., 2014). Intriguingly, WASH contributes to *M. marinum* growth, and the WASH and Arp2/3 complexes can be observed at the MCV at 24 hpi (Kolonko et al., 2014). However, the F-actin coat of the MCV is almost completely lost and treatment with LatA does not alter the association of p80 or VatA with the MCV (Kolonko et al., 2014). Kil2, a *D. discoideum* P-type ATPase involved in intra-phagosomal killing of *Klebsiella*, does not play any role in the establishment of the MCV nor in *M. marinum* intracellular replication (Lelong et al., 2011). In addition, the *D. discoideum* homolog of coronin, a mammalian protein involved in the organization of the actin cytoskeleton that positively modulates intracellular mycobacterial growth in macrophages (Jayachandran et al., 2007), appears heterogeneously localized at the MCV but

TABLE 1 | *M. marinum* infection stages in *D. discoideum* and methods used for their analysis.

Infection stage	Method used for analysis	*D. discoideum* strains/markers		*M. marinum* strains/markers	
1. Phagocytosis	FACS (Sattler et al., 2013)	wt	–	wt	pMSP12::GFP
	IFA (Hagedorn et al., 2009)	wt	F-actin (phalloidin)	wt	pMSP12::GFP
	InfectChip (Delince et al., 2016)	wt	–	wt	pCherry10
	Live microscopy (Hagedorn et al., 2009)	wt	GFP-ABD	wt	pR2Hyg
	TEM (Hagedorn et al., 2009)	wt	–	wt	–
2. Niche establishment	IFA (Hagedorn and Soldati, 2007; Kolonko et al., 2014)	wt, *wshA*-	ArpC4-GFP, calmodulin, cathepsin D, Coronin-GFP, F-actin, p80, vacuolins, VMC, VatA, GFP-WASH	wt, L1D	pCherry3, pMSP12::GFP
	Live microscopy (Kolonko et al., 2014; Barisch et al., 2015a,b; Gerstenmaier et al., 2015; Barisch and Soldati, 2017b; Cardenal-Muñoz et al., 2017)	wt	ABD-GFP, AmtA-mCherry/GFP, DQ Green BSA, LysoSensor Green, NR, GFP-Rab5a, GFP-Rab7a, GFP-Rab11c, TRITC-dextran, VacA-GFP, VatB-RFP, VatM-GFP	wt, ΔRD1	pCherry3/10, pMSP12::DsRed/GFP, Vibrant DyeCycle Ruby
	TEM (Cardenal-Muñoz et al., 2017)	wt	–	wt	–
3. MCV membrane damage	IFA (Cardenal-Muñoz et al., 2017)	wt, *atg1*-	Atg8a, GFP-p62, Ub (FK2)	wt, ΔCE	pCherry10
	Immunoblot (Cardenal-Muñoz et al., 2017)	wt	p-4E-BP1 (T70), Abp1, p-Raptor (S863)	wt, ΔRD1	pCherry10, pMSP12::DsRed
	Live microscopy (Cardenal-Muñoz et al., 2017)	wt, *atg1*-	GFP-Atg8a, GFP-Atg18, DQ Green BSA, GFP-Ub	wt, ΔRD1, ΔRD1::RD1-2F9	pCherry10, pMSP12::DsRed, Vibrant DyeCycle Ruby
	qPCR (Cardenal-Muñoz et al., 2017)	wt	*atg1*, *atg8a*, *atg8b*, *p62*	wt, ΔRD1	–
4. MCV membrane repair	IFA (Cardenal-Muñoz et al., 2017)	wt, *atg1*-, *atg1*- Atg1-GFP, *atg8*-	Ub (FK2)	wt	pCherry10
	Immunoblot (Cardenal-Muñoz et al., 2017)	wt	p-4E-BP1 (T70), Abp1, p-Raptor (S863)	wt, ΔRD1	pCherry10, pMSP12::DsRed
	Live microscopy (Cardenal-Muñoz et al., 2017)	wt	GFP-Lamtor1, GFP-Lst8, GFP-Raptor, GFP-Rheb	wt, ΔRD1	pCherry10, pMSP12::DsRed
	TEM (Cardenal-Muñoz et al., 2017)	wt, *atg1*-	–	wt	–
5. Bacteria replication within the MCV	FACS (Hagedorn and Soldati, 2007; Hagedorn et al., 2009; Lelong et al., 2011; Kolonko et al., 2014)	wt, *kil2*-, *racH*-, *vacB*-, *wshA*-	MB38::ESAT-6	wt, L1D, ΔRD1	pMSP12::GFP
	IFA (Solomon et al., 2003; Hagedorn and Soldati, 2007; Lelong et al., 2011)	wt, *kil2*-, *racH*-, *vacB*-	vacuolins, coronin-GFP, p80	wt, L1D	*map24*::GFP, pMSP12::GFP
	Luminescence recording in microplate reader (Ouertatani-Sakouhi et al., 2017)	wt	–	wt	pMV306::*lux*
	TEM (Hagedorn et al., 2009)	wt	–	wt	–

(Continued)

TABLE 1 | Continued

Infection stage	Method used for analysis	*D. discoideum* strains/markers		*M. marinum* strains/markers	
6. MCV rupture	IFA (Hagedorn and Soldati, 2007; Hagedorn et al., 2009; Lelong et al., 2011; Cardenal-Muñoz et al., 2017)	wt, *kil2-*, *racH-*, *vacA-*, *vacB-*	MB38::ESAT-6, p80, Ub (KF2), vacuolins	wt, ΔRD1	pCherry10, pMSP12::GFP
	Live microscopy (Barisch et al., 2015b)	wt	VacA-GFP	wt	pCherry10
	TEM (Hagedorn et al., 2009)	wt, *racH-*	–	wt, ΔRD1	–
7. Escape from the MCV	IFA (Hagedorn and Soldati, 2007; Hagedorn et al., 2009; Gerstenmaier et al., 2015; Cardenal-Muñoz et al., 2017)	wt, *racH-*, *vacA- vacB-*	Atg8a, F-actin (phalloidin), MB38::ESAT-6, GFP-p62/Sqstm1, p80, Ub (FK2), vacuolins	wt, ΔRD1	pCherry10, pMSP12::GFP
	Live microscopy (Barisch et al., 2015a,b; Barisch and Soldati, 2017b)	wt	AmtA-mCherry/GFP, RFP/GFP-Plin, VacA-GFP	wt, ΔRD1	pCherry10
	TEM (Hagedorn et al., 2009)	wt, *racH-*	–	wt, ΔRD1	–
8. Cytosolic replication	Luminescence recording in microplate reader (Cardenal-Muñoz et al., 2017)	wt, *atg1-*, *atg8a-*, *p62-*	–	wt, ΔRD1	pMV306::*lux*
9.1. Egress by ejection	CLEM (Gerstenmaier et al., 2015)	wt	F-actin (Lifeact-GFP)	wt	pCherry3
	FACS (Gerstenmaier et al., 2015)	wt, *atg1-*	PI	wt	pMSP12::GFP
	IFA (Hagedorn et al., 2009; Kolonko et al., 2014; Gerstenmaier et al., 2015)	wt, *atg1-*, *atg5-*, *atg6-*, *atg7-*, *p62/sqstm1-*, *racH-*, *vacA-*, *vacB-*, *wshA-*, *wshA-* GFP-WASH	GFP-2xFYVE, Arp3, Atg8a, GFP-Atg18, Coronin, F-actin (phalloidin), GFP, MB38::ESAT-6, myoII, myoB, GFP-p62/Sqstm1, p80, PM4C4, Ub (FK2)	wt, ΔRD1	anti-mar, pCherry3, pMSP12::GFP, pR2Hyg
	Live microscopy (Hagedorn et al., 2009; Gerstenmaier et al., 2015)	wt	ABD-GFP, GFP-ABD, DAPI, TRITC-dextran	wt	pMSP12::GFP, pR2Hyg
	TEM (Gerstenmaier et al., 2015)	wt, *atg1-*	–	wt	–
9.2. Egress by host cell death	FACS (Gerstenmaier et al., 2015)	wt, *atg1-*	PI	wt	pMSP12::GFP
	InfectChip (Delince et al., 2016)	wt	–	wt	pCherry10
9.3. Exocytosis	IFA (Hagedorn et al., 2009)	wt	GFP-ABD, F-actin (phalloidin), p80, PM4C4, vacuolin	wt	pMSP12::GFP
	InfectChip (Delince et al., 2016)	wt	–	wt	pCherry10
	Live microscopy (Gerstenmaier et al., 2015)	wt	ABD-GFP, TRITC-dextran	wt	pMSP12::GFP
	SEM (Hagedorn et al., 2009)	wt	–	wt	–
	TEM (Hagedorn et al., 2009)	wt	–	wt	–
10. Intercellular dissemination	Dissemination/Transmission assay [fixed fluorescence microscopy (Hagedorn et al., 2009) or FACS (Gerstenmaier et al., 2015)]	wt, *atg1-*, *racH-*	GFP-ABD, Lifeact-RFP	wt	pMSP12::GFP, pR2Hyg
	IFA (Hagedorn et al., 2009)	wt	F-actin (phalloidin), p80	wt	pMSP12::GFP

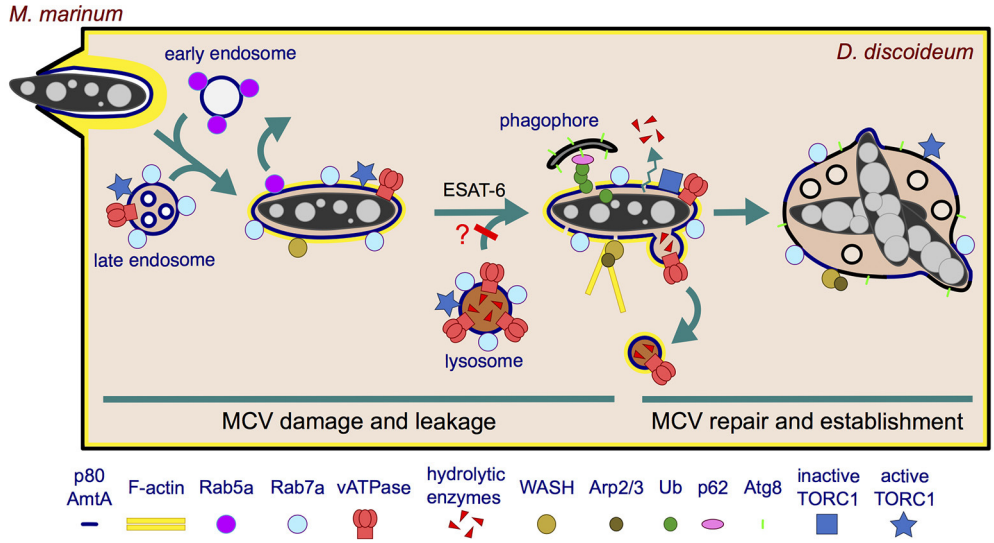

FIGURE 2 | Establishment of the MCV during the first 12 h of infection. *M. marinum* is engulfed by an F-actin-positive phagocytic cup, resulting in an early phagosome that likely fuses sequentially with early and late endosomes. Rab5a is rapidly recycled from the MCV, which transiently acquires characteristics of a late endosome (Rab7a$^+$, vATPase$^+$, active TORC1$^+$) but does not accumulate hydrolases. The undetectable level of hydrolases might result from defects in delivery, efficient recycling or leakage out of the MCV. In the case lysosomes do fuse with the MCV and deliver hydrolases, these might be retrieved by a mechanism dependent on WASH and Arp2/3 complexes. These complexes induce actin polymerization at the MCV, contributing to the retrieval of the vATPase and possibly hydrolases. In addition, *M. marinum* secretes ESAT-6 that damages the membrane, which renders the MCV leaky for ions and possibly lysosomal enzymes. Moreover, present evidence does not exclude the possibility that lysosomal fusion with the MCV is blocked. The membrane perforations induce an autophagic response in *D. discoideum*: TORC1 is inactivated and induces transcription of autophagy genes and formation of phagophores. The phagophores are recruited to the damaged MCV to repair the membrane and possibly deliver nutrients. *M. marinum* consequently survives and proliferates within a repaired and permissive MCV.

seems to negatively regulate the uptake or early survival and proliferation of *M. marinum* (Solomon et al., 2003). These data suggest that other host factors must be responsible for the support of the *M. marinum* intracellular replication in this amoeba.

One of the bacterial effectors required for the successful proliferation of *M. marinum* within *D. discoideum* is MAG24-1 (Solomon et al., 2003; Hagedorn and Soldati, 2007), a PE-PGRS protein also essential for replication in mammalian macrophages, frogs and flies (Ramakrishnan et al., 2000; Dionne et al., 2003). Actually, due to its role in intracellular growth, MAG24-1 can be used as a tool to monitor the proliferation of *M. marinum* mutant strains in *D. discoideum* by simply following the expression of GFP under the control of the *mag24-1* promoter in bacteria carrying the map24::GFP vector (Hagedorn and Soldati, 2007) (Supplementary Table 1). Another factor essential for optimal *M. marinum* intracellular growth is the ESX-1 secretion system, responsible for the rupture of the phagosomes containing *M. marinum* and its release into *D. discoideum* cytosol at the end of this infection phase (21–37 hpi) (Hagedorn and Soldati, 2007; Hagedorn et al., 2009). Mtb and *M. avium* can be seen in *D. discoideum* within spacious compartments that accumulate vacuolin but, contrary to Mtb, the ESX-1-deficient *M. avium* (Houben et al., 2014) does not escape its MCV (Hagedorn et al., 2009). A functional ESX-1 is important for optimal *M. marinum* proliferation (Hagedorn et al., 2009; Cardenal-Muñoz et al., 2017), and the exogenous expression of *M. marinum* ESAT-6 in *D. discoideum* rescues the inefficient intracellular replication of ΔRD1 bacteria (Hagedorn et al., 2009). The role of ESX-1 in phagosomal escape and intracellular proliferation of *M. marinum* and Mtb has also been described in mammalian cells (Stamm et al., 2003; Gao et al., 2004; Volkman et al., 2004; Tan et al., 2006; Simeone et al., 2015; Zhang et al., 2016). In addition to ESX-1, other mycobacterial factors have been shown to contribute to phagosomal rupture. The mycobacterial cell wall components phthiocerol dimycocerosates (PDIMs) have been revealed essential for ESAT-6 activity, suggesting some sort of cooperativity not yet understood (Augenstreich et al., 2017).

The *D. discoideum* ammonium transporter AmtA is a useful marker to determine whether or not mycobacteria are inside a compartment, since its fluorescent versions ubiquitously localize to all the endosomes and the MCV (Barisch et al., 2015b; Barisch and Soldati, 2017b) (Supplementary Table 4). Methods based on fluorescence resonance energy transfer (FRET), such as FRET-based microscopy or flow cytometry, have been performed in macrophages infected with Mtb and *M. marinum* to detect the mycobacteria-mediated phagosome disruption (Simeone et al., 2012, 2015; Acosta et al., 2014).

Late *M. marinum* Infection Phase (~37–72 hpi)

After 37 hpi, when *M. marinum* has escaped its MCV, the intracellular bacterial load stabilizes and even decreases (Hagedorn and Soldati, 2007). This might be the result of the convergence between recapture and killing of cytosolic bacteria in lytic compartments, and the release of the bacteria to the extracellular medium or neighboring cells (**Figure 1**). Events of recapture have not been reported so far in *D. discoideum*, but in macrophages cytosolic *M. marinum* is ubiquitinated

and recaptured into non-autophagic double membrane compartments (LAMP-1-positive, LC3/Atg8-negative) (Collins et al., 2009). It was proposed that ESCRT, a protein machinery that sorts ubiquitinated cargo to degradation into intraluminal vesicles (Schmidt and Teis, 2012), would deliver these bacteria to multivesicular bodies (MVB) and finally to lysosomes, but the bactericidal activity of these putative recapture compartments was not established (Collins et al., 2009).

Regarding release, and as a consequence of the wide range of strategies used by bacteria to survive and replicate within their hosts, multiple egress strategies have emerged in the course of evolution (Friedrich et al., 2012) (**Figure 1** and **Table 1**). In some cases, egress implies the disruption of one or several host membranes, which may lead to the host cell death. Mycobacteria modulate the death of their host cells, inducing apoptotic or necrotic processes with different biological implications. These processes vary depending on the mycobacterial species, host cell types, and infection stage (reviewed in Aguilo et al., 2013; Srinivasan et al., 2014). In this context, many studies have associated ESX-1 activity and mycobacterial vacuolar escape to an increased host cell cytotoxicity and death (Hsu et al., 2003; Derrick and Morris, 2007; Kaku et al., 2007; Kinhikar et al., 2010; Simeone et al., 2012; Augenstreich et al., 2017). Thus, incubation with purified ESAT-6, as well as infection with wild-type (wt) Mtb and *M. marinum* but not with ΔRD1 mutant bacteria, lyse epithelial and red blood cells and macrophages (Hsu et al., 2003; Gao et al., 2004). This is of special relevance since mycobacterial egress from its host might influence spread of the infection in a tissue. Similarly, by using a microfluidic device (the InfectChip) to microscopically monitor single-cell long-term infection in *D. discoideum*, it has been shown that a quarter of the phagocytosed *M. marinum* induces death and lysis of the amoebae, contributing to bacteria release (Delince et al., 2016).

Alternative non-lytic mechanisms of bacterial egress also occur during mycobacterial infection in *D. discoideum*. For instance, release of *M. marinum* within the first hours of infection, when most of the bacilli are still intravacuolar, thereby suggesting an exocytic process, can be induced by mild starvation of *D. discoideum* (Delince et al., 2016). This phenomenon is likely akin to the known massive exocytosis of lysosomal enzymes that *D. discoideum* undergoes upon starvation (Smith et al., 2010). In addition, bacterial ejection occurs at later time points (or earlier if the MOI is increased to 50–100, Gerstenmaier et al., 2015) once mycobacteria have escaped the MCV and accessed the host cytosol (Hagedorn et al., 2009). During ejection, *M. marinum* and Mtb, but not the ESX-1-deficient *M. avium*, use the actin cytoskeleton of *D. discoideum* to form an actin-based short barrel structure formed at the plasma membrane, called the ejectosome, through which they exit the cell (Hagedorn et al., 2009). In this context, some *D. discoideum* actin-binding proteins such as coronin and myosin IB are enriched at the ejectosome (Hagedorn et al., 2009) (Supplementary Table 4). In addition, ejection cannot occur in amoebae lacking the actin polymerization complex WASH (Kolonko et al., 2014). Strikingly, other markers of the actin cytoskeleton such as the actin nucleator complex Arp2/3 and myosin II are not enriched at the ejectosome, suggesting that this structure may assemble *de novo* during ejection (Hagedorn et al., 2009). It has been proposed that the *D. discoideum* plasma membrane reseals at the posterior of the bacterium after ejection, preventing the amoebal lysis or leakage (Gerstenmaier et al., 2015) (section *D. discoideum* Plasma Membrane Damage and Sealing at Later Time Points). Exclusion of DAPI (a membrane-impermeant DNA binding dye) from the nuclei of live amoebae during ejection demonstrates that *M. marnium* does not kill or induce leakage of its host while egressing by this mean (Hagedorn et al., 2009).

Exocytosis and ejection can be discriminated by fluorescence microscopy with various *D. discoideum* markers. For instance, only during exocytosis the intracellular pole of the egressing bacterium is positive for endosomal and MCV markers such as p80 and vacuolins. In addition, the extracellular part of the exocytosed bacterium is free of any plasma membrane marker (Hagedorn et al., 2009; Gerstenmaier et al., 2015). On the contrary, upon ejection, extracellular Mtb and *M. marinum* are wrapped in plasma membrane remnants positive for p80 or PM4C4 (Supplementary Table 4). Clumps of bacteria can be exocytosed, but ejectosomes, which are often observed to form clusters, only release individual bacteria (Hagedorn et al., 2009).

Once bacteria exit the cell, neighboring cells might become new hosts. Within macrophages, a subpopulation of cytosolic *M. marinum* sheds its ubiquitinated cell wall possibly to avoid recapture into lysosomes. These bacteria induce the polymerization of actin tails and spread via actin-dense filopodia that can be caught by other cells (Stamm et al., 2003; Collins et al., 2009; Hagedorn et al., 2009). However, and presumably due to the high rates of actin turnover, cytosolic *M. marinum* does not form persistent actin tails in *D. discoideum*, but events of cell-to-cell transmission synchronized with actin-based ejection are observed (Hagedorn et al., 2009). *D. discoideum* RacH, mentioned before to contribute to the maturation of the MCV, also assists *M. marinum* in its release from the amoeba and the subsequent intercellular dissemination. Accordingly, ejection of *M. marinum* is not observed in *racH*-cells (Hagedorn et al., 2009), and the population of infected *racH*- amoebae almost fully retain all bacteria until 37 hpi (Hagedorn and Soldati, 2007; Hagedorn et al., 2009) (Supplementary Table 3). In agreement with these results, quantitative dissemination assays have confirmed the positive role of RacH in *M. marinum* cell-to-cell spread. In these fluorescence microscopy assays, an unlabeled donor *D. discoideum* strain (wt or *racH*-) was infected with red fluorescent *M. marinum*, and a wt acceptor strain expressing GFP was added to the infection after 12 h. Transmission from *racH*-infected cells to wt cells was reduced over eight-fold (Hagedorn et al., 2009).

M. MARINUM INDUCES MEMBRANE DAMAGE THAT IS COUNTERACTED BY *D. DISCOIDEUM*

Rupture of host membranes by bacterial pathogens is achieved by the well-orchestrated secretion of lipases, proteases and pore-forming toxins. This is the case of vacuolar bacteria such as *Mycobacterium*, *Shigella*, *Listeria,* or *Salmonella*, which escape to

the host cytosol via the disruption of their vacuole. Although the membranolytic activity of the mycobacteria ESX-1 secretion system is widely accepted, it has been proposed that ESX-1-dependent membrane disruptions do not require ESAT-6 activity in physiological conditions in macrophages (Conrad et al., 2017). Instead, the perforations would occur upon direct contact of Mtb and *M. marinum* ESX-1 with host MCV membranes (Conrad et al., 2017), which would confine the membranolytic activity to the bacterial poles, where the ESX-1 is enriched (Carlsson et al., 2009). Incompatible with this proposed model, *M. marinum* mutants specifically lacking only ESAT-6 and CFP10 (ΔCE) in an otherwise intact RD1 locus are defective in hemolysis, cytolysis, and cytotoxicity (Gao et al., 2004). Similarly, the virulent Mtb H37Rv strain with a 12 amino acids deletion in ESAT-6 shows impaired membranolytic activity in the THP-1 human macrophages (Houben et al., 2012). Regarding CFP10, it has been shown that the protein dissociates from ESAT-6 in acidic conditions similar to those encountered within the phagosome, and it does not disrupt artificial liposomes on its own (de Jonge et al., 2007). As a consequence, CFP10 has been proposed to act as a chaperone of ESAT-6, conferring stability or protection against proteases. Despite the fact that the structures of ESAT-6 and CFP10 have been solved (Renshaw et al., 2005), it is not yet well-understood how ESAT-6 induces membrane disruptions.

Perforation and Repair of the MCV Membrane at Early Time Points

M. marinum resides inside a phagosome that shields it against the host intracellular immune responses but limits nutrient access. Maybe as a reaction, the bacterium creates a porous vacuole which might appear ideal to obtain unrestricted access to nutrients. Indeed, very early during infection of *D. discoideum*, *M. marinum* induces ESX-1-dependent damages in the MCV membrane, which results in the decoration of cytosol-exposed bacteria with Ub already at 1.5 hpi (Cardenal-Muñoz et al., 2017). This MCV membrane damage leads to a well-orchestrated early autophagic response consisting in: (i) transient downregulation of TORC1 and upregulation of transcription of autophagy genes such as *atg1*, the two paralogs *atg8a* and *atg8b*, and *p62*, (ii) enhanced formation of autophagosomes, and (iii) recruitment of the xenophagy machinery (Ub, GFP-p62, and Atg8a) to the damaged MCV. These responses to MCV damage are significantly reduced or even abolished when *M. marinum* lacks the RD1 locus and, more specifically, ESAT-6 and CFP-10 (Cardenal-Muñoz et al., 2017).

However, contrary to the increased bacterial killing expected from an enhanced xenophagic response, *M. marinum* survives and proliferates within *D. discoideum* by blocking the autophagic flux and its subsequent degradation within autolysosomes (Cardenal-Muñoz et al., 2017). Once again, the main player involved in this blockage is the mycobacterial ESX-1 secretion system, also shown to block the autophagic flux in human cells infected with Mtb (Romagnoli et al., 2012). Along these lines, even though 40–50% of the early *M. marinum* MCVs are positive for the autophagosomal marker Atg8a and for markers of acidic compartments [vATPase LysoSensor Green and neutral red (NR) (Hagedorn and Soldati, 2007; Kolonko et al., 2014; Cardenal-Muñoz et al., 2017)], and assuming that the presence of Rab7 on the MCV (Cardenal-Muñoz et al., 2017) should ensure fusion with late endosomes and lysosomes (Zhang et al., 2009), the MCVs containing wt bacteria are devoid of lysosomal enzymes and degradative activity, as demonstrated by the lack of cathepsin D and proteolysis-dependent DQ-Green BSA fluorescence (Hagedorn and Soldati, 2007; Cardenal-Muñoz et al., 2017). This suggests that the ESX-1-induced membrane damage make MCVs leaky for hydrolytic enzymes. This MCV leakage, together with the retrieval of the vATPase, and possibly hydrolases, by WASH- and Arp2/3-dependent polymerization of actin[see section Early *M. marinum* Infection Phase (∼0–12 hpi) and **Figure 2**], would affect both autophagic flux and killing of mycobacteria. Interestingly, depletion of hydrolases from the acidic *Salmonella*-containing compartment (SCV) has already been described, although the mechanism is different. *Salmonella* subverts the Rab9-dependent retrograde trafficking of mannose-6-phosphate receptors in human cells, which results in fusion of the SCV with lysosomes that are reduced in hydrolytic enzymes (McGourty et al., 2012).

The membrane damage inflicted by *Salmonella* induces an amino acid starvation response in the host cell that inhibits TOR and induces autophagy and membrane repair, leading to the normalization of the amino acid levels and the reactivation of TOR at the surface of SCVs (Tattoli et al., 2012a,b; Kreibich et al., 2015). Interestingly, it has been recently shown that mammalian TRIM16, a member of the TRIM family, recognizes the endomembrane perturbations induced by Mtb ESX-1 and affects TORC1 activity, inducing autophagy to protect macrophages from damage (Chauhan et al., 2016). The role of autophagy in mediating membrane repair during *D. discoideum* infection with *M. marinum* has also been recently proposed (Cardenal-Muñoz et al., 2017). After downregulation of TORC1 and induction of the autophagic response mentioned above, *D. discoideum* Lst8 (a TORC1 component) and two TORC1 activators, the Rheb GTPase and Lamtor1 [a member of the guanine nucleotide exchange factor (GEF) Ragulator complex] localize to damaged MCVs coinciding with reactivation of TORC1 at 7 hpi (Cardenal-Muñoz et al., 2017) (**Figure 2**). In addition, EM inspection of infected amoebae lacking the major autophagy initiator Atg1 (ULK in humans) (Mesquita et al., 2015) reveals that most bacteria escape very early to the cytosol (1 hpi), followed by a striking increased load of highly ubiquitinated cytosolic bacteria that cannot be degraded by xenophagy. This suggests that the autophagy pathway of *D. discoideum* is required for the repair of the MCV membranes, preventing the escape of mycobacteria to the cytosol. It remains unclear why *M. marinum* accelerates its growth only after 24 hpi in the *atg1*-amoebae (Cardenal-Muñoz et al., 2017). One plausible explanation is that autophagy would not only recognize damage and repair the MCV, but it could also provide *M. marinum* with cytoplasmic nutrients such as membranes and lipid droplets (LDs) by the fusion of autophagosomes with the MCV (see section *M. marinum* Exploits *D. discoideum* Lipids).

D. discoideum Plasma Membrane Damage and Sealing at Later Time Points

Despite the function of autophagy in membrane repair during early infection, most *M. marinum* bacilli are able to break completely their MCV and finally access the *D. discoideum* cytosol (Hagedorn and Soldati, 2007). As previously described, *M. marinum* perforates the plasma membrane of *D. discoideum* to egress through an actin-based ejectosome (Hagedorn et al., 2009). The ESX1 secretion system, and more specifically secreted ESAT-6, are required for ejection of the bacteria (Hagedorn et al., 2009). This is demonstrated by restoration of ejection of the ΔRD1 mutant by ectopic expression of *M. marinum* ESAT-6 in *D. discoideum* (Hagedorn et al., 2009). Despite this perforation, the integrity of the *D. discoideum* plasma membrane is continuously maintained during and after ejection by the autophagy machinery (**Figure 1**). This is necessary to avoid lytic cell death and to improve cell-to-cell transmission of the bacteria (Gerstenmaier et al., 2015). Accordingly, the autophagosomal markers Atg8, GFP-p62, and Ub are present at a pocket formed around the intracellular distal pole of ejecting *M. marinum* (Gerstenmaier et al., 2015). On the contrary, GFP-Atg18 and GFP-2xFYVE, two reporters of expanding phagophores (Calvo-Garrido et al., 2014; Mesquita et al., 2016), are less or rarely present, respectively (Gerstenmaier et al., 2015). This, together with the fact that the transcription levels of autophagy genes remain unchanged at these late stages of infection (Cardenal-Muñoz et al., 2017), suggest that *M. marinum* exploits pre-formed autophagosomes during its ejection.

The core autophagy machinery of *D. discoideum* (Atg1, Atg5, Atg6, and Atg7) is required for the recruitment of Atg8 to the distal pole of ejecting *M. marinum* (Supplementary Table 3). Strikingly, *atg1-* cells can form the actin-based structure of ejectosomes, but these are not functional for cell-to-cell transmission (Gerstenmaier et al., 2015). In addition, the selective receptor p62 is not required for the recruitment of Atg8 to the ejecting bacterium (Gerstenmaier et al., 2015). This, together with the fact that *M. marinum* grows normally within *p62*-cells (Cardenal-Muñoz et al., 2017), suggest that alternative autophagy receptors might exist in *D. discoideum*. Interesingly, the ESX-1 secretion system, which induces the recruitment of autophagic markers to bacteria escaping the MCV (Cardenal-Muñoz et al., 2017), does not play a role in the localization of Atg8 to bacteria during ejection (Gerstenmaier et al., 2015). This was shown by co-infecting cells with wt and either *M. marinum* ΔRD1 or the non-pathogenic *M. smegmatis* (whose ESAT-6 is inactive in membrane disruption). In these cells both bacteria form ejectosomes and recruit Atg8 to their distal pole (Gerstenmaier et al., 2015).

M. MARINUM EXPLOITS *D. DISCOIDEUM* LIPIDS

Inside their hosts, pathogens are restricted to a limited supply of nutrients. For instance, to drive proliferation, intracellular bacteria need to exploit a suitable energy source (Abu Kwaik, 2015; Abu Kwaik and Bumann, 2015). In recent years, it has become evident that *Mycobacterium* spp. access host lipids (Peyron et al., 2008; Caire-Brandli et al., 2014) to gain energy via β-oxidation and the glyoxylate shunt (McKinney et al., 2000; Munoz-Elias and McKinney, 2005). The importance of lipids for Mtb, but also for other *Mycobacterium* spp., is supported by the high number of genes (more than 250) harbored in the Mtb genome and required for lipid and fatty acid (FA) metabolism (Cole et al., 1998). The encoded proteins have diverse roles in cell wall synthesis, formation of intracytosolic lipid inclusions (ILIs) and production of energy (reviewed in Dumas and Haanappel, 2017). Strikingly, 100 of these genes exclusively encode proteins involved in the five reactions of β-oxidation (Cole et al., 1998). Interestingly, the chromosome of *M. marinum* is 50% larger than the one of Mtb (6.6 million base pairs compared to 4.4 million), which is also reflected by a higher number of genes involved in lipid metabolism (Stinear et al., 2008). For instance, the genome of *M. marinum* encodes 32 *fadD* acyl-CoA synthase paralog, compared with 23 in Mtb. This larger genome likely reflects the capacity of *M. marinum* to infect and produce a tuberculosis-like disease in a larger range of environmental hosts compared to Mtb (Stinear et al., 2000).

Lipid Droplets Are Recruited to the MCV during the Early Infection Phase

Despite the increasing evidence pointing to a central role of lipids during Mtb infection, the basic cellular mechanisms by which pathogenic mycobacteria exploit host lipids are still poorly understood. One of the major characteristics of tuberculosis is the appearance of foamy macrophages during chronic infection. The accumulation of LDs that leads to the foamy characteristics of the respective host cells was observed during Mtb infection (reviewed in Russell et al., 2009), but also in infections with *M. bovis* (D'Avila et al., 2006) and *M. leprae* (de Mattos et al., 2012). By using *D. discoideum* as a model for foamy macrophages, it was recently shown that host LDs move to the MCV within minutes after phagocytosis (**Figure 3**, step 1; Barisch et al., 2015b). The clustering of host LDs at the MCV can be monitored by live microscopy using Bodipy 493/503 as a neutral lipid marker for LDs that were induced by feeding cells with exogenous FAs prior to infection. We propose that host LDs might be translocated into the MCV by a process similar to lipophagy (**Figure 3**, step 1b), a selective autophagy pathway for LDs (reviewed in Schulze et al., 2017), or by a fusion-like process similar to that observed in a macrophage/*M. avium* infection model system (Caire-Brandli et al., 2014) (**Figure 3**, step 2). In analogy to LD-bilayer or LD-LD fusion (Thiam et al., 2013), the phospholipid monolayer of an LD might first fuse with the outer leaflet of the MCV membrane leading to the release of the hydrophobic core lipids into the membrane bilayer of the MCV. In a second step, a new LD-like structure might bud into the lumen of the MCV (for more detailed information, please see (Barisch and Soldati, 2017a).

Host Lipid Distribution at the *M. marinum* Proliferation Phase

At later infection stages (19 hpi), LD-like structures disappear, but neutral lipids and sterols, which can be detected by Bodipy

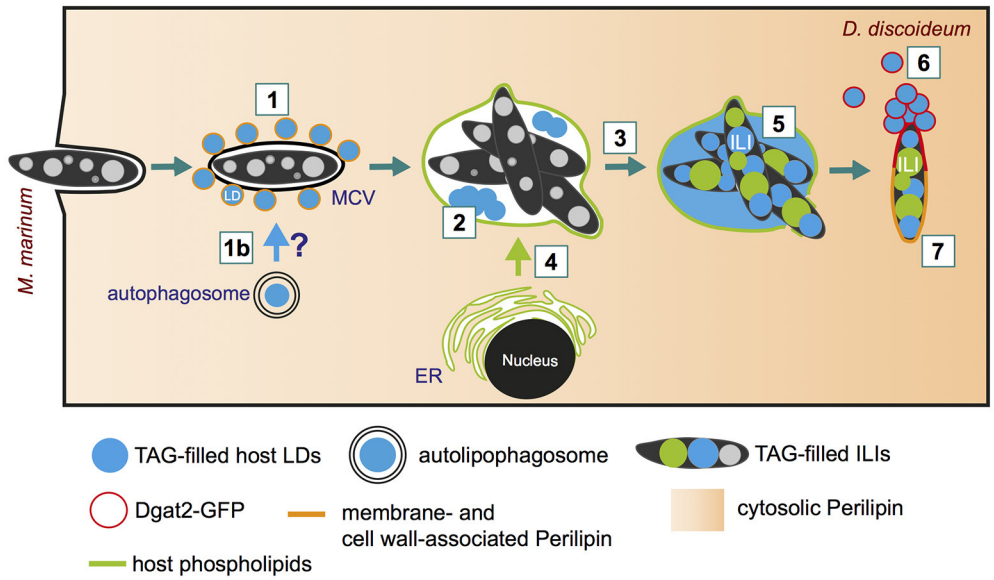

FIGURE 3 | Lipid distribution and re-arrangement during infection. (1) Soon after bacteria uptake (10 min post-infection), host lipid droplets (LDs) are clustered around the MCV (Barisch et al., 2015b). (1b) Indicates the possibility of LDs capture and translocation via lipophagy (Barisch and Soldati, 2017a); (2) LDs might be imported into the MCV by a mechanism similar to phagosomal fusion; (3) Neutral lipids (and sterols) accumulate within the MCV at late infection stages; (4) Host phospholipids are transferred to the MCV by membrane trafficking (Barisch and Soldati, 2017b); (5) Host triacylglycerols (TAGs) and phospholipids serve as fatty acid (FA) source for bacterial intracytosolic lipid inclusion (ILI) formation (Barisch et al., 2015b); (6) Dgat2-positive LDs aggregate at bacteria poles as soon as the MCV breaks, leading to the coalescence of LDs onto the *M. marinum* cell wall and the complete surrounding of the bacteria by Dgat2 (Barisch and Soldati, 2017a); (7) The *D. discoideum* homolog of perilipin reaches *M. marinum* from the cytosol and targets the bacterial cell wall with the help of amphipathic and hydrophobic domains (Barisch et al., 2015b; Barisch and Soldati, 2017b).

493/503 and filipin staining, are homogenously distributed within the MCV (**Figure 3**, step 3; Barisch et al., 2015b). Interestingly, these observations are in agreement with the fact that mycobacteria are one of the rare species able to catabolize host sterols and, more precisely, cholesterol (Pandey and Sassetti, 2008; Senaratne et al., 2008). By labeling *D. discoideum* with Topfluor-Lysophosphatidylcholine (Topfluor-LysoPC), a fluorescent phospholipid precursor, it was observed by live microscopy that host phospholipids accumulate at the membranes of the MCV, most likely by standard membrane trafficking (**Figure 3**, step 4; Barisch and Soldati, 2017b).

Strikingly, intravacuolar bacteria accumulate considerably more ILIs when *D. discoideum* cells are treated with exogenous FAs (**Figure 3**, step 5). Not only the FAs released from host triacylglycerols (TAGs) but also those from phospholipids are used by *M. marinum* for ILI formation (**Figure 3**, step 5; Barisch and Soldati, 2017b). This was shown by thin layer chromatography (TLC) using a *D. discoideum dgat1/2* double mutant, which is depleted in both diacyglycerol O-acyltransferases Dgat1 and Dgat2. This mutant shuttles excessive lipids into phospholipids, and does not synthesize TAGs and generate LDs (Du et al., 2013; Barisch and Soldati, 2017b). Interestingly, by measuring bacteria growth with the help of high-content microscopy and a luminescence-based assay, it was observed that *M. marinum* growth was unaffected in the *dgat1/2* double mutant (Barisch and Soldati, 2017b) leading to the conclusion that host phospholipids can successfully substitute for host TAGs. The transfer of host lipids to the intracellular pathogen can also be monitored by live-cell microscopy. To this end, host cells are labeled with Topfluor-LysoPC prior to infection. Strikingly, fluorescently-labeled host phospholipids become first enriched at the membrane of the MCV 10 min post-infection, and inside the bacteria at 21 hpi. Consequently, it was proposed that host lipids are transferred to the MCV by membrane trafficking and then further processed by bacterial or host phospholipases to facilitate uptake of FAs into the bacteria (Barisch and Soldati, 2017b).

Recently, the question whether Mtb has enzymes to successfully cleave/hydrolyse host lipids was addressed (Singh et al., 2017). The authors propose that host lipids are cleaved by Msh1, which is upregulated upon hypoxic conditions, and secreted into the host cytosol, where it hydrolyses TAGs. For *M. marinum*, it has been shown that the formation of ILIs depends on its type VII secretion system ESX-5, presumably thanks to the absorption of nutrients such as FAs through membrane porins or channels that are formed into the outer membrane of *M. marinum* by this ESX-5 apparatus (Ates et al., 2015). In the case of Mtb, FAs are transported into the bacteria via the mammalian cell entry 1 (Mce1) complex and LucA that interacts with subunits of the complex and coordinates its activity, and which is required for full virulence of Mtb *in vivo* (Nazarova et al., 2017).

The reason why intracellular mycobacteria accumulate ILIs during infection is so far poorly understood. One possibility is that these bacteria use ILIs as an energy source. For instance, it has been shown that in macrophages infected with *M. avium* and

without any additional fat source, LDs are rapidly depleted from the macrophages, immediately followed by ILIs depletion from the pathogens (Caire-Brandli et al., 2014). Moreover, with the help of an *in vitro* dormancy model, it was proposed that *M. bovis* BCG uses the TAGs released from ILIs as an energy source during reactivation from dormancy (Low et al., 2009). In addition, when the synthesis of TAGs is inhibited in *Drosophila melanogaster*, the accumulation of host LDs induced by *M. marinum* infection is also prevented, and the mycobacteria-LDs association, as well as the number of intracellular viable *M. marinum*, are reduced (Pean et al., 2017). Furthermore, ILI-rich mycobacteria have been shown to be more tolerant to rifampicin, isoniazid, ethambutol, and ciprofloxacin (Hammond et al., 2015). Finally, an antioxidant role of LDs (or ILIs) was proposed recently (Bailey et al., 2015).

Importantly, host lipids might not only be used by these bacteria as an energy source but also as building blocks for cell wall lipids. The core of the mycobacterial cell wall consists of mycolic acids that are esterified to arabinogalactan (AGs) polysaccharides, which are in turn covalently attached to a peptidoglycan backbone (reviewed in Brennan, 2003; Jackson, 2014). This core structure serves as anchor for extractible "free lipids" such as PDIMs and phenolic glycolipids (PGLs). One unique feature of pathogenic *Mycobacterium* spp. is their antibiotic resistance that is conferred by the "mycomembrane," the impermeable lipid bilayer that is formed by the mycolic acids and the free lipids (Jackson, 2014). During infection, PDIMs are involved in Mtb uptake (Astarie-Dequeker et al., 2009), block of phagosomal maturation and acidification arrest (Pethe et al., 2004; Stewart et al., 2005), in escape to the cytosol and egress from the host cells (Quigley et al., 2017). In addition, PDIMs are essential for the multiplication and persistence of Mtb in the lungs of infected mice (Cox et al., 1999), and Mtb strains inhibited in PDIM synthesis are more susceptible to killing by an early innate host response (Day et al., 2014). Corroborating this, it has been demonstrated that FAs released from host LDs are used by Mtb to synthesize PDIMs (Lee et al., 2013).

PDIMs are also implicated in the virulence of *M. marinum*. Like Mtb in macrophages, *M. marinum* synthesizes PDIMs (and TAGs) from FAs released from *D. discoideum* LDs and phospholipids (Barisch and Soldati, 2017b). To monitor lipid transfer from the host to the pathogen, *D. discoideum* lipids can be labeled by using fluorescent FAs such as Bodipy 558/568 C12 or Topfluor-LysoPC prior to infection (Barisch and Soldati, 2017b). The incorporation of the fluorescent label into *D. discoideum* and *M. marinum* lipids can be detected by TLC and fluorescent lipid species can be identified with the help of fluorescent standard lipids.

A transposon insertion in the *M. marinum tesA* gene, encoding a putative type II thioesterase, leads to an altered cell wall without PDIMs and PGLs and the subsequent lack of the permeability barrier (Alibaud et al., 2011). As a consequence, the *M. marinum tesA* mutant is attenuated in *D. discoideum* and in zebrafish embryos (Alibaud et al., 2011). Inhibitor and gene mutations altering the PDIMs and PGLs of *M. marinum* affect its virulence in *D. discoideum* and adult zebrafish, respectively (Yu et al., 2012; Ouertatani-Sakouhi et al., 2017). In addition, Cambier et al., elegantly described how Mtb and *M. marinum* preferentially recruit and infect permissive macrophages while microbicidal ones are evaded (Cambier et al., 2014). This bypass of the innate immune system was proposed to be the result of cell-surface-associated PDIMs hiding underlying pathogen-associated molecular patterns (PAMPs).

LD Proteins Target Cytosolic *M. marinum* at Late Infection Phases

At later infection stages (42 hpi), LD proteins such as the *D. discoideum* homolog of perilipin as well as Dgat2 localize to cytosolic *M. marinum* (**Figure 3**, steps 6 and 7; Barisch et al., 2015b; Barisch and Soldati, 2017b). Perilipin belongs to the class II of LD proteins, which bind the LD surface through hydrophobic and amphipatic domains, and circulates between LDs and the cytosol. During infection, perilipin is proposed to partition into the waxy mycobacterial cell wall in a similar way, via its amphipathic and hydrophobic regions (Barisch and Soldati, 2017a). Importantly, by using a luminescence-based assay to measure intracellular *M. marinum* growth, it became evident that in a *D. discoideum* perilipin (*plnA*) mutant, bacteria growth is inhibited starting from 20 hpi, the time at which *M. marinum* reaches the cytosol (Barisch et al., 2015b). Consequently, it was proposed that perilipin might exert a barrier function, protecting the *M. marinum* cell wall during the cytosolic phase of the infection from degradative host processes such as neutral lipases.

Dgat2 belongs to the class I of LD proteins, which bind the LD surface through an hydrophobic hairpin motif, and is exclusively localized at LDs. Consequently, Dgat2 is transferred to the waxy cell wall of *M. marinum* by coalescence with LDs and lateral diffusion (Barisch and Soldati, 2017b).

THE END OF THE ROMANCE: USING *D. DISCOIDEUM* TO UNCOVER THERAPEUTIC TARGETS IN *M. MARINUM*

D. discoideum Plaque Assays

As for animals, *M. marinum* is pathogenic for *D. discoideum*. Contrary to the food bacterium *Klebsiella*, the growth of *D. discoideum* is restricted when plated on *M. marinum* lawns (Ouertatani-Sakouhi et al., 2017). Researchers have made use of this growth incapacity to perform genetic and chemical screens for the search of virulence genes and anti-mycobacterial compounds. For instance, *M. marinum* TesA, a putative type II thioesterase required for the synthesis of the cell wall lipids PDIMs and PGLs, was identified in a *D. discoideum* plaque assay where a *M. marinum* transposon mutant library was screened for bacterial attenuation. The role of TesA in virulence was further confirmed during infection of zebrafish embryos, and the *tesA* gene was proposed as a possible genetic target for disruption in human mycobacterial pathogens (Alibaud et al., 2011). In addition, another plaque assay screen of *M. marinum* transposon mutants allowed Chen and collaborators to discover that two genes, *mmar_2318* and *mmar_2319*, involved in the biosynthesis of lipooligosaccharide (LOS) contribute to *M. marinum* virulence in *D. discoideum* and limit bacterial

entry in human macrophages (Chen et al., 2015) (Supplementary Table 2). Chemical screens can also be performed in amoebae (Ouertatani-Sakouhi et al., 2017; Trofimov et al., in press). For instance, drugs targeting the *M. marinum* cell wall have been recently identified to block/decrease *M. marinum* virulence by inhibiting bacterial aggregation and permeability, sliding motility and/or intracellular replication within *D. discoideum* (Ouertatani-Sakouhi et al., 2017). All these findings highlight *D. discoideum* as an alternative host for the screening of *Mycobacterium* virulence factors and potential antibacterial compounds.

High throughput Screening

Since the advent of next-generation sequencing (NGS) technologies, numerous methods to investigate the host-pathogen interaction at different levels (i.e., RNA, DNA, and proteins) have been developed. Among them, RNA sequencing (RNA-Seq) is becoming the standard to analyze the transcripts of each actor involved in a bacterial infection, either independently (bacteria or host) or simultaneously (bacteria and host) by dual RNA-Seq (Saliba et al., 2017; Westermann et al., 2017). This method has been used to describe the gene expression profile of *M. marinum* during exponential and stationary growth (Wang et al., 2013), as well as under stress conditions (Pettersson et al., 2015). In addition, it has allowed to determine the contribution of specific cells (neutrophils and macrophages) to the innate immune response against *M. marinum*, Mtb, and *M. bovis* (Schnappinger et al., 2003; Nalpas et al., 2015; Kenyon et al., 2017) and to identify genes such as *whiB4*, which encodes a protein regulating the PE/PPE genes and is required for *M. marinum* and Mtb virulence (Chawla et al., 2012; Wu et al., 2017). Moreover, a recent metabolomics study coupled to dual RNA-Seq allowed to reconstruct the dietary map of Mtb during macrophage infection (Zimmermann et al., 2017). Since the RNA-Seq methodology has already been established in *D. discoideum* (Miranda et al., 2013), it will be of high interest to perform dual RNA-seq in the *D. discoideum—M. marinum* infection model.

Another NGS method is transposon sequencing (Tn-Seq), which allows the analysis of fitness and genetic interactions in microorganisms by using random transposon insertion libraries in bacteria (van Opijnen et al., 2009; DeJesus and Ioerger, 2013; DeJesus et al., 2013, 2017a,b; van Opijnen and Camilli, 2013; Nambi et al., 2015) Thanks to this method, various researchers have identified essential genes for Mtb growth and cholesterol metabolism (Griffin et al., 2011; Zhang et al., 2012; DeJesus and Ioerger, 2013) and have investigated the Mtb virulence factors required for survival in human dendritic cells (Mendum et al., 2015). Concerning *M. marinum*, only one study has been published so far (Weerdenburg et al., 2015), in which the authors identified ∼300 genes essential for survival of the bacteria *in vitro*. These genes are mostly shared with Mtb and correspond to 6% of the total coding sequences. The authors investigated the strategies used by *M. marinum* to exploit different phagocytic cells, from protozoan and vertebrate origin. The behavior of the *M. marinum* transposon mutant pool was highly similar between the two mammalian cell lines (human THP-1 monocytes and mouse RAW264.7 macrophages) and between the two amoebae *D. discoidum* and *A. castellani*, while an intermediate behavior was observed in cells derived from fish (carp CLC leukocytes), probably due to their higher similarity with natural *M. marinum* hosts. Thus, the authors concluded that *M. marinum* has both conserved and host-specific virulence determinants. Regarding the conserved virulence factors, transposon interruption of PDIMs, ESX-1, or Mce1/4 leads to high attenuation of *M. marinum* virulence in multiple hosts. In addition, a new virulence factor of *M. marinum* was highlighted and validated *in vivo*, the *cpsA* gene. This gene encodes a protein of the LytR family of transcriptional regulators and has been recently demonstrated to be required for *M. marinum* cell wall integrity and virulence in the zebrafish model (Wang et al., 2015; Weerdenburg et al., 2015). Moreover, amoebae-specific pathways have been pointed out by the authors. For instance, transposon insertions in multiple genes involved in biosynthesis of vitamin B_{12} highly increased fitness of *M. marinum* in *Acanthamoeba*, while they had no or little impact on the bacteria within the other host cells (Weerdenburg et al., 2015). To conclude, *M. marinum* uses specific mechanisms to adapt to different intracellular environments. Some specific requirements for infection of mammalian cells are not applicable for protozoa infection, and *vice versa*.

Finally, REMI sequencing (REMI-Seq) has recently been developed for *D. discoideum* by the group of C. Thompson (https://thethompsonlab.wordpress.com/mutant-library/). The REMI method was first described in *Saccharomyces* (Schiestl and Petes, 1991) and then adapted to *D. discoideum* (Kuspa and Loomis, 1992; Kuspa, 2006). The technique comprises the integration of linear DNA into eukaryotic genomes for insertional mutagenesis. Combining REMI with NGS, a genome-wide collection of tagged mutants can be created to investigate host genes. However, REMI-Seq has not yet been used in the context of mycobacterial infection. Therefore, this tool, combined with other methods described above, are promising and innovative approaches that could help identify genes and pathways involved in mycobacteria-host interaction.

CONCLUDING REMARKS

In this review, we have described the so far known processes involved in the intracellular cycle of *M. marinum* within the amoeba *D. discoideum*. The comparison with studies carried out in human cells with Mtb revealed that the infection cycles of both bacteria share numerous similarities. However, many of the virulence mechanisms used by both pathogens to subvert the immune response of their hosts remain to be elucidated. We propose the *D. discoideum—M. marinum* system as a suitable and powerful model to study infection by tuberculous mycobacteria.

It needs to be noticed that not all the markers listed here were monitored in all the listed strains, and vice versa.

Please see main text and supplementary tables for more details. IFA, immunofluorescence assay; TEM, transmission electron microscopy; qPCR, quantitative polymerase chain reaction; SEM, scanning electron microscopy; CLEM, correlative light and electron microscopy.

AUTHOR CONTRIBUTIONS

EC-M, CB, LL, and AL-J wrote the original draft. EC-M and CB drew the figures and prepared the tables. EC-M, CB, LL, and TS reviewed and edited the draft. TS supervised this work.

FUNDING

The TS laboratory is supported by multiple grants from the Swiss National Science Foundation, and TS is a member of iGE3 (www.ige3.unige.ch) as well as of the COST Actions BM1203 EU-ROS and CA15138 TRANSAUTOPHAGY.

SUPPLEMENTARY MATERIAL

The Supplementary Material for this article can be found online at: https://www.frontiersin.org/articles/10.3389/fcimb.2017.00529/full#supplementary-material

REFERENCES

Abdallah, A. M., Gey van Pittius, N. C., Champion, P. A., Cox, J., Luirink, J., Vandenbroucke-Grauls, C. M., et al. (2007). Type VII secretion–mycobacteria show the way. *Nat. Rev. Microbiol.* 5, 883–891. doi: 10.1038/nrmicro1773

Abu Kwaik, Y. (2015). Nutrition-based evolution of intracellular pathogens. *Environ. Microbiol. Rep.* 7, 2–3. doi: 10.1111/1758-2229.12236

Abu Kwaik, Y., and Bumann, D. (2015). Host delivery of favorite meals for intracellular pathogens. *PLoS Pathog.* 11:e1004866. doi: 10.1371/journal.ppat.1004866

Acosta, Y., Zhang, Q., Rahaman, A., Ouellet, H., Xiao, C., Sun, J., et al. (2014). Imaging cytosolic translocation of Mycobacteria with two-photon fluorescence resonance energy transfer microscopy. *Biomed. Opt. Express* 5, 3990–4001. doi: 10.1364/BOE.5.003990

Aguilo, N., Marinova, D., Martin, C., and Pardo, J. (2013). ESX-1-induced apoptosis during mycobacterial infection: to be or not to be, that is the question. *Front. Cell. Infect. Microbiol.* 3:88. doi: 10.3389/fcimb.2013.00088

Alibaud, L., Rombouts, Y., Trivelli, X., Burguiere, A., Cirillo, S. L., Cirillo, J. D., et al. (2011). A *Mycobacterium marinum* TesA mutant defective for major cell wall-associated lipids is highly attenuated in *Dictyostelium discoideum* and zebrafish embryos. *Mol. Microbiol.* 80, 919–934. doi: 10.1111/j.1365-2958.2011.07618.x

Arafah, S., Kicka, S., Trofimov, V., Hagedorn, M., Andreu, N., Wiles, S., et al. (2013). Setting up and monitoring an infection of *Dictyostelium discoideum* with mycobacteria. *Methods Mol. Biol.* 983, 403–417. doi: 10.1007/978-1-62703-302-2_22

Astarie-Dequeker, C., Le Guyader, L., Malaga, W., Seaphanh, F. K., Chalut, C., Lopez, A., et al. (2009). Phthiocerol dimycocerosates of *M. tuberculosis* participate in macrophage invasion by inducing changes in the organization of plasma membrane lipids. *PLoS Pathog* 5:e1000289. doi: 10.1371/journal.ppat.1000289

Ates, L. S., Ummels, R., Commandeur, S., van de Weerd, R., Sparrius, M., Weerdenburg, E., et al. (2015). Essential ROLE of the ESX-5 secretion system in outer membrane permeability of pathogenic mycobacteria. *PLoS Genet.* 11:e1005190. doi: 10.1371/journal.pgen.1005190

Aubry, A., Mougari, F., Reibel, F., and Cambau, E. (2017). *Mycobacterium marinum*. *Microbiol. Spectr.* 5. doi: 10.1128/microbiolspec.TNMI7-0038-2016

Augenstreich, J., Arbues, A., Simeone, R., Haanappel, E., Wegener, A., Sayes, F., et al. (2017). ESX-1 and phthiocerol dimycocerosates of *Mycobacterium tuberculosis* act in concert to cause phagosomal rupture and host cell apoptosis. *Cell. Microbiol.* 19:e12726. doi: 10.1111/cmi.12726

Bailey, A. P., Koster, G., Guillermier, C., Hirst, E. M., MacRae, J. I., Lechene, C. P., et al. (2015). Antioxidant role for lipid droplets in a stem cell niche of Drosophila. *Cell* 163, 340–353. doi: 10.1016/j.cell.2015.09.020

Barisch, C., López-Jiménez, A. T., and Soldati, T. (2015a). Live imaging of *Mycobacterium marinum* infection in *Dictyostelium discoideum*. *Methods Mol. Biol.* 1285, 369–385. doi: 10.1007/978-1-4939-2450-9_23

Barisch, C., Paschke, P., Hagedorn, M., Maniak, M., and Soldati, T. (2015b). Lipid droplet dynamics at early stages of *Mycobacterium marinum* infection in Dictyostelium. *Cell. Microbiol.* 17, 1332–1349. doi: 10.1111/cmi.12437

Barisch, C., and Soldati, T. (2017a). Breaking fat! How Mycobacteria and other intracellular pathogens manipulate lipid droplets. *Biochimie* 141, 54–61. doi: 10.1016/j.biochi.2017.06.001

Barisch, C., and Soldati, T. (2017b). *Mycobacterium marinum* degrades both triacylglycerols and phospholipids from its Dictyostelium host to synthesise its own triacylglycerols and generate lipid inclusions. *PLoS Pathog.* 13:e1006095. doi: 10.1371/journal.ppat.1006095

Barondes, S. H., Cerra, R. F., Cooper, D. N., Haywood-Reid, P. L., and Roberson, M. M. (1984). Localization of soluble endogenous lectins and their ligands at specific extracellular sites. *Biol. Cell* 51, 165–172. doi: 10.1111/j.1768-322X.1984.tb00295.x

Barry, N. P., and Bretscher, M. S. (2010). Dictyostelium amoebae and neutrophils can swim. *Proc. Natl. Acad. Sci. U.S.A.* 107, 11376–11380. doi: 10.1073/pnas.1006327107

Bitter, W., Houben, E. N., Bottai, D., Brodin, P., Brown, E. J., Cox, J. S., et al. (2009). Systematic genetic nomenclature for type VII secretion systems. *PLoS Pathog.* 5:e1000507. doi: 10.1371/journal.ppat.1000507

Bottai, D., Di Luca, M., Majlessi, L., Frigui, W., Simeone, R., Sayes, F., et al. (2012). Disruption of the ESX-5 system of *Mycobacterium tuberculosis* causes loss of PPE protein secretion, reduction of cell wall integrity and strong attenuation. *Mol. Microbiol.* 83, 1195–1209. doi: 10.1111/j.1365-2958.2012.08001.x

Boulais, J., Trost, M., Landry, C. R., Dieckmann, R., Levy, E. D., Soldati, T., et al. (2010). Molecular characterization of the evolution of phagosomes. *Mol. Syst. Biol.* 6:423. doi: 10.1038/msb.2010.80

Boyle, K. B., and Randow, F. (2013). The role of 'eat-me' signals and autophagy cargo receptors in innate immunity. *Curr. Opin. Microbiol.* 16, 339–348. doi: 10.1016/j.mib.2013.03.010

Bozzaro, S., and Eichinger, L. (2011). The professional phagocyte *Dictyostelium discoideum* as a model host for bacterial pathogens. *Curr. Drug Targets* 12, 942–954. doi: 10.2174/138945011795677782

Brennan, P. J. (2003). Structure, function, and biogenesis of the cell wall of *Mycobacterium tuberculosis*. *Tuberculosis* 83, 91–97. doi: 10.1016/S1472-9792(02)00089-6

Brenz, Y., Ohnezeit, D., Winther-Larsen, H. C., and Hagedorn, M. (2017). Nramp1 and NrampB contribute to resistance against Francisella in Dictyostelium. *Front. Cell. Infect. Microbiol.* 7:282. doi: 10.3389/fcimb.2017.00282

Caire-Brändli, I., Papadopoulos, A., Malaga, W., Marais, D., Canaan, S., Thilo, L., et al. (2014). Reversible lipid accumulation and associated division arrest of *Mycobacterium avium* in lipoprotein-induced foamy macrophages may resemble key events during latency and reactivation of tuberculosis. *Infect. Immun.* 82, 476–490. doi: 10.1128/IAI.01196-13

Calvo-Garrido, J., Carilla-Latorre, S., Kubohara, Y., Santos-Rodrigo, N., Mesquita, A., Soldati, T., et al. (2010). Autophagy in Dictyostelium: genes and pathways, cell death and infection. *Autophagy* 6, 686–701. doi: 10.4161/auto.6.6.12513

Calvo-Garrido, J., and Escalante, R. (2010). Autophagy dysfunction and ubiquitin-positive protein aggregates in Dictyostelium cells lacking Vmp1. *Autophagy* 6, 100–109. doi: 10.4161/auto.6.1.10697

Calvo-Garrido, J., King, J. S., Muñoz-Braceras, S., and Escalante, R. (2014). Vmp1 regulates PtdIns3P signaling during autophagosome formation in *Dictyostelium discoideum*. *Traffic* 15, 1235–1246. doi: 10.1111/tra.12210

Cambier, C. J., Takaki, K. K., Larson, R. P., Hernandez, R. E., Tobin, D. M., Urdahl, K. B., et al. (2014). Mycobacteria manipulate macrophage recruitment through coordinated use of membrane lipids. *Nature* 505, 218–222. doi: 10.1038/nature12799

Cardenal-Muñoz, E., Arafah, S., Lopez-Jimenez, A. T., Kicka, S., Falaise, A., Bach, F., et al. (2017). *Mycobacterium marinum* antagonistically induces an autophagic response while repressing the autophagic flux in a TORC1- and ESX-1-dependent manner. *PLoS Pathog.* 13:e1006344. doi: 10.1371/journal.ppat.1006344

Carlsson, F., Joshi, S. A., Rangell, L., and Brown, E. J. (2009). Polar localization of virulence-related Esx-1 secretion in mycobacteria. *PLoS Pathog.* 5:e1000285. doi: 10.1371/journal.ppat.1000285

Chauhan, S., Kumar, S., Jain, A., Ponpuak, M., Mudd, M. H., Kimura, T., et al. (2016). TRIMs and galectins globally cooperate and TRIM16 and Galectin-3 co-direct autophagy in endomembrane damage homeostasis. *Dev. Cell* 39, 13–27. doi: 10.1016/j.devcel.2016.08.003

Chawla, M., Parikh, P., Saxena, A., Munshi, M., Mehta, M., Mai, D., et al. (2012). *Mycobacterium tuberculosis* WhiB4 regulates oxidative stress response to modulate survival and dissemination *in vivo*. *Mol. Microbiol.* 85, 1148–1165. doi: 10.1111/j.1365-2958.2012.08165.x

Chen, Y. Y., Yang, F. L., Wu, S. H., Lin, T. L., and Wang, J. T. (2015). *Mycobacterium marinum* mmar_2318 and mmar_2319 are responsible for lipooligosaccharide biosynthesis and virulence toward Dictyostelium. *Front. Microbiol.* 6:1458. doi: 10.3389/fmicb.2015.01458

Clarke, M., Köhler, J., Arana, Q., Liu, T., Heuser, J., and Gerisch, G. (2002). Dynamics of the vacuolar H(+)-ATPase in the contractile vacuole complex and the endosomal pathway of Dictyostelium cells. *J. Cell. Sci.* 115(Pt 14), 2893–2905.

Cole, S. T., Brosch, R., Parkhill, J., Garnier, T., Churcher, C., Harris, D., et al. (1998). Deciphering the biology of *Mycobacterium tuberculosis* from the complete genome sequence. *Nature* 393, 537–544. doi: 10.1038/31159

Collins, C. A., De Mazière, A., van Dijk, S., Carlsson, F., Klumperman, J., and Brown, E. J. (2009). Atg5-independent sequestration of ubiquitinated mycobacteria. *PLoS Pathog.* 5:e1000430. doi: 10.1371/journal.ppat.1000430

Conrad, W. H., Osman, M. M., Shanahan, J. K., Chu, F., Takaki, K. K., Cameron, J., et al. (2017). Mycobacterial ESX-1 secretion system mediates host cell lysis through bacterium contact-dependent gross membrane disruptions. *Proc. Natl. Acad. Sci. U.S.A.* 114, 1371–1376. doi: 10.1073/pnas.1620133114

Cooper, D. N., and Barondes, S. H. (1984). Colocalization of discoidin-binding ligands with discoidin in developing *Dictyostelium discoideum*. *Dev. Biol.* 105, 59–70. doi: 10.1016/0012-1606(84)90261-6

Cooper, D. N., Lee, S. C., and Barondes, S. H. (1983). Discoidin-binding polysaccharide from *Dictyostelium discoideum*. *J. Biol. Chem.* 258, 8745–8750.

Cox, J. S., Chen, B., McNeil, M., and Jacobs, W. R. Jr. (1999). Complex lipid determines tissue-specific replication of *Mycobacterium tuberculosis* in mice. *Nature* 402, 79–83. doi: 10.1038/47042

Daffe, M., Laneelle, M. A., and Lacave, C. (1991). Structure and stereochemistry of mycolic acids of *Mycobacterium marinum* and *Mycobacterium ulcerans*. *Res. Microbiol.* 142, 397–403. doi: 10.1016/0923-2508(91)90109-N

D'Avila, H., Melo, R. C., Parreira, G. G., Werneck-Barroso, E. H. C., Castro-Faria-Neto, and Bozza, P. T. (2006). *Mycobacterium bovis* bacillus Calmette-Guerin induces TLR2-mediated formation of lipid bodies: intracellular domains for eicosanoid synthesis *in vivo*. *J. Immunol.* 176, 3087–3097. doi: 10.4049/jimmunol.176.5.3087

Day, T. A., Mittler, J. E., Nixon, M. R., Thompson, C., Miner, M. D., Hickey, M. J., et al. (2014). *Mycobacterium tuberculosis* strains lacking surface lipid phthiocerol dimycocerosate are susceptible to killing by an early innate host response. *Infect. Immun.* 82, 5214–5222. doi: 10.1128/IAI.01340-13

Decostere, A., Hermans, K., and Haesebrouck, F. (2004). Piscine mycobacteriosis: a literature review covering the agent and the disease it causes in fish and humans. *Vet. Microbiol.* 99, 159–166. doi: 10.1016/j.vetmic.2003.07.011

DeJesus, M. A., Gerrick, E. R., Xu, W., Park, S. W., Long, J. E., Boutte, C. C., et al. (2017a). Comprehensive essentiality analysis of the *Mycobacterium tuberculosis* genome via saturating transposon mutagenesis. *MBio* 8, e02133-16. doi: 10.1128/mBio.02133-16

DeJesus, M. A., and Ioerger, T. R. (2013). A Hidden Markov Model for identifying essential and growth-defect regions in bacterial genomes from transposon insertion sequencing data. *BMC Bioinformatics* 14:303. doi: 10.1186/1471-2105-14-303

DeJesus, M. A., Nambi, S., Smith, C. M., Baker, R. E., Sassetti, C. M., and Ioerger, T. R. (2017b). Statistical analysis of genetic interactions in Tn-Seq data. *Nucleic Acids Res.* 45:e93. doi: 10.1093/nar/gkx128

DeJesus, M. A., Zhang, Y. J., Sassetti, C. M., Rubin, E. J., Sacchettini, J. C., and Ioerger, T. R. (2013). Bayesian analysis of gene essentiality based on sequencing of transposon insertion libraries. *Bioinformatics* 29, 695–703. doi: 10.1093/bioinformatics/btt043

de Jonge, M. I., Pehau-Arnaudet, G., Fretz, M. M., Romain, F., Bottai, D., Brodin, P., et al. (2007). ESAT-6 from *Mycobacterium tuberculosis* dissociates from its putative chaperone CFP-10 under acidic conditions and exhibits membrane-lysing activity. *J. Bacteriol.* 189, 6028–6034. doi: 10.1128/JB.00469-07

Delincé, M. J., Bureau, J. B., López-Jiménez, A. T., Cosson, P., Soldati, T., and McKinney, J. D. (2016). A microfluidic cell-trapping device for single-cell tracking of host-microbe interactions. *Lab Chip* 16, 3276–3285. doi: 10.1039/C6LC00649C

de Mattos, K. A., Sarno, E. N., Pessolani, M. C., and Bozza, P. T. (2012). Deciphering the contribution of lipid droplets in leprosy: multifunctional organelles with roles in Mycobacterium leprae pathogenesis. *Mem. Inst. Oswaldo Cruz* 107(Suppl. 1), 156–166. doi: 10.1590/S0074-02762012000900023

Derrick, S. C., and Morris, S. L. (2007). The ESAT6 protein of *Mycobacterium tuberculosis* induces apoptosis of macrophages by activating caspase expression. *Cell. Microbiol.* 9, 1547–1555. doi: 10.1111/j.1462-5822.2007.00892.x

dictyBase (2004). *dictyBase*. Available online at: http://dictybase.org/

Dionne, M. S., Ghori, N., and Schneider, D. S. (2003). *Drosophila melanogaster* is a genetically tractable model host for *Mycobacterium marinum*. *Infect. Immun.* 71, 3540–3550. doi: 10.1128/IAI.71.6.3540-3550.2003

Dominguez-Martin, E., Cardenal-Munoz, E., King, J. S., Soldati, T., Coria, R., and Escalante, R. (2017). Methods to monitor and quantify autophagy in the social amoeba *Dictyostelium discoideum*. *Cells* 6:18. doi: 10.3390/cells6030018

Dormann, D., Vasiev, B., and Weijer, C. J. (2000). The control of chemotactic cell movement during *Dictyostelium morphogenesis*. *Philos. Trans. R. Soc. Lond. B Biol. Sci.* 355, 983–991. doi: 10.1098/rstb.2000.0634

Du, F., Edwards, K., Shen, Z., Sun, B., De Lozanne, A., Briggs, S., et al. (2008). Regulation of contractile vacuole formation and activity in Dictyostelium. *EMBO J.* 27, 2064–2076. doi: 10.1038/emboj.2008.131

Du, X., Barisch, C., Paschke, P., Herrfurth, C., Bertinetti, O., Pawolleck, N., et al. (2013). Dictyostelium lipid droplets host novel proteins. *Eukaryot. Cell* 12, 1517–1529. doi: 10.1128/EC.00182-13

Duleh, S. N., and Welch, M. D. (2010). WASH and the Arp2/3 complex regulate endosome shape and trafficking. *Cytoskeleton* 67, 193–206. doi: 10.1002/cm.20437

Dumas, F., and Haanappel, E. (2017). Lipids in infectious diseases - The case of AIDS and tuberculosis. *Biochim. Biophys. Acta* 1859(9 Pt B), 1636–1647. doi: 10.1016/j.bbamem.2017.05.007

Dunn, J. D., Bosmani, C., Barisch, C., Raykov, L., Lefrançois, L. H., Cardenal-Muñoz, E., et al. (2018). Eat prey, live: *Dictyostelium discoideum* as a model for cell-autonomous defenses. *Front. Immunol.* 8:1906. doi: 10.3389/fimmu.2017.01906

Eichinger, L., Pachebat, J. A., Glockner, G., Rajandream, M. A., Sucgang, R., Berriman, M., et al. (2005). The genome of the social amoeba *Dictyostelium discoideum*. *Nature* 435, 43–57. doi: 10.1038/nature03481

Eichinger, L., and Rivero, F. (2013). *Dictyostelium discoideum Protocols. Methods in Molecular Biology,* Vol. 57. Heidelberg: Humana Press; Springer Verlag.

Eitle, E., Keller, T., Parish, C. R., and Parish, R. W. (1993). Polysaccharides influence the aggregation of *Dictyostelium discoideum* cells and bind to developmentally regulated cell surface proteins. *Exp. Cell Res.* 205, 374–382. doi: 10.1006/excr.1993.1100

Friedrich, N., Hagedorn, M., Soldati-Favre, D., and Soldati, T. (2012). Prison break: pathogens' strategies to egress from host cells. *Microbiol. Mol. Biol. Rev.* 76, 707–720. doi: 10.1128/MMBR.00024-12

Gao, L. Y., Guo, S., McLaughlin, B., Morisaki, H., Engel, J. N., and Brown, E. J. (2004). A mycobacterial virulence gene cluster extending RD1 is required for cytolysis, bacterial spreading and ESAT-6 secretion. *Mol. Microbiol.* 53, 1677–1693. doi: 10.1111/j.1365-2958.2004.04261.x

Gerasimova, A., Kazakov, A. E., Arkin, A. P., Dubchak, I., and Gelfand, M. S. (2011). Comparative genomics of the dormancy regulons in mycobacteria. *J. Bacteriol.* 193, 3446–3452. doi: 10.1128/JB.00179-11

Gerstenmaier, L., Pilla, R., Herrmann, L., Herrmann, H., Prado, M., Villafano, G. J., et al. (2015). The autophagic machinery ensures nonlytic transmission of mycobacteria. *Proc. Natl. Acad. Sci. U.S.A.* 112, E687–E692. doi: 10.1073/pnas.1423318112

Gey Van Pittius, N. C., Gamieldien, J., Hide, W., Brown, G. D., Siezen, R. J., and Beyers, A. D. (2001). The ESAT-6 gene cluster of *Mycobacterium tuberculosis* and other high G+C Gram-positive bacteria. *Genome Biol.* 2:RESEARCH0044.

Griffin, J. E., Gawronski, J. D., Dejesus, M. A., Ioerger, T. R., Akerley, B. J., and Sassetti, C. M. (2011). High-resolution phenotypic profiling defines genes essential for mycobacterial growth and cholesterol catabolism. *PLoS Pathog.* 7:e1002251. doi: 10.1371/journal.ppat.1002251

Groschel, M. I., Sayes, F., Simeone, R., Majlessi, L., and Brosch, R. (2016). ESX secretion systems: mycobacterial evolution to counter host immunity. *Nat. Rev. Microbiol.* 14, 677–691. doi: 10.1038/nrmicro.2016.131

Hagedorn, M., Rohde, K. H., Russell, D. G., and Soldati, T. (2009). Infection by tubercular mycobacteria is spread by nonlytic ejection from their amoeba hosts. *Science* 323, 1729–1733. doi: 10.1126/science.1169381

Hagedorn, M., and Soldati, T. (2007). Flotillin and RacH modulate the intracellular immunity of Dictyostelium to *Mycobacterium marinum* infection. *Cell. Microbiol.* 9, 2716–2733. doi: 10.1111/j.1462-5822.2007.00993.x

Hammond, R. J., Baron, V. O., Oravcova, K., Lipworth, S., and Gillespie, S. H. (2015). Phenotypic resistance in mycobacteria: is it because I am old or fat that I resist you? *J. Antimicrob. Chemother.* 70, 2823–2827. doi: 10.1093/jac/dkv178

Houben, D., Demangel, C., van Ingen, J., Perez, J., Baldeon, L., Abdallah, A. M., et al. (2012). ESX-1-mediated translocation to the cytosol controls virulence of mycobacteria. *Cell. Microbiol.* 14, 1287–1298. doi: 10.1111/j.1462-5822.2012.01799.x

Houben, E. N., Korotkov, K. V., and Bitter, W. (2014). Take five - Type VII secretion systems of Mycobacteria. *Biochim. Biophys. Acta* 1843, 1707–1716. doi: 10.1016/j.bbamcr.2013.11.003

Hsu, T., Hingley-Wilson, S. M., Chen, B., Chen, M., Dai, A. Z., Morin, P. M., et al. (2003). The primary mechanism of attenuation of bacillus Calmette-Guerin is a loss of secreted lytic function required for invasion of lung interstitial tissue. *Proc. Natl. Acad. Sci. U.S.A.* 100, 12420–12425. doi: 10.1073/pnas.1635213100

Jackson, M. (2014). The mycobacterial cell envelope-lipids. *Cold Spring Harb. Perspect. Med.* 4:a021105 . doi: 10.1101/cshperspect.a021105

Jamwal, S. V., Mehrotra, P., Singh, A., Siddiqui, Z., Basu, A., and Rao, K. V. (2016). Mycobacterial escape from macrophage phagosomes to the cytoplasm represents an alternate adaptation mechanism. *Sci. Rep.* 6:23089. doi: 10.1038/srep23089

Jayachandran, R., Sundaramurthy, V., Combaluzier, B., Mueller, P., Korf, H., Huygen, K., et al. (2007). Survival of mycobacteria in macrophages is mediated by coronin 1-dependent activation of calcineurin. *Cell* 130, 37–50. doi: 10.1016/j.cell.2007.04.043

Kaku, T., Kawamura, I., Uchiyama, R., Kurenuma, T., and Mitsuyama, M. (2007). RD1 region in mycobacterial genome is involved in the induction of necrosis in infected RAW264 cells via mitochondrial membrane damage and ATP depletion. *FEMS Microbiol. Lett.* 274, 189–195. doi: 10.1111/j.1574-6968.2007.00838.x

Kenyon, A., Gavriouchkina, D., Zorman, J., Napolitani, G., Cerundolo, V., and Sauka-Spengler, T. (2017). Active nuclear transcriptome analysis reveals inflammasome-dependent mechanism for early neutrophil response to *Mycobacterium marinum*. *Sci. Rep.* 7:6505. doi: 10.1038/s41598-017-06099-x

Kicka, S., Trofimov, V., Harrison, C., Ouertatani-Sakouhi, H., McKinney, J., Scapozza, L., et al. (2014). Establishment and validation of whole-cell based fluorescence assays to identify anti-mycobacterial compounds using the *Acanthamoeba castellanii-Mycobacterium marinum* host-pathogen system. *PLoS ONE* 9:e87834. doi: 10.1371/journal.pone.0087834

Kimura, T., Jain, A., Choi, S. W., Mandell, M. A., Schroder, K., Johansen, T., et al. (2015). TRIM-mediated precision autophagy targets cytoplasmic regulators of innate immunity. *J. Cell Biol.* 210, 973–989. doi: 10.1083/jcb.201503023

King, J. S., Veltman, D. M., and Insall, R. H. (2011). The induction of autophagy by mechanical stress. *Autophagy* 7, 1490–1499. doi: 10.4161/auto.7.12.17924

Kinhikar, A. G., Verma, I., Chandra, D., Singh, K. K., Weldingh, K., Andersen, P., et al. (2010). Potential role for ESAT6 in dissemination of *M. tuberculosis* via human lung epithelial cells. *Mol. Microbiol.* 75, 92–106. doi: 10.1111/j.1365-2958.2009.06959.x

Kolonko, M., Geffken, A. C., Blumer, T., Hagens, K., Schaible, U. E., and Hagedorn, M. (2014). WASH-driven actin polymerization is required for efficient mycobacterial phagosome maturation arrest. *Cell. Microbiol.* 16, 232–246. doi: 10.1111/cmi.12217

Kreibich, S., Emmenlauer, M., Fredlund, J., Rämö, P., Munz, C., Dehio, C., et al. (2015). Autophagy proteins promote repair of endosomal membranes damaged by the Salmonella type three secretion system 1. *Cell Host Microbe* 18, 527–537. doi: 10.1016/j.chom.2015.10.015

Kuspa, A. (2006). Restriction enzyme-mediated integration (REMI) mutagenesis. *Methods Mol. Biol.* 346, 201–209. doi: 10.1385/1-59745-144-4:201

Kuspa, A., and Loomis, W. F. (1992). Tagging developmental genes in Dictyostelium by restriction enzyme-mediated integration of plasmid DNA. *Proc. Natl. Acad. Sci. U.S.A.* 89, 8803–8807. doi: 10.1073/pnas.89.18.8803

Lampe, E. O., Brenz, Y., Herrmann, L., Repnik, U., Griffiths, G., Zingmark, C., et al. (2015). Dissection of Francisella-host cell interactions in *Dictyostelium discoideum*. *Appl. Environ. Microbiol.* 82, 1586–1598. doi: 10.1128/AEM.02950-15

Lee, W., VanderVen, B. C., Fahey, R. J., and Russell, D. G. (2013). Intracellular *Mycobacterium tuberculosis* exploits host-derived fatty acids to limit metabolic stress. *J. Biol. Chem.* 288, 6788–6800. doi: 10.1074/jbc.M112.445056

Lelong, E., Marchetti, A., Gueho, A., Lima, W. C., Sattler, N., Molmeret, M., et al. (2011). Role of magnesium and a phagosomal P-type ATPase in intracellular bacterial killing. *Cell. Microbiol.* 13, 246–258. doi: 10.1111/j.1462-5822.2010.01532.x

Lerena, M. C., and Colombo, M. I. (2011). *Mycobacterium marinum* induces a marked LC3 recruitment to its containing phagosome that depends on a functional ESX-1 secretion system. *Cell. Microbiol.* 13, 814–835. doi: 10.1111/j.1462-5822.2011.01581.x

Loomis, W. F. (2014). Cell signaling during development of Dictyostelium. *Dev. Biol.* 391, 1–16. doi: 10.1016/j.ydbio.2014.04.001

Low, K. L., Rao, P. S., Shui, G., Bendt, A. K., Pethe, K., Dick, T., et al. (2009). Triacylglycerol utilization is required for regrowth of *in vitro* hypoxic nonreplicating *Mycobacterium bovis* bacillus Calmette-Guerin. *J. Bacteriol.* 191, 5037–5043. doi: 10.1128/JB.00530-09

Madley, I. C., and Hames, B. D. (1981). An analysis of discoidin I binding sites in *Dictyostelium discoideum* (NC4). *Biochem. J.* 200, 83–91. doi: 10.1042/bj2000083

Mandell, M. A., Jain, A., Arko-Mensah, J., Chauhan, S., Kimura, T., Dinkins, C., et al. (2014). TRIM proteins regulate autophagy and can target autophagic substrates by direct recognition. *Dev. Cell* 30, 394–409. doi: 10.1016/j.devcel.2014.06.013

Maniak, M. (2011). Dictyostelium as a model for human lysosomal and trafficking diseases. *Semin. Cell Dev. Biol.* 22, 114–119. doi: 10.1016/j.semcdb.2010.11.001

McGourty, K., Thurston, T. L., Matthews, S. A., Pinaud, L., Mota, L. J., and Holden, D. W. (2012). Salmonella inhibits retrograde trafficking of mannose-6-phosphate receptors and lysosome function. *Science* 338, 963–967. doi: 10.1126/science.1227037

McKinney, J. D., Höner zu Bentrup, K., Muñoz-Elías, E. J., Miczak, A., Chen, B., Chan, W. T., et al. (2000). Persistence of *Mycobacterium tuberculosis* in macrophages and mice requires the glyoxylate shunt enzyme isocitrate lyase. *Nature* 406, 735–738. doi: 10.1038/35021074

Mendum, T. A., Wu, H., Kierzek, A. M., and Stewart, G. R. (2015). Lipid metabolism and Type VII secretion systems dominate the genome scale virulence profile of *Mycobacterium tuberculosis* in human dendritic cells. *BMC Genomics* 16:372. doi: 10.1186/s12864-015-1569-2

Mesquita, A., Cardenal-Munoz, E., Dominguez, E., Munoz-Braceras, S., Nunez-Corcuera, B., Phillips, B. A., et al. (2016). Autophagy in Dictyostelium: mechanisms, regulation and disease in a simple biomedical model. *Autophagy* 13, 24–40. doi: 10.1080/15548627.2016.1226737

Mesquita, A., Tabara, L. C., Martinez-Costa, O., Santos-Rodrigo, N., Vincent, O., and Escalante, R. (2015). Dissecting the function of Atg1 complex in Dictyostelium autophagy reveals a connection with the pentose phosphate pathway enzyme transketolase. *Open Biol.* 5:150088. doi: 10.1098/rsob.150088

Miranda, E. R., Rot, G., Toplak, M., Santhanam, B., Curk, T., Shaulsky, G., et al. (2013). Transcriptional profiling of Dictyostelium with RNA sequencing. *Methods Mol. Biol.* 983, 139–171. doi: 10.1007/978-1-62703-302-2_8

Mukai, A., Ichiraku, A., and Horikawa, K. (2016). Reliable handling of highly A/T-rich genomic DNA for efficient generation of knockin strains of *Dictyostelium discoideum*. *BMC Biotechnol.* 16:37. doi: 10.1186/s12896-016-0267-8

Munoz-Elias, E. J., and McKinney, J. D. (2005). *Mycobacterium tuberculosis* isocitrate lyases 1 and 2 are jointly required for *in vivo* growth and virulence. *Nat. Med.* 11, 638–644. doi: 10.1038/nm1252

Nakatogawa, H. (2015). Regulated degradation: controlling the stability of autophagy gene transcripts. *Dev. Cell* 34, 132–134. doi: 10.1016/j.devcel.2015.07.002

Nalpas, N. C., Magee, D. A., Conlon, K. M., Browne, J. A., Healy, C., McLoughlin, K. E., et al. (2015). RNA sequencing provides exquisite insight into the manipulation of the alveolar macrophage by tubercle bacilli. *Sci. Rep.* 5:13629. doi: 10.1038/srep13629

Nambi, S., Long, J. E., Mishra, B. B., Baker, R., Murphy, K. C., Olive, A. J., et al. (2015). The oxidative stress network of *Mycobacterium tuberculosis* reveals coordination between radical detoxification systems. *Cell Host Microbe* 17, 829–837. doi: 10.1016/j.chom.2015.05.008

Nazarova, E. V., Montague, C. R., La, T., Wilburn, K. M., Sukumar, N., Lee, W., et al. (2017). Rv3723/LucA coordinates fatty acid and cholesterol uptake in *Mycobacterium tuberculosis*. *Elife* 6:e26969. doi: 10.7554/eLife.26969

Nichols, J. M., Veltman, D., and Kay, R. R. (2015). Chemotaxis of a model organism: progress with Dictyostelium. *Curr. Opin. Cell Biol.* 36, 7–12. doi: 10.1016/j.ceb.2015.06.005

Noad, J. A., von der Malsburg, Pathe, C., Michel, M. A., Komander, D., and Randow, F. (2017). LUBAC-synthesized linear ubiquitin chains restrict cytosol-invading bacteria by activating autophagy and NF-kappaB. *Nat. Microbiol.* 2:17063. doi: 10.1038/nmicrobiol.2017.63

Otto, G. P., Wu, M. Y., Kazgan, N., Anderson, O. R., and Kessin, R. H. (2004). Dictyostelium macroautophagy mutants vary in the severity of their developmental defects. *J. Biol. Chem.* 279, 15621–15629. doi: 10.1074/jbc.M311139200

Ouertatani-Sakouhi, H., Kicka, S., Chiriano, G., Harrison, C. F., Hilbi, H., Scapozza, L., et al. (2017). Inhibitors of *Mycobacterium marinum* virulence identified in a *Dictyostelium discoideum* host model. *PLoS ONE* 12:e0181121. doi: 10.1371/journal.pone.0181121

Pallen, M. J. (2002). The ESAT-6/WXG100 superfamily – and a new Gram-positive secretion system? *Trends Microbiol.* 10, 209–212. doi: 10.1016/S0966-842X(02)02345-4

Pandey, A. K., and Sassetti, C. M. (2008). Mycobacterial persistence requires the utilization of host cholesterol. *Proc. Natl. Acad. Sci. U.S.A.* 105, 4376–4380. doi: 10.1073/pnas.0711159105

Parikka, M., Hammaren, M. M., Harjula, S. K., Halfpenny, N. J., Oksanen, K. E., Lahtinen, M. J., et al. (2012). *Mycobacterium marinum* causes a latent infection that can be reactivated by gamma irradiation in adult zebrafish. *PLoS Pathog.* 8:e1002944. doi: 10.1371/journal.ppat.1002944

Patterson, D. J. (1980). Contractile vacuoles and associated structures: their organization and function. *Biol. Rev.* 55, 1–46. doi: 10.1111/j.1469-185X.1980.tb00686.x

Pean, C. B., Schiebler, M., Tan, S. W., Sharrock, J. A., Kierdorf, K., Brown, K. P., et al. (2017). Regulation of phagocyte triglyceride by a STAT-ATG2 pathway controls mycobacterial infection. *Nat. Commun.* 8:14642. doi: 10.1038/ncomms14642

Pethe, K., Swenson, D. L., Alonso, S., Anderson, J., Wang, C., and Russell, D. G. (2004). Isolation of *Mycobacterium tuberculosis* mutants defective in the arrest of phagosome maturation. *Proc. Natl. Acad. Sci. U.S.A.* 101, 13642–13647. doi: 10.1073/pnas.0401657101

Pettersson, B. M., Das, S., Behra, P. R., Jordan, H. R., Ramesh, M., Mallick, A., et al. (2015). Comparative sigma factor-mRNA levels in *Mycobacterium marinum* under stress conditions and during host infection. *PLoS ONE* 10:e0139823. doi: 10.1371/journal.pone.0139823

Peyron, P., Vaubourgeix, J., Poquet, Y., Levillain, F., Botanch, C., Bardou, F., et al. (2008). Foamy macrophages from tuberculous patients' granulomas constitute a nutrient-rich reservoir for *M. tuberculosis* persistence. *PLoS Pathog* 4:e1000204. doi: 10.1371/journal.ppat.1000204

Pym, A. S., Brodin, P., Brosch, R., Huerre, M., and Cole, S. T. (2002). Loss of RD1 contributed to the attenuation of the live tuberculosis vaccines *Mycobacterium bovis* BCG and *Mycobacterium microti*. *Mol. Microbiol.* 46, 709–717. doi: 10.1046/j.1365-2958.2002.03237.x

Quigley, J., Hughitt, V. K., Velikovsky, C. A., Mariuzza, R. A., El-Sayed, N. M., and Briken, V. (2017). The cell wall lipid PDIM contributes to phagosomal escape and host cell exit of *Mycobacterium tuberculosis*. *MBio* 8:e00148-17. doi: 10.1128/mBio.00148-17

Ramakrishnan, L. (2004). Using *Mycobacterium marinum* and its hosts to study tuberculosis. *Curr. Sci.* 86, 82–92. Available online at: https://iths.pure.elsevier.com/en/publications/using-mycobacterium-marinum-and-its-hosts-to-study-tuberculosis

Ramakrishnan, L., Federspiel, N. A., and Falkow, S. (2000). Granuloma-specific expression of Mycobacterium virulence proteins from the glycine-rich PE-PGRS family. *Science* 288, 1436–1439. doi: 10.1126/science.288.5470.1436

Raper, K. B. (1935). *Dictyostelium discoideum*, a new species of slime mold from decaying forest leaves. *J. Agric. Res.* 50, 135–147.

Renshaw, P. S., Lightbody, K. L., Veverka, V., Muskett, F. W., Kelly, G., Frenkiel, T. A., et al. (2005). Structure and function of the complex formed by the tuberculosis virulence factors CFP-10 and ESAT-6. *EMBO J.* 24, 2491–2498. doi: 10.1038/sj.emboj.7600732

Romagnoli, A., Etna, M. P., Giacomini, E., Pardini, M., Remoli, M. E., Corazzari, M., et al. (2012). ESX-1 dependent impairment of autophagic flux by *Mycobacterium tuberculosis* in human dendritic cells. *Autophagy* 8, 1357–1370. doi: 10.4161/auto.20881

Rosel, D., Khurana, T., Majithia, A., Huang, X., Bhandari, R., and Kimmel, A. R. (2012). TOR complex 2 (TORC2) in Dictyostelium suppresses phagocytic nutrient capture independently of TORC1-mediated nutrient sensing. *J. Cell. Sci.* 125(Pt 1), 37–48. doi: 10.1242/jcs.077040

Rosen, S. D., Kafka, J. A., Simpson, D. L., and Barondes, S. H. (1973). Developmentally regulated, carbohydrate-binding protein in *Dictyostelium discoideum*. *Proc. Natl. Acad. Sci. U.S.A.* 70, 2554–2557. doi: 10.1073/pnas.70.9.2554

Rosengarten, R. D., Santhanam, B., Fuller, D., Katoh-Kurasawa, M., Loomis, W. F., Zupan, B., et al. (2015). Leaps and lulls in the developmental transcriptome of *Dictyostelium discoideum*. *BMC Genomics* 16:294. doi: 10.1186/s12864-015-1491-7

Russell, D. G., Cardona, P. J., Kim, M. J., Allain, S., and Altare, F. (2009). Foamy macrophages and the progression of the human tuberculosis granuloma. *Nat. Immunol.* 10, 943–948. doi: 10.1038/ni.1781

Ryu, Y. J., Koh, W. J., and Daley, C. L. (2016). Diagnosis and treatment of nontuberculous mycobacterial lung disease: clinicians' perspectives. *Tuberc. Respir. Dis.* 79, 74–84. doi: 10.4046/trd.2016.79.2.74

Saliba, A. E., Santos S., and Vogel, J. (2017). New RNA-seq approaches for the study of bacterial pathogens. *Curr. Opin. Microbiol.* 35, 78–87. doi: 10.1016/j.mib.2017.01.001

Sattler, N., Monroy, R., and Soldati, T. (2013). Quantitative analysis of phagocytosis and phagosome maturation. *Methods Mol. Biol.* 983, 383–402. doi: 10.1007/978-1-62703-302-2_21

Schiestl, R. H., and Petes, T. D. (1991). Integration of DNA fragments by illegitimate recombination in Saccharomyces cerevisiae. *Proc. Natl. Acad. Sci. U.S.A.* 88, 7585–7589. doi: 10.1073/pnas.88.17.7585

Schmidt, O., and Teis, D. (2012). The ESCRT machinery. *Curr. Biol.* 22, R116–R120. doi: 10.1016/j.cub.2012.01.028

Schnappinger, D., Ehrt, S., Voskuil, M. I., Liu, Y., Mangan, J. A., Monahan, I. M., et al. (2003). Transcriptional adaptation of *Mycobacterium tuberculosis* within macrophages: insights into the phagosomal environment. *J. Exp. Med.* 198, 693–704. doi: 10.1084/jem.20030846

Schulze, R. J., Sathyanarayan, A., and Mashek, D. G. (2017). Breaking fat: the regulation and mechanisms of lipophagy. *Biochim. Biophys. Acta* 1862(10 Pt B), 1178–1187. doi: 10.1016/j.bbalip.2017.06.008

Senaratne, R. H., Sidders, B., Sequeira, P., Saunders, G., Dunphy, K., Marjanovic, O., et al. (2008). *Mycobacterium tuberculosis* strains disrupted in mce3 and mce4 operons are attenuated in mice. *J. Med. Microbiol.* 57(Pt 2), 164–170. doi: 10.1099/jmm.0.47454-0

Serafini, A., Boldrin, F., Palu, G., and Manganelli, R. (2009). Characterization of a *Mycobacterium tuberculosis* ESX-3 conditional mutant: essentiality and rescue by iron and zinc. *J. Bacteriol.* 191, 6340–6344. doi: 10.1128/JB.00756-09

Serafini, A., Pisu, D., Palu, G., Rodriguez, G. M., and Manganelli, R. (2013). The ESX-3 secretion system is necessary for iron and zinc homeostasis in *Mycobacterium tuberculosis*. *PLoS ONE* 8:e78351. doi: 10.1371/journal.pone.0078351

Shevchuk, O., Batzilla, C., Hagele, S., Kusch, H., Engelmann, S., Hecker, M., et al. (2009). Proteomic analysis of Legionella-containing phagosomes isolated from Dictyostelium. *Int. J. Med. Microbiol.* 299, 489–508. doi: 10.1016/j.ijmm.2009.03.006

Siegrist, M. S., Steigedal, M., Ahmad, R., Mehra, A., Dragset, M. S., Schuster, B. M., et al. (2014). Mycobacterial Esx-3 requires multiple components for iron acquisition. *MBio* 5, e01073–e01014. doi: 10.1128/mBio.01073-14

Siegrist, M. S., Unnikrishnan, M., McConnell, M. J., Borowsky, M., Cheng, T. Y., Siddiqi, N., et al. (2009). Mycobacterial Esx-3 is required for mycobactin-mediated iron acquisition. *Proc. Natl. Acad. Sci. U.S.A.* 106, 18792–18797. doi: 10.1073/pnas.0900589106

Simeone, R., Bobard, A., Lippmann, J., Bitter, W., Majlessi, L., Brosch, R., et al. (2012). Phagosomal rupture by *Mycobacterium tuberculosis* results in toxicity and host cell death. *PLoS Pathog.* 8:e1002507. doi: 10.1371/journal.ppat.1002507

Simeone, R., Sayes, F., Song, O., Groschel, M. I., Brodin, P., Brosch, R., et al. (2015). Cytosolic access of *Mycobacterium tuberculosis*: critical impact of phagosomal acidification control and demonstration of occurrence *in vivo*. *PLoS Pathog.* 11:e1004650. doi: 10.1371/journal.ppat.1004650

Singh, K. H., Jha, B., Dwivedy, A., Choudhary, E., AG. N., Ashraf, A., et al. (2017). Characterization of a secretory hydrolase from *Mycobacterium tuberculosis* sheds critical insight into host lipid utilization by *M. tuberculosis*. *J. Biol. Chem.* 292, 11326–11335. doi: 10.1074/jbc.M117.794297

Smith, E. W., Lima, W. C., Charette, S. J., and Cosson, P. (2010). Effect of starvation on the endocytic pathway in Dictyostelium cells. *Eukaryot. Cell* 9, 387–392. doi: 10.1128/EC.00285-09

Solomon, J. M., Leung, G. S., and Isberg, R. R. (2003). Intracellular replication of *Mycobacterium marinum* within *Dictyostelium discoideum*: efficient replication in the absence of host coronin. *Infect. Immun.* 71, 3578–3586. doi: 10.1128/IAI.71.6.3578-3586.2003

Sorensen, A. L., Nagai, S., Houen, G., Andersen, P., and Andersen, A. B. (1995). Purification and characterization of a low-molecular-mass T-cell antigen secreted by *Mycobacterium tuberculosis*. *Infect. Immun.* 63, 1710–1717.

Srinivasan, L., Ahlbrand, S., and Briken, V. (2014). Interaction of *Mycobacterium tuberculosis* with host cell death pathways. *Cold Spring Harb. Perspect. Med.* 4:a022459. doi: 10.1101/cshperspect.a022459

Stamm, L. M., Morisaki, J. H., Gao, L. Y., Jeng, R. L., McDonald, K. L., Roth, R., et al. (2003). *Mycobacterium marinum* escapes from phagosomes and is propelled by actin-based motility. *J. Exp. Med.* 198, 1361–1368. doi: 10.1084/jem.20031072

Steiner, B., Weber, S., and Hilbi, H. (2017). Formation of the Legionella-containing vacuole: phosphoinositide conversion, GTPase modulation and ER dynamics. *Int. J. Med. Microbiol.* doi: 10.1016/j.ijmm.2017.08.004

Stevense, M., Chubb, J. R., and Muramoto, T. (2011). Nuclear organization and transcriptional dynamics in Dictyostelium. *Dev. Growth Differ.* 53, 576–586. doi: 10.1111/j.1440-169X.2011.01271.x

Stewart, G. R., Patel, J., Robertson, B. D., Rae, A., and Young, D. B. (2005). Mycobacterial mutants with defective control of phagosomal acidification. *PLoS Pathog.* 1, 269–278. doi: 10.1371/journal.ppat.0010033

Stinear, T. P., Jenkin, G. A., Johnson, P. D., and Davies, J. K. (2000). Comparative genetic analysis of *Mycobacterium ulcerans* and *Mycobacterium marinum* reveals evidence of recent divergence. *J. Bacteriol.* 182, 6322–6330. doi: 10.1128/JB.182.22.6322-6330.2000

Stinear, T. P., Seemann, T., Harrison, P. F., Jenkin, G. A., Davies, J. K., Johnson, P. D., et al. (2008). Insights from the complete genome sequence of *Mycobacterium marinum* on the evolution of *Mycobacterium tuberculosis*. *Genome Res.* 18, 729–741. doi: 10.1101/gr.075069.107

Tan, T., Lee, W. L., Alexander, D. C., Grinstein, S., and Liu, J. (2006). The ESAT-6/CFP-10 secretion system of *Mycobacterium marinum* modulates phagosome maturation. *Cell. Microbiol.* 8, 1417–1429. doi: 10.1111/j.1462-5822.2006.00721.x

Tattoli, I., Philpott, D. J., and Girardin, S. E. (2012a). The bacterial and cellular determinants controlling the recruitment of mTOR to the Salmonella-containing vacuole. *Biol. Open* 1, 1215–1225. doi: 10.1242/bio.201 22840

Tattoli, I., Sorbara, M. T., Vuckovic, D., Ling, A., Soares, F., Carneiro, L. A., et al. (2012b). Amino acid starvation induced by invasive bacterial pathogens triggers an innate host defense program. *Cell Host Microbe* 11, 563–575. doi: 10.1016/j.chom.2012.04.012

Thiam, A. R., Farese, R. V. Jr., and Walther, T. C. (2013). The biophysics and cell biology of lipid droplets. *Nat. Rev. Mol. Cell Biol.* 14, 775–786. doi: 10.1038/nrm3699

Thurston, T. L., Boyle, K. B., Allen, M., Ravenhill, B. J., Karpiyevich, M., Bloor, S., et al. (2016). Recruitment of TBK1 to cytosol-invading Salmonella induces WIPI2-dependent antibacterial autophagy. *EMBO J.* 35, 1779–1792. doi: 10.15252/embj.201694491

Thurston, T. L., Ryzhakov, G., Bloor, S., von Muhlinen, N., and Randow, F. (2009). The TBK1 adaptor and autophagy receptor NDP52 restricts the proliferation of ubiquitin-coated bacteria. *Nat. Immunol.* 10, 1215–1221. doi: 10.1038/ni.1800

Tobin, D. M., and Ramakrishnan, L. (2008). Comparative pathogenesis of *Mycobacterium marinum* and *Mycobacterium tuberculosis*. *Cell. Microbiol.* 10, 1027–1039. doi: 10.1111/j.1462-5822.2008.01133.x

Tonjum, T., Welty, D. B., Jantzen, E., and Small, P. L. (1998). Differentiation of *Mycobacterium ulcerans*, *M. marinum*, and *M. haemophilum*: mapping of their relationships to *M. tuberculosis* by fatty acid profile analysis, DNA-DNA hybridization, and 16S rRNA gene sequence analysis. *J. Clin. Microbiol.* 36, 918–925.

Tosetti, N., Croxatto, A., and Greub, G. (2014). Amoebae as a tool to isolate new bacterial species, to discover new virulence factors and to study the host-pathogen interactions. *Microb. Pathog.* 77, 125–130. doi: 10.1016/j.micpath.2014.07.009

Trofimov, V., Kicka, S., Mucaria, S., Hanna, N., Ramon-Olayo, F., Vela-González Del Peral, L. et al. (in press). Phenotypic screening of antimycobacterial compounds in alternative infection models identifies anti-infectives and their molecular targets in cell wall-related pathways. *Sci. Rep.*

Unnikrishnan, M., Constantinidou, C., Palmer, T., and Pallen, M. J. (2017). The enigmatic Esx proteins: looking beyond Mycobacteria. *Trends Microbiol.* 25, 192–204. doi: 10.1016/j.tim.2016.11.004

Urwyler, S., Nyfeler, Y., Ragaz, C., Lee, H., Mueller, L. N., Aebersold, R., et al. (2009). Proteome analysis of Legionella vacuoles purified by magnetic immunoseparation reveals secretory and endosomal GTPases. *Traffic* 10, 76–87. doi: 10.1111/j.1600-0854.2008.00851.x

van Opijnen, T., Bodi, K. L., and Camilli, A. (2009). Tn-seq: high-throughput parallel sequencing for fitness and genetic interaction studies in microorganisms. *Nat. Methods* 6, 767–772. doi: 10.1038/nmeth.1377

van Opijnen, T., and Camilli, A. (2013). Transposon insertion sequencing: a new tool for systems-level analysis of microorganisms. *Nat. Rev. Microbiol.* 11, 435–442. doi: 10.1038/nrmicro3033

Veltman, D. M., Akar, G., Bosgraaf, L., and Van Haastert, P. J. (2009a). A new set of small, extrachromosomal expression vectors for *Dictyostelium discoideum*. *Plasmid* 61, 110–118. doi: 10.1016/j.plasmid.2008.11.003

Veltman, D. M., Keizer-Gunnink, I., and Haastert, P. J. (2009b). An extrachromosomal, inducible expression system for *Dictyostelium discoideum*. *Plasmid* 61, 119–125. doi: 10.1016/j.plasmid.2008.11.002

Volkman, H. E., Clay, H., Beery, D., Chang, J. C., Sherman, D. R., and Ramakrishnan, L. (2004). Tuberculous granuloma formation is enhanced by a mycobacterium virulence determinant. *PLoS Biol.* 2:e367. doi: 10.1371/journal.pbio.0020367

Wang, Q., Zhu, L., Jones, V., Wang, C., Hua, Y., Shi, X., et al. (2015). CpsA, a LytR-CpsA-Psr family protein in *Mycobacterium marinum*, is required for cell wall integrity and virulence. *Infect. Immun.* 83, 2844–2854. doi: 10.1128/IAI.03081-14

Wang, S., Dong, X., Zhu, Y., Wang, C., Sun, G., Luo, T., et al. (2013). Revealing of *Mycobacterium marinum* transcriptome by RNA-seq. *PLoS ONE* 8:e75828. doi: 10.1371/journal.pone.0075828

Watts, D. J., and Ashworth, J. M. (1970). Growth of myxameobae of the cellular slime mould *Dictyostelium discoideum* in axenic culture. *Biochem. J.* 119, 171–174. doi: 10.1042/bj1190171

Weber, S., and Hilbi, H. (2014). Live cell imaging of phosphoinositide dynamics during Legionella infection. *Methods Mol. Biol.* 1197, 153–167. doi: 10.1007/978-1-4939-1261-2_9

Weerdenburg, E. M., Abdallah, A. M., Rangkuti, F., Abd El Ghany, M., Otto, T. D., Adroub, S. A., et al. (2015). Genome-wide transposon mutagenesis indicates that *Mycobacterium marinum* customizes its virulence mechanisms

for survival and replication in different hosts. *Infect. Immun.* 83, 1778–1788. doi: 10.1128/IAI.03050-14

Westermann, A. J., Barquist, L., and Vogel, J. (2017). Resolving host-pathogen interactions by dual RNA-seq. *PLoS Pathog.* 13:e1006033. doi: 10.1371/journal.ppat.1006033

Wiegand, S., Kruse, J., Gronemann, S., and Hammann, C. (2011). Efficient generation of gene knockout plasmids for *Dictyostelium discoideum* using one-step cloning. *Genomics* 97, 321–325. doi: 10.1016/j.ygeno.2011.02.001

Williams, J. G. (2006). Transcriptional regulation of Dictyostelium pattern formation. *EMBO Rep.* 7, 694–698. doi: 10.1038/sj.embor.7400714

World Health Organization (2015). Global Tuberculosis Report 2015. Available online at: http://apps.who.int/iris/bitstream/10665/191102/1/9789241565059_eng.pdf

Wu, J., Ru, H. W., Xiang, Z. H., Jiang, J., Wang, Y. C., Zhang, L., et al. (2017). WhiB4 Regulates the PE/PPE gene family and is essential for virulence of *Mycobacterium marinum*. *Sci. Rep.* 7:3007. doi: 10.1038/s41598-017-03020-4

Wullschleger, S., Loewith, R., and Hall, M. N. (2006). TOR signaling in growth and metabolism. *Cell* 124, 471–484. doi: 10.1016/j.cell.2006.01.016

Yu, J., Tran, V., Li, M., Huang, X., Niu, C., Wang, D., et al. (2012). Both phthiocerol dimycocerosates and phenolic glycolipids are required for virulence of *Mycobacterium marinum*. *Infect. Immun.* 80, 1381–1389. doi: 10.1128/IAI.06370-11

Zhang, M., Chen, L., Wang, S., and Wang, T. (2009). Rab7: roles in membrane trafficking and disease. *Biosci. Rep.* 29, 193–209. doi: 10.1042/BSR20090032

Zhang, Q., Wang, D., Jiang, G., Liu, W., Deng, Q., Li, X., et al. (2016). EsxA membrane-permeabilizing activity plays a key role in mycobacterial cytosolic translocation and virulence: effects of single-residue mutations at glutamine 5. *Sci. Rep.* 6:32618. doi: 10.1038/srep32618

Zhang, Y. J., Ioerger, T. R., Huttenhower, C., Long, J. E., Sassetti, C. M., Sacchettini, J. C., et al. (2012). Global assessment of genomic regions required for growth in *Mycobacterium tuberculosis*. *PLoS Pathog.* 8:e1002946. doi: 10.1371/journal.ppat.1002946

Zimmermann, M., Kogadeeva, M., Gengenbacher, M., McEwen, G., Mollenkopf, H. J., Zamboni, N., et al. (2017). Integration of metabolomics and transcriptomics reveals a complex diet of *Mycobacterium tuberculosis* during early macrophage infection. *mSystems* 2:e00057-17. doi: 10.1128/mSystems.00057-17

Conflict of Interest Statement: The authors declare that the research was conducted in the absence of any commercial or financial relationships that could be construed as a potential conflict of interest.

frontiers in Cellular and Infection Microbiology

ORIGINAL RESEARCH
published: 11 January 2018
doi: 10.3389/fcimb.2017.00536

Differential Effects of Iron, Zinc, and Copper on *Dictyostelium discoideum* Cell Growth and Resistance to *Legionella pneumophila*

Simona Buracco[1], *Barbara Peracino*[1], *Claudia Andreini*[2], *Enrico Bracco*[3] *and Salvatore Bozzaro*[1]*

[1] Department of Clinical and Biological Sciences, University of Torino, Turin, Italy, [2] Magnetic Resonance Center (CERM), University of Florence, Florence, Italy, [3] Department of Oncology, University of Torino, Turin, Italy

Iron, zinc, and copper play fundamental roles in eucaryotes and procaryotes, and their bioavailability regulates host-pathogen interactions. For intracellular pathogens, the source of metals is the cytoplasm of the host, which in turn manipulates intracellular metal traffic following pathogen recognition. It is established that iron is withheld from the pathogen-containing vacuole, whereas for copper and zinc the evidence is unclear. Most infection studies in mammals have concentrated on effects of metal deficiency/overloading at organismal level. Thus, zinc deficiency or supplementation correlate with high risk of respiratory tract infection or recovery from severe infection, respectively. Iron, zinc, and copper deficiency or overload affects lymphocyte proliferation/maturation, and thus the adaptive immune response. Whether they regulate innate immunity at macrophage level is open, except for iron. The early identification in a mouse mutant susceptible to mycobacterial infection of the iron transporter Nramp1 allowed dissecting Nramp1 role in phagocytes, from the social amoeba *Dictyostelium* to macrophages. Nramp1 regulates iron efflux from the phagosomes, thus starving pathogenic bacteria for iron. Similar studies for zinc or copper are scant, due to the large number of copper and zinc transporters. In *Dictyostelium*, zinc and copper transporters include 11 and 6 members, respectively. To assess the role of zinc or copper in *Dictyostelium*, cells were grown under conditions of metal depletion or excess and tested for resistance to *Legionella pneumophila* infection. Iron shortage or overload inhibited *Dictyostelium* cell growth within few generations. Surprisingly, zinc or copper depletion failed to affect growth. Zinc or copper overloading inhibited cell growth at, respectively, 50- or 500-fold the physiological concentration, suggesting very efficient control of their homeostasis, as confirmed by Inductively Coupled Plasma Mass Spectrometry quantification of cellular metals. *Legionella* infection was inhibited or enhanced in cells grown under iron shortage or overload, respectively, confirming a major role for iron in controlling resistance to pathogens. In contrast, zinc and copper

OPEN ACCESS

Edited by:
Thierry Soldati,
Université de Genève, Switzerland

Reviewed by:
Olivier Neyrolles,
Centre National de la Recherche Scientifique (CNRS), France
Hubert Hilbi,
University of Zurich, Switzerland

***Correspondence:**
Salvatore Bozzaro
salvatore.bozzaro@unito.it

Received: *31 October 2017*
Accepted: *26 December 2017*
Published: *11 January 2018*

Citation:
Buracco S, Peracino B, Andreini C, Bracco E and Bozzaro S (2018) Differential Effects of Iron, Zinc, and Copper on Dictyostelium discoideum Cell Growth and Resistance to Legionella pneumophila. Front. Cell. Infect. Microbiol. 7:536. doi: 10.3389/fcimb.2017.00536

depletion or excess during growth did not affect *Legionella* infection. Using Zinpyr-1 as fluorescent sensor, we show that zinc accumulates in endo-lysosomal vesicles, including phagosomes, and the contractile vacuole. Furthermore, we provide evidence for permeabilization of the *Legionella*-containing vacuole during bacterial proliferation.

Keywords: *Dictyostelium discoideum*, *Legionella pneumophila*, host-pathogen interactions, phagocytosis, Nramp1, NrampB, divalent metals, Zinpyr-1

INTRODUCTION

Transition metals, such as iron, zinc, copper, or manganese, play fundamental roles in many biological processes in both procaryotes and eucaryotes. Thanks to their ability to easily shift between different oxidation states, they act as co-factors of enzymes, and it is estimated that 30–45% of known enzymes are metalloproteins containing one of these metals (Andreini et al., 2008; Waldron et al., 2009). Among the transition metals, iron is the most abundant in living organisms. By shifting between the ferric and the ferrous forms, iron catalyzes redox reactions that are essential for processes such as respiration, oxygen transport, metabolic energy production, and gene regulation (Andreini et al., 2008; Pantopoulos et al., 2012). Whereas, iron is mostly present in the environment as insoluble ferric form, copper is easily bioavailable in the soluble Cu^{2+} cupric form (Festa and Thiele, 2011). Similarly to iron, copper is involved in redox reactions, regulating the activity of enzymes, such as the respiratory chain cytochrome c oxidase and the Cu-Zn superoxide dismutase (Tapiero and Tew, 2003; Rubino and Franz, 2012). Zinc is the second most abundant transition metal in living organisms after iron, is incorporated in about 10% of human proteins and necessary for over 300 enzymes (Andreini et al., 2011). In contrast to iron and copper, zinc is redox-inert, but has many structural and catalytic roles, stabilizing negative charges of the substrates or organizing protein subdomains in zinc motifs (Tapiero and Tew, 2003; Cerasi et al., 2013; Maret, 2013).

Excess iron, copper, or zinc are toxic, as they perturb the redox potential, producing highly reactive hydroxyl radicals (copper and iron), bind to sulfide and thiol groups, thus destabilizing iron-sulfur clusters (copper and zinc), or interfere with the metabolism of other ions, displacing them from their binding proteins (Letelier et al., 2005; Dupont et al., 2011; Imlay, 2014). Thus, cells have developed complex mechanisms to regulate import, export, and storage of transition metals (Stafford et al., 2013; Bird, 2015; Weiss and Carver, 2017).

Tight regulation of transition metal bioavailability is also a vital part of host-pathogen interactions. In bacteria, transition metals are involved in metabolism and regulation of virulence as a mechanism of host invasion, and many opportunistic pathogens, such as pathogenic strains of *Escherichia* or *Klebsiella*, *Mycobacteria*, *Salmonella*, or *Legionella*, have developed sophisticated sensing, uptake, and export mechanisms to accumulate transition metals according to their physiological needs (Graham et al., 2009; Dupont et al., 2011; Rowland and Niederweis, 2012; Porcheron et al., 2013; Braymer and Giedroc, 2014; Neyrolles et al., 2015; Skaar and Raffatellu, 2015; Capdevila et al., 2016).

The source of transition metals for intracellular pathogens is the cytoplasm of the host cell, which in turn can manipulate metal uptake and intracellular traffic following pathogen recognition. Several lines of evidence support the notion that iron and manganese are withheld from the phagosome, or the pathogen-containing vacuole, to prevent reconstruction by the engulfed bacteria of Fe-S clusters and the use of Mn^{2+} as a protectant against reactive oxygen species (Weinberg, 2000; Kehres and Maguire, 2003; Nairz et al., 2010; Lisher and Giedroc, 2013). Iron efflux from phagosomes by the Nramp1 transporter, both in mammalian macrophage and the lower professional phagocyte *Dictyostelium discoideum*, is such a paradigmatic case of starvation strategy, or so-called "nutritional immunity" (Appelberg, 2006; Cellier, 2012; Bozzaro et al., 2013a). In contrast to iron, copper, and zinc are presumably used as a mechanism to poison bacterial pathogens (Wagner et al., 2005; White et al., 2009; Botella et al., 2012; Soldati and Neyrolles, 2012; Djoko et al., 2015), though zinc sequestration as antibacterial weapon has also been described (Stafford et al., 2013; Vignesh et al., 2013; Djoko et al., 2015; Besold et al., 2016). Copper withdrawal has been shown to play a role for resistance to fungal pathogens, raising the possibility that it may be used also for bacteria (Besold et al., 2016). Except for iron, most studies with mammals provide only indirect evidence of the role of copper or zinc in immune defense, while an understanding of the underlying processes at macrophage level is lacking or very limited (White et al., 2009). Indeed, most infection studies have concentrated on microbial mechanisms of defense against metal poisoning or on the effects of metal deficiency or overload at organismal level, both in laboratory animals and in epidemiological studies with humans (Prohaska and Lukasewycz, 1981; Chaturvedi and Henderson, 2014; Prasad, 2014; Pasricha and Drakesmith, 2016). These studies have shown the importance of zinc or copper for several physiological processes, including proper development of the immune system, lymphocyte differentiation, and adaptive immunity (Bonaventura et al., 2015; Weiss and Carver, 2017). Their role in cell-autonomous defense mechanisms, i.e., innate immunity, at the level of monocytes or macrophages, is less clear. It has been shown that both free zinc and copper accumulate in endosomal vesicles, including phagosomes, in response to inflammatory signals and mycobacterial infection (Wagner et al., 2005; Botella et al., 2011), and that silencing of the Cu-ATPase ATP7A impairs macrophage bactericidal activity (White et al., 2009). Enhanced expression of a mycobacterial P-type ATPase, CtpC, which favors zinc efflux, has been also reported, with a

ctpc-null mutant growing poorly in macrophages (Botella et al., 2011).

For assessing the role of zinc or copper, macrophage cell lines or explanted monocytes could be grown in defined serum-free media, which contain, however, traces of transition metals in addition to proprietary components. Addition of extracellular or intracellular metal chelators to circumvent this limitation often fails, as they are not specific for a given metal and may have other unknown effects, stripping metals from exposed cellular proteins (Kay, 2004). A valid alternative is the use of single-celled amoebae or protozoa, which are the natural hosts of many bacterial pathogens that occasionally infect animals or humans. It is generally recognized that the ability of many bacterial pathogens to grow in macrophages and cause animal or human diseases is a consequence of their adaptation and survival in the normally hostile amoeboid niche, which is the training ground for evolution of virulence traits (Greub and Raoult, 2004; Casadevall, 2008; Cosson and Soldati, 2008; Salah et al., 2009; Erken et al., 2013; Tosetti et al., 2014). An established amoeboid model organism for phagocytosis and host-pathogen interactions is the social amoeba *D. discoideum*. *Dictyostelium* cells are free-living soil amoebae that grow by engulfing and digesting bacteria, and as such they are potential hosts of pathogens (Bozzaro et al., 2008, 2013a; Cosson and Soldati, 2008). Being haploid and amenable to molecular genetic techniques, *Dictyostelium* offers many advantages for identifying and characterizing host genes involved in resistance to pathogens (Bozzaro and Eichinger, 2011). Studies in the last decade have shown that *Dictyostelium* cells share with mammalian macrophages not only the basic phagocytic machinery, but also many mechanisms of innate and nutritional immunity (Bozzaro et al., 2008, 2013a; Cosson and Soldati, 2008; Soldati and Neyrolles, 2012; Nasser et al., 2013; Gaudet et al., 2016). Concerning transition metals, *Dictyostelium* cells share with macrophages the expression of the Nramp1 iron transporter in the phagolysosome, which is essential for proton-driven iron efflux from the phagosome, thus potentially starving bacteria for iron and manganese (Forbes and Gros, 2003; Courville et al., 2006; Peracino et al., 2006; Buracco et al., 2015). In agreement with this function, *nramp1* KO mutants display increased susceptibility to infection by *L. pneumophila* and *M. avium* (Peracino et al., 2006). *L. pneumophila* was also shown to hinder H^+ V-ATPase, but not Nramp1, recruitment to the *Legionella*-containing macropinosome, thus manipulating Nramp1 activity (Peracino et al., 2010). *Dictyostelium* is also unique among amoebae and protozoa, for encoding in the genome a second Nramp protein, NrampB (formerly Nramp2), belonging to the prototypical Nramp family (Courville et al., 2006; Peracino et al., 2013). NrampB, is expressed in the membrane of the contractile vacuole, and, together with Nramp1, appears to regulate iron homeostasis by transporting iron across the membrane of the contractile vacuole. Mutants defective in NrampB display also increased susceptibility to *Legionella*, suggesting that perturbation of iron homeostasis affects host-pathogen interactions (Bozzaro et al., 2013a).

The *Dictyostelium* genome encodes three SLC31 (CTR) copper transporters, and three P-type Cu-ATPases, one of which is a homolog of the human ATP7A P-type ATPase (The Dictyostelium webpage: http://www.dictybase.org). Both ATP7A and the CTR protein p80 are localized in the plasma membrane and transitorily in phagosomes (Ravanel et al., 2001; Burlando et al., 2002; Hagedorn and Soldati, 2007). ATP7A activity in the plasma membrane is apparently responsible for the refractoriness of *Dictyostelium* cells to high copper concentrations in medium (Burlando et al., 2002; Balbo and Bozzaro, 2008), whereas its transient recruitment to the phagosomal membrane points to a potential involvement in pumping copper in the phagosomal lumen, favoring a potential toxic effect of this metal on bacteria (Hao et al., 2016). The p80 copper transporter could, instead, be involved in copper efflux from the phagosome, but no functional studies have been done in this regard. The zinc transporter family includes 11 members, with seven ZIP and four ZNT family members (Sunaga et al., 2008; The Dictyostelium webpage: http://www.dictybase.org), but no data are available on their localization in phagosome and their potential involvement in host-pathogen interactions.

To assess a role for zinc or copper in *Dictyostelium* phagocytosis and defense mechanisms against bacterial pathogens, and given the large number of transporters for these metals, we have followed in this paper a holistic approach, based on cultivation of wild type cells or Nramp1 knockout mutant in a minimal medium depleted of, or overloaded with either zinc, copper, or iron. The rationale is that extensive growth in media deprived of or with high content of a given metal, should results in either metal deficiency or overload in cells, thus potentially altering their resistance to pathogens. We show here that iron, but not copper or zinc deficiency affects cell growth. Metal excess results in inhibition of cell growth, with the cells being much more sensitive to iron than to copper or zinc overloading. Cells grown under iron depleting or overloading conditions, show, respectively, resistance to or exacerbation of *L. pneumophila* infection, whereas *Legionella* intracellular growth is unaltered by depletion or overloading with copper or zinc. Thus, it appears that zinc and copper, in contrast to iron, play a minor role in *Dictyostelium* resistance against *Legionella*. We provide also evidence for very tight regulation of copper and zinc homeostasis in *Dictyostelium*, which can in part explain these results, and for accumulation of free zinc ions in vesicles of the endo-lysosomal pathway and in the contractile vacuole.

MATERIALS AND METHODS

Cell and Bacterial Strains and Culture Methods

Dictyostelium discoideum parental strain AX2 and the Nramp1-KO mutant were used. The Nramp1-KO mutant or cells producing Nramp1-RFP and NrampB-RFP were generated previously in the lab (Peracino et al., 2006; Buracco et al., 2015). AX2 cells producing calnexin-GFP (Müller-Taubenberger, 2001) and the 389-2 vector for the expression of mRFPmars (Fischer et al., 2004) were provided by Annette Müller-Taubenberger. For generating AX2 cells producing CshA-RFP, the *cshA* gene

was cloned into the EcoR1 site of the 389-2 vector (C-terminal mRFPmars). AX2 cells producing CshA-RFP or RFP alone were generated by electroporation (Pang et al., 1999), and transformants were selected on plates in nutrient medium containing 10 μg/ml G418. All strains were cultured axenically in AX2 axenic medium (AX2M) (Watts and Ashworth, 1970) or in the growth media listed in **Table 1** (Franke and Kessin, 1977). In all cases, cells were grown in Erlenmayer flasks under shaking at 150 rpm at 22°C on a gyratory shaker in a climatic cabinet (Kueh ner, Basel, Switzerland) as previously described (Peracino et al., 2013). Blasticidin at the concentration of 10 μg/ml was added to the Nramp1-KO mutant. Cells producing GFP- or RFP-fused proteins were cultured in the presence of 10–30 μg/ml G418.

Escherichia coli B2 strain, *Klebsiella aerogenes,* and *Salmonella typhimurium* (ATCC number 14028) were used. Pre-cultures of bacteria were maintained in LB agar.

Legionella pneumophila Corby producing GFP or Ds-red Express were provided by Michael Steinert and grown on buffered charcoal yeast extract agar (BCYE; 10 g/l ACES, 10 g/l yeast extract, 2g/l activated charcoal powder, 15 g/l agar, 3.3 mM L-cysteine, 0.6 mM $Fe(NO_3)_3$ (Feeley et al., 1979) supplemented with 5 μg/ml chloramphenicol. Bacteria were incubated for 72 h at 37°C and 5% CO_2 (Fajardo et al., 2004; Peracino et al., 2013).

Cell Growth Assays

Exponentially growing AX2 cells were washed twice in 0.017 M Soerensen Na/K phosphate buffer (pH 6.0) and resuspended at a final concentration of 5×10^4 cells/ml in the different media listed in **Table 1**. The required metal concentration was added from a stock solution of the salt dissolved in water and filtered. For iron, the stock solution was freshly prepared to avoid formation of precipitates. Cells were grown under shaking and growth was assessed daily over a period of 1 to 3 weeks, when required by subculturing the cells in the same medium shortly before they reached the stationary phase. Cell number was counted using a hemocytometer Bürker chamber. For some experiments, growth was also assessed in M2 and M3 medium with addition of 50, 100, or 500 μM zinc extracellular chelator 2-{[Bis(2-pyridinylmethyl)amino]ethylamino}benzenesulfonic acid hydrate sodium salt ZX1 (Strem Chemicals Inc., Newburyport, USA) (Pan et al., 2011) or 50, 100, or 500 μM of copper extracellular chelator trientine hydrochloride (Sigma-Aldrich, St Louis, MO, USA).

TABLE 1 | Minimal media used for cell growth.

	Metal added (μM)		
	Fe	**Zn**	**Cu**
FM*	100	8	0.6
M1	0	8	0.6
M1+	10–200	8	0.6
M2	100	0	0.6
M2+	100	80–800	0.6
M3	100	8	0
M3+	100	8	6–600

**As indicated in the recipe of the FM medium defined in Franke and Kessin (1977). M1 to M3: medium composition as in FM, except for the metal indicated.*

Cell Development on Non-nutrient Agar Plates

AX2 cells were grown for 24 h in M1 ± Fe medium or for 480 h in M2 ± Zn or M3 ± Cu medium. Cells were then harvested from culture media, washed twice in Soerensen phosphate buffer and resuspended in the same buffer a concentration of 1×10^7 cells/ml. Aliquots of 50 μl were plated on agar plates buffered with Soerensen phosphate buffer at a density of about 3×10^5 cells per cm^2, and incubated at 23°C (Peracino et al., 2013). Images were acquired using a Wild M3Z Stereomicroscope (Wild Heerbrugg, Switzerland) supplied with a MicrOcular 3.0 MP Electronic Eyepiece (Bresser GmbH, Rhede, Germany).

Cell Growth on Bacteria

A single colony of bacteria was picked from plate and bacteria were grown in LB medium overnight with shaking. The next day, 50 μl of the bacterial culture were spread in each well of a 24-well N-agar (1 g of peptone, 1 g of glucose, 15 g of agar in 1 l of Soerensen phosphate buffer) for *E.coli B/2* and *S. typhimurium*, or SM-agar (10 g of bactopeptone, 1 g of yeast extract, 10 g of glucose, 1 g of $MgSO_4$ $7(H_2O)$, 2.5 g of KH_2PO_4, 1 g of Na_2HPO_4 $2(H_2O)$, 18 g of agar in 1 l of water) for *K. aerogenes*, and further grown overnight at 22°C. AX2 cells were grown as previously described in the minimal media listed in **Table 1**. Cells were then washed twice in Soerensen phosphate buffer and serial dilutions were plated on the dry bacterial lawn, as described in Froquet et al. (2008). Pictures of the appearance and widening of growth plaques were acquired daily with a scanner.

Legionella pneumophila Uptake and Infection Assays

AX2 or Nramp1-KO cells grown in the media listed in **Table 1** were washed twice in Soerensen phosphate buffer containing 50 μM CaCl2, resuspended in the corresponding culture medium without glucose containing 5 μg/ml chloramphenicol, and 1.0×10^5 cells were plated in 96-well tissue culture plates. For every condition, cells were tested in triplicates for a series of time points ranging from 0 to 96 hpi. As control, AX2 cells grown in axenic medium and resuspended in low fluorescence medium (LoFlo Medium supplemented with yeast extract, Formedium, Norfolk, UK) containing 5 μg/ml chloramphenicol were used. Freshly collected *L. pneumophila* Corby producing GFP were added to *Dictyostelium* cells at a MOI (Multiplicity Of Infection) of 1:1 and immediately centrifuged at 600 g for 10 min at room temperature to synchronize infection. Plates were incubated at 25°C and samples were collected every 24 h (Hägele et al., 2000; Skriwan et al., 2002). Uninfected cells were used as a control. Flow cytometry analysis was performed according to Tiaden et al. (2013), using a CyAn ADP Analyzer (Beckman Coulter, Brea, CA, USA). Cells were identified based on forward and side scatter parameters. GFP fluorescence was measured in the FL1

channel (excitation wavelength: 488 nm; emission: 530–540 nm), and the mean fluorescence was determined for at least 10,000 cells. For some experiments, 25 μM membrane-permeable zinc chelator N,N,N′,N′-Tetrakis(2-pyridylmethyl)ethylenediamine (TPEN) (Sigma-Aldrich, St Louis, MO, USA) was added to the infection medium.

For the uptake assay, cells were grown as described and infected with *L. pneumophila* Corby producing GFP at a MOI of 10:1. After centrifugation, cells were detached and analyzed by flow cytometry at 0 and 40 min post-infection. For every time, duplicates were tested and the percentage of fluorescent cells was recorded.

Data analysis was carried out using FlowJo software (FlowJo LLC, Oregon USA).

In Vivo Microscopy and Fluorescence Imaging

Cells infected with *L. pneumophila* producing GFP or Ds-red Express were plated in black 96-well tissue culture μ-plates (ibidi GmbH, Planegg/Martinsried, Germany) and incubated at 25°C. Confocal series images were taken daily on an inverted Zeiss LSM800 with AiryScan (Carl Zeiss, Inc., Oberkochen, Germany) equipped with a Plan-Apochromat 63x/1.40 DIC Oil-immersion objective. For excitation, a 488 nm Diode laser was used and its emission collected with a 495–519 nm filter for GFP and a 592–614 nm filter for RFP. Phase contrast was recorded simultaneously.

For monitoring zinc intracellular localization, cells producing Nramp1 or NrampB-RFP or AX2 cells mixed with TRITC-labeled *E. coli* (MOI 100:1) were used. Cells were washed and resuspended in Soerensen phosphate buffer and incubated for 30 min with 5 μM Zinpyr-1 fluorescent probe (Abcam, Cambridge, UK). Non-incorporated probe was removed by washing with Soerensen buffer and the cells were plated on glass coverslips. Images were acquired as previously described.

Metal Analysis by Inductively Coupled Plasma Mass Spectrometry (ICP-MS)

AX2 cells were grown for 24 h in M1 ± Fe medium or for 480 h in M2 ± Zn or M3 ± Cu media. A total of 10^8 cells were washed five times in Soerensen phosphate buffer and pelleted in Eppendorf tubes. Digestion was performed by adding 1 ml of concentrated HNO_3 (70%) to each sample. After complete dissolution, samples were further digested by applying microwave heating (Milestone MicroSYNTH, Microwave labstation equipped with an optical fiber temperature control and HPR-1000/6M six position high-pressure reactor, Bergamo, Italy). After digestion, the volume of each sample was brought to 3 ml with ultrapure water, filtered with 0.45 mm filter and analyzed by ICP-MS, using a Thermo Scientific ELEMENT 2 ICP-MS (Finnigan, Rodano, Italy) (Fiorito et al., 2012). The same analysis was also performed on 800 μl of M2 or M3 medium. The quantification was obtained through a calibration curve measured by using six Fe/Cu/Zn absorption standard solutions (Sigma-Aldrich) in the range 0.0025–0.3 μg/ml. Samples with metals concentrations higher than the upper limit were diluted opportunely. Sample digestion and metal quantifications were carried out by the facility of the Molecular Imaging Center (Department of Chemistry, University of Torino, Italy).

RESULTS

Effects of Transition Metal Depletion or Overloading on Growth of Wild Type AX2 Cells

We first investigated how alterations in the availability of iron, copper, or zinc would affect *Dictyostelium* cell growth. This was achieved by evaluating AX2 wild type cell growth in a defined FM minimal medium (Franke and Kessin, 1977), in which the concentrations of single metals was modified. The FM minimal medium contains 100 μM $FeCl_3$, 8 μM $ZnSO_4$, and 0.6 μM $CuSO_4$ (Franke and Kessin, 1977). We omitted or added to the original recipe one of these three metals at varying concentrations, as summarized in **Table 1**. AX2 cells exponentially growing in AX2 medium (AX2M) were diluted in these minimal media to an initial concentration of 5×10^4 cells/ml, and growth was evaluated under shaking for 1 to 3 weeks. As previously reported, cell growth is optimal at an iron concentration of 100 μM, but inhibited after a few generations if iron is omitted or the amount increased to 200 μM (**Figure 1A** and Peracino et al., 2010). In sharp contrast, cell growth up to 10^7/ml was unaffected in M2 or M3 medium or with up to 20- or 200-fold excess of zinc or copper, respectively, compared to control FM (**Figures 1B,C**). Higher concentrations of copper led to a delay in the rate of cell duplication and total inhibition with 1,000-fold excess (**Figure 1C**). In the case of zinc, a toxic effect was observed with 50 or 100-fold excess (**Figure 1B**).

To assess whether cell growth would be affected by prolonged incubation in medium without added zinc or copper or with high, but non-toxic, concentrations of zinc or copper, namely 20- or 200-fold excess, respectively, cells were re-diluted in the same medium, shortly before reaching the stationary phase, and cell growth measured over 480 h. As shown in **Figure 1D**, no significant changes in the rate of cell doubling time was observed. Thus, *Dictyostelium* cells appear to be very efficient in controlling high concentrations of copper or zinc. More surprising is that their growth rate is unaffected by depletion of either metal. A preliminary analysis of the metal proteome, by using a modified metal predator as bioinformatic tool (Valasatava et al., 2016), shows that the *Dictyostelium* genome encodes 840 zinc- and 250 iron-binding proteins, corresponding to 6.6 and 2%, respectively, of the entire proteome. There are fewer copper-binding proteins: about 40. Especially for zinc, one would expect that zinc shortage in the medium would have detrimental effects for the activity of the zinc-binding proteins, many of which are involved in basic cellular processes, such as transcription, translation, cell replication, and protein turnover. We thus tested whether incubation for 480 h, i.e., about 24 generations, in M2 or M3 medium led to a shrinkage in cell volume, but no significant changes in size with control cells were found (M2: 4.8 ± 0.9 μl; M3: 5.2 ± 1.5 μl; FM: 4.7 ± 1.8 μl, in all cases per 10^7 cells). Addition to M2 or M3 medium of extracellular zinc chelator

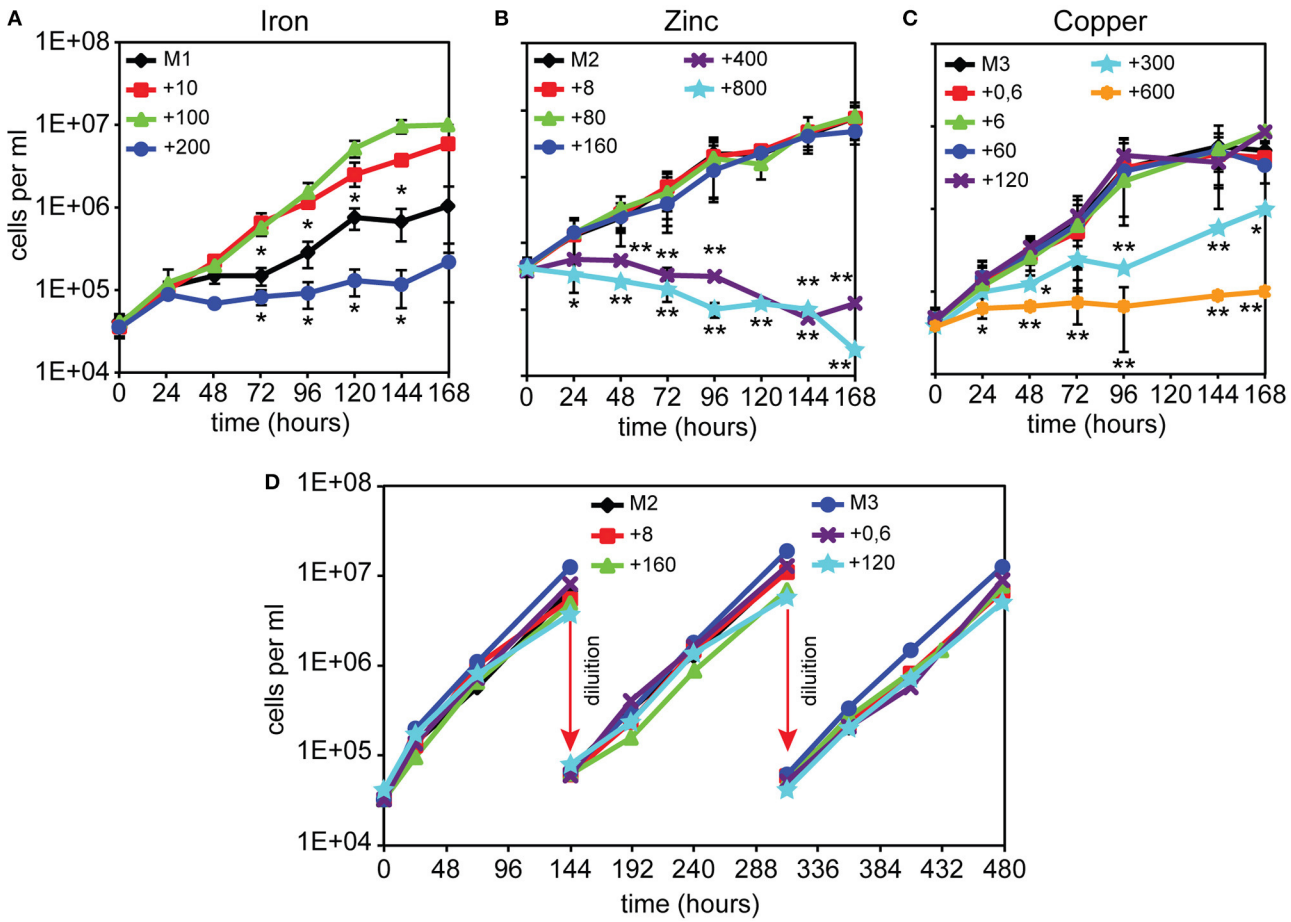

FIGURE 1 | *Dictyostelium* cell growth in minimal medium with or without $FeCl_3$, $ZnSO_4$, or $CuSO_4$ supplementation. **(A)** In the absence of iron, AX2 cells were able to replicate for 4–5 generations, albeit very slowly, before reaching a plateau. Cells grew well with 10 or 100 μM iron, whereas with 200 μM iron growth was impaired. Modified from Peracino et al. (2013). **(B–D)** Both zinc and copper deprivation did not affect AX2 cell replication. Only with 300 μM copper, growth was severely reduced and stopped completely at twice the concentration, while 400 and 800 μM zinc caused cell death. Exponentially growing AX2 cells were diluted in minimal medium with or without the indicated amounts of iron chloride **(A)**, zinc sulfate **(B)**, or copper sulfate **(C)**, incubated under shaking and counted for growth at the indicated times. **(D)** Cells were grown in the indicated amounts of zinc or copper and, before entering the stationary phase, subcultured by dilution for two additional weeks (arrows). For simplicity, only a few counts are shown. Mean values of at least three experiments with error bars (±SD) are shown. The asterisks denote significant difference compared with cells growth in minimal medium containing normal metal concentration (100 μM for iron, 8 μM for zinc, and 0.6 μM for copper). Two-tailed *t*-test assuming unequal variance: $*P < 0.05$, $**P < 0.01$. **(D)** Mean values of at least two experiments are shown. The numbers indicate metal concentration in μM. All media used are described in **Table 1**.

ZX1 or copper chelator trientine hydrochloride at concentrations varying between 50 and 500 μM also failed to affect cell growth.

Copper and Zinc Concentration in Cells Growing in Medium Depleted or Overloaded with Metals

Presuming there are no other sources of these metals in the medium, at any cell doubling the intracellular amount of iron, zinc, or copper should halve. Initially, cells contain the metals engulfed with the axenic medium and might undergo some duplication rounds, as observed for iron (**Figure 1A**), but this does not explain the ability of the cells to sustain more than 20 generations in the absence of external zinc or copper (**Figures 1B,C**). However, even in minimal medium without added metals, metal contamination cannot be excluded, particularly due to amino acids. Indeed most amino acids contain up to 0.5–5 ppm iron, zinc or copper, based on manufacturer sheets. In addition, metals can leach from the glassware and, depending on their composition, from some plastics used for cell culture and treatment (Kay, 2004).

To get an unbiased measure of the amount of zinc or copper in medium and in cells, we measured their concentrations by using Inductively Coupled Plasma Mass Spectrometry (ICP-MS). In the nominally metal-free M2 and M3 medium, 0.58 and 0.028 μM zinc or copper, respectively, were detected, amounting to 7.26 and 4.67% the concentration of zinc or copper, respectively, present in the standard FM medium (**Table 2**). When cells subcultured for 3 weeks in M2 or M3 medium were analyzed by ICP-MS, we found that 10^7 cells still contained about 84 or 3.1 ng of zinc

TABLE 2 | ICP-MS analysis of media.

	[Me] (μM)	
	Zn	**Cu**
FM*	8	0.6
M2	0.581	
M3		0.028

**The concentration of metals added to the FM medium are reported. The nominally metal-free media M2 and M3 were subjected to ICP-MS analysis as described in Material and Methods.*

TABLE 3 | Cellular metal content (ICP-MS).

Growth in:	Me/10^7 cells (ng)		
	Fe	**Zn**	**Cu**
AX2M	31.1 ± 19.1	93.5 ± 20.1	6 ± 0.1
FM	68.9 ± 0.3	96.2 ± 11.2	6 ± 0.4
M1	17.3 ± 0.2		
M2		84 ± 4.2	
M2+160		253.4 ± 10.5	
M3			3.1 ± 0.4
M3+120			14.6 ± 0.1

Total concentration of Zn or Cu measured by ICP-MS in lysates from cells grown for 24 h in M1 ± Fe or for 3 weeks in M2 ± Zn or M3 ± Cu. Cells growing in AX2M and FM were tested after 24 h for Fe, and 3 weeks for Zn and Cu. Data are means ± SD of one experiment in duplicate. The cell lysate concentrations are based on 10^8 cells in ∼130 μl.

or copper, respectively, i.e., about 87 and 51% of the amount present in cells growing in standard minimal medium or AX2 medium. In cells incubated with a 20 or 200-fold excess of zinc or copper, respectively, the cellular concentration increased of only 2.7- and 2.4-fold, respectively, compared to FM or AX2 medium (**Table 3**). Normalized for cell volume, the intracellular copper concentration in *Dictyostelium* is 6 ± 0.7 and 30.6 ± 0.3 μM for cells grown in, respectively, nominally copper-free medium or medium containing 120 μM Cu. The intracellular zinc concentration amounts to 243 ± 12.3 to 912 ± 37.7 μM in cells grown in, respectively, nominally zinc-free medium or in presence of 160 μM zinc. The intracellular values are, at least for zinc, comparable to those found in many eukaryotic cells (Krezel and Maret, 2006; Colvin et al., 2008; Vignesh et al., 2013; Kambe et al., 2015). While incubation in M2 or M3 medium slightly affected the intracellular amount of zinc or copper after 3 weeks of culture, just 24 h of growth in M1 medium (corresponding to 1 cell doubling) were sufficient to halve the iron cellular content (**Table 3**). ICP-MS analysis in cells incubated with excess of iron could not be performed for the persistence in the sample of iron precipitates that would bias the measure.

These results indicate that, unlike iron, *Dictyostelium* cells are extremely efficient in acquiring and storing copper and zinc, maintaining intracellular levels sufficient to support growth, even when the concentration of these metals, particularly zinc, in the medium is strongly reduced. Similarly, their high tolerance toward both zinc and copper toxicity seems to derive from their high efficiency in extruding excessive amounts of these metals from the cell.

Effects of Iron, Zinc, and Copper Shortage or Overload on Growth on Bacteria and Development

Cells previously grown under deficiency or overloading of iron, zinc, or copper were tested for development on agar. For iron, we employed the same conditions used for the growth assay (**Figure 1A**): cells were incubated in nominally iron-free M1 medium or with iron supplementation for 24 h, washed in Soerensen phosphate buffer and then analyzed for development. Cells grown in M1 developed normally. Cells grown in M1 plus 200 μM iron developed with normal timing (**Figure 2A**), but formed very large streams, which underwent fragmentation into multiple mounds that developed to fruiting bodies (**Figure 2B**). In the case of copper or zinc overloading, we tested concentrations that produced no toxic effects on cell growth, and the cells were grown for 3 weeks (**Figure 1D**), before being washed and assayed for development. Cells were able to develop and form fruiting bodies similarly to control cells, except for cells grown in M2 medium which failed to complete development and were arrested at the mound stage (**Figure 2A**). Cells grown in a 200-fold excess of copper formed loose mounds, which elongated to small fruiting bodies, though many cells failed to aggregate (**Figure 2A**).

To assess whether previous growth under metal deficiency or overloading affected phagocytosis and growth on non-pathogenic bacteria, cells grown as just described were also plated on agar with *E. coli B/2*, *K. aerogenes,* or *S. thyphimurium*, and the increase in size of the colonies scored every 24 h. The growth rate was similar for cells grown under iron, zinc, or copper deficiency or overload on all three bacterial lawns, indicating that phagocytosis and bacterial digestion are unaffected by the previous growth conditions of the cells. In all cases, fruiting bodies were also formed in the middle of the plaque (**Figure S1**).

Dynamics of *Legionella* Infection Analyzed by Flow Cytometry and Live-Cell Imaging

The effects of metal deficiency or overload on *Dictyostelium* resistance to pathogenic bacteria, was studied with *Legionella pneumophila*. *L. pneumophila* infection was monitored, as schematized in **Figure 3**, by confocal microscopy and by measuring in flow cytometry cellular fluorescence due to intracellular proliferation of GFP-producing bacteria, and cytotoxicity as changes in cellular physical parameters. In control cells grown in AX2 medium and incubated with *Legionella*, the intracellular fluorescence increased over time, reaching a peak 72 h post-infection (hpi), and decreasing thereafter (**Figure 4A**). Concomitantly, the percentage of dead cells (identified as a smaller and granulous population) incremented, exceeding 80% at 72–96 hpi (**Figure 4B**). Indeed, as observed by confocal microscopy, *Legionella* started to replicate inside the infected cells soon after its entry, with about 5–15 bacteria/cell 24 hpi, continuing to proliferate until filling almost completely

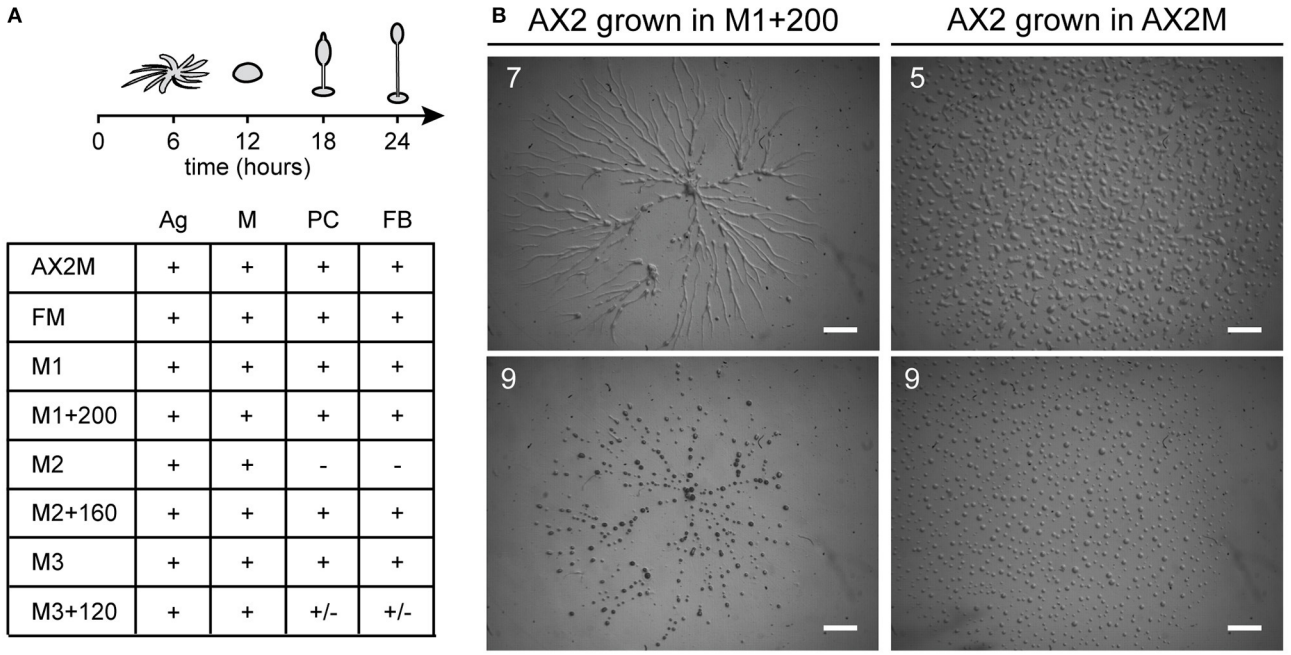

	Ag	M	PC	FB
AX2M	+	+	+	+
FM	+	+	+	+
M1	+	+	+	+
M1+200	+	+	+	+
M2	+	+	-	-
M2+160	+	+	+	+
M3	+	+	+	+
M3+120	+	+	+/-	+/-

FIGURE 2 | Effects of metal deficiency or overload on *Dictyostelium* development. AX2 cells were pre-incubated for 24 h in M1 ± Fe, or for 3 weeks in M2 ± Zn, or M3 ± Cu. Thereafter, cells were washed in Soerensen phosphate buffer, plated on non-nutrient phosphate agar and monitored over time in a stereomicroscope. **(A)** (Top) Schematic representation of development with timing: stream formation (aggregation, Ag), mounds (M), pre-culminants (PC), and mature fruiting bodies (FB). (Bottom) Developmental stages reached by cells grown in the indicated medium. Symbols indicate: "+" stage reached at the indicated time; "–" developmental stage not reached; "+/–" stage reached, but with alterations in time or morphology. Results from three different experiments. **(B)** AX2 cells grown in M1+200 for 24 h, in contrast to cells grown in AX2 medium (on the right), formed very elongated streams that fragmented in multiple mounds. The numbers indicate hours from the beginning of cell starvation. Scale bar: 1 mm.

the cell. The host cells lost the amoeboid form, rounding up and detaching from the bottom of the well by around 24 hpi. From 72 hpi, but strongly at 96 hpi, we noticed the presence of cellular debris and an increase in the number of extracellular bacteria, indicating cell lysis (**Figure 4C**). Under the conditions used, *Legionella* cannot grow extracellularly, thus an increase in the number of extracellular bacteria can only be the result of leakage from lysed cells. This explains also the reduction of cellular mean fluorescence measured at 96 hpi (**Figure 4A**).

After its entry, *L. pneumophila* forms a replication-permissive compartment inside the host cell, known as the *Legionella*-containing vacuole (LCV) (Horwitz, 1983; Lu and Clarke, 2005; Steiner et al., 2017). We observed that, even at later stages of infection, the bacteria appeared to be packed together, as if contained in a cellular compartment (**Figure 4C** and **Movie S1**). We infected *Dictyostelium* cells producing calnexin-GFP with a RFP-producing *Legionella* strain. Calnexin is an ER-specific protein that was previously demonstrated to be recruited to LCVs (Fajardo et al., 2004; Ragaz et al., 2008), where it remains for at least 8–14 hpi (Urwyler et al., 2009; Weber et al., 2014). Using this marker, we evidenced the presence of a membrane surrounding the large mass of replicating bacteria even at 48 hpi (**Figure 5A**), indicating that the LCV continues to tightly interact with the ER also at advanced stages of infection. The membrane integrity of the LCV was then evaluated by infecting cells producing free RFP or CshA-RFP. The citrate synthase CshA is a cytosolic protein, composed of 492 amino acid residues and containing a peroxisomal targeting PTS2 sequence, which by interacting with Pex7 leads to its transport to peroxisomes (Huang et al., 2004). In CshA-RFP producing cells peroxisomes are labeled, in addition to a diffused labeling of the cytosol, due to the synthesized, but not yet transported, protein. Cellular compartments whose membrane is not permeable appear as "black holes" in RFP or CshA-RFP producing cells. At 24 hpi the replicating legionellae were clearly contained within a RFP or CshA-RFP impermeable membrane (**Figures 5C,D**). In some cells the RFP or CshA-RFP labeling diffused between bacteria, suggesting that the LCV membrane had become permeable to the fluorescent proteins (**Figures 5C,D**). As infection progressed, the proportion of cells showing the latter condition increased. Since RFP is smaller than CshA-RFP (27 kDa vs. at least 75 kDa for the CshA-RFP non-complexed with Pex7), we calculated the percentage of LCVs showing co-localization of with either RFP or CshA-RFP at each time point. As shown in **Figure 5B**, at 24 hpi only 44% of LCVs were positive for CshA-RFP against 88% for RFP, with a gradual increase to 94 or 90% at 72 hpi for RFP or CshA-RFP, respectively. It is worth mentioning that no peroxisomes were found mixed with legionellae within the LCV, even at 72 hpi, but only free RFP or CshA-RFP.

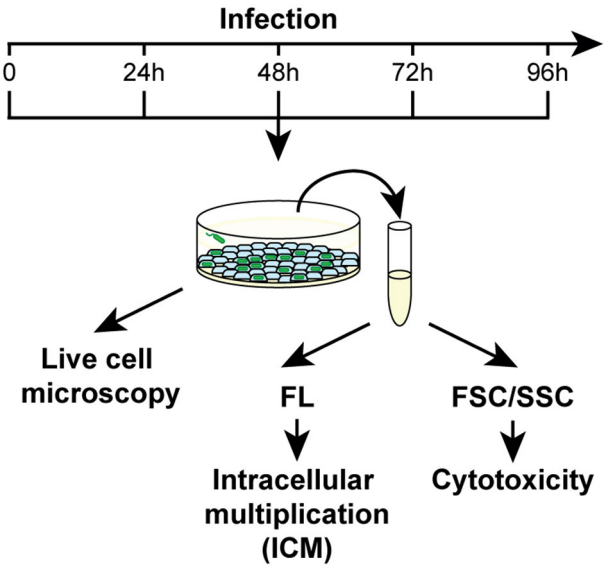

FIGURE 3 | Work flow for *Legionella* infection assays. *Dictyostelium* cells were infected with GFP producing *L. pneumophila* in 96-well plates at MOI 1:1 and analyzed daily by confocal microscopy or by flow cytometry. For the latter, two different parameters were acquired: the increase of mean fluorescence over time as a measure of the intracellular replication of bacteria, and changes in the FSC/SSC pattern as indicators of cytotoxicity. Concomitantly, cells were monitored by confocal microscopy. Abbreviations are as follows: *FL* fluorescence, *FSC/SSC* forward/sideward scatter channel.

From these data we conclude that the LCV continues to be surrounded by a membrane even at later stages of infection, with the membrane becoming gradually permeable to proteins of increasing molecular size between 24 and 72 h after its formation, with no egression of bacteria in the cytosol, but dispersal into the extracellular milieu following cell lysis.

Legionella Uptake and Infection in AX2 or Nramp1-KO Cells Grown in Minimal Medium with or without Iron Supplementation

We followed *Legionella* infection in AX2 cells grown for 24 h in minimal medium containing 0, 100, or 200 μM $FeCl_3$. In cells deprived of iron during growth, *Legionella* intracellular replication was strongly reduced (**Figure 6A**) and the percentage of dead cells did not increase significantly over time (**Figure 6B**). These data were confirmed by live microscopy: at 72 hpi, only a very small number of cells were infected with bacteria (**Figure 6C**).

When cells previously grown in the presence of iron were tested, *Legionella* intracellular growth was significantly higher compared to the condition of iron shortage, with the number of intracellular bacteria rapidly increasing during the first 48 hpi, and starting to decrease concomitantly with a boost in the percentage of dead cells (**Figures 6A,B**). Indeed, by confocal microscopy we observed already at 48 hpi and strongly at 72 hpi an increase in the number of extracellular bacteria and of lysed cells (**Figure 6C**). No differences were detected when the amount of iron in the growth medium was doubled to 200 μM (**Figures 6A,B**). Despite the inhibition of growth induced by the latter concentration of iron (**Figure 1A**), no increase in the percentage of dead cells was observed in the uninfected control (4.8% of dead cells compared to 77.3% in infected cells at 72 hpi). Therefore, the cytotoxic effect observed in infected cells is not due to the metal, but to the rapid proliferation of the bacteria. Adding iron during the infection assay to cells previously grown in the presence of iron facilitated *Legionella* intracellular growth, with a maximal value already reached at 24 hpi (**Figure 6A**).

We also tested whether iron could affect *Legionella* uptake. AX2 cells were grown for 24 h in M1 ± Fe, as previously described. Thereafter, they were washed, resuspended in nominally iron-free medium, co-centrifuged with GFP-producing *Legionella* (MOI 10:1) and incubated for 40 min at 25°C. Uptake was measured as increase of the percentage of fluorescent (i.e., harboring bacteria) cells. When cells grown in M1 were assayed, only about 23% of them were fluorescent, rising to 38% 40 min post-infection (**Figure 7**). In cells grown in M1 plus 100 or 200 μM iron, the percentage of fluorescent cells was already significantly higher at time 0 (47–50%), and further increased over 66% after 40 min, with no differences between 100 and 200 μM Fe (**Figure 7**). It is worth mentioning that though the number of infected cells increased, the mean number of *Legionella* per cell did not increase significantly, as confirmed by confocal microscopy. Thus, growing cells in the presence or absence of iron affects both uptake and infection of *Legionella*.

We previously showed that *Dictyostelium* Nramp1 is rapidly recruited from the Golgi to phagosomes and macropinosomes. Here it mediates iron efflux to the cytosol and, by doing so, it confers resistance to infection by intracellular pathogens, such as *Legionella* and *Mycobacterium avium* (Peracino et al., 2006, 2013; Buracco et al., 2015). Similarly to AX2 cells, when Nramp1-KO cells were grown for 24 h in M1 medium, infection was significantly reduced in both parameters, *Legionella* intracellular replication and bacteria-triggered cytotoxicity (**Figure 8**). In cells grown in the presence of iron and infected in a medium containing the same concentration of the metal, *Legionella* intracellular growth reached again a peak at 24 hpi and then started to decrease over time (**Figure 8A**). At the same time, the percentage of dead cells increased steadily, exceeding 80% at 72 hpi (**Figure 8B**). Thus, iron deficiency or overload has similar effects on *Legionella* infection in cells lacking Nramp1 and parental cells, though in the Nramp1-KO mutant intracellular growth of *Legionella* was more rapid, consistent with its increased susceptibility to infection (Peracino et al., 2006).

Effects of Altering Zinc or Copper Availability on *Legionella* Infection

We tested whether zinc or copper exert similar effects as iron. AX2 cells grown for 168 h in M2 ± Zn or M3 ± Cu were infected and analyzed by flow cytometry. Under all conditions tested, neither bacterial intracellular proliferation nor cytotoxicity were significantly altered compared to the control incubated in standard FM medium (**Figure 9**). As

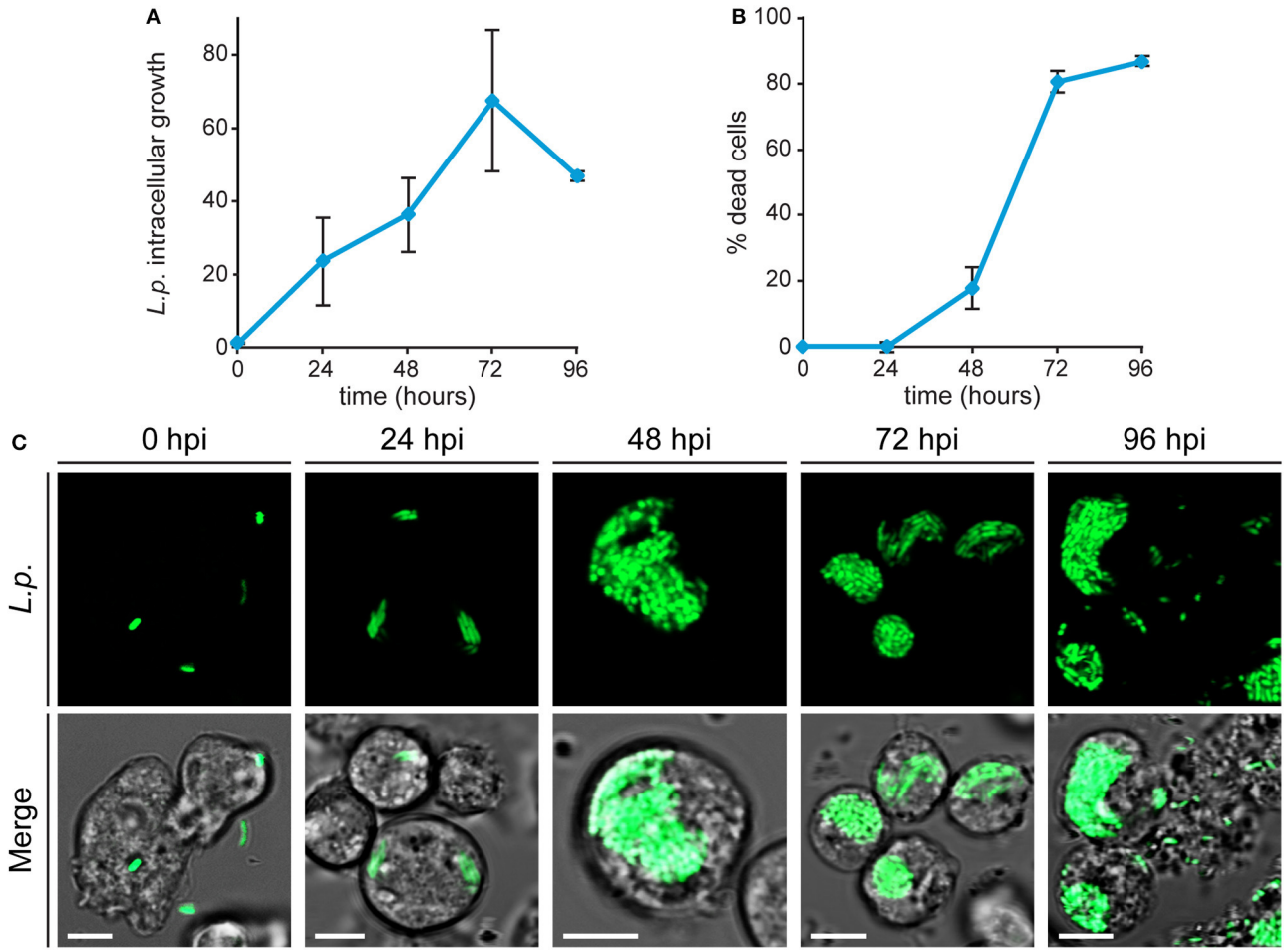

FIGURE 4 | *Legionella* infection in *Dictyostelium* cells. **(A,B)** AX2 cells growing axenically were infected with GFP-producing *L. pneumophila* and monitored by flow cytometry. The intracellular growth of *Legionella* was assessed by measuring the mean fluorescence of GFP-producing *L. pneumophila* within AX2 cells and *L. pneumophila*-triggered cytotoxicity by determining the percentage of dead cells. For ICG, the trend in different experiments was similar, although the absolute values varied strongly between replicates, due to changes in cell autofluorescence. Thus, *Legionella* replication was expressed as mean fold-increase in fluorescence intensity relative to the autofluorescence of the corresponding non-infected cells. All measurements are mean values of seven different experiments with error bars (±SD). **(C)** Confocal fluorescence images of infected living cells at different times post-infection. (Top) GFP-producing *Legionella* and (Bottom) merge with corresponding phase-contrast. In intact cells, the proliferating bacteria are packed together, except for extracellular bacteria in lysed cells (96 hpi). Scale bars: 5 μm.

shown in **Table 3**, omitting zinc or copper in the culture medium affects only minimally the cellular concentration of these metals, particularly for zinc, compared to the standard FM medium, with no inhibitory effect on cell growth, though in the case of zinc postaggregative development is blocked. In some experiments the intracellular zinc chelator TPEN was added during *Legionella* infection to cells previously grown in M2 medium, but no effects on *Legionella* growth or cytotoxicity were observed compared to the M2 medium (**Figure 9**). The absence of significant differences in *Legionella* infection between cells grown in nominally-free metal medium, supplemented in the case of zinc with TPEN during infection, or at the highest concentrations of metal tested suggests to us that zinc and copper play a minor role in *Dictyostelium* resistance to *Legionella* infection.

Intracellular Distribution of Free Zinc Ions in *Dictyostelium* Cells

To better understand if free zinc ions could play a role in predation and infection, we investigated their intracellular localization using the cell-permeable fluorogenic Zn^{2+} reporter Zinpyr-1, which fluoresces in the pH range 3.5 to 8 upon binding Zn^{2+} and is highly selective for the labile Zn^{2+} pool (Burdette et al., 2001; Figueroa et al., 2014). When the probe was administered to AX2 cells producing the iron transporter Nramp1-RFP, the fluorescent signal accumulated in vesicles coated with Nramp1-RFP (**Figure 10A**). Nramp1 traffics between trans-Golgi and endosomes, including macropinosomes, phagosomes, and endolysosomes, but is not found in postlysosomal vesicles (Peracino et al., 2006). In cells producing the iron transporter NrampB-RFP, we

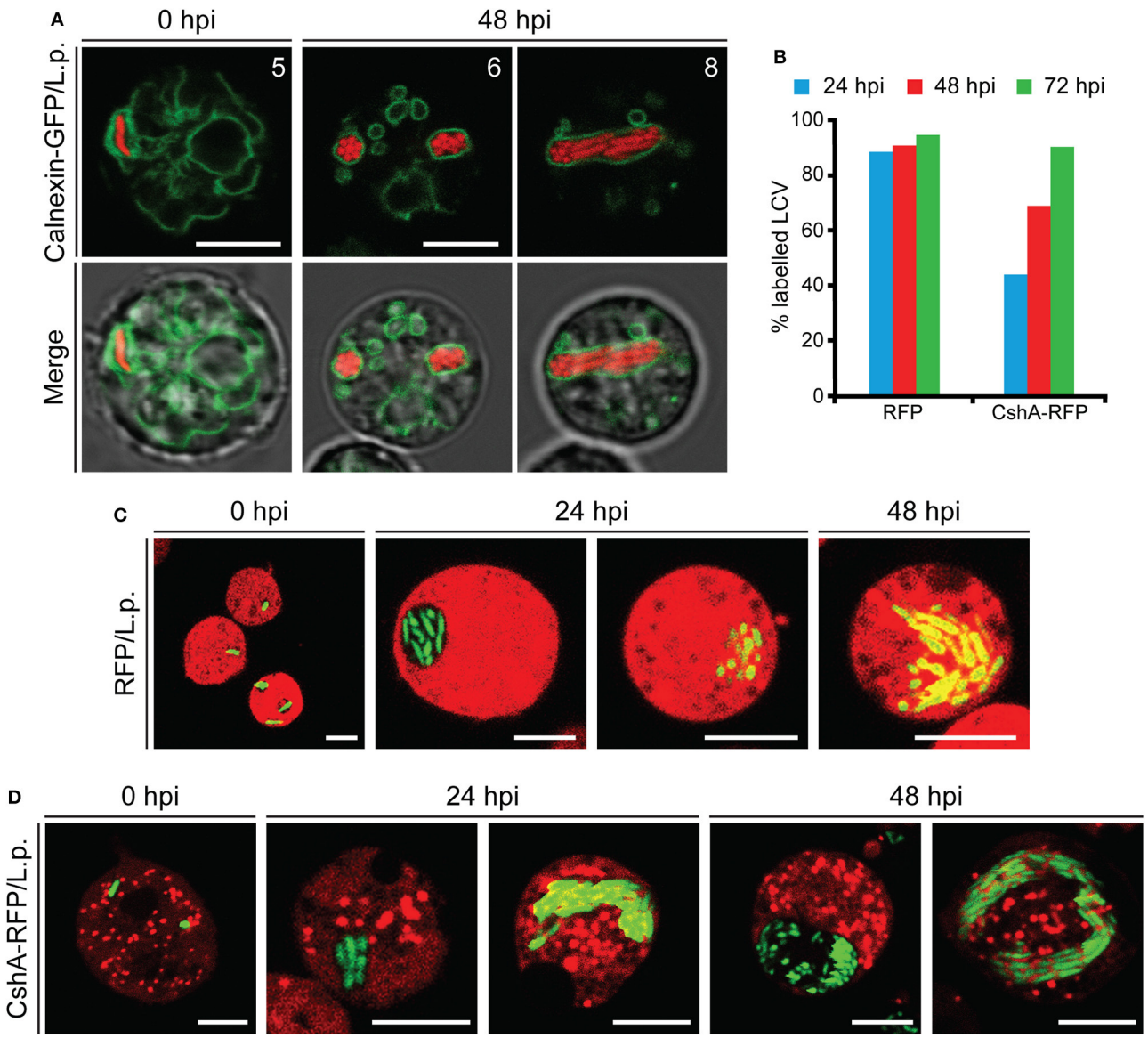

FIGURE 5 | Characterization of the LCV membrane during *Legionella* infection. **(A)** Confocal images of living AX2 cells producing Calnexin-GFP and infected with RFP-producing *L. pneumophila*. The double exposure (red and green fluorescence) shows the presence of a membrane surrounding the replicating bacteria even at 48 hpi. The numbers indicate distance from the bottom surface of the cell (μm). **(B–D)** Co-localization of RFP or CshA-RFP with the LCV. AX2 cells expressing free RFP or CshA-RFP were infected with GFP-producing *L. pneumophila* and confocal images acquired every 24 h post-infection **(C,D)**. The small organelles labeled with CshA-RFP in **(D)** are peroxisomes. **(B)** The number of LCVs labeled with the cytosolic fluorescent proteins was quantified analyzing at least 30 cells for each time point and expressed as percentage of the total. For all confocal images, red and green fluorescence merge is shown. The diffusion of free-RFP or CshA-RFP fluorescence inside the LCV allows evaluating the integrity of the LCV membrane. Scale bars: 5 μm.

observed also transient labeling of the contractile vacuole (CV) membrane, with a faint labeling inside the vacuole, most evident under continuous Zinpyr-1 loading (**Figure 10B**). NrampB is localized exclusively in the membrane of the CV tubule network (Peracino et al., 2013). Since Zinpyr-1 under continuous loading failed to label other membranes, including the plasma membrane, the fluorescence in the CV membrane cannot be due to some unspecific effect of Zinpyr-1 diffusing across the membrane bilayer. As additional control, we incubated cells treated with the intracellular membrane-permeable chelator TPEN with Zinpyr-1 under continuous loading. As shown in **Figure 10C**, the Zinpyr-1 fluorescence is undetectable both at the level of the contractile vacuole and endosomal vesicles. We conclude that the Zinpyr-1 fluorescence in the CV is due to chelation of free zinc ions being transported across the CV membrane. No differences in Zinpyr-1 cellular localization were observed in cells grown in M2 medium ± Zn. In cells incubated with TRITC-labeled *E. coli*, we observed co-localization of

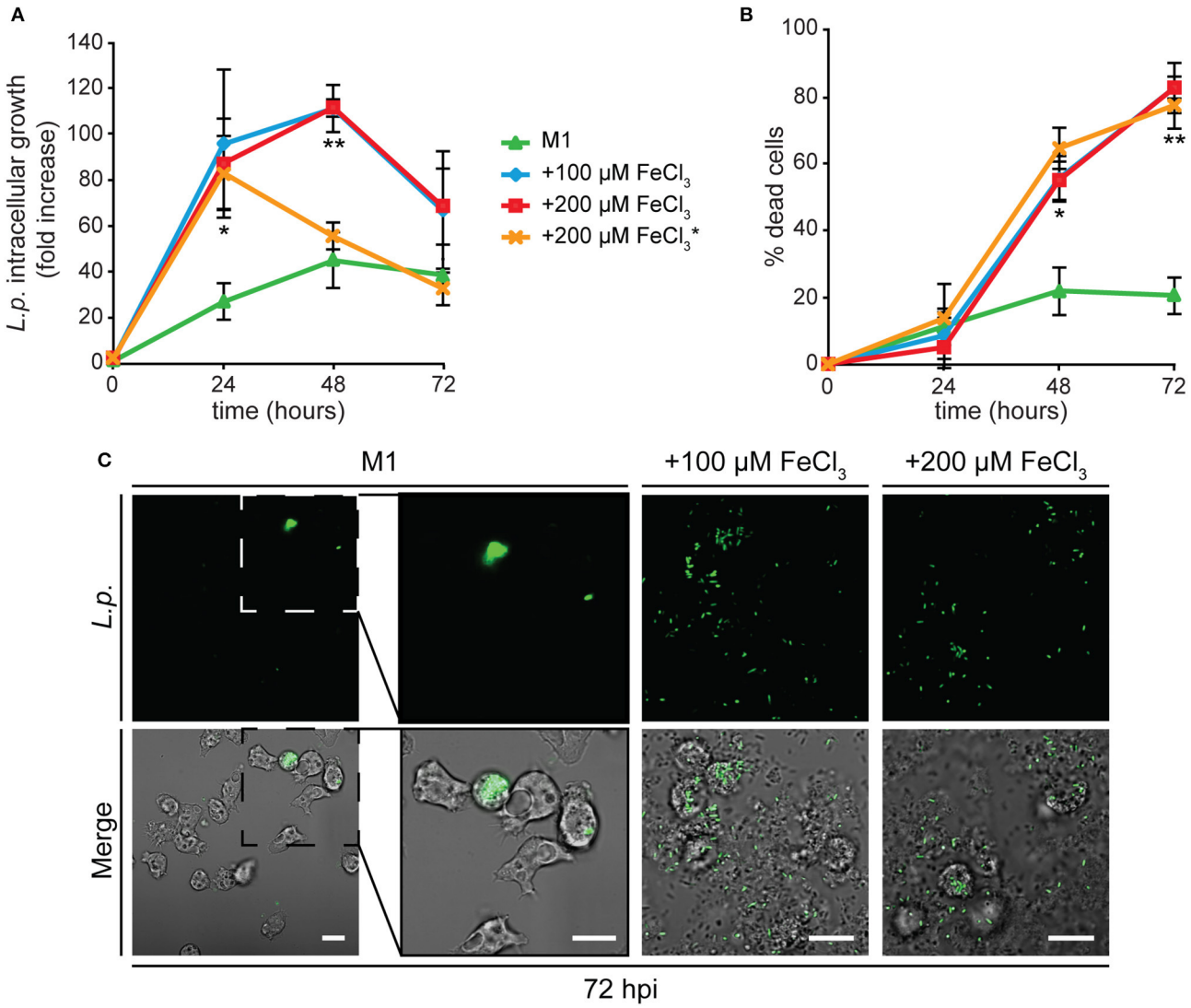

FIGURE 6 | Alterations in cellular iron content affect *Legionella* infection in *Dictyostelium*. **(A,B)** AX2 cells were grown for 24 h in M1 ± Fe and infected with GFP-producing *L. pneumophila*. In some experiments with cells grown in M1+200 μM iron, iron at the same concentration was added to the medium during infection (*). The intracellular growth (ICG) of *Legionella* **(A)** and cytotoxicity **(B)** were measured by flow cytometry as in **Figure 4**. AX2 cell growth in M1 results in strongly reduced *Legionella* growth and cytotoxicity, whereas growth in iron-rich media stimulates both *Legionella* intracellular growth and induced cytotoxicity. The presence of iron in the medium during infection induces earlier bacterial leakage from infected cells, shifting the fluorescence peak from 48 to 24 hpi. Mean values of two to four experiments in triplicate with error bars (±SD). $^{*}P < 0.05$ or $^{**}P < 0.01$ (two-tailed Student's *t*-test, assuming unequal variance) vs. the condition of growth in M1. **(C)** Confocal images of infected cells at 72 hpi. Green fluorescence and merge with corresponding phase-contrast are shown. In M1 only few cells are infected with *Legionella* after 72 h and no bacteria are visible in the extracellular medium. On the contrary, many extracellular bacteria and lysed cells are visible when cells were grown in the presence of iron. Scale bars: 5 μm.

the fluorescent probe also with the bacteria in phagosomes (**Figure 10D**).

Thus, in *Dictyostelium* cells, free zinc ions accumulate in vesicles of the endo-lysosomal pathway, including phagosomes. The transient labeling of the CV membrane and the faint labeling inside the CV suggests that excess free zinc is transported across the CV membrane, where it could be stored or secreted extracellularly. Similar experiments with copper could not be done, as fluorescent reporters for copper are not commercially available.

DISCUSSION

The high number of copper and zinc transporters in *Dictyostelium* makes difficult a targeted genetic approach to decipher the role of these metals in host-pathogen interactions, in contrast to what has been possible with the Nramp iron transporters (Peracino et al., 2006, 2013). In this paper we have followed an indirect approach, by growing cells under conditions of metal deficiency or overload and then testing the cells for resistance to infection by *L. pneumophila*, which is a very

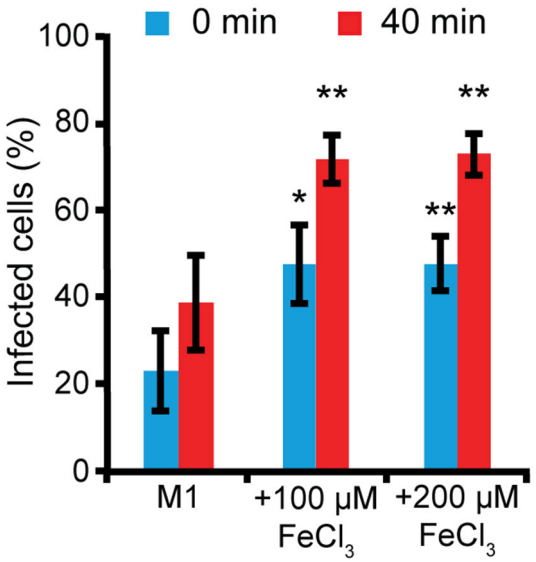

FIGURE 7 | Iron deficiency or overload affects *L. pneumophila* uptake. AX2 cells grown for 24 h in M1 medium ± Fe were infected with GFP-producing *L. pneumophila* at MOI 10:1 and analyzed by flow cytometry. Bacteria uptake was measured as the percentage of *Dictyostelium* cells harboring GFP-positive *L. pneumophila* at 0 and 40 min post-infection. In the nominally iron-free M1 medium, bacteria uptake was significantly reduced compared to cells grown in the presence of iron. Mean values of three different experiments with error bars (±SD) are shown. *$P < 0.05$ or **$P < 0.01$ (two-tailed Student's *t*-test, assuming unequal variance) vs. the corresponding time of the condition in M1.

well-studied pathogen for these cells under laboratory conditions (Hägele et al., 2000; Solomon and Isberg, 2000; Peracino et al., 2006; Hilbi et al., 2007; Steinert, 2011; Bozzaro et al., 2013b; Hoffmann et al., 2014).

We used a minimal culture medium (FM Medium) made of amino acids, glucose, a few selected vitamins and trace elements (Franke and Kessin, 1977), whose concentration could be modified. As contamination of pico- to nano-molar traces of metals could derive from reagents (in particular amino acids), glass or other materials (Kay, 2004), the culture medium could not be totally depleted of iron, copper, or zinc, as confirmed by the ICP-MS analysis. The nominally zinc- or copper-free medium still contained, respectively, 7.26 and 4.6% of metal, compared to the standard FM medium. What is more important, the metal concentration in cells growing for more than 20 generations in these nominally zinc- or copper-free media was only slightly reduced compared to cells growing in FM medium, namely of about 15 and 50% for zinc and copper, respectively. Cell growth in media containing 276- or 4,285-fold zinc or copper, respectively, compared to the concentration in the nominally metal-free media, resulted in an increase of only 3- and about 5-fold cellular zinc or copper, respectively, after 24 cell doublings. These data indicate that *Dictyostelium* cells possess very tight regulatory mechanisms of uptake, storing and release of these metals, which can explain why the cell growth rate was absolutely unaffected in media within such a broad range of external zinc or copper concentrations. Only at higher concentrations of copper and zinc, inhibitory and toxic effects on cell growth were detectable, confirming previous results (Burlando et al., 2002; Balbo and Bozzaro, 2008). The high tolerance, at least for copper, could be linked to the activity of one or more MNK Cu-ATPases, whose expression in the plasma membrane is enhanced by addition of salts (Burlando et al., 2002; Hao et al., 2016). For zinc, nothing is known on the cellular localization and activity of the transporters (Sunaga et al., 2008).

In the case of iron, the cellular concentration was reduced to a quarter after 24 h incubation, and about two duplications, in nominally iron-free medium compared to FM medium. We have confirmed that iron is essential for cell growth, with the growth rate being slowed down and cell duplication inhibited within few generations in both nominally iron-free medium and iron overload (Peracino et al., 2013). Iron overload led to formation of very large aggregating streams, which underwent fragmentation. A similar phenotype has been already described for the Nramp1/NrampB double knockout mutant (Peracino et al., 2010), and recalls the streamer mutants, some of which are defective in cGMP phosphodiesterase (Ross and Newell, 1979; Newell and Liu, 1992), suggesting a possible regulation of chemotaxis by iron homeostasis that needs further investigation.

Interestingly, the intracellular growth of *Legionella* was strongly inhibited in cells grown in nominally iron-free medium, but enhanced in cells exposed during growth to 100 or 200 µM iron. Addition of iron to the medium during infection further stimulated *Legionella* growth in iron overloaded cells. The uptake of *Legionella* was also affected by iron, in that the number of cells ingesting *Legionella* was higher in the population grown under iron overload, though the mean number of *Legionella* per cell was constant. Whether this is due to iron being secreted by the iron-overloaded cells, thus stimulating bacterial attachment to the cell surface, is unclear. Increased *Legionella* uptake due to extracellular iron has been recently described in macrophages (O'Connor et al., 2016).

Similar results were obtained with the Nramp1 knockout mutant. The iron transporter Nramp1 mediates iron efflux from the phagosome, and its inactivation increases susceptibility to *L. pneumophila*, *M. avium,* and *F. tularensis* (Peracino et al., 2006; Buracco et al., 2015; Brenz et al., 2017). Growing the mutant cells in nominally iron-free medium for 24 h strongly inhibited *Legionella* intracellular growth, whereas cell growth under iron overload enhanced its susceptibility to infection to a higher level than in the parental cells, consistent with a higher accumulation of iron in the LCV, due to inactivation of Nramp1 (Buracco et al., 2015). Remarkably, *Legionella* intracellular proliferation in iron overloaded cells was so rapid that already at 48 hpi almost all cells underwent lysis with dispersal of the bacteria in the extracellular milieu. Taken together, these results indicate that a condition of iron starvation is protective for *Dictyostelium* cells against *Legionella* infection whereas high iron cellular content predisposes to rapid infection.

Iron is essential for *Legionella* growth and expression of virulence genes (Robey and Cianciotto, 2002; Cianciotto, 2015; Portier et al., 2015). In *Dictyostelium*, the source of iron for *Legionella* is the macropinosome, where the bacterium is

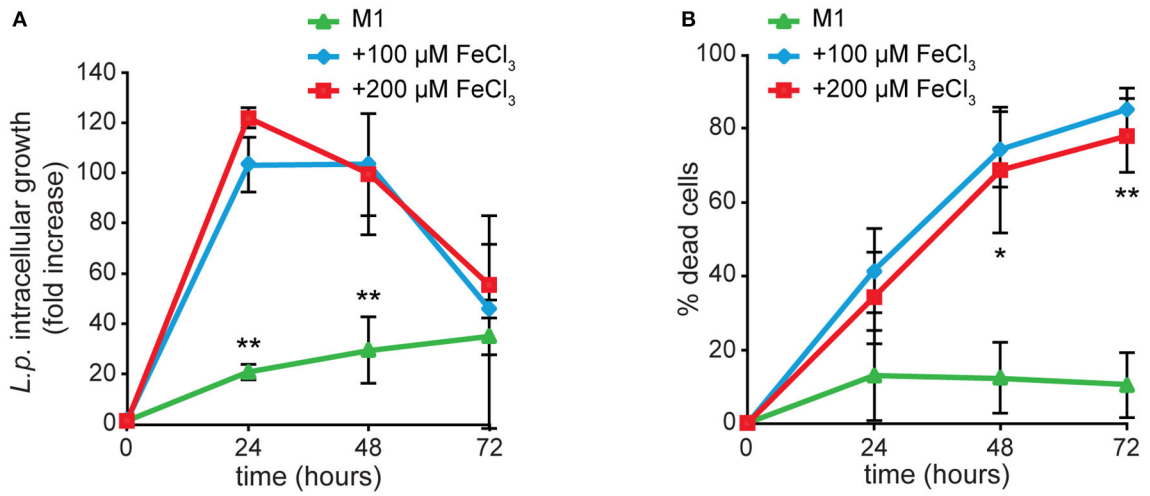

FIGURE 8 | Iron effects on *L. pneumophila* intracellular replication and cytotoxicity in Nramp1-KO mutant. Infection was evaluated in Nramp1-KO cells as previously described for AX2 cells in **Figure 5**, in the presence of iron in the infection medium at the same concentrations used for cell growth. Flow cytometry analysis of ICM **(A)** and cytotoxicity **(B)** are shown. In cells lacking Nramp1, growth in M1 affected bacterial replication and cytotoxicity similarly to AX2, whereas growth in the presence of iron stimulated *Legionella* infection to a higher degree than in AX2 (see **Figure 5**). Mean values of at least two experiments in triplicate with error bars (±SD). $^{*}P < 0.05$ or $^{**}P < 0.01$ (two-tailed Student's *t*-test, assuming unequal variance) vs. the condition of 100 μM $FeCl_3$.

taken up (Peracino et al., 2010). By pumping iron outside the macropinosome via Nramp1, *Dictyostelium* attempts to starve *Legionella* for iron, but *Legionella* can manipulate Nramp1 activity, by avoiding recruitment to the macropinosome of the V-H^+ ATPase (Peracino et al., 2010), and inhibiting its activity via the Dot/Icm substrate SidK (Xu et al., 2010). The V-H^+ ATPase is essential for Nramp1-mediated iron efflux (Buracco et al., 2015), thus iron accumulation transforms the macropinosome in a replication-permissive LCV (Steiner et al., 2017). If so, then a condition of iron starvation during cell growth, resulting in less iron being available in the macropinosome, independently of Nramp1 activity, will result in increased resistance of the host cell to *Legionella* infection, while iron overload will increase susceptibility to infection. Recently, an inhibitory effect of iron depletion on *Legionella* infection has been shown in macrophages treated with the iron chelator deferoxamine mesylate during infection or in *Acanthamoeba castellanii* infected in iron-free buffer (O'Connor et al., 2016). In the case of *A. castellanii*, the experimental conditions were different from those used in our experiments, as *A. castellanii* was grown in iron-containing medium and only the infection assay was done in iron-free buffer, which could explain the rather mild effect reported by the authors.

We have shown that *Legionella* proliferation occurs inside the LCV up to cell lysis, with the LCV in close contact to, if not fused with the endoplasmic reticulum (ER) membrane even up to later stages of infection. Association with the ER has been already described at early stages of infection, presumably induced by *Legionella* for acquiring new membrane for the LCV (Fajardo et al., 2004; Lu and Clarke, 2005; Urwyler et al., 2009; Weber et al., 2014; Steiner et al., 2017). Our data suggest that this process sets forth up to later stages.

Interestingly, the LCV membrane becomes gradually permeable between 24 and 48 hpi, allowing diffusion in the vacuole of cytosolic proteins first of lower (27 kDa) and later of higher molecular mass (about 76 kDa), but the bacteria remain packed together and do not egress into the cytosol, suggesting that, though permeable to proteins, the LCV membrane does not allow exit of the bacteria before cell lysis. Vacuole disruption shortly before cell lysis has been reported (Creasey and Isberg, 2012), but the present data suggest that *Legionella* induces permeability of the vacuole in the proliferation phase, possibly to get easy access to nutrients of the host. The dynamics of permeability by using fluorescent probes of increasing molecular size will be reported elsewhere. We failed to detect in the extracellular space clumps of bacteria, which could suggest non-lytic release in LCV's, as described in *A. castellanii* (Berk et al., 1998; Chen et al., 2004; Lau and Ashbolt, 2009).

In sharp contrast to iron, variation in cellular zinc or copper content over a range of, respectively, 3- to 5-fold did not significantly affect timing or extent of *Legionella* intracellular growth. For both, the infection rate was slower, though statistically not significant or borderline, in cells grown in nominally zinc or copper-free medium compared to cells with 5-fold more intracellular copper. If any, this would suggest that a higher intracellular zinc or copper concentration is not toxic for *Legionella*. In the case of zinc, *Dictyostelium* cells with the lowest zinc concentration were blocked at mound stage, suggesting that a suboptimal zinc concentration is deleterious for development. Zinc ions have been shown to enhance pre-stalk to stalk differentiation (Kubohara and Okamoto, 1994) and a family of three ZNT zinc transporters has been shown to be expressed at postaggregative stage in pre-stalk cells (Sunaga et al., 2008).

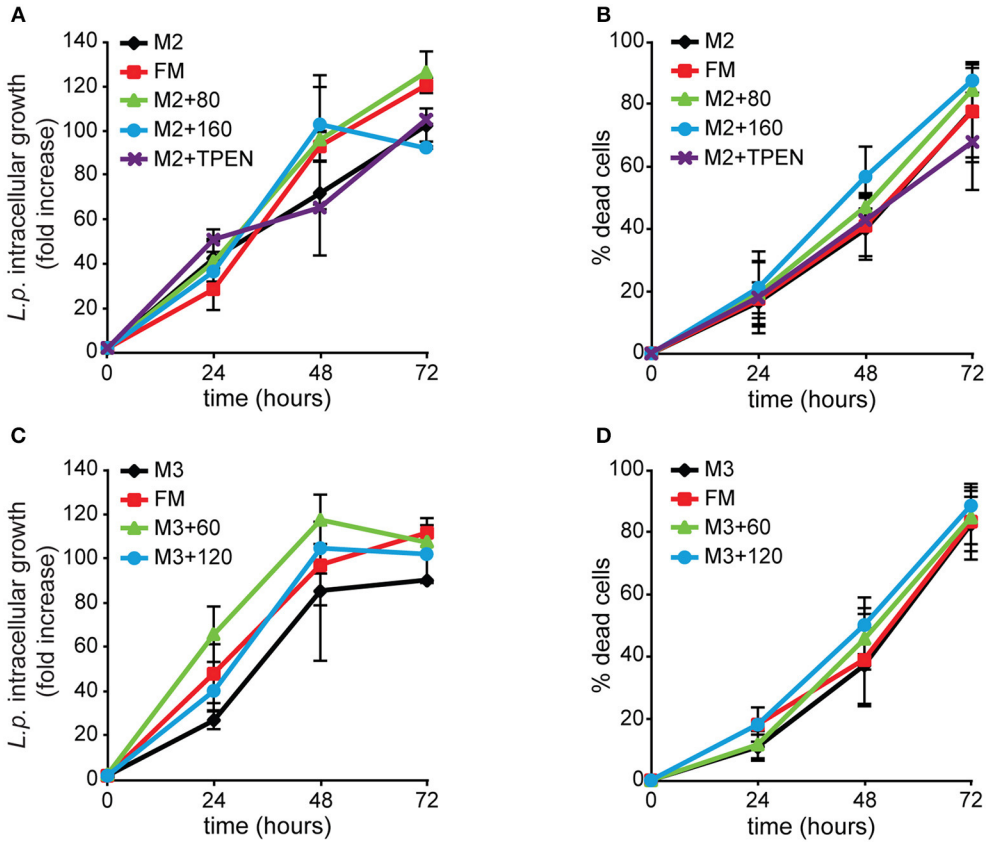

FIGURE 9 | Alterations of zinc or copper availability do not affect *Legionella* infection in *Dictyostelium* cells. AX2 cells were grown for 3 weeks (24 generations) in **(A,B)** M2 ± Zn or **(C,D)** M3 ± Cu medium and then infected with GFP-producing *L. pneumophila*. ICG and cytotoxicity were evaluated as previously described in **Figure 4**, with the first expressed as mean fold-increase in fluorescence intensity relative to the autofluorescence of the corresponding non-infected cells. Omitting or adding zinc or copper in cell growth medium did not significantly affect *Legionella* intracellular growth and induced cytotoxicity compared to FM medium. In the case of zinc, adding the intracellular chelator TPEN during infection failed to have any effect. Infection in cells grown in M3 + 6 μM Cu was comparable to the other conditions and, for simplicity, it was removed from the graphics. Mean values of three different experiments with error bars (±SD). **(C)** $P = 0.054$, at 24 hpi for M3 compared to M3 + 60 μM. The numbers indicate metal and chelator concentration in μM.

By using the iron fluorescent reporter calcein, we showed previously that iron is rapidly depleted from endo-lysosomal vesicles via Nramp1 (Buracco et al., 2015). By using the membrane-permeable zinc fluorescent reporter Zinpyr-1, we have now shown that free zinc ions accumulate in vesicles of the endo-lysosomal pathway, including phagosomes, and in the contractile vacuole. Free zinc in other cellular compartments or in the cytosol was below detection with this fluorescent reporter. Zinc transport across the membrane of the contractile vacuole is consistent with the proposed CV role as store or sink for metals (Bozzaro et al., 2013a; Peracino et al., 2013). By using bacteria expressing a copper and a reactive oxygen species biosensor, Hao et al. (2016) showed that copper and reactive oxygen species accumulate in *Dictyostelium* phagosomes upon bacterial phagocytosis. Thus, both zinc and copper are found in *Dictyostelium* phagosomes, consistent with a potential intoxicating role against pathogens, as suggested for macrophages (Babu and Failla, 1990; Wagner et al., 2005; White et al., 2009; Ward et al., 2010; Botella et al., 2011; Chaturvedi and Henderson, 2014; Djoko et al., 2015), though the evidence, at least for zinc, is less clear, and zinc sequestration, likely as it occurs for iron, has been also proposed as defense mechanism (Kehl-Fie and Skaar, 2010; Vignesh et al., 2013).

We have no evidence for phagocytosis inducing a burst of zinc in endocytic vesicles, as shown in macrophages with non-pathogenic bacteria (Botella et al., 2011). We used TRITC-labeled *E. coli*, which are not alive, whereas Botella and coworkers used living bacteria. If this would be the reason, then it would not be phagocytosis *per se* that triggers zinc accumulation, but a cellular response to the ingested living bacteria. Alternatively, the different results can be explained with the different zinc reporters used, Zinpyr-1 in this paper and FluoZin-3 in the Botella et al. (2011) paper. It is worth mentioning that Zinpyr-1 is more specific and selective for free zinc than FluoZin-3 (Figueroa et al., 2014). Further experiments are required to distinguish between these possibilities.

Our data suggest that, in contrast to iron, changes in cellular zinc or copper play a minor role in *Dictyostelium* resistance to pathogens, at least with *L. pneumophila*. Whether this holds true for other pathogens, such as mycobacteria, is under investigation.

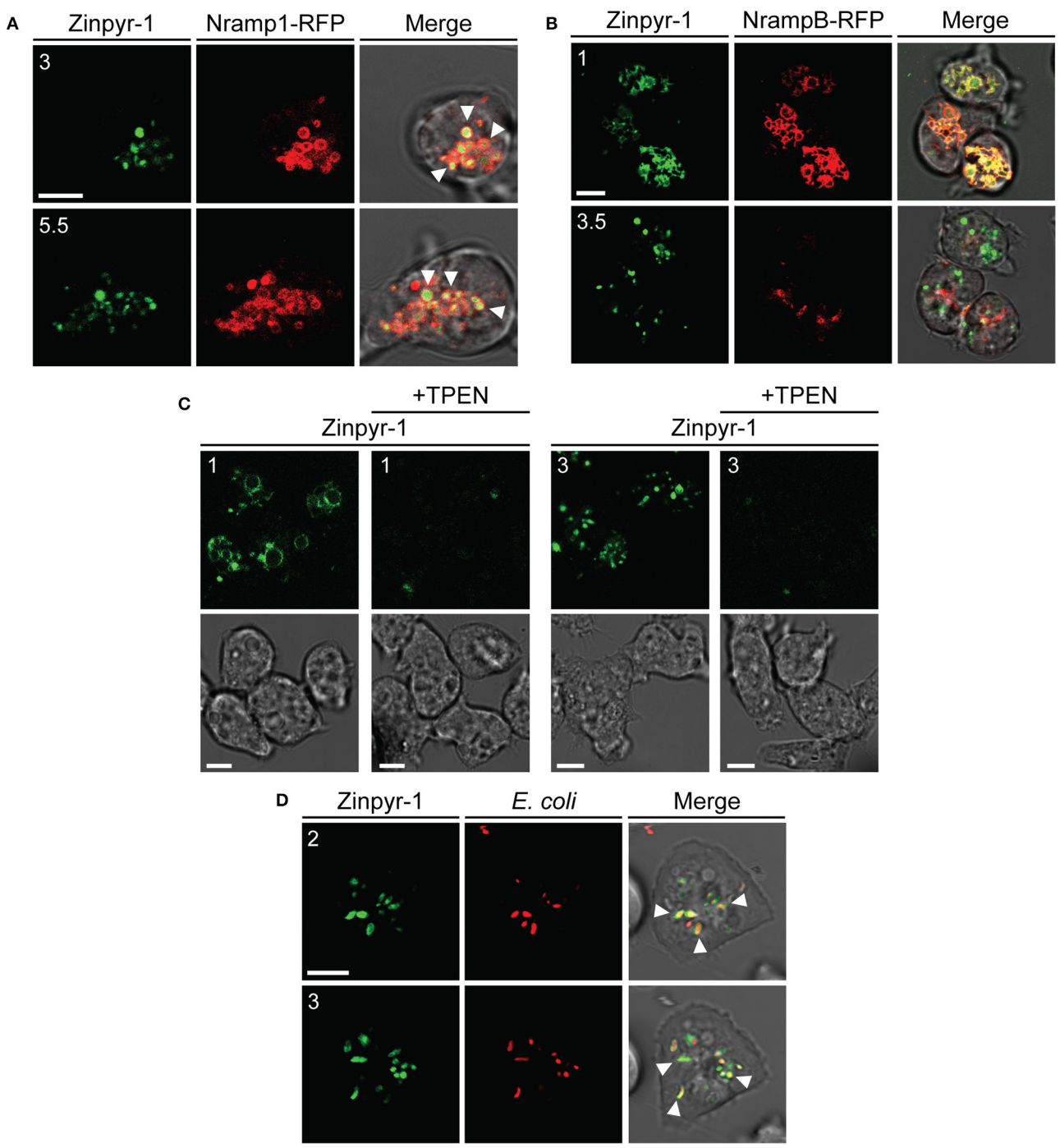

FIGURE 10 | Free zinc ions accumulate in endo-lysosomal vesicles and in the contractile vacuole network. **(A)** AX2 cells producing Nramp1-RFP were washed, resuspended in Soerensen phosphate buffer and incubated with the fluorescent zinc chelator Zinpyr-1 for 30 min. Cells were then washed and resuspended in the same buffer. After plating on glass coverslips, confocal series images were taken. Coincidence of Nramp1-RFP and Zinpyr-1 was detected in almost all vesicles, as indicated by some arrowheads. **(B)** NrampB-RFP producing cells were washed, resuspended in Soerensen phosphate buffer and loaded continuously with Zinpyr-1. Images of cells 30 min after the start of the incubation are shown. The fluorescent zinc reporter labeled the membrane of the contractile vacuole network, identified by NrampB-RFP label, and, faintly, the CV lumen. For all confocal images, red, green fluorescence and merge with corresponding phase-contrast are shown sequentially. **(C)** AX2 cells were washed, resuspended in Soerensen phosphate buffer and incubated with Zinpyr-1 in the presence or not of the zinc intracellular chelator TPEN (25 μM). Green fluorescence (Top) and phase-contrast (Bottom) are shown. In the presence of the chelator, Zinpyr-1 labeling in both contractile vacuole and endo-lysosomal vesicles disappears, indicating that the observed fluorescent signal is not a result of some unspecific effects of Zinpyr-1, but of its interaction with free zinc. **(D)** Living AX2 cells were pulsed with TRITC-labeled *E. coli* and Zinpyr-1 for 30 min, washed and plated on glass coverslips. Confocal section images were taken. Zinpyr-1 green fluorescence co-localized with engulfed bacteria, as indicated by some arrows. The numbers indicate distance from the bottom surface of the cell (in μm). Scale bars: 5 μm.

A shortcoming of our experimental approach is the apparently very high efficiency of *Dictyostelium* cells to cope with conditions of zinc or copper starvation or overloading. To which extent this is typical of *Dictyostelium* cells or is a common feature of other cells, including macrophages, is unknown. The experimental approach described here offers now the opportunity to identify, in a transcriptomic study, the genes responsible for this high homeostatic adaptation to zinc and copper deprivation or intoxication. From the site of the pathogen, the same approach can be used to identify potential mutants in metal dependent virulence genes.

There is an analogy between the conditions used in this paper and those encountered with humans affected by transition metal deficiency or overloading, due to nutritional or environmental problems. In particular, iron or zinc deficiency is a global nutritional problem, with negative health consequences, including anemia, impaired immune function and neurological diseases. Dietary iron supplementation to prevent micronutrient deficiency in areas with a high burden of infectious diseases is a double–edged weapon, as it can exacerbate morbidity and mortality from infectious diseases (Oppenheimer, 2001; Soofi et al., 2013; Pasricha and Drakesmith, 2016). Similarly, in patients undergoing multiple blood transfusion, the risk of infections is higher, and iron therapy in patients at high risk of infection has been questioned (Ozment and Turi, 2009; Weiss and Carver, 2017). The previous (Peracino et al., 2006; Buracco et al., 2015) and present results with the professional phagocyte *Dictyostelium* support this caution, offering a mechanistic explanation for the iron effects on infection that holds true also for macrophages. Concerning copper, but in particular zinc, further studies are required with macrophages isolated from animals exposed to metal deficiency or overloading. Identifying the genes responsible in *Dictyostelium* for the tight regulation of zinc and copper homeostasis and for their transport in phagosomes can shed some light on cellular zinc and copper store and mobilization, and the genetic basis of antimicrobial metal transport, also in macrophages.

AUTHOR CONTRIBUTIONS

SBu and SBo designed the experiments; SBu conducted the experiments, acquired, and analyzed the data; BP generated the *Dictyostelium* KO mutants and the plasmids for RFP-fused proteins and helped with some experiments; CA was responsible for the bioinformatic analysis of the metalloproteome. EB cloned the cshA gene, generated, and characterized cells expressing CshA-RFP. SBu and SBo wrote the manuscript; all approved the paper.

ACKNOWLEDGMENTS

We thank Annette Mueller Taubenberger for AX2 cells producing GFP and for the 389-2 vector (C-terminal mRFPmars), Michael Steinert for the *L. pneumophila* Corby producing GFP and Ds-red Express. We are grateful to the Dictybase team (www.dictybase.org) for maintenance of the Dictyostelid genome database, and Alessandra Viale of the Molecular Imaging Center (Department of Chemistry, University of Torino, Italy) for ICP-MS analysis. This work was supported by a research grant of the Compagnia San Paolo/Università di Torino (12-CSP-C03-065).

SUPPLEMENTARY MATERIAL

The Supplementary Material for this article can be found online at: https://www.frontiersin.org/articles/10.3389/fcimb.2017.00536/full#supplementary-material

Movie S1 | 3-D reconstruction of AX2 cells infected with GFP-producing *L. pneumophila* 48 hpi. 3-D projections of a single AX2 cell infected with GFP-tagged *L. pneumophila* were generated and animated with the confocal microscope LSM800 software (Zen Software, Carl Zeiss, Inc., Oberkochen, Germany) in.avi format. The movie shows bacteria contained in high number inside the infected cell. Legionellae are not spread in the cell, but are packed together in a "ring"-like structure, presumably around the nucleus.

Figure S1 | Plaque formation by AX2 cells previously grown in media depleted or overloaded with iron, zinc, or copper. Ax2 cells were grown in M1 ± Fe for 24 h or in M2 ± Zn or M3 ± Cu for 3 weeks. Cells were then washed, resuspended in Soerensen buffer, and serial dilutions were plated on a lawn of *E. coli* B2, *S. typhimurium,* or *K. aerogenes*, as described in Materials and Methods. Pictures of the appearance and widening of growth plaques were acquired daily with a scanner. Images of the lowest dilution used (10 cells per well) are shown that were acquired 3 or 4 days after plating. No significant differences in growth were observed. Numbers indicate metal concentration in μM (Top) or time in days (on the right).

REFERENCES

Andreini, C., Bertini, I., and Cavallaro, G. (2011). Minimal functional sites allow a classification of zinc sites in proteins. *PLoS ONE* 6:e26325. doi: 10.1371/journal.pone.0026325

Andreini, C., Bertini, I., Cavallaro, G., Holliday, G. L., and Thornton, J. M. (2008). Metal ions in biological catalysis: from enzyme databases to general principles. *J. Biol. Inorg. Chem.* 13, 1205–1218. doi: 10.1007/s00775-008-0404-5

Appelberg, R. (2006). Macrophage nutriprive antimicrobial mechanisms. *J. Leukoc. Biol.* 79, 1117–1128. doi: 10.1189/jlb.0206079

Babu, U., and Failla, M. L. (1990). Respiratory burst and candidacidal activity of peritoneal macrophages are impaired in copper-deficient rats. *J. Nutr.* 120, 1692–1699.

Balbo, A., and Bozzaro, S. (2008). A novel bioassay for evaluating soil bio-hazards using Dictyostelium as biosensor: validation and application to the Bio-Bio project. *Fresenius Environ. Bull.* 17, 1137–1143.

Berk, S. G., Ting, R. S., Turner, G. W., and Ashburn, R. J. (1998). Production of respirable vesicles containing live *Legionella pneumophila* cells by two Acanthamoeba spp. *Appl. Environ. Microbiol.* 64, 279–286.

Besold, A. N., Culbertson, E. M., and Culotta, V. C. (2016). The Yin and Yang of copper during infection. *J. Biol. Inorg. Chem.* 21, 137–144. doi: 10.1007/s00775-016-1335-1

Bird, A. J. (2015). Cellular sensing and transport of metal ions: implications in micronutrient homeostasis. *J. Nutr. Biochem.* 26, 1103–1115. doi: 10.1016/j.jnutbio.2015.08.002

Bonaventura, P., Benedetti, G., Albarède, F., and Miossec, P. (2015). Zinc and its role in immunity and inflammation. *Autoimmun. Rev.* 14, 277–285. doi: 10.1016/j.autrev.2014.11.008

Botella, H., Peyron, P., Levillain, F., Poincloux, R., Poquet, Y., Brandli, I., et al. (2011). Mycobacterial p(1)-type ATPases mediate resistance to zinc poisoning in human macrophages. *Cell Host Microbe* 10, 248–259. doi: 10.1016/j.chom.2011.08.006

Botella, H., Stadthagen, G., Lugo-Villarino, G., de Chastellier, C., and Neyrolles, O. (2012). Metallobiology of host-pathogen interactions: an intoxicating new insight. *Trends Microbiol.* 20, 106–112. doi: 10.1016/j.tim.2012.01.005

Bozzaro, S., Bucci, C., and Steinert, M. (2008). Phagocytosis and host–pathogen interactions in dictyostelium with a look at macrophages. *Int. Rev. Cell Mol. Biol.* 271, 253–300. doi: 10.1016/S1937-6448(08)01206-9

Bozzaro, S., Buracco, S., and Peracino, B. (2013a). Iron metabolism and resistance to infection by invasive bacteria in the social amoeba *Dictyostelium discoideum*. *Front. Cell. Infect. Microbiol.* 3:50. doi: 10.3389/fcimb.2013.00050

Bozzaro, S., and Eichinger, L. (2011). The professional phagocyte *Dictyostelium discoideum* as a model host for bacterial pathogens. *Curr. Drug Targets* 12, 942–954. doi: 10.2174/138945011795677782

Bozzaro, S., Peracino, B., and Eichinger, L. (2013b). Dictyostelium host response to legionella infection: strategies and assays. *Methods Mol. Biol.* 954, 417–438. doi: 10.1007/978-1-62703-161-5_26

Braymer, J. J., and Giedroc, D. P. (2014). Recent developments in copper and zinc homeostasis in bacterial pathogens. *Curr. Opin. Chem. Biol.* 19, 59–66. doi: 10.1016/j.cbpa.2013.12.021

Brenz, Y., Ohnezeit, D., Winther-Larsen, H. C., and Hagedorn, M. (2017). Nramp1 and NrampB contribute to resistance against francisella in Dictyostelium. *Front. Cell. Infect. Microbiol.* 7:282. doi: 10.3389/fcimb.2017.00282

Buracco, S., Peracino, B., Cinquetti, R., Signoretto, E., Vollero, A., Imperiali, F., et al. (2015). Dictyostelium Nramp1, which is structurally and functionally similar to mammalian DMT1 transporter, mediates phagosomal iron efflux. *J. Cell Sci.* 128, 3304–3316. doi: 10.1242/jcs.173153

Burdette, S. C., Walkup, G. K., Spingler, B., Tsien, R. Y., and Lippard, S. J. (2001). Fluorescent Sensors for Zn 2+ based on a Fluorescein platform: synthesis, properties and intracellular distribution. *J. Am. Chem. Soc.* 123, 7831–7841. doi: 10.1021/ja010059l

Burlando, B., Evangelisti, V., Dondero, F., Pons, G., Camakaris, J., and Viarengo, A. (2002). Occurrence of {Cu-ATPase} in Dictyostelium: possible role in resistance to copper. *Biochem. Biophys. Res. Commun.* 291, 476–483. doi: 10.1006/bbrc.2002.6463

Capdevila, D. A., Wang, J., and Giedroc, D. P. (2016). Bacterial strategies to maintain zinc metallostasis at the host-pathogen interface. *J. Biol. Chem.* 291, 20858–20868. doi: 10.1074/jbc.R116.742023

Casadevall, A. (2008). Evolution of intracellular pathogens. *Annu. Rev. Microbiol.* 62, 19–33. doi: 10.1146/annurev.micro.61.080706.093305

Cellier, M. F. (2012). Nutritional immunity: homology modeling of Nramp metal import. *Adv. Exp. Med. Biol.* 946, 335–351. doi: 10.1007/978-1-4614-0106-3_19

Cerasi, M., Ammendola, S., and Battistoni, A. (2013). Competition for zinc binding in the host-pathogen interaction. *Front. Cell. Infect. Microbiol.* 3:108. doi: 10.3389/fcimb.2013.00108

Chaturvedi, K. S., and Henderson, J. P. (2014). Pathogenic adaptations to host-derived antibacterial copper. *Front. Cell. Infect. Microbiol.* 4:3. doi: 10.3389/fcimb.2014.00003

Chen, J., de Felipe, K. S., Clarke, M., Lu, H., Anderson, O. R., Segal, G., et al. (2004). Legionella effectors that promote nonlytic release from protozoa. *Science* 303, 1358–1361. doi: 10.1126/science.1094226

Cianciotto, N. P. (2015). An update on iron acquisition by *Legionella pneumophila*: new pathways for siderophore uptake and ferric iron reduction. *Future Microbiol.* 10, 841–851. doi: 10.2217/fmb.15.21

Colvin, R. A., Bush, A. I., Volitakis, I., Fontaine, C. P., Thomas, D., Kikuchi, K., et al. (2008). Insights into Zn2+ homeostasis in neurons from experimental and modeling studies. *Am. J. Physiol. Cell Physiol.* 294, C726–C742. doi: 10.1152/ajpcell.00541.2007

Cosson, P., and Soldati, T. (2008). Eat, kill or die: when amoeba meets bacteria. *Curr. Opin. Microbiol.* 11, 271–276. doi: 10.1016/j.mib.2008.05.005

Courville, P., Chaloupka, R., and Cellier, M. F. (2006). Recent progress in structure–function analyses of Nramp proton-dependent metal-ion transporters. *Biochem. Cell Biol.* 84, 960–978. doi: 10.1139/o06-193

Creasey, E. A., and Isberg, R. R. (2012). The protein SdhA maintains the integrity of the Legionella-containing vacuole. *Proc. Natl. Acad. Sci. U.S.A.* 109, 3481–3486. doi: 10.1073/pnas.1121286109

Djoko, K. Y., Ong, C. Y., Walker, M. J., and McEwan, A. G. (2015). The role of copper and zinc toxicity in innate immune defense against bacterial pathogens. *J. Biol. Chem.* 290, 18954–18961. doi: 10.1074/jbc.R115.647099

Dupont, C. L., Grass, G., and Rensing, C. (2011). Copper toxicity and the origin of bacterial resistance—new insights and applications. *Metallomics* 3, 1109–1118. doi: 10.1039/c1mt00107h

Erken, M., Lutz, C., and McDougald, D. (2013). The rise of pathogens: predation as a factor driving the evolution of human pathogens in the environment. *Microb. Ecol.* 65, 860–868. doi: 10.1007/s00248-013-0189-0

Fajardo, M., Schleicher, M., Noegel, A., Bozzaro, S., Killinger, S., Heuner, K., et al. (2004). Calnexin, calreticulin and cytoskeleton-associated proteins modulate uptake and growth of *Legionella pneumophila* in *Dictyostelium discoideum*. *Microbiology* 150, 2825–2835. doi: 10.1099/mic.0.27111-0

Feeley, J. C., Gibson, R. J., Gorman, G. W., Langford, N. C., Rasheed, J. K., Mackel, D. C., et al. (1979). Charcoal-yeast extract agar: primary isolation medium for *Legionella pneumophila*. *J. Clin. Microbiol.* 10, 437–441.

Festa, R. A., and Thiele, D. J. (2011). Copper: an essential metal in biology. *Curr. Biol.* 21, R877–R883. doi: 10.1016/j.cub.2011.09.040

Figueroa, J. A. L., Vignesh, K. S., Deepe, G. S., and Caruso, J. (2014). Selectivity and specificity of small molecule fluorescent dyes/probes used for the detection of Zn2+ and Ca2+ in cells. *Metallomics* 6, 301–315. doi: 10.1039/C3MT00283G

Fiorito, V., Geninatti Crich, S., Silengo, L., Altruda, F., Aime, S., and Tolosano, E. (2012). Assessment of iron absorption in mice by ICP-MS measurements of (57)Fe levels. *Eur. J. Nutr.* 51, 783–789. doi: 10.1007/s00394-011-0256-6

Fischer, M., Haase, I., Simmeth, E., Gerisch, G., and Müller-Taubenberger, A. (2004). A brilliant monomeric red fluorescent protein to visualize cytoskeleton dynamics in Dictyostelium. *FEBS Lett.* 577, 227–232. doi: 10.1016/j.febslet.2004.09.084

Forbes, J. R., and Gros, P. (2003). Iron, manganese, and cobalt transport by Nramp1 (Slc11a1) and Nramp2 (Slc11a2) expressed at the plasma membrane. *Blood* 102, 1884–1892. doi: 10.1182/blood-2003-02-0425

Franke, J., and Kessin, R. (1977). A defined minimal medium for axenic strains of *Dictyostelium discoideum*. *Proc. Natl. Acad. Sci. U.S.A.* 74, 2157–2161. doi: 10.1073/pnas.74.5.2157

Froquet, R., Lelong, E., Marchetti, A., and Cosson, P. (2008). *Dictyostelium discoideum*: a model host to measure bacterial virulence. *Nat. Protoc.* 4, 25–30. doi: 10.1038/nprot.2008.212

Gaudet, R. G., Bradfield, C. J., and MacMicking, J. D. (2016). Evolution of cell-autonomous effector mechanisms in macrophages versus non-immune cells. *Microbiol. Spectr.* 4, 1–30. doi: 10.1128/microbiolspec.MCHD-0050-2016

Graham, A. I., Hunt, S., Stokes, S. L., Bramall, N., Bunch, J., Cox, A. G., et al. (2009). Severe zinc depletion of *Escherichia coli*. *J. Biol. Chem.* 284, 18377–18389. doi: 10.1074/jbc.M109.001503

Greub, G., and Raoult, D. (2004). Microorganisms resistant to free-living amoebae. *Clin. Microbiol. Rev.* 17, 413–433. doi: 10.1128/CMR.17.2.413-433.2004

Hagedorn, M., and Soldati, T. (2007). Flotillin and RacH modulate the intracellular immunity of Dictyostelium to *Mycobacterium marinum* infection. *Cell. Microbiol.* 9, 2716–2733. doi: 10.1111/j.1462-5822.2007.00993.x

Hägele, S., Köhler, R., Merkert, H., Schleicher, M., Hacker, J., and Steinert, M. (2000). *Dictyostelium discoideum*: a new host model system for intracellular pathogens of the genus Legionella. *Cell. Microbiol.* 2, 165–171. doi: 10.1046/j.1462-5822.2000.00044.x

Hao, X., Lüthje, F., Rønn, R., German, N. A., Li, X., Huang, F., et al. (2016). A role for copper in protozoan grazing – two billion years selecting for bacterial copper resistance. *Mol Microbiol.* 102, 628–641 doi: 10.1111/mmi.13483

Hilbi, H., Weber, S. S., Ragaz, C., Nyfeler, Y., and Urwyler, S. (2007). Environmental predators as models for bacterial pathogenesis. *Environ. Microbiol.* 9, 563–575. doi: 10.1111/j.1462-2920.2007.01238.x

Hoffmann, C., Harrison, C. F., and Hilbi, H. (2014). The natural alternative: protozoa as cellular models for Legionella infection. *Cell. Microbiol.* 16, 15–26. doi: 10.1111/cmi.12235

Horwitz, M. A. (1983). Formation of a novel phagosome by the Legionnaires' disease bacterium (*Legionella pneumophila*) in human monocytes. *J. Exp. Med.* 158, 1319–1331.

Huang, Y.-C., Chen, Y.-H., Lo, S.-R., Liu, C.-I., Wang, C.-W., and Chang, W.-T. (2004). Disruption of the peroxisomal citrate synthase CshA affects cell growth and multicellular development in *Dictyostelium discoideum*. *Mol. Microbiol.* 53, 81–91. doi: 10.1111/j.1365-2958.2004.04109.x

Imlay, J. A. (2014). The mismetallation of enzymes during oxidative stress. *J. Biol. Chem.* 289, 28121–28128. doi: 10.1074/jbc.R114.588814

Kambe, T., Tsuji, T., Hashimoto, A., and Itsumura, N. (2015). The physiological, biochemical, and molecular roles of zinc transporters in zinc homeostasis and metabolism. *Physiol. Rev.* 95, 749–784. doi: 10.1152/physrev.00035.2014

Kay, A. R. (2004). Detecting and minimizing zinc contamination in physiological solutions. *BMC Physiol.* 4:4. doi: 10.1186/1472-6793-4-4

Kehl-Fie, T. E., and Skaar, E. P. (2010). Nutritional immunity beyond iron: a role for manganese and zinc. *Curr. Opin. Chem. Biol.* 14, 218–224. doi: 10.1016/j.cbpa.2009.11.008

Kehres, D. G., and Maguire, M. E. (2003). Emerging themes in manganese transport, biochemistry and pathogenesis in bacteria. *FEMS Microbiol. Rev.* 27, 263–290. doi: 10.1016/S0168-6445(03)00052-4

Krezel, A., and Maret, W. (2006). Zinc-buffering capacity of a eukaryotic cell at physiological pZn. *J. Biol. Inorg. Chem.* 11, 1049–1062. doi: 10.1007/s00775-006-0150-5

Kubohara, Y., and Okamoto, K. (1994). Specific induction by zinc of Dictyostelium stalk cell differentiation. *Exp. Cell Res.* 214, 367–372. doi: 10.1006/excr.1994.1269

Lau, H. Y., and Ashbolt, N. J. (2009). The role of biofilms and protozoa in Legionella pathogenesis: implications for drinking water. *J. Appl. Microbiol.* 107, 368–378. doi: 10.1111/j.1365-2672.2009.04208.x

Letelier, M. E., Lepe, A. M., Faúndez, M., Salazar, J., Marín, R., Aracena, P., et al. (2005). Possible mechanisms underlying copper-induced damage in biological membranes leading to cellular toxicity. *Chem. Biol. Interact.* 151, 71–82. doi: 10.1016/j.cbi.2004.12.004

Lisher, J. P., and Giedroc, D. P. (2013). Manganese acquisition and homeostasis at the host-pathogen interface. *Front. Cell. Infect. Microbiol.* 3:91. doi: 10.3389/fcimb.2013.00091

Lu, H., and Clarke, M. (2005). Dynamic properties of Legionella-containing phagosomes in *Dictyostelium amoebae*. *Cell Microbiol.* 7, 995–1007. doi: 10.1111/j.1462-5822.2005.00528.x

Maret, W. (2013). Zinc biochemistry: from a single zinc enzyme to a key element of life. *Adv. Nutr.* 4, 82–91. doi: 10.3945/an.112.003038

Müller-Taubenberger, A. (2001). Calreticulin and calnexin in the endoplasmic reticulum are important for phagocytosis. *EMBO J.* 20, 6772–6782. doi: 10.1093/emboj/20.23.6772

Nairz, M., Schroll, A., Sonnweber, T., and Weiss, G. (2010). The struggle for iron - a metal at the host-pathogen interface. *Cell Microbiol.* 12, 1691–1702. doi: 10.1111/j.1462-5822.2010.01529.x

Nasser, W., Santhanam, B., Miranda, E. R., Parikh, A., Juneja, K., Rot, G., et al. (2013). Bacterial discrimination by dictyostelid amoebae reveals the complexity of ancient interspecies interactions. *Curr. Biol.* 23, 862–872. doi: 10.1016/j.cub.2013.04.034

Newell, P. C., and Liu, G. (1992). Streamer F mutants and chemotaxis of Dictyostelium. *Bioessays* 14, 473–479. doi: 10.1002/bies.950140708

Neyrolles, O., Wolschendorf, F., Mitra, A., and Niederweis, M. (2015). Mycobacteria, metals, and the macrophage. *Immunol. Rev.* 264, 249–263. doi: 10.1111/imr.12265

O'Connor, T. J., Zheng, H., VanRheenen, S. M., Ghosh, S., Cianciotto, N. P., and Isberg, R. R. (2016). Iron limitation triggers early egress by the intracellular bacterial pathogen *Legionella pneumophila*. *Infect. Immun.* 84, 2185–2197. doi: 10.1128/IAI.01306-15

Oppenheimer, S. J. (2001). Iron and its relation to immunity and infectious disease. *J. Nutr.* 131, 616S–635S.

Ozment, C. P., and Turi, J. L. (2009). Iron overload following red blood cell transfusion and its impact on disease severity. *Biochim. Biophys. Acta* 1790, 694–701. doi: 10.1016/j.bbagen.2008.09.010

Pan, E., Zhang, X. A., Huang, Z., Krezel, A., Zhao, M., Tinberg, C. E., et al. (2011). Vesicular zinc promotes presynaptic and inhibits postsynaptic long-term potentiation of mossy fiber-CA3 synapse. *Neuron* 71, 1116–1126. doi: 10.1016/j.neuron.2011.07.019

Pang, K. M., Lynes, M. A., and Knecht, D. A. (1999). Variables controlling the expression level of exogenous genes in Dictyostelium. *Plasmid* 41, 187–197. doi: 10.1006/plas.1999.1391

Pantopoulos, K., Porwal, S. K., Tartakoff, A., and Devireddy, L. (2012). Mechanisms of mammalian iron homeostasis. *Biochemistry* 51, 5705–5724. doi: 10.1021/bi300752r

Pasricha, S.-R., and Drakesmith, H. (2016). Iron deficiency anemia: problems in diagnosis and prevention at the population level. *Hematol. Oncol. Clin. North Am.* 30, 309–325. doi: 10.1016/j.hoc.2015.11.003

Peracino, B., Balest, A., and Bozzaro, S. (2010). Phosphoinositides differentially regulate bacterial uptake and Nramp1-induced resistance to Legionella infection in Dictyostelium. *J. Cell Sci.* 123, 4039–4051. doi: 10.1242/jcs.072124

Peracino, B., Buracco, S., and Bozzaro, S. (2013). The Nramp (Slc11) proteins regulate development, resistance to pathogenic bacteria and iron homeostasis in *Dictyostelium discoideum*. *J. Cell Sci.* 126, 301–311. doi: 10.1242/jcs.116210

Peracino, B., Wagner, C., Balest, A., Balbo, A., Pergolizzi, B., and Noegel, A. A., et al. (2006). Function and mechanism of action of Dictyostelium Nramp1 (Slc11a1) in bacterial infection. *Traffic* 7, 22–38. doi: 10.1111/j.1600-0854.2005.00356.x

Porcheron, G., Garénaux, A., Proulx, J., Sabri, M., and Dozois, C. M. (2013). Iron, copper, zinc, and manganese transport and regulation in pathogenic Enterobacteria: correlations between strains, site of infection and the relative importance of the different metal transport systems for virulence. *Front. Cell. Infect. Microbiol.* 3:90. doi: 10.3389/fcimb.2013.00090

Portier, E., Zheng, H., Sahr, T., Burnside, D. M., Mallama, C., Buchrieser, C., et al. (2015). IroT/mavN, a new iron-regulated gene involved in *Legionella pneumophila* virulence against amoebae and macrophages. *Environ. Microbiol.* 17, 1338–1350. doi: 10.1111/1462-2920.12604

Prasad, A. S. (2014). Impact of the discovery of human zinc deficiency on health. *J. Trace Elem. Med. Biol.* 28, 357–363. doi: 10.1016/j.jtemb.2014.09.002

Prohaska, J. R., and Lukasewycz, O. A. (1981). Copper deficiency suppresses the immune response of mice. *Science* 213, 559–561. doi: 10.1126/science.7244654

Ragaz, C., Pietsch, H., Urwyler, S., Tiaden, A., Weber, S. S., and Hilbi, H. (2008). The *Legionella pneumophila* phosphatidylinositol-4 phosphate-binding type IV substrate SidC recruits endoplasmic reticulum vesicles to a replication-permissive vacuole. *Cell Microbiol.* 10, 2416–2433. doi: 10.1111/j.1462-5822.2008.01219.x

Ravanel, K., de Chassey, B., Cornillon, S., Benghezal, M., Zulianello, L., Gebbie, L., et al. (2001). Membrane sorting in the endocytic and phagocytic pathway of *Dictyostelium discoideum*. *Eur. J. Cell Biol.* 80, 754–764. doi: 10.1078/0171-9335-00215

Robey, M., and Cianciotto, N. P. (2002). *Legionella pneumophila* feoAB promotes ferrous iron uptake and intracellular infection. *Infect. Immun.* 70, 5659–5669. doi: 10.1128/IAI.70.10.5659-5669.2002

Ross, F. M., and Newell, P. C. (1979). Genetics of aggregation pattern mutations in the cellular slime mould *Dictyostelium discoideum*. *J. Gen. Microbiol.* 115, 289–300. doi: 10.1099/00221287-115-2-289

Rowland, J. L., and Niederweis, M. (2012). Resistance mechanisms of *Mycobacterium tuberculosis* against phagosomal copper overload. *Tuberculosis* 92, 202–210. doi: 10.1016/j.tube.2011.12.006

Rubino, J. T., and Franz, K. J. (2012). Coordination chemistry of copper proteins: how nature handles a toxic cargo for essential function. *J. Inorg. Biochem.* 107, 129–143. doi: 10.1016/j.jinorgbio.2011.11.024

Salah, I. B., Ghigo, E., and Drancourt, M. (2009). Free-living amoebae, a training field for macrophage resistance of mycobacteria. *Clin. Microbiol. Infect.* 15, 894–905. doi: 10.1111/j.1469-0691.2009.03011.x

Skaar, E. P., and Raffatellu, M. (2015). Metals in infectious diseases and nutritional immunity. *Metallomics* 7, 926–928. doi: 10.1039/C5MT90021B

Skriwan, C., Fajardo, M., Hägele, S., Horn, M., Wagner, M., Michel, R., et al. (2002). Various bacterial pathogens and symbionts infect the amoeba *Dictyostelium discoideum*. *Int. J. Med. Microbiol.* 291, 615–624. doi: 10.1078/1438-4221-00177

Soldati, T., and Neyrolles, O. (2012). Mycobacteria and the intraphagosomal environment: take it with a pinch of salt(s)! *Traffic* 13, 1042–1052. doi: 10.1111/j.1600-0854.2012.01358.x

Solomon, J. M., and Isberg, R. R. (2000). Growth of *Legionella pneumophila* in *Dictyostelium discoideum*: a novel system for genetic analysis of host-pathogen interactions. *Trends Microbiol.* 8, 478–480. doi: 10.1016/S0966-842X(00)01852-7

Soofi, S., Cousens, S., Iqbal, S. P., Akhund, T., Khan, J., Ahmed, I., et al. (2013). Effect of provision of daily zinc and iron with several micronutrients on growth and morbidity among young children in Pakistan: a cluster-randomised trial. *Lancet* 382, 29–40. doi: 10.1016/S0140-6736(13)60437-7

Stafford, S. L., Bokil, N. J., Achard, M. E., Kapetanovic, R., Schembri, M. A., McEwan, A. G., et al. (2013). Metal ions in macrophage antimicrobial

pathways: emerging roles for zinc and copper. *Biosci. Rep.* 33:e00049. doi: 10.1042/BSR20130014

Steiner, B., Weber, S., and Hilbi, H. (2017). Formation of the Legionella-containing vacuole: phosphoinositide conversion, GTPase modulation and ER dynamics. *Int. J. Med. Microbiol.* doi: 10.1016/j.ijmm.2017.08.004. [Epub ahead of print].

Steinert, M. (2011). Pathogen-host interactions in Dictyostelium, Legionella, Mycobacterium and other pathogens. *Semin. Cell Dev. Biol.* 22, 70–76. doi: 10.1016/j.semcdb.2010.11.003

Sunaga, N., Monna, M., Shimada, N., Tsukamoto, M., and Kawata, T. (2008). Expression of zinc transporter family genes in Dictyostelium. *Int. J. Dev. Biol.* 52, 377–381. doi: 10.1387/ijdb.072389ns

Tapiero, H., and Tew, K. D. (2003). Trace elements in human physiology and pathology: zinc and metallothioneins. *Biomed. Pharmacother.* 57, 399–411. doi: 10.1016/S0753-3322(03)00081-7

Tiaden, A. N., Kessler, A., and Hilbi, H. (2013). Analysis of legionella infection by flow cytometry. *Methods Mol. Biol.* 954, 233–249. doi: 10.1007/978-1-62703-161-5_14

Tosetti, N., Croxatto, A., and Greub, G. (2014). Amoebae as a tool to isolate new bacterial species, to discover new virulence factors and to study the host–pathogen interactions. *Microb. Pathog.* 77, 125–130. doi: 10.1016/j.micpath.2014.07.009

Urwyler, S., Nyfeler, Y., Ragaz, C., Lee, H., Mueller, L. N., Aebersold, R., et al. (2009). Proteome analysis of Legionella vacuoles purified by magnetic immunoseparation reveals secretory and endosomal GTPases. *Traffic* 10, 76–87. doi: 10.1111/j.1600-0854.2008.00851.x

Valasatava, Y., Rosato, A., Banci, L., and Andreini, C. (2016). MetalPredator: a web server to predict iron-sulfur cluster binding proteomes. *Bioinformatics* 32, 2850–2852. doi: 10.1093/bioinformatics/btw238.

Vignesh, K. S., Figueroa, J. A., Porollo, A., Caruso, J. A., and Deepe, G. S. (2013). Granulocyte macrophage-colony stimulating factor induced Zn sequestration enhances macrophage superoxide and limits intracellular pathogen survival. *Immunity* 39, 697–710. doi: 10.1016/j.immuni.2013.09.006

Wagner, D., Maser, J., Lai, B., Cai, Z., Barry, C. E., Höner Zu Bentrup, K., et al. (2005). Elemental analysis of *Mycobacterium avium*-, *Mycobacterium tuberculosis*-, and *Mycobacterium smegmatis*-containing phagosomes indicates pathogen-induced microenvironments within the host cell's endosomal system. *J. Immunol.* 174, 1491–1500. doi: 10.4049/jimmunol.174.3.1491

Waldron, K. J., Rutherford, J. C., Ford, D., and Robinson, N. J. (2009). Metalloproteins and metal sensing. *Nature* 460, 823–830. doi: 10.1038/nature08300

Ward, S. K., Abomoelak, B., Hoye, E. A., Steinberg, H., and Talaat, A. M. (2010). CtpV: a putative copper exporter required for full virulence of *Mycobacterium tuberculosis*. *Mol. Microbiol.* 77, 1096–1110. doi: 10.1111/j.1365-2958.2010.07273.x

Watts, D. J., and Ashworth, J. M. (1970). Growth of myxameobae of the cellular slime mould *Dictyostelium discoideum* in axenic culture. *Biochem. J.* 119, 171–174.

Weber, S., Wagner, M., and Hilbi, H. (2014). Live-cell imaging of phosphoinositide dynamics and membrane architecture during Legionella infection. *MBio* 5, e00839-13. doi: 10.1128/mBio.00839-13

Weinberg, E. D. (2000). Modulation of intramacrophage iron metabolism during microbial cell invasion. *Microbes Infect.* 2, 85–89. doi: 10.1016/S1286-4579(00)00281-1

Weiss, G., and Carver, P. L. (2017). Role of divalent metals in infectious disease susceptibility and outcome. *Clin. Microbiol. Infect.* 24, 16–23. doi: 10.1016/j.cmi.2017.01.018

White, C., Lee, J., Kambe, T., Fritsche, K., and Petris, M. J. (2009). A role for the ATP7A copper-transporting ATPase in macrophage bactericidal activity. *J. Biol. Chem.* 284, 33949–33956. doi: 10.1074/jbc.M109.070201

Xu, L., Shen, X., Bryan, A., Banga, S., Swanson, M. S., and Luo, Z.-Q. (2010). Inhibition of host vacuolar H+-ATPase activity by a *Legionella pneumophila* effector. *PLoS Pathog.* 6:e1000822. doi: 10.1371/journal.ppat.1000822.

Conflict of Interest Statement: The authors declare that the research was conducted in the absence of any commercial or financial relationships that could be construed as a potential conflict of interest.

frontiers in Cellular and Infection Microbiology

ORIGINAL RESEARCH
published: 30 January 2018
doi: 10.3389/fcimb.2018.00008

Inorganic Polyphosphate Is Essential for *Salmonella* Typhimurium Virulence and Survival in *Dictyostelium discoideum*

Macarena A. Varas[1], Sebastián Riquelme-Barrios[2], Camila Valenzuela[2], Andrés E. Marcoleta[3], Camilo Berríos-Pastén[3], Carlos A. Santiviago[2] and Francisco P. Chávez[1]**

[1] *Laboratorio de Microbiología de Sistemas, Departamento de Biología, Facultad de Ciencias, Universidad de Chile, Santiago, Chile,* [2] *Laboratorio de Microbiología, Departamento de Bioquímica y Biología Molecular, Facultad de Ciencias Químicas y Farmacéuticas, Universidad de Chile, Santiago, Chile,* [3] *Laboratorio de Biología Estructural y Molecular, Departamento de Biología, Facultad de Ciencias, Universidad de Chile, Santiago, Chile*

Inorganic polyphosphate (polyP) deficiency in enteric bacterial pathogens reduces their ability to invade and establish systemic infections in different hosts. For instance, inactivation of the polyP kinase gene (*ppk*) encoding the enzyme responsible for polyP biosynthesis reduces invasiveness and intracellular survival of *Salmonella enterica* serovar Typhimurium (*S.* Typhimurium) in epithelial cells and macrophages *in vitro*. In addition, the virulence *in vivo* of a *S.* Typhimurium Δ*ppk* mutant is significantly reduced in a murine infection model. In spite of these observations, the role played by polyP during the *Salmonella*-host interaction is not well understood. The social amoeba *Dictyostelium discoideum* has proven to be a useful model for studying relevant aspects of the host-pathogen interaction. In fact, many intracellular pathogens can survive within *D. discoideum* cells using molecular mechanisms also required to survive within macrophages. Recently, we established that *S.* Typhimurium is able to survive intracellularly in *D. discoideum* and identified relevant genes linked to virulence that are crucial for this process. The aim of this study was to determine the effect of a polyP deficiency in *S.* Typhimurium during its interaction with *D. discoideum*. To do this, we evaluated the intracellular survival of wild-type and Δ*ppk* strains of *S.* Typhimurium in *D. discoideum* and the ability of these strains to delay the social development of the amoeba. In contrast to the wild-type strain, the Δ*ppk* mutant was unable to survive intracellularly in *D. discoideum* and enabled the social development of the amoeba. Both phenotypes were complemented using a plasmid carrying a copy of the *ppk* gene. Next, we simultaneously evaluated the proteomic response of both *S.* Typhimurium and *D. discoideum* during host-pathogen interaction via global proteomic profiling. The analysis of our results allowed the identification of novel molecular signatures that give insight into *Salmonella-Dictyostelium* interaction. Altogether, our results indicate that inorganic polyP is essential for *S.* Typhimurium virulence and survival in *D. discoideum*. In addition,

OPEN ACCESS

Edited by:
Thierry Soldati,
Université de Genève, Switzerland

Reviewed by:
Francisco Ramos-Morales,
Universidad de Sevilla, Spain
Salvatore Bozzaro,
Università degli Studi di Torino, Italy
Richard H. Gomer,
Texas A&M University College Station, United States

***Correspondence:**
Carlos A. Santiviago
csantiviago@ciq.uchile.cl
Francisco P. Chávez
fpchavez@uchile.cl

Received: *03 November 2017*
Accepted: *09 January 2018*
Published: *30 January 2018*

Citation:
Varas MA, Riquelme-Barrios S, Valenzuela C, Marcoleta AE, Berríos-Pastén C, Santiviago CA and Chávez FP (2018) Inorganic Polyphosphate Is Essential for Salmonella Typhimurium Virulence and Survival in Dictyostelium discoideum. Front. Cell. Infect. Microbiol. 8:8. doi: 10.3389/fcimb.2018.00008

we have validated the use of global proteomic analyses to simultaneously evaluate the host-pathogen interaction of *S.* Typhimurium and *D. discoideum*. Furthermore, our infection assays using these organisms can be exploited to screen for novel anti-virulence molecules targeting inorganic polyP biosynthesis.

Keywords: *Salmonella*, *Dictyostelium*, polyphosphate, *ppk*, virulence, intracellular survival, proteomics

INTRODUCTION

The ability of *Dictyostelium discoideum* cells to feed on bacteria has prompted the development of virulence assays for identifying host defense mechanisms and deciphering bacterial virulence factors (Cosson et al., 2002; Froquet et al., 2009). Basic cellular processes such as phagocytosis, phagosomal development and autophagy, are evolutionarily well conserved between *Dictyostelium* and macrophages (Hägele et al., 2000; Bozzaro and Eichinger, 2011; Dunn et al., 2018). Consequently, *D. discoideum* has been established as a model to study host-pathogen interaction in a wide range of pathogenic bacteria such as *Legionella*, *Salmonella, Francisella*, *Mycobacterium,* and *Pseudomonas*, among others (Pukatzki et al., 2002; Hagedorn and Soldati, 2007; Weber et al., 2014; Lampe et al., 2015; Bravo-Toncio et al., 2016; Riquelme et al., 2016; Cardenal-Muñoz et al., 2017). Unlike mammalian phagocytes, *D. discoideum* is amenable to a diverse array of genetic manipulations facilitating the *in vivo* identification of host susceptibility determinants and pathogen virulence factors (Carilla-Latorre et al., 2008; Hasselbring et al., 2011; Pan et al., 2011; Tosetti et al., 2014; Zhang et al., 2016). However, *in vivo* host-pathogen interaction during bacterial infection in *D. discoideum* remains poorly understood.

Salmonella enterica serovar Typhimurium (*S.* Typhimurium) is a foodborne pathogen causative of gastroenteritis in a variety of warm-blooded animals that largely relies on its ability to survive inside host cells. Relevant genes required for this process are located in pathogenicity islands such as SPI-1 and SPI-2, which encode two independent type III secretion systems (T3SS-1 and T3SS-2, respectively) that inject effector proteins into host cells and are critical during different stages of infection (reviewed in Haraga et al., 2008). In a previous study, we showed that *S.* Typhimurium genes linked to virulence are required to survive in *D. discoideum*, including those encoding factors involved in the biosynthesis of aromatic compounds, the production of a lipopolysaccharide containing a complete O-antigen, T3SS-1, T3SS-2, the type VI secretion system (T6SS) encoded in SPI-6 and the PhoP/PhoQ two-component system (Riquelme et al., 2016). Hence, *S.* Typhimurium exploits a common set of molecular mechanisms to survive within amoeba and animal host cells, supporting the use of *D. discoideum* as a model for host-pathogen interactions and to study the cellular processes that are affected during infection.

We are particularly interested in inorganic polyphosphate (polyP) metabolism because this biopolymer is important for *D. discoideum* development and predation, and for virulence in many bacterial pathogens (Zhang et al., 2005; Brown and Kornberg, 2008). In fact, we have demonstrated that polyP biosynthesis is essential for *P. aeruginosa* PAO1 virulence toward this amoeba (Bravo-Toncio et al., 2016). Inorganic polyP is an abundant and ubiquitous biopolymer that has been conserved in every cell in nature. In the last decades, an increasing number of physiological functions have been reported for polyP in bacteria (Brown and Kornberg, 2008). Due to their phosphoanhydride bonds similar to those in ATP and their properties as polyanions, polyP serve as microbial phosphagen in a variety of biochemical reactions, as a buffer against alkalis, and as a metal storage and metal-chelating agent. In addition, recent studies have revealed the importance of polyP metabolism in signaling and regulatory processes, cell viability and proliferation, and as modulator of microbial stress response (Gray and Jakob, 2015). In numerous pathogenic bacteria, inactivation of the polyP kinase gene (*ppk*) encoding the enzyme responsible for polyP biosynthesis causes defects in biofilm formation, quorum sensing, motility, general stress and stringent responses, and production of virulence factors (Rao et al., 1998; Rashid and Kornberg, 2000; Rashid et al., 2000a,b; Brown and Kornberg, 2008; Varela et al., 2010; Varas et al., 2017). In *S.* Typhimurium, inorganic polyP is essential for long-term survival and virulence factors production (Kim et al., 2002). However, the exact mechanism that links polyP metabolism and *Salmonella* virulence remains to be elucidated.

In this study, we used *D. discoideum* as a host model to study the link between polyP biosynthesis and virulence in *S.* Typhimurium. To this end, we assessed the intracellular survival of *S.* Typhimurium wild-type and Δ*ppk* strains in the amoeba, and the effect of these strains in the social development of the host. Our results indicate that inorganic polyP is essential during *S.* Typhimurium infection of *D. discoideum*. Also, we used global proteomic profiling to get a global view of host cellular responses toward infection that gave insight into *Salmonella-Dictyostelium* interaction.

MATERIALS AND METHODS

Bacterial Strains and Culture Conditions

The bacterial strains used in this study are listed in **Table 1**. All *S.* Typhimurium strains are derivatives of the wild-type, virulent strain 14028s (Fields et al., 1986). Bacteria were routinely grown at 37°C with agitation in Luria-Bertani (LB) medium (10 g/L tryptone, 5 g/L yeast extract, 5 g/L NaCl). When required, LB medium was supplemented with ampicillin (Amp, 100 mg/L), chloramphenicol (Cam, 20 mg/L) or kanamycin (Kan, 75 mg/L). LB medium was solidified by the addition of agar (15 g/L). All procedures involving the use of pathogenic organisms were conducted following the guidelines in the Biosafety Manual of the National Commission of Scientific and Technological Research

TABLE 1 | Bacteria and *Dictyostelium* strains used in this study.

Strains	Features	Source or reference
***Salmonella* Typhimurium**		
14028s	Wild-type, virulent strain	Laboratory collection
Δ*ppk*	14028s Δ*ppk*::Cam	This study
Δ*ppk*/pPPK	14028s Δ*ppk*::Cam/pPPK	This study
Δ*aroA*	14028s Δ*aroA*::Kan	This study
Escherichia coli		
B/r (DBS0348878)	Wild-type strain	Dicty Stock Center (dictyBase)
Dictyostelium discoideum		
AX4 (DBS0302402)	*axeA1 axeB1 axeC1*	Dicty Stock Center (dictyBase)

TABLE 2 | Primers used in this study.

Name	Sequence
aroA_H1+P1	GTTGAGTTTCATGGAATCCCTGACGTTACAACCCAT CGCGGTGCAGGCTGGAGCTGCTTC
aroA_H2+P2	AACAGAAGACTTAGGCAGGCGTACTCATTCGCGCCA GTTGCATATGAATATCCTCCTTAG
aroA_Out5	GCGCGCCTCTATCTATAACG
aroA_Out3	TTTTTCATACTAATCTTCCGTTGA
ppk_(H1+P1)	ATGGGTCAGGAAAAGCTATATATCGAGAAAGAACT GAGCTGTGTAGGCTGGAGCTGCTTC
ppk_(H2+P2)	TTAGTCTGGTTGCTCGAGTGATTTGATGTAGTCATA AATTCATATGAATATCCTCCTTAG
ppk_Out5	ACAGGACTGCGTCTGCTTGCCG
ppk_Out3	CTGCATTGCGCCGTCAACCACG
pBAD_Forward	ATGCCATAGCATTTTTATCC
pBAD_Reverse	GATTTAATCTGTATCAGG

Underlined sequences correspond to the region that anneals to the 5′ or 3′ end of the antibiotic-resistance cassette in template vectors pCLF2 and pCLF4.

(CONICYT), and were approved by the Institutional Biosafety Committee of Universidad de Chile, Campus Norte.

Construction of Mutant Strains

All *S.* Typhimurium mutants were generated by the Lambda Red recombination method (Datsenko and Wanner, 2000) with modifications (Santiviago et al., 2009), using plasmid pCLF4 (Kan^R, GenBank accession number EU629214) or pCLF2 (Cam^R, GenBank accession number HM047089) as template. Correct allelic replacement in these mutants was confirmed by PCR amplification using primers flanking the substitution site. All primers for PCR amplifications are listed in **Table 2**.

Construction of Complementing Plasmid pPPK

A DNA fragment containing the *ppk* gene (including its promoter region) was amplified from the genome of *S.* Typhimurium strain 14028s using *Taq* DNA polymerase (Invitrogen) and primers ppk_Out5 and ppk_Out3 (**Table 2**). The PCR product was purified from 1% agarose gels using the "QIAquick Gel Extraction Kit" (QIAGEN) and cloned into pBAD-TOPO using the "pBAD-TOPO TA Expression Kit" (Invitrogen). The presence and orientation of the insert in the recombinant plasmid generated (pPPK) was confirmed by PCR amplification using combinations of primers ppk_Out5, ppk_Out3, pBAD_Forward and pBAD_Reverse (**Table 2**). Finally, *S.* Typhimurium Δ*ppk* was transformed by electroporation with plasmid pPPK for complementation assays.

Dictyostelium Culture Conditions

D. discoideum strain AX4 was obtained from Dicty Stock Center (Kreppel et al., 2004; Basu et al., 2013; Fey et al., 2013), and cultured according to standard protocols (Fey et al., 2007). Briefly, amoebae were maintained at 22°C in SM medium (10 g/L glucose, 10 g/L peptone, 1 g/L yeast extract, 1 g/L $MgSO_4 \times 7H_2O$, 1.9 g/L KH_2PO_4, 0.6 g/L K_2HPO_4, 20 g/L agar), growing on a confluent lawn of *Escherichia coli* B/r. Before development and intracellular survival assays, amoebae were grown in the absence of bacteria (axenic cultures) at 22°C with agitation (180 rpm) in liquid HL5 medium (14 g/L tryptone, 7 g/L yeast extract, 0.35 g/L Na_2HPO_4, 1.2 g/L KH_2PO_4, 14 g/L glucose, pH 6.3). When required, media were supplemented with streptomycin (Stp; 300 mg/L) and Amp (100 mg/L). Amoebae were harvested in early exponential phase ($1–1.5 \times 10^6$ cells/mL) and centrifuged at $500 \times g$ for 10 min at 4°C. The supernatant was discarded and the pellet was adjusted to 1×10^6 cells/mL in HL5 medium for development assays or washed three times using Soerensen buffer (2 g/L KH_2PO_4, 0.36 g/L $Na_2HPO_4 \times 2H_2O$, pH 6.0) for intracellular survival assays. The population of viable amoebae was evaluated by Trypan blue exclusion and counting in a Neubauer chamber.

Development Assay

Individual wells of a 24-well plate containing N agar (Soerensen buffer supplemented with 1 g/L peptone, 1 g/L glucose and 20 g/L agar) were inoculated with 30 μL of a stationary-phase culture from each bacterial strain to be evaluated. The plate was incubated overnight at 22°C to generate bacterial lawns. The next day, 10 μL of a cellular suspension containing 1×10^4 *D. discoideum* AX4 cells in HL5 was spotted in the middle of each well and the plate was further incubated at 22°C for 6 days. Amoebae were monitored daily and the developmental phase reached ("aggregation," "elevation," and "culmination") was scored. A score of "1" was assigned when amoebae aggregated forming a phagocytosis plaque. A score of "2" was assigned when elevated structures, such as "slugs" or "fingers", were observed all across the surface of the agar in the well. A score of "3" was assigned when fruiting bodies were formed all across the surface of the agar in the well. Intermediate states among two developmental phases were recorded as average values of the corresponding scores. In addition, representative images of *D. discoideum* development were obtained at days 2 and 4 using an Olympus MVX10 stereomicroscope.

Intracellular Survival Assay

Intracellular survival assays were performed as described previously (Riquelme et al., 2016). Briefly, each bacterial strain to

be assessed was grown to stationary phase, harvested and washed twice with Soerensen buffer. Next, $\sim 2 \times 10^7$ *D. discoideum* AX4 cells were mixed with each bacterial strain until reaching a multiplicity of infection (MOI) of 100 bacteria/amoeba in 10 mL of Soerensen buffer. After 1 h of co-incubation at 22°C with agitation (180 rpm), the extracellular bacteria were removed by three sequential washing steps using Soerensen buffer. The infected amoebae were suspended in 10 mL of Soerensen buffer ($t = 0$) and further incubated at 22°C with agitation (180 rpm). Aliquots were obtained at 0, 1, 3, 4.5, and 6 h post infection. The population of viable amoebae were determined at each time point. In parallel, infected amoebae recovered at each time point were lysed with 0.2% Triton X-100 and loads of intracellular bacteria were estimated by serial dilutions and plating on LB agar. Statistical significance was determined using a one-way ANOVA and two-way ANOVA with Fisher's LSD post-test.

Global Proteomic Profiling Using Q-Exactive Mass Spectrometry

For proteomic analyses, $\sim 1 \times 10^6$ amoeba cells were obtained from individual intracellular survival assays after 6 h of infection with the wild-type strain or the Δ*ppk* mutant. Uninfected amoebae were used as control condition. Amoebae from each experimental condition were concentrated by centrifugation at $500 \times g$ for 10 min, quick-frozen, and kept at −80°C until further use. Global proteomic profiles from samples representing the different experimental conditions were obtained from Bioproximity, LLC (USA). In each case, a unique proteomic analysis was performed using a pool of cells from three independent assays. Protein denaturation, digestion and desalting of samples were prepared using the filter-assisted sample preparation (FASP) method (Wiśniewski et al., 2009). Briefly, the samples were digested using trypsin, and each digestion mixture was analyzed by ultra-high pressure liquid chromatography (UHPLC-MS/MS) coupled to a high resolution, high mass accuracy quadrupole-Orbitrap mass spectrometer (Q-Exactive, Thermo Fisher). For protein quantification, intensity measurements derived from the area-under-the-curve of the MS/MS scan for each peptide ion identification were summed for each sample. These values were averaged across all samples and a normalization factor determined and applied for each sample (Zhang et al., 2010). MS/MS data were compared with the most recent protein sequence libraries available from UniProtKB. Proteins were required to have one or more unique peptides detected across the analyzed samples with an *e*-value ≤ 0.0001.

Proteomes from each experimental condition were compared using an online tool that generates Venn diagrams and lists of proteins detected in any given condition (http://bioinformatics.psb.ugent.be/webtools/Venn/). The proteins detected in 2 experimental conditions were analyzed by calculating $\log_2$ values of condition_1/condition_2 detection ratios. Enrichment for a protein in a particular condition was considered when the corresponding calculated value was >0.6 (∼1.5 fold enrichment).

Analysis of *D. discoideum* Proteins Detected by Global Proteomic Profiling

D. discoideum proteins were identified from Q-proteomics data using library ID: 44689 (PubMed Taxonomy database), which include proteomes of strains AX2, AX3 y AX4. Proteins were classified according to the predicted functions annotated in the *Clusters of Orthologous Groups of Proteins* (COGs) database (Tatusov et al., 2000). The UniProtKB ID of each protein was mapped to the COGs database of the Social Amoeba Comparative Genome Browser (SACGB, http://sacgb.leibniz-fli.de/cgi/cog.pl?ssi=free), and the EggNOG database of orthologous groups and functional annotation (Jensen et al., 2008). To do this, both databases were downloaded, and mappings were performed using custom Python scripts. Using this approach we were able to assign COG categories for ∼80% of all proteins detected in each experimental condition.

In addition, overrepresentation analyses were performed using the *Protein Annotation Through Evolutionary Relationship* (PANTHER) tool (http://www.pantherdb.org/), a comprehensive system that combines gene function, ontology, pathways and statistical analysis tools that enable the analysis of large-scale, genome-wide data from sequencing, proteomics or gene expression experiments (Mi et al., 2013, 2016). To do this, the UniProtKB IDs from the different sets of detected protein were used as input in PANTHER. This tool was able to map the UniProtKB ID for ∼96% of all proteins detected in each experimental condition. The results of overrepresentation analyses were filtered according to three annotation data sets: "Biological process", "Cellular component", and "Reactome pathways". The cut-off for the analyses was set to $P < 0.05$.

Analysis of Bacterial Proteins Detected by Global Proteomic Profiling

S. Typhimurium proteins were identified from Q-proteomics data using the libraries ID: 588858 and ID: 99287 (PubMed Taxonomy database), which include proteomes of strains 14028s and LT2. Virulence-related proteins were assigned following inspections of databases PATRIC_VF, VFDB and VICTORS, using tools available at the Pathosystems Resource Integration Center web site (PATRIC; www.patricbrc.org). Also, proteins encoded in genes located in close proximity to known virulence determinants, as well as genes located within *Salmonella* pathogenicity islands (SPIs) or prophages, were identified and analyzed using Artemis V.14, IslandViewer 3, Pathogenicity Island DataBase (PAIDB v2.0), PHAST and Islander (Rutherford et al., 2000; Zhou et al., 2011; Dhillon et al., 2015; Hudson et al., 2015; Yoon et al., 2015).

RESULTS AND DISCUSSION

Inorganic Polyphosphate Is Essential for *S.* Typhimurium Virulence in *D. discoideum*

To evaluate the role played by polyP biosynthesis in the virulence of *S.* Typhimurium in *D. discoideum*, we constructed a Δ*ppk* derivative of the wild-type, virulent strain 14028s. This mutant is impaired in the synthesis of polyP. In addition, the mutant was

transformed with a plasmid harboring a wild-type version of *ppk* (i.e., pPPK) to confirm the specificity of the effects attributed to the inactivation of this gene in our assays.

Previous reports indicate that virulent pathogenic bacteria delay the social development of *D. discoideum*, while attenuated or non-pathogenic bacteria allow its rapid progression (within 3–4 days in our experimental conditions). Thus, assessing the effect of a given bacterial strain on the social development of *D. discoideum* can be used to evaluate its virulence (Sillo et al., 2011; Bravo-Toncio et al., 2016; Ouertatani-Sakouhi et al., 2017). Notably, this host-pathogen interaction model has been recently used to identify compounds that inhibit bacterial virulence (Bravo-Toncio et al., 2016; Ouertatani-Sakouhi et al., 2017). Therefore, we compared the effect of feeding *D. discoideum* with the wild-type strain or its Δ*ppk* derivative on the social development of the amoeba. In addition, a Δ*aroA* derivative of strain 14028s (known to be attenuated in murine infection models Sebkova et al., 2008), and *Escherichia coli* B/r (routinely used to feed *D. discoideum* during growth under laboratory conditions Fey et al., 2007) were included in our assay as attenuated and non-pathogenic controls, respectively.

The different bacterial strains were inoculated on N agar and incubated overnight to generate bacterial lawns. Then, *D. discoideum* cells were deposited on top of each bacterial lawn and the plates were monitored for 6 days to follow the progression of *D. discoideum* development, which mainly involves three sequential stages: aggregation, elevation, and culmination (**Figure 1**). *E. coli* B/r allowed the rapid progression of the development, culminating within 3 to 4 days, where mature fruiting bodies were predominant (**Figure 1**). A similar phenotype was observed in the case of the Δ*aroA* mutant, indicating that this strain is not virulent for *D. discoideum*. This observation is in agreement with previous reports indicating that an *aroA* mutant of *S.* Typhimurium is unable to survive intracellularly in this amoeba (Riquelme et al., 2016). On the contrary, the wild-type strain produced a delay in the development of the amoeba where only the aggregation phase was reached after 6 days of co-incubation (**Figure 1**). This phenotype was not observed in the case of the Δ*ppk* mutant, which allowed the development of the amoebae until reaching the elevation phase at 6 days of co-incubation. Of note, the Δ*ppk* mutant harboring plasmid pPPK showed a wild-type phenotype

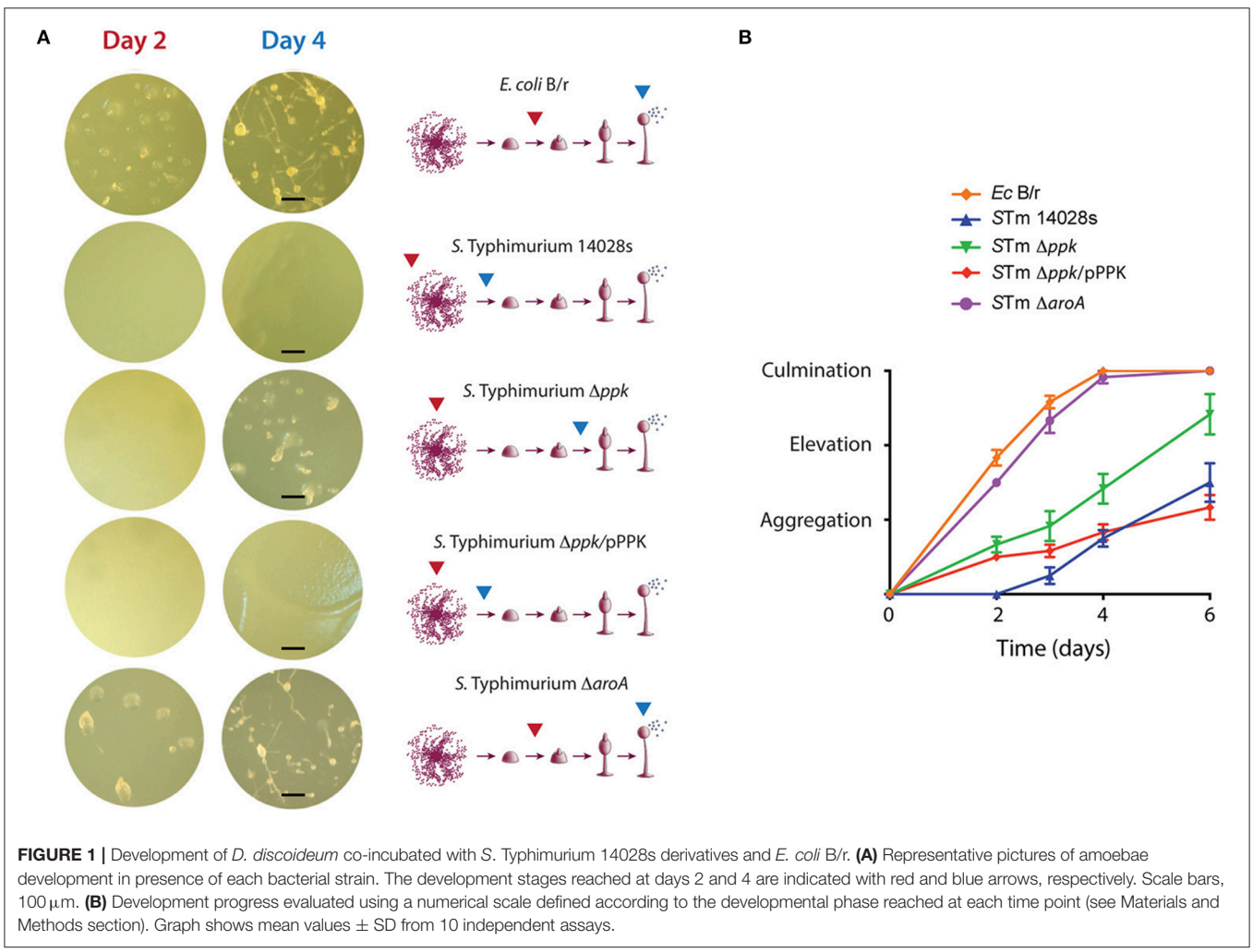

FIGURE 1 | Development of *D. discoideum* co-incubated with *S.* Typhimurium 14028s derivatives and *E. coli* B/r. **(A)** Representative pictures of amoebae development in presence of each bacterial strain. The development stages reached at days 2 and 4 are indicated with red and blue arrows, respectively. Scale bars, 100 μm. **(B)** Development progress evaluated using a numerical scale defined according to the developmental phase reached at each time point (see Materials and Methods section). Graph shows mean values ± SD from 10 independent assays.

(**Figure 1**). These results indicate that polyP synthesis is essential for *S.* Typhimurium virulence in *D. discoideum.*

Our observations on the interaction of *S.* Typhimurium with *D. discoideum* are consistent with a previous study that evaluated the virulence of the pathogen by assessing its effect on the social development of the amoeba. The authors reported that *Dictyostelium* growth on a lawn of wild-type *S.* Typhimurium causes the aberrant development of the amoeba, or even resulted in cell death depending on nutrient conditions of the medium used for the assay. Both phenotypes required a functional T3SS-2 (Sillo et al., 2011). Additionally, the effect observed for a polyP deficiency on the social development of the amoeba has been also reported in the case of *P. aeruginosa* (Zhang et al., 2005; Bravo-Toncio et al., 2016) highlighting the essential role played by polyP biosynthesis in bacterial virulence using this model organism.

Inorganic Polyphosphate Is Essential for *S.* Typhimurium Survival in *D. discoideum*

Recently, we reported that wild-type *S.* Typhimurium can survive within *D. discoideum* and requires relevant genes linked to virulence for this process (Riquelme et al., 2016). To evaluate the role played by polyP in the intracellular survival of *S.* Typhimurium in *D. discoideum*, we performed infection assays where vegetative amoebae were co-incubated with the wild-type strain or its Δ*ppk* derivative. At different times post infection, intracellular bacteria were recovered from infected amoebae and titrated. The attenuated Δ*aroA* mutant was included as a control in our assays.

First, we evaluated the internalization of each mutant strain after 1 h of co-incubation with the amoebae, and observed that Δ*ppk* and Δ*aroA* mutants were internalized at higher levels than the wild-type strain. In contrast, the Δ*ppk* mutant harboring plasmid pPPK was internalized at wild-type levels (**Figure 2A**). Then, we evaluated the intracellular survival of each strain at different times post infection and observed that the wild-type strain was able to survive and replicate in the amoebae. On the contrary, the Δ*ppk* mutant was defective for intracellular survival at all time points evaluated. The same phenotype was observed in the case of the attenuated Δ*aroA* mutant. The intracellular survival of the Δ*ppk* mutant harboring plasmid pPPK was comparable to that shown by the wild-type strain (**Figure 2B**). It is worth mentioning that no effect in amoeba viability was observed during the course of these experiments (**Figure 2C**), indicating that the differences observed in the titers of intracellular bacteria are not attributable to changes in the number of viable amoebae.

Overall, our results indicate that polyP synthesis is essential for *S.* Typhimurium to survive intracellularly in *D. discoideum.* These observations are in line with a previous study indicating that a Δ*ppk* mutant of *S.* Typhimurium is deficient for intracellular survival in RAW 264.7 murine macrophages (Kim et al., 2002). In addition, several studied indicate that *S.* Typhimurium *ppk* mutants present a variety of phenotypes, including defective long-term survival *in vitro*, defective responses to oxidative stress and starvation, sensitivity to polymyxin, intolerance to acid and heat, impaired invasiveness in HEp-2 epithelial cells, and loss of swimming motility, all of which strongly influence virulence (Kim et al., 2002; McMeechan

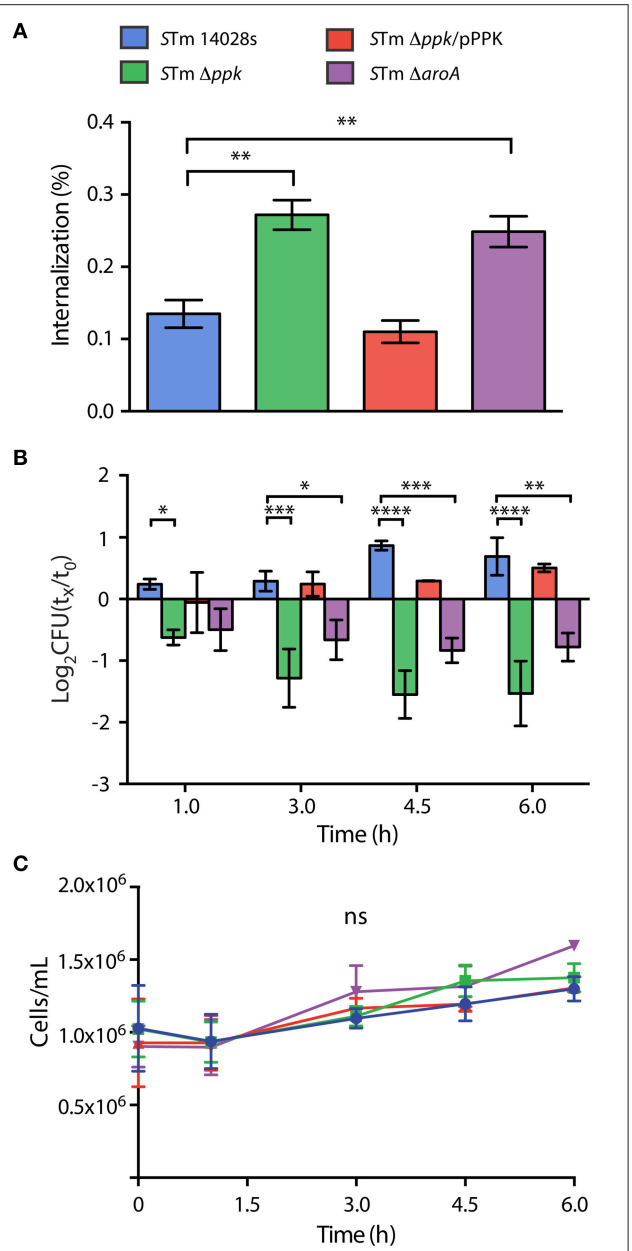

FIGURE 2 | Internalization and intracellular survival of *S.* Typhimurium 14028s derivatives in *D. discoideum*. **(A)** Percentage of internalized bacteria after 1 hour of co-incubation, calculated as 100 × ($CFU_{t=0}$/$CFU_{inoculum}$). Statistical significance was determined using a one-way ANOVA with Fisher's LSD post-test (** = p <0.005). **(B)** Intracellular survival at different times post infection, expressed as $\log_2(CFU_{t=x}/CFU_{t=0})$. Statistical significance was determined using a two-way ANOVA with Fisher's LSD post-test (* = $p < 0.05$, ** = $p < 0.005$, *** = $p < 0.001$, **** = p <0.0001). **(C)** Population of viable amoebae at each time point expressed as cells/mL. Statistical significance was determined using a two-way ANOVA with Fisher's LSD post-test (ns = not significant). Graphs in panels **(A–C)** show mean values ± SD from 5 independent assays. The color code in panel **(A)** is also valid for panels **(B,C)**.

et al., 2007; Cheng and Sun, 2009). Accordingly, it has been reported that a *ppk* mutant of *S.* Typhimurium was attenuated in orally-infected Rhode Island Red chickens and BALB/c mice (McMeechan et al., 2007).

Global Proteomic Profiling of *Dictyostelium-Salmonella* Interaction

In order to determine the global response of *D. discoideum* to infections with *S.* Typhimurium wild type or its Δ*ppk* mutant derivative, we performed a global proteomic profiling of such interactions. To achieve this, the amoebae were co-incubated with each bacterial strain until reaching 6 h of infection. This time was chosen because the intracellular survival of both strains in *D. discoideum* showed the highest differences (**Figure 2B**). Non-infected amoebae were used as control condition. Next, shotgun proteomic profiling of infected and control amoebae were performed by UHPLC-MS/MS (Q-proteomics). Thus, 1779, 1950, and 1850 proteins were detected in samples of amoebae infected with the wild-type strain, amoebae infected with the Δ*ppk* mutant, and uninfected amoebae, respectively (**Table S1**).

A total of 258, 250, and 336 proteins were exclusively detected in non-infected amoebae, in amoebae infected with the wild-type strain, or in amoebae infected with the Δ*ppk* mutant, respectively. Additionally, 1277 proteins were detected in all three experimental conditions tested (**Figure 3A**). Considering that these proteins could be interesting if they show significant differences in expression levels, we carried out a comparative analysis of proteins detected in pairs of experimental conditions

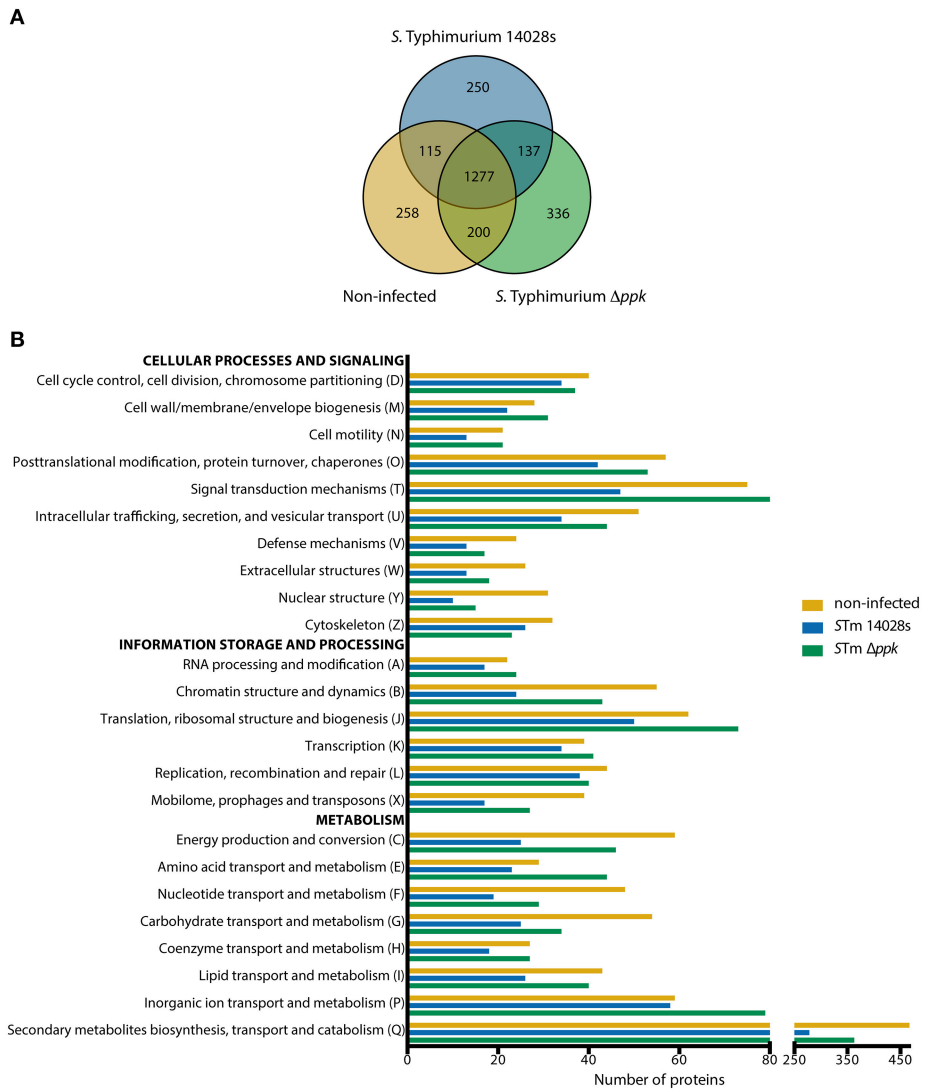

FIGURE 3 | COG functional categorization of *D. discoideum* proteins detected during infection with *S.* Typhimurium strains. **(A)** Venn diagram of *D. discoideum* proteins detected in uninfected amoebae or in amoebae infected with *S.* Typhimurium wild-type or its Δ*ppk* derivative. **(B)** Graph showing number of proteins detected in each experimental condition and classified according to COG functional categories (see Materials and Methods section). COG categories were further grouped in three main classes: "Cellular processes and signaling", "Information storage and processing", and "Metabolism".

(i.e., non-infected amoebae vs. infected with the wild-type strain; non infected amoebae vs. infected with the Δ*ppk* mutant; and amoebae infected with the wild-type strain vs. infected with the Δ*ppk* mutant) to determine enrichment in a particular condition (cut-off: ∼1.5 fold change). Proteins found exclusively or enriched in a given experimental condition were classified according to COG categories, which in turn were grouped in three main classes: "Cellular processes and signaling", "Information storage and processing", and "Metabolism" (**Table S2**). For most COG categories, the total number of proteins detected from non-infected amoebae was similar to those detected from amoebae infected with the Δ*ppk* mutant, in contrast to proteins detected in amoebae infected with the wild-type strain (**Figure 3B**). This was particularly evident in the case of COG categories "Posttranslational modification, protein turnover, chaperones", "Signal transduction mechanisms", "Intracellular trafficking, secretion, and vesicular transport" (associated with "Cellular processes and signaling"), "Chromatin structure and dynamics", "Translation, ribosomal structure, and biogenesis", "Mobilome, prophages, and transposons" (associated with "Information storage and processing"), "Energy production and conversion", "Nucleotide transport and metabolism", "Carbohydrate transport and metabolism", "Coenzyme transport and metabolism", "Lipid transport an metabolism", and "Secondary metabolites biosynthesis, transport and catabolism" (associated with "Metabolism"; **Figure 3B**).

Additionally, proteins that were exclusive or significantly enriched in each experimental condition were identified and used to perform overrepresentation analyses using the PANTHER tool (**Table S3**). The results were filtered according to three annotation data sets: "Biological process", "Cellular component", and "Reactome pathways" (**Table 3**). Overrepresented groups of proteins detected in *D. discoideum* infected with either *S.* Typhimurium strain include those involved in endomembrane trafficking, actin cytoskeleton organization, social development, chemotaxis and response to cAMP, immune system, response to bacteria, ubiquitination and proteasome degradation.

Regarding endomembrane trafficking, common overrepresented proteins include those involved in Secretion of lysosomal enzymes (GO:0033299), Exocytosis (GO:0006887), Phagocytosis (GO:0006909), Early phagosome (GO:0032009), Endosome (GO:0005768), Signaling by Rho GTPases (R-DDI-194315), Rho GTPases Activate WASPs and WAVEs (R-DDI-5663213), and Fc gamma receptor (FCGR) dependent phagocytosis (R-DDI-2029480). Overrepresented proteins in amoebae infected with the wild-type strain include those involved in Rab protein signal transduction (GO:0032482), Positive regulation of guanyl-nucleotide exchange factor activity (GO:1905099), Regulation of vacuole fusion, non-autophagic (GO:0032889), Lysosomal lumen acidification (GO:0007042), Protein localization to lysosome (GO:0061462), Vesicle transport along microtubule (GO:0047496), Phosphatidylinositol phosphorylation (GO:0046854), Phosphatidylinositol-mediated signaling (GO:0048015), G beta:gamma signaling through PI3Kgamma (R-DDI-392451), and PI3K Cascade (R-DDI-109704). On the other hand, overrepresented proteins in amoebae infected with the Δ*ppk* mutant include those linked to Phosphatidylinositol 3-kinase signaling (GO:0014065), Phosphatidylinositol 3-kinase complex (GO:0005942), Regulation of exocytosis (GO:0017157), Vacuolar acidification (GO:0007035), Late endosome to vacuole transport (GO:0045324), Establishment of protein localization to vacuole (GO:0072666), Post-lysosomal vacuole (GO:0032195), Late endosome (GO:00057770), and Lysosome (GO:0005764). It is well known that *S.* Typhimurium delivers T3SS-2 effector proteins that interfere with the maturation of the endocytic route in eukaryotic host cells in order to avoid phagolysosomal fusion. This process results in a unique vacuolar compartment referred to as the *Salmonella*-containing vacuole (SCV), where this pathogen resides (Haraga et al., 2008; LaRock et al., 2015). We have described that inactivation of T3SS-2 abolishes the intracellular survival of *S.* Typhimurium in *D. discoideum* (Riquelme et al., 2016). Accordingly, our analysis suggest that wild-type *S.* Typhimurium resides in an intracellular compartment of *D. discoideum* comparable to an early endosome, while the Δ*ppk* mutant resides in a compartment that ultimately fuses with the lysosome, explaining the defective intracellular survival phenotype shown by this strain in the amoeba (**Figure 2**).

Most overrepresented proteins associated with the response to bacterial infection were detected in amoeba infected with either strain of *S.* Typhimurium. These proteins include those linked to Immune System (R-DDI-168256), Innate Immune System (R-DDI-168249), Adaptive Immune System (R-DDI-1280218), Cross-presentation of soluble exogenous antigens (endosomes) (R-DDI-1236978), Antigen processing: Ubiquitination & Proteasome degradation (R-DDI-983168), and ROS, RNS production in response to bacteria (R-DDI-1222556). No overrepresented proteins were exclusively detected in infections with the wild-type strain, while overrepresented proteins only detected during infections with the Δ*ppk* mutant include those associated with Metabolism of nitric oxide (R-DDI-202131) and eNOS activation and regulation (R-DDI-203765). These proteins (SprA/Q54GP3, PtsA/Q1ZXI0, and GchA/Q94465) are required for the *de novo* biosynthesis of tetrahydrobiopterin, an essential co-factor for the aromatic amino acid hydroxylases and nitric oxide synthases in mammals (Thöny et al., 2000; Choi et al., 2006; Vásquez-Vivar, 2009). These results indicate that *D. discoideum* infected with either wild-type or Δ*ppk S.* Typhimurium generates a robust response that includes production of ROS and RNS in order to eliminate the pathogen.

Proteins exclusively detected in *D. discoideum* infected with the wild-type strain indicate that the pathogen induces DNA damage in the host. This is revealed by a number of proteins involved in Positive regulation of single strand break repair (GO:1903518), Positive regulation of DNA repair (GO:0045739), DNA ligation involved in DNA repair (GO:0051103), Site of double-strand break (GO:0035861), and Cell death signaling via NRAGE, NRIF, and NADE (R-DDI-204998), the latter being a process associated with apoptotic cell death. It is tempting to speculate that this DNA damage is the result of excessive ROS/RNS production in response to the pathogen.

TABLE 3 | Overrepresentation analysis of *D. discoideum* proteins detected during infections with *S*. Typhimurium wild type and Δ*ppk*.

A. *D. discoideum* infected with *S*. Typhimurium wild type

Biological process	**Fold enrichment**	***p*-value**
Actin filament reorganization (GO:0090527)	20.47	4.77E-02
Protein sulfation (GO:0006477)	20.47	4.77E-02
Positive regulation of protein localization to cell surface (GO:2000010)	20.47	4.77E-02
Anaerobic respiration (GO:0009061)	20.47	4.77E-02
Cell-cell signaling (GO:0007267)	20.47	4.77E-02
Rab protein signal transduction (GO:0032482)	20.47	4.77E-02
Positive regulation of single strand break repair (GO:1903518)	20.47	4.77E-02
Positive regulation of DNA repair (GO:0045739)	20.47	4.77E-02
Positive regulation of guanyl-nucleotide exchange factor activity (GO:1905099)	20.47	4.77E-02
Regulation of vacuole fusion, non-autophagic (GO:0032889)	20.47	4.77E-02
Lysosomal lumen acidification (GO:0007042)	20.47	4.77E-02
Secretion of lysosomal enzymes (GO:0033299)	12.28	2.02E-03
Protein localization to lysosome (GO:0061462)	10.24	1.68E-02
Negative regulation of phagocytosis (GO:0050765)	8.53	3.51E-04
Vesicle transport along microtubule (GO:0047496)	8.19	2.54E-02
Aerobic respiration (GO:0009060)	6.43	1.80E-06
DNA ligation involved in DNA repair (GO:0051103)	6.14	1.35E-02
Regulation of aggregate size involved in sorocarp development (GO:0031157)	5.69	2.10E-03
Response to reactive oxygen species (GO:0000302)	5.51	3.44E-04
Phosphatidylinositol phosphorylation (GO:0046854)	5.46	6.69E-03
Phosphatidylinositol-mediated signaling (GO:0048015)	4.82	1.02E-02
Response to cAMP (GO:0051591)	4.72	2.66E-02
Positive regulation of actin filament polymerization (GO:0030838)	4.09	3.93E-03
Defense response to bacterium (GO:0042742)	3.56	2.74E-02
Chemotaxis to cAMP (GO:0043327)	2.63	8.39E-03
Exocytosis (GO:0006887)	2.52	1.59E-02
Phagocytosis (GO:0006909)	2.44	9.34E-03
Aggregation involved in sorocarp development (GO:0031152)	1.87	2.46E-02
Cellular component	**Fold enrichment**	***p*-value**
Proteasome core complex, beta-subunit complex (GO:0019774)	20.47	4.77E-02
Actomyosin, actin portion (GO:0042643)	20.47	4.77E-02
Site of double-strand break (GO:0035861)	20.47	4.77E-02
Nuclear SCF ubiquitin ligase complex (GO:0043224)	20.47	4.77E-02
Vacuolar proton-transporting V-type ATPase, V1 domain (GO:0000221)	13.65	9.73E-03
Early phagosome (GO:0032009)	7.31	7.00E-04
Proteasome core complex, alpha-subunit complex (GO:0019773)	5.85	4.66E-02
Phagolysosome (GO:0032010)	5.12	3.28E-03
Endosome (GO:0005768)	2.16	8.59E-03
Reactome pathways	**Fold enrichment**	***p*-value**
G beta:gamma signaling through Pl3Kgamma (R-DDI-392451)	20.47	4.77E-02
Antigen presentation: Folding, assembly and peptide loading of class I MHC (R-DDI-983170)	10.24	1.68E-02
Cell death signaling via NRAGE, NRIF and NADE (R-DDI-204998)	6.51	1.26E-04
Rho GTPases Activate WASPs and WAVEs (R-DDI-5663213)	6.40	1.26E-03
ROS, RNS production in response to bacteria (R-DDI-1222556)	6.14	1.35E-02
Iron uptake and transport (R-DDI-917937)	6.14	1.35E-02
Pl3K Cascade (R-DDI-109704)	5.12	2.17E-02
Cytosolic sensors of pathogen-associated DNA (R-DDI-1834949)	4.39	3.21E-02

(Continued)

TABLE 3 | Continued

Reactome pathways	**Fold enrichment**	***p*-value**
Cellular response to heat stress (R-DDI-3371556)	4.31	1.48E-02
Fc gamma receptor (FCGR) dependent phagocytosis (R-DDI-2029480)	4.24	3.34E-03
Signaling by Rho GTPases (R-DDI-194315)	3.32	3.64E-04
Cross-presentation of soluble exogenous antigens (endosomes) (R-DDI-1236978)	3.10	2.42E-02
Immune System (R-DDI-168256)	3.00	2.94E-07
Innate Immune System (R-DDI-168249)	2.58	4.63E-04
Adaptive Immune System (R-DDI-1280218)	2.53	2.39E-03
Antigen processing: Ubiquitination & Proteasome degradation (R-DDI-983168)	2.34	2.34E-02
Cellular responses to stress (R-DDI-2262752)	2.32	4.78E-02

B. *D. discoideum* infected with *S.* Typhimurium Δ*ppk*

Biological process	**Fold enrichment**	***p*-value**
Positive regulation of sporulation (GO:0043938)	16.14	7.06E-03
Negative regulation of phagocytosis (GO:0050765)	8.07	1.23E-04
Arp2/3 complex-mediated actin nucleation (GO:0034314)	6.92	9.83E-03
Phosphatidylinositol 3-kinase signaling (GO:0014065)	6.46	3.91E-02
Regulation of exocytosis (GO:0017157)	6.46	3.91E-02
Secretion of lysosomal enzymes (GO:0033299)	6.46	3.91E-02
Regulation of protein ubiquitination (GO:0031396)	6.05	1.40E-02
Vacuolar acidification (GO:0007035)	6.05	1.40E-02
Negative regulation of actin filament polymerization (GO:0030837)	5.95	2.20E-04
Regulation of positive chemotaxis (GO:0050926)	5.38	1.91E-02
Response to cAMP (GO:0051591)	4.97	9.25E-03
Late endosome to vacuole transport (GO:0045324)	4.97	9.25E-03
Aerobic respiration (GO:0009060)	4.61	8.67E-05
Chemotaxis to cAMP (GO:0043327)	4.15	6.93E-07
Establishment of protein localization to vacuole (GO:0072666)	4.04	8.75E-03
Response to bacterium (GO:0009617)	3.99	3.18E-07
Actin filament polymerization (GO:0030041)	3.77	3.02E-03
Phagocytosis (GO:0006909)	3.65	2.21E-06
Response to oxidative stress (GO:0006979)	3.28	2.40E-04
Exocytosis (GO:0006887)	2.73	2.90E-03
Aggregation involved in sorocarp development (GO:0031152)	1.82	1.78E-02
Cellular component	**Fold enrichment**	***p*-value**
Post-lysosomal vacuole (GO:0032195)	10.76	1.53E-02
Proton-transporting V-type ATPase, V1 domain (GO:0033180)	6.92	9.83E-03
Arp2/3 protein complex (GO:0005885)	6.46	3.74E-03
Early phagosome (GO:0032009)	5.76	1.98E-03
Proteasome complex (GO:0000502)	5.26	8.14E-07
Phosphatidylinositol 3-kinase complex (GO:0005942)	4.04	3.96E-02
Proteasome core complex (GO:0005839)	4.04	1.84E-02
Endosome (GO:0005768)	2.36	8.82E-04
Late endosome (GO:00057770)	2.36	8.82E-04
Lysosome (GO:0005764)	1.79	3.99E-02
Reactome pathways	**Fold enrichment**	***p*-value**
eNOS activation and regulation (R-DDI-203765)	12.11	2.10E-03
Metabolism of nitric oxide (R-DDI-202131)	12.11	2.10E-03
ROS, RNS production in response to bacteria (R-DDI-1222556)	8.07	4.51E-04

(Continued)

TABLE 3 | Continued

Reactome pathways	Fold enrichment	*p*-value
Iron uptake and transport (R-DDI-917937)	6.73	1.02E-03
Cross-presentation of soluble exogenous antigens (endosomes) (R-DDI-1236978)	6.36	2.47E-07
Rho GTPases Activate WASPs and WAVEs (R-DDI-5663213)	5.04	3.50E-03
Fc gamma receptor (FCGR) dependent phagocytosis (R-DDI-2029480)	3.90	2.51E-03
Innate Immune System (R-DDI-168249)	3.35	5.65E-08
Signaling by Rho GTPases (R-DDI-194315)	3.05	2.87E-04
Antigen processing: Ubiquitination & Proteasome degradation (R-DDI-983168)	3.00	5.52E-04
Immune System (R-DDI-168256)	2.93	2.06E-08
Adaptive Immune System (R-DDI-1280218)	2.77	1.41E-04

Overrepresentation analyses were performed using PANTHER (http://www.pantherdb.org/). UniProtKB IDs from exclusive and significantly-enriched proteins of D. discoideum detected during infections with the wild-type strain or the Δppk mutant were used as input. The results were filtered according to 3 annotation data sets: "Biological process," "Cellular component," and "Reactome pathways." The cut-off for the analyses was set to $p < 0.05$.

Furthermore, this DNA damage needs to be repaired by the amoeba in order to resume growth and development. This is in agreement with the ability of *S.* Typhimurium to delay the social development of *D. discoideum* according to our development assay (**Figure 1**). In addition, two proteins linked to Protein sulfation (GO:0006477) (i.e., Kil1/Q556K8 and Phg1a/Q55FP0) were only detected in amoeba infected with the wild-type strain. Both proteins have been implicated in *D. discoideum* killing of intracellular *K. pneumoniae* (Benghezal et al., 2006; Cosson and Soldati, 2008; Le Coadic et al., 2013). Of note, protein sulfation has been implicated in decreased bacterial adherence to eukaryotic cells and reduced T3SS-dependent cytotoxicity (Blondel et al., 2016). Thus, variations in sulfation levels on the surface of *D. discoideum* generated during *S.* Typhimurium infection may explain differences in internalization observed between the wild-type and attenuated strains Δ*ppk* and Δ*aroA* in our infection assays (**Figure 2A**).

Intracellular pathogens need to cope with a hostile environment inside the host during infection. Thus, our global proteomic profiles of *D. discoideum* proteins suggest that the amoeba recognizes wild-type *S.* Typhimurium and elicits a strong response that includes production of toxic ROS and RNS. Nevertheless, the pathogen manipulates the endocytic pathway of the host to generate an intracellular replicative niche to survive this cell-autonomous defense response. On the contrary, after recognition the Δ*ppk* mutant appears to be unable to subvert the amoebal autonomous defense mechanism and to survive the unfavorable conditions within the host. This idea is in agreement with the phenotypes reported for null mutants of *ppk* in several bacterial pathogens (Rao et al., 1998; Rashid and Kornberg, 2000; Rashid et al., 2000a,b; Kim et al., 2002; McMeechan et al., 2007; Brown and Kornberg, 2008; Varela et al., 2010; Gray and Jakob, 2015; Varas et al., 2017). In addition the mutant seems to be incapable to modify the endocytic pathway, ending in a degradative intracellular compartment. Consequently, the Δ*ppk* mutant is unable to survive within the amoeba and to subvert the social development of this host.

In addition to *D. discoideum* proteins, we attempted to identify *S.* Typhimurium proteins expressed during the infection of the amoeba with the wild-type strain or the Δ*ppk* mutant. Using our Q-proteomics approach we were able to detect a limited number of bacterial proteins, most probably due to their low relative abundance in each sample in comparison to *D. discoideum* proteins. Thus, a total of 54 and 34 proteins were identified in infections of amoeba cells with the wild-type strain and the Δ*ppk* mutant, respectively. A group of seven proteins was detected in amoebae infected with either strain (**Figure 4A**). The identities of all *S.* Typhimurium proteins detected are listed in **Table 4**. The location of genes encoding all these proteins in the genome of *S.* Typhimurium 14028s is shown in **Figure 4B**. The list of detected proteins was compared with a list of 469 classic virulence-related proteins included in databases PATRIC_VF, VFDB and VICTORS using tools implemented in PATRIC (www.patricbrc.org). We identified 11 *S.* Typhimurium proteins linked to virulence in amoebae infected with the wild-type strain, and 4 of these proteins in amoebae infected with the Δ*ppk* mutant, respectively (proteins highlighted in bold type in **Table 4**).

The limited amount of *S.* Typhimurium proteins detected in our global proteomic profiling impeded us conducting an insightful comparative analysis in order to understand differences between infections of *D. discoideum* with the wild-type strain and the Δ*ppk* mutant. However, it is worth mentioning a particular group of *S.* Typhimurium proteins detected during amoebae infections that includes AroA, SprB, STM14_0329, H-NS, Fis, ArcB, NuoG, EntC, IbpB, CsgB, StiC, and FliK.

AroA is a 3-enolpyruvylshikimate-5-phosphate synthetase that is crucial for biosynthesis of aromatic compounds. As a result, *Salmonella aroA* null-mutants are highly attenuated in different infection models (Hoiseth and Stocker, 1981; Stocker et al., 1983; Cooper et al., 1990) and present strong defects in survival within macrophages (Fields et al., 1986; Lowe et al., 1999) and in *D. discoideum* (Riquelme et al., 2016). This protein was detected in amoebae infected with both *S.* Typhimurium wild-type and Δ*ppk* strains.

SprB is a transcription factor from the LuxR/UhaP family that is encoded in SPI-1. This protein regulates the coordinate expression of SPI-1 and SPI-4 genes during *Salmonella* infection (Saini and Rao, 2010). STM14_0329 (also known as SciO and TssK) is one of the 13 core components of the T6SS encoded

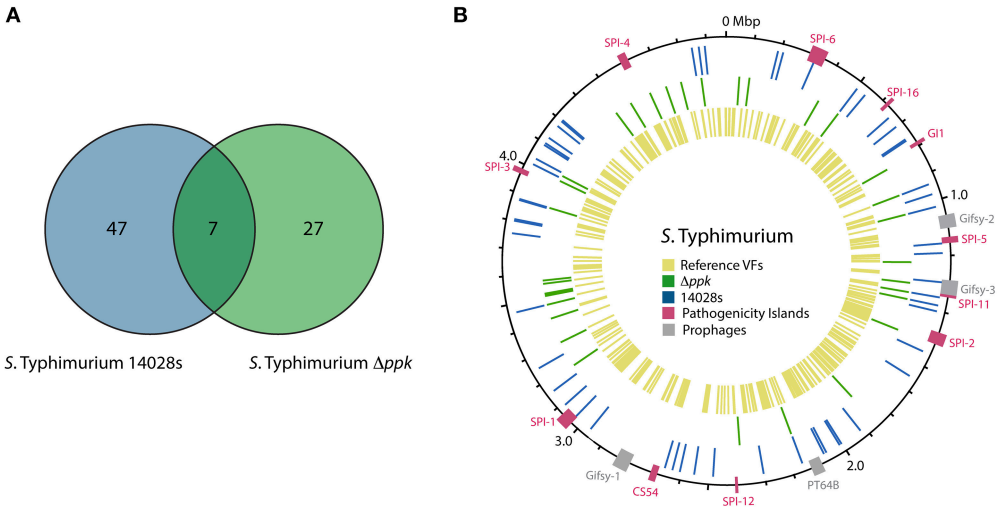

FIGURE 4 | *S.* Typhimurium proteins detected by global proteomic profiling during infection of *D. discoideum*. **(A)** Venn diagram of *S.* Typhimurium proteins detected during infection of *D. discoideum* with the wild-type strain or its Δ*ppk* derivative. **(B)** Circular representation of *S.* Typhimurium 14028s chromosome. Boxes in magenta and gray indicate regions corresponding to known *Salmonella* pathogenicity islands (SPIs) and prophages, respectively. Blue and green lines indicate the location of genes encoding proteins detected during the infection with the wild-type strain or its Δ*ppk* derivative, respectively. Yellow lines indicate the location of genes encoding virulence-associated proteins listed in databases PATRIC_VF, VFDB, and VICTORS (see Materials and Methods section).

in SPI-6 (Blondel et al., 2009; Journet and Cascales, 2016). T6SS are versatile weapons exploited by numerous bacterial pathogens to target either eukaryotic host cells or competitor bacteria (Cianfanelli et al., 2016; Hachani et al., 2016; Journet and Cascales, 2016). Noteworthy, we have recently described that null mutations in *S.* Typhimurium genes encoding essential components of T3SS-1 and SPI-6 T6SS cause intracellular survival defects in *D. discoideum* (Riquelme et al., 2016).

The nucleoid-associated protein H-NS selectively silences horizontally-acquired genes by direct binding to DNA sequences with high TA content in the genome, including all major SPIs in *S.* Typhimurium (Lucchini et al., 2006; Navarre et al., 2006). Accordingly, *hns* mutations are highly pleiotropic in *S.* Typhimurium (Hinton et al., 1992) and produce attenuated strains (Harrison et al., 1994). A recent study indicates that the fitness defects presented by *hns* mutants of *S.* Typhimurium are mainly due to a misregulation of SPI-1 genes (Ali et al., 2014). The factor for inversion stimulation (Fis) is a nucleoid-associated protein that influences the topological state of DNA in the cell by direct binding to DNA and by modulating DNA gyrase and topoisomerase I gene expression. As in the case of H-NS, Fis acts as a key regulator of virulence in *S.* Typhimurium mainly by controlling the coordinate expression of genes located in several SPIs, as well as genes involved in motility (reviewed in Duprey et al., 2014). Therefore, *fis* mutants of *S.* Typhimurium are defective for intracellular survival in macrophages (O Cróinín et al., 2006; Wang et al., 2013). ArcB is the sensor component of the master regulatory two-component system ArcA/ArcB, that controls the expression of several genes and operons encoding proteins linked to the metabolic shift from anaerobic to aerobic conditions, and the enzymatic defenses of bacteria against ROS (Evans et al., 2011). It is worth mentioning that H-NS, Fis and ArcB were only detected in amoebae infected with the Δ*ppk* mutant, perhaps reflecting adjustments required to cope with the pleiotropic phenotypes presented by this kind of mutant.

NuoG is a subunit of the NADH dehydrogenase I complex. *S.* Gallinarum Δ*nuoG* mutants are attenuated in chicken and show reduced survival and multiplication in the reticuloendothelial system of this host (Zhang-Barber et al., 1998; Turner et al., 2003). Noteworthy, it has been reported that NuoG is involved in detoxification of ROS produced by macrophages during *M. tuberculosis* infection (Miller et al., 2010). Thus, it is tempting to speculate that NuoG can play a similar role during *S.* Typhimurium infection of *D. discoideum*.

EntC is an isochorismate synthase involved in the biosynthesis of catecholate siderophores enterobactin and salmochelin, produced by *Salmonella* (and other bacterial pathogens) to capture iron from the host during infection (reviewed in Fischbach et al., 2006). It has been established that production of salmochelin is essential for full virulence of *S.* Typhimurium in mice (Crouch et al., 2008). Furthermore, the production of enterobactin and salmochelin is required for *S.* Typhimurium to survive in macrophages at early stages of infection, and these siderophores protect the pathogen against reactive oxygen species produced by macrophages during the infective process (Achard et al., 2013). Our results suggest that *S.* Typhimurium produces catecholate siderophores inside *D. discoideum*, perhaps contributing to the intracellular survival of this pathogen.

IbpB is a small heat-shock protein (sHSP) being member of a widely conserved family of ATP-independent molecular chaperones that bind to misfolded proteins and protect them from irreversible aggregation (Laskowska et al., 1996; Lee et al., 1997). It has been reported that *E. coli* chaperones IbpB and IbpA are substrates for the ATP-dependent Lon protease (Bissonnette

TABLE 4 | *S.* Typhimurium proteins detected during infections of *D. discoideum* with the wild-type strain or the Δ*ppk* mutant.

Locus tag in strain 14028s	Locus tag in strain LT2	Gene name	Product
A. Infection with the wild-type strain			
STM14_0190	STM0158	*acnB*	Bifunctional aconitate hydratase 2/2-methylisocitrate dehydratase
STM14_0207	STM0175	*stiC*	Putative fimbrial usher
STM14_0329	STM0281	–	Putative cytoplasmic protein
STM14_0529	**STM0447**	***tig***	**Trigger factor**
STM14_0564	STM0479	–	Putative transposase
STM14_0693	STM0595	*entC*	Isochorismate synthase
STM14_0743	STM0636	*ybeD*	Hypothetical protein
STM14_0806	STM0691	–	Tricarballylate dehydrogenase
STM14_0815	STM0698	*pgm*	Phosphoglucomutase
STM14_1013	**STM0863**	***dacC***	**D-alanyl-D-alanine carboxypeptidase fraction C**
STM14_1056	STM0939	*ybjD*	Hypothetical protein
STM14_1106	**STM0978**	***aroA***	**3-phosphoshikimate 1-carboxyvinyltransferase**
STM14_1259	STM1109	–	Putative periplasmic protein
STM14_1309	STM1143	*csgB*	Curlin minor subunit
STM14_1432	–	–	Phage replication protein O
STM14_1515	**STM1255**	–	**Putative ABC transporter periplasmic binding protein**
STM14_1565	**STM1290**	***gapA***	**Glyceraldehyde-3-phosphate dehydrogenase**
STM14_1590	STM1310	*nadE*	NAD synthetase
STM14_1770	STM1468	*fumA*	Fumarase A
STM14_1884	STM1561	–	Putative lipoprotein
STM14_2183	STM1806	*nhaB*	Sodium/proton antiporter
STM14_2303	STM1894	*ruvB*	Holliday junction DNA helicase B
STM14_2313	–	–	Hypothetical protein
STM14_2383	STM1963	*amyA*	Cytoplasmic alpha-amylase
STM14_2395	STM1974	*fliK*	Flagellar hook-length control protein
STM14_2515	STM2027	*cbiH*	Precorrin-3B C17-methyltransferase
STM14_2658	STM2155	*metG*	Methionyl-tRNA synthetase
STM14_2864	STM2323	*nuoG*	NADH dehydrogenase subunit G
STM14_2938	STM2389	*fadI*	3-ketoacyl-CoA thiolase
STM14_2999	STM2441	*cysA*	Sulfate/thiosulfate transporter subunit
STM14_3031	STM2472	*maeB*	Malic enzyme
STM14_3058	–	–	Hypothetical protein
STM14_3368	STM2792	*gabT*	4-aminobutyrate aminotransferase
STM14_3463	STM2866	*sprB*	Transcriptional regulator
STM14_3529	STM2926	*pcm*	Protein-L-isoaspartate O-methyltransferase
STM14_3594	STM2980	*ygdE*	Putative RNA 2'-O-ribose methyltransferase
STM14_3709	STM3069	*pgk*	Phosphoglycerate kinase
STM14_3969	**STM3286**	***infB***	**Translation initiation factor IF-2**
STM14_4299	STM3571	*ftsY*	Cell division protein FtsY
STM14_4345	STM3610	*yhjG*	Putative inner membrane protein
STM14_4351	STM3614	*dctA*	C4-dicarboxylate transporter DctA
STM14_4431	STM3674	*lyxK*	L-xylulose kinase
STM14_4435	**STM3678**	–	**Putative regulatory protein (AraC family)**
STM14_4585	STM3796A	–	Integral membrane protein
STM14_4614	STM3822	*torA*	Trimethylamine N-oxide reductase subunit
STM14_4665	STM3869	*atpF*	F0F1 ATP synthase subunit B
STM14_4675	STM3878	*yieM*	Hypothetical protein
STM14_4698	STM3901	*ilvG*	Acetolactate synthase 2 catalytic subunit
STM14_4760	STM3957	*pldA*	Phospholipase A
STM14_4785	STM3738	*yigC*	3-octaprenyl-4-hydroxybenzoate decarboxylase

(Continued)

TABLE 4 | Continued

Locus tag in strain 14028s	Locus tag in strain LT2	Gene name	Product
STM14_4789	STM3983	*fadB*	Multifunctional fatty acid oxidation complex subunit alpha
STM14_5386	STM4489	–	Putative DNA helicase
STM14_5404	STM4503	–	Putative inner membrane protein
STM14_5437	STM4525	*hsdM*	DNA methylase M
B. Infection with the Δ*ppk* mutant			
STM14_0055	STM0046	*ileS*	Isoleucyl-tRNA synthetase
STM14_0100	STM0084	–	Putative sulfatase
STM14_0417	STM0357	*mod*	DNA methylase
STM14_0529	**STM0447**	***tig***	**Trigger factor**
STM14_0870	STM0748	*tolB*	Translocation protein TolB
STM14_0992	STM0798	*uvrB*	Excinuclease ABC subunit B
STM14_1013	**STM0863**	***dacC***	**D-alanyl-D-alanine carboxypeptidase fraction C**
STM14_1106	**STM0978**	***aroA***	**3-phosphoshikimate 1-carboxyvinyltransferase**
STM14_1353	STM1182	*flgJ*	Peptidoglycan hydrolase
STM14_1459/STM14_3188	STM2605	–	Prophage head-tail preconnector
STM14_1515	**STM1255**	–	**Putative ABC transporter periplasmic binding protein**
STM14_1565	**STM1290**	***gapA***	**Glyceraldehyde-3-phosphate dehydrogenase**
STM14_1723	STM1426	*ribE*	Riboflavin synthase subunit alpha
STM14_2116	STM1751	*hns*	Global DNA-binding transcriptional dual regulator H-NS
STM14_2516	STM2028	*cbiG*	Cobalamin biosynthesis protein CbiG
STM14_2753	STM2227	*yejL*	Hypothetical protein
STM14_3634	STM3010	*aas*	Bifunctional acyl-[acyl carrier protein] synthetase/2-acylglycerophosphoethanolamine acyltransferase
STM14_3771	STM3122	–	Putative arylsulfatase
STM14_3899	STM3220	*ygjO*	Putative methyltransferase
STM14_3969	**STM3286**	***infB***	**Translation initiation factor IF-2**
STM14_4016	STM3328	*arcB*	Aerobic respiration control sensor protein ArcB
STM14_4020	STM3330	*gltB*	Glutamate synthase subunit alpha
STM14_4022	STM3332	*yhcG*	Putative cytoplasmic protein
STM14_4067	STM3373	*mreC*	Cell wall structural complex MreBCD transmembrane component MreC
STM14_4083	STM3385	*fis*	DNA-binding protein Fis
STM14_4435	**STM3678**	–	**Putative regulatory protein (AraC family)**
STM14_4568	STM3787	*uhpT*	Sugar phosphate antiporter
STM14_4599	STM3808	*ibpB*	Heat shock chaperone IbpB
STM14_4982	STM4146	*tuf_2*	Elongation factor Tu
STM14_5066	STM4213	–	Putative phage tail sheath protein
STM14_5155	STM4285	*fdhF*	Formate dehydrogenase
STM14_5237	STM4356	*yjeF*	Hypothetical protein
STM14_5312	STM4421	–	Putative NAD-dependent aldehyde dehydrogenase
STM14_5395	STM4498	–	Putative inner membrane protein

Bold type indicates proteins detected during infection with either the wild-type strain or the Δppk mutant. Red indicates classic virulence-related proteins included in databases PATRIC_VF, VFDB, and VICTORS that were identified using tools implemented in PATRIC (www.patricbrc.org).

et al., 2010). In addition, polyP forms a complex with Lon and stimulates the degradation of selected proteins (Kuroda et al., 2001, 2006; Nomura et al., 2004; Kuroda, 2006). Thus, there is a functional link between IbpB, Lon and the biosynthesis of polyP during the bacterial stress response.

Among the bacterial proteins detected in amoebae infected with wild-type *S.* Typhimurium we found CsgB, StiC, and FliK, which are associated to the assembly of proteinaceous structures such as fimbriae and flagellum, respectively. This is noteworthy because it is generally accepted that this kind of surface structures are repressed upon invasion of host cells. CsgB participates in the assembly of the curli fimbriae, favoring the polymerization of its major component CsgA (reviewed in Evans and Chapman, 2014). Curli fimbriae are amyloid fibers that act as scaffolding agents in biofilms of *E. coli* and *Salmonella*, providing increased resistance to desiccation and to sodium hypochlorite, and being extremely resistant to proteolysis and chemical denaturation (Chapman et al., 2002; White et al., 2006). These fimbriae have been linked

to cell-cell contacts, and to adherence to various eukaryotic cells, tissues, and abiotic surfaces, thus promoting community behavior and host colonization, playing an important role in the initial stages of the infection process (Barnhart and Chapman, 2006). To our knowledge, there are no previous reports on the expression of CsgB when *Salmonella* resides inside host cells. StiC is an usher protein encoded in one of the 11 chaperone-usher fimbrial gene clusters in the genome of *S.* Typhimurium (Jarvik et al., 2010). Chaperone-usher fimbriae normally have one or more structural subunits, which are exported and assembled on the bacterial surface by cognate periplasmic chaperone proteins and an outer-membrane usher protein. Some of them have demonstrated roles in binding to different receptors, persisting in specific niches, promoting infections, or forming biofilms (Weening et al., 2005; Clayton et al., 2008; Yue et al., 2012). The *stiABCH* gene cluster encodes a class γ-fimbriae, characterized for harboring subunits comprising the domains PFAM00419 or COG3539 (Nuccio and Bäumler, 2007). To our knowledge, no previous studies have addressed the specific contribution of this fimbrial operon to *S.* Typhimurium virulence. However, a previous study showed that the chaperone-usher SEF14 fimbriae are essential for an efficient uptake and survival of *S.* Enteritidis in murine macrophages, suggesting that they may be required at stages beyond the initial host colonization (Edwards et al., 2000). FliK is the protein that controls the length of the flagellar hook, and is encoded in one of the 17 operons composing the flagellar regulon of *S.* Typhimurium (Chilcott and Hughes, 2000). The flagellum is required for bacterial access to the intestinal epithelium, adherence to several tissues, and immune modulation (Rossez et al., 2015). Although flagellum assembly is normally prevented inside host cells, it was previously reported that intracellular *Salmonella* triggers swelling of macrophages (referred to as "oncotic macrophages") in a process where flagellated bacilli intermittently escape from infected host cells (Sano et al., 2007).

CONCLUSIONS

Overall, our results indicate that polyP biosynthesis is crucial for virulence and intracellular survival of *S.* Typhimurium in *D. discoideum*. In addition, we have validated the use of global proteomic analyses to gain insight into the host-pathogen interaction of *D. discoideum* and *S.* Typhimurium. The analysis of host proteins related to endocytic pathway, immune response, cell death, cytoskeleton dynamics, and developmental process revealed mechanisms that may explain the phenotypes shown by a *S.* Typhimurium strain lacking polyP during *D. discoideum* infection. Thus, our work demonstrates that unbiased high-throughput proteomics can be used as a powerful approach to provide new perspectives on host-pathogen interactions. Furthermore, our infection and development assays using these organisms can be exploited to screen for novel anti-virulence molecules targeting inorganic polyP biosynthesis.

AUTHOR CONTRIBUTIONS

MV, SR-B, CV, CS, and FC: Conceived and designed the experiments; MV, SR-B, CV, and AM: Performed the experiments; MV, SR-B, CV, AM, CB-P, CS, and FC: Analyzed the data; MV, CB-P, CS, and FC: Contributed with reagents/animals/materials/analysis tools; MV, AM, CS, and FC: Wrote the paper. All authors read and approved the final manuscript.

FUNDING

This work was supported in part by FONDECYT grants 1120209 (to FC), 1140754 and 1171844 (to CS). MV was supported by CONICYT fellowship 21120431 and FONDECYT grant 3170449. SR-B and CV were supported by CONICYT fellowships 21160818 and 21140615, respectively.

ACKNOWLEDGMENTS

We are indebted to Nicole Molina for technical support.

SUPPLEMENTARY MATERIAL

The Supplementary Material for this article can be found online at: https://www.frontiersin.org/articles/10.3389/fcimb.2018.00008/full#supplementary-material

Table S1 | List of all proteins detected in uninfected amoebae, and in amoebae infected with *S.* Typhimurium wild type or Δ*ppk*, and their corresponding PANTHER annotation.

Table S2 | Proteins found exclusively or enriched in a given experimental condition, classified according to COG categories.

Table S3 | Overrepresentation analysis for proteins found exclusively or enriched in amoebae infected with *S.* Typhimurium wild type or Δ*ppk*.

REFERENCES

Achard, M. E., Chen, K. W., Sweet, M. J., Watts, R. E., Schroder, K., Schembri, M. A., et al. (2013). An antioxidant role for catecholate siderophores in *Salmonella*. *Biochem. J.* 454, 543–549. doi: 10.1042/BJ20121771

Ali, S. S., Soo, J., Rao, C., Leung, A. S., Ngai, D. H., Ensminger, A. W., et al. (2014). Silencing by H-NS potentiated the evolution of *Salmonella*. *PLoS Pathog.* 10:e1004500. doi: 10.1371/journal.ppat.1004500

Barnhart, M. M., and Chapman, M. R. (2006). Curli biogenesis and function. *Annu. Rev. Microbiol.* 60, 131–147. doi: 10.1146/annurev.micro.60.080805.142106

Basu, S., Fey, P., Pandit, Y., Dodson, R., Kibbe, W. A., and Chisholm, R. L. (2013). DictyBase 2013: integrating multiple Dictyostelid species. *Nucleic Acids Res.* 41, D676–D683. doi: 10.1093/nar/gks1064.

Benghezal, M., Fauvarque, M. O., Tournebize, R., Froquet, R., Marchetti, A., Bergeret, E., et al. (2006). Specific host genes required for the killing of *Klebsiella* bacteria by phagocytes. *Cell Microbiol.* 8, 139–148. doi: 10.1111/j.1462-5822.2005.00607.x

Bissonnette, S. A., Rivera-Rivera, I., Sauer, R. T., and Baker, T. A. (2010). The IbpA and IbpB small heat-shock proteins are substrates of the AAA+ Lon protease. *Mol. Microbiol.* 75, 1539–1549. doi: 10.1111/j.1365-2958.2010.07070.x

Blondel, C. J., Jiménez, J. C., Contreras, I., and Santiviago, C. A. (2009). Comparative genomic analysis uncovers 3 novel loci encoding type six

secretion systems differentially distributed in *Salmonella* serotypes. *BMC Genomics* 10:354. doi: 10.1186/1471-2164-10-354

Blondel, C. J., Park, J. S., Hubbard, T. P., Pacheco, A. R., Kuehl, C. J., Walsh, M. J., et al. (2016). CRISPR/Cas9 screens reveal requirements for host cell sulfation and fucosylation in bacterial type III secretion system-mediated cytotoxicity. *Cell Host Microbe* 20, 226–237. doi: 10.1016/j.chom.2016.06.010

Bozzaro, S., and Eichinger, L. (2011). The professional phagocyte *Dictyostelium discoideum* as a model host for bacterial pathogens. *Curr. Drug Targets* 12, 942–954. doi: 10.2174/138945011795677782

Bravo-Toncio, C., Álvarez, J. A., Campos, F., Ortíz-Severín, J., Varas, M., Cabrera, R., et al. (2016). *Dictyostelium discoideum* as a surrogate host-microbe model for antivirulence screening in *Pseudomonas aeruginosa* PAO1. *Int. J. Antimicrob. Agents* 47, 403–409. doi: 10.1016/j.ijantimicag.2016.02.005

Brown, M. R., and Kornberg, A. (2008). The long and short of it - polyphosphate, PPK and bacterial survival. *Trends Biochem. Sci.* 33, 284–290. doi: 10.1016/j.tibs.2008.04.005

Cardenal-Muñoz, E., Arafah, S., López-Jiménez, A. T., Kicka, S., Falaise, A., Bach, F., et al. (2017). *Mycobacterium marinum* antagonistically induces an autophagic response while repressing the autophagic flux in a TORC1- and ESX-1-dependent manner. *PLoS Pathog.* 13:e1006344. doi: 10.1371/journal.ppat.1006344

Carilla-Latorre, S., Calvo-Garrido, J., Bloomfield, G., Skelton, J., Kay, R. R., Ivens, A., et al. (2008). *Dictyostelium* transcriptional responses to *Pseudomonas aeruginosa*: common and specific effects from PAO1 and PA14 strains. *BMC Microbiol.* 8:109. doi: 10.1186/1471-2180-8-109

Chapman, M. R., Robinson, L. S., Pinkner, J. S., Roth, R., Heuser, J., Hammar, M., et al. (2002). Role of *Escherichia coli* curli operons in directing amyloid fiber formation. *Science* 295, 851–855. doi: 10.1126/science.1067484

Cheng, Y., and Sun, B. (2009). Polyphosphate kinase affects oxidative stress response by modulating cAMP receptor protein and *rpoS* expression in *Salmonella* Typhimurium. *J. Microbiol. Biotechnol.* 19, 1527–1535. doi: 10.4014/jmb.0903.03030

Chilcott, G. S., and Hughes, K. T. (2000). Coupling of flagellar gene expression to flagellar assembly in *Salmonella enterica* serovar Typhimurium and *Escherichia coli*. *Microbiol. Mol. Biol. Rev.* 64, 694–708. doi: 10.1128/MMBR.64.4.694-708.2000

Choi, Y. K., Kong, J. S., and Park, Y. S. (2006). Functional role of sepiapterin reductase in the biosynthesis of tetrahydropteridines in *Dictyostelium discoideum* Ax2. *Biochim. Biophys. Acta* 1760, 877–882. doi: 10.1016/j.bbagen.2005.11.017

Cianfanelli, F. R., Monlezun, L., and Coulthurst, S. J. (2016). Aim, load, fire: the type VI secretion system, a bacterial nanoweapon. *Trends Microbiol.* 24, 51–62. doi: 10.1016/j.tim.2015.10.005

Clayton, D. J., Bowen, A. J., Hulme, S. D., Buckley, A. M., Deacon, V. L., Thomson, N. R., et al. (2008). Analysis of the role of 13 major fimbrial subunits in colonisation of the chicken intestines by *Salmonella enterica* serovar Enteritidis reveals a role for a novel locus. *BMC Microbiol.* 8:228. doi: 10.1186/1471-2180-8-228

Cooper, G. L., Nicholas, R. A., Cullen, G. A., and Hormaeche, C. E. (1990). Vaccination of chickens with a *Salmonella enteritidis aroA* live oral *Salmonella* vaccine. *Microb. Pathog.* 9, 255–265. doi: 10.1016/0882-4010(90)90014-H

Cosson, P., and Soldati, T. (2008). Eat, kill or die: when amoeba meets bacteria. *Curr. Opin. Microbiol.* 11, 271–276. doi: 10.1016/j.mib.2008.05.005

Cosson, P., Zulianello, L., Join-Lambert, O., Faurisson, F., Gebbie, L., Benghezal, M., et al. (2002). *Pseudomonas aeruginosa* virulence analyzed in a *Dictyostelium discoideum* host system. *J. Bacteriol.* 184, 3027–3033. doi: 10.1128/JB.184.11.3027-3033.2002

Crouch, M. L., Castor, M., Karlinsey, J. E., Kalhorn, T., and Fang, F. C. (2008). Biosynthesis and IroC-dependent export of the siderophore salmochelin are essential for virulence of *Salmonella enterica* serovar Typhimurium. *Mol. Microbiol.* 67, 971–983. doi: 10.1111/j.1365-2958.2007.06089.x

Datsenko, K. A., and Wanner, B. L. (2000). One-step inactivation of chromosomal genes in *Escherichia coli* K-12 using PCR products. *Proc. Natl. Acad. Sci. U.S.A.* 97, 6640–6645. doi: 10.1073/pnas.120163297

Dhillon, B. K., Laird, M. R., Shay, J. A., Winsor, G. L., Lo, R., Nizam, F., et al. (2015). IslandViewer 3: more flexible, interactive genomic island discovery, visualization and analysis. *Nucleic Acids Res.* 43, W104–W108. doi: 10.1093/nar/gkv401

Dunn, J. D., Bosmani, C., Barisch, C., Raykov, L., Lefrançois, L. H., Cardenal-Muoz, E., et al. (2018). Eat prey, live: *Dictyostelium discoideum* as a model for cell-autonomous defenses. *Front. Immunol.* 8:1906. doi: 10.3389/fimmu.2017.01906

Duprey, A., Reverchon, S., and Nasser, W. (2014). Bacterial virulence and Fis: adapting regulatory networks to the host environment. *Trends Microbiol.* 22, 92–99. doi: 10.1016/j.tim.2013.11.008

Edwards, R. A., Schifferli, D. M., and Maloy, S. R. (2000). A role for *Salmonella* fimbriae in intraperitoneal infections. *Proc. Natl. Acad. Sci. U.S.A.* 97, 1258–1262. doi: 10.1073/pnas.97.3.1258

Evans, M. L., and Chapman, M. R. (2014). Curli biogenesis: order out of disorder. *Biochim. Biophys. Acta* 1843, 1551–1558. doi: 10.1016/j.bbamcr.2013.09.010

Evans, M. R., Fink, R. C., Vazquez-Torres, A., Porwollik, S., Jones-Carson, J., McClelland, M., et al. (2011). Analysis of the ArcA regulon in anaerobically grown *Salmonella enterica* sv. Typhimurium. *BMC Microbiol.* 11:58. doi: 10.1186/1471-2180-11-58

Fey, P., Dodson, R. J., Basu, S., and Chisholm, R. L. (2013). One stop shop for everything *Dictyostelium*: dictyBase and the Dicty Stock Center in 2012. *Methods Mol. Biol.* 983, 59–92. doi: 10.1007/978-1-62703-302-2_4

Fey, P., Kowal, A. S., Gaudet, P., Pilcher, K. E., and Chisholm, R. L. (2007). Protocols for growth and development of *Dictyostelium discoideum*. *Nat. Protoc.* 2, 1307–1316. doi: 10.1038/nprot.2007.178

Fields, P. I., Swanson, R. V., Haidaris, C. G., and Heffron, F. (1986). Mutants of *Salmonella typhimurium* that cannot survive within the macrophage are avirulent. *Proc. Natl. Acad. Sci. U.S.A.* 83, 5189–5193. doi: 10.1073/pnas.83.14.5189

Fischbach, M. A., Lin, H., Liu, D. R., and Walsh, C. T. (2006). How pathogenic bacteria evade mammalian sabotage in the battle for iron. *Nat. Chem. Biol.* 2, 132–138. doi: 10.1038/nchembio771

Froquet, R., Lelong, E., Marchetti, A., and Cosson, P. (2009). *Dictyostelium discoideum*: a model host to measure bacterial virulence. *Nat. Protoc.* 4, 25–30. doi: 10.1038/nprot.2008.212

Gray, M. J., and Jakob, U. (2015). Oxidative stress protection by polyphosphate - new roles for an old player. *Curr. Opin. Microbiol.* 24, 1–6. doi: 10.1016/j.mib.2014.12.004

Hachani, A., Wood, T. E., and Filloux, A. (2016). Type VI secretion and anti-host effectors. *Curr. Opin. Microbiol.* 29, 81–93. doi: 10.1016/j.mib.2015.11.006

Hagedorn, M., and Soldati, T. (2007). Flotillin and RacH modulate the intracellular immunity of *Dictyostelium* to *Mycobacterium marinum* infection. *Cell Microbiol.* 9, 2716–2733. doi: 10.1111/j.1462-5822.2007.00993.x

Hägele, S., Köhler, R., Merkert, H., Schleicher, M., Hacker, J., and Steinert, M. (2000). *Dictyostelium discoideum*: a new host model system for intracellular pathogens of the genus *Legionella*. *Cell Microbiol.* 2, 165–171. doi: 10.1046/j.1462-5822.2000.00044.x

Haraga, A., Ohlson, M. B., and Miller, S. I. (2008). *Salmonellae* interplay with host cells. *Nat. Rev. Microbiol.* 6, 53–66. doi: 10.1038/nrmicro1788

Harrison, J. A., Pickard, D., Higgins, C. F., Khan, A., Chatfield, S. N., Ali, T., et al. (1994). Role of *hns* in the virulence phenotype of pathogenic salmonellae. *Mol. Microbiol.* 13, 133–140. doi: 10.1111/j.1365-2958.1994.tb00408.x

Hasselbring, B. M., Patel, M. K., and Schell, M. A. (2011). *Dictyostelium discoideum* as a model system for identification of *Burkholderia pseudomallei* virulence factors. *Infect. Immun.* 79, 2079–2088. doi: 10.1128/IAI.01233-10

Hinton, J. C., Santos, D. S., Seirafi, A., Hulton, C. S., Pavitt, G. D., and Higgins, C. F. (1992). Expression and mutational analysis of the nucleoid-associated protein H-NS of *Salmonella typhimurium*. *Mol. Microbiol.* 6, 2327–2337. doi: 10.1111/j.1365-2958.1992.tb01408.x

Hoiseth, S. K., and Stocker, B. A. (1981). Aromatic-dependent *Salmonella typhimurium* are non-virulent and effective as live vaccines. *Nature* 291, 238–239. doi: 10.1038/291238a0

Hudson, C. M., Lau, B. Y., and Williams, K. P. (2015). Islander: a database of precisely mapped genomic islands in tRNA and tmRNA genes. *Nucleic Acids Res.* 43, D48–D53. doi: 10.1093/nar/gku1072

Jarvik, T., Smillie, C., Groisman, E. A., and Ochman, H. (2010). Short-term signatures of evolutionary change in the *Salmonella enterica* serovar Typhimurium 14028 genome. *J. Bacteriol.* 192, 560–567. doi: 10.1128/JB.01233-09

Jensen, L. J., Julien, P., Kuhn, M., von Mering, C., Muller, J., Doerks, T., et al. (2008). eggNOG: automated construction and annotation of orthologous groups of genes. *Nucleic Acids Res.* 36, D250–D254. doi: 10.1093/nar/gkm796

Journet, L., and Cascales, E. (2016). The Type VI secretion system in *Escherichia coli* and related species. *EcoSal Plus*. doi: 10.1128/ecosalplus.ESP-0009-2015

Kim, K. S., Rao, N. N., Fraley, C. D., and Kornberg, A. (2002). Inorganic polyphosphate is essential for long-term survival and virulence factors in *Shigella* and *Salmonella* spp. *Proc. Natl. Acad. Sci. U.S.A.* 99, 7675–7680. doi: 10.1073/pnas.112210499

Kreppel, L., Fey, P., Gaudet, P., Just, E., Kibbe, W. A., Chisholm, R. L., et al. (2004). dictyBase: a new *Dictyostelium discoideum* genome database. *Nucleic Acids Res.* 32, D332–D333. doi: 10.1093/nar/gkh138

Kuroda, A. (2006). A polyphosphate-lon protease complex in the adaptation of *Escherichia coli* to amino acid starvation. *Biosci. Biotechnol. Biochem.* 70, 325–331. doi: 10.1271/bbb.70.325

Kuroda, A., Nomura, K., Ohtomo, R., Kato, J., Ikeda, T., Takiguchi, N., et al. (2001). Role of inorganic polyphosphate in promoting ribosomal protein degradation by the Lon protease in *E. coli*. *Science* 293, 705–708. doi: 10.1126/science.1061315

Kuroda, A., Nomura, K., Takiguchi, N., Kato, J., and Ohtake, H. (2006). Inorganic polyphosphate stimulates Lon-mediated proteolysis of nucleoid proteins in *Escherichia coli*. *Cell Mol. Biol.* 52, 23–29. doi: 10.1170/T723

Lampe, E. O., Brenz, Y., Herrmann, L., Repnik, U., Griffiths, G., Zingmark, C., et al. (2015). Dissection of *Francisella*-host cell interactions in *Dictyostelium discoideum*. *Appl. Environ. Microbiol.* 82, 1586–1598. doi: 10.1128/AEM.02950-15

LaRock, D. L., Chaudhary, A., and Miller, S. I. (2015). Salmonellae interactions with host processes. *Nat. Rev. Microbiol.* 13, 191–205. doi: 10.1038/nrmicro3420

Laskowska, E., Wawrzynów, A., and Taylor, A. (1996). IbpA and IbpB, the new heat-shock proteins, bind to endogenous *Escherichia coli* proteins aggregated intracellularly by heat shock. *Biochimie* 78, 117–122. doi: 10.1016/0300-9084(96)82643-5

Le Coadic, M., Froquet, R., Lima, W. C., Dias, M., Marchetti, A., and Cosson, P. (2013). Phg1/TM9 proteins control intracellular killing of bacteria by determining cellular levels of the Kil1 sulfotransferase in *Dictyostelium*. *PLoS ONE* 8:e53259. doi: 10.1371/journal.pone.0053259

Lee, G. J., Roseman, A. M., Saibil, H. R., and Vierling, E. (1997). A small heat shock protein stably binds heat-denatured model substrates and can maintain a substrate in a folding-competent state. *EMBO J.* 16, 659–671. doi: 10.1093/emboj/16.3.659

Lowe, D. C., Savidge, T. C., Pickard, D., Eckmann, L., Kagnoff, M. F., Dougan, G., et al. (1999). Characterization of candidate live oral *Salmonella typhi* vaccine strains harboring defined mutations in *aroA*, *aroC*, and *htrA*. *Infect. Immun.* 67, 700–707.

Lucchini, S., Rowley, G., Goldberg, M. D., Hurd, D., Harrison, M., and Hinton, J. C. (2006). H-NS mediates the silencing of laterally acquired genes in bacteria. *PLoS Pathog.* 2:e81. doi: 10.1371/journal.ppat.0020081

McMeechan, A., Lovell, M. A., Cogan, T. A., Marston, K. L., Humphrey, T. J., and Barrow, P. A. (2007). Inactivation of *ppk* differentially affects virulence and disrupts ATP homeostasis in *Salmonella enterica* serovars Typhimurium and Gallinarum. *Res. Microbiol.* 158, 79–85. doi: 10.1016/j.resmic.2006.10.008

Mi, H., Muruganujan, A., Casagrande, J. T., and Thomas, P. D. (2013). Large-scale gene function analysis with the PANTHER classification system. *Nat .Protoc.* 8, 1551–1566. doi: 10.1038/nprot.2013.092

Mi, H., Poudel, S., Muruganujan, A., Casagrande, J. T., and Thomas, P. D. (2016). PANTHER version 10: expanded protein families and functions, and analysis tools. *Nucleic Acids Res.* 44, D336–D342. doi: 10.1093/nar/gkv1194

Miller, J. L., Velmurugan, K., Cowan, M. J., and Briken, V. (2010). The type I NADH dehydrogenase of *Mycobacterium tuberculosis* counters phagosomal NOX2 activity to inhibit TNF-alpha-mediated host cell apoptosis. *PLoS Pathog.* 6:e1000864. doi: 10.1371/journal.ppat.1000864

Navarre, W. W., Porwollik, S., Wang, Y., McClelland, M., Rosen, H., Libby, S. J., et al. (2006). Selective silencing of foreign DNA with low GC content by the H-NS protein in *Salmonella*. *Science* 313, 236–238. doi: 10.1126/science.1128794

Nomura, K., Kato, J., Takiguchi, N., Ohtake, H., and Kuroda, A. (2004). Effects of inorganic polyphosphate on the proteolytic and DNA-binding activities of Lon in *Escherichia coli*. *J. Biol. Chem.* 279, 34406–34410. doi: 10.1074/jbc.M404725200

Nuccio, S. P., and Bäumler, A. J. (2007). Evolution of the chaperone/usher assembly pathway: fimbrial classification goes Greek. *Microbiol. Mol. Biol. Rev.* 71, 551–575. doi: 10.1128/MMBR.00014-07

O Cróinín, T., Carroll, R. K., Kelly, A., and Dorman, C. J. (2006). Roles for DNA supercoiling and the Fis protein in modulating expression of virulence genes during intracellular growth of *Salmonella enterica* serovar Typhimurium. *Mol. Microbiol.* 62, 869–882. doi: 10.1111/j.1365-2958.2006.05416.x

Ouertatani-Sakouhi, H., Kicka, S., Chiriano, G., Harrison, C. F., Hilbi, H., Scapozza, L., et al. (2017). Inhibitors of *Mycobacterium marinum* virulence identified in a *Dictyostelium discoideum* host model. *PLoS ONE* 12:e0181121. doi: 10.1371/journal.pone.0181121

Pan, Y. J., Lin, T. L., Hsu, C. R., and Wang, J. T. (2011). Use of a *Dictyostelium* model for isolation of genetic loci associated with phagocytosis and virulence in *Klebsiella pneumoniae*. *Infect. Immun.* 79, 997–1006. doi: 10.1128/IAI.00906-10

Pukatzki, S., Kessin, R. H., and Mekalanos, J. J. (2002). The human pathogen *Pseudomonas aeruginosa* utilizes conserved virulence pathways to infect the social amoeba *Dictyostelium discoideum*. *Proc. Natl. Acad. Sci. U.S.A.* 99, 3159–3164. doi: 10.1073/pnas.052704399

Rao, N. N., Liu, S., and Kornberg, A. (1998). Inorganic polyphosphate in *Escherichia coli*: the phosphate regulon and the stringent response. *J. Bacteriol.* 180, 2186–2193.

Rashid, M. H., and Kornberg, A. (2000). Inorganic polyphosphate is needed for swimming, swarming, and twitching motilities of *Pseudomonas aeruginosa*. *Proc. Natl. Acad. Sci. U.S.A.* 97, 4885–4890. doi: 10.1073/pnas.060030097

Rashid, M. H., Rao, N. N., and Kornberg, A. (2000a). Inorganic polyphosphate is required for motility of bacterial pathogens. *J. Bacteriol.* 182, 225–227. doi: 10.1128/JB.182.1.225-227.2000

Rashid, M. H., Rumbaugh, K., Passador, L., Davies, D. G., Hamood, A. N., Iglewski, B. H., et al. (2000b). Polyphosphate kinase is essential for biofilm development, quorum sensing, and virulence of *Pseudomonas aeruginosa*. *Proc. Natl. Acad. Sci. U.S.A.* 97, 9636–9641. doi: 10.1073/pnas.170283397

Riquelme, S., Varas, M., Valenzuela, C., Velozo, P., Chahin, N., Aguilera, P., et al. (2016). Relevant genes linked to virulence are required for *Salmonella* Typhimurium to survive intracellularly in the social amoeba *Dictyostelium discoideum*. *Front. Microbiol.* 7:1305. doi: 10.3389/fmicb.2016.01305

Rossez, Y., Wolfson, E. B., Holmes, A., Gally, D. L., and Holden, N. J. (2015). Bacterial flagella: twist and stick, or dodge across the kingdoms. *PLoS Pathog.* 11:e1004483. doi: 10.1371/journal.ppat.1004483

Rutherford, K., Parkhill, J., Crook, J., Horsnell, T., Rice, P., Rajandream, M. A., et al. (2000). Artemis: sequence visualization and annotation. *Bioinformatics* 16, 944–945. doi: 10.1093/bioinformatics/16.10.944

Saini, S., and Rao, C. V. (2010). SprB is the molecular link between *Salmonella* pathogenicity island 1 (SPI1) and SPI4. *J. Bacteriol.* 192, 2459–2462. doi: 10.1128/JB.00047-10

Sano, G., Takada, Y., Goto, S., Maruyama, K., Shindo, Y., Oka, K., et al. (2007). Flagella facilitate escape of *Salmonella* from oncotic macrophages. *J. Bacteriol.* 189, 8224–8232. doi: 10.1128/JB.00898-07

Santiviago, C. A., Reynolds, M. M., Porwollik, S., Choi, S. H., Long, F., Andrews-Polymenis, H. L., et al. (2009). Analysis of pools of targeted *Salmonella* deletion mutants identifies novel genes affecting fitness during competitive infection in mice. *PLoS Pathog.* 5:e1000477. doi: 10.1371/journal.ppat.1000477

Sebkova, A., Karasova, D., Crhanova, M., Budinska, E., and Rychlik, I. (2008). *aro* mutations in *Salmonella enterica* cause defects in cell wall and outer membrane integrity. *J. Bacteriol.* 190, 3155–3160. doi: 10.1128/JB.00053-08

Sillo, A., Matthias, J., Konertz, R., Bozzaro, S., and Eichinger, L. (2011). *Salmonella typhimurium* is pathogenic for *Dictyostelium* cells and subverts the starvation response. *Cell Microbiol.* 13, 1793–1811. doi: 10.1111/j.1462-5822.2011.01662.x

Stocker, B. A., Hoiseth, S. K., and Smith, B. P. (1983). Aromatic-dependent "*Salmonella* sp." as live vaccine in mice and calves. *Dev. Biol. Stand* 53, 47–54.

Tatusov, R. L., Galperin, M. Y., Natale, D. A., and Koonin, E. V. (2000). The COG database: a tool for genome-scale analysis of protein functions and evolution. *Nucleic Acids Res.* 28, 33–36. doi: 10.1093/nar/28.1.33

Thöny, B., Auerbach, G., and Blau, N. (2000). Tetrahydrobiopterin biosynthesis, regeneration and functions. *Biochem. J.* 347(Pt 1), 1–16. doi: 10.1042/bj3470001

Tosetti, N., Croxatto, A., and Greub, G. (2014). Amoebae as a tool to isolate new bacterial species, to discover new virulence factors and to study the host-pathogen interactions. *Microb. Pathog.* 77, 125–130. doi: 10.1016/j.micpath.2014.07.009

Turner, A. K., Barber, L. Z., Wigley, P., Muhammad, S., Jones, M. A., Lovell, M. A., et al. (2003). Contribution of proton-translocating proteins to the virulence of *Salmonella enterica* serovars Typhimurium, Gallinarum,

and Dublin in chickens and mice. *Infect. Immun.* 71, 3392–3401. doi: 10.1128/IAI.71.6.3392-3401.2003

Varas, M., Valdivieso, C., Mauriaca, C., Ortíz-Severín, J., Paradela, A., Poblete-Castro, I., et al. (2017). Multi-level evaluation of *Escherichia coli* polyphosphate related mutants using global transcriptomic, proteomic and phenomic analyses. *Biochim. Biophys. Acta* 1861, 871–883. doi: 10.1016/j.bbagen.2017.01.007

Varela, C., Mauriaca, C., Paradela, A., Albar, J. P., Jerez, C. A., and Chávez, F. P. (2010). New structural and functional defects in polyphosphate deficient bacteria: a cellular and proteomic study. *BMC Microbiol.* 10:7. doi: 10.1186/1471-2180-10-7

Vásquez-Vivar, J. (2009). Tetrahydrobiopterin, superoxide, and vascular dysfunction. *Free Radic. Biol. Med.* 47, 1108–1119. doi: 10.1016/j.freeradbiomed.2009.07.024

Wang, H., Liu, B., Wang, Q., and Wang, L. (2013). Genome-wide analysis of the *Salmonella* Fis regulon and its regulatory mechanism on pathogenicity islands. *PLoS ONE* 8:e64688. doi: 10.1371/journal.pone.0064688

Weber, S., Wagner, M., and Hilbi, H. (2014). Live-cell imaging of phosphoinositide dynamics and membrane architecture during *Legionella* infection. *MBio* 5, e00839–e00813. doi: 10.1128/mBio.00839-13

Weening, E. H., Barker, J. D., Laarakker, M. C., Humphries, A. D., Tsolis, R. M., and Bäumler, A. J. (2005). The *Salmonella enterica* serotype Typhimurium *lpf*, *bcf*, *stb*, *stc*, *std*, and *sth* fimbrial operons are required for intestinal persistence in mice. *Infect. Immun.* 73, 3358–3366. doi: 10.1128/IAI.73.6.3358-3366.2005

White, A. P., Gibson, D. L., Kim, W., Kay, W. W., and Surette, M. G. (2006). Thin aggregative fimbriae and cellulose enhance long-term survival and persistence of *Salmonella*. *J. Bacteriol.* 188, 3219–3227. doi: 10.1128/JB.188.9.3219-3227.2006

Wiśniewski, J. R., Zougman, A., Nagaraj, N., and Mann, M. (2009). Universal sample preparation method for proteome analysis. *Nat. Methods* 6, 359–362. doi: 10.1038/nmeth.1322

Yoon, S. H., Park, Y. K., and Kim, J. F. (2015). PAIDB v2.0: exploration and analysis of pathogenicity and resistance islands. *Nucleic Acids Res.* 43, D624–D630. doi: 10.1093/nar/gku985

Yue, M., Rankin, S. C., Blanchet, R. T., Nulton, J. D., Edwards, R. A., and Schifferli, D. M. (2012). Diversification of the *Salmonella* fimbriae: a model of macro- and microevolution. *PLoS ONE* 7:e38596. doi: 10.1371/journal.pone.0038596

Zhang, G., Ueberheide, B. M., Waldemarson, S., Myung, S., Molloy, K., Eriksson, J., et al. (2010). Protein quantitation using mass spectrometry. *Methods Mol. Biol.* 673, 211–222. doi: 10.1007/978-1-60761-842-3_13

Zhang, H., Gómez-García, M. R., Brown, M. R., and Kornberg, A. (2005). Inorganic polyphosphate in *Dictyostelium discoideum*: influence on development, sporulation, and predation. *Proc. Natl. Acad. Sci. U.S.A.* 102, 2731–2735. doi: 10.1073/pnas.0500023102

Zhang, X., Zhuchenko, O., Kuspa, A., and Soldati, T. (2016). Social amoebae trap and kill bacteria by casting DNA nets. *Nat. Commun.* 7:10938. doi: 10.1038/ncomms10938

Zhang-Barber, L., Turner, A. K., Dougan, G., and Barrow, P. A. (1998). Protection of chickens against experimental fowl typhoid using a *nuoG* mutant of *Salmonella* serotype Gallinarum. *Vaccine* 16, 899–903. doi: 10.1016/S0264-410X(97)00300-9

Zhou, Y., Liang, Y., Lynch, K. H., Dennis, J. J., and Wishart, D. S. (2011). PHAST: a fast phage search tool. *Nucleic Acids Res.* 39, W347–W352. doi: 10.1093/nar/gkr485

Conflict of Interest Statement: The authors declare that the research was conducted in the absence of any commercial or financial relationships that could be construed as a potential conflict of interest.

frontiers in Cellular and Infection Microbiology

METHODS
published: 02 March 2018
doi: 10.3389/fcimb.2018.00062

Quantification of Live Bacterial Sensing for Chemotaxis and Phagocytosis and of Macropinocytosis

*Netra P. Meena and Alan R. Kimmel**

Laboratory of Cellular and Developmental Biology, National Institute of Diabetes and Digestive and Kidney Diseases, The National Institutes of Health, Bethesda, MD, United States

Initial immunological defense mechanisms to pathogen invasion rely on innate pathways of chemotaxis and phagocytosis, original to ancient phagocytes. Although chemotaxis has been well-studied in mammalian and model systems using purified chemoattractants in defined conditions, directed movement toward live bacteria has been more difficult to assess. *Dictyostelium discoideum* is a professional phagocyte that chemotaxes toward bacteria during growth-phase in a process to locate nutrient sources. Using *Dictyostelium* as a model, we have developed a system that is able to quantify chemotaxis to very high sensitivity. Here, *Dictyostelium* can detect various chemoattractants at concentrations <1 nM. Given this exceedingly sensitive signal response, *Dictyostelium* will migrate directionally toward live gram positive and gram negative bacteria, in a highly quantifiable manner, and dependent upon bacterially-secreted chemoattractants. Additionally, we have developed a real-time, quantitative assay for phagocytosis of live gram positive and gram negative bacteria. To extend the analyses of endocytic functions, we further modified the system to quantify cellular uptake *via* macropinocytosis of smaller (<100 kDa) molecules. These various approaches provide novel means to dissect potential for identification of novel chemoattractants and mechanistic factors that are essential for chemotaxis, phagocytosis, and/or macropinocytosis and for more detailed understanding in host-pathogen interactive defenses.

Keywords: cell migration, *Bacillus*, *Pseudomonas*, *E. coli*, pterin, cAMP, innate immunity, *Dictyostelium*

OPEN ACCESS

Edited by:
Thierry Soldati,
Université de Genève, Switzerland

Reviewed by:
Robert Roger Kay,
Medical Research Council, United Kingdom
Salvatore Bozzaro,
Università degli Studi di Torino, Italy

****Correspondence:***
Alan R. Kimmel
alank@helix.nih.gov

Received: *31 October 2017*
Accepted: *13 February 2018*
Published: *02 March 2018*

Citation:
Meena NP and Kimmel AR (2018) Quantification of Live Bacterial Sensing for Chemotaxis and Phagocytosis and of Macropinocytosis. Front. Cell. Infect. Microbiol. 8:62. doi: 10.3389/fcimb.2018.00062

1. INTRODUCTION

Host–pathogen interactions are crucial aspects to the immune response. Innate immunity comprises generalized defense to invading microorganisms and involves cellular functions, including chemotaxis and phagocytosis, that can be traced at least 1 billion years (Cosson and Soldati, 2008; Jin et al., 2008; Bozzaro and Eichinger, 2011), where ancient professional phagocytes utilized the pathways in a search for and an uptake of new nutrient sources. Thus, similar molecular processes, including receptor signaling and directed cytoskeletal mobilization, are essential for both destruction of pathogenic bacteria by macrophage and neutrophils, and for nutrient capture by *Dictyostelium discoideum* (Cosson and Soldati, 2008; Jin et al., 2008; Bozzaro and Eichinger, 2011). Significantly, the ease in genetic manipulation of *Dictyostelium* (Basu et al., 2013) has made it an ideal model for mechanistic studies of these processes.

Dictyostelium can rapidly sense multiple chemoattractants in very broad and dynamic concentration gradients (Jin, 2013; Artemenko et al., 2014; Nichols et al., 2015). We established a new quantitative system for high-throughput chemoattractant gradient perception at very low concentration (<1 nM) sensitivity and then extended conditions for use of live bacteria as the source for secreted chemoattractants (Meena and Kimmel, 2017). This further permitted analyses to understand simultaneous response to multiple chemoattractants and to identify bacterially secreted factors. Beyond, we have modified the system to examine functions secondary to chemotaxis that are essential for target removal through phagocytosis and macropinocytosis.

Procedural details are, thus, presented for quantification of chemotaxis in real-time to both purified ligands, individually, or in multiple combinations, or to live bacteria. We also outline specific approaches for quantifying cellular uptake of large (>1 μm) particles by phagocytosis or of molecules (<100 kDa) by macropinocytosis, again in a real-time and high-throughput mode.

2. MATERIALS AND EQUIPMENT

2.1. Solutions

1. *Dictyostelium* growth medium: D3-T Medium KD Medical, cat # D3-T001 (Composition/1L: 7.15 g proteose peptone, 7.15 g peptone A, 7.15 g yeast extract, 15.3 g glucose, 0.52 g Na_2HPO_4*$7H_2O$, 0.48 g KH_2PO_4 – pH 6.4).
2. Phosphate Buffer (PB): 5 mM Na_2HPO_4, 5 mM NaH_2PO_4, adjusted to pH 6.5.
3. cAMP: 1 mM in PB, dilute as needed.
4. Folate, Pterin, and Methopterin: 50 mM in PB, neutralized as needed with 1 N NaOH. All of these compounds are light sensitive; for most consistent results, prepare fresh and keep in a light-tight vial.
5. LB medium: KD Medical, cat # BLF-7030.
6. Nutrient broth: BD, cat # 234000.
7. Tryptic soya broth: BD, cat # 211825.

2.2. Supplies

1. *Dictyostelium discoideum*, strain Ax3: dictyBase (http://dictybase.org).
2. Shaker Incubator: New Brunswick Innova 44 incubator shaker.
3. The IncuCyte® Live Cell Analysis System: Essen Bioscience, cat # 4582.
4. *Escherichia coli*, Strain *Dh5α*: Thermo Fisher Scientific, cat # C404010.
5. *Bacillus cereus*: ATCC® 14579™.
6. *Micrococcus luteus*: ATCC® 4698™.
7. *Pseudomonas fluorescens*: ATCC® 31086™.
8. pHrodo™ Red Dextran, 10,000 MW: ThermoFisher Scientific, cat # P10361.
9. Spectrophotometer: GE Healthcare/Amersham Biosciences Ultrospec 3100 Pro UV/Visible Spectrophotometer # 80-2112-31.
10. Lab-TeK 4-well-chambered slide: ThermoFisher Scientific, cat # 155383.
11. Lab-TeK 8-well-chambered slide: ThermoFisher Scientific, cat # 155411.
12. Confocal Microscope: LSM 780 confocal/multiphoton microscope, Carl Zeiss, Thornwood, NY, USA.
13. Chemotaxis 96 well plate: Essen BioScience, cat # 4648.
14. 96 well, flat bottom plate for phagocytosis and macropinocytosis: Corning, cat # 3596.
15. Bovine serum albumin (BSA): Sigma-Aldrich, cat # A3803.
16. pHrodo™ Phagocytosis particle labeling kit: Thermo Fisher Scientific, cat # A100267.

3. PROCEDURES AND RESULTS

3.1. Chemotaxis by Growth Phase *Dictyostelium* to Chemoattractants, Folate, Methopterin, Pterin, and cAMP

3.1.1. Growth and Preparation of Dictyostelium

3.1.1.1. Grow *Dictyostelium* in D3-T Medium at 22°C in shaking culture, at ∼200 rpm, to 1 × 10^6 cells/mL.

3.1.1.2. Centrifuge cells at 22°C for 5 min at 500 × *g*.

3.1.1.3. Wash cells once with 10 mM phosphate buffer (PB), pH 6.5 at 22°C.

3.1.1.4. Resuspend cells at 1.5–4.5 × 10^4 cells/mL in PB, by gentle tapping of the bottom of tube.

3.1.2. Quantification of Dictyostelium Chemotaxis to Chemical Ligands

3.1.2.1. Coat both the upper and lower chambers of the chemotaxis plates with 1% Bovine serum albumin (BSA) in PB, adding 60 μL of 1% BSA to top chamber and 160 μL to the bottom well. Incubate the plates at room temperature.

3.1.2.2. After 1 h, temporarily move the upper part of the plate to a new plate bottom and carefully remove the BSA from each well of the upper plate chamber without touching the membrane.

3.1.2.3. Add 60 μL (1–3 × 10^3) of growing *Dictyostelium* (from **3.1.1.4.**) in PB to the upper well of a BSA-treated chemotaxis plate. Avoid creating air bubbles at the surface of the membrane.

3.1.2.4. Completely remove BSA from each well of the BSA-treated bottom plate and add 200 μL PB with or without chemoattractants at desired concentrations (e.g., 0–1 mM).

3.1.2.5. After adding both cells and chemoattractants to their respective parts of the chemotaxis plate, reassemble the original plate. Carefully place the upper part of the chemotaxis plate on top of the lower part of the plate, and avoid generating any air bubbles in the process.

3.1.2.6. Transfer the assembled plate into the IncuCyte chamber, at 22°C. Using a 10x objective lens, collect cell images from both the top and under surface of the membrane, over a desired time (e.g., 1.5–4 h), at 15 min intervals. Export the data into Microsoft Excel for processing.

3.1.3. Results

Dictyostelium grow as single cells that migrate to bacterially secreted pterin-derived folate moieties and to cAMP (Meena and Kimmel, 2017), in a search for nutrient sources. Assaying chemotaxis of growth-phase *Dictyostelium* had been a great challenge (Veltman et al., 2014). However, we developed a highly sensitive, quantitative, and reproducible method for chemotaxis of growth-phase *Dictyostelium* that is easily modified and optimized for most single-cell types (Meena and Kimmel, 2017).

The approach adapts the IncuCyte® live-cell analysis system from Essen Bioscience for real-time imaging of chemotaxis in a 96-well format. IncuCyte® uses high definition phase contrast imaging and ClearView Cell Migration Plates. The scan intervals, digital zoom, and imaging channels are set manually. But following, image acquisition is fully automated, as are integrated real-time data analyses and full time-course metrics, with application of the IncuCyte® Chemotaxis Cell Migration Software Module. The specialized 96-well chemotaxis dish is comprised of three sections: a transparent lid, an upper well plate (which will contain cells to be assayed), and a bottom well plate (which will have chemoattractants). A membrane of uniformly-spaced 8 μm pores separates each aligned upper and bottom chamber well.

Chemoattractant gradients are established by chemical diffusion from the bottom wells, through the membrane pores, into the upper wells. Cell migration results from the movement of cells out of the upper well, through the membrane toward the bottom well, and chemotaxis is quantified over time, by imaging cells that had migrated from the upper well base to the under surface of the membrane within the bottom chamber. The assays are highly reproducible, with generally <10% non-specific directed migration to phosphate buffer controls [**Figure 1** (Meena and Kimmel, 2017)]. In addition, by comparing migration toward buffer controls, using cells incubated in the presence or absence of chemoattractants, we can assess a potential chemokinetic contribution to random

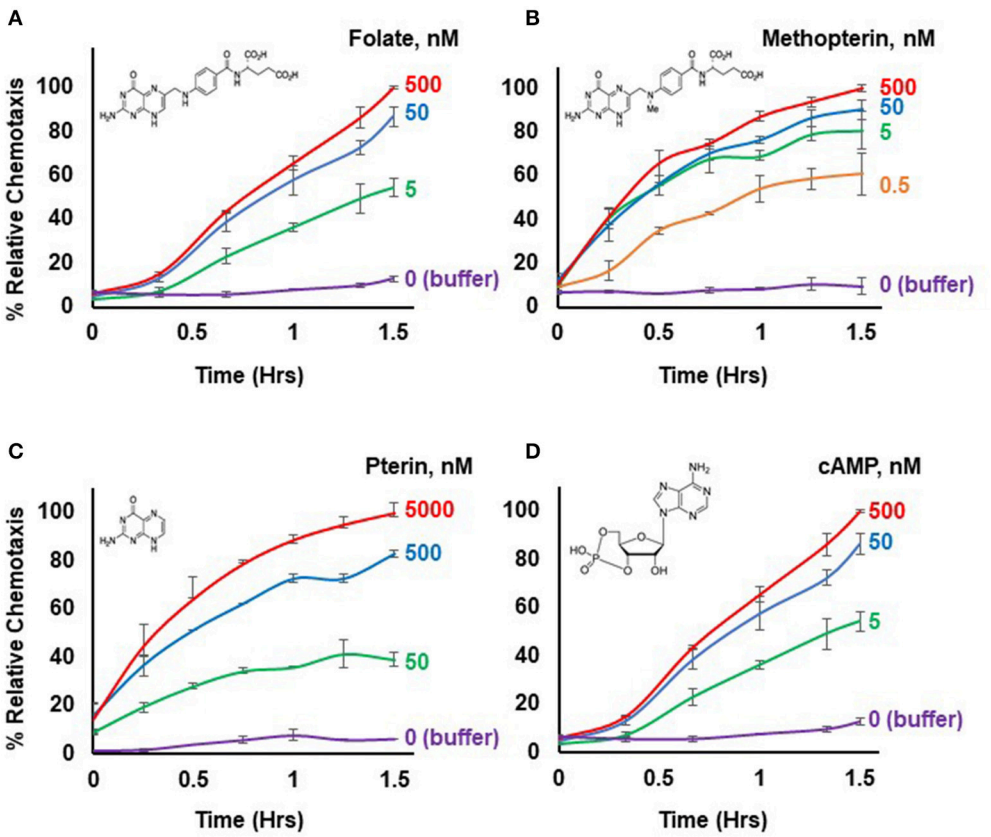

FIGURE 1 | Chemotactic dose-responses to different chemoattractants. **(A)** Time-course quantification of *Dictyostelium* migration to various dose concentrations of folate. Relative chemotaxis is normalized to 500 nM folate at 1.5 h; no additional chemotaxis is observed with folate increased to 5,000 nM (see **Figure 2**). Standard deviations are shown based upon three replicates. The structure of folate is shown. **(B)** Time-course quantification of *Dictyostelium* migration to various dose concentrations of methopterin. Relative chemotaxis is normalized to 500 nM methopterin at 1.5 h. Standard deviations are shown based upon three replicates. The structure of methopterin is shown. **(C)** Time-course quantification of *Dictyostelium* migration to various dose concentrations of pterin. Relative chemotaxis is normalized to 5,000 nM pterin at 1.5 h. Standard deviations are shown based upon three replicates. The structure of pterin is shown. **(D)** Time-course quantification of *Dictyostelium* migration to various dose concentrations of cAMP. Relative chemotaxis is normalized to 500 nM cAMP at 1.5 h; no additional chemotaxis is observed with cAMP increased to 5,000 nM (see **Figure 2**). Standard deviations are shown based upon three replicates. The structure of cAMP is shown.

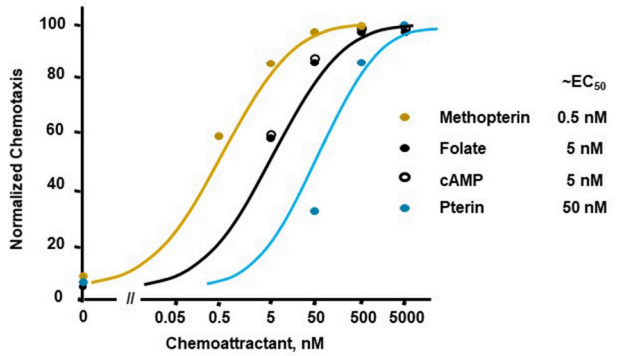

FIGURE 2 | Quantified dose-responses for *Dictyostelium* chemotaxis to different chemoattractants. Curve fits are shown for an indicated EC_{50}. Symbols presented are means from three separate experiments at 1.5 h, as derived from data as per **Figure 1**.

migration (Meena and Kimmel, 2017). Chemokinesis may increase operative backgrounds to ∼15%, for fully responsive cells (Meena and Kimmel, 2017).

Figure 1 illustrates a typical chemotactic dose-response, time-course for migration of growth-phase *Dictyostelium* toward four different chemoattractants. Folate, methopterin, and pterin represent 3 structurally related moieties that interact with the same chemoattractant receptor (NPM and ARK, in preparation), but at differing activating affinities, in the order of methopterin>folate>pterin (NPM and ARK, in preparation); the EC_{50} for chemotaxis of each is consistent with these affinity differences (**Figure 2**). Separately, we also show high chemosensitivity of growth-phase *Dictyostelium* to the unrelated chemoattractant cAMP (**Figures 1D**, **2**), which interacts with a distinct chemoattractant receptor (Liao et al., 2013; Meena and Kimmel, 2016, 2017).

3.2. Chemotaxis of Growth Phase *Dictyostelium* to Live Bacteria

3.2.1. Growth and Preparation of Growth Phase Dictyostelium

Follow all steps in **3.1.1.**

3.2.2. Growth of Bacteria

3.2.2.1. Grow *Escherichia coli* in LB medium at 37°C, in shaking culture at ∼200 rpm, to OD_{600} <1.

3.2.2.2. Grow *Bacillus cereus* in Nutrient broth medium at 30°C, in shaking culture at ∼200 rpm, to OD_{600} <1.

3.2.2.3. Grow *Pseudomonas fluorescens* in Nutrient broth medium at 28°C, in shaking culture at ∼200 rpm, to OD_{600} <1.

3.2.2.4. Grow *Micrococcus luteus* in Tryptic soya broth medium at 30°C, in shaking culture at ∼200 rpm, to OD_{600} <1.

3.2.3. Preparation of Bacteria for Chemotaxis

3.2.3.1. Wash bacteria three times in PB, with centrifugation at ∼6,000 rpm, room temperature for 2 min.

3.2.3.2. Resuspend bacteria in PB at 2.5×10^8 cells/ml.

3.2.4. Quantification of Chemotaxis Using Bacteria as Signaling Agents

3.2.4.1 Prepare chemotaxis plates with *Dictyostelium* in the upper chamber wells following steps **3.1.2.1–3.1.2.3.**

3.2.4.2. Remove BSA completely from each well of the treated bottom plate and add PB with bacteria at the desired cell number (e.g., $0–50 \times 10^6$ bacteria) to the bottom well of the plate.

3.2.4.3. After adding both *Dictyostelium* and bacteria to their respective parts of the chemotaxis plate, reassemble the original plate. Carefully place upper part of the plate on top of the lower part of the chemotaxis plate, avoid generating any air bubble in this process.

3.2.4.4. Transfer the assembled plate into the IncuCyte chamber, at 22°C. Using a 10x objective lens, collect cell images from both the top, and under surface of the membrane, over a desired time (e.g., 1.5–4 h.), at 15 min intervals. Export the data into Microsoft Excel for processing.

3.2.5. Results

The response sensitivity of growth-phase *Dictyostelium* to <1 nM concentrations of various chemoattractants suggested that the assay might be sufficiently effective to detect directed migration to live bacteria secreting endogenous compounds, which act as chemoattractants to *Dictyostelium*. Indeed, we had previously demonstrated that *Dictyostelium* would chemotax to both *Klebsiela planticola* and *Bacillus subtilis* (Meena and Kimmel, 2017). Relative chemotaxis was directly correlated to cell number, indicating an excellent dose-dependent quantifiable response. We also showed that chemotaxis relied on folate- and/or cAMP-dependent signaling pathways and that secreted cAMP could be detected by bioassay (Meena and Kimmel, 2017).

Here, we extend the system to define conditions for quantifiable chemotaxis to other live bacterial species. *Dictyostelium* show strong chemotactic response to both gram positive (*Bacillus cereus, Micrococcus luteus*) and gram negative (*Escherichia coli, Pseudomonas fluorescens*) bacteria (**Figure 3**), in a manner similar to that of purified chemoattractants (see **Figure 1**). Physio-chemical analyses confirm the secretion of cAMP and/or folate, by the various bacteria.

3.3. Phagocytosis of Live Bacteria by Growth Phase *Dictyostelium*

3.3.1. Growth and Preparation of Growth Phase Dictyostelium

Follow all steps in **3.1.1.**

3.3.2. Growth and Preparation of Bacteria

Follow all steps in **3.2.2.** and **3.2.3.**

3.3.3. Preparation of pHrodo®-Labeled Live Bacteria

3.3.3.1. pHrodo™ is a fluorogenic dye that exhibits a dramatic increase in fluorescence at an acidified pH. Thus, pHrodo®-labeled bacteria show minimal basal fluorescence, but upon phagocytosis by *Dictyostelium* and transport to lysosomes, detected fluorescence increases. ∼2 x 10^9 bacteria from **3.2.3.** were centrifuged

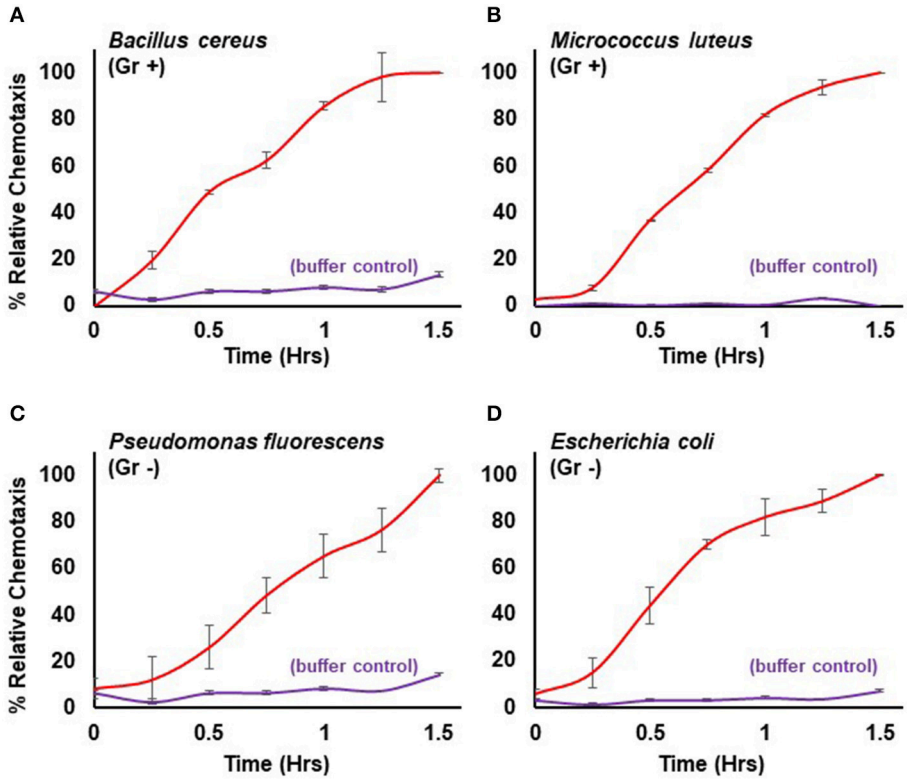

FIGURE 3 | Quantified chemotaxis to live bacteria. Time-course quantification of WT *Dictyostelium* migration to 5 × 10^7 cells of **(A)** gram positive (Gr +) *Bacillus cereus*, **(B)** gram positive (Gr+) *Micrococcus luteus*, **(C)** gram negative (Gr -) *Pseudomonas fluorescens*, and **(D)** gram negative (Gr–) *Escherichia coli*; buffer controls are included for each. Relative chemotaxis is normalized to values at 1.5 h. Standard deviations are shown based upon three replicates.

for 2 min at 12,000 rpm and resuspended in ∼50 μL of Component C (ThermoFisher Scientific, pHrodo™ Phagocytosis particle labeling kit). Succinimidyl ester dye (10 mM) was added to 0.5 mM and incubated for 45 min at room temperature. To prevent cell lethality during pHrodo®-labeling, toxic compounds (e.g., methanol) were eliminated from the labeling.

3.3.3.2. To remove non-complexed dye, bacteria were washed three times at 12,000 rpm with Component C. All pHrodo®-labeled bacteria species were viable, as observed by cell division and motility, when re-cultured in growth medium.

3.3.4. Quantification of Phagocytosis of Live Bacteria

3.3.4.1. ∼0.9 x 10^5 *Dictyostelium* from **3.1.2.4.** in 100 μL PB were added to each phagocytosis/macropinocytosis plate well and allowed to adhere to the well base for 1–5 min.

3.3.4.2. ∼1 x 10^7 (∼10-fold the number of *Dictyostelium* cells) of pHrodo®-labeled live bacteria from **3.3.3.2.** in 100 μL of PB were added to each well. In parallel, for negative controls, three wells had bacteria, without added *Dictyostelium*.

3.3.4.3. Transfer the plate to the IncuCyte chamber, at 22°C. Using a 10x objective lens, collect cell images in the visible and rhodamine detection ([Excitation/Emission (nm) 560/585]), a desired time (e.g., 1.5–4 h), at 15 min intervals. Export the data into Microsoft Excel for processing.

3.3.5. Phagocytosis of pHrodo-Labeled Bacteria Using Immunofluorescence Microscopy

3.3.5.1. Follow all steps in **3.1.1.** to obtain growth phase *Dictyostelium*.

3.3.5.2. Follow all steps in **3.3.3.** to obtain pHrodo-labeled bacteria.

3.3.5.3. Phagocytosis of pHrodo-labeled bacteria by *Dictyostelium* can also be visualized by confocal microscopy. Briefly, add 400 μL of pHrodo-labeled live bacteria 8 × 10^6 /mL in PB and 400 μL of *Dictyostelium* at 1.0 x 10^6 /mL in PB to a well of a 4-well Lab-Tec chambered slide and incubate at 22°C for 15 min, to allow cells to adhere.

3.3.5.4. DIC and fluorescent [Excitation/Emission (nm) 560/585] images were acquired at varying times by confocal/multiphoton microscopy using a 100x oil objective lens and processed using Zeiss ZEN software.

3.3.6. Results

In addition to chemotaxis, professional phagocytes are defined by an ability to engulf large (>1 μM) particles, for nutrient uptake, directed killing of invading unicellular organisms, and/or

removal of cell debris (Lim et al., 2017). Essential to phagocytic processes is the acidification of phagosomes through a vesicle trafficking pathway leading to foreign particle destruction (Levin et al., 2016). We have taken advantage of the rhodamine probe pHrodo® that has minimal fluorescence in a pH neutral milieu, but which displays enhanced (∼10x) fluorescence at decreasing pH (Kapellos et al., 2016). We developed non-toxic conditions to surface label various bacterial species with pHrodo®, thus enabling a quantifiable mode for the dynamic determination of bacterial internalization. Further, the pHrodo®-labeled bacteria remain fully viable and continue to serve as functional sources for chemoattraction of *Dicytostelium* (Meena and Kimmel, 2017).

Figure 4 shows a time-dependent increase in fluorescence upon phagocytosis of pHrodo®-labeled gram positive and gram negative bacteria by *Dictyostelium* and their transport into acidified intracellular vesicles; in the absence of *Dictyostelium*, fluorescence remains comparatively low throughout the time-course. The functional difference in fluorescent intensity is well visualized by confocal microscopy (**Figure 4**). Extracellular bacteria have very low level fluorescence, whereas, following phagocytosis, intracellular vesicles of *Dictyostelium* become progressively, highly, and specifically fluorescent (Meena and Kimmel, 2017).

3.4. Macropinocytosis of pHrodo®Red Dextran by Growth Phase *Dictyostelium*

3.4.1. Macropinocytosis of pHrodo®Red Dextran Using Immunofluorescence Microscopy

3.4.1.1. Follow all steps in **3.1.1.** to obtain growth phase *Dictyostelium*.

3.4.1.2. As per phagocytosis, macropinocytosis by *Dictyostelium* can be monitored by assessing fluorescence changes of pHrodo coupled to dextran, 10K, upon cellular internalization. For confocal microscopy, first add 300 μL of *Dictyostelium* at 1.0×10^6 /mL in PB to a well of an 8-well Lab-Tec chambered slide and incubate at 22°C for 15 min, to allow cells to adhere. Subsequently, add 300 μL of pHrodo-Red Dextran at 30 μg/mL.

3.4.1.3. DIC and fluorescent [Excitation/Emission (nm) 560/585] images were acquired at varying times by confocal/multiphoton microscopy using a 100x oil objective lens and processed using Zeiss ZEN software.

3.4.2. Quantification of Macropinocytosis of pHrodo-Red Dextran

3.4.2.1. $\sim 0.9 \times 10^5$ *Dictyostelium* from **3.1.1.** in 100 μL PB were added to each phagocytosis/macropinocytosis plate well and allowed to adhere to the well base for 1–5 min.

3.4.2.2. 100 μL of pHrodo® Red Dextran suspension in PB (0–4 μg) was then added to each well. In parallel, for negative controls, three wells had pHrodo® Red Dextran, without added *Dictyostelium*.

3.4.2.3. Transfer the plate to the IncuCyte chamber, at 22°C. Using a 10x objective lens, collect cell images in the visible and rhodamine detection [Excitation/Emission (nm) 560/585], a desired time (e.g., 1.5–4 h), at 15 min intervals. Export the data into Microsoft Excel for processing.

3.4.3. Results

Certain cells of the immune system (e.g., macrophage and dendritic) utilize macropinocytosis in a central role for antigen uptake, processing, and presentation during pathogen defense (Lim and Gleeson, 2011; Marques et al., 2017). In *Dictyostelium*, macropinocytosis plays a role for nutrient uptake (Bloomfield et al., 2015). Macropinocytosis, however, is a distinct pathway to phagocytosis (Lim and Gleeson, 2011; Levin et al., 2016; Marques et al., 2017); the former functions for cellular uptake of fluid-phase elements, whereas the latter is focused to large particle recognition. Still, the macropinosome and phagosome systems have certain commonality with the endosomal/lysosomal pathway and vesicle acidification (Lim and Gleeson, 2011; Levin et al., 2016; Marques et al., 2017). Therefore, we utilized the pH-sensitive probe pHrodo® dextran 10K that has minimal fluorescence at neutral pH, but displays dramatic enhancement of fluorescence as the pH decreases during macropinocytosis, with endosome maturation, and fusion with lysosomes.

The principle of the macropinocytosis assay perfectly parallels that of phagocytosis and is, thus, readily observed by confocal fluorescence microscopy (**Figure 5A**) or by high-throughput measurement, where, following a lag, there is a time-dependent increase in fluorescence upon macropinocytosis of pHrodo®-labeled dextran by *Dictyostelium* and transport into acidified intracellular vesicles is highly quantifiable (**Figure 5B**). In the absence of *Dictyostelium*, fluorescence of pHrodo®-labeled dextran remains unchanged.

The observed kinetics do differ from that generally observed using FITC-dextran and shaking assays, where uptake is linear for ∼120 min, which then plateaus. Several physical parameter distinctions underlie these kinetic differences. With FITC-dextran, intracellular fluorescence can be detected upon immediate uptake, whereas pHrodo®-labeled dextran must first traffic through acidic vesicles to become fluorescent. In suspension assays, *Dictyostelium* are exposed to continuous and non-varying concentrations of FITC-dextran, from 0 time. In the IncuCyte system, *Dictyostelium* are first adhered at 0 time, before pHrodo®-labeled dextran is added; chemical diffusion and cell movement can lead to a further time-lag for maximal dextran-cell interactions. Collectively, these factors contribute to non-linear (lag phase) curves during initial stages, and relative kinetic delays throughout the time-course. Following the lag, we see linearity for ∼120 min, which begins to plateau for the lower pHrodo®-labeled dextran input ratios.

4. DISCUSSION

We have applied a high-throughput platform for quantified time-course assays of chemotaxis, phagocytosis, and macropinocytosis. Although we developed these for *Dictyostelium*, they are easily adaptable to phagocytic cells of any species. The 96-well format permits pharmaceutical or small molecule evaluations for each, with sufficient scale for multiple controls and replicates. As each process is unique,

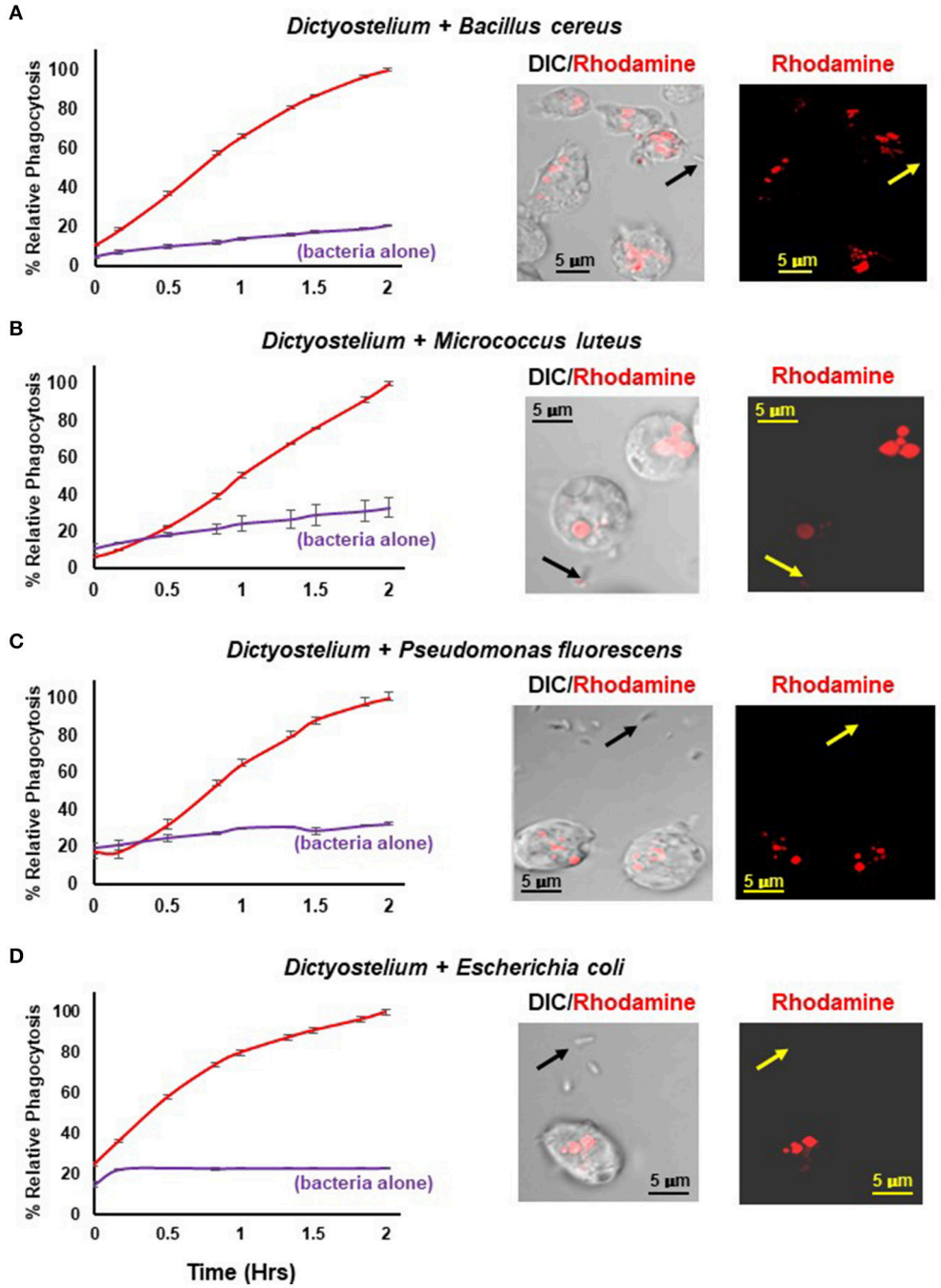

FIGURE 4 | Quantified phagocytosis of live bacteria. Left panels show time-course phagocytosis quantification by WT *Dictyostelium* of pHrodo®-labeled **(A)** *Bacillus cereus*, **(B)** *Micrococcus luteus*, **(C)** *Pseudomonas fluorescens*, and **(D)** *Escherichia coli*; bacteria-alone controls are included for each. Standard deviations are shown based upon three replicates and normalized to values of 2 h. Right panels show confocal images for DIC and rhodamine fluorescence after 2 hrs of phagocytosis. Arrows indicate pHrodo®-bacteria with low level fluorescence outside of *Dictyostelium*. **(A)** *Bacillus cereus*, **(C)** *Pseudomonas fluorescens*, and **(D)** *Escherichia coli* are rod-like, whereas **(B)** *Micrococcus luteus* is coccoid; at an increased magnification, their typical rounded, clumped-cell characteristic is apparent.

their combined and distinct set of quantitative assay parameters must be considered when comparing to other approaches. Thus, quantifications rely on collective cellular response, and cannot simply separate the contribution of each individual component. While we have had success with continuous assay in excess of 6 h, we generally limit data collection to <2 h, where physiological differences between cells at their start and end points are minimized. We have confirmed utility for genetic screens in network pathway testing (Meena and Kimmel, 2017) and, thus, identified specific receptors,

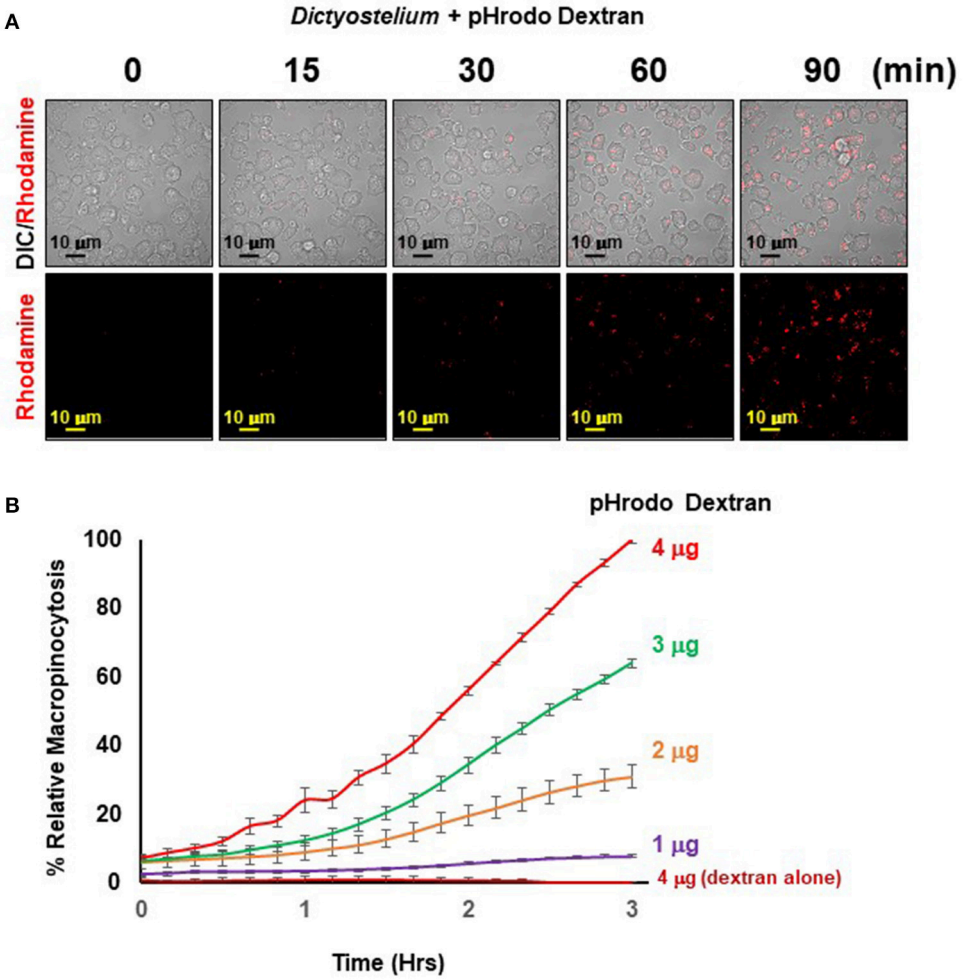

FIGURE 5 | Quantified macropinocytosis by *Dictyostelium*. **(A)** DIC and rhodamine fluorescent images of pHrodo® -labeled Dextran (in red) engulfed by WT *Dictyostelium* over time. **(B)** Time-course macropinocytosis quantification by WT *Dictyostelium* of pHrodo®-labeled Dextran; a dextran-alone control is included. Standard deviations are shown based upon three replicates and normalized to values for 4 µg pHrodo®-Dextran at 3 h.

G proteins, etc. as essential or non-essential components in these pathways.

Although the chemotaxis data provide direct quality proof for high sensitivity at <1 nM chemoattractant concentrations, the data have significant complexity to interpretation, which differ for purified ligands or live bacteria as the chemoattractant source. Whereas the system does not provide direct quantification of migratory speed, directionality, or cell-shape change with comparison of WT and mutant cells as do single-cell, time-course chemoattractant response assays, it presents an effective complementary alterative that is highly quantifiable, in a high-throughput manner. It is, for example, highly effective to analyze response to live bacteria, receptor affinity response, essential pathway genes, novel chemoattractants, and small molecule targets, where multiple independent replicates and controls require precise temporal parallel evaluations.

After careful evaluation of diverse experiments and algorithms involving multiple replicates and controls, we conclude that precise normalizations provide the most consistent and reproducible data for interpretation, in comparison to scoring absolute numbers of migratory cells. Values for relative chemotaxis reach a plateau with time, independent of chemoattractant concentration, or bacterial numbers used [see **Figures 1**, **3** (Meena and Kimmel, 2017)]. Nonetheless, this is not simply because there are no migratory cells remaining in the upper well chamber at the time of the plateau. Several other factors are contributory. First, for chemotaxis, we image the number of cells associated with the bottom of the transmembrane at a given time point. However, this association is transitory, and eventually cells will drop off the membrane into the bottom well and be lost to the chemotaxis cell count. Even as new cells continuously reach the membrane, they are in balance with the cell numbers that have become dissociated, thus contributing to a chemotactic plateau appearance. Second, *Dictyostelium* continuously secrete enzymes that inactivate chemoattractants folate or cAMP; a deaminase (Pan and Wurster, 1978) oxidizes

the essential amino group at position 2 of the pyrimidine ring (see **Figure 1**), while a phosphodiesterase converts cAMP into 5′-AMP (Franke and Kessin, 1992; Brzostowski and Kimmel, 2006). As these inactivating enzymes accumulate, they can create a buffer area around migrating cells that reduces chemoattractant gradient strength stimulation of naïve cells, and, thus, reduce their chemotactic response (Tweedy et al., 2016; Meena and Kimmel, 2017).

The chemoattractant gradients established are neither linear nor static, with variations occurring in both signal strength and gradient steepness. Initially, for ligand chemotaxis, concentrations detected by cells in the upper well chamber are relatively low, but with a very steep chemoattractant gradient. However, with time, as the ligand concentration in the upper well rises progressively, the steepness of the gradient diminishes in parallel. For bacteria as chemoattractant sources, it is even more complex. The available levels of chemoattractant is ever increasing, with their continued secretion by bacteria and accumulation in the wells of the lower chamber altering the shape of the gradient.

Apart from dissecting mechanistic pathways for chemotaxis, we are also interested to identify the chemical composition of bacterially secreted chemoattractants. We have applied several approaches to this. The mixing of saturating levels of any specific chemoattractant with cells plated in the upper well chamber will desensitize cells for chemotactic response to that same chemoattractant, but will not compete with unrelated chemoattractants in the bottom chamber wells (Meena and Kimmel, 2017). Alternatively, we have used *Dictyostelium* lacking components of known pathways to determine the presence or absence of known chemoattractants. Finally, we applied physio-chemical assays of bacterially secreted compounds for potential to identify novel molecules. Other factors need to be considered for cellular migration to bacteria that secrete more than a single type chemoattractant. Although folate and cAMP bind and activate different G protein coupled receptors, their downstream intracellular paths converge (Liao et al., 2013; Meena and Kimmel, 2017). Thus, although low sub-saturating levels (e.g., 1 nM) of folate and cAMP elicit greater chemotactic response when provided in combination than with either alone (Meena and Kimmel, 2017), no differences are seen between a single or mixed ligand preparation when either or both are at signal saturation (e.g., 1 μM). Accordingly, if a bacterial population can secrete multiple chemoattractants to saturating levels overall cell migration might remain unaltered, even if signal response were fully suppressed for one ligand.

Chemotaxis orients cell movement toward component targets for directed removal and destruction. Since phagocytosis serves as a primary process for this latter cellular function, we developed an engulfment assay of live bacteria that would precisely parallel chemotaxis and allow co-analyses to define common and unique pathways. We labeled bacteria with the rhodamine based probe pHrodo® that exhibits enhanced fluorescence with decreasing pH, and quantified phagocytic rates as a function of an increase in fluorescence, upon the internalization of pHrodo®-bacteria and trafficking into acidified intracellular vesicles. The phagocytosis assay is highly quantitative in real-time, and the 96-well format facilitates the dissection of molecular pathways, and evaluation of sensitivity to pharmaceutical agents.

Our labeling conditions do not compromise bacterial viability and pHrodo®-bacteria remain strongly chemoattractant for *Dictyostelium* (Meena and Kimmel, 2017). Moreover, we have demonstrated that *Dictyostelium* lacking chemosensitivity to pHrodo®-bacteria, through the loss of chemoattractant receptor function, retain full phagocytic capacity, thus, separating essential dependency of these cellular processes (Meena and Kimmel, 2017).

We have further demonstrated cell-viable labeling and quantitative phagocytosis of multiple gram negative and gram positive bacterial species and suggest that these procedures are adaptable to virtually any bacteria, providing an excellent extension to existing tools for dynamic studies of host-pathogen interactions during chemotaxis and phagocytosis.

Macropinocytosis is another highly regulated pathway for endocytosis, which, like phagocytosis, is essential in pathogen defense (Lim and Gleeson, 2011; Marques et al., 2017). Although both phagocytosis and macropinocytosis are actin-dependent pathways, they separately involve many distinct molecular elements (Lim and Gleeson, 2011; Bloomfield et al., 2015; Levin et al., 2016; Lim et al., 2017; Marques et al., 2017). Macropinocytosis is well-coordinated to signaling response for cytoskeletal remodeling for fluid phase uptake and, although many components and regulators are known, their precise sequence in event activations is still poorly defined. Since most macropinocytosis assays have limited real-time and/or high-throughput outputs, we consequently used pHrodo®-dextran as a fluorescent read-out, as per phagocytosis. Our results have demonstrated defined conditions for highly quantitative measurements of macropinocytosis in *Dictyostelium* in a physiological, but high-throughput, setting.

We anticipate that the multiple assays described here will have significant utility in application for functional host-pathogen studies.

AUTHOR CONTRIBUTIONS

All authors listed have made a substantial, direct and intellectual contribution to the work, and approved it for publication.

FUNDING

This work was supported by the Intramural Research Program of the National Institute of Diabetes and Digestive and Kidney Diseases, National Institutes of Health.

ACKNOWLEDGMENTS

We thank our colleagues who have contributed to defining the excellence of *Dictyostelium* as a model for the study of chemotaxis, phagocytosis, and macropinocytosis and, especially, dictyBase (http://dictybase.org/).

REFERENCES

Artemenko, Y., Lampert, T. J., and Devreotes, P. N. (2014). Moving towards a paradigm: common mechanisms of chemotactic signaling in Dictyostelium and mammalian leukocytes. *Cell. Mol. Life Sci.* 71, 3711–3747. doi: 10.1007/s00018-014-1638-8

Basu, S., Fey, P., Pandit, Y., Dodson, R., Kibbe, W. A., and Chisholm, R. L. (2013). DictyBase 2013: integrating multiple Dictyostelid species. *Nucleic Acids Res.* 41, D676–D683. doi: 10.1093/nar/gks1064

Bloomfield, G., Traynor, D., Sander, S. P., Veltman, D. M., Pachebat, J. A., and Kay, R. R. (2015). Neurofibromin controls macropinocytosis and phagocytosis in Dictyostelium. *Elife* 4:e04940. doi: 10.7554/eLife.04940

Bozzaro, S., and Eichinger, L. (2011). The professional phagocyte *Dictyostelium discoideum* as a model host for bacterial pathogens. *Curr. Drug Targets* 12, 942–954. doi: 10.2174/138945011795677782

Brzostowski, J. A., and Kimmel, A. R. (2006). Nonadaptive regulation of ERK2 in Dictyostelium: implications for mechanisms of cAMP relay. *Mol. Biol. Cell* 17, 4220–4227. doi: 10.1091/mbc.E06-05-0376

Cosson, P., and Soldati, T. (2008). Eat, kill or die: when amoeba meets bacteria. *Curr. Opin. Microbiol.* 11, 271–276. doi: 10.1016/j.mib.2008.05.005

Franke, J., and Kessin, R. H. (1992). The cyclic nucleotide phosphodiesterases of *Dictyostelium discoideum*: molecular genetics and biochemistry. *Cell. Signal.* 4, 471–478. doi: 10.1016/0898-6568(92)90016-2

Jin, T. (2013). Gradient sensing during chemotaxis. *Curr. Opin. Cell Biol.* 25, 532–537. doi: 10.1016/j.ceb.2013.06.007

Jin, T., Xu, X., and Hereld, D. (2008). Chemotaxis, chemokine receptors and human disease. *Cytokine* 44, 1–8. doi: 10.1016/j.cyto.2008.06.017

Kapellos, T. S., Taylor, L., Lee, H., Cowley, S. A., James, W. S., Iqbal, A. J., et al. (2016). A novel real time imaging platform to quantify macrophage phagocytosis. *Biochem. Pharmacol.* 116, 107–119. doi: 10.1016/j.bcp.2016.07.011

Levin, R., Grinstein, S., and Canton, J. (2016). The life cycle of phagosomes: formation, maturation, and resolution. *Immunol. Rev.* 273, 156–179. doi: 10.1111/imr.12439

Liao, X. H., Buggey, J., Lee, Y. K., and Kimmel, A. R. (2013). Chemoattractant stimulation of TORC2 is regulated by receptor/G protein-targeted inhibitory mechanisms that function upstream and independently of an essential GEF/Ras activation pathway in Dictyostelium. *Mol. Biol. Cell* 24, 2146–2155. doi: 10.1091/mbc.E13-03-0130

Lim, J. J., Grinstein, S., and Roth, Z. (2017). Diversity and versatility of phagocytosis: roles in innate immunity, tissue remodeling, and homeostasis. *Front. Cell. Infect. Microbiol.* 7:191. doi: 10.3389/fcimb.2017.00191

Lim, J. P., and Gleeson, P. A. (2011). Macropinocytosis: an endocytic pathway for internalising large gulps. *Immunol. Cell Biol.* 89, 836–843. doi: 10.1038/icb.2011.20

Marques, P. E., Grinstein, S., and Freeman, S. A. (2017). SnapShot: macropinocytosis. *Cell* 169, 766-766.e1. doi: 10.1016/j.cell.2017.04.031

Meena, N. P., and Kimmel, A. R. (2016). Biochemical responses to chemically distinct chemoattractants during the growth and development of Dictyostelium. *Methods Mol. Biol.* 1407, 141–151. doi: 10.1007/978-1-4939-3480-5_11

Meena, N. P., and Kimmel, A. R. (2017). Chemotactic network responses to live bacteria show independence of phagocytosis from chemoreceptor sensing. *Elife* 6:e24627. doi: 10.7554/eLife.24627

Nichols, J. M., Veltman, D., and Kay, R. R. (2015). Chemotaxis of a model organism: progress with Dictyostelium. *Curr. Opin. Cell Biol.* 36, 7–12. doi: 10.1016/j.ceb.2015.06.005

Pan, P., and Wurster, B. (1978). Inactivation of the chemoattractant folic acid by cellular slime molds and identification of the reaction product. *J. Bacteriol.* 136, 955–959.

Tweedy, L., Knecht, D. A., Mackay, G. M., and Insall, R. H. (2016). Self-generated chemoattractant gradients: attractant depletion extends the range and robustness of chemotaxis. *PLoS Biol.* 14:e1002404. doi: 10.1371/journal.pbio.1002404

Veltman, D. M., Lemieux, M. G., Knecht, D. A., and Insall, R. H. (2014). PIP(3)-dependent macropinocytosis is incompatible with chemotaxis. *J. Cell Biol.* 204, 497–505. doi: 10.1083/jcb.201309081

Conflict of Interest Statement: The authors declare that the research was conducted in the absence of any commercial or financial relationships that could be construed as a potential conflict of interest.

frontiers in Cellular and Infection Microbiology

MINI REVIEW
published: 05 December 2017
doi: 10.3389/fcimb.2017.00497

Exploring Virulence Determinants of Filamentous Fungal Pathogens through Interactions with Soil Amoebae

Silvia Novohradská[1,2], *Iuliia Ferling*[1,2] *and Falk Hillmann*[1]*

[1] *Evolution of Microbial Interactions, Leibniz Institute for Natural Product Research and Infection Biology-Hans Knöll Institute, Jena, Germany,* [2] *Institute of Microbiology, Friedrich Schiller University Jena, Jena, Germany*

Infections with filamentous fungi are common to all animals, but attention is rising especially due to the increasing incidence and high mortality rates observed in immunocompromised human individuals. Here, *Aspergillus fumigatus* and other members of its genus are the leading causative agents. Attributes like their saprophytic life-style in various ecological niches coupled with nutritional flexibility and a broad host range have fostered the hypothesis that environmental predators could have been the actual target for some of their virulence determinants. In this mini review, we have merged the recent findings focused on the potential dual-use of fungal defense strategies against innate immune cells and soil amoebae as natural phagocytes. Well-established virulence attributes like the melanized surface of fungal conidia or their capacity to produce toxic secondary metabolites have also been found to be protective against the model amoeba *Dictyostelium discoideum.* Some of the recent advances during interaction studies with human cells have further promoted the adaptation of other amoeba infection models, including the wide-spread generalist *Acanthamoeba castellanii*, or less prominent representatives like *Vermamoeba vermiformis.* We further highlight prospects and limits of these natural phagocyte models with regard to the infection biology of filamentous fungi and in comparison to the phagocytes of the innate immune system.

Keywords: dictyostelium, acanthamoeba, aspergillus, phagocytosis, macrophages, amoebae

OPEN ACCESS

Edited by:
Sascha Thewes,
Freie Universität Berlin, Germany

Reviewed by:
Sven Krappmann,
University of Erlangen-Nuremberg, Germany
Marie-Helene Rodier,
CHU/Faculté de Médecine, France

***Correspondence:**
Falk Hillmann
falk.hillmann@leibniz-hki.de

Received: *14 September 2017*
Accepted: *20 November 2017*
Published: *05 December 2017*

Citation:
Novohradská S, Ferling I and Hillmann F (2017) Exploring Virulence Determinants of Filamentous Fungal Pathogens through Interactions with Soil Amoebae. Front. Cell. Infect. Microbiol. 7:497. doi: 10.3389/fcimb.2017.00497

ENVIRONMENTALLY ACQUIRED FUNGAL PATHOGENS

Fungi are ubiquitous in nature, inhabiting various ecological niches. Even among those which thrive as saprophytes and do not exhibit any host requirement for survival, there are pathogens which cause devastating diseases in humans and animals resulting in thousands of deaths every year (Brown et al., 2012). Classical examples include filamentous fungi like *Aspergillus fumigatus* and *Fusarium* sp., but also several dimorphic fungi such as *Blastomyces dermatitidis* or *Histoplasma capsulatum,* and the yeast *Cryptococcus neoformans*, have environmental reservoirs. One of the most prevalent groups of fungi in the environment is represented by the aspergilli (Shelton et al., 2002). With several hundred species, only a few of them have a considerable impact on human health: *A. fumigatus, A. flavus, A. terreus, A. nidulans,* and *A. niger*.

Aspergillus fumigatus is one of the most important air-borne fungal pathogens, living ubiquitously in terrestrial environments. This fungus disseminates by releasing thousands of

asexual spores (conidia) from each conidiophore which, upon inhalation, pass through the nasal cavity and reach the alveoli. Most of them are expelled by mucocilliary clearance while the residual ones are eliminated by macrophages and neutrophils of an immunocompetent host. In the case of an immunodeficient host, conidia swell and grow into a mycelium. Once the fungus overcomes the natural immune barrier, it can cause asthma-associated allergies, sinusitis, allergic bronchopulmonary aspergillosis (ABPA) and, in the worst case, life-threatening invasive aspergillosis (IA), occasionally reaching mortality rates even beyond 50% due to rapid progression and misdiagnosis (Brown et al., 2012). Aspergilli can also infect wild and domestic animals nearly encompassing all major phyla including corals, honey bees, reptiles, and warm-blooded animals such as birds, mammals, and non-human primates (reviewed by Seyedmousavi et al., 2015). Another group of environmental filamentous fungi represent exclusively entomogenous pathogens, such as *Metarhizium anisopliae* or *Beauveria bassiana.* Microscopic examination and phagocytosis assays with these fungi suggested that their ability to adhere to the insect cuticle, penetrate through the haemocoel using hydrolyzing enzymes, and ultimately survive phagocytic haemocytes may be a consequence of adaptations that have been acquired early in evolution to avoid predation by soil amoebae (Bidochka et al., 2010).

Unlike *Aspergillus, C. neoformans* is not ubiquitous in the soil; rather it has been isolated from areas frequented by pigeons, chickens, turkeys, and other avian species. After inhalation of infectious particles, *Cryptococcus* resides in the lung alveoli where it can persist and replicate while a thick polysaccharide capsule surrounding the yeast cell helps to avoid its killing by macrophages. Other studies have shown that *Cryptococcus* is also able to survive intracellularly, even a few hour after phagocytosis (Feldmesser et al., 2000). Dissemination to the brain results in severe meningoencephalitis, especially in immunocompromised patients. On the other hand, *C. gatii* which has been isolated from trees, mainly causes pulmonary infections in an immunocompetent host (García-Rodas and Zaragoza, 2012; Kwon-Chung et al., 2014).

Among other environmentally acquired pathogenic fungi, thermally dimorphic fungi such as *Histoplasma capsulatum*, *Blastomyces dermatitidis*, and *Coccidioides immitis* are especially clinically relevant and classified as Biosafety Level 3 (BSL3) organisms. Despite their divergent phylogeny, they all share similar patterns of existence: temperature-dependent morphological dimorphism, pulmonary infectivity, and endemism. After the inhalation of conidia, transformation into a yeast-form is crucial to promote pathogenicity through escape from phagocytosis, modulation of the cytotoxic environment of the phagolysosome or enhanced degradation of reactive oxygen species (Boyce and Andrianopoulos, 2015).

Considering the diversity of environmental niches and strategies to survive and replicate within a variety of mammalian hosts, the aforementioned virulence attributes may confer a dual-use capability to defend against phagocytes in both animal hosts and the environment. Moreover, such parallels gave rise to the idea that selective pressures in the environment have led to the emergence and maintenance of these traits that have later supported virulence in higher eukaryotes. Although the filamentous life style of aspergilli suggests little need for any specific attributes to avoid or withstand any phagocytes, their infectious and reproductive stage is formed by small, unicellular conidia which are easily ingested by such cells. A number of profound studies over the last years have uncovered a multitude of mechanisms which aid in the escape and defense of these fungi against their opponents of human or environmental origin (**Table 1**).

FUNGAL RESISTANCE TO INNATE IMMUNE CELLS AND SOIL AMOEBAE

Macrophages and neutrophil granulocytes are the most prominent representatives among innate immune cells which counteract fungal pathogens. Alveolar macrophages are the first line of defense against IA by killing inhaled conidia and initiating the pro-inflammatory response that recruits neutrophils to the site of infection (reviewed by Brakhage et al., 2010). As a consequence, patients with reduced numbers of macrophages have long been known to be at a higher risk to develop IA (Brakhage, 2005). A number of *in-vitro* studies suggest that even macrophages from immunocompetent individuals show variable killing efficiencies of ingested fungal conidia ranging from 10 to 90% as summarized in Philippe et al. (2003). The same study demonstrated that fungal conidia are especially resistant to killing when remaining in a dormant state or when the confronting macrophages are derived from immunosuppressed donors. Overall, most of these results are based on counts of colony forming units (CFUs) and certain methodological issues, such as the time of co-incubation, conidial aggregation or the incomplete experimental removal of non-ingested conidia, could have also contributed to the heterogeneous killing rates that have been reported. A similar assay with *Dictyostelium discoideum* revealed that conidia were readily ingested but remained viable over more than 24 h based on the number of CFUs (Hillmann et al., 2015). Even the comparably robust pathogen *Acanthamoeba castellanii* ingested conidia within the first hour of their interaction, but no signs of digestion were observed at any stage (Van Waeyenberghe et al., 2013). Along this line, co-incubation of *A. fumigatus* or *Fusarium oxysporum* conidia with the common water contaminant *Vermamoeba vermiformis* did not result in any reduction of viable conidia, but instead phagocytic uptake promoted filamentation and growth of the fungus (Cateau et al., 2014; Maisonneuve et al., 2016).

RECOGNITION AND PROCESSING OF FUNGAL CONIDIA BY HUMAN AND ENVIRONMENTAL PHAGOCYTES

Given their role as a first line of defense, studies on the recognition and phagocytic processing of fungal conidia by macrophages have a long-standing history, mainly with regard to aspergilli. The surface of their conidia represents the immediate interface and pathogen-associated molecular patterns (PAMPs) include cell wall constituents like α- and β-glucans, chitins, galactomannans, and other polysaccharides. However, these are

TABLE 1 | Fungal virulence determinants studied using amoeba model systems.

Amoeba model	Fungal pathogen	Virulence factor studied	References
HUMAN PATHOGENIC FUNGI			
A. castellanii	*C. neoformans*	Capsule, melanin, phospholipase production	Steenbergen et al., 2001; Chrisman et al., 2010
		Comparative transcriptomic study	Derengowski et al., 2013
		Extracellular vesicles, glucuronoxylomannan of capsule	Rizzo et al., 2017
	H. capsulatum	Yeast-to-hyphae transition	Steenbergen et al., 2004
	S. schenckii		
	B. dermatitidis		
	A. fumigatus	Phagocytic escape	Van Waeyenberghe et al., 2013
A. castellanii *Naegleria gruberi*	*A. fumigatus* *A. terreus*	Diffusible compound with anti-amoebic properties	Hobson, 2000
D. discoideum	*C. neoformans*	Capsule, melanin	Steenbergen et al., 2003
	A. fumigatus	DHN-melanin, gliotoxin	Hillmann et al., 2015
		Trypacidin	Mattern et al., 2015
	A. terreus	Asp-melanin	Geib et al., 2016
	S. cerevisiae *C. albicans* *C. glabrata*	Flocculation Hyphae formation	Koller et al., 2016
ENTOMOPATHOGENIC FUNGI			
A. castellanii	*M. anisopliae* *B. bassiana*	Phagocytic escape and survival	Bidochka et al., 2010
OTHER			
Giant vampyrellid soil amoebae *Protostelium mycophaga*	Various soil-borne species, Plant pathogenic fungi	First feeding trials to assess the ability of soil amoeba to attack, perforate and lyse the spores of different soil fungi	Old and Darbyshire, 1978; Chakraborty et al., 1983; Old et al., 1985; Chakraborty and Old, 1986 Olive and Stoianovitch, 1960

usually masked by a proteinaceous, hydrophobic rodlet layer which is immunologically inert and diminishes the recognition by immune cells (Aimanianda et al., 2009). The green-gray dihydroxynapthalene (DHN)-melanin pigment coating dormant conidia is another surface component assumed to play a similar role in *A. fumigatus* (Jahn et al., 1997; Tsai et al., 1998; Chai et al., 2010). These protective layers are lost during swelling and subsequent germination of the conidia (**Figure 1**), exposing the PAMPs and allowing recognition, as demonstrated for strains of *A. fumigatus* lacking the DHN melanin pigment which were ingested by macrophages at higher rates than wild type strains (Luther et al., 2007). Interestingly, nearly identical ratios were observed with *D. discoideum*. Conidia of the wild-type, covered by green DHN-melanin, were taken up, but at least threefold less efficiently than the white conidia of the melanin deficient mutant (Hillmann et al., 2015). These data suggest that hiding "prey"-associated molecular patterns could be an asset to escape also from environmental predators and hence, well suited to be studied in an amoeba model.

Swollen conidia of *A. fumigatus* that have lost their DHN-melanin cover expose cell wall β-glucans which activate the Dectin-1/Syk kinase/NADPH signaling cascade in macrophages (Luther et al., 2007; Ma et al., 2012). After recognition and internalization, phagolysosome maturation is initiated through assembly of the NADPH oxidase and LC3-associated phagocytosis (LAP) (Akoumianaki et al., 2016). Melanized conidia of *A. fumigatus* are able to inhibit the crucial process of phagolysosomal maturation at the acidification step which contributes to their significantly reduced killing rates relative to melanin deficient conidia (Jahn et al., 2002; Thywißen et al., 2011, **Figure 1**). In sharp contrast, melanized conidia were shown to inhibit the apoptosis of macrophages by activating the PI3-kinase/Akt signaling pathway (Volling et al., 2011).

The chemically distinct Asp-melanin of *Aspergillus terreus* does not inhibit phagolysosomal acidification in macrophages or *D. discoideum* (**Figure 1**), indicating that even closely related fungi, such as *A. fumigatus* and *A. terreus*, apply different persistence and propagation strategies inside the harsh phagolysosomes of macrophages and some environmental phagocytes (Slesiona et al., 2012; Geib et al., 2016).

PHAGOCYTE-ESCAPE MECHANISMS OF *A. FUMIGATUS*

Apart from conidial killing, macrophage encounters with *A. fumigatus* may also result in disruption of the host cell by the elongation of the hyphae (**Figure 1**). Here, *Aspergillus fumigatus* conidia swell up and initiate growth despite the nutrient-scarce environment of the phagolysosome thereby exploiting their glyoxylate cycle and siderophore machinery to overcome the limited supply of carbon and iron, respectively (Behnsen et al., 2007; Schrettl et al., 2010). It seems likely that these pathways could also be active during conidial processing in environmental phagocytes as this escape strategy was well documented during the interaction with *A. castellanii* as well as *D. discoideum*, resulting in host cell lysis for both amoebae (Van Waeyenberghe et al., 2013; Hillmann et al., 2015). Some of the consequences

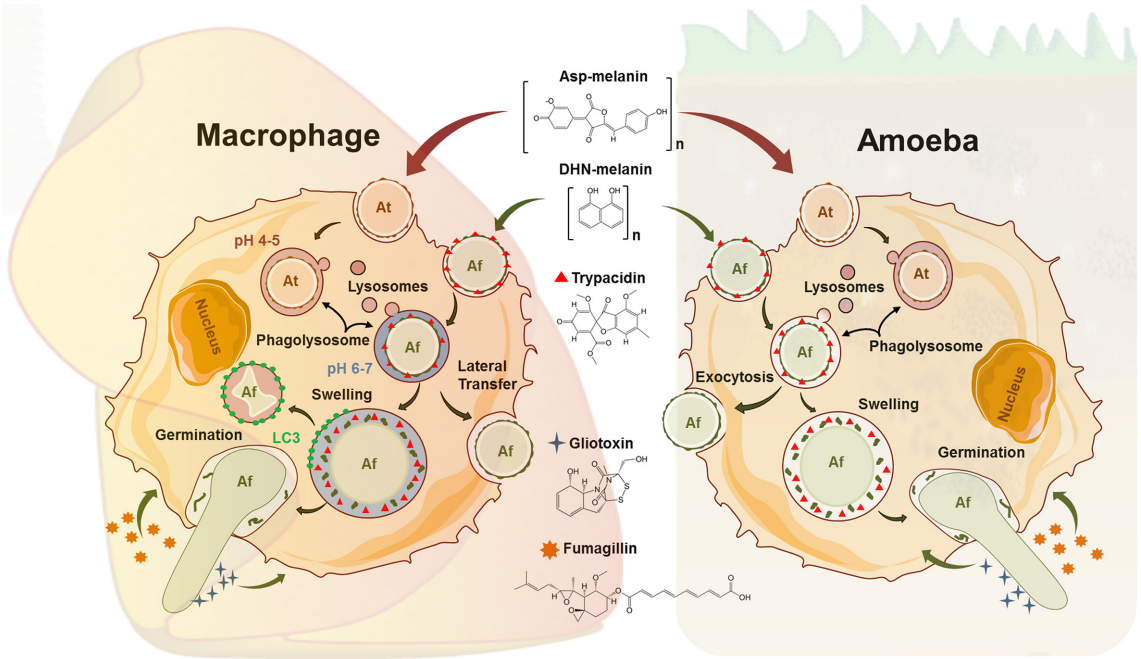

FIGURE 1 | Comparative schematic view on parallel events in the phagocytic processing of fungal conidia from *Aspergillus fumigatus* (Af) and *Aspergillus terreus* (At) in macrophages and amoeba. The latter summarizes results from *A. castellanii* (Ac) and *D. discoideum* (Dd). The conidial pigments Asp-melanin (At) and DHN-melanin (Af) are complex polymers and the final-known intermediate structure is displayed. Ingested spores of At can persist in acidified phagolysosomes (PLs) in macrophages. Acidification of At containing PLs occurs also in *D. discoideum*. In macrophages, Af can either be killed *via* the LC3 dependent pathway, laterally transferred to other cells, or undergo swelling and germination. Exocytosis (Ac), swelling (Ac, Dd) and germination (Ac, Dd) of Af conidia has also been documented in amoeba, while killing by amoeba has not been reported. The spore-borne trypacidin, and the secreted gliotoxin and fumagillin are all made by *A. fumigatus* only and are all known to affect macrophages as well as Dd.

of intracellular fungal germination on the host cell were only recently resolved for human alveolar macrophages. Orchestrated by calcineurin, the infected host cell can complete exocytosis of the fungus containing endosome, followed by the lateral transfer to neighboring cells as part of programmed necrosis (Shah et al., 2016). In perspective of the well-studied social behavior of *D. discoideum,* this amoeba model seems to be especially promising for future studies on such intercellular or altruistic processes. It has become obvious that filamentous fungi can be tough opponents of innate immune cells, but questions on the origin of such anti-immune properties of filamentous fungi remain open. Amoeba models could help to close the knowledge gaps which cannot be addressed from *in vitro* studies with human cells.

AMOEBAE PREDATION AS AN EVOLUTIONARY TRAINING GROUND FOR FILAMENTOUS FUNGAL PATHOGENS

Free living amoebae (FLA) are ubiquitous unicellular protozoa, distributed worldwide in various environments such as soil, water, or air. Mycophagous species, either opportunists or specialists, are widespread and have been isolated over the past 60 years (Olive and Stoianovitch, 1960; Old and Darbyshire, 1978; Chakraborty et al., 1983; Old et al., 1985; Chakraborty and Old, 1986). One of the first mycophagous amoebae ever described was *Protostelium mycophagum* (Olive and Stoianovitch, 1960). It has been isolated alongside the pink-pigmented yeast *Rhodotorula mucilaginosa,* but it can also feed on *Phoma* sp., *Ustilago violacea, Sporobolomyces* sp., and *Cryptococcus laurentii* (Spiegel et al., 2006). Other mycophagous soil amoebae from the genera *Thecamoeba, Arachnula,* and *Vampyrella* have been shown to suppress the growth of the plant pathogenic fungus *Gaeumannomyces graminis* var. *tritici* and therefore significantly contribute to the reduction of "take-all" wheat crops disease caused by this fungus (Chakraborty et al., 1983).

In environments where fungi have encountered constant protozoal predation and competition for nutrients, they must have developed strategies to counteract phagocytic uptake or intracellular passage. Consequently, the same determinants that were effective against amoeba predation, could have later promoted the survival of fungi in a human host. The coincidental evolution hypothesis suggests that virulence factors have evolved as a response to more ordinary selection pressures than for virulence *per se* (Erken et al., 2013). Several studies using free-living amoeba *A. castellanii* and more recently *D. discoideum* have supported this hypothesis for yeast-like fungi and have underlined the suitability of these models to study basic fungal virulence determinants (Steenbergen et al., 2001, 2004; Chrisman et al., 2010; Derengowski et al., 2013; Koller et al., 2016; Rizzo et al., 2017, see **Table 1** for an overview).

Aspergillus fumigatus requires no obvious residence inside the mammalian host to survive and replicate; it appears to lack classical virulence factors and its pathogenicity primarily depends on host impairment. Therefore, it is conceivable that the ability to counteract the compromised immune system was partially tuned from the long-term interplay between fungi and their predators in their natural environment. Such fungivorous organisms are by no means limited to amoebae, but also include higher animals like nematodes, mites, or insects. For instance, a primary study on *A. nidulans* demonstrated that the multitude of fungal low-molecular-mass compounds known as secondary metabolites could present a selective advantage against predation by the fungivorous springtail *Folsomia candida* (Rohlfs et al., 2007).

Such defensive actions could also provide protection against microscopic predators, as active components have been shown to diffuse from the non-germinating spores and inhibit certain functions of phagocytosis (Slight et al., 1996). The anti-amoebae effects of diffusates from clinical and environmental isolates of *A. fumigatus* and *A. terreus* have been described on *Naegleria gruberi*, proposing it as a primary function of such metabolites (Hobson, 2000). Even at the early stages of a direct interaction, mycotoxins are encountered immediately by the ingesting phagocytes, as it has recently been shown for the amoebicidal polyketide trypacidin which resides primarily on the surface of the *A. fumigatus* spore (Gauthier et al., 2012; Mattern et al., 2015, **Figure 1**). Following germination and escape, further potent, soluble toxins are synthesized.

Among them, the sesquiterpene fumagillin was one of the first for which amoebacidal properties were observed and has initially been used for the treatment of infections caused by *Entamoeba histolytic*a (Killough et al., 1952). Fumagillin (**Figure 1**) and its synthetic analogs thereby irreversibly inhibit the methionine aminopeptidase-2 (MetAP2), making them promising therapeutic candidates against malaria parasites, trypanosomes, or other amoebae (Arico-Muendel et al., 2009). When using *D. discoideum* as a model, however, cytotoxic effects on the phagocytes could largely be attributed to the non-ribosomal peptide gliotoxin (Hillmann et al., 2015). The toxic and immunosuppressive properties of gliotoxin, the prototype of the epidithiodioxopiperazine (ETP)-type mycotoxins, are directed toward the host's immune effector cells *via* the activity of its unusual intramolecular disulfide bridge (**Figure 1**). Several target molecules for gliotoxin have been well described, including the NADPH oxidase of polymorphonuclear leukocytes or central regulatory hubs like the phosphatidylinositol 3,4,5-trisphosphate metabolism and the transcription factor NFκB (Pahl et al., 1996; Tsunawaki et al., 2004; Schlam et al., 2016). Among these studies, Schlam and colleagues have shown that gliotoxin further prevents integrin activation in immortalized and primary macrophages and interferes with actin dynamics. As both of these are essential instruments during phagocytosis and membrane ruffling, such pathways may be attractive targets in the defense against FLA. Previously it was thought that gliotoxin production is restricted only to clinical isolates of *A. fumigatus*; however, it was demonstrated recently that the vast majority (>96%) of both environmental and clinical isolates of aspergilli are able to produce this mycotoxin (Kupfahl et al., 2008; Scharf et al., 2012). Consequently, it is only plausible to suspect that fungi have maintained their whole repertoire of active secondary metabolites to counteract not only their numerous competitors, but also predators in their natural environment whose numbers and diversity have long been underestimated. A recent study supports this conclusion by demonstrating that mycophagous protists are abundant, taxonomically widespread, and central ecological players in the soil food web (Geisen et al., 2016).

PERSPECTIVES

Both *Dictyostelium discoideum* and *Acanthamoeba castellanii* have been extensively studied as model organisms in terms of phagocytic interactions, mainly due to the similarity with human macrophages (Tosetti et al., 2014). As unicellular eukaryotes, with a compartmentalized cytoplasm, relatively small size, and active chemotactic movement they exemplify an ideal non-mammalian model for host-pathogen interactions and microbial infections. Both amoebae are easy to cultivate (either on bacteria or axenically), giving high cell yields with defined identity. Besides, working with these model organisms is highly advantageous in terms of genetic malleability combined with a profound knowledge of its phagocytic pathways (Eichinger et al., 2005; Siddiqui and Khan, 2012). A major advantage of *D. discoideum* over *A. castellanii* is the well annotated genome, the high number of molecular tools and protocols, and the wide availability of targeted mutants that are easily accessible at www.dictybase.org (Eichinger et al., 2005; Bozzaro and Eichinger, 2011; Fey et al., 2013). However, the fact that prolonged subcultivations and axenization of native amoeba cultures may have led to the accumulation of undesired mutations and loss of original phagocytic abilities has to be taken into consideration. Another drawback of *D. discoideum* is its limited maximal survival temperature of roughly 27°C, which may be unfavorable for some fungi that may express their full virulence potential only at temperatures around 37°C. However, at present there is little support for the idea that filamentous fungi like *A. fumigatus* tend to regulate their general virulence attributes strictly in response to higher temperatures. In fact, a recent study revealed that 11 of 37 clusters encoding for the biosynthesis of secondary metabolites were activated by a temperature shift from 37 to 30°C, including those coding for DHN-melanin, gliotoxin, and trypacidin (Lind et al., 2016). Nevertheless, when using amoebae as a tool to study the origin of fungal virulence, it is important to keep in mind that throughout their evolution, fungi have also encountered many other soil-dwelling predators that may have contributed to the emergence of fungal virulence determinants. Certainly not all virulence traits are equally beneficial to protect fungi in different hosts, giving rise to a number of different invertebrate animal models which have been used to study fungal pathogenesis (Desalermos et al., 2012). Very little is known about the interaction of soil amoebae and fungi in their natural environment. It is plausible, that not every amoeba is amenable to infection by every fungal pathogen. Furthermore, bacteria are the preferential prey for *D. discoideum*, while *A. castellanii* was originally discovered as a contaminant in yeast cultures (Castellani, 1930). Even if fungal infection biologists have successfully exploited these two established amoeba models, further studies on the evolution of fungal virulence may call

for an inclusion of natural fungivorous predators from the Amoebozoa phylum.

AUTHOR CONTRIBUTIONS

SN, IF, and FH wrote the initial version of the manuscript. IF and SN prepared illustrations. FH revised the manuscript. All authors read and approved the final version.

ACKNOWLEDGMENTS

Research in the authors lab is supported by a fellowship of the DFG funded excellence graduate school "Jena School of Microbial Communication"—JSMC (to SN), a grant of the European Social Fund ESF "Europe for Thuringia" (2015 FGR 0097) and DFG grant HI 1574/2-1.

REFERENCES

Aimanianda, V., Bayry, J., Bozza, S., Kniemeyer, O., Perruccio, K., Elluru, S. R., et al. (2009). Surface hydrophobin prevents immune recognition of airborne fungal spores. *Nature* 460, 1117–1121. doi: 10.1038/nature08264

Akoumianaki, T., Kyrmizi, I., Valsecchi, I., Gresnigt, M. S., Samonis, G., Drakos, E., et al. (2016). *Aspergillus* cell wall melanin blocks LC3-associated phagocytosis to promote pathogenicity. *Cell Host Microbe* 19, 79–90. doi: 10.1016/j.chom.2015.12.002

Arico-Muendel, C., Centrella, P. A., Contonio, B. D., Morgan, B. A., O'Donovan, G., Paradise, C. L., et al. (2009). Antiparasitic activities of novel, orally available fumagillin analogs. *Bioorg. Med. Chem. Lett.* 19, 5128–5131. doi: 10.1016/j.bmcl.2009.07.029

Behnsen, J., Narang, P., Hasenberg, M., Gunzer, F., Bilitewski, U., Klippel, N., et al. (2007). Environmental dimensionality controls the interaction of phagocytes with the pathogenic fungi *Aspergillus fumigatus* and *Candida albicans*. *PLoS Pathog.* 3:e13. doi: 10.1371/journal.ppat.0030013

Bidochka, M. J., Clark, D. C., Lewis, M. W., and Keyhani, N. O. (2010). Could insect phagocytic avoidance by entomogenous fungi have evolved via selection against soil amoeboid predators? *Microbiology* 156, 2164–2171. doi: 10.1099/mic.0.038216-0

Boyce, K. J., and Andrianopoulos, A. (2015). Fungal dimorphism: the switch from hyphae to yeast is a specialized morphogenetic adaptation allowing colonization of a host. *FEMS Microbiol. Rev.* 39, 797–811. doi: 10.1093/femsre/fuv035

Bozzaro, S., and Eichinger, L. (2011). The professional phagocyte *Dictyostelium discoideum* as a model host for bacterial pathogens. *Curr. Drug Targets* 12, 942–954. doi: 10.2174/138945011795677782

Brakhage, A. A. (2005). Systemic fungal infections caused by *Aspergillus* species: epidemiology, infection process and virulence determinants. *Curr. Drug Targets* 6, 875–886. doi: 10.2174/138945005774912717

Brakhage, A. A., Bruns, S., Thywissen, A., Zipfel, P. F., and Behnsen, J. (2010). Interaction of phagocytes with filamentous fungi. *Curr. Opin. Microbiol.* 13, 409–415. doi: 10.1016/j.mib.2010.04.009

Brown, G. D., Denning, D. W., Gow, N. A. R., Levitz, S. M., Netea, M. G., and White, T. C. (2012). Hidden killers: human fungal infections. *Sci. Transl. Med.* 4:165rv113. doi: 10.1126/scitranslmed.3004404

Castellani, A. (1930). An amoeba found in culture of yeast: preliminary note. *J. Trop. Med. Hyg.* 33:160

Cateau, E., Hechard, Y., Fernandez, B., and Rodier, M. H. (2014). Free living amoebae could enhance *Fusarium oxysporum* growth. *Fungal Ecol.* 8, 12–17. doi: 10.1016/j.funeco.2013.12.006

Chai, L. Y., Netea, M. G., Sugui, J., Vonk, A. G., van de Sande, W. W., Warris, A., et al. (2010). *Aspergillus fumigatus* conidial melanin modulates host cytokine response. *Immunobiology* 215, 915–920. doi: 10.1016/j.imbio.2009.10.002

Chakraborty, S., and Old, K. M. (1986). Ultrastructure and description of a fungus-feeding amoeba, *Trichamoeba mycophaga* n. sp. (Amoebidae, Amoebea), from Australia. *J. Eukaryot. Microbiol.* 33, 564–569. doi: 10.1111/j.1550-7408.1986.tb05663.x

Chakraborty, S., Old, K. M., and Warcup, J. H. (1983). Amoebae from a take-all suppressive soil which feed on *Gaeumannomyces graminis tritici* and other soil fungi. *Soil Biol. Biochem.* 15, 17–24. doi: 10.1016/0038-0717(83)90113-X

Chrisman, C. J., Alvarez, M., and Casadevall, A. (2010). Phagocytosis of *Cryptococcus neoformans* by, and nonlytic exocytosis from *Acanthamoeba castellanii*. *Appl. Environ. Microbiol.* 76, 6056–6062. doi: 10.1128/AEM.00812-10

Derengowski Lda, S., Paes, H. C., Albuquerque, P., Tavares, A. H., Fernandes, L., Silva-Pereira, I., et al. (2013). The transcriptional response of *Cryptococcus neoformans* to ingestion by *Acanthamoeba castellanii* and macrophages provides insights into the evolutionary adaptation to the mammalian host. *Eukaryot. Cell* 12, 761–774. doi: 10.1128/EC.00073-13

Desalermos, A., Fuchs, B. B., and Mylonakis, E. (2012). Selecting an invertebrate model host for the study of fungal pathogenesis. *PLoS Pathog.* 8:e1002451. doi: 10.1371/journal.ppat.1002451

Eichinger, L., Pachebat, J. A., Glöckner, G., Rajandream, M. A., Sucgang, R., Berriman, M., et al. (2005). The genome of the social amoeba *Dictyostelium discoideum*. *Nature* 435, 43–57. doi: 10.1038/nature03481

Erken, M., Lutz, C., and McDougald, D. (2013). The rise of pathogens: predation as a factor driving the evolution of human pathogens in the environment. *Microb. Ecol.* 65, 860–868. doi: 10.1007/s00248-013-0189-0

Feldmesser, M., Kress, Y., Novikoff, P., and Casadevall, A. (2000). *Cryptococcus neoformans* is a facultative intracellular pathogen in murine pulmonary infection. *Infect. Immun.* 68, 4225–4237. doi: 10.1128/IAI.68.7.4225-4237.2000

Fey, P., Dodson, R. J., Basu, S., and Chisholm, R. L. (2013). "One stop shop for everything Dictyostelium: dictyBase and the Dicty Stock Center in 2012," in *Dictyostelium Discoideum Protocols,* eds L. Eichinger, and F. Rivero (Totowa, NJ: Humana Press), 59–92.

García-Rodas, R., and Zaragoza, O. (2012). Catch me if you can: phagocytosis and killing avoidance by *Cryptococcus neoformans*. *FEMS Immunol. Med. Microbiol.* 64, 147–161. doi: 10.1111/j.1574-695X.2011.00871.x

Gauthier, T., Wang, X., Sifuentes Dos Santos, J., Fysikopoulos, A., Tadrist, S., Canlet, C., et al. (2012). Trypacidin, a spore-borne toxin from *Aspergillus fumigatus*, is cytotoxic to lung cells. *PLoS ONE* 7:e29906. doi: 10.1371/journal.pone.0029906

Geib, E., Gressler, M., Viediernikova, I., Hillmann, F., Jacobsen, I. D., Nietzsche, S., et al. (2016). A non-canonical melanin biosynthesis pathway protects *Aspergillus terreus* conidia from environmental stress. *Cell Chem. Biol.* 23, 587–597. doi: 10.1016/j.chembiol.2016.03.014

Geisen, S., Koller, R., Hünninghaus, M., Dumack, K., Urich, T., and Bonkowski, M. (2016). The soil food web revisited: diverse and widespread mycophagous soil protists. *Soil Biol. Biochem.* 94, 10–18. doi: 10.1016/j.soilbio.2015.11.010

Hillmann, F., Novohradská, S., Mattern, D. J., Forberger, T., Heinekamp, T., Westermann, M., et al. (2015). Virulence determinants of the human pathogenic fungus *Aspergillus fumigatus* protect against soil amoeba predation. *Environ. Microbiol.* 17, 2858–2869. doi: 10.1111/1462-2920.12808

Hobson, R. P. (2000). The effects of diffusates from the spores of *Aspergillus fumigatus* and *A. terreus* on human neutrophils, *Naegleria gruberi* and *Acanthamoeba castellanii*. *Med. Mycol.* 38, 133–141. doi: 10.1080/mmy.38.2.133.141

Jahn, B., Koch, A., Schmidt, A., Wanner, G., Gehringer, H., Bhakdi, S., et al. (1997). Isolation and characterization of a pigmentless-conidium mutant of *Aspergillus fumigatus* with altered conidial surface and reduced virulence. *Infect. Immun.* 65, 5110–5117.

Jahn, B., Langfelder, K., Schneider, U., Schindel, C., and Brakhage, A. A. (2002). PKSP-dependent reduction of phagolysosome fusion and intracellular kill of *Aspergillus fumigatus* conidia by human monocyte-derived macrophages. *Cell Microbiol.* 4, 793–803. doi: 10.1046/j.1462-5822.2002.00228.x

Killough, J. H., Magill, G. B., and Smith, R. C. (1952). The treatment of amebiasis with fumagillin. *Science* 115, 71–72. doi: 10.1126/science.115.2977.71

Koller, B., Schramm, C., Siebert, S., Triebel, J., Deland, E., Pfefferkorn, A. M., et al. (2016). *Dictyostelium discoideum* as a novel host system to study

the interaction between phagocytes and yeasts. *Front. Microbiol.* 7:1665. doi: 10.3389/fmicb.2016.01665

Kupfahl, C., Michalka, A., Lass-Flörl, C., Fischer, G., Haase, G., Ruppert, T., et al. (2008). Gliotoxin production by clinical and environmental *Aspergillus fumigatus* strains. *Int. J. Med. Microbiol.* 298, 319–327. doi: 10.1016/j.ijmm.2007.04.006

Kwon-Chung, K. J., Fraser, J. A., Doering, T. L., Wang, Z., Janbon, G., Idnurm, A., et al. (2014). *Cryptococcus neoformans* and *Cryptococcus gattii*, the etiologic agents of cryptococcosis. *Cold Spring Harb. Perspect Med.* 4:a019760. doi: 10.1101/cshperspect.a019760

Lind, A. L., Smith, T. D., Saterlee, T., Calvo, A. M., and Rokas, A. (2016). Regulation of secondary metabolism by the velvet complex is temperature-responsive in *Aspergillus*. *G3(Bethesda)* 6, 4023–4033. doi: 10.1534/g3.116.033084

Luther, K., Torosantucci, A., Brakhage, A. A., Heesemann, J., and Ebel, F. (2007). Phagocytosis of *Aspergillus fumigatus* conidia by murine macrophages involves recognition by the dectin-1 beta-glucan receptor and Toll-like receptor 2. *Cell Microbiol.* 9, 368–381. doi: 10.1111/j.1462-5822.2006.00796.x

Ma, J., Becker, C., Lowell, C. A., and Underhill, D. M. (2012). Dectin-1-triggered recruitment of light chain 3 protein to phagosomes facilitates major histocompatibility complex class II presentation of fungal-derived antigens. *J. Biol. Chem.* 287, 34149–34156. doi: 10.1074/jbc.M112.382812

Maisonneuve, E., Cateau, E., Kaaki, S., and Rodier, M.-H. (2016). *Vermamoeba vermiformis-Aspergillus fumigatus* relationships and comparison with other phagocytic cells. *Parasitol. Res.* 115, 4097–4105. doi: 10.1007/s00436-016-5182-3

Mattern, D. J., Schoeler, H., Weber, J., Novohradská, S., Kraibooj, K., Dahse, H. M., et al. (2015). Identification of the antiphagocytic trypacidin gene cluster in the human-pathogenic fungus *Aspergillus fumigatus*. *Appl. Microbiol. Biotechnol.* 99, 10151–10161. doi: 10.1007/s00253-015-6898-1

Old, K. M., Chakraborty, S., and Gibbs, R. (1985). Fine structure of a new mycophagous amoeba and its feeding on *Cochliobolus sativus*. *Soil Biol. Biochem.* 17, 645–655. doi: 10.1016/0038-0717(85)90042-2

Old, K. M., and Darbyshire, J. F. (1978). Soil fungi as food for giant amoebae. *Soil Biol. Biochem.* 10, 93–100. doi: 10.1016/0038-0717(78)90077-9

Olive, L. S., and Stoianovitch, C. (1960). Two new members of the Acrasiales. *Bull. Torr. Botan. Club.* 87, 1–20. doi: 10.2307/2483057

Pahl, H. L., Krauss, B., Schulze-Osthoff, K., Decker, T., Traenckner, E. B., Vogt, M., et al. (1996). The immunosuppressive fungal metabolite gliotoxin specifically inhibits transcription factor NF-kappaB. *J. Exp. Med.* 183, 1829–1840. doi: 10.1084/jem.183.4.1829

Philippe, B., Ibrahim-Granet, O., Prévost, M. C., Gougerot-Pocidalo, M. A., Sanchez Perez, M., Van der Meeren, A., et al. (2003). Killing of *Aspergillus fumigatus* by alveolar macrophages is mediated by reactive oxidant intermediates. *Infect. Immun.* 71, 3034–3042. doi: 10.1128/IAI.71.6.3034-3042.2003

Rizzo, J., Albuquerque, P. C., Wolf, J. M., Nascimento, R., Pereira, M. D., Nosanchuk, J. D., et al. (2017). Analysis of multiple components involved in the interaction between *Cryptococcus neoformans* and *Acanthamoeba castellanii*. *Fungal Biol.* 121, 602–614. doi: 10.1016/j.funbio.2017.04.002

Rohlfs, M., Albert, M., Keller, N. P., and Kempken, F. (2007). Secondary chemicals protect mould from fungivory. *Biol. Lett.* 3, 523–525. doi: 10.1098/rsbl.2007.0338

Scharf, D. H., Heinekamp, T., Remme, N., Hortschansky, P., Brakhage, A. A., and Hertweck, C. (2012). Biosynthesis and function of gliotoxin in *Aspergillus fumigatus*. *Appl. Microbiol. Biotechnol.* 93, 467–472. doi: 10.1007/s00253-011-3689-1

Schlam, D., Canton, J., Carreño, M., Kopinski, H., Freeman, S. A., Grinstein, S., et al. (2016). Gliotoxin suppresses macrophage immune function by subverting phosphatidylinositol 3,4,5-trisphosphate homeostasis. *MBio* 7, 02242-15. doi: 10.1128/mBio.02242-15

Schrettl, M., Ibrahim-Granet, O., Droin, S., Huerre, M., Latgé, J.-P., and Haas, H. (2010). The crucial role of the *Aspergillus fumigatus* siderophore system in interaction with alveolar macrophages. *Microb. Infect.* 12, 1035–1041. doi: 10.1016/j.micinf.2010.07.005

Seyedmousavi, S., Guillot, J., Arné, P., de Hoog, G. S., Mouton, J. W., Melchers, W. J., et al. (2015). *Aspergillus* and aspergilloses in wild and domestic animals: a global health concern with parallels to human disease. *Med. Mycol.* 53, 765–797. doi: 10.1093/mmy/myv067

Shah, A., Kannambath, S., Herbst, S., Rogers, A., Soresi, S., Carby, M., et al. (2016). Calcineurin orchestrates lateral transfer of *Aspergillus fumigatus* during macrophage cell death. *Am. J. Respir. Crit. Care Med.* 194, 1127–1139. doi: 10.1164/rccm.201601-0070OC

Shelton, B. G., Kirkland, K. H., Flanders, W. D., and Morris, G. K. (2002). Profiles of airborne fungi in buildings and outdoor environments in the United States. *Appl. Environ. Microbiol.* 68, 1743–1753. doi: 10.1128/AEM.68.4.1743-1753.2002

Siddiqui, R., and Khan, N. A. (2012). Biology and pathogenesis of *Acanthamoeba*. *Parasit. Vectors* 5:6. doi: 10.1186/1756-3305-5-6

Slesiona, S., Gressler, M., Mihlan, M., Zaehle, C., Schaller, M., Barz, D., et al. (2012). Persistence versus escape: *Aspergillus terreus* and *Aspergillus fumigatus* employ different strategies during interactions with macrophages. *PLoS ONE* 7:e31223. doi: 10.1371/journal.pone.0031223

Slight, J., Nicholson, W. J., Mitchell, C. G., Pouilly, N., Beswick, P. H., Seaton, A., et al. (1996). Inhibition of the alveolar macrophage oxidative burst by a diffusible component from the surface of the spores of the fungus *Aspergillus fumigatus*. *Thorax* 51, 389–396. doi: 10.1136/thx0.51.4.389

Spiegel, F. W., Shadwick, J. D., and Hemmes, D. E. (2006). A new ballistosporous species of Protostelium. *Mycologia* 98, 144–148 doi: 10.1080/15572536.2006.11832721

Steenbergen, J. N., Nosanchuk, J. D., Malliaris, S. D., and Casadevall, A. (2003). *Cryptococcus neoformans* virulence in enhanced after growth in the genetically malleable host *Dictyostelium discoideum*. *Infect Immun.* 9, 4862–4872. doi: 10.1128/IAI.71.9.4862-4872.2003

Steenbergen, J. N., Nosanchuk, J. D., Malliaris, S. D., and Casadevall, A. (2004). Interaction of *Blastomyces dermatitidis, Sporothrix schenckii,* and *Histoplasma capsulatum* with *Acanthamoeba castellanii*. *Infect. Immun.* 72, 3478–3488. doi: 10.1128/IAI.72.6.3478-3488.2004

Steenbergen, J. N., Shuman, H. A., and Casadevall, A. (2001). *Cryptococcus neoformans* interactions with amoebae suggest an explanation for its virulence and intracellular pathogenic strategy in macrophages. *Proc. Natl. Acad. Sci. U.S.A.* 98, 15245–15250. doi: 10.1073/pnas.261418798

Thywißen, A., Heinekamp, T., Dahse, H. M., Schmaler-Ripcke, J., Nietzsche, S., Zipfel, P. F., et al. (2011). Conidial dihydroxynaphthalene melanin of the human pathogenic fungus *Aspergillus fumigatus* interferes with the host endocytosis pathway. *Front. Microbiol.* 2:96. doi: 10.3389/fmicb.2011.00096

Tosetti, N., Croxatto, A., and Greub, G. (2014). Amoebae as a tool to isolate new bacterial species, to discover new virulence factors and to study the host-pathogen interactions. *Microb. Pathog.* 77, 125–130. doi: 10.1016/j.micpath.2014.07.009

Tsai, H. F., Chang, Y. C., Washburn, R. G., Wheeler, M. H., and Kwon-Chung, K. J. (1998). The developmentally regulated alb1 gene of *Aspergillus fumigatus*: its role in modulation of conidial morphology and virulence. *J. Bacteriol.* 180, 3031–3038.

Tsunawaki, S., Yoshida, L. S., Nishida, S., Kobayashi, T., and Shimoyama, T. (2004). Fungal metabolite gliotoxin inhibits assembly of the human respiratory burst NADPH oxidase. *Infect. Immun.* 72, 3373–3382. doi: 10.1128/IAI.72.6.3373-3382.2004

Van Waeyenberghe, L., Bare, J., Pasmans, F., Claeys, M., Bert, W., Haesebrouck, F., et al. (2013). Interaction of *Aspergillus fumigatus* conidia with *Acanthamoeba castellanii* parallels macrophage-fungus interactions. *Environ. Microbiol. Rep.* 5, 819–824. doi: 10.1111/1758-2229.12082

Volling, K., Thywissen, A., Brakhage, A. A., and Saluz, H. P. (2011). Phagocytosis of melanized *Aspergillus* conidia by macrophages exerts cytoprotective effects by sustained PI3K/Akt signalling. *Cell Microbiol.* 13, 1130–1148. doi: 10.1111/j.1462-5822.2011.01605.x

Conflict of Interest Statement: The authors declare that the research was conducted in the absence of any commercial or financial relationships that could be construed as a potential conflict of interest.

frontiers in Cellular and Infection Microbiology

ORIGINAL RESEARCH
published: 09 April 2018
doi: 10.3389/fcimb.2018.00108

Cryptococcus neoformans Escape From *Dictyostelium* Amoeba by Both WASH-Mediated Constitutive Exocytosis and Vomocytosis

Rhys A. Watkins[1,2†], *Alexandre Andrews*[1,2†], *Charlotte Wynn*[1,2], *Caroline Barisch*[3], *Jason S. King*[1,4*] *and Simon A. Johnston*[1,2*]

[1] Bateson Centre, University of Sheffield, Sheffield, United Kingdom, [2] Department of Infection Immunity and Cardiovascular Disease, Medical School, University of Sheffield, Sheffield, United Kingdom, [3] Department of Biochemistry, Faculty of Science, University of Geneva, Geneva, Switzerland, [4] Department of Biomedical Sciences, University of Sheffield, Sheffield, United Kingdom

Cryptococcus neoformans is an environmental yeast that can cause opportunistic infections in humans. As infecting animals does not form part of its normal life-cycle, it has been proposed that the virulence traits that allow cryptococci to resist immune cells were selected through interactions with environmental phagocytes such as amoebae. Here, we investigate the interactions between *C. neoformans* and the social amoeba *Dictyostelium discoideum*. We show that like macrophages, *D. discoideum* is unable to kill *C. neoformans* upon phagocytosis. Despite this, we find that the yeast pass through the amoebae with an apparently normal phagocytic transit and are released alive by constitutive exocytosis after ~80 min. This is the canonical pathway in amoebae, used to dispose of indigestible material after nutrient extraction. Surprisingly however, we show that upon either genetic or pharmacological blockage of constitutive exocytosis, *C. neoformans* still escape from *D. discoideum* by a secondary mechanism. We demonstrate that constitutive exocytosis-independent egress is stochastic and actin-independent. This strongly resembles the non-lytic release of cryptococci by vomocytosis from macrophages, which do not perform constitutive exocytosis and normally retain phagocytosed material. Our data indicate that vomocytosis is functionally redundant for escape from amoebae, which thus may not be the primary driver for its evolutionary selection. Nonetheless, we show that vomocytosis of *C. neoformans* is mechanistically conserved in hosts ranging from amoebae to man, providing new avenues to understand this poorly-understood but important virulence mechanism.

Keywords: cryptococcus, *Dictyostelium*, amoeba, pathogen, exocytosis, cryptococcosis, vomocytosis, WASH

OPEN ACCESS

Edited by:
Sascha Thewes,
Freie Universität Berlin, Germany

Reviewed by:
Charley Christian Staats,
Federal University of Rio Grande do Sul (UFRGS), Brazil
Sascha Brunke,
Leibniz-Institut für Naturstoff-Forschung und Infektionsbiologie and Hans Knöll Institut, Germany

***Correspondence:**
Jason S. King
jason.king@sheffield.ac.uk
Simon A. Johnston
s.a.johnston@sheffield.ac.uk

† These authors have contributed equally to this work.

Received: *24 November 2017*
Accepted: *19 March 2018*
Published: *09 April 2018*

Citation:
Watkins RA, Andrews A, Wynn C, Barisch C, King JS and Johnston SA (2018) Cryptococcus neoformans Escape From Dictyostelium Amoeba by Both WASH-Mediated Constitutive Exocytosis and Vomocytosis. Front. Cell. Infect. Microbiol. 8:108. doi: 10.3389/fcimb.2018.00108

INTRODUCTION

Cryptococcus neoformans is a basidiomycete yeast found globally in a wide variety of natural environments. Unusually for an environmental yeast, *C. neoformans* is also a pathogen of animals. Most significant is the fatal infection of the severely immunocompromised, with cryptococcal meningitis caused by *C. neoformans* responsible for 15% of AIDS-related deaths (Rajasingham et al., 2017). The interaction of *C. neoformans* with its host is highly complex, and what differentiates normal immunity from the development of life

threatening cryptococcal meningitis is well defined (Tenforde et al., 2017).

Macrophages have been repeatedly demonstrated to be critical for protection against *C. neoformans* infection. However, macrophages may also have a role in pathogenesis in the immunocompromised as cryptococci are able to grow and survive within macrophages and may use macrophages as a Trojan horse to disseminate from the lung. *In vitro*, almost every aspect of macrophage antimicrobial activity is either avoided or manipulated by *C. neoformans*, which are able to survive and replicate intracellularly, following uptake by phagocytosis (Johnston and May, 2013; Ballou and Johnston, 2017). Survival traits include the generation of a characteristic polysaccharide capsule, which is both anti-phagocytic and helps protect the yeast from the host antimicrobial machinery if it is engulfed, as well as melanin production which serves as a potent antioxidant—protecting the yeast from the phagosomal oxidative attack and the immunomodulatory activity of cell wall chitin (Casadevall et al., 2000; Nosanchuk and Casadevall, 2006; Wiesner et al., 2015).

An additional pathogenic mechanism is the remarkable ability of *C. neoformans* to promote its non-lytic expulsion from host cells in a process known as vomocytosis (Alvarez and Casadevall, 2006; Ma et al., 2006). This enables the yeast to escape whilst leaving the host phagocyte intact, thus preventing immune stimulation and promoting dissemination. Whilst it has been shown that vomocytosis is suppressed by host actin polymerization (Johnston and May, 2010) and can be modulated by host Annexin A2 and Mitogen Activated Protein kinase (ERK5) activity (Stukes et al., 2016; Gilbert et al., 2017) little is known of the underlying molecular mechanisms underlying expulsion. Nonetheless, vomocytosis has been observed in both cell culture and *in vivo* models and is thought to significantly contribute to *C. neoformans* virulence (Alvarez and Casadevall, 2006; Ma et al., 2006; Bojarczuk et al., 2016; Johnston et al., 2016; Gilbert et al., 2017).

As with other opportunistic pathogens, it is unlikely that interactions with mammalian macrophages have been the evolutionary drivers of *C. neoformans* virulence. Cryptococci are free-living fungi with a life cycle that is not dependent on infecting an animal host. It has therefore been proposed that the mechanisms that allow *C. neoformans* to survive and grow in macrophages have primarily evolved to avoid predation by phagocytes in its natural environment, such as amoebae (Steenbergen et al., 2001; Casadevall, 2012; Watkins et al., 2017).

Like leukocytes, amoebae are professional phagocytes, using their chemotactic and phagocytic abilities to capture and kill environmental microbes for food. Despite the large evolutionary distance between them, much of the machinery and mechanisms for phagocytosis and phagosome maturation are highly conserved between amoebae and mammalian immune cells (Boulais et al., 2010). Traits that have evolved to help yeast and bacteria avoid being killed by amoebae in the environment are therefore likely to have similar effects when they encounter mammalian immune cells.

Previous studies have demonstrated similarities in the interactions between *C. neoformans* with amoebae and macrophages. *C. neoformans* is able to both survive phagocytosis and replicate intracellularly within *Acanthamoeba castellanii,* ultimately being released alive without causing lysis of the host amoeba (Steenbergen et al., 2001; Chrisman et al., 2010). Due to its amenability to genetic manipulation, the social amoeba *Dictyostelium discoideum* has been used a model host for a number of human pathogens and is also susceptible to *C. neoformans* infection (Steenbergen et al., 2003). Importantly, passage through *D. discoideum* caused a stimulation in *C. neoformans* capsule expansion and melanization together with a corresponding increase in subsequent virulence in mice (Steenbergen et al., 2003). Interactions with amoebae can therefore directly influence interactions between *C. neoformans* and mammalian immune cells.

The fate of internalized material in animal cells is variable and complex. There are examples of the expulsion of internalized material from a variety of cell types, particularly in the context of antigen presentation (Chen and Jondal, 2004; Peters et al., 2006; Griffiths et al., 2012; Le Roux et al., 2012; Turner et al., 2016). However, animal macrophages (notably tissue resident cells, such as alveolar macrophage) have the ability to retain particulate matter that may otherwise be damaging (Bai et al., 2015). In contrast, the constitutive exocytosis of phagocytosed material by amoeba has been demonstrated in diverse species including *D. discoideum, Amoeba proteus, Entamoeba histolytica* and *A. castellanii* (Weisman and Korn, 1967; Ravdin et al., 1988; Christofidou-Solomidou and Stockem, 1992; Clarke et al., 2010) and thus appears to be a necessary and general feature of free-living amoebae. Therefore macrophages and amoebae differ in their retention of phagocytosed material.

Recently it was shown that constitutive exocytosis in *D. discoideum* is dependent on the activity of the WASH (WASP And SCAR Homolog) complex (Carnell et al., 2011). WASH is a direct activator of the ARP2/3 (Actin Related Protein 2/3) complex, causing the polymerization of actin on the surface of vesicles and driving membrane protein sorting and recycling (Derivery et al., 2009; Gomez and Billadeau, 2009; Zech et al., 2011; Seaman et al., 2013). Whilst an early phase of WASH activity drives the retrieval of cell surface proteins from phagosomes (Buckley et al., 2016), a second phase of activity occurs after 40–60 min of digestion, driving the removal of the vacuolar (V)-ATPase and phagosomal neutralization. This facilitates hydrolase retrieval (King et al., 2013) and is a prerequisite for exocytosis. Consequently *D. discoideum* cells lacking WASH have a complete block in constitutive exocytosis (Carnell et al., 2011).

As constitutive exocytosis represents the normal mechanism of non-lytic release of phagosomal contents, we hypothesized that this may be involved in the escape of live *C. neoformans* from amoebae. We show that *C. neoformans* survive phagocytosis by *D. discoideum*, but follow an apparently normal phagosomal transit and are normally released alive by WASH-dependent constitutive exocytosis. However, when constitutive exocytosis is blocked, *C. neoformans* still escape in a WASH and actin-independent manner reminiscent of vomocytosis. This

demonstrates redundant, mechanistically different egress mechanisms with implications for the understanding of the evolutionary drivers of cryptococcal virulence.

MATERIALS AND METHODS

Strains and Cell Culture

For all experiments the Ax2 axenic strain of *D. discoideum* was used, both as "wild type" as well as the parental of the previously published *WASH*-mutant strain (Carnell et al., 2011). *D. discoideum* were cultured in filter-sterilized HL-5 medium (Formedium, Norfolk, UK) at 22°C. Cells expressing GFP fused to the vatM subunit of the vacuolar-ATPase were generated using plasmid pMJC25 (Carnell et al., 2011).

Unless otherwise stated, *C. neoformans* var. grubii (serotype A) strain H99α stably expressing mCherry was used (Gibson et al., in review). The previously published *plb1* and *cap59* mutants were generated from the alternative wild-type parent H99, which was used as control when appropriate (Chen et al., 2000; Voelz et al., 2010). *C. neoformans* were grown in YPD medium at 28°C prior to experiments, but washed and resuspended in HL5 medium before infecting *D. discoideum*. *C. neoformans* were heat-killed by incubation at 65°C for 30 min, before washing in PBS. UV-killing was performed by exposure of *C. neoformans* cultures to 4 J of UV using a UVIlink CL-5087 cross-linker illuminator. Killing was always confirmed by plating samples on YPD agar to check absence of growth.

Infections and Microscopy

Prior to imaging, 2×10^6 *D. discoideum* cells were seeded in 2 ml HL5 medium in glass-bottom 35 mm dishes (Mat-Tek), left to adhere for 30 min. Then 2×10^5 *C. neoformans* cells, 4.5 μm green fluorescent YG unmodified beads (Polysciences Inc., Pennsylvania, USA), or TRITC-labeled heat killed *S. cerevisiae* (kind gift from Thierry Soldati; University of Geneva) were added prior to imaging. This differed for latrunculin treatment experiments: amoebae were mixed with yeast at a ratio of 1:1 and left for 1 h for phagocytosis to occur before addition of 5 μm Latrunculin A (Cayman chemical Co.).

Long term time-lapse movies were recorded using a Nikon TI- E with a CFI Plan Apochromat λ 20x N.A.0.75 at 22°C. Images were captured on a large-format Andor Neo 5.5 s CMOS camera for 12 h, imaging 4 fields of view every 30 s. Transit times were determined as the time from phagocytosis to release. Events where cells could not be tracked for a minimum of 500 min post-phagocytosis were excluded from the analysis.

Spinning disc microscopy was performed on a Perkin-Elmer Ultraview VoX spinning disk confocal microscope running on an Olympus 1 × 81 body with an UplanSApo 60x oil immersion objective (NA 1.4). Images were captured on a Hamamatsu C9100-50 EM-CCD camera.

Statistical Analysis

Mann Whitney test was used to test significance between continuous data and Fisher's exact test for categorical data. *P*-values below 0.05 (with modification for multiplicity of testing) were considered statistically significant. All statistical tests were performed with GraphPad Prism version 7.

RESULTS

Cryptococcus neoformans Is Constitutively Exocytosed by Amoebae

To determine whether *C. neoformans* utilizes a pathogen-specific mechanism of release or follows the normal phagocytic pathway of engulfment and constitutive exocytosis in amoeba we first compared the transit of *C. neoformans* with that of inert particles.

Using time lapse microscopy, we followed the phagocytosis and release of *C. neoformans* compared to heat killed non-pathogenic yeast *Saccharomyces cerevisiae* and 4.0 μm latex beads by *D. discoideum*. All three cargoes were of a similar size (between 3 and 5 μm) and all were exocytosed from amoebae (**Figures 1A–C**). However, unlike the vomocytosis of *C. neoformans* from macrophages which happens stochastically and inefficiently over a period of many hours (Ma et al., 2006; Johnston and May, 2010), 100% of phagosomes fused with the plasma membrane, exocytosing their contents within 4 h of engulfment in all cases.

Surprisingly, whilst we attempted to use killed *C. neoformans* as controls, both heat- or UV-killing of the yeast reduced phagocytosis by *D. discoideum* by 90% (**Figure 1H**). This effect was further compounded in *WASH*-null amoebae, in which phagocytosis of UV-killed *C. neoformans* was never observed in 3 independent experiments, consistent with previous reports of phagocytosis defects in these mutants due to reduced surface levels of phagocytic receptors (Buckley et al., 2016). The reason why killed *C. neoformans* resist phagocytosis is unclear, but it was not possible to observe sufficient events for analysis and therefore heat-killed *S. cerevisiae* were used as non-pathogenic controls in subsequent experiments.

From the time-lapse movies, we were able to define precise transit times for phagosomes containing the different cargoes, tracking individual particles from engulfment to release (**Figures 1D–F**). Comparison of the transit time demonstrated that both fungal cells took slightly longer to complete the phagocytic cycle than latex beads however, there was no significant difference between heat killed *S. cerevisiae* and *C. neoformans* (median transit time latex beads = 61 min, heat killed *S. cerevisiae* = 82 min and *C. neoformans* = 84 min, **Figure 1G**). Importantly the *C. neoformans* were able to resist killing by the amoebae and were exocytosed alive, as indicated by subsequent budding and dividing after egress consistent with previous studies (Steenbergen et al., 2003). Therefore, despite their ability to survive phagocytosis by *D. discoideum*, transit time of *C. neoformans* is indistinguishable from normal constitutive exocytosis.

The V-ATPase Is Rapidly Recruited to Phagosomes Containing *C. neoformans* and Removed Prior to Exocytosis

Unlike the vomocytosis of cryptococci, a number of molecular requirements for constitutive exocytosis in amoebae have

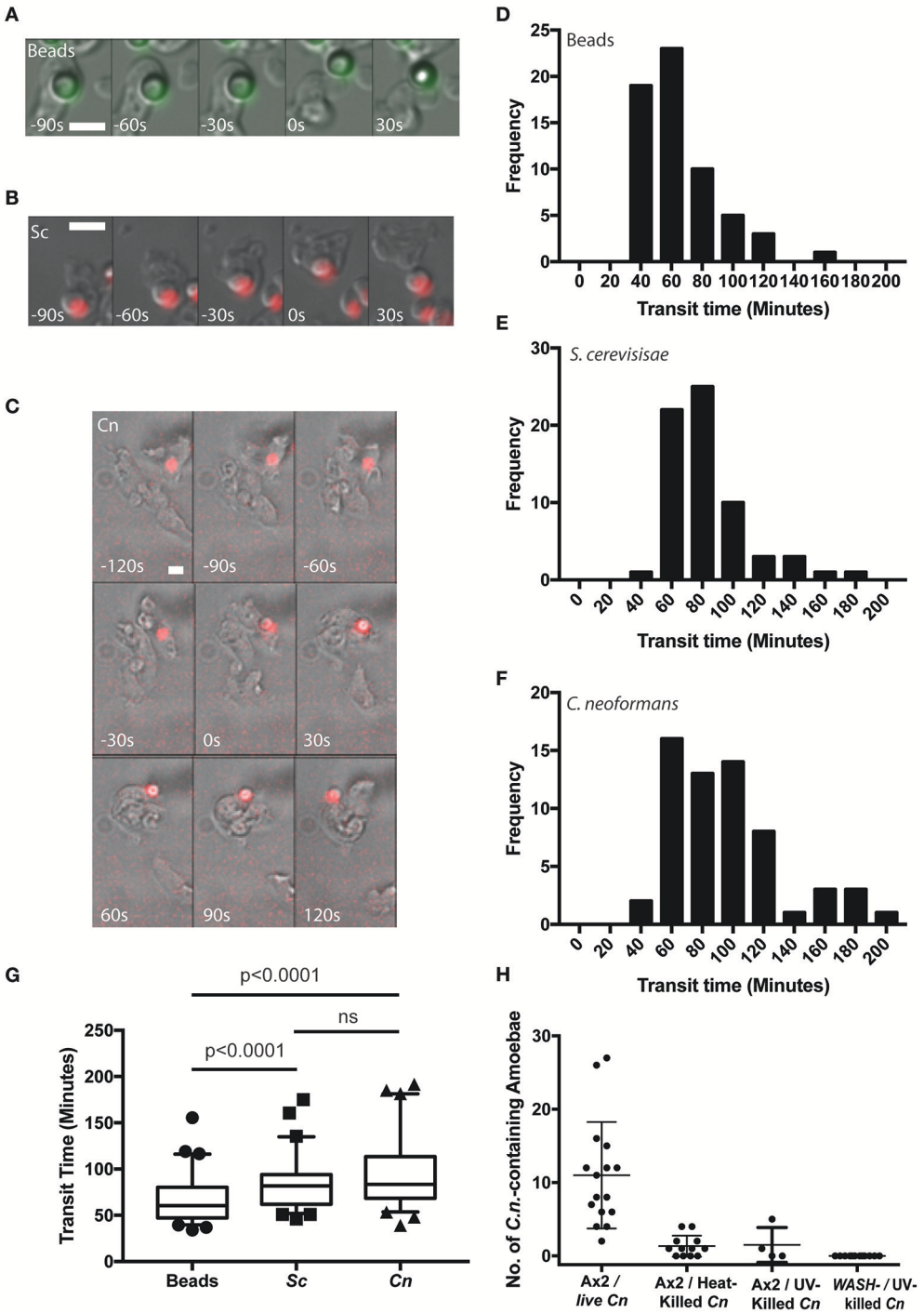

FIGURE 1 | *Cryptococcus neoformans* is constitutively exocytosed from *Dictyostelium discoideum* amoeba. **(A–C)** Example exocytosis of **(A)** 4.5 um green fluorescent latex beads (images start at 40 min after phagocytosis) **(B)** heat killed *Saccharomyces cerevisiae* (images start at 60 min after phagocytosis) and **(C)** *C. neoformans* strain Kn99mCherry from wild type *D. discoideum* strain Ax2 (images start at 60 min after phagocytosis). Time 0 s indicates point of exocytosis. Scale bars 5 μm. **(D–F)** Frequency histograms of combined transit times measured from three independent 12 h time lapses. **(D)** Latex beads 126 transit times. **(E)** Heat killed *S. cerevisiae* 66 transit times. **(F)** *C. neoformans* 57 transit times. **(G)** Comparison of transit times for latex beads, heat killed *S. cerevisiae* and *C. neoformans*. **(H)** Quantification of phagocytic events for live, heat killed and UV killed cryptococci in Ax2 and WASH null cells. *P*-values are Mann-Whitney test.

been identified. We therefore next asked whether passage of *C. neoformans* through *D. discoideum* followed the normal path of maturation and constitutive exocytosis.

During normal transit, phagosomes rapidly accumulate the V-ATPase and acidify within 2–3 min of engulfment; the V-ATPase is subsequently retained for ∼45 min to allow digestion before retrieval and phagolysosomal neutralization prior to constitutive exocytosis (Clarke et al., 2002, 2010). Using cells expressing GFP-fused to the VatM subunit of the V-ATPase, we monitored recruitment to phagosomes following engulfment of cryptococci. V-ATPase was present, on average, within 114 ± 44 s (**Figure 2A**, S.D., $n = 6$) of phagocytosis consistent with published data for inert phagosomes (Clarke et al., 2002; Buckley et al., 2016). To test if V-ATPase recruitment was maintained, we also measured the proportion of *C. neoformans*-containing phagosomes positive for GFP-VatM after 20 min incubation of cryptococci with amoebae—before any post-lysosomal transitions should have occurred (**Figure 1F**). V-ATPase was clearly visible on 90.0% of phagosomes (68/76 from three independent experiments). However, when we looked after 1 h, we were able to observe recycling of the V-ATPase from live (budding) *C. neoformans*-containing phagosomes prior to exocytosis (**Figure 2B**). Both phagosomal transit time and V-ATPase dynamics are therefore unaffected by pathogenic *C. neoformans* indicating that the normal mode of release is through canonical constitutive exocytosis.

C. neoformans Can Escape From Amoebae by Both WASH-Dependent and -Independent Mechanisms

To test the hypothesis that Cryptococci-containing phagosomes are normally expelled through the constitutive exocytosis pathway, we investigated exocytosis in *WASH*-null cells. In *D. discoideum,* WASH is essential for V-ATPase recycling and constitutive exocytosis, allowing us to specifically genetically ablate this pathway (Carnell et al., 2011).

In agreement with previous studies we found that phagosomes containing heat killed *S. cerevisiae* were never released from *WASH*-null amoebae within our 12 h period of observation (**Figure 3A**). In contrast, phagosomes containing *C. neoformans* were still exocytosed but with significantly altered dynamics (**Figure 3B**). Whilst >90% of *C. neoformans*-containing phagosomes are exocytosed within 2 h in wild type amoebae (**Figure 1F**), release from *WASH*-null cells was much more variable with between 20 and 60% escaping over 12 h (**Figure 3C**). Cryptococcus-containing phagosome transit was much slower through *WASH*-null cells with very little overlap with the exocytosis from wild-type amoebae (ca. **Figures 1F**, **3C**) and was much less synchronous, appearing to occur stochastically any time from 3 to >10 h (**Figure 3D**). Notably, both this variation and timing is comparable to that reported for vomocytosis of cryptococci from animal cells (Johnston and May, 2010).

The actin cytoskeleton is a negative regulator of vomocytosis in mammals, but essential for constitutive phagosome exocytosis in *D. discoideum* (Ma et al., 2006; Carnell et al., 2011). Therefore, we predicted that inhibition of actin polymerization would copy the phenotype of *WASH*-null *Dictyostelium* for both heat killed *S. cerevisiae* and *C. neoformans* containing phagosomes. When we measured the percentage exocytosis of heat killed *S. cerevisiae* containing phagosomes we found that while 100% of phagosomes were exocytosed by untreated amoebae we only observed a single exocytosis event out of 90 phagosomes analyzed over 12 h when actin polymerization was blocked by latrunculin A treatment after phagocytosis (**Figure 3E**). In contrast, ∼20% of *C. neoformans*-containing phagosomes in latrunculin A-treated amoebae were released over the same period (**Figure 3F**). Transit times were again significantly longer than with untreated amoebae, and were indistinguishable to the phenotype observed with *WASH*-null amoebae (**Figure 3G**). Thus, whilst cryptococci are normally released by constitutive exocytosis from *D. discoideum,* they can also escape by a mechanistically different route upon either pharmacological or genetic blockade of the constitutive pathway, highly reminiscent of vomocytosis.

C. neoformans Mutants *cap59* and *plb1* Do Not Exhibit Defects in Vomocytosis in Amoebae

We next tested whether cryptococcal virulence factors that affect vomocytosis from mammalian cells play conserved roles in egress from *D. discoideum*. *C. neoformans* mutants with defects in polysaccharide capsule formation or deletion of the phospholipase PLB1 both exhibit reduced rates of vomocytosis and pathogenicity in animal cells (Cox et al., 2001; Noverr et al., 2003; Chayakulkeeree et al., 2011; Evans et al., 2015). However, when we measured the rates of release of acapsular *cap59* and *plb1* mutant strains from wild-type *D. discoideum* we found that release of both mutants was unaffected: there were no significant differences in either frequency or transit time compared to the parental *C. neoformans* strain (H99) both with and without blockage of the constitutive pathway with latrunculin A (**Figures 4A,B**). This was an intriguing finding, suggesting differences in the signaling pathways to vomocytosis between amoebae and macrophages but a conservation of molecular mechanism.

In the Absence of Constitutive Exocytosis *C. neoformans* Can Persist and Grow Intracellularly

Constitutive exocytosis of indigestible phagosomal material is critical for organisms that rely on phagocytosis for nutrition. Furthermore, amoebae may ingest microbes such as cryptococci that are able to actively resist phagosomal killing. Therefore, we investigated if, in the absence of constitutive exocytosis, cryptococci posed a greater threat to amoebae.

We observed no cell lysis of either wild-type or *WASH*-null cells infected with *C. neoformans* as indicated by the continued motility of the amoebae throughout the phagocytic cycle and after fungi egress. Low levels of amoeba lysis were observed upon latrunculin A treatment, most likely due to the severe effects of complete actin depolymerization. Killing and digestion

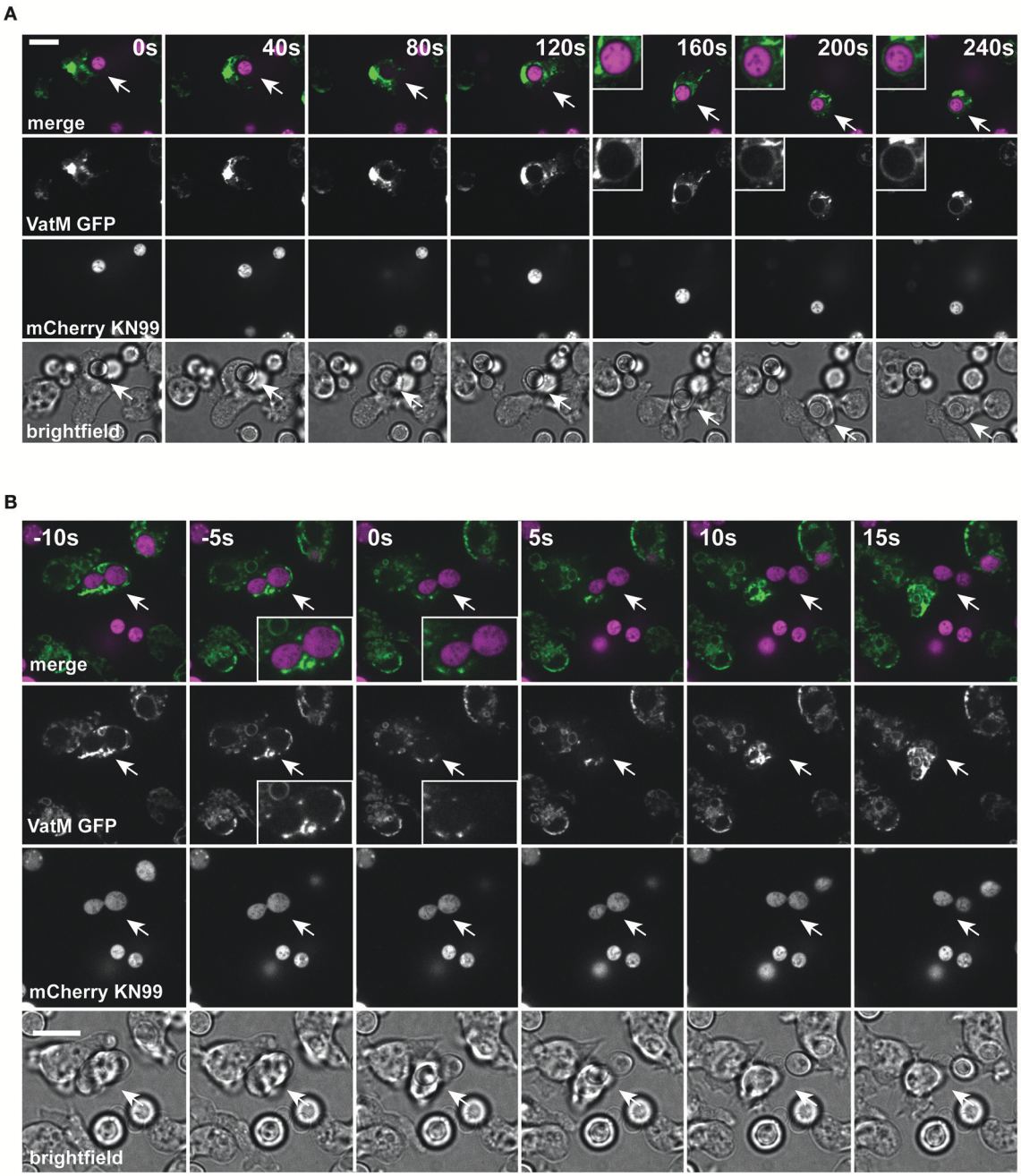

FIGURE 2 | Phagosomes containing *Cryptococcus neoformans* acquire V-ATPase following phagocytosis that is lost prior to exocytosis. **(A)** Confocal time lapse microscopy of *C. neoformans* phagocytosis by wild type *D. discoideum* strain Ax2. Representative time lapse from three independent experiments. Images were captured every 10 s. VatM is a subunit of the *D. discoideum* V-ATPase complex. Arrow indicates phagocytosed cryptococcal cell. Inset box is a magnification of phagosome containing cryptococcal cell demonstrating acquisition of V-ATPase. **(B)** Confocal time lapse microscopy of *C. neoformans* exocytosis by wild type *D. discoideum* strain Ax2. Representative time lapse from three independent experiments. Images were captured every 5 s. Arrow indicates exocytosed cryptococcal cell. Inset box is a magnification of exocytosed cryptococcal cell demonstrating absence of V-ATPase prior to exocytosis. Scale bars 10 μm.

of yeast is indicated by the transformation of the phagosome to a granular and irregular shape, whereas growth can be inferred from yeast budding. When constitutive exocytosis was blocked with latrunculin A on average, more than 80% of cryptococci persisted within *Dictyostelium* phagosomes without signs of death and digestion, with 13% actively budding over the 12 h of the experiment (**Figures 5A,B**). In this respect the *plb1* mutant behaved similarly to wild type cryptococci. The acapsular strain *cap59* was phagocytosed twice as efficiently as the wild type cryptococcus strain (11 internalized *cap59* cryptococci per 100

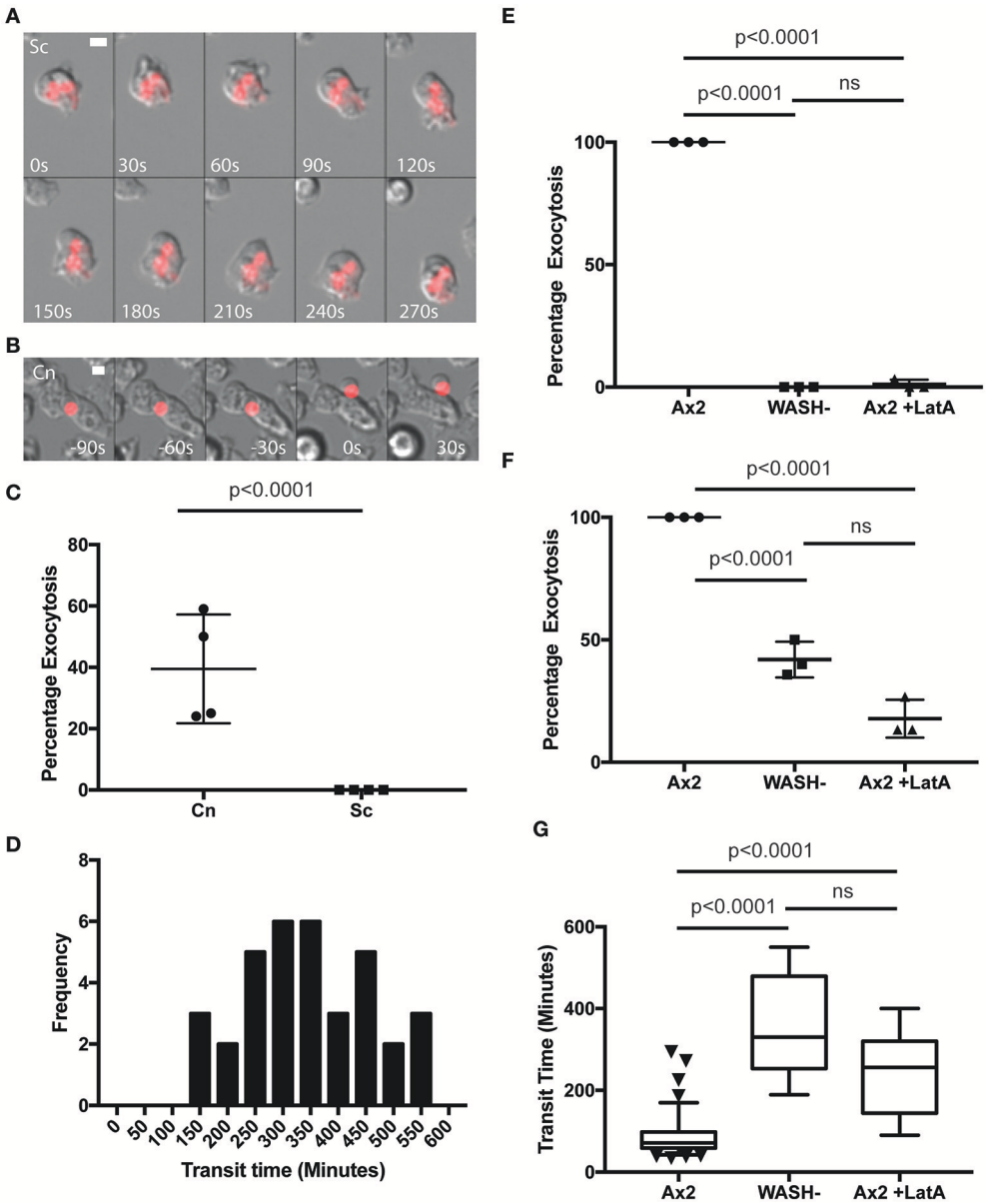

FIGURE 3 | Exocytosis of *Cryptococcus neoformans* from *Dictyostelium* is dependent on WASH and the actin cytoskeleton. **(A)** Heat killed *S. cerevisiae* are not exocytosed from WASH null *D. discoideum*. Example from 12 h time lapse imaging of heat killed *S. cerevisiae* in WASH null *D. discoideum* representative of 60 phagosomes containing heat killed *S. cerevisiae* from three independent experiments (images start at 500 min after phagocytosis). **(B)** *C. neoformans* are exocytosed from WASH null *D. discoideum*. Example from 12 h time lapse imaging representative of 62 phagosomes containing *C. neoformans* from three independent experiments (images start at 200 min after phagocytosis). Scale bars 5 μm. **(C)** Quantification of the percentage of exocytosis of *C. neoformans* and heat killed *S. cerevisiae* from WASH null *D. discoideum* from three independent 12 h time lapses. **(D)** Frequency histogram of combined 35 transit times measured from three independent 12 h time lapses. **(E)** Exocytosis of heat killed *S. cerevisiae* from wild type Ax2 but not WASH null or latrunculin A treated Ax2 *D. discoideum.* Quantification of the percentage of exocytosis from three independent 12 h time lapses. Total of 60 phagosomes were analyzed from each condition. *P*-values are Fishers test. **(F)** Exocytosis of *C. neoformans* from wild type Ax2, WASH null, and latrunculin A treated *D. discoideum.* Quantification of the percentage of exocytosis from three independent 12 h time lapses. Total of 60 phagosomes were analyzed from each condition. *P*-values are Fishers test. **(G)** Transit times of *C. neoformans* through WASH null and latrunculin A treated Ax2 *D. discoideum* are not significantly different. *P*-values are Mann-Whitney test.

amoeba vs. 5.3 cryptococci per 100 amoeba, 300 amoeba analyzed from three independent experiments). However, the acapsular *cap59* strain appeared to be growth-arrested within *D. discoideum* phagosomes, as budding was never observed (0/90 phagosomes, $P = 0.0011$ compared to H99, Fishers test; **Figure 5B**). Whilst this is consistent with other studies (Feldmesser et al., 2000; Steenbergen et al., 2001) surprisingly, we also never observed the collapse of *cap59*-containing phagosomes within the 12 h

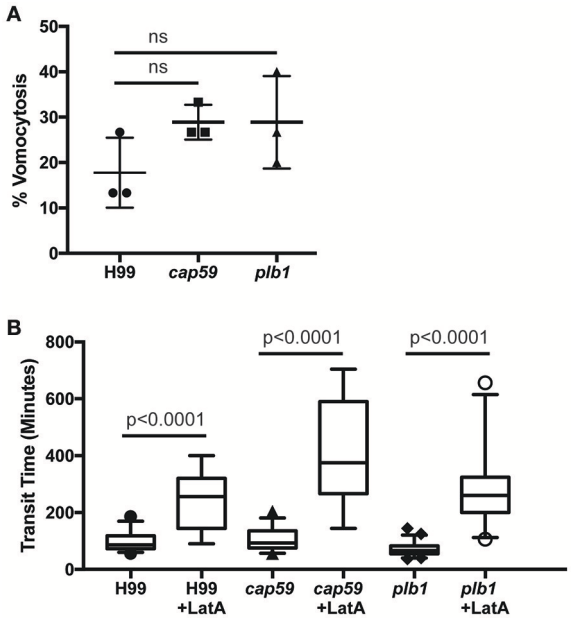

FIGURE 4 | Exocytosis and vomocytosis of *C. neoformans cap59* and *plb1* mutants are indistinguishable from wild type H99. **(A)** Quantification of the percentage of non-constitutive exocytosis of *C. neoformans* mutants from wild-type Ax2 *D. discoideum* treated with latrunculin A from three independent 12 h time lapses. Total of 45 phagosomes were analyzed for wild type H99, 90 for *cap59* and 90 for *plb1*. *P*-values are Fisher's exact test. **(B)** Transit times of *C. neoformans* H99 wild type, mutant *cap59* and *plb1*. Phagosomes analyzed the same as **(A)**. *P*-values for between cryptococcal strain significance tests are non-significant in all cases. *P*-values are Mann-Whitney test.

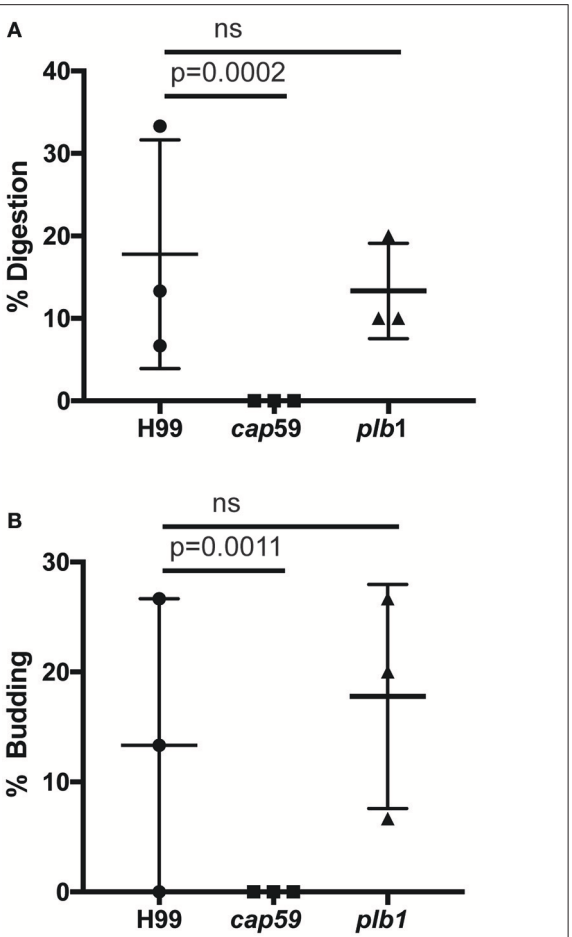

FIGURE 5 | Outcomes of interaction between cryptococcal cells and amoebae with inhibition of constitutive exocytosis. Quantification of outcome from three independent 12 h time lapses. Numbers of phagosomes analyzed the same as **Figure 4A**. **(A)** Percentage of fungal cells digested by amoebae over 12 h. **(B)** Percentage of fungal cells that budded while intracellular in amoebae over 12 h. *P*-values are Fisher's exact test.

indicating yeast death. This implies that either acapsular cells survive under growth arrest, or that death of *cap59* cells occurs over a longer period than we are able to observe in this assay. Nonetheless, in the absence of constitutive exocytosis, yeast are able to replicate intracellularly within the retained phagosomes.

DISCUSSION

In this work we have investigated the interactions between the environmental yeast *C. neoformans* and an environmental amoeba, *D. discoideum*. As *C. neoformans* can evade human immune cells and cause opportunistic infection in immunocompromised individuals we sought to test the hypothesis that the yeast virulence mechanisms had evolved to protect against amoebae in the environment.

In agreement with previous reports (Steenbergen et al., 2003), we found that *C. neoformans* were almost completely impervious to predation by *D. discoideum*; we consistently observed lower rates of *C. neoformans* phagocytosis compared to other particles, and even when the yeast were engulfed the amoebae were unable to kill them. This is similar to the interactions with mammalian macrophages, indicating that *C. neoformans* employs similar phagocyte evasion strategies. Chief amongst these is the characteristic cryptococcal capsule which is highly anti-phagocytic and also provides protection from oxidative attack. Consistent with this both we, and others found capsule deficient yeasts were unable to grow within amoebae (Steenbergen et al., 2001, 2003) and we found that the acapsular strain was taken up twice as frequently as the wild type.

Whilst *C. neoformans* typically persist and proliferate in macrophages for many hours before escaping by vomocytosis, we found they passed through *D. discoideum* via an apparently normal phagosomal transit in just ∼80 min. This short time period provides limited opportunity for intracellular growth of fungal cells or the lysis of amoebae. Whilst others have shown that *C. neoformans* are able to grow (and therefore extract nutrients) when co-incubated with amoebae over several days (Steenbergen et al., 2001, 2003). The relatively short amount of time spent inside the amoeba implies that much of this growth is extracellular and intracellular growth has not been directly demonstrated by high resolution time lapse imaging (Steinman

et al., 1976; Derengowski et al., 2013; Fu and Casadevall, 2018). We were unable to identify intracellular proliferation in the absence of the constitutive exocytosis inhibition. It therefore seems unlikely that *C. neoformans* has successfully evolved mechanisms to support intracellular replication within amoebae that exhibit rapid phagosomal transit, as demonstrated for *D. discoideum, Amoeba proteus, Entamoeba histolytica* and *A. castellanii* (Weisman and Korn, 1967; Ravdin et al., 1988; Christofidou-Solomidou and Stockem, 1992; Clarke et al., 2010).

Although *D. discoideum* are unable to kill phagocytosed *C. neoformans* the transit time is identical to that of heat-killed non-pathogenic yeast. This suggests that there is no major subversion of normal phagosome maturation. Consistent with this we find that the V-ATPase is both recruited, and retrieved from phagosomes with normal dynamics. This is in contrast to a recent study in macrophages, demonstrating that *C. neoformans* is able to disrupt phagosome maturation to inhibit acidification and proteolysis to permit intracellular proliferation (Smith et al., 2015). As the crypotococcal-containing phagosome in macrophages is permeabilized shortly after phagocytosis by macrophages (Tucker and Casadevall, 2002) V-ATPase delivery may be intact in both systems, but ineffective due to proton leakage.

Surprisingly, although *C. neoformans* are released alive from *D. discoideum* by canonical, WASH-dependent constitutive exocytosis, we found they were still expelled when the constitutive pathway was blocked. This second pathway strongly resembles vomocytosis from macrophages, being non-lytic, stochastic and inhibited by actin (Alvarez and Casadevall, 2006; Ma et al., 2006; Johnston and May, 2010). Vomocytosis remains mechanistically poorly understood and defined, but it seems highly likely that the WASH-independent egress of *C. neoformans* from *D. discoideum* is an analogous process.

Whilst laboratory strains have mutations that facilitate macropinocytosis and phagocytosis of large particles, wild-type isolates of *D. discoideum* are bacterivores and cannot engulf yeasts (Bloomfield et al., 2015). Therefore although *D. discoideum* provides a genetically tractable model for amoebae in general, it is highly unlikely to be an environmental host for cryptococci. The high phagocytic throughput of amoebae necessitates a mechanism to dispose of indigestible material, and unlike macrophages, there is no advantage in retaining phagosomes indefinitely to restrict an inflammatory response. As constitutive exocytosis appears to be sufficient for successful escape of *C. neoformans* on its own, the evolutionary drivers of a secondary, redundant escape mechanism are unclear. Whether other, more environmentally-relevant amoeba behave differently, or another environmental interaction altogether selects for this virulence trait requires further study.

Whatever the evolutionary basis, we have shown that vomocytosis-like egress is a mechanistically distinct process from constitutive exocytosis and is conserved in hosts from *D. discoideum* to man. The genetic tractability of *Dictyostelium* amoebae present an unparalleled opportunity to study the molecular cell biology of host cryptococcal interactions, and the differences in the environmental niche of *C. neoformans* and infection of humans.

AUTHOR CONTRIBUTIONS

RW, AA, CW, and CB performed experiments and data analysis. Initial concept, funding, experimental design were undertaken by JK and SJ. All authors prepared and edited the manuscript.

ACKNOWLEDGMENTS

We would like to thank Thierry Soldati for assistance and support developing this project. This work was supported by a Royal Society University Research Fellowship UF140624 to JK, and Medical Research Council and Department for International Development Career Development Award Fellowship MR/J009156/1 to SJ. We are grateful for a Microbiology Society Harry Smith Vacation studentship to support CW. RW was supported by a Bateson Centre BMedSci scholarship. Microscopy studies were supported by an MRC grant (G0700091) and a Wellcome Trust grant (GR077544AIA).

REFERENCES

Alvarez, M., and Casadevall, A. (2006). Phagosome extrusion and host-cell survival after *Cryptococcus neoformans* phagocytosis by macrophages. *Curr. Biol.* 16, 2161–2165. doi: 10.1016/j.cub.2006.09.061

Bai, Y., Brugha, R. E., Jacobs, L., Grigg, J., Nawrot, T. S., and Nemery, B. (2015). Carbon loading in airway macrophages as a biomarker for individual exposure to particulate matter air pollution - a critical review. *Environ. Int.* 74, 32–41. doi: 10.1016/j.envint.2014.09.010

Ballou, E. R., and Johnston, S. A. (2017). The cause and effect of Cryptococcus interactions with the host. *Curr. Opin. Microbiol.* 40, 88–94. doi: 10.1016/j.mib.2017.10.012

Bloomfield, G., Traynor, D., Sander, S. P., Veltman, D. M., Pachebat, J. A., and Kay, R. R. (2015). Neurofibromin controls macropinocytosis and phagocytosis in *Dictyostelium*. *eLife* 4:e04940. doi: 10.7554/eLife.04940

Bojarczuk, A., Miller, K. A., Hotham, R., Lewis, A., Ogryzko, N. V., Kamuyango, A. A., et al. (2016). *Cryptococcus neoformans* intracellular proliferation and capsule size determines early macrophage control of infection. *Sci. Rep.* 6:21489. doi: 10.1038/srep21489

Boulais, J., Trost, M., Landry, C. R., Dieckmann, R., Levy, E. D., Soldati, T., et al. (2010). Molecular characterization of the evolution of phagosomes. *Mol. Syst. Biol.* 6:423. doi: 10.1038/msb.2010.80

Buckley, C. M., Gopaldass, N., Bosmani, C., Johnston, S. A., Soldati, T., Insall, R. H., et al. (2016). WASH drives early recycling from macropinosomes and phagosomes to maintain surface phagocytic receptors. *Proc. Natl. Acad. Sci. U.S.A.* 113, E5906–E5915. doi: 10.1073/pnas.1524532113

Carnell, M., Zech, T., Calaminus, S. D., Ura, S., Hagedorn, M., Johnston, S. A., et al. (2011). Actin polymerization driven by WASH causes V-ATPase retrieval and vesicle neutralization before exocytosis. *J. Cell Biol.* 193, 831–839. doi: 10.1083/jcb.201009119

Casadevall, A. (2012). Amoeba provide insight into the origin of virulence in pathogenic fungi. *Adv. Exp. Med. Biol.* 710, 1–10. doi: 10.1007/978-1-4419-5638-5_1

Casadevall, A., Rosas, A. L., and Nosanchuk, J. D. (2000). Melanin and virulence in *Cryptococcus neoformans*. *Curr. Opin. Microbiol.* 3, 354–358. doi: 10.1016/S1369-5274(00)00103-X

Chayakulkeeree, M., Johnston, S. A., Oei, J. B., Lev, S., Williamson, P. R., Wilson, C. F., et al. (2011). SEC14 is a specific requirement

for secretion of phospholipase B1 and pathogenicity of *Cryptococcus neoformans*. *Mol. Microbiol.* 80, 1088–1101. doi: 10.1111/j.1365-2958.2011.07632.x

Chen, L., and Jondal, M. (2004). Alternative processing for MHC class I presentation by immature and CpG-activated dendritic cells. *Eur. J. Immunol.* 34, 952–960. doi: 10.1002/eji.200324359

Chen, S. C., Wright, L. C., Golding, J. C., and Sorrell, T. C. (2000). Purification and characterization of secretory phospholipase B, lysophospholipase and lysophospholipase/transacylase from a virulent strain of the pathogenic fungus *Cryptococcus neoformans*. *Biochem. J.* 347(Pt 2), 431–439. doi: 10.1042/bj3470431

Chrisman, C. J., Alvarez, M., and Casadevall, A. (2010). Phagocytosis of *Cryptococcus neoformans* by, and nonlytic exocytosis from, *Acanthamoeba* castellanii. *Appl. Environ. Microbiol.* 76, 6056–6062. doi: 10.1128/AEM.00812-10

Christofidou-Solomidou, M., and Stockem, W. (1992). Induced pinocytosis and endosomal pathways in *Amoeba proteus*. *Eur. J. Protistol.* 28, 56–70. doi: 10.1016/S0932-4739(11)80320-2

Clarke, M., Köhler, J., Arana, Q., Liu, T., Heuser, J., and Gerisch, G. (2002). Dynamics of the vacuolar H^+-ATPase in the contractile vacuole complex and the endosomal pathway of *Dictyostelium* cells. *J. Cell Sci.* 115, 2893–2905.

Clarke, M., Maddera, L., Engel, U., and Gerisch, G. (2010). Retrieval of the vacuolar H-ATPase from phagosomes revealed by live cell imaging. *PLoS ONE* 5:e8585. doi: 10.1371/journal.pone.0008585

Cox, G. M., McDade, H. C., Chen, S. C., Tucker, S. C., Gottfredsson, M., Wright, L. C., et al. (2001). Extracellular phospholipase activity is a virulence factor for *Cryptococcus neoformans*. *Mol. Microbiol.* 39, 166–175. doi: 10.1046/j.1365-2958.2001.02236.x

Derengowski, L. da. S., Paes, H. C., Albuquerque, P., Tavares, A. H. F. P., Fernandes, L., Silva-Pereira, I., et al. (2013). The transcriptional response of *Cryptococcus neoformans* to ingestion by *Acanthamoeba castellanii* and macrophages provides insights into the evolutionary adaptation to the mammalian host. *Eukaryot. Cell* 12, 761–774. doi: 10.1128/EC.00073-13

Derivery, E., Sousa, C., Gautier, J. J., Lombard, B., Loew, D., and Gautreau, A. (2009). The Arp2/3 activator WASH controls the fission of endosomes through a large multiprotein complex. *Dev. Cell* 17, 712–723. doi: 10.1016/j.devcel.2009.09.010

Evans, R. J., Li, Z., Hughes, W. S., Djordjevic, J. T., Nielsen, K., and May, R. C. (2015). Cryptococcal phospholipase B1 is required for intracellular proliferation and control of titan cell morphology during macrophage infection. *Infect. Immun.* 83, 1296–1304. doi: 10.1128/IAI.03104-14

Feldmesser, M., Kress, Y., Novikoff, P., and Casadevall, A. (2000). *Cryptococcus neoformans* is a facultative intracellular pathogen in murine pulmonary infection. *Infect. Immun.* 68, 4225–4237. doi: 10.1128/IAI.68.7.4225-4237.2000

Fu, M. S., and Casadevall, A. (2018). Divalent metal cations potentiate the predatory capacity of amoeba for *Cryptococcus neoformans*. *Appl. Environ. Microbiol.* 84: e01717-17. doi: 10.1128/AEM.01717-17

Gilbert, A. S., Seoane, P. I., Sephton-Clark, P., Bojarczuk, A., Hotham, R., Giurisato, E., et al. (2017). Vomocytosis of live pathogens from macrophages is regulated by the atypical MAP kinase ERK5. *Sci Adv* 3:e1700898. doi: 10.1126/sciadv.1700898

Gomez, T. S., and Billadeau, D. D. (2009). A FAM21-containing WASH complex regulates retromer-dependent sorting. *Dev. Cell* 17, 699–711. doi: 10.1016/j.devcel.2009.09.009

Griffiths, R. E., Kupzig, S., Cogan, N., Mankelow, T. J., Betin, V. M. S., Trakarnsanga, K., et al. (2012). Maturing reticulocytes internalize plasma membrane in glycophorin A-containing vesicles that fuse with autophagosomes before exocytosis. *Blood* 119, 6296–6306. doi: 10.1182/blood-2011-09-376475

Johnston, S. A., and May, R. C. (2010). The human fungal pathogen *Cryptococcus neoformans* escapes macrophages by a phagosome emptying mechanism that is inhibited by Arp2/3 complex-mediated actin polymerisation. *PLoS Pathog.* 6:e1001041. doi: 10.1371/journal.ppat.1001041

Johnston, S. A., and May, R. C. (2013). Cryptococcus interactions with macrophages: evasion and manipulation of the phagosome by a fungal pathogen. *Cell. Microbiol.* 15, 403–411. doi: 10.1111/cmi.12067

Johnston, S. A., Voelz, K., and May, R. C. (2016). *Cryptococcus neoformans* thermotolerance to avian body temperature is sufficient for extracellular growth but not intracellular survival in macrophages. *Sci. Rep.* 6:20977. doi: 10.1038/srep20977

King, J. S., Gueho, A., Hagedorn, M., Gopaldass, N., Leuba, F., Soldati, T., et al. (2013). WASH is required for lysosomal recycling and efficient autophagic and phagocytic digestion. *Mol. Biol. Cell* 24, 2714–2726. doi: 10.1091/mbc.E13-02-0092

Le Roux, D., Le Bon, A., Dumas, A., Taleb, K., Sachse, M., Sikora, R., et al. (2012). Antigen stored in dendritic cells after macropinocytosis is released unprocessed from late endosomes to target B cells. *Blood* 119, 95–105. doi: 10.1182/blood-2011-02-336123

Ma, H., Croudace, J. E., Lammas, D. A., and May, R. C. (2006). Expulsion of live pathogenic yeast by macrophages. *Curr. Biol.* 16, 2156–2160. doi: 10.1016/j.cub.2006.09.032

Nosanchuk, J. D., and Casadevall, A. (2006). Impact of melanin on microbial virulence and clinical resistance to antimicrobial compounds. *Antimicrob. Agents Chemother.* 50, 3519–3528. doi: 10.1128/AAC.00545-06

Noverr, M. C., Cox, G. M., Perfect, J. R., and Huffnagle, G. B. (2003). Role of PLB1 in pulmonary inflammation and cryptococcal eicosanoid production. *Infect. Immun.* 71, 1538–1547. doi: 10.1128/IAI.71.3.1538-1547.2003

Peters, S., Reinthal, E., Blitgen-Heinecke, P., Bartz-Schmidt, K. U., and Schraermeyer, U. (2006). Inhibition of lysosomal degradation in retinal pigment epithelium cells induces exocytosis of phagocytic residual material at the basolateral plasma membrane. *Ophthalmic Res.* 38, 83–88. doi: 10.1159/000090268

Rajasingham, R., Smith, R. M., Park, B. J., Jarvis, J. N., Govender, N. P., Chiller, T. M., et al. (2017). Global burden of disease of HIV-associated cryptococcal meningitis: an updated analysis. *Lancet Infect. Dis.* 17, 873–881. doi: 10.1016/S1473-3099(17)30243-8

Ravdin, J. I., Murphy, C. F., and Schlesinger, P. H. (1988). The cellular regulation of vesicle exocytosis by *Entamoeba histolytica*. *J. Protozool.* 35, 159–163.

Seaman, M. N., Gautreau, A., and Billadeau, D. D. (2013). Retromer-mediated endosomal protein sorting: all WASHed up! *Trends Cell Biol.* 23, 522–528. doi: 10.1016/j.tcb.2013.04.010

Smith, L. M., Dixon, E. F., and May, R. C. (2015). The fungal pathogen *Cryptococcus neoformans* manipulates macrophage phagosome maturation. *Cell. Microbiol.* 17, 702–713. doi: 10.1111/cmi.12394

Steenbergen, J. N., Nosanchuk, J. D., Malliaris, S. D., and Casadevall, A. (2003). *Cryptococcus neoformans* virulence is enhanced after growth in the genetically malleable host *Dictyostelium discoideum*. *Infect. Immun.* 71, 4862–4872. doi: 10.1128/IAI.71.9.4862-4872.2003

Steenbergen, J. N., Shuman, H. A., and Casadevall, A. (2001). *Cryptococcus neoformans* interactions with amoebae suggest an explanation for its virulence and intracellular pathogenic strategy in macrophages. *Proc. Natl. Acad. Sci. U.S.A.* 98, 15245–15250. doi: 10.1073/pnas.261418798

Steinman, R. M., Brodie, S. E., and Cohn, Z. A. (1976). Membrane flow during pinocytosis. A stereologic analysis. *J. Cell Biol.* 68, 665–687.

Stukes, S., Coelho, C., Rivera, J., Jedlicka, A. E., Hajjar, K. A., and Casadevall, A. (2016). The membrane phospholipid binding protein annexin A2 promotes phagocytosis and nonlytic exocytosis of *Cryptococcus neoformans* and impacts survival in fungal infection. *J. Immunol.* 197, 1252–1261. doi: 10.4049/jimmunol.1501855

Tenforde, M. W., Scriven, J. E., Harrison, T. S., and Jarvis, J. N. (2017). Immune correlates of HIV-associated cryptococcal meningitis. *PLoS Pathog.* 13:e1006207. doi: 10.1371/journal.ppat.1006207

Turner, C. T., Fuller, M., Hopwood, J. J., Meikle, P. J., and Brooks, D. A. (2016). Drug induced exocytosis of glycogen in Pompe disease. *Biochem. Biophys. Res. Commun.* 479, 721–727. doi: 10.1016/j.bbrc.2016.09.145

Tucker, S. C., and Casadevall, A. (2002). Replication of *Cryptococcus neoformans* in macrophages is accompanied by phagosomal permeabilization and accumulation of vesicles containing polysaccharide in the cytoplasm. *Proc. Natl. Acad. Sci. U.S.A.* 99, 3165–3170. doi: 10.1073/pnas.052702799

Voelz, K., Johnston, S. A., Rutherford, J. C., and May, R. C. (2010). Automated analysis of cryptococcal macrophage parasitism using GFP-tagged cryptococci. *PLoS ONE* 5:e15968. doi: 10.1371/journal.pone.0015968

Watkins, R. A., King, J. S., and Johnston, S. A. (2017). Nutritional requirements and their importance for virulence of pathogenic

Cryptococcus species. *Microorganisms.* 5:E65. doi: 10.3390/microorganisms5040065

Weisman, R. A., and Korn, E. D. (1967). Phagocytosis of latex beads by *Acanthamoeba*. I. Biochemical properties. *Biochemistry* 6, 485–497. doi: 10.1021/bi00854a017

Wiesner, D. L., Specht, C. A., Lee, C. K., Smith, K. D., Mukaremera, L., Lee, S. T., et al. (2015). Chitin recognition via chitotriosidase promotes pathologic type-2 helper T cell responses to cryptococcal infection. *PLoS Pathog.* 11:e1004701. doi: 10.1371/journal.ppat.1004701

Zech, T., Calaminus, S. D., Caswell, P., Spence, H. J., Carnell, M., Insall, R. H., et al. (2011). The Arp2/3 activator WASH regulates alpha5beta1-integrin-mediated invasive migration. *J. Cell Sci.* 124(Pt 22), 3753–3759. doi: 10.1242/jcs.080986

Conflict of Interest Statement: The authors declare that the research was conducted in the absence of any commercial or financial relationships that could be construed as a potential conflict of interest.

frontiers in Cellular and Infection Microbiology

MINI REVIEW
published: 11 January 2018
doi: 10.3389/fcimb.2017.00527

Amoebae, Giant Viruses, and Virophages Make Up a Complex, Multilayered Threesome

*Jan Diesend, Janis Kruse, Monica Hagedorn and Christian Hammann**

Ribogenetics Biochemistry Lab, Department of Life Sciences and Chemistry, Jacobs University Bremen, Bremen, Germany

Viral infection had not been observed for amoebae, until the *Acanthamoeba polyphaga* mimivirus (APMV) was discovered in 2003. APMV belongs to the nucleocytoplasmatic large DNA virus (NCLDV) family and infects not only *A. polyphaga*, but also other professional phagocytes. Here, we review the *Megavirales* to give an overview of the current members of the *Mimi-* and *Marseilleviridae* families and their structural features during amoebal infection. We summarize the different steps of their infection cycle in *A. polyphaga and Acanthamoeba castellani*. Furthermore, we dive into the emerging field of virophages, which parasitize upon viral factories of the *Megavirales* family. The discovery of virophages in 2008 and research in recent years revealed an increasingly complex network of interactions between cell, giant virus, and virophage. Virophages seem to be highly abundant in the environment and occupy the same niches as the *Mimiviridae* and their hosts. Establishment of metagenomic and co-culture approaches rapidly increased the number of detected virophages over the recent years. Genetic interaction of cell and virophage might constitute a potent defense machinery against giant viruses and seems to be important for survival of the infected cell during mimivirus infections. Nonetheless, the molecular events during co-infection and the interactions of cell, giant virus, and virophage have not been elucidated, yet. However, the genetic interactions of these three, suggest an intricate, multilayered network during amoebal (co-)infections. Understanding these interactions could elucidate molecular events essential for proper viral factory activity and could implicate new ways of treating viruses that form viral factories.

Keywords: *Acanthamoeba polyphaga* mimivirus (APMV), virophage, nucleocytoplasmatic large DNA virus (NCLDV), mimivirus, pathogen defense

OPEN ACCESS

Edited by:
Thierry Soldati,
Université de Genève, Switzerland

Reviewed by:
Guruprasad R. Medigeshi,
Translational Health Science and Technology Institute, India
Bernard La Scola,
Aix-Marseille University, France

****Correspondence:***
Christian Hammann
c.hammann@jacobs-university.de

Received: *15 October 2017*
Accepted: *13 December 2017*
Published: *11 January 2018*

Citation:
Diesend J, Kruse J, Hagedorn M and Hammann C (2018) Amoebae, Giant Viruses, and Virophages Make Up a Complex, Multilayered Threesome. Front. Cell. Infect. Microbiol. 7:527. doi: 10.3389/fcimb.2017.00527

INTRODUCTION TO GIANT VIRUSES

The discovery of giant viruses in the early 2000s led to a mind shift in the field of virology with respect to the potential origins of viruses (La Scola et al., 2003; Raoult et al., 2004). Originally, viruses were thought of as submicroscopic particles with a self-evident denial that viruses might exist, whose size would be large enough to be resolved with a simple light microscope (Lwoff, 1957; Raoult, 2013). Due to this mindset, the large, gram-positive particles in an *Acanthamoeba polyphaga* population were at first erroneously classified as bacteria (Birtles et al., 1997; La Scola et al., 2003; Raoult et al., 2007). Only the absence of ribosomal DNA in the presumed bacterium, led to the discovery and definition of the *A. polyphaga* mimivirus (APMV) in 2003 (La Scola et al., 2003).

The acronym mimivirus (for mimicking microbe) reflects the resemblance to bacteria upon gram staining. At the same time, the discovery of APMV was the first ever report of a virus infecting amoebae. Amongst other features that are detailed below, APMV is unusual as it contains a large genome of 1.14 Mbp, thereby even surpassing the genome size of some bacterial species (Raoult et al., 2004). APMV particles are characterized by an up to 700 nm large capsid (**Figure 1A**), which is well above the resolution of a simple light microscope. Once it was established that giant DNA viruses of amoebae exist, many more such viruses, belonging to the nucleoplasmatic large DNA viruses (NCLDV) were found in the environment, as well as within a wide range of host organisms from humans, monkeys, and oysters (Boughalmi et al., 2013a; Dornas et al., 2014; Andrade et al., 2015). *Ex vivo* studies of human cell lines revealed that APMV is capable of infecting myeloid and mononuclear blood cells and interferes with the type I Interferon system (Silva et al., 2014). In addition, a distantly APMV-related NCLDV family member has been shown to productively infect T-lymphocytes under laboratory conditions (Popgeorgiev et al., 2013). In 2008, a small particle called Sputnik 1 (La Scola et al., 2008) was discovered in *A. polyphaga*, which parasitizes viral factories of giant viruses. Due to the functional similarity to bacteriophages in mediating lateral gene transfer, Sputnik was classified as a virophage (La Scola et al., 2008). Here, we will review the expanding family of virophages and discuss the implications for giant virus reproduction inside amoebae.

THE DIVERSE FAMILIES OF GIANT VIRUSES THAT INFECT AMOEBAE

The discovery of APMV sparked the interest in giant viruses and spawned a contemporary research field of its own (La Scola et al., 2003). Up until today, two giant virus families belonging to the NCLDV have been described that primarily infect amoebae: the *Mimiviridae* and the *Marseilleviridae* (**Figure 1B**). The latter has the *A. polyphaga* marseillevirus (APMaV) as founding member, which was discovered in 2009 (Boyer et al., 2009; Colson et al., 2013). In the last decade, nine additional viruses have been associated with the *Marseilleviridae* group (Colson et al., 2017). The *Acanthamoeba castellani* lausannevirus (ACLaV) was discovered by incubating water from the Seine river in France with *A. castellani*, a close relative of *A. polyphaga* (Thomas et al., 2011). ACLaV is the first known giant virus to encode histone-like proteins, which could point towards a DNA packaging mechanism similar to eukaryotes (Thomas et al., 2011). The Cannes 8 virus (Ca8V) (La Scola et al., 2010) and the Senegal virus (SNGV) (Lagier et al., 2012) have been isolated using similar co-culture methods and are grouped with the *Marseilleviridae*. The icosahedral capsid of the *Marseilleviridae* is between 190 and 250 nm in diameter (Colson et al., 2013). Like the genome of the *Mimiviridae*, the 370,000 bp dsDNA genome is encased in a lipid bilayer and encodes about 450 proteins (Boyer et al., 2009; La Scola et al., 2010; Thomas et al., 2011; Lagier et al., 2012). Both, *Mimiviridae* and *Marseilleviridae*, share only nine core genes with all NCLDVs (**Figure 1C**) and 180 genes are shared with at least two of the NCLDV families (Yutin et al., 2009; Yutin and Koonin, 2012). Based on the discovery of APMV and its complex genome, it was suggested to incorporate viruses into the tree of life by defining them as capsid-encoding organisms contrary to the ribosome-encoding organisms, which are represented by eukarya, bacteria, and archaea (Raoult and Forterre, 2008).

APMV—THE BEST STUDIED GIANT VIRUS OF AMOEBAE

APMV was the first giant virus to be discovered (La Scola et al., 2008) and confronted the scientific community with features never observed in a virus before. Its capsid size and genetic complexity with many genes usually found in eukaryotic and prokaryotic cells challenged the Lwoff's characteristics of a virus (Raoult et al., 2004; Raoult and Forterre, 2008). The AT-rich 1.14 Mbp APMV genome features an impressive number of 979 protein-encoding genes in a dense arrangement (Raoult et al., 2004; Legendre et al., 2011). Several of its genes are only found in giant viruses of amoebae and code for virus-atypical proteins involved in DNA repair, protein folding, tRNA synthesis and translation, and more (Raoult et al., 2004). In addition, the APMV genome displays some plasticity and encodes self-splicing introns, inteins, and a specific set of mobile genetic elements called transpovirons (Desnues et al., 2012). Furthermore, the genome contains many genes likely acquired via horizontal gene transfer, paralogous genes, and so called ORFans, genes that encode proteins with unknown function (Suhre, 2005; Filée et al., 2007; Moreira and Brochier-Armanet, 2008; Forterre, 2010). Many of these genes are shared with the poxviruses, phycodnaviruses, and other NCLDVs (Filée et al., 2007). ORFans represent roughly 50% of genes and about 40% of the APMV proteome, which results in a high number of factors with unknown functions that might act during viral replication and morphogenesis (Renesto et al., 2006). Alike "classical" viruses, APMV genes are partly under the control of early and late stage-specific promoters (Raoult et al., 2004; Suhre et al., 2005).

The APMV particles possess remarkable structural features, separating them from the classical structures of viruses (**Figure 1A**). In its center, the viral DNA, mRNAs and proteins are packed into the core compartment (Xiao et al., 2009; Kuznetsov et al., 2013) and enclosed by a lipid membrane. Among the pre-packed proteins are 12 enzymes involved in transcription, five in DNA repair, two in RNA modification, and five in protein modification (Renesto et al., 2006). The central compartment is surrounded by an approximately 340 nm-large lipid bilayer and a secondary bilayer directly underneath an icosahedral capsid. This is comprised of major capsid proteins and features a five-branch proteinaceous structure, the "stargate," at one vortex (Kuznetsov et al., 2013). The capsid itself is covered by a compact layer of about 120–140 nm long, heavily glycosylated fibrils, which potentially facilitate the attachment of APMV to its host cells (Rodrigues et al., 2015).

As of now, only four fiber associated proteins (FAP1-4) have been functionally associated with either fibril biosynthesis or as components of the fibrils (Sobhy et al., 2015). FAP1 is an aryl

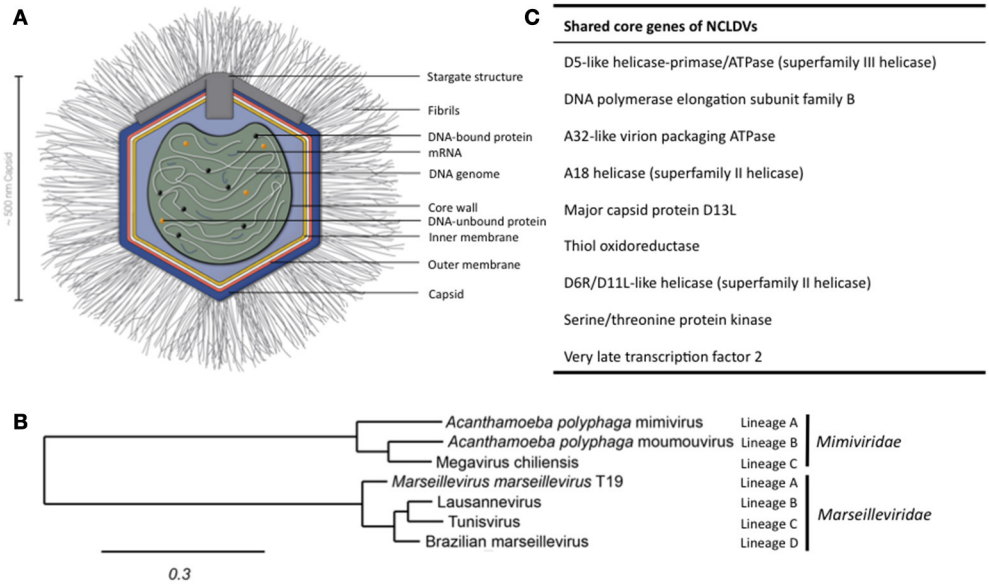

FIGURE 1 | Structure of APMV and the core genes and relationship of giant viruses. **(A)** Viral particles of APMV feature a viral core with the genome, mRNAs, and prefabricated proteins. This core is surrounded by the indicated membranes and the capsid structure that contains a pentagonal, star-shaped structure termed "stargate," which is involved in the release of the viral core into the host cell's cytosol upon phagocytosis. The capsid is decorated with a compact layer of fibrils. For details see main text. **(B)** Cladogram displaying the relationships of the different lineages of the *Mimiviridae* and *Marseilleviridae*. Since the discovery of APMV, over 100 new mimivirus strains have been characterized using samples of various origins in amoebal co-culture methods (Pagnier et al., 2013; Khalil et al., 2016a,b). All *Mimiviridae* share a capsid size between 370 and 600 nm and a 1.02–1.26 Mb AT-rich genome which encodes about 1.000 putative proteins (Colson et al., 2017). Based on sequence homology, the *Mimiviridae* can be divided into three distinct lineages: lineage A with APMV as prototype and a total of 18 members, as reviewed recently (Colson et al., 2017), lineage B with the moumouvirus as prototype and four additional members (Yoosuf et al., 2012; Colson et al., 2017), and lineage C with Megavirus chiliensis as prototype and a total of 12 members (Arslan et al., 2011; Colson et al., 2017). The tree was created using the sequences of the D13 major capsid proteins of the indicated prototype viruses using Phylogeny.fr, with the relative evolutionary distance indicated (Dereeper et al., 2008, 2010). **(C)** List of nine genes conserved throughout all NCLDV families.

alcohol oxidase, which catalyzes the degradation of lignin or lignin derivatives. This suggests that APMV might also be able to infect lignin-containing algae (Klose et al., 2015; Rodrigues et al., 2015). However, the fibrils and associated proteins are not essential for the productive infection of amoebae: during long-term intraamoebal culture (150 generations), the responsible genes are lost (Boyer et al., 2011; Rodrigues et al., 2015). This indicates that the genomic complexity of APMV might be maintained to allow for a broad host range. If so, only a subset of its diverse molecular tools would come in use to enter and infect individual hosts.

INFECTION CYCLES OF GIANT VIRUSES IN AMOEBAE

Even though the replication cycle of most giant viruses differ in aspects like nuclear involvement, duration, assembly, and release of the viral progeny, key steps in the infection appear to be conserved, as summarized recently (Colson et al., 2017). For example, all known giant viruses enter the host cell by phagocytosis and release their DNA into the cytosol in a similar manner (Ghigo et al., 2008). Furthermore, viral replication takes place in specialized endoplasmatic reticulum (ER)-derived compartments that are found in the cytosol and are called viral factories (Xiao et al., 2009; Mutsafi et al., 2010; Kuznetsov et al., 2013).

After uptake, the virus resides in a *de-novo* phagosome. Subsequently, the phagosomal and viral membranes fuse, which allows the release of the viral core, that contains the genome, proteins, and mRNAs into the cytosol (Zauberman et al., 2008; Mutsafi et al., 2010). Alike the well-described poxvirus (Broyles, 2003), the structural integrity of the viral core seems to be retained until viral factories arise (Claverie et al., 2009; Mutsafi et al., 2010). Intriguingly, recent experiments suggest that viral transcription might be initiated already before the release of the viral core (Mutsafi et al., 2014). Once in the cytosol, replication of the viral genome begins immediately and the expression of early stage genes leads to the formation of early viral factories (Suzan-Monti et al., 2007; Mutsafi et al., 2013, 2014). The replication cycle is confined to the cytosol, again a trait shared with the poxvirus (La Scola et al., 2003; Claverie et al., 2009). This also suggests that giant viruses (like the poxvirus) must carry transcription complexes to initiate transcription immediately after infection (Resch et al., 2007; Claverie et al., 2009). In later stages of infection, these viral factories merge into one large cytosolic compartment for replication and capsid assembly (Suzan-Monti et al., 2007; Mutsafi et al., 2014). It should be noted that viral factories are not chaotic, but rather appear to feature distinct assembly lines for their progeny. The viral

factory is made up of functional regions playing discrete roles in replication, capsid assembly, DNA packaging, and attachment of fibrils (Suzan-Monti et al., 2007; Mutsafi et al., 2014). In the outermost layer of the viral factory, the internal membrane layers of APMV are assembled from host-derived membrane vesicles, which are thought to rupture, thereby forming open single-layer membrane sheets (Mutsafi et al., 2013). Capsid assembly occurs around these membrane sheets and is scaffolded by the major capsid protein L425 (Mutsafi et al., 2013). Upon capsid formation, the genome is deposited into the empty viral particle through a transient interstice distal from the "stargate" structure (Zauberman et al., 2008). There is little evidence for a nuclear stage of giant viruses. However, the nuclei of *A. polyphaga* and *A. castellani* exhibit transient changes in their morphology during the early stages of infection with members of the *Marseilleviridae* family (Arantes et al., 2016). This indicates that nuclear host factors might play a role in the APMV replication, a notion that is supported by a two-fold decrease of the nuclear size in infected *A. polyphaga* cells (Colson et al., 2017). This might be due to a substantial redistribution of nuclear factors for viral replication, transcription or other processes (Colson et al., 2017). Albeit indirectly, this scenario is supported by data on the cytoplasmic replication of the Vaccinia virus (a poxvirus), to which mimivirus replication bears similarities (Mutsafi et al., 2010) and for which the involvement of nuclear enzymes has been demonstrated (Oh and Broyles, 2005).

VIROPHAGES AS PARASITES OF THE MEGAVIRALES

The description of *Megavirales* infection of amoebae was followed by the discovery of the fascinating virophage Sputnik in 2008 (La Scola et al., 2008). Sputnik was found infecting the viral factories of the mamavirus, a close relative of APMV (La Scola et al., 2008). Replication of the Sputnik virophages inside APMV-infected *A. castellani* cells is deleterious to APMV replication and results in abortive DNA replication and disruption of capsid biogenesis (La Scola et al., 2008). There is an ongoing discussion on the classification of virophages, that are denoted in several articles as satellite viruses (Krupovic and Cvirkaite-Krupovic, 2011; Blanc et al., 2015; Koonin and Krupovic, 2017). Satellite viruses are characterized by their dependency on factors of a helper virus. However, the Sputnik genomes itself encodes factors involved in viral replication (La Scola et al., 2008), suggesting that Sputnik can be classified as a virus, rather than a defective viral particle or sub-viral agent (Fischer, 2011; Desnues and Raoult, 2012).

All known members of the virophage family parasitizing on giant viruses are categorized into the large virus-dependent or -associated (*Lavida-*)*viridae* family that is divided into the *Sputnikvirus* and *Mavirus* genera (Krupovic et al., 2016). At the species level, the *Sputnikvirus* genus can be differentiated into the APMV-dependent Sputnik virophage and the APMV-dependent Zamilon virophage (**Table 1**), while *Mavirus* genus contains only the *Cafeteria roenbergensis* virus (CroV)-dependent mavirus (Krupovic et al., 2016).

Virophage replication has been extensively studied in particular for Sputnik, Zamilon and mavirus. Studies on amoebae infected with different mimiviruses revealed that Sputnik virophages can parasitize mimiviruses from all *Mimiviridae* lineages but apparently not the *Marseilleviridae* lineages (Gaia et al., 2013). Sputnik replicates inside mamavirus-infected *A. castellani* cells within the viral factories, nonetheless, with different kinetics as the mamavirus and at multiple hot spots inside the factory (La Scola et al., 2008). In APMVs viral factories, Sputnik infection results in the emergence of newly generated particles 6 h post infection with a concomitant decrease of infective APMV particles (Ogata and Claverie, 2008). The 18,343-kilobase circular dsDNA genome of Sputnik possesses 21 partly overlapping open-reading frames (ORFs) encoding for several factors involved in DNA replication (La Scola et al., 2008). Interestingly, four of the ORFs are strongly homologous to APMV-encoded genes (La Scola et al., 2008; Gaia et al., 2013). Since Sputnik virophages encodes a lambda-type integrase, the molecular tools for genomic integration are present (La Scola et al., 2008). Indeed, an integration of the Sputnik genome into the genome of the Lentille virus, a relative of APMV, could be observed experimentally (Desnues et al., 2012). There is no indication of Sputnik genome integration into the host cell genome, in line with the lack of indications for a nuclear phase.

The Zamilon virophage (belonging to the *Sputnikvirus* genus) was discovered together with the Mont1 mimivirus in soil samples from Tunisia (Boughalmi et al., 2013a; Gaia et al., 2014). The 60 nm-wide, spherical virophage carries a 17,276 bp dsDNA genome encoding 20 genes. Although Zamilon shares 76% of its genomic sequence with Sputnik, Zamilon can only infect lineages B and C (Gaia et al., 2014). Furthermore, the tv_L8 protein, encoded in the transpovirons of the Monve mimivirus, shares significant homology with the ORF8-encoded protein of Zamilon (Gaia et al., 2014). This suggests that an exchange of genetic material can in principle occur between the giant virus and the Zamilon virophage within co-infected amoebae, although this has not been observed experimentally so far.

The Maverick-related virus (mavirus), lonely member of the *Mavirus* genus, parasitizes the viral factories of CroV that infects the marine heterotrophic nanoflagellate *C. roenbergensis* (Fischer et al., 2010; Fischer and Suttle, 2011). Although this review is predominantly concerned with infection of amoebae, mavirus is included here for its unique features for a virophage. Its 19,063 bp circular genome possesses 20 ORFs including a retroviral integrase, an unsual, protein-primed DNA polymerase, plus four additional proteins, all of which are also found conserved in Maverick/Polinton (MP) retroelements (Fischer and Suttle, 2011; Krupovic et al., 2014, 2016). Additionally, the termini of the mavirus genome consist of long terminal repeats similar to those found in MP retroelements (Yutin et al., 2013; Krupovic et al., 2016). Both findings suggest that these retroelements might have originated from mavirus genome integration events in mavirus co-infected cells (Fischer and Suttle, 2011; Krupovic et al., 2016). Nonetheless, this hypothesis for the origins of MP retroelements remains to be tested experimentally. Fischer and Hackl (2016) succeeded to monitor the integration of mavirus into the *C. roenbergensis* genome by co-infection with a low multiplicity of infection of CroV. Intriguingly, genes in the

TABLE 1 | Overview of the *Mimiviridae* and *Marseilleviridae* families and experimentally shown virophage infections.

Family	L[a]	Name	Place discovered	Size [nm]	References	GenBank Acc. No.	Genome size [kbp]	No. of ORFs (predicted)	GC%	Virophage	References
Mimiviridae	A	*A. polyphaga* mimivirus	Bradford, England	750	La Scola et al., 2003	NC_014649.1	1,182	979	28	Sputnik	La Scola et al., 2008
	A	*A. polyphaga* mamavirus	Paris, France	750	Colson et al., 2011	JF801956.1	1,192	1023	28	Sputnik	La Scola et al., 2008
	A	Hirudovirus	Tunisia	520	Boughalmi et al., 2013a	KF493731.1	1,155	992	28	No report	
	A	Niemeyer virus	Belo Horizonte, Brazil	620	Boratto et al., 2015	KT599914.1	1,299	1003	28	No report	
	A	Samba virus	Negro River, Brazil	570	Campos et al., 2014; Assis et al., 2015	KF959826.2	1,181	971	28	Rio Negro	Campos et al., 2014
	A	Amazonian virus	Negro River, Brazil		Assis et al., 2015	KM982403	1,180	979	27	No report	
	A	Kroon virus	Lagoa Santa, Brazil		Assis et al., 2015	KM982402.1	1,222	944	27	No report	
	A	Oyster virus	Florianópolis, Brazil		Assis et al., 2015	KM982401.1	1,200	948	27	No report	
	A	Pointe-Rouge 1 virus	Marseille, France	390	La Scola et al., 2010	LN871174.1	1,151			Sputnik	Gaia et al., 2013
	A	Longchamps virus		450	La Scola et al., 2010	LN871173.1	1,104			Sputnik	Gaia et al., 2013
	A	Fauteuil virus		600	La Scola et al., 2010	LN871163.1	1,181			Sputnik	Gaia et al., 2013
	A	Terra2 virus	Marseille, France	370	La Scola et al., 2010; Yoosuf et al., 2014b	KF527228.1	1,167	890	28	Sputnik	Gaia et al., 2013
	A	Pointe-Rouge 2 virus	Marseille, France	500	La Scola et al., 2010	LN871172.1	1,163			Sputnik	Gaia et al., 2013
	A	Lactour virus		450	La Scola et al., 2010	CXOL00000000.1*	1,181			Sputnik	Gaia et al., 2013
	A	Lentille virus	Marseille, France	500	La Scola et al., 2010	AFYC00000000.1*	1,193	807		Sputnik	La Scola et al., 2010
	A	Shirakomae virus	Nagano, Japan		Takemura et al., 2016	AP017645.1	1,183	996		No report	
	A	Kasaii virus	Tokyo, Japan		Takemura et al., 2016	AP017644.1	1,183	996		No report	
	A	Bombay virus	Mumbai, India	435	Chatterjee et al., 2016b	KU761889.1	1,182	898	28	No report	
	B	*A. polyphaga* moumouvirus	South-East France	420	La Scola et al., 2010; Yoosuf et al., 2012	NC020104.1	1,021	930		Sputnik	Gaia et al., 2013
	B	Monve virus		390	La Scola et al., 2010	JN885994-6001*	1,015			Sputnik	Gaia et al., 2013
	B	Saudi moumouvirus	Jeddah, Saudi Arabia	500	Bajrai et al., 2016	KY110734.1	1,046	868	26	No report	
	B	Goulette virus			Boughalmi et al., 2013c	KC008572.1	1,017	979		No report	
	C	Megavirus chiliensis	Las Cruces, Chile	700	Arslan et al., 2011	JN258408.1	1,259	1120	25	No report	
	C	LBA111 virus	Tunisia	550	Saadi et al., 2013a	JX885207.1	1,231	1183		No report	
	C	Courdo 11 virus	Saint-Raphael, France	450	La Scola et al., 2010; Yoosuf et al., 2014a	JX975216.1	1,246	1166		Sputnik	Gaia et al., 2013

(Continued)

TABLE 1 | Continued

Family	L[a]	Name	Place discovered	Size [nm]	References	GenBank Acc. No.	Genome size [kbp]	No. of ORFs (predicted)	GC%	Virophage	References
	C	Courdo 7 virus	France	400	La Scola et al., 2010	JN885990-3	1,000			Sputnik	Gaia et al., 2013
	C	Terra1 virus	Marseille, France	420	La Scola et al., 2010; Yoosuf et al., 2014b	KF527229.1	1,234	1055	25	Sputnik	Gaia et al., 2013
	C	Shan virus	Marseille, France	640	Saadi et al., 2013b	LN868520.1	1,259			No report	
	C	Courdo5 virus		400	La Scola et al., 2010	LN868540.1	0,922			Sputnik	Gaia et al., 2013
	C	Powai Lake megavirus	Mumbai, India	425	Chatterjee et al., 2016a	KU877344.1	1,209	996	25	No report	
	C	Bus virus		400	La Scola et al., 2010	LN868539.1	1,229			Sputnik	Gaia et al., 2013
	C	Avenue 9 virus			Boughalmi et al., 2013c	LN867403.1	1,214			No report	
	C	Montpellier 3 virus	Montpellier, France	370	La Scola et al., 2010	LN868518.1	1,243			Sputnik	Gaia et al., 2013
	C	Mont1 virus	Tunisia	500	Boughalmi et al., 2013c					Zamilon	Gaia et al., 2014
Marseilleiviridae	A	*Marseillevirus marseillevirus* T19	Paris, France	250	Boyer et al., 2009	NC_013756	0,368	457	45	No report	
	A	Giant blood marseillevirus	Marseille, France	220	Popgeorgiev et al., 2013	PRJNA185405*	0,357	617	45	No report	
	A	Cannes8 virus	Cannes, France	190	La Scola et al., 2010; Aherfi et al., 2013	KF261120	0,374	484		No report	
	A	Senegalvirus	N'diop, Senegal	200	Lagier et al., 2012	JF909596-602*	0,373			No report	
	A	Melbournevirus	Melbourne, Australia	200	Doutre et al., 2014	KM275475.1	0,369	403	45	No report	
	B	Lausannevirus	Seine River, France	200	Thomas et al., 2011	NC_015326	0,347	450		No report	
	B	Port-Miou virus	Port-Miou Calanque, France	200	Doutre et al., 2015	KT428292.1	0,349	410		No report	
	B	Noumeavirus	Noumea, New Caledonia	200	Fabre et al., 2017	NC_033775	0,376	452	43	No report	
	C	Tunisvirus	Tunis, Tunisia	250	Boughalmi et al., 2013c; Aherfi et al., 2014	KF483846.1	0,380	484	43	No report	
	C	Insectomime virus	Tunis, Tunisia	225	Boughalmi et al., 2013b	KF527888.1	0,387	477	43	No report	
	C	Tokyovirus A1	Arakawa River, Japan	200	Takemura, 2016	AP017398.1	0,373	487		No report	
	D	Brazilian marseillevirus	Belo Horizonte, Brazil	250	Dornas et al., 2015, 2016	NC_029692	0,362	491	43	No report	
	E	Golden marseillevirus	Guaíba Lake, Brazil	200	Dos Santos et al., 2016	KT835053.1	0,361	483	43	No report	

**Genomes with separate available contigs or only raw sequencing data.*
[a]*Lineage.*

mavirus genome possess promoter sequences similar to the late stage promoter of CroV (Fischer and Hackl, 2016). As a consequence, re-infection of *C. roenbergensis* carrying the integrated mavirus genome with CroV resulted in inhibition of CroV DNA replication, concomitantly with an increased survival of *C. roenbergensis* (Fischer and Hackl, 2016).

Other virophages have been discovered by metagenomic analysis of water samples [e.g., the Organic Lake virophage (Yau et al., 2011), the Yellowstone Lake virophages (Zhou et al., 2013, 2015)]. However, the viral and cellular host for these remain to be determined (Krupovic et al., 2016), unlike the situation of the Rio Negro virophage that has the Samba virus as viral host (Campos et al., 2014).

OUTLOOK

Since the discovery of its first member APMV in 2003, new giant viruses are discovered continuously in samples from all over the world and added to the *Megavirales* family. The addition of virophages as parasites of giant viruses, their high abundance in the environment, and the genetic interactions between cell, giant virus, and virophage, suggest an intricate, multilayered network during amoebal co- and super-infections. Future studies of these dynamic interactions could elucidate the inner mechanics of viral factories.

AUTHOR CONTRIBUTIONS

All authors designed the mini review. JD: generated the figures and drafted the text; MH and CH: wrote the manuscript.

FUNDING

This work is supported by a grant of the Tönjes-Vagt-Stiftung Bremen, Germany.

REFERENCES

Aherfi, S., Boughalmi, M., Pagnier, I., Fournous, G., La Scola, B., Raoult, D., et al. (2014). Complete genome sequence of Tunisvirus, a new member of the proposed family Marseilleviridae. *Arch. Virol.* 159, 2349–2358. doi: 10.1007/s00705-014-2023-5

Aherfi, S., Pagnier, I., Fournous, G., Raoult, D., La Scola, B., and Colson, P. (2013). Complete genome sequence of Cannes 8 virus, a new member of the proposed family "Marseilleviridae." *Virus Genes* 47, 550–555. doi: 10.1007/s11262-013-0965-4

Andrade, K. R., Boratto, P. P. V. M., Rodrigues, F. P., Silva, L. C. F., Dornas, F. P., Pilotto, M. R., et al. (2015). Oysters as hot spots for mimivirus isolation. *Arch. Virol.* 160, 477–482. doi: 10.1007/s00705-014-2257-2

Arantes, T. S., Rodrigues, R. A. L., Dos Santos Silva, L. K., Oliveira, G. P., Souza, H. L. D., Khalil, J. Y., et al. (2016). The large Marseillevirus explores different entry pathways by forming giant infectious vesicles. *J. Virol.* 90, 5246–5255. doi: 10.1128/JVI.00177-16

Arslan, D., Legendre, M., Seltzer, V., Abergel, C., and Claverie, J.-M. (2011). Distant Mimivirus relative with a larger genome highlights the fundamental features of Megaviridae. *Proc. Natl. Acad. Sci. U.S.A.* 108, 17486–17491. doi: 10.1073/pnas.1110889108

Assis, F. L., Bajrai, L., Abrahao, J. S., Kroon, E. G., Dornas, F. P., Andrade, K. R., et al. (2015). Pan-genome analysis of Brazilian lineage A amoebal mimiviruses. *Viruses* 7, 3483–3499. doi: 10.3390/v7072782

Bajrai, L. H., de Assis, F. L., Azhar, E. I., Jardot, P., Robert, C., Abrahão, J., et al. (2016). Saudi Moumouvirus, the first group B mimivirus isolated from Asia. *Front. Microbiol.* 7:2029. doi: 10.3389/fmicb.2016.02029

Birtles, R. J., Rowbotham, T. J., Storey, C., Marrie, T. J., and Raoult, D. (1997). Chlamydia-like obligate parasite of free-living amoebae. *Lancet* 349, 925–926. doi: 10.1016/S0140-6736(05)62701-8

Blanc, G., Gallot-Lavallée, L., and Maumus, F. (2015). Provirophages in the Bigelowiella genome bear testimony to past encounters with giant viruses. *Proc. Natl. Acad. Sci. U.S.A.* 112, E5318–E5326. doi: 10.1073/pnas.1506469112

Boratto, P. V., Arantes, T. S., Silva, L. C. F., Assis, F. L., Kroon, E. G., La Scola, B., et al. (2015). Niemeyer virus: a new mimivirus group A isolate harboring a set of duplicated aminoacyl-tRNA synthetase genes. *Front. Microbiol.* 6:1256. doi: 10.3389/fmicb.2015.01256

Boughalmi, M., Pagnier, I., Aherfi, S., Colson, P., Raoult, D., and La Scola, B. (2013a). First isolation of a giant virus from wild Hirudo medicinalis leech: Mimiviridae isolation in Hirudo medicinalis. *Viruses* 5, 2920–2930. doi: 10.3390/v5122920

Boughalmi, M., Pagnier, I., Aherfi, S., Colson, P., Raoult, D., and La Scola, B. (2013b). First isolation of a Marseillevirus in the Diptera Syrphidae Eristalis tenax. *Intervirology* 56, 386–394. doi: 10.1159/000354560

Boughalmi, M., Saadi, H., Pagnier, I., Colson, P., Fournous, G., Raoult, D., et al. (2013c). High-throughput isolation of giant viruses of the Mimiviridae and Marseilleviridae families in the Tunisian environment. *Environ. Microbiol.* 15, 2000–2007. doi: 10.1111/1462-2920.12068

Boyer, M., Azza, S., Barrassi, L., Klose, T., Campocasso, A., Pagnier, I., et al. (2011). Mimivirus shows dramatic genome reduction after intraamoebal culture. *Proc. Natl. Acad. Sci. U.S.A.* 108, 10296–10301. doi: 10.1073/pnas.1101118108

Boyer, M., Yutin, N., Pagnier, I., Barrassi, L., Fournous, G., Espinosa, L., et al. (2009). Giant Marseillevirus highlights the role of amoebae as a melting pot in emergence of chimeric microorganisms. *Proc. Natl. Acad. Sci. U.S.A.* 106, 21848–21853. doi: 10.1073/pnas.0911354106

Broyles, S. S. (2003). Vaccinia virus transcription. *J. Gen. Virol.* 84, 2293–2303. doi: 10.1099/vir.0.18942-0

Campos, R. K., Boratto, P. V., Assis, F. L., Aguiar, E. R. G. R., Silva, L. C. F., Albarnaz, J. D., et al. (2014). Samba virus: a novel mimivirus from a giant rain forest, the Brazilian Amazon. *Virol. J.* 11:95. doi: 10.1186/1743-422X-11-95

Chatterjee, A., Ali, F., Bange, D., and Kondabagil, K. (2016a). Complete genome sequence of a new megavirus family member isolated from an Inland Water Lake for the First Time in India. *Genome Announc.* 4:e00402-16. doi: 10.1128/genomeA.00402-16

Chatterjee, A., Ali, F., Bange, D., and Kondabagil, K. (2016b). Isolation and complete genome sequencing of Mimivirus bombay, a Giant Virus in sewage of Mumbai, India. *Genomics Data* 9, 1–3. doi: 10.1016/j.gdata.2016.05.013

Claverie, J.-M., Grzela, R., Lartigue, A., Bernadac, A., Nitsche, S., Vacelet, J., et al. (2009). Mimivirus and Mimiviridae: giant viruses with an increasing number of potential hosts, including corals and sponges. *J. Invertebr. Pathol.* 101, 172–180. doi: 10.1016/j.jip.2009.03.011

Colson, P., La Scola, B., Levasseur, A., Caetano-Anollés, G., and Raoult, D. (2017). Mimivirus: leading the way in the discovery of giant viruses of amoebae. *Nat. Rev. Microbiol.* 15, 243–254. doi: 10.1038/nrmicro.2016.197

Colson, P., Pagnier, I., Yoosuf, N., Fournous, G., La Scola, B., and Raoult, D. (2013). "Marseilleviridae," a new family of giant viruses infecting amoebae. *Arch. Virol.* 158, 915–920. doi: 10.1007/s00705-012-1537-y

Colson, P., Yutin, N., Shabalina, S. A., Robert, C., Fournous, G., La Scola, B., et al. (2011). Viruses with More Than 1,000 Genes: Mamavirus, a New *Acanthamoeba polyphaga* mimivirus Strain, and Reannotation of Mimivirus Genes. *Genome Biol. Evol.* 3, 737–742. doi: 10.1093/gbe/evr048

Dereeper, A., Audic, S., Claverie, J.-M., and Blanc, G. (2010). BLAST-EXPLORER helps you building datasets for phylogenetic analysis. *BMC Evol. Biol.* 10:8. doi: 10.1186/1471-2148-10-8

Dereeper, A., Guignon, V., Blanc, G., Audic, S., Buffet, S., Chevenet, F., et al. (2008). Phylogeny.fr: robust phylogenetic analysis for the non-specialist. *Nucleic Acids Res.* 36, W465–W469. doi: 10.1093/nar/gkn180

Desnues, C., La Scola, B., Yutin, N., Fournous, G., Robert, C., Azza, S., et al. (2012). Provirophages and transpovirons as the diverse mobilome of giant viruses. *Proc. Natl. Acad. Sci. U.S.A.* 109, 18078–18083. doi: 10.1073/pnas.1208835109

Desnues, C., and Raoult, D. (2012). Virophages question the existence of satellites. *Nat. Rev. Microbiol.* 10:234. doi: 10.1038/nrmicro2676-c3

Dornas, F. P., Assis, F. L., Aherfi, S., Arantes, T., Abrahão, J. S., Colson, P., et al. (2016). A Brazilian Marseillevirus is the founding member of a lineage in family Marseilleviridae. *Viruses* 8:76. doi: 10.3390/v8030076

Dornas, F. P., Khalil, J. Y. B., Pagnier, I., Raoult, D., Abrahão, J., and La Scola, B. (2015). Isolation of new Brazilian giant viruses from environmental samples using a panel of protozoa. *Front. Microbiol.* 6:1086. doi: 10.3389/fmicb.2015.01086

Dornas, F. P., Rodrigues, F. P., Boratto, P. V. M., Silva, L. C. F., Ferreira, P. C. P., Bonjardim, C. A., et al. (2014). Mimivirus circulation among wild and domestic mammals, Amazon Region, Brazil. *Emerging Infect. Dis.* 20, 469–472. doi: 10.3201/eid2003.131050

Dos Santos, R. N., Campos, F. S., Medeiros De Albuquerque, N. R., Finoketti, F., Côrrea, R. A., Cano-Ortiz, L., et al. (2016). A new marseillevirus isolated in Southern Brazil from Limnoperna fortunei. *Sci. Rep.* 6:35237. doi: 10.1038/srep35237

Doutre, G., Arfib, B., Rochette, P., Claverie, J.-M., Bonin, P., and Abergel, C. (2015). Complete genome sequence of a new member of the Marseilleviridae recovered from the Brackish submarine spring in the Cassis Port-Miou Calanque, France. *Genome Announc.* 3:e01148-15. doi: 10.1128/genomeA.01148-15

Doutre, G., Philippe, N., Abergel, C., and Claverie, J.-M. (2014). Genome analysis of the first Marseilleviridae representative from Australia indicates that most of its genes contribute to virus fitness. *J. Virol.* 88, 14340–14349. doi: 10.1128/JVI.02414-14

Fabre, E., Jeudy, S., Santini, S., Legendre, M., Trauchessec, M., Couté, Y., et al. (2017). Noumeavirus replication relies on a transient remote control of the host nucleus. *Nat. Commun.* 8:15087. doi: 10.1038/ncomms15087

Filée, J., Siguier, P., and Chandler, M. (2007). I am what I eat and I eat what I am: acquisition of bacterial genes by giant viruses. *Trends Genet.* 23, 10–15. doi: 10.1016/j.tig.2006.11.002

Fischer, M. G. (2011). Sputnik and Mavirus: more than just satellite viruses. *Nat. Rev. Microbiol.* 10:78. doi: 10.1038/nrmicro2676-c1

Fischer, M. G., Allen, M. J., Wilson, W. H., and Suttle, C. A. (2010). Giant virus with a remarkable complement of genes infects marine zooplankton. *Proc. Natl. Acad. Sci. U.S.A.* 107, 19508–19513. doi: 10.1073/pnas.1007615107

Fischer, M. G., and Hackl, T. (2016). Host genome integration and giant virus-induced reactivation of the virophage mavirus. *Nature* 540:288. doi: 10.1038/nature20593

Fischer, M. G., and Suttle, C. A. (2011). A virophage at the origin of large DNA transposons. *Science* 332:231. doi: 10.1126/science.1199412

Forterre, P. (2010). Giant viruses: conflicts in revisiting the virus concept. *Intervirology* 53, 362–378. doi: 10.1159/000312921

Gaia, M., Benamar, S., Boughalmi, M., Pagnier, I., Croce, O., Colson, P., et al. (2014). Zamilon, a novel virophage with Mimiviridae host specificity. *PLoS ONE* 9:e94923. doi: 10.1371/journal.pone.0094923

Gaia, M., Pagnier, I., Campocasso, A., Fournous, G., Raoult, D., and La Scola, B. (2013). Broad spectrum of Mimiviridae virophage allows its isolation using a mimivirus reporter. *PLoS ONE* 8:e61912. doi: 10.1371/journal.pone.0061912

Ghigo, E., Kartenbeck, J., Lien, P., Pelkmans, L., Capo, C., Mege, J.-L., et al. (2008). Ameobal pathogen mimivirus infects macrophages through phagocytosis. *PLoS Pathog.* 4:e1000087. doi: 10.1371/journal.ppat.1000087

Khalil, J. Y. B., Andreani, J., and La Scola, B. (2016a). Updating strategies for isolating and discovering giant viruses. *Curr. Opin. Microbiol.* 31, 80–87. doi: 10.1016/j.mib.2016.03.004

Khalil, J. Y. B., Robert, S., Reteno, D. G., Andreani, J., Raoult, D., and La Scola, B. (2016b). High-throughput isolation of giant viruses in liquid medium using automated flow cytometry and fluorescence staining. *Front. Microbiol.* 7:26. doi: 10.3389/fmicb.2016.00026

Klose, T., Herbst, D. A., Zhu, H., Max, J. P., Kenttämaa, H. I., and Rossmann, M. G. (2015). A mimivirus enzyme that participates in viral entry. *Structure* 23, 1058–1065. doi: 10.1016/j.str.2015.03.023

Koonin, E. V., and Krupovic, M. (2017). Polintons, virophages and transpovirons: a tangled web linking viruses, transposons and immunity. *Curr. Opin. Virol.* 25, 7–15. doi: 10.1016/j.coviro.2017.06.008

Krupovic, M., Bamford, D. H., and Koonin, E. V. (2014). Conservation of major and minor jelly-roll capsid proteins in Polinton (Maverick) transposons suggests that they are bona fide viruses. *Biol. Direct* 9:6. doi: 10.1186/1745-6150-9-6

Krupovic, M., and Cvirkaite-Krupovic, V. (2011). Virophages or satellite viruses? *Nat. Rev. Microbiol.* 9:762. doi: 10.1038/nrmicro2676

Krupovic, M., Kuhn, J. H., and Fischer, M. G. (2016). A classification system for virophages and satellite viruses. *Arch. Virol.* 161, 233–247. doi: 10.1007/s00705-015-2622-9

Kuznetsov, Y. G., Klose, T., Rossmann, M., and Mcpherson, A. (2013). Morphogenesis of mimivirus and its viral factories: an atomic force microscopy study of infected cells. *J. Virol.* 87, 11200–11213. doi: 10.1128/JVI.01372-13

Lagier, J.-C., Armougom, F., Million, M., Hugon, P., Pagnier, I., Robert, C., et al. (2012). Microbial culturomics: paradigm shift in the human gut microbiome study. *Clin. Microbiol. Infect.* 18, 1185–1193. doi: 10.1111/1469-0691.12023

La Scola, B., Audic, S., Robert, C., Jungang, L., Lamballerie, X. D., Drancourt, M., et al. (2003). A giant virus in amoebae. *Science* 299:2033. doi: 10.1126/science.1081867

La Scola, B., Campocasso, A., N'dong, R., Fournous, G., Barrassi, L., Flaudrops, C., et al. (2010). Tentative characterization of new environmental giant viruses by MALDI-TOF mass spectrometry. *Intervirology* 53, 344–353. doi: 10.1159/000312919

La Scola, B., Desnues, C., Pagnier, I., Robert, C., Barrassi, L., Fournous, G., et al. (2008). The virophage as a unique parasite of the giant mimivirus. *Nature* 455, 100–104. doi: 10.1038/nature07218

Legendre, M., Santini, S., Rico, A., Abergel, C., and Claverie, J.-M. (2011). Breaking the 1000-gene barrier for Mimivirus using ultra-deep genome and transcriptome sequencing. *Virol. J.* 8:99. doi: 10.1186/1743-422X-8-99

Lwoff, A. (1957). The concept of virus. *J. Gen. Microbiol.* 17, 239–253. doi: 10.1099/00221287-17-2-239

Moreira, D., and Brochier-Armanet, C. (2008). Giant viruses, giant chimeras: the multiple evolutionary histories of Mimivirus genes. *BMC Evol. Biol.* 8:12. doi: 10.1186/1471-2148-8-12

Mutsafi, Y., Fridmann-Sirkis, Y., Milrot, E., Hevroni, L., and Minsky, A. (2014). Infection cycles of large DNA viruses: emerging themes and underlying questions. *Virology* 466–467, 3–14. doi: 10.1016/j.virol.2014.05.037

Mutsafi, Y., Shimoni, E., Shimon, A., and Minsky, A. (2013). Membrane assembly during the infection cycle of the giant Mimivirus. *PLoS Pathog.* 9:e1003367. doi: 10.1371/journal.ppat.1003367

Mutsafi, Y., Zauberman, N., Sabanay, I., and Minsky, A. (2010). Vaccinia-like cytoplasmic replication of the giant Mimivirus. *Proc. Natl. Acad. Sci. U.S.A.* 107, 5978–5982. doi: 10.1073/pnas.0912737107

Ogata, H., and Claverie, J.-M. (2008). How to infect a mimivirus. *Science* 321:1305. doi: 10.1126/science.1164839

Oh, J., and Broyles, S. S. (2005). Host cell nuclear proteins are recruited to cytoplasmic vaccinia virus replication complexes. *J. Virol.* 79, 12852–12860. doi: 10.1128/JVI.79.20.12852-12860.2005

Pagnier, I., Reteno, D.-G. I., Saadi, H., Boughalmi, M., Gaia, M., Slimani, M., et al. (2013). A decade of improvements in Mimiviridae and Marseilleviridae isolation from amoeba. *Intervirology* 56, 354–363. doi: 10.1159/000354556

Popgeorgiev, N., Boyer, M., Fancello, L., Monteil, S., Robert, C., Rivet, R., et al. (2013). Marseillevirus-like virus recovered from blood donated by asymptomatic humans. *J. Infect. Dis.* 208, 1042–1050. doi: 10.1093/infdis/jit292

Raoult, D. (2013). TRUC or the need for a new microbial classification. *Intervirology* 56, 349–353. doi: 10.1159/000354269

Raoult, D., Audic, S., Robert, C., Abergel, C., Renesto, P., Ogata, H., et al. (2004). The 1.2-megabase genome sequence of Mimivirus. *Science* 306, 1344–1350. doi: 10.1126/science.1101485

Raoult, D., and Forterre, P. (2008). Redefining viruses: lessons from Mimivirus. Nat. *Rev. Microbiol.* 6, 315–319. doi: 10.1038/nrmicro1858

Raoult, D., La Scola, B., and Birtles, R. (2007). The discovery and characterization of Mimivirus, the largest known virus and putative pneumonia agent. *Clin. Infect. Dis.* 45, 95–102. doi: 10.1086/518608

Renesto, P., Abergel, C., Decloquement, P., Moinier, D., Azza, S., Ogata, H., et al. (2006). Mimivirus giant particles incorporate a large fraction of anonymous and unique gene products. *J. Virol.* 80, 11678–11685. doi: 10.1128/JVI.00940-06

Resch, W., Hixson, K. K., Moore, R. J., Lipton, M. S., and Moss, B. (2007). Protein composition of the vaccinia virus mature virion. *Virology* 358, 233–247. doi: 10.1016/j.virol.2006.08.025

Rodrigues, R. A. L., Dos Santos Silva, L. K., Dornas, F. P., Oliveira, D. B. D., Magalhães, T. F. F., Santos, D. A., et al. (2015). Mimivirus fibrils are important for viral attachment to the microbial world by a diverse glycoside interaction repertoire. *J. Virol.* 89, 11812–11819. doi: 10.1128/JVI.01976-15

Saadi, H., Pagnier, I., Colson, P., Cherif, J. K., Beji, M., Boughalmi, M., et al. (2013a). First isolation of mimivirus in a patient with pneumonia. *Clin. Infect. Dis.* 57, e127–e134. doi: 10.1093/cid/cit354

Saadi, H., Reteno, D. G. I., Colson, P., Aherfi, S., Minodier, P., Pagnier, I., et al. (2013b). Shan virus: a new mimivirus isolated from the stool of a Tunisian Patient with pneumonia. *Intervirology* 56, 424–429. doi: 10.1159/000354564

Silva, L. C. F., Almeida, G. M. F., Oliveira, D. B., Dornas, F. P., Campos, R. K., La Scola, B., et al. (2014). A resourceful giant: APMV is able to interfere with the human type I interferon system. *Microbes Infect.* 16, 187–195. doi: 10.1016/j.micinf.2013.11.011

Sobhy, H., La Scola, B., Pagnier, I., Raoult, D., and Colson, P. (2015). Identification of giant Mimivirus protein functions using RNA interference. *Front. Microbiol.* 6:345. doi: 10.3389/fmicb.2015.00345

Suhre, K. (2005). Gene and genome duplication in *Acanthamoeba polyphaga* Mimivirus. *J. Virol.* 79, 14095–14101. doi: 10.1128/JVI.79.22.14095-14101.2005

Suhre, K., Audic, S., and Claverie, J.-M. (2005). Mimivirus gene promoters exhibit an unprecedented conservation among all eukaryotes. *Proc. Natl. Acad. Sci. U.S.A.* 102, 14689–14693. doi: 10.1073/pnas.0506465102

Suzan-Monti, M., La Scola, B., Barrassi, L., Espinosa, L., and Raoult, D. (2007). Ultrastructural characterization of the giant volcano-like virus factory of *Acanthamoeba polyphaga* Mimivirus. *PLoS ONE* 2:e328. doi: 10.1371/journal.pone.0000328

Takemura, M. (2016). Draft genome sequence of tokyovirus, a member of the family Marseilleviridae Isolated from the Arakawa River of Tokyo, Japan. *Genome Announc.* 4:e00429-16. doi: 10.1128/genomeA.00429-16

Takemura, M., Mikami, T., and Murono, S. (2016). Nearly complete genome sequences of two mimivirus strains isolated from a Japanese Freshwater Pond and River Mouth. *Genome Announc.* 4:e01378-16. doi: 10.1128/genomeA.01378-16

Thomas, V., Bertelli, C., Collyn, F., Casson, N., Telenti, A., Goesmann, A., et al. (2011). Lausannevirus, a giant amoebal virus encoding histone doublets. *Environ. Microbiol.* 13, 1454–1466. doi: 10.1111/j.1462-2920.2011.02446.x

Xiao, C., Kuznetsov, Y. G., Sun, S., Hafenstein, S. L., Kostyuchenko, V. A., Chipman, P. R., et al. (2009). Structural studies of the giant mimivirus. *PLoS Biol.* 7:e92. doi: 10.1371/journal.pbio.1000092

Yau, S., Lauro, F. M., Demaere, M. Z., Brown, M. V., Thomas, T., Raftery, M. J., et al. (2011). Virophage control of antarctic algal host–virus dynamics. *Proc. Natl. Acad. Sci. U.S.A.* 108, 6163–6168. doi: 10.1073/pnas.1018221108

Yoosuf, N., Pagnier, I., Fournous, G., Robert, C., La Scola, B., Raoult, D., et al. (2014a). Complete genome sequence of Courdo11 virus, a member of the family Mimiviridae. *Virus Genes* 48, 218–223. doi: 10.1007/s11262-013-1016-x

Yoosuf, N., Pagnier, I., Fournous, G., Robert, C., Raoult, D., La Scola, B., et al. (2014b). Draft genome sequences of Terra1 and Terra2 viruses, new members of the family Mimiviridae isolated from soil. *Virology* 452–453, 125–132. doi: 10.1016/j.virol.2013.12.032

Yoosuf, N., Yutin, N., Colson, P., Shabalina, S. A., Pagnier, I., Robert, C., et al. (2012). Related giant viruses in distant locations and different habitats: *Acanthamoeba polyphaga* moumouvirus represents a third lineage of the Mimiviridae that is close to the megavirus lineage. *Genome Biol. Evol.* 4, 1324–1330. doi: 10.1093/gbe/evs109

Yutin, N., and Koonin, E. V. (2012). Hidden evolutionary complexity of Nucleo-Cytoplasmic Large DNA viruses of eukaryotes. *Virol. J.* 9:161. doi: 10.1186/1743-422X-9-161

Yutin, N., Raoult, D., and Koonin, E. V. (2013). Virophages, polintons, and transpovirons: a complex evolutionary network of diverse selfish genetic elements with different reproduction strategies. *Virol. J.* 10:158. doi: 10.1186/1743-422X-10-158

Yutin, N., Wolf, Y. I., Raoult, D., and Koonin, E. V. (2009). Eukaryotic large nucleo-cytoplasmic DNA viruses: clusters of orthologous genes and reconstruction of viral genome evolution. *Virol. J.* 6:223. doi: 10.1186/1743-422X-6-223

Zauberman, N., Mutsafi, Y., Halevy, D. B., Shimoni, E., Klein, E., Xiao, C., et al. (2008). Distinct DNA exit and packaging portals in the virus *Acanthamoeba polyphaga* mimivirus. *PLoS Biol.* 6:e114. doi: 10.1371/journal.pbio.0060114

Zhou, J., Sun, D., Childers, A., Mcdermott, T. R., Wang, Y., and Liles, M. R. (2015). Three novel virophage genomes discovered from Yellowstone Lake metagenomes. *J. Virol.* 89, 1278–1285. doi: 10.1128/JVI.03039-14

Zhou, J., Zhang, W., Yan, S., Xiao, J., Zhang, Y., Li, B., et al. (2013). Diversity of virophages in metagenomic data sets. *J. Virol.* 87, 4225–4236. doi: 10.1128/JVI.03398-12

Conflict of Interest Statement: The authors declare that the research was conducted in the absence of any commercial or financial relationships that could be construed as a potential conflict of interest.

frontiers in Cellular and Infection Microbiology

MINI REVIEW
published: 22 March 2018
doi: 10.3389/fcimb.2018.00077

From Phagocytes to Immune Defense: Roles for Coronin Proteins in *Dictyostelium* and Mammalian Immunity

*Mayumi Mori, Ravindra Mode and Jean Pieters**

Biozentrum, University of Basel, Basel, Switzerland

Microbes have interacted with eukaryotic cells for as long as they have been co-existing. While many of these interactions are beneficial for both the microbe as well as the eukaryotic cell, several microbes have evolved into pathogenic species. For some of these pathogens, host cell invasion results in irreparable damage and thus host cell destruction, whereas others use the host to avoid immune detection and elimination. One of the latter pathogens is *Mycobacterium tuberculosis*, arguably one of the most notorious pathogens on earth. In mammalian macrophages, *M. tuberculosis* manages to survive within infected macrophages by avoiding intracellular degradation in lysosomes using a number of different strategies. One of these is based on the recruitment and phagosomal retention of the host protein coronin 1, that is a member of the coronin protein family and a mammalian homolog of coronin A, a protein identified in *Dictyostelium*. Besides mediating mycobacterial survival in macrophages, coronin 1 is also an important regulator of naïve T cell homeostasis. How, exactly, coronin 1 mediates its activity in immune cells remains unclear. While in lower eukaryotes coronins are involved in cytoskeletal regulation, the functions of the seven coronin members in mammals are less clear. *Dictyostelium* coronins may have maintained multiple functions, whereas the mammalian coronins may have evolved from regulators of the cytoskeleton to modulators of signal transduction. In this minireview, we will discuss the different studies that have contributed to understand the molecular and cellular functions of coronin proteins in mammals and *Dictyostelium.*

Keywords: coronins, *Dictyostelium discoideum*, Mycobacterium, phagocytes, immune cells

OPEN ACCESS

Edited by:
Sascha Thewes,
Freie Universität Berlin, Germany

Reviewed by:
Maria Isabel Colombo,
Universidad Nacional de Cuyo, Argentina
Barbara Walzog,
Ludwig-Maximilians-Universität München, Germany

****Correspondence:***
Jean Pieters
jean.pieters@unibas.ch

Received: *13 October 2017*
Accepted: *27 February 2018*
Published: *22 March 2018*

Citation:
Mori M, Mode R and Pieters J (2018) From Phagocytes to Immune Defense: Roles for Coronin Proteins in Dictyostelium and Mammalian Immunity. Front. Cell. Infect. Microbiol. 8:77. doi: 10.3389/fcimb.2018.00077

INTRODUCTION

All eukaryotes are surrounded by microorganisms that on the one hand fulfill important roles in providing symbiotic support for eukaryotic life, and at the same time can pose a threat in the form of virulent bacteria, causing infections, disease and death.

For both lower eukaryotes such as the amoeba *Dictyostelium discoideum*, as well as mammalian macrophages, the first encounter with microbes, especially bacteria, results in the activation of phagocytic processes leading to engulfment of the bacteria within phagosomes, followed by lysosomal digestion (Flannagan et al., 2012). When bacteria serve as nutrients, as is the case for *Dictyostelium*, lysosomal degradation will allow the availability of amino acids,

lipids, and other molecules that serve the need for *Dictyostelium* growth (Allen and Aderem, 1996). In case of bacteria being phagocytosed by mammalian cells such as dendritic cells and macrophages, the end point is usually inactivation of the pathogen, as well as presentation of pathogen fragments to the immune system in order to activate effector lymphocytes (T cells) for the generation of adaptive immune responses (Pieters, 2000; Blum et al., 2013).

Phagocytosis is an ancient and evolutionary conserved mechanism (Aderem and Underhill, 1999). Indeed, the basic mechanisms regulating the formation of a phagocytic cup, internalization of the bacteria and the transfer from phagosomes to lysosomes are conserved from lower eukaryotes such as *Dictyostelium* to mammalian phagocytes, including macrophages, neutrophils and dendritic cells. Phagocytosis involves cell surface recognition through different plasma membrane receptors that transmit signals through a variety of pathways to the cytoskeleton in order to allow plasma membrane deformation to accommodate the incoming particles/bacteria (Flannagan et al., 2012).

Virulence Strategies Employed by Pathogenic Microbes

Whereas the encounter of mammalian phagocytes with bacteria most often results in its destruction and activation of specific immunity, many pathogenic bacteria have evolved a diverse array of strategies to circumvent phagocytosis and lysosomal destruction. For example, several pathogens, including *Neisseria* spp., *Pseudomonas* spp., *Streptococcus* spp., and *Salmonella* spp. are known to avoid phagocytic uptake (Sarantis and Grinstein, 2012). Also, certain pathogens, including *Listeria* spp. and *Shigella* spp. are engulfed by phagocytic cells but rapidly transfer to the cytosol where they can proliferate and spread (Hamon et al., 2012; Mellouk and Enninga, 2016). Yet other bacilli such as *Brucella* spp. and *Salmonella* spp. enter the phagocyte through phagocytosis but divert to the endoplasmic reticulum (*Brucella* spp.) or the Golgi (*Salmonella* spp.) instead of being delivered to lysosomes (Celli and Gorvel, 2004; Escoll et al., 2016). Furthermore, some pathogens are phagocytosed and delivered to lysosomes and subsequently withstand the hostile environment of the lysosomal pathway through the release of neutralizing factors (Voth and Heinzen, 2007).

Several pathogens use more than one of these strategies to circumvent host cell destruction; in fact, one of the most notorious pathogens, *Mycobacterium tuberculosis*, has evolved multiple mechanisms to avoid killing by immune cells as well as recognition by the adaptive immune system. For example, *M. tuberculosis* manipulates the host ability to detect and internalize the bacilli through pathogen-associated molecular patterns (PAMPs) (Stamm et al., 2015). Also, once inside the host cell, *M. tuberculosis* uses a range of strategies to avoid destruction, including manipulation of V-ATPase levels to avoid lysosomal acidification (Rohde et al., 2007), expression of genes that allow the bacilli to withstand the low pH of the endosomal/lysosomal pathway (Vandal et al., 2008), neutralizing reactive nitrogen and oxygen species (Shiloh and Nathan, 2000), resisting delivery to autophagosomes (Deretic, 2005; Romagnoli et al., 2012), counter-balancing iron depletion encountered upon phagocytosis (Weiss and Schaible, 2015) and interfering with lysosomal delivery following phagocytosis (Pieters, 2008; Gengenbacher and Kaufmann, 2012).

Inhibition of lysosomal delivery is an important trait of pathogenic mycobacteria, and the bacilli devote considerable efforts toward achieving that goal (Rohde et al., 2007; Pieters, 2008). This is achieved through the release of molecules, both signaling molecules, lipids and proteins (Cowley et al., 2004; Walburger et al., 2004; Hmama et al., 2015; Lovewell et al., 2016), as well as through the recruitment of host factors allowing mycobacterial escape from lysosomal degradation.

Role for Coronin 1 in the Interaction of *M. tuberculosis* With Macrophages

One of the host proteins co-opted by *M. tuberculosis* to avoid lysosomal killing is coronin 1 (encoded by the *coro1a* gene; for a discussion on the coronin nomenclature see; Pieters et al., 2013), a ∼51 kD protein that is located in the macrophage cytosol and cell cortex. Coronin 1, also known as P57 or TACO, for Tryptophan Aspartate containing Coat protein, was identified in a search for host components potentially involved in the intracellular survival of mycobacteria within macrophages (Ferrari et al., 1999). Coronin 1 is a member of the highly conserved family of coronin proteins whose members are expressed across the eukaryotic kingdom and are characterized by the presence of a central WD (tryptophan-aspartate) 40 repeat that in coronin 1-folds in a 7-bladed beta propeller (Suzuki et al., 1995; Okumura et al., 1998; Gatfield et al., 2005; Appleton et al., 2006). Coronin 1 is highly expressed in all hematopoietic cells as well as to a lower degree in neurons (Ferrari et al., 1999; Nal et al., 2004; Jayachandran et al., 2014). Upon entry of pathogenic mycobacteria into macrophages, coronin 1 is retained on phagosomes containing viable, but not killed mycobacteria and its retention on phagosomes prevents intracellular killing of *M. tuberculosis* through activation of the Ca^{2+}/calcineurin pathway (Jayachandran et al., 2007). Apart from *M. tuberculosis*, *M. leprae* as well as virulent *H. pylori* recruit coronin 1 to their intracellular niche, although the exact consequences of coronin 1 retention for pathogen survival in these latter cases remain unclear (Zheng and Jones, 2003; Suzuki et al., 2006).

CORONINS IN DICTYOSTELIUM

Coronin was initially isolated as a 55 kD actin/myosin-interacting molecule from *Dictyostelium discoideum* lysates (de Hostos et al., 1991). Subsequently, it was realized that *Dictyostelium* also expresses a so-called "tandem" coronin containing a duplicated tryptophan-aspartate repeat-containing region, now referred to as coronin B (Shina et al., 2010). Coronin B assembles with actin and deletion of this coronin in *Dictyostelium* was shown to both enhance as well as reduce phagocytosis, dependent on the particles to be internalized (Shina et al., 2010). Coronin B was proposed to act upstream of the suppressor of cAMP receptor (SCAR) and Wiskott-Aldrich syndrome protein

(WASp) (Swaminathan et al., 2015) which connect signals from G protein-coupled receptors and cell surface tyrosine receptors to the actin cytoskeleton, respectively (Bear et al., 1998; Pollitt and Insall, 2009).

In *Dictyostelium*, coronin A is involved in a diverse array of activities, including cell motility, cAMP-mediated chemotaxis, and cytokinesis (de Hostos et al., 1993; Nagasaki et al., 2002). Given the initial isolation of coronin A with actin/myosin, the roles for coronin A in the above-mentioned activities have been attributed to the capacity of *Dictyostelium* coronin A in modulating the F-actin cytoskeleton. Coronin A is localized within regions of actin turnover (Maniak et al., 1995; Heinrich et al., 2008), leading to the conclusion that *Dictyostelium* coronin A is a regulator of the F-actin cytoskeleton, thereby modulating chemotaxis, cell motility and cytokinesis; it should however be noted that *Dictyostelium* lacking coronin A do not show an obvious alteration in the assembly or localization of actin filaments (de Hostos et al., 1993). Separate work using yeast coronin (Crn1) has shown that while deletion of yeast Crn1 does not result in an aberrant F-actin cytoskeleton (Heil-Chapdelaine et al., 1998; Goode et al., 1999), Crn1 binds to and bundles F-actin *in vitro* (Goode et al., 1999) as well as can modulate F-actin polymerization either positively (Liu et al., 2011) or negatively (Humphries et al., 2002) in an actin-related protein 2/3 (ARP2/3) complex-dependent manner. Indeed, yeast Crn1 possesses a number of regions of homology with actin- and tubulin-binding proteins, including microtubule- and F-actin/ARP2/3-interacting domains (Liu et al., 2011), that are lacking in most other coronins (Eckert et al., 2011).

More recent work that revisited the role for coronin A in *Dictyostelium* found that coronin A is important for the initiation of multicellular differentiation following deprivation of nutrients (Vinet et al., 2014); in *Dictyostelium*, nutrient starvation induces the aggregation of individual amoebae into a multicellular structure ultimately forming a fruiting body. Such aggregation is mediated by the second messenger cAMP, that functions both as a chemoattractant as well as an intracellular signal mediating gene transcription. Aggregation is initiated by cell density and nutrient-sensing factors released by the starving culture that induce the expression of genes involved in multicellular aggregation (Devreotes, 1989; Loomis, 2014). It was found that coronin A plays an essential role in the initiation of this developmental program by being involved in the response to factors secreted during the transition from growth to development of the cells. Since application of cAMP to coronin A-deficient cells is sufficient to restore chemotaxis and multicellular aggregation, coronin A appears to be dispensable for the cAMP relay as well as for processes downstream of cAMP. Also, the fact that folate chemotaxis occurs normally in the absence of coronin A argues against an exclusive role for coronin A in cytoskeletal remodeling (Vinet et al., 2014). Furthermore, consistent with earlier results showing that F-actin rearrangement is not required for the initiation of cAMP signaling (Parent et al., 1998; Kriebel et al., 2008), coronin A-dependent induction of genes required for development such as *aca* and *carA* does not require F-actin-based rearrangement (Vinet et al., 2014).

These data suggests that instead of modulating F-actin, coronin A is responsible for the sensing of factors secreted in the conditioned medium (Vinet et al., 2014). Coronin A may function downstream of conditioned medium factor (CMF) (Jain et al., 1992; Yuen et al., 1995), or possibly other, as yet undefined factors that are essential for the initiation of cAMP-dependent chemotaxis and aggregation. Whether the motility and cytokinesis defects observed upon coronin A deletion (de Hostos et al., 1993; Vinet et al., 2014) are related to a possible function of coronin A in the modulation of the cAMP pathway or linked to a role for coronin A in F-actin-mediated processes remains to be clarified. In this context, it is interesting to note that in *Dictyostelium*, myosin-independent cytokinesis (one of the two types of cytokinesis, the other one being myosin-II-dependent, see Nagasaki et al., 2002; Li, 2007) has been linked to both coronin A as well as AmiA (also known as Pianissimo, a target of rapamycin complex (TORC) 2-associated protein) that in *Dictyostelium* is a cytosolic regulator of adenylate cyclase (Pergolizzi et al., 2002). Furthermore, recent work implicated coronin A in regulating the availability of GTP-Rac through a domain with homology to a Cdc42- and Rac-interactive binding (CRIB) motif for activation of downstream effectors, thereby being responsible for myosin II disassembly (Swaminathan et al., 2014). Interestingly, this CRIB-like domain was found to be dispensable for the role of coronin A in cytokinesis, since expression of a mutant coronin A lacking Rac binding activity rescued the cytokinesis defect of coronin A-deficient cells (Swaminathan et al., 2014). This suggest that coronin A domains distinct from the CRIB-like motif are involved in the regulation of cytokinesis.

The precise role for *Dictyostelium* coronins in the modulation of bacterial uptake and survival is less clear. A role for coronin A in phagocytosis appears to be dependent on the type of cargo that is internalized; upon coronin A deletion, phagocytosis of *E. coli* and yeast particles is reduced, while uptake of *Mycobacterium marinum* is enhanced (Maniak et al., 1995; Solomon et al., 2003). Also, it should be noted that yeast phagocytosis is increased upon coronin B deletion (Shina et al., 2011). Furthermore, while coronin A becomes enriched on newly formed phagosomes, it is rapidly dissociated once the bacteria have been fully internalized (Maniak et al., 1995; Rauchenberger et al., 1997; Lu and Clarke, 2005; Hagedorn and Soldati, 2007). For both *M. marinum* as well as *Legionella pneumonia*, deletion of coronin A renders *Dictyostelium* more permissive for intracellular bacterial growth (Solomon et al., 2000, 2003). These data suggest that in *Dictyostelium* coronin A may play a protective role for the host, although the mechanisms involved remain unclear.

CORONIN 1 FUNCTION IN MAMMALIAN LEUKOCYTES

As described above, in resting macrophages, the only role for coronin 1 appears to be the modulation of the intracellular trafficking and survival of *M. tuberculosis* (Jayachandran et al., 2007, 2008). Given the proposed role for *Dictyostelium* coronin A in the modulation of F-actin-dependent processes such as

chemotaxis and cytokinesis, it was initially anticipated that its mammalian homolog in macrophages, coronin 1, also modulates F-actin. However, in macrophages depleted for coronin 1 either by short interference (si)RNA or gene ablation, actin-dependent functions appear to be unperturbed as judged by the analysis of cell motility, macropinocytosis and membrane ruffling (Jayachandran et al., 2007, 2008). In contrast to studies using macrophages from coronin 1-deficient mice (Jayachandran et al., 2007) or J774 macrophages depleted for coronin 1 by siRNA (Jayachandran et al., 2008), TAT-mediated transduction of the WD repeat domain of coronin 1 in RAW 264.7 macrophages and neutrophils was shown to affect early phagocytosis (Yan et al., 2005, 2007); this may reflect differences in the experimental setup (such as time to allow uptake) or differential requirements for coronin 1 in phagocytosis in different macrophage and/or cell types; alternatively, especially given the propensity of coronin 1 mutants to cause aggregation, the introduction of misfolded protein domains may compromise cellular functions such as chemotaxis and phagocytosis (Gatfield et al., 2005). Whereas coronin 1 does not appear to be required for the functionality of resting macrophages, during an inflammatory stimulus coronin 1 is responsible for reprogramming the uptake pathway from phagocytosis to macropinocytosis in order to rapidly eliminate pathogens, a function that is dependent on activation of phosphoinositol (PI)-3-kinase (Bosedasgupta and Pieters, 2014). Furthermore, coronin 1 is largely dispensable for the functioning of B cells, mast cells, dendritic cells and natural killer cells, although the latter have been described to be affected by coronin 1 mutation in human (Moshous et al., 2013; Mace and Orange, 2014; Jayachandran and Pieters, 2015; Tchang et al., 2017). Also, coronin 1 was found to be dispensable for neutrophil function and recruitment in an *in vivo* model of liver injury and concanavanin A-induced hepatitis (Combaluzier and Pieters, 2009; Siegmund et al., 2013); in humans, coronin 1 has been associated with neutrophil survival and recent work has implicated coronin 1 in integrin-mediated functioning (Moriceau et al., 2009; Pick et al., 2017).

The in-depth analysis of coronin 1-deficient mice revealed that besides protecting intracellular mycobacteria from degradation within macrophages, a major function of coronin 1 is to regulate peripheral naïve T cell homeostasis; upon depletion of coronin 1, naïve T cells are virtually absent despite a normal development and selection in the thymus (Föger et al., 2006; Haraldsson et al., 2008; Mueller et al., 2008; Shiow et al., 2008; Lang et al., 2017). The role for coronin 1 in maintaining peripheral naïve T cells is conserved in humans: deletion or mutation of the *coro1a* gene has been reported to result in a selective depletion of naïve T cells (Moshous et al., 2013; Yee et al., 2016), or, when *coro1a* deletion or mutation is combined with other genetic aberrations, in more complex phenotypes including B and NK cell deficits besides the naïve T cell depletion (Shiow et al., 2009; Mace and Orange, 2014; Stray-Pedersen et al., 2014; Punwani et al., 2015; Yee et al., 2016). The mechanism underlying coronin 1-dependent naïve T cell survival remains controversial; in one study, coronin 1 was suggested to modulate the F-actin cytoskeleton, thereby regulating T cell survival (Föger et al., 2006); however, separate studies showed that altered F-actin levels do not correlate with T cell viability nor are other actin-dependent leukocyte functions affected by coronin 1 deletion (Jayachandran et al., 2007; Mueller et al., 2011). Instead, coronin 1-deficient T cells were shown to be unable to respond to a range of T cell stimuli and the defect was narrowed down to be at the level of activation of the Ca^{2+}/calcineurin pathway (Haraldsson et al., 2008; Mueller et al., 2008).

Further analysis of mice lacking coronin 1 revealed an important function of this coronin family member in neurons, where it regulates Ca^{2+}- and cAMP-dependent signaling thereby modulating various neuronal activities, including cognition and behavior as well as target innervation (Jayachandran et al., 2014; Suo et al., 2014). It is also interesting to note that *M. tuberculosis* is known to subvert host cAMP signaling (Agarwal et al., 2009), and retention of coronin 1 at the phagosomal membrane may be part of this strategy. Whether and how Ca^{2+} and cAMP signaling are interconnected and whether coronin 1-dependent cAMP signaling plays a role in T cell homeostasis and mycobacterial survival within macrophages remains to be analyzed.

A CONCERTED ROLE FOR CORONINS IN *DICTYOSTELIUM* AND MAMMALS?

The available information on the role for coronins in *Dictyostelium* and mammals suggests that these proteins play diverse roles in a number of physiological processes. The hallmark of all coronin protein family members is their central WD40 repeat, that folds into a beta propeller structure. Beta-propellers, also known as beta-transducin repeats, form structural domains that are involved in protein-protein interaction (Smith, 2008). Both in *Dictyostelium* as well as in mammalian cells, several coronin family members colocalize with and are associated with actin (de Hostos et al., 1991; Shina et al., 2010; Pieters et al., 2013) whereas for a number of mammalian coronin proteins (coronin 2, 5, and 7) actin binding remains unclear (see e.g., Rybakin et al., 2004; Cai et al., 2007). It of course remains possible, especially in mammals with up to 7 coronin molecules being expressed, that the role for coronins in actin rearrangement is redundant and therefore single deletions may not result in an actin-dependent phenotype. On the other hand, it could be that the interaction of coronin molecules with the actin cytoskeleton ensures a local source of coronin molecules to allow conversion of extracellular signals into local changes in the cortical actin cytoskeleton (Wang et al., 1998; Eichinger et al., 1999; Gatfield et al., 2005). Such a role for coronins is consistent not only with their sequence as well as structural homology with the beta subunit of trimeric G proteins that function downstream of G protein-coupled receptor molecules (de Hostos et al., 1991; Gatfield et al., 2005; Appleton et al., 2006), but also with the activities of *Dictyostelium* coronin A and mammalian coronin 1 in the modulation of Ca^{2+}- and cAMP-dependent signal transduction pathways (Jayachandran et al., 2014; Suo et al., 2014; Vinet et al., 2014). Also, recent work linking coronins to the activation of small GTP binding proteins, that are well known regulators of the actin cytoskeleton (Berzat and Hall, 2010; Castro-Castro et al., 2011; Swaminathan et al., 2014), suggests

that coronins may be placed upstream of F-actin reorganization. Interestingly, in both *Dictyostelium* as well as mammalian cells, the role for coronin in the activation of Ca^{2+}/cAMP signaling could be separated from a potential involvement in F-actin rearrangement (Mueller et al., 2007, 2011; Jayachandran et al., 2014; Vinet et al., 2014). How, exactly, coronin molecules are being regulated is unknown. Also, the molecules upstream of coronin 1 possibly involved in the sensing of extracellular signals remain to be identified. In light of the here described roles for mammalian and *Dictyostelium* coronins in the trafficking and survival of intracellular pathogens, elucidation of these upstream receptor molecules may also shed light on the intricate relationship of pathogenic microbes and their eukaryotic hosts.

AUTHOR CONTRIBUTIONS

All authors listed have made a substantial, direct and intellectual contribution to the work, and approved it for publication.

ACKNOWLEDGMENTS

We thank Rajesh Jayachadran and Tohnyui Ndinyanka Fabrice for critical comments on the manuscript. Work in the Pieters Laboratory is supported by the Swiss National Science Foundation, the Swiss Multiple Sclerosis Society, the Novartis Foundation for Medical-Biological Research, the Gebert Ruef Foundation and the Canton of Basel.

REFERENCES

Aderem, A., and Underhill, D. M. (1999). Mechanisms of phagocytosis in macrophages. *Annu. Rev. Immunol.* 17, 593–623. doi: 10.1146/annurev.immunol.17.1.593

Agarwal, N., Lamichhane, G., Gupta, R., Nolan, S., and Bishai, W. R. (2009). Cyclic AMP intoxication of macrophages by a *Mycobacterium tuberculosis* adenylate cyclase. *Nature* 460, 98–102. doi: 10.1038/nature08123

Allen, L. A., and Aderem, A. (1996). Mechanisms of phagocytosis. *Curr. Opin. Immunol.* 8, 36–40. doi: 10.1016/S0952-7915(96)80102-6

Appleton, B. A., Wu, P., and Wiesmann, C. (2006). The crystal structure of murine coronin-1: a regulator of actin cytoskeletal dynamics in lymphocytes. *Structure* 14, 87–96. doi: 10.1016/j.str.2005.09.013

Bear, J. E., Rawls, J. F., and Saxe, C. L. III. (1998). SCAR, a WASP-related protein, isolated as a suppressor of receptor defects in late Dictyostelium development. *J. Cell Biol.* 142, 1325–1335. doi: 10.1083/jcb.142.5.1325

Berzat, A., and Hall, A. (2010). Cellular responses to extracellular guidance cues. *EMBO J.* 29, 2734–2745. doi: 10.1038/emboj.2010.170

Blum, J. S., Wearsch, P. A., and Cresswell, P. (2013). Pathways of antigen processing. *Annu. Rev. Immunol.* 31, 443–473. doi: 10.1146/annurev-immunol-032712-095910

Bosedasgupta, S., and Pieters, J. (2014). Inflammatory stimuli reprogram macrophage phagocytosis to macropinocytosis for the rapid elimination of pathogens. *PLoS Pathog.* 10:e1003879. doi: 10.1371/journal.ppat.1003879

Cai, L., Marshall, T. W., Uetrecht, A. C., Schafer, D. A., and Bear, J. E. (2007). Coronin 1B coordinates Arp2/3 complex and cofilin activities at the leading edge. *Cell* 128, 915–929. doi: 10.1016/j.cell.2007.01.031

Castro-Castro, A., Ojeda, V., Barreira, M., Sauzeau, V., Navarro-Lérida, I., Muriel, O., et al. (2011). Coronin 1A promotes a cytoskeletal-based feedback loop that facilitates Rac1 translocation and activation. *EMBO J.* 30, 3913-3927. doi: 10.1038/emboj.2011.310

Celli, J., and Gorvel, J. P. (2004). Organelle robbery: brucella interactions with the endoplasmic reticulum. *Curr. Opin. Microbiol.* 7, 93–97. doi: 10.1016/j.mib.2003.11.001

Combaluzier, B., and Pieters, J. (2009). Chemotaxis and phagocytosis in neutrophils is independent of coronin 1. *J. Immunol.* 182, 2745–2752. doi: 10.4049/jimmunol.0801812

Cowley, S., Ko, M., Pick, N., Chow, R., Downing, K. J., Gordhan, B. G., et al. (2004). The *Mycobacterium tuberculosis* protein serine/threonine kinase PknG is linked to cellular glutamate/glutamine levels and is important for growth *in vivo*. *Mol. Microbiol.* 52, 1691–1702. doi: 10.1111/j.1365-2958.2004.04085.x

de Hostos, E. L., Bradtke, B., Lottspeich, F., Guggenheim, R., and Gerisch, G. (1991). Coronin, an actin binding protein of *Dictyostelium discoideum* localized to cell surface projections, has sequence similarities to G protein beta subunits. *EMBO J.* 10, 4097–4104.

de Hostos, E. L., Rehfuess, C., Bradtke, B., Waddell, D. R., Albrecht, R., Murphy, J., et al. (1993). Dictyostelium mutants lacking the cytoskeletal protein coronin are defective in cytokinesis and cell motility. *J. Cell Biol.* 120, 163–173. doi: 10.1083/jcb.120.1.163

Deretic, V. (2005). Autophagy in innate and adaptive immunity. *Trends Immunol.* 26, 523–528. doi: 10.1016/j.it.2005.08.003

Devreotes, P. (1989). *Dictyostelium discoideum*: a model system for cell-cell interactions in development. *Science* 245, 1054–1058. doi: 10.1126/science.2672337

Eckert, C., Hammesfahr, B., and Kollmar, M. (2011). A holistic phylogeny of the coronin gene family reveals an ancient origin of the tandem-coronin, defines a new subfamily, and predicts protein function. *BMC Evol. Biol.* 11:268. doi: 10.1186/1471-2148-11-268

Eichinger, L., Lee, S. S., and Schleicher, M. (1999). Dictyostelium as model system for studies of the actin cytoskeleton by molecular genetics. *Microsc. Res. Tech.* 47, 124–134. doi: 10.1002/(SICI)1097-0029(19991015)47:2<124::AID-JEMT5>3.0.CO;2-8

Escoll, P., Mondino, S., Rolando, M., and Buchrieser, C. (2016). Targeting of host organelles by pathogenic bacteria: a sophisticated subversion strategy. *Nat. Rev. Microbiol.* 14, 5–19. doi: 10.1038/nrmicro.2015.1

Ferrari, G., Langen, H., Naito, M., and Pieters, J. (1999). A coat protein on phagosomes involved in the intracellular survival of mycobacteria. *Cell* 97, 435–447.

Flannagan, R. S., Jaumouillé, V., and Grinstein, S. (2012). The cell biology of phagocytosis. *Annu. Rev. Pathol.* 7, 61–98. doi: 10.1146/annurev-pathol-011811-132445.

Föger, N., Rangell, L., Danilenko, D. M., and Chan, A. C. (2006). Requirement for coronin 1 in T lymphocyte trafficking and cellular homeostasis. *Science* 313, 839–842. doi: 10.1126/science.1130563

Gatfield, J., Albrecht, I., Zanolari, B., Steinmetz, M. O., and Pieters, J. (2005). Association of the leukocyte plasma membrane with the actin cytoskeleton through coiled coil-mediated trimeric coronin 1 molecules. *Mol. Biol. Cell* 16, 2786–2798. doi: 10.1091/mbc.E05-01-0042

Gengenbacher, M., and Kaufmann, S. H. (2012). *Mycobacterium tuberculosis*: success through dormancy. *FEMS Microbiol. Rev.* 36, 514–532. doi: 10.1111/j.1574-6976.2012.00331.x.

Goode, B. L., Wong, J. J., Butty, A. C., Peter, M., McCormack, A. L., Yates, J. R., et al. (1999). Coronin promotes the rapid assembly and cross-linking of actin filaments and may link the actin and microtubule cytoskeletons in yeast. *J. Cell Biol.* 144, 83–98. doi: 10.1083/jcb.144.1.83

Hagedorn, M., and Soldati, T. (2007). Flotillin and RacH modulate the intracellular immunity of Dictyostelium to *Mycobacterium marinum* infection. *Cell. Microbiol.* 9, 2716–2733. doi: 10.1111/j.1462-5822.2007.00993.x

Hamon, M. A., Ribet, D., Stavru, F., and Cossart, P. (2012). Listeriolysin O: the Swiss army knife of Listeria. *Trends Microbiol.* 20, 360–368. doi: 10.1016/j.tim.2012.04.006

Haraldsson, M. K., Louis-Dit-Sully, C. A., Lawson, B. R., Sternik, G., Santiago-Raber, M. L., Gascoigne, N. R., et al. (2008). The lupus-related Lmb3 locus contains a disease-suppressing Coronin-1A gene mutation. *Immunity* 28, 40–51. doi: 10.1016/j.immuni.2007.11.023

Heil-Chapdelaine, R. A., Tran, N. K., and Cooper, J. A. (1998). The role of Saccharomyces cerevisiae coronin in the actin and microtubule cytoskeletons. *Curr. Biol.* 8, 1281–1284. doi: 10.1016/S0960-9822(07)00539-8

Heinrich, D., Youssef, S., Schroth-Diez, B., Engel, U., Aydin, D., Blümmel, J., et al. (2008). Actin-cytoskeleton dynamics in non-monotonic cell spreading. *Cell Adh. Migr.* 2, 58–68. doi: 10.4161/cam.2.2.6190

Hmama, Z., Peña-Díaz, S., Joseph, S., and Av-Gay, Y. (2015). Immunoevasion and immunosuppression of the macrophage by *Mycobacterium tuberculosis*. *Immunol. Rev.* 264, 220–232. doi: 10.1111/imr.12268

Humphries, C. L., Balcer, H. I., D'Agostino, J. L., Winsor, B., Drubin, D. G., Barnes, G., et al. (2002). Direct regulation of Arp2/3 complex activity and function by the actin binding protein coronin. *J. Cell Biol.* 159, 993–1004. doi: 10.1083/jcb.200206113

Jain, R., Yuen, I. S., Taphouse, C. R., and Gomer, R. H. (1992). A density-sensing factor controls development in Dictyostelium. *Genes Dev.* 6, 390–400. doi: 10.1101/gad.6.3.390

Jayachandran, R., Gatfield, J., Massner, J., Albrecht, I., Zanolari, B., and Pieters, J. (2008). RNA interference in J774 macrophages reveals a role for coronin 1 in mycobacterial trafficking but not in actin-dependent processes. *Mol. Biol. Cell* 19, 1241–1251. doi: 10.1091/mbc.E07-07-0640

Jayachandran, R., Liu, X., Bosedasgupta, S., Müller, P., Zhang, C. L., Moshous, D., et al. (2014). Coronin 1 regulates cognition and behavior through modulation of cAMP/protein kinase A signaling. *PLoS Biol.* 12:e1001820. doi: 10.1371/journal.pbio.1001820

Jayachandran, R., and Pieters, J. (2015). Regulation of immune cell homeostasis and function by coronin 1. *Int. Immunopharmacol.* 28, 825–828. doi: 10.1016/j.intimp.2015.03.045.

Jayachandran, R., Sundaramurthy, V., Combaluzier, B., Mueller, P., Korf, H., Huygen, K., et al. (2007). Survival of mycobacteria in macrophages is mediated by coronin 1-dependent activation of calcineurin. *Cell* 130, 37–50. doi: 10.1016/j.cell.2007.04.043

Kriebel, P. W., Barr, V. A., Rericha, E. C., Zhang, G., and Parent, C. A. (2008). Collective cell migration requires vesicular trafficking for chemoattractant delivery at the trailing edge. *J. Cell Biol.* 183, 949–961. doi: 10.1083/jcb.200808105

Lang, M. J., Mori, M., Ruer-Laventie, J., and Pieters, J. (2017). A coronin 1-dependent decision switch in juvenile mice determines the population of the peripheral naive T cell compartment. *J. Immunol.* 199, 2421–2431. doi: 10.4049/jimmunol.1700438

Li, R. (2007). Cytokinesis in development and disease: variations on a common theme. *Cell. Mol. Life Sci.* 64, 3044–3058. doi: 10.1007/s00018-007-7285-6

Liu, S. L., Needham, K. M., May, J. R., and Nolen, B. J. (2011). Mechanism of a concentration-dependent switch between activation and inhibition of Arp2/3 complex by coronin. *J. Biol. Chem.* 286, 17039–17046. doi: 10.1074/jbc.M111.219964

Loomis, W. F. (2014). Cell signaling during development of Dictyostelium. *Dev. Biol.* 391, 1–16. doi: 10.1016/j.ydbio.2014.04.001

Lovewell, R. R., Sassetti, C. M., and VanderVen, B. C. (2016). Chewing the fat: lipid metabolism and homeostasis during *M. tuberculosis* infection. *Curr. Opin. Microbiol.* 29, 30–36. doi: 10.1016/j.mib.2015.10.002

Lu, H., and Clarke, M. (2005). Dynamic properties of Legionella-containing phagosomes in Dictyostelium amoebae. *Cell. Microbiol.* 7, 995–1007. doi: 10.1111/j.1462-5822.2005.00528.x

Mace, E. M., and Orange, J. S. (2014). Lytic immune synapse function requires filamentous actin deconstruction by Coronin 1A. *Proc. Natl. Acad. Sci. U.S.A.* 111, 6708–6713. doi: 10.1073/pnas.1314975111

Maniak, M., Rauchenberger, R., Albrecht, R., Murphy, J., and Gerisch, G. (1995). Coronin involved in phagocytosis: dynamics of particle-induced relocalization visualized by a green fluorescent protein Tag. *Cell* 83, 915–924. doi: 10.1016/0092-8674(95)90207-4

Mellouk, N., and Enninga, J. (2016). Cytosolic access of intracellular bacterial pathogens: the shigella paradigm. *Front. Cell. Infect. Microbiol.* 6:35. doi: 10.3389/fcimb.2016.00035

Moriceau, S., Kantari, C., Mocek, J., Davezac, N., Gabillet, J., Guerrera, I. C., et al. (2009). Coronin-1 is associated with neutrophil survival and is cleaved during apoptosis: potential implication in neutrophils from cystic fibrosis patients. *J. Immunol.* 182, 7254–7263. doi: 10.4049/jimmunol.0803312

Moshous, D., Martin, E., Carpentier, W., Lim, A., Callebaut, I., Canioni, D., et al. (2013). Whole-exome sequencing identifies Coronin-1A deficiency in 3 siblings with immunodeficiency and EBV-associated B-cell lymphoproliferation. *J. Allergy Clin. Immunol.* 131, 1594–1603. doi: 10.1016/j.jaci.2013.01.042

Mueller, P., Liu, X., and Pieters, J. (2011). Migration and homeostasis of naive T cells depends on coronin 1-mediated prosurvival signals and not on coronin 1-dependent filamentous actin modulation. *J. Immunol.* 186, 4039–4050. doi: 10.4049/jimmunol.1003352

Mueller, P., Massner, J., Jayachandran, R., Combaluzier, B., Albrecht, I., Gatfield, J., et al. (2008). Regulation of T cell survival through coronin-1-mediated generation of inositol-1,4,5-trisphosphate and calcium mobilization after T cell receptor triggering. *Nat. Immunol.* 9, 424–431. doi: 10.1038/ni1570

Mueller, P., Quintana, A., Griesemer, D., Hoth, M., and Pieters, J. (2007). Disruption of the cortical actin cytoskeleton does not affect store operated Ca^{2+} channels in human T-cells. *FEBS Lett.* 581, 3557–3562. doi: 10.1016/j.febslet.2007.06.068

Nagasaki, A., de Hostos, E. L., and Uyeda, T. Q. (2002). Genetic and morphological evidence for two parallel pathways of cell-cycle-coupled cytokinesis in Dictyostelium. *J. Cell Sci.* 115(Pt 10), 2241–2251.

Nal, B., Carroll, P., Mohr, E., Verthuy, C., Da Silva, M. I., Gayet, O., et al. (2004). Coronin-1 expression in T lymphocytes: insights into protein function during T cell development and activation. *Int. Immunol.* 16, 231–240. doi: 10.1093/intimm/dxh022

Okumura, M., Kung, C., Wong, S., Rodgers, M., and Thomas, M. L. (1998). Definition of family of coronin-related proteins conserved between humans and mice: close genetic linkage between coronin-2 and CD45-associated protein. *DNA Cell Biol.* 17, 779–787. doi: 10.1089/dna.1998.17.779

Parent, C. A., Blacklock, B. J., Froehlich, W. M., Murphy, D. B., and Devreotes, P. N. (1998). G protein signaling events are activated at the leading edge of chemotactic cells. *Cell* 95, 81–91.

Pergolizzi, B., Peracino, B., Silverman, J., Ceccarelli, A., Noegel, A., Devreotes, P., et al. (2002). Temperature-sensitive inhibition of development in Dictyostelium due to a point mutation in the piaA gene. *Dev. Biol.* 251, 18–26. doi: 10.1006/dbio.2002.0809

Pick, R., Begandt, D., Stocker, T. J., Salvermoser, M., Thome, S., Böttcher, R. T., et al. (2017). Coronin 1A, a novel player in integrin biology, controls neutrophil trafficking in innate immunity. *Blood* 130, 847–858. doi: 10.1182/blood-2016-11-749622

Pieters, J. (2000). MHC class II-restricted antigen processing and presentation. *Adv. Immunol.* 75, 159–208. doi: 10.1016/S0065-2776(00)75004-8

Pieters, J. (2008). *Mycobacterium tuberculosis* and the macrophage: maintaining a balance. *Cell Host Microbe* 3, 399–407. doi: 10.1016/j.chom.2008.05.006

Pieters, J., Müller, P., and Jayachandran, R. (2013). On guard: coronin proteins in innate and adaptive immunity. *Nat. Rev. Immunol.* 13, 510–518. doi: 10.1038/nri3465

Pollitt, A. Y., and Insall, R. H. (2009). WASP and SCAR/WAVE proteins: the drivers of actin assembly. *J. Cell Sci.* 122(Pt 15), 2575–2578. doi: 10.1242/jcs.023879

Punwani, D., Pelz, B., Yu, J., Arva, N. C., Schafernak, K., Kondratowicz, K., et al. (2015). Coronin-1A: immune deficiency in humans and mice. *J. Clin. Immunol.* 35, 100–107. doi: 10.1007/s10875-015-0130-z.

Rauchenberger, R., Hacker, U., Murphy, J., Niewöhner, J., and Maniak, M. (1997). Coronin and vacuolin identify consecutive stages of a late, actin-coated endocytic compartment in Dictyostelium. *Curr. Biol.* 7, 215–218. doi: 10.1016/S0960-9822(97)70093-9

Rohde, K., Yates, R. M., Purdy, G. E., and Russell, D. G. (2007). *Mycobacterium tuberculosis* and the environment within the phagosome. *Immunol. Rev.* 219, 37–54. doi: 10.1111/j.1600-065X.2007.00547.x

Romagnoli, A., Etna, M. P., Giacomini, E., Pardini, M., Remoli, M. E., Corazzari, M., et al. (2012). ESX-1 dependent impairment of autophagic flux by *Mycobacterium tuberculosis* in human dendritic cells. *Autophagy* 8, 1357–1370. doi: 10.4161/auto.20881

Rybakin, V., Stumpf, M., Schulze, A., Majoul, I. V., Noegel, A. A., and Hasse, A. (2004). Coronin 7, the mammalian POD-1 homologue, localizes to the Golgi apparatus. *FEBS Lett.* 573, 161–167. doi: 10.1016/j.febslet.2004.07.066

Sarantis, H., and Grinstein, S. (2012). Subversion of phagocytosis for pathogen survival. *Cell Host Microbe* 12, 419–431. doi: 10.1016/j.chom.2012.09.001

Shiloh, M. U., and Nathan, C. F. (2000). Reactive nitrogen intermediates and the pathogenesis of Salmonella and mycobacteria. *Curr. Opin. Microbiol.* 3, 35–42. doi: 10.1016/S1369-5274(99)00048-X

Shina, M. C., Müller-Taubenberger, A., Unal, C., Schleicher, M., Steinert, M., Eichinger, L., et al. (2011). Redundant and unique roles of coronin proteins in Dictyostelium. *Cell. Mol. Life Sci. CMLS* 68, 303–313. doi: 10.1007/s00018-010-0455-y

Shina, M. C., Unal, C., Eichinger, L., Muller-Taubenberger, A., Schleicher, M., Steinert, M., et al. (2010). A Coronin7 homolog with functions in actin-driven processes. *J. Biol. Chem.* 285, 9249–9261. doi: 10.1074/jbc.M109.083725

Shiow, L. R., Paris, K., Akana, M. C., Cyster, J. G., Sorensen, R. U., and Puck, J. M. (2009). Severe combined immunodeficiency (SCID) and attention deficit hyperactivity disorder (ADHD) associated with a Coronin-1A mutation and a chromosome 16p11.2 deletion. *Clin. Immunol.* 131, 24–30. doi: 10.1016/j.clim.2008.11.002

Shiow, L. R., Roadcap, D. W., Paris, K., Watson, S. R., Grigorova, I. L., Lebet, T., et al. (2008). The actin regulator coronin 1A is mutant in a thymic egress-deficient mouse strain and in a patient with severe combined immunodeficiency. *Nat. Immunol.* 9, 1307–1315. doi: 10.1038/ni.1662

Siegmund, K., Lee, W. Y., Tchang, V. S., Stiess, M., Terracciano, L., Kubes, P., et al. (2013). Coronin 1 is dispensable for leukocyte recruitment and liver injury in concanavalin A-induced hepatitis. *Immunol. Lett.* 153, 62–70. doi: 10.1016/j.imlet.2013.06.005

Smith, T. F. (2008). Diversity of WD-repeat proteins. *Subcell. Biochem.* 48, 20–30. doi: 10.1007/978-0-387-09595-0_3.

Solomon, J. M., Leung, G. S., and Isberg, R. R. (2003). Intracellular replication of *Mycobacterium marinum* within *Dictyostelium discoideum*: efficient replication in the absence of host coronin. *Infect. Immun.* 71, 3578–3586. doi: 10.1128/IAI.71.6.3578-3586.2003

Solomon, J. M., Rupper, A., Cardelli, J. A., and Isberg, R. R. (2000). Intracellular growth of Legionella pneumophila in *Dictyostelium discoideum*, a system for genetic analysis of host-pathogen interactions. *Infect. Immun.* 68, 2939–2947. doi: 10.1128/IAI.68.5.2939-2947.2000

Stamm, C. E., Collins, A. C., and Shiloh, M. U. (2015). Sensing of *Mycobacterium tuberculosis* and consequences to both host and bacillus. *Immunol. Rev.* 264, 204–219. doi: 10.1111/imr.12263

Stray-Pedersen, A., Jouanguy, E., Crequer, A., Bertuch, A. A., Brown, B. S., Jhangiani, S. N., et al. (2014). Compound heterozygous CORO1A mutations in siblings with a mucocutaneous-immunodeficiency syndrome of epidermodysplasia verruciformis-HPV, molluscum contagiosum and granulomatous tuberculoid leprosy. *J. Clin. Immunol.* 34, 871–890. doi: 10.1007/s10875-014-0074-8

Suo, D., Park, J., Harrington, A. W., Zweifel, L. S., Mihalas, S., and Deppmann, C. D. (2014). Coronin-1 is a neurotrophin endosomal effector that is required for developmental competition for survival. *Nat. Neurosci.* 17, 36–45. doi: 10.1038/nn.3593

Suzuki, K., Nishihata, J., Arai, Y., Honma, N., Yamamoto, K., Irimura, T., et al. (1995). Molecular cloning of a novel actin-binding protein, p57, with a WD repeat and a leucine zipper motif. *FEBS Lett.* 364, 283–288. doi: 10.1016/0014-5793(95)00393-N

Suzuki, K., Takeshita, F., Nakata, N., Ishii, N., and Makino, M. (2006). Localization of CORO1A in the macrophages containing Mycobacterium leprae. *Acta Histochem. Cytochem.* 39, 107–112. doi: 10.1267/ahc.06010

Swaminathan, K., Müller-Taubenberger, A., Faix, J., Rivero, F., and Noegel, A. A. (2014). A Cdc42- and Rac-interactive binding (CRIB) domain mediates functions of coronin. *Proc. Natl. Acad. Sci. U.S.A.* 111, E25–E33. doi: 10.1073/pnas.1315368111

Swaminathan, K., Stumpf, M., Müller, R., Horn, A. C., Schmidbauer, J., Eichinger, L., et al. (2015). Coronin7 regulates WASP and SCAR through CRIB mediated interaction with Rac proteins. *Sci. Rep.* 5:14437. doi: 10.1038/srep14437

Tchang, V. S. Y., Stiess, M., Siegmund, K., Karrer, U., and Pieters, J. (2017). Role for coronin 1 in mouse NK cell function. *Immunobiology* 222, 291–300. doi: 10.1016/j.imbio.2016.09.011

Vandal, O. H., Pierini, L. M., Schnappinger, D., Nathan, C. F., and Ehrt, S. (2008). A membrane protein preserves intrabacterial pH in intraphagosomal *Mycobacterium tuberculosis*. *Nat. Med.* 14, 849–854. doi: 10.1038/nm.1795

Vinet, A. F., Fiedler, T., Studer, V., Froquet, R., Dardel, A., Cosson, P., et al. (2014). Initiation of multicellular differentiation in *Dictyostelium discoideum* is regulated by coronin A. *Mol. Biol. Cell* 25, 688–701. doi: 10.1091/mbc.E13-04-0219

Voth, D. E., and Heinzen, R. A. (2007). Lounging in a lysosome: the intracellular lifestyle of Coxiella burnetii. *Cell. Microbiol.* 9, 829–840. doi: 10.1111/j.1462-5822.2007.00901.x.

Walburger, A., Koul, A., Ferrari, G., Nguyen, L., Prescianotto-Baschong, C., Huygen, K., et al. (2004). Protein kinase G from pathogenic mycobacteria promotes survival within macrophages. *Science* 304, 1800–1804. doi: 10.1126/science.1099384

Wang, Y., Liu, J., and Segall, J. E. (1998). MAP kinase function in amoeboid chemotaxis. *J. Cell Sci.* 111 (Pt 3), 373–383.

Weiss, G., and Schaible, U. E. (2015). Macrophage defense mechanisms against intracellular bacteria. *Immunol. Rev.* 264, 182–203. doi: 10.1111/imr.12266

Yan, M., Collins, R. F., Grinstein, S., and Trimble, W. S. (2005). Coronin-1 function is required for phagosome formation. *Mol. Biol. Cell* 16, 3077–3087. doi: 10.1091/mbc.E04-11-0989

Yan, M., Di Ciano-Oliveira, C., Grinstein, S., and Trimble, W. S. (2007). Coronin function is required for chemotaxis and phagocytosis in human neutrophils. *J. Immunol.* 178, 5769–5778. doi: 10.4049/jimmunol.178.9.5769

Yee, C. S., Massaad, M. J., Bainter, W., Ohsumi, T. K., Föger, N., Chan, A. C., et al. (2016). Recurrent viral infections associated with a homozygous CORO1A mutation that disrupts oligomerization and cytoskeletal association. *J. Allergy Clin. Immunol.* 137, 879-888.e872. doi: 10.1016/j.jaci.2015.08.020

Yuen, I. S., Jain, R., Bishop, J. D., Lindsey, D. F., Deery, W. J., Van Haastert, P. J., et al. (1995). A density-sensing factor regulates signal transduction in Dictyostelium. *J. Cell Biol.* 129, 1251–1262. doi: 10.1083/jcb.129.5.1251

Zheng, P. Y., and Jones, N. L. (2003). Helicobacter pylori strains expressing the vacuolating cytotoxin interrupt phagosome maturation in macrophages by recruiting and retaining TACO (coronin 1) protein. *Cell. Microbiol.* 5, 25–40. doi: 10.1046/j.1462-5822.2003.00250.x

Conflict of Interest Statement: The authors declare that the research was conducted in the absence of any commercial or financial relationships that could be construed as a potential conflict of interest.

frontiers in Cellular and Infection Microbiology

ORIGINAL RESEARCH
published: 15 March 2018
doi: 10.3389/fcimb.2018.00073

The Saposin-Like Protein AplD Displays Pore-Forming Activity and Participates in Defense Against Bacterial Infection During a Multicellular Stage of *Dictyostelium discoideum*

Ranjani Dhakshinamoorthy[1†], *Moritz Bitzhenner*[1], *Pierre Cosson*[2], *Thierry Soldati*[3] and *Matthias Leippe*[1*]

[1] Zoological Institute, Comparative Immunobiology, University of Kiel, Kiel, Germany, [2] Department of Cell Physiology and Metabolism, Faculty of Medicine, University of Geneva, Geneva, Switzerland, [3] Department of Biochemistry, Faculty of Science, University of Geneva, Geneva, Switzerland

OPEN ACCESS

Edited by:
Patricia Ann Champion, University of Notre Dame, United States

Reviewed by:
Falk Hillmann, Leibniz-Institut für Naturstoff-Forschung und Infektionsbiologie, Hans Knöll Institut, Germany
Serge Ankri, Technion – Israel Institute of Technology, Israel

***Correspondence:**
Matthias Leippe
mleippe@zoologie.uni-kiel.de

[†]**Present Address:**
Ranjani Dhakshinamoorthy, Department of Biotechnology, Bhupat and Jyoti Mehta School of Biosciences, Indian Institute of Technology Madras, Chennai, India

Received: 22 November 2017
Accepted: 27 February 2018
Published: 15 March 2018

Citation:
Dhakshinamoorthy R, Bitzhenner M, Cosson P, Soldati T and Leippe M (2018) The Saposin-Like Protein AplD Displays Pore-Forming Activity and Participates in Defense Against Bacterial Infection During a Multicellular Stage of Dictyostelium discoideum. Front. Cell. Infect. Microbiol. 8:73. doi: 10.3389/fcimb.2018.00073

Due to their archaic life style and microbivor behavior, amoebae may represent a source of antimicrobial peptides and proteins. The amoebic protozoon *Dictyostelium discoideum* has been a model organism in cell biology for decades and has recently also been used for research on host-pathogen interactions and the evolution of innate immunity. In the genome of *D. discoideum,* genes can be identified that potentially allow the synthesis of a variety of antimicrobial proteins. However, at the protein level only very few antimicrobial proteins have been characterized that may interact directly with bacteria and help in fighting infection of *D. discoideum* with potential pathogens. Here, we focus on a large group of gene products that structurally belong to the saposin-like protein (SAPLIP) family and which members we named provisionally Apls (amoebapore-like peptides) according to their similarity to a comprehensively studied antimicrobial and cytotoxic pore-forming protein of the protozoan parasite *Entamoeba histolytica*. We focused on AplD because it is the only Apl gene that is reported to be primarily transcribed further during the multicellular stages such as the mobile slug stage. Upon knock-out (KO) of the gene, *aplD*$^{-}$ slugs became highly vulnerable to virulent *Klebsiella pneumoniae*. *AplD*$^{-}$ slugs harbored bacterial clumps in their interior and were unable to slough off the pathogen in their slime sheath. Re-expression of AplD in *aplD*$^{-}$ slugs rescued the susceptibility toward *K. pneumoniae*. The purified recombinant protein rAplD formed pores in liposomes and was also capable of permeabilizing the membrane of live *Bacillus megaterium*. We propose that the multifarious Apl family of *D. discoideum* comprises antimicrobial effector polypeptides that are instrumental to interact with bacteria and their phospholipid membranes. The variety of its members would allow a complementary and synergistic action against a variety of microbes, which the amoeba encounters in its environment.

Keywords: amoebapore, antimicrobial peptides, *Dictyostelium discoideum*, host-pathogen interactions, saposin-like proteins, slugs, Sentinel cells, innate immunity

INTRODUCTION

Amoebozoa are interesting models to study the early evolution of innate immunity (Leippe, 1999). The social amoeba *Dictyostelium discoideum*, a genetically tractable model for the study of cell biology, has recently become a powerful model organism in infection biology. In particular, it has been employed as a surrogate host for human pathogens such as *Legionella* (Farbrother et al., 2006), Mycobacteria (Hagedorn and Soldati, 2007; Hagedorn et al., 2009), and *Pseudomonas* (Cosson et al., 2002; Alibaud et al., 2008). In its amoebic stage, *D. discoideum* phagocytoses microbes and thereby resembles phagocytes of the innate immune system (Cosson and Soldati, 2008). Upon starvation, the amoebae aggregate and undergo a programmed differentiation and morphogenesis. One of the specific stages is the so-called slug, formed by the aggregation of about 100,000 amoebae, which will eventually differentiate into a fruiting body. Among slug cells, Sentinel cells represent a simple and efficient immune system. These phagocytes patrol the slug body to capture toxic compounds and invading bacteria. The Sentinel cells are continuously shed behind in the slime sheath of migrating slugs (Chen et al., 2007). These immune-like phagocytes have recently been reported to possess the capacity to produce extracellular DNA traps around the pathogen/foreign body (Zhang et al., 2016) in a way similar to phagocytes of vertebrates and invertebrates (Brinkmann et al., 2004; Robb et al., 2014). These features make of *D. discoideum* an even more attractive model to trace back the conserved functions of the innate immune system across evolution from protozoans to metazoans (Chen et al., 2007; Hagedorn et al., 2009; Zhang and Soldati, 2016).

Despite these promising results, the knowledge about the arsenal that *D. discoideum* employs to kill phagocytosed microbes and to combat potential pathogens is still scarce. The only example of an antimicrobial effector characterized at the protein level is the AlyA lysozyme, which had been isolated from amoebic extracts and found to be able to degrade bacterial cell walls (Müller et al., 2005).

According to the information derived from the genome project, *D. discoideum* possesses at least 15 genes potentially coding for lysozymes belonging to several different classes of these hydrolytic enzymes (Eichinger and Noegel, 2005; Müller et al., 2005). Beside the family of Alys, putative *Entamoeba*-type lysozymes, phage-type lysozymes, and C-type lysozymes (LyCs) can be identified in databases (Müller et al., 2005).

Another multifarious gene family of *D. discoideum*, which products may target bacterial membranes and thereby kill bacteria directly, is the one coding for saposin-like proteins (SAPLIPs). Structurally, SAPLIPs are characterized by four or five compactly packed alpha-helices, and are typically stabilized by three disulfide bonds built by a conserved array of six cysteine residues (Liepinsh et al., 1997). Functionally, SAPLIPs fulfill various biological functions, but the members of this family have in common that they interact with lipids and membranes (Munford et al., 1995; Bruhn, 2005; Kolter et al., 2005). SAPLIPS with antimicrobial activity can be found in phylogenetically diverse organisms ranging from protozoans to mammals (Leippe et al., 1991; Andersson et al., 1995; Peña et al., 1997).

In pathogenic amoebae, saposin-like proteins are well-known as pore-forming proteins that permeabilize the membranes of bacteria and human host cells (Leippe, 2014). The most comprehensively studied member of amoebic SAPLIPs is amoebapore A from *E. histolytica,* the tertiary structure revealed the characteristic SAPLIP fold (Hecht et al., 2004). We therefore provisionally termed the putative SAPLIPs of which *D. discoideum* Apls for amoebapore-like peptides.

Dictyostelium discoideum possesses 17 Apl genes that potentially can give rise to 33 SAPLIP peptides given that larger precursor proteins containing more than one SAPLIP domain (also termed saposin B domain) might be processed to release several mature SAPLIPs, as exemplified for the name-giving saposins (O'Brien and Kishimoto, 1991) and for naegleriapores of the free-living amoeba *Naegleria fowleri* (Herbst et al., 2004). Such an enormous variety of SAPLIPs in one species is only known so far from *C. elegans*, a nematode that also feeds on microbes (Roeder et al., 2010).

In D. discoideum, one may speculate that these proteins act complementarily and synergistically and constitute an important part of the antimicrobial armamentarium during its unicellular and multicellular stages. Nonetheless, functions other than killing of bacteria by membrane permeabilization have been reported for amoebic SAPLIPs (Michalek and Leippe, 2015).

In the present study, we have chosen AplD among the plethora of potential *D. discoideum* SAPLIPs for a more detailed functional study because it became apparent that: (i) the primary translation product comprises a single SAPLIP domain preceded by a putative signal peptide as known for amoebapores; (ii) the gene has been reported to be differentially expressed upon bacterial challenge; and (iii) most importantly with respect to immunity, *aplD* is reported to be primarily transcribed during the multicellular stages (Dicty express: https://dictyexpress.research.bcm.edu/bcm/#/all?genes=DDB_G0293010).

At the protein level, we characterized the ability of AplD to permeabilize the membranes of live bacteria and liposomes by monitoring quantitatively the activity of a recombinantly expressed protein (rAplD). *In vivo*, we phenotypically analyzed the effect of ablation of *aplD* on amoebic growth on various bacterial lawns, on bacterial killing in the amoebic stage, and on the slug's capacity to fight a bacterial infection.

MATERIALS AND METHODS

Bacterial Cultures

Various bacterial strains were used in the study (Supplementary Table 1). The bacterial cultures were grown at 220 rpm at 37 °C for 12 to 14 h in Luria-Bertani medium.

Dictyostelium discoideum Cultures

Ax2 obtained from the Dicty stock center was used for generating the *apl* and *lyC* KO mutants. Ax2 amoebae were grown in maltose-HL5 medium and blasticidin (8 μg/ml)-containing maltose-HL5 medium was used to select the KOs. The *D. discoideum* cells transfected with prestalk reporter

(*ecmAO*-RFP), prespore reporter (*pSA*-RFP) plasmids, and *aplD*$^{-}$/[act6]:*aplD*.FLAG cells [rescue strain; mentioned as *aplD*$^{-}$(+)] were cultured in maltose-HL5 medium complemented with G418 (10 μg/ml) and blasticidin (8 μg/ml).

Creation of KO Vectors

Short gene fragments from the 5′ and 3′ regions of *apl* and *lyC* genes were amplified by PCR and ligated appropriately at the 5′ and 3′ flanking ends of the blasticidin resistance (Bsr) gene present in the pLPBLP gene disruption vector as described in Faix et al. (2004). Before transfection, the KO vectors were subjected to DNA sequencing (Eurofins MWG operon, Germany) to verify vector orientations and mutations.

Plasmids

pLPBLP, *ecmAO*-RFP, *pSA*-RFP, and pD*neo*2a-3xFLAG plasmids were received from the Dicty stock center.

Targeted Gene Ablations in *D. discoideum*

Gene disruptions were achieved by homologous recombination between the respective *apl*s and *lyC*s with their corresponding KO vectors. Ax2 cells (2×10^7) were sedimented at $560 \times g$ at RT for 5 min. The pellet was resuspended in 1 ml ice-cold electroporation (EP) buffer (10 mM K_2HPO_4, 10 mM KH_2PO_4, 50 mM sucrose, pH 6.2.), washed at 10,000 × *g* at RT for 2 min, and briefly incubated on ice. The respective linearized KO vector was resolved in 100 μl ice-cold EP^{++} buffer (EP buffer containing 1 mM $MgSO_4$, 1 mM $NaHCO_3$, 1 μM $CaCl_2$, and 1 mM ATP, pH 6.2) and subsequently mixed with Ax2. Immediately, this cell mixture was transferred to 2-mm gap electroporation cuvette (BTX electroporation cuvettes, Harvard apparatus) and electroporation was carried out at 300 V, 2 ms time constant with five square pulses, including 5-s intervals inbetween the pulses, using a BTX 830 electroporator (Harvard apparatus). After 10 min incubation on ice, the cell suspension was transferred to Petri dishes that contain 10 ml maltose-HL5 medium and incubated at 22°C. Blasticidin (8 μg/ml) selection was introduced 24 h later. Blasticidin-resistant clones had appeared after a week and were aspirated from the Petri dishes and seeded in 24-well plates (both from Sarstedt, Germany) for PCR analyses.

Identification of KO Clones

Cell lysates were prepared from the blasticidin-resistant clones following the method described in Charette and Cosson (2004). As described in Faix et al. (2004) three different PCR analyses were performed to verify the *apl* and *lyC* KO vectors insertion in 5′–3′ orientation at the *apl* and *lyC* loci. PCR screening results for *aplD* KO clones are shown in the Supplementary Figure 1. KO vectors (vector control, VC) and Ax2 genomic DNA (wild-type, WT) were used as respective controls for PCR analyses. The KO clones were confirmed for gene ablation at the respective gene locus by performing Southern hybridization (Supplementary Figure 2), using the DIG-High prime DNA labeling and detection starter kit II (Roche), following manufacturer's instructions. A probe was generated for the Bsr-resistance gene sequence, which spans for 249 base pairs and dioxygenin (DIG) was used as the labeling agent.

Construction of an *aplD* Rescue Strain

The cDNA sequence of *aplD* was amplified by PCR and cloned under the Actin 6 promoter (*act6*) of pDneo2a-3xFLAG vector (Dubin and Nellen, 2010). The 3′ end of *aplD* cDNA was fused to the FLAG gene. Finally, the pDneo2a-3xFLAG[*act6*/*aplD*] plasmid was transfected into *aplD*$^{-}$ cells. AplD-FLAG fusion protein expression in the rescue strain [*aplD*$^{-}$(+)] was confirmed by Western blot analysis (Supplementary Figure 3). After separation by SDS-PAGE, proteins were transferred onto a polyvynilidene fluoride membrane and the blot was incubated with a mouse anti-FLAG M2 monoclonal antibody (Sigma Life Science) and subsequently developed using a goat anti-mouse IgG (H+L) conjugated to alkaline phosphatase (Jackson ImmunoResearch).

AplD Transcriptional Profiling

To analyse transcription in axenic cultures, RNA was isolated from axenically grown *D. discoideum* amoebae (5×10^6 cells) and the first strand cDNA was synthesized using the RNA template (cDNA synthesis kit, Invitrogen). Quantitative RT-PCR (qRT-PCR) was performed using the cDNA template as described by the manufacturer (qRT-PCR mix, TAKARA and Light cycler, Roche). For analysis of xenic cultures, Ax2 cells were mixed with bacteria (ratio 1:10) and the amoebae-bacteria cell suspensions were incubated at 140 rpm and 22°C for 8 h. Subsequently, the xenic Ax2 cells were washed three times at $425 \times g$ at 4°C for 2 min to remove excess bacteria. cDNA was synthesized and qRT-PCR analyses were performed as described above. *AplD* transcription in axenic Ax2 amoebae was considered as reference to determine the *aplD* expression in xenic Ax2. Each symbol denotes individual experiment. The house keeping genes tested were *Ig7* (*rnlA*) and Glyceraldehyde-3-phosphate dehydrogenase (*GAPDH*). The bacterial strains tested include *Kp*LM21, *B. subtilis*, and PT531 (see Supplementary Table 1). For analysis during development, axenic Ax2 cells were washed with Sörensen's buffer (SB) at $510 \times g$ and 22°C for 7 min. The cell pellets were resuspended in 100 μl SB and deposited on SB agar (1%) plates. Subsequently, the plates were incubated in a dark, moist chamber at 22°C and RNA was isolated from the starving amoebae (0 h), streaming cells (8 h), mounds (12 h), slugs (16 h), and fruiting bodies (24 h) and qRT-PCR was performed in duplicates. *AplD* expression in the starving amoebae (0 h) was considered as reference to quantify the *aplD* expression at other stages of development (Sillo et al., 2008). Three independent development experiments were performed and the bars represent standard deviation.

Growth of *Dictyostelium* on Bacterial Lawns

Bacterial growth assays were performed on routinely used SM agar medium, which was devoid of glucose. SM agar plates were prepared as described in Froquet et al. (2009). Varying number (10^4, 10^3, 10^2, and 10^1) of *D. discoideum* amoebae were deposited on the bacterial lawn layered on SM agar plates and incubated in the dark at 22°C. Five days later, the KOs were scored for their plaque forming abilities by having Ax2 as comparative controls. Three independent experiments were performed with triplicates

(see Supplementary Table 1 for details on the bacterial strains tested).

Intracellular Killing of Bacteria by *Dictyostelium*

Dictyostelium discoideum amoebae were mixed with bacteria (100:1) and incubated at 140 rpm, 22°C. The total number of viable bacteria was measured at the indicated time points by following the method detailed in Benghezal et al. (2006). The rate of killing of *K. pneumoniae* bacteria by amoebae was quantified by counting the number of colony forming units (CFU) at each time point. Three independent experiments were performed.

Dictyostelium discoideum Development

Dictyostelium discoideum cells were washed with SB and deposited on SB agar (1%) plates at a cell density 5×10^5 cells/cm^2. Subsequently, plates were incubated in a dark, moist chamber at 22°C. The morphogenetic stages were imaged under the stereomicroscope (Olympus ULWCD 0.30) at time points mentioned (Supplementary Figure 4). *Dictyostelium discoideum* development on SB agar was monitored in three independent experiments.

Prestalk (pst) and Prespore (psp) Slug Patterns

Slug pattern analyses were performed as described in Parkinson et al. (2009). For prestalk reporter (*ecmAO*-RFP) examination, *D. discoideum* amoebae carrying the *ecmAO*-RFP plasmid were mixed with *D. discoideum* amoebae at 20:80 ratio and seeded on a SB agar (1%) plate at a cell density 5×10^5 cells/cm^2. For prespore reporter (*pSA*-RFP) examination, *D. discoideum* amoebae (20%) were mixed with *D. discoideum* amoebae marked with *pSA*-RFP (80%) and deposited on SB agar plates. The plates were incubated in a dark, moist chamber at 22°C until the migrating slugs were formed and were imaged under the stereomicroscope (Olympus ULWCD 0.30) (Supplementary Figure 4). Two independent experiments were performed in duplicates and at least ten slugs were imaged per plate.

Slugs Infection

Dictyostelium discoideum cells were harvested from Petri dishes, 2.5×10^7 cells were sedimented, and the pellets were resuspended in 50 µl SB. This high density cell suspension was deposited on SB agar (1%) plates and incubated in a dark, moist chamber with an unidirectional light source until migrating slugs were formed (∼18 h). Slug infection experiments were performed following Chen et al. (2007) with some modifications. The slugs were injured with a sterile needle (23G × $1^{1/4}$, B|BRAUN Injekt F) and a dense bacterial suspension, which was prepared from an overnight culture, was layered on the injured slugs. *K. pneumoniae* expressing GFP reporter (*Kp*GFP) and *E. coli* expressing DsRed reporter were used for infecting the injured slugs (see Supplementary Table 1). The slugs infected with *Ec* DsRed were imaged under the stereo microscope (Olympus ULWCD 0.30) 8 h post infection and those slugs infected with *Kp*GFP were imaged 20 h and 24 h post infection. *Kp*GFP was grown with ampicillin (1 mg/ml) for 12 h at 37°C. *Ec* DsRed was grown with isopropyl β-D-1-thiogalactopyranoside (IPTG, 100 mM) and kanamycin (150 µg/ml). Three independent experiments were performed and at least ten slugs were imaged per experiment for each strain [Ax2, *aplD*$^-$, and *aplD*$^-$(+)].

Sentinel Cells Examination

Dictyostelium discoideum cells were allowed to form slugs on SB agar (1%) plates containing ethidium bromide (EtBr, 3 µg/ml) as described in Chen et al. (2007). After 3 h, Sentinel cells present in the migrating slugs were visualized under the stereomicroscope (Olympus ULWCD 0.30). Three independent experiments were performed and at least ten slugs were imaged per experiment for each strain (Ax2 and *aplD*$^-$).

Recombinant Protein Production and Purification

The nucleotide sequence encoding putatively mature AplD (DDB0216216) was codon optimized for bacterial expression and synthesized by GeneArt (Regensburg, Germany). The cDNA was ligated into the pET-32a (+) (Novagen) expression vector containing an ampicillin resistance gene using *KpnI* and *XhoI* cleavage sites. The resulting plasmid encodes a fusion protein, which comprised an N-terminal thioredoxin followed by a hexahistidine (His_6) tag and contained thrombin and tobacco etch virus (TEV) protease cleavage sites preceding the primary structure of AplD. TEV cleavage yielded a product with the amino acid sequence as follows: GEIDNNQCQICELLVKDIIE GLTANQSVEVIEHGLNLICDHIPLHVRVCKQFVDSNFQKIV QFIENHDDPQEICEKCGVC. The protein was recombinantly expressed in *E. coli* C 43 at 37°C after induction with 0.5 mM IPTG for 6 h and extracted by sonication on ice (Sonoplus HD 2200 sonicator, MS-73 titanium microtip, Bandelin electronic GmbH, Germany). The fusion protein in the soluble fraction was purified by immobilized-metal affinity chromatography (IMAC) using a TALON resin (Clontech, Saint-Germain-en-Laye, France) and subsequent anion-exchange chromatography (1-ml Resource Q column, GE Healthcare) using an Äkta purifier system (model P-900; GE Healthcare) and 20 mM Tris-HCl, pH 7.0 with a continous linear gradient of 0-1 M NaCl for elution. The N-terminal tag was removed by cleavage with TEV protease (ProTEV Plus protease, Promega) at 30°C overnight. The cleaved product was subjected again to IMAC and anion-exchange chromatography (Mini Q column 4.6/50, GE Healthcare, Solingen, Germany) to remove the fusion partner and the TEV from recombinant AplD. After final purification, the apparently homogeneous protein fraction was lyophilized, redissolved, and dialyzed against 10 mM sodium phosphate, pH 6.8.

Purity was proven by tricine-SDS polyacrylamid gel (SDS PAGE) using 13% separation gels (Schägger and von Jagow, 1987) and SeeBluePlus2 (Invitrogen) as standard protein marker for molecular masses. Protein concentration was determined with the BCA assay (Pierce, Thermo Scientific, Bonn, Germany). The molecular mass of recombinant AplD was determined by mass spectrometry in linear mode using a 4700 Proteomic Analyzer MALDI-TOF/TOF mass spectrometer (Life Technologies, Darmstadt, Germany).

Assays for Membrane-Permeabilizing Activities

Pore-forming activity using the liposome depolarisation assay (Leippe et al., 1991) and permeabilization of cytoplasmic membranes of live bacteria using the fluorescent dye SYTOX Green (Herbst et al., 2002) were measured as described previously. Briefly, in the liposome-depolarization assay a valinomycin-induced diffusion potential across the membrane of liposomes prepared from asolectin, a crude mixture of soy bean phospholipids, resulted in quenching of the enclosed fluorescent dye. Application of a pore-forming protein disrupts the membrane potential and the fluorescence intensity increases by the release of the dye. An increase of 5% within 1 min after addition of the pore-forming agent at 25°C is defined as one activity unit. In the membrane-permeabilization assay the fluorescent dye SYTOX Green (Invitrogen) is added to *Bacillus megaterium*, *E. coli*, *Klebsiella aerogenes*, *K. pneumonia Kp*LM21, or *K. pneumoniae* K^- as viable target giving a signal while intercalating in DNA. Accordingly, only when the bacterial plasma membrane become compromised, e.g., by an antimicrobial protein, fluorescence appears. The values were expressed as the mean of three independent experiments. Kinetics of the membrane permeabilization of *B. megaterium* were monitored in that fluorescence was measured for different doses at various time points and presented as a representative example from four replicates with similar results. The synthetic peptides alamethicin and cecropin P1 served as positive controls in the activity assays (Sigma, Taufkirchen, Germany).

RESULTS

The Multifarious Apl Family

In the genome of *D. discoideum,* we detected 17 genes that may code for Apl proteins containing a single or several SAPLIP domains (**Figure 1**). The sequences of *apl* A-R and the corresponding putative proteins can be retrieved from the *D. discoideum* database (www.dictybase.org) using apl* as a query. Their primary translation products each contain a predicted signal peptide that may allow trafficking of the precursor proteins to lysosomal compartments. Proteolytic processing of larger precursors can result in 33 mature peptides with one SAPLIP domain. An N-terminal glycosylation site can be predicted for nearly all of them.

Apl Mutants Were Defective for Growth on Virulent LM21 *K. pneumoniae*

The permissiveness of various bacteria for amoebic growth is routinely assessed by testing the ability of *D. discoideum* mutants to generate growth plaques on bacteria lawns. This strategy has led to the identification of several bacterial virulence genes (Cosson et al., 2002; Pukatzki et al., 2002; Benghezal et al., 2007; Alibaud et al., 2008). Here, we adapted the method to test the growth abilities of *D. discoideum* Ax2 strain in which genes potentially coding for antimicrobial proteins (*apl*s and *lyC*s) have been disrupted. To quantitate the degree of bacterial virulence, varying number of *D. discoideum* cells were spotted on bacterial lawns and the growth plaques

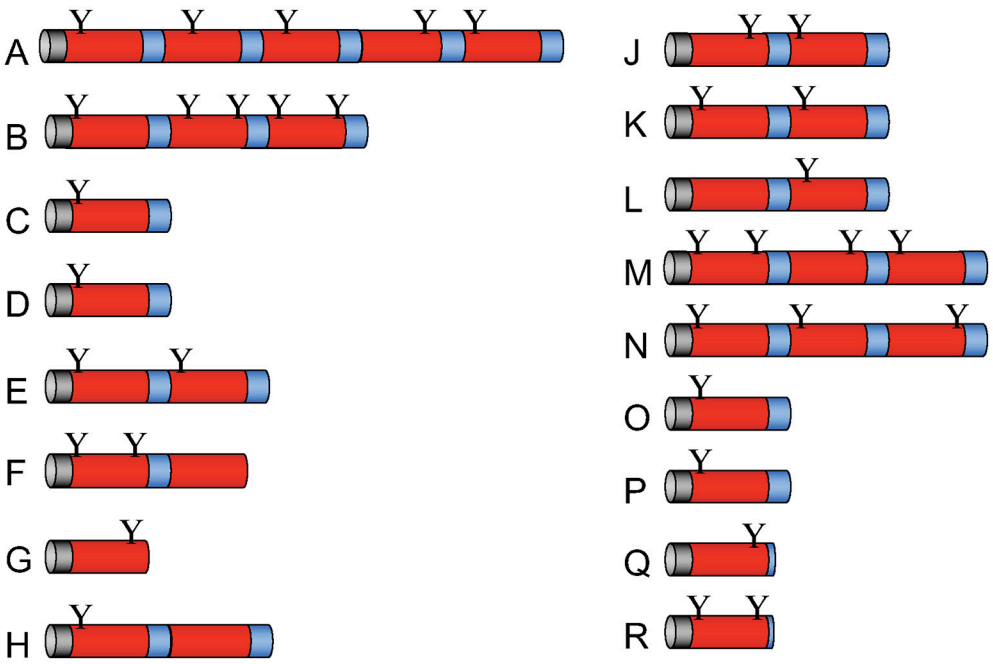

FIGURE 1 | Molecular architecture of Apl precursor proteins. The *D. discoideum* genome contains 17 genes that potentially code for saposin-like proteins (SAPLIPs) with some similarity to amoebapores provisionally termed Apls. The primary translation products of *apl*s named from A to R (omitting I) contain between one and five SAPLIP domains (also termed saposin B domain). After processing, these preproproteins potentially give rise to 33 different mature polypeptides. Signal peptides (gray), SAPLIP domains (red), putative linker regions and end regions (blue), and potential N-glycosylation sites (Y) are depicted.

were monitored after 5 days. It became apparent that *aplD*$^{-}$ was defective for growth on *Kp*LM21, a clinical isolate and two *apl* mutants, *aplD*$^{-}$ and *aplP*$^{-}$, were non-permissive for growth on *K*$^{-}$, a capsule defective *Kp* strain (**Figure 2A**). In the case of Ax2, even 10 amoebae were sufficient to create growth plaques on *K*$^{-}$ and *Kp*LM21, whereas at least 10,000 amoebae of *aplD*$^{-}$ and at least thousand amoebae of *aplP*$^{-}$ were required to generate visible plaques on *K*$^{-}$. Likewise, *Kp*LM21 allowed plaque formation only when 10,000 *aplD*$^{-}$ amoebae were deposited (**Figure 2A**). We also found that *D. discoideum* with a KO of the gene encoding the C-type lysozyme 2, *lyC2*$^{-}$, was defective for growth on *K*$^{-}$ (Supplementary Figure 5). The growth abilities of *Apl*s and *lyC*s mutants on bacteria such as *B. subtilis*, *E. coli Br*, non-pathogenic *K. pneumoniae*, and *P. aeruginosa* are summarized in a scheme (**Figure 2B**).

Vegetative *aplD*$^{-}$ Amoebae Efficiently Kill *K. pneumoniae Kp*LM21

As described in Benghezal et al. (2006), we performed a specific assay to investigate whether *aplD*$^{-}$ amoebae are defective in phagocytosis and/or killing of *Kp*LM21. These assays measure the total number of live bacteria remaining at indicated time points. We found that *aplD*$^{-}$ amoebae were able to phagocytose and kill *Klebsiella aerogenes* and *Kp*LM21 as efficiently as the wild-type Ax2 (**Figure 3**). This indicates that AplD is not essential for intracellular killing of *K. pneumoniae* bacteria in free-living *Dictyostelium* amoebae.

AplD Upregulation Upon Exposure to *Kp*LM21

To examine whether the expression of *aplD* is regulated by exposure to various bacteria, we measured the level of the *aplD* mRNA by qRT-PCR. Contact with *Kp*LM21 increased *aplD* at least three-fold, but contact with *Bacillus subtilis* did not induce a significant change. In contrast, exposure to *Pseudomonas aeruginosa* PT531 downregulated *aplD* on average about 6-fold (**Figure 4A**). Analyses of *aplD* regulation during *D. discoideum* development on non-nutrient KK2 agar showed that *aplD* was weakly expressed in axenic conditions, but was strongly upregulated during late development stages, starting from the mound stage [12 h] and slug stage [16 h], and peaking at fruiting body stage [24 h] (**Figure 4B**). This profile is comparable to the *aplD* transcriptional regulation observed in Ax4 grown on bacteria and subjected to development on SB agar (Dicty express, Supplementary Figure 6). The transcriptional regulation of antimicrobial genes during the growth phase of *D. discoideum* might be essential to adapt to various food sources, but also combat various pathogens. It has been reported that amoebae stop feeding during development. Therefore, the main purpose for the *aplD* upregulation might be an extracellular role in cellular defenses inside the multicellular

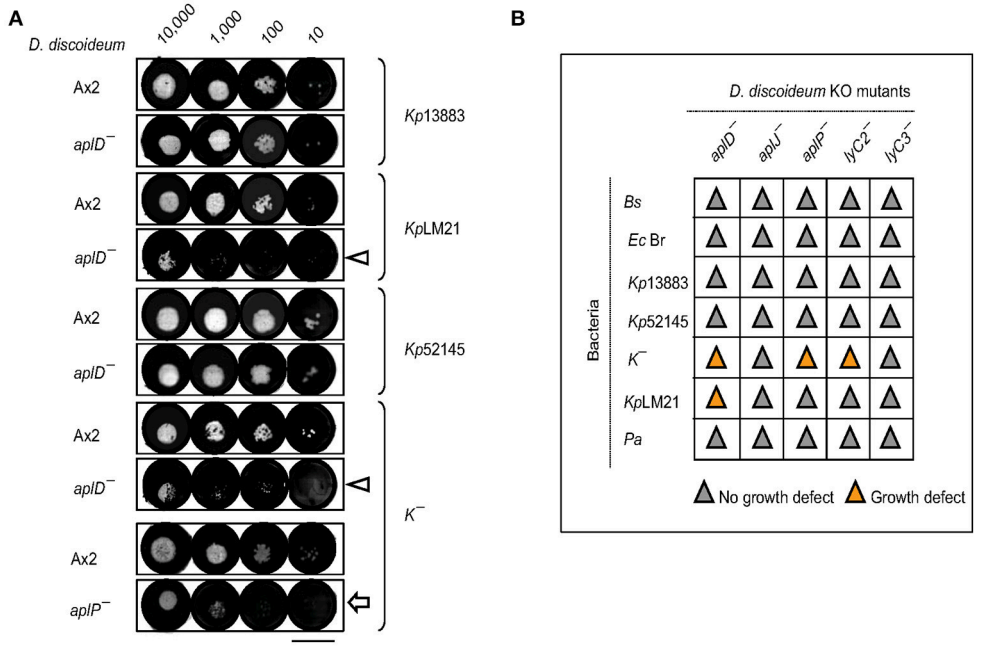

FIGURE 2 | Growth defects of *AplD*$^{-}$ and *aplP*$^{-}$ cells on virulent *K. pneumoniae*. **(A)** *D. discoideum* growth abilities on various *K. pneumoniae* were tested by depositing indicated number of amoebae on *K. pneumoniae* lawns that were prepared on SM agar. *D. discoideum* amoebae were fed with *Kp*13883, *Kp*LM21, *Kp*52145, and *K*$^{-}$. Arrowheads indicate *aplD*$^{-}$ cells growth defects on *Kp*LM21 and *K*$^{-}$. Arrow represents *aplP*$^{-}$ growth impairment on *K*$^{-}$. Scale bar, 1.5 cm. **(B)** Growth abilities of *aplD*$^{-}$, *aplJ*$^{-}$, *aplP*$^{-}$, *lyC2*$^{-}$ (see Supplementary Figure 5), and *lyC3*$^{-}$ were tested on *B. subtilis* (*Bs*), *E. coli* B/r (*Ec* Br), *K. pneumoniae* strains (*Kp*13883, *Kp*52145, *K*$^{-}$, and *Kp*LM21), and *P. aeruginosa* (*Pa*). Gray and yellow colors demonstrate the absence and presence of *D. discoideum* growth plaques on bacteria (see Supplementary Table 1 for bacterial strain details).

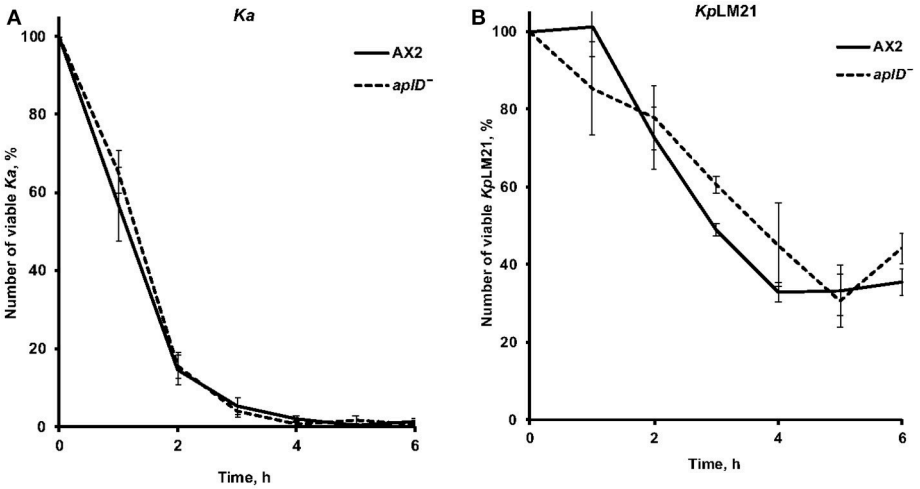

FIGURE 3 | *AplD*$^{-}$ cells kill efficiently *Klebsiella pneumoniae*. **(A)** The ability of *D. discoideum* to ingest and kill non-virulent *K. aerogenes Ka* was tested by mixing amoebae and bacteria and measuring the total number of viable bacteria at the indicated time points. **(B)** The same assay was performed using virulent *K. pneumoniae Kp*LM21. Ax2 was used as comparative control. Each curve is the average of three independent experiments, bars represent standard error of the mean.

structures or inside phagocytic Sentinel cells. Interestingly, upregulation of *aplD* during development, in particular at late stages, is several folds higher than during exposure to *Kp*LM21.

AplD^{-} Slugs Are Vulnerable to *K. pneumoniae*

To test the idea that AplD is primarily instrumental in multicellular stages of *D. discoideum*, we infected slugs derived from *aplD*$^{-}$ amoebae with a *K. pneumoniae* (*Kp*) strain that expressed GFP. Unlike wild type slugs, at 20 h post *Kp* infection, *aplD*$^{-}$ slugs showed bacterial deposits both on their surface and in their body. At 24 h post *Kp* infection, *aplD*$^{-}$ slugs showed *Kp* clumps mainly inside. Additionally, *aplD*$^{-}$ slugs were not successful in sloughing off *Kp* in their slime sheath (**Figure 5**). By contrast, *aplD*$^{-}$ slugs were able to shed *E. coli* in their slime sheath as early as 8 h post infection (**Figure 5**). As the major defense mechanism reported so far in *D. discoideum* slugs is based on the phagocytic nature of Sentinel cells, we examined whether *aplD*$^{-}$ slugs possess a functional population of these cells. As evidenced by the uptake of the fluid-phase tracer EtBr, *aplD*$^{-}$ slugs were capable of generating Sentinel cells that internalized the toxic dye and were sloughed off during migration (**Figure 6**) and *aplD*$^{-}$ did not depict any prominent developmental defect (Supplementary Figure 4).

Klebsiella Pneumoniae Susceptibility Was Rescued in *aplD*$^{-}$(+) Amoebae and Slugs

As described above, *aplD*$^{-}$ amoebae were restricted for growth on *K. pneumoniae*, *K*$^{-}$, and *Kp*LM21, and *aplD*$^{-}$ slugs were vulnerable to *Kp* infections. We tested whether restoration of *aplD* expression in *aplD*$^{-}$ would rescue the phenotypic defects. Constitutive expression of *aplD* in *aplD*$^{-}$ amoebae, termed *aplD*$^{-}$(+), under the control of the *act6* promoter of an extra-chromosomal vector rescued the formation of plaques on *K*$^{-}$ but showed only partial rescue on *Kp*LM21 lawns (**Figure 7**). Bacterial clearing was observed on *Kp*LM21 lawns when 10^4 and 10^3 amoebae were deposited, but not with 10^2 and 10^1 amoebae. This observation might indicate that spatio-temporal regulation of *aplD* expression is crucial for full functionality. *AplD*$^{-}$(+) slugs infected with *Kp* were able to clear off *Kp* by sloughing them off in their slime sheath. It appeared that the interior of *aplD*$^{-}$(+) slugs was virtually free of *Kp* deposits and clumps (**Figure 5**).

In-Vitro Functional Analysis of the Protein AplD

AplD was heterologously synthesized in *E. coli* as a fusion protein and subsequently the thioredoxin-His_6 tag was removed by proteolytic cleavage. The final product was purified to apparent homogeneity by repeated steps of IMAC and anion-exchange chromatography (**Figure 8A**). Analysis by MALDI-TOF mass spectrometry confirmed the molecular identity of rAplD. It revealed an experimental average mass of 9,070.8 Da, which is in good agreement with the calculated molecular mass (9,070.3 Da) provided that six cysteine residues are involved in disulfide bonds. The recombinant protein was tested for its pore-forming and bacterial-membrane permeabilizing activities *in vitro*. AplD formed pores in liposomes composed of asolectin. At mildly acidic pH (5.2), AplD depolarized liposomal membranes with similar activity as the prototype of a pore-forming peptide, alamethicin (**Figure 8B**). AplD acted in a pH-dependent manner. The protein displayed the highest pore-forming activity at pH 4.4 and gave decreasing values with increasing pH (**Figure 8C**). In the Sytox-Green assay, performed exemplarily with *B. megaterium,* it became apparent that AplD is capable of permeabilizing the cytoplasmic membranes of

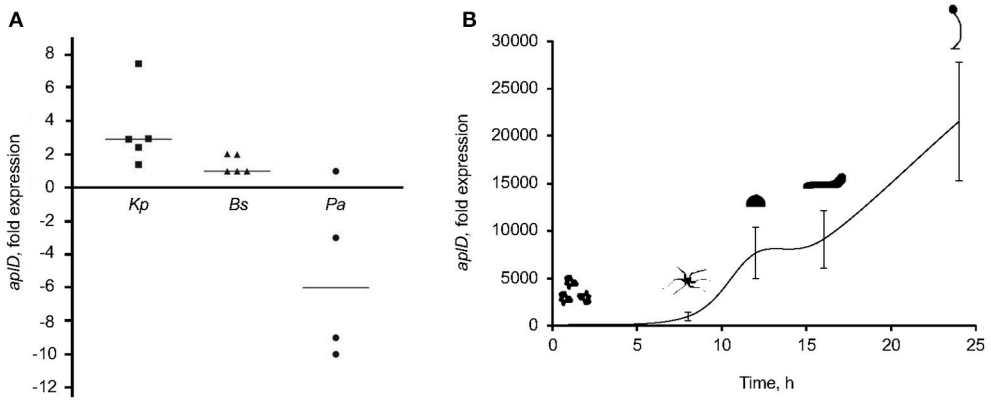

FIGURE 4 | *AplD* upregulation upon *K. pneumoniae* feeding and during late development. **(A)** *AplD* transcription profile in xenic Ax2 cultures were examined by mixing amoebae with bacteria at an 1:10 ratio and measuring *aplD* transcript levels by qRT-PCR. *AplD* fold expression in xenic Ax2 cultures were determined based on *aplD* transcription in axenic Ax2 cultures. Bacterial strains tested were *K. pneumoniae* (*Kp*LM21), *B. subtilis* (*Bs*), and *P. aeruginosa* (*Pa*). Each symbol denotes the data from an individual experiment and the bar represents the median thereof. **(B)** *AplD* regulation during Ax2 development was tested by subjecting Ax2 for development on KK2 agar plates and quantifying *aplD* transcription at different morphogenetic stages by qRT-PCR. *AplD* expression at 0 h was considered as reference to determine *aplD* fold expression at subsequent development stages. $n = 3$, bars represent standard deviation.

live bacteria. Membrane-permeabilizing activity increased with time. After 2 min, virtually no activity was detectable, but already after 5 min bacteria with compromised membranes appeared, particularly at higher protein concentrations. After 1 h, approximately 50% of the bacteria were permeabilized by AplD at 2.5 μM (**Figure 8D**). We could not detect bacterial membrane permeabilization with up to 5 μM AplD in the same assay when we used Gram-negative bacteria, *K. pneumoniae* LM21, *K. pneumoniae* K^-, *K. aerogenes*, or *E. coli*, as target cells (data not shown) indicating that the outer membrane of these species constitutes an additional barrier for AplD for reaching the bacterial cytoplasmic membrane.

DISCUSSION

Dictyostelium discoideum is a non-pathogenic, unicellular host used for bacterial and fungal risk assessment studies (Cosson et al., 2002; Alibaud et al., 2008; Koller et al., 2016) and the outcomes from such studies remain surprisingly similar to the observations made in animal hosts (Benghezal et al., 2006; Hagedorn et al., 2009). Although *D. discoideum* serves as a versatile system to explore bacterial virulence genes and their mechanisms of action, not much is known about the effector molecules of *D. discoideum* and their mode of action to defend against pathogens. In *D. discoideum*, host-pathogen interaction studies can be attempted both at the single-cell phagocyte stage and during the multicellular stages of its life cycle. Interestingly, the single-cell and multicellular phases are clearly separated and involve differential regulation of gene expression. During the growth phase, *D. discoideum* internalizes microbes by phagocytosis and the resulting phagosome fuses with lysosome, a compartment that houses hydrolytic enzymes and antimicrobial peptides, leading to efficient killing and degradation of the microbes to fulfill the nutritional need of the growing amoeba.

However, several intracellular pathogens have evolved mechanisms to block phago-lysosome fusion and to exploit the phagosomal compartment as their replication hub (Hagedorn et al., 2009; Shevchuk et al., 2014). During the multicellular stages of development, the antibacterial defense mechanisms are even more sophisticated. For example, in the slug formed mainly of non-phagocytic prespore and prestalk cells, about 1% of the cells, called the Sentinel cells retain their phagocytic ability. The foreign bodies and poisonous compounds that enter the slug are swallowed by these cells and finally get sloughed off the migrating slug and remain in the slime sheath, where they are entangled within extracellular DNA traps (Zhang and Soldati, 2016; Zhang et al., 2016). Mechanistically, this helps to restrict microbial infection and/or the accumulation of toxins. The present study reveals for the first time the specific involvement of the AplD gene product in antimicrobial defense during multicellular stages of development. In addition, *aplD* expression is differentially regulated by exposure to different bacteria, e.g., induced in the presence of *K. pneumoniae* and repressed in the presence of *P. aeruginosa*.

These *in vivo* evidences strongly suggest that Apl peptides are involved in antimicrobial defense, but a direct membrane-lysing activity had not been reported so far. Here, we show that purified, recombinant AplD displayed pore-forming activity in the minimalistic system of liposomes and also readily permeabilized the membranes of the live Gram-positive bacterium *B. megaterium* as monitored by the Sytox green assay. However, an activity against Gram-negative bacteria was not detected at the concentrations employed. One might speculate that AplD can also permeabilize *Klebsiella*, provided that the outer membrane does not hamper the access to the primary target, the bacterial plasma cell membrane. The antimicrobial efficacy of the relatively negatively charged AplD might be substantially enhanced by the synergistic action of other antimicrobial proteins, e.g., Apls with a more positive net charge,

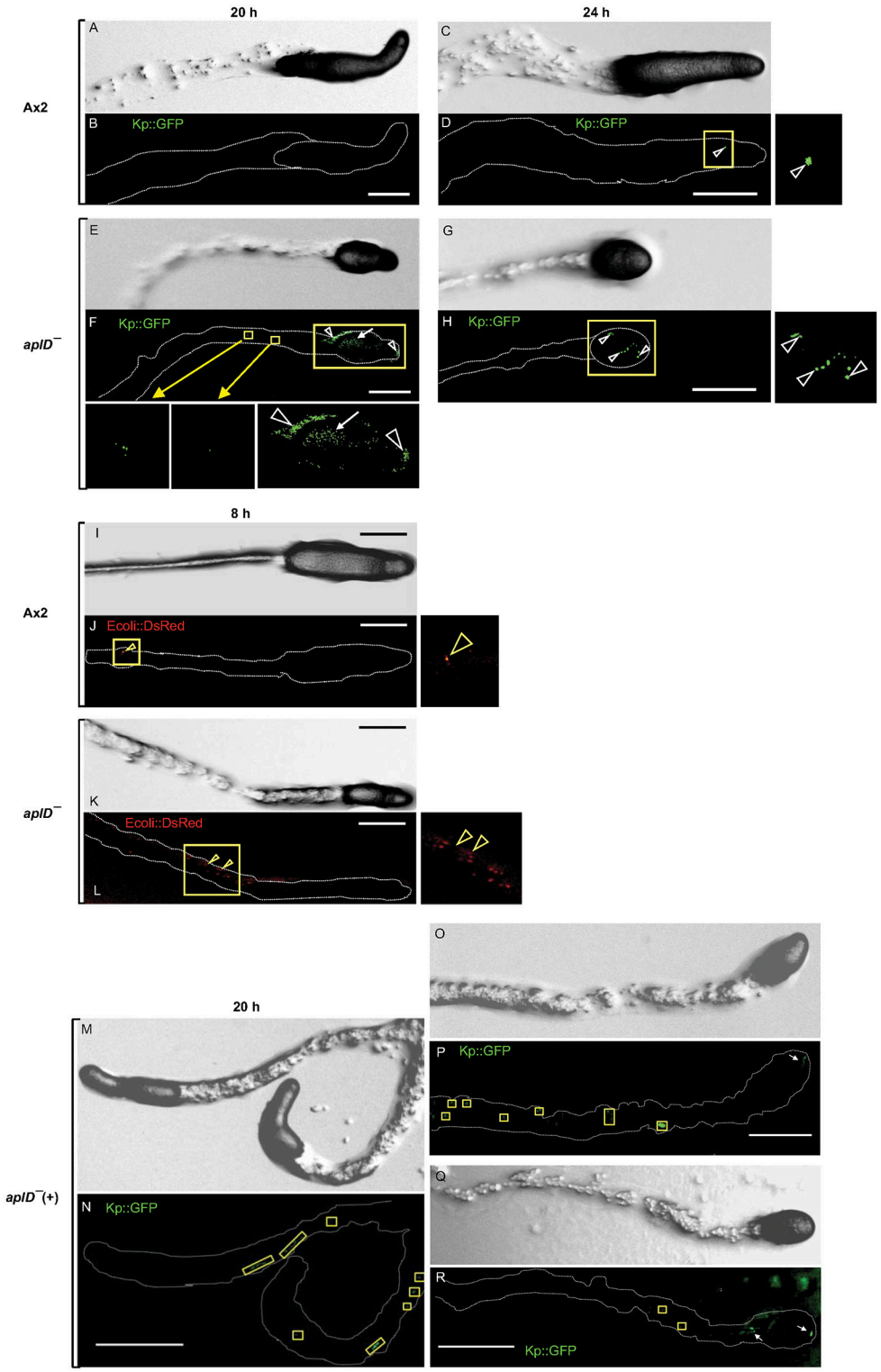

FIGURE 5 | Susceptibility of slugs to infection with *Klebsiella* and *E. coli*. Migrating *D. discoideum* slugs were injured with a fine needle and infected with GFP-expressing *K. pneumoniae* (*Kp*GFP). Slugs were imaged at 20 and 24 h post *Kp*GFP infection. Differential Interference Contrast (DIC) images of Ax2 **(A,C)** and *aplD*$^{-}$ slugs **(E,G)** at 20 and 24 h post infection are represented. *Kp*GFP infections in Ax2 **(B,D)** and *aplD*$^{-}$ slugs **(F,H)** at 20 and 24 h post infection are shown under green fluorescence filter. *Kp*GFP infection in Ax2 slug imaged 24 h post *Kp*GFP infection **(D)** is also magnified. *Kp*GFP infection on slug surface (arrowheads) and slug interior (arrow) and in the slime sheath of *aplD*$^{-}$ slug at 20 h post infection are magnified in the insets below. *Kp*GFP clumps inside *aplD*$^{-}$ slug 24 h post infection **(H)** is

(Continued)

FIGURE 5 | magnified in the adjacent panel. *AplD*$^{-}$ slugs sloughed off *E. coli* in their slime sheaths. DIC images of Ax2 and *aplD*$^{-}$ slugs **(I,K)** 8 h post infection with *E. coli* DsRed are represented. *E. coli* DsRed clumps (arrowheads) in Ax2 **(J)** and *aplD*$^{-}$ **(L)** slime sheaths (boxes) are shown under red fluorescence filter and are also magnified in the respective insets. *AplD*$^{-}$(+) slugs sloughed off *Kp*GFP in their slime sheaths. *AplD*$^{-}$(+) slugs were infected with *Kp*GFP as described earlier and were imaged 20 h post *Kp*GFP infection. DIC images of *aplD*$^{-}$(+) slugs are shown in **(M,O,Q)**. *K. pneumoniae* infections in *aplD*$^{-}$(+) slugs are shown under green fluorescence filter in **(N,P,R)**. *AplD*$^{-}$(+) slime sheaths showing *Kp*GFP deposits (boxes) and clumps in the slug interior (arrows) at 20 h post infection are depicted. Scale bars, 100 μm.

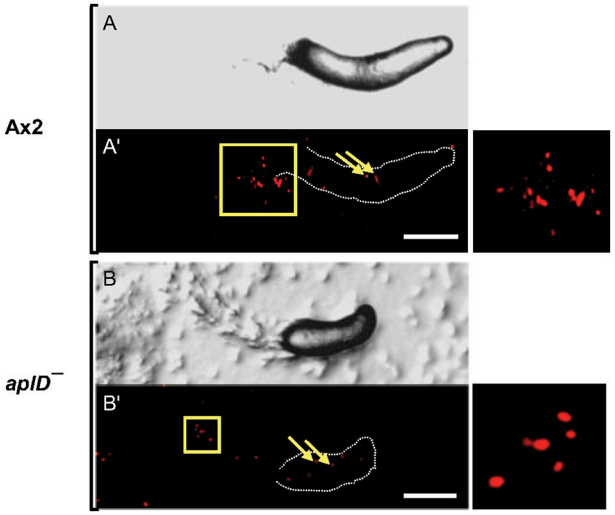

FIGURE 6 | Sentinel cells were unaffected in *aplD*$^{-}$ slugs. Ax2 and *aplD*$^{-}$ slugs were allowed to migrate on EtBr-containing (3 μg/ml) agar for 3 h. DIC images of Ax2 and *aplD*$^{-}$ slugs **(A,B)** imaged under a stereomicroscope are represented. Sentinel cells inside Ax2 and *aplD*$^{-}$ slugs **(A',B')** are shown under red fluorescence filter (arrows). Sentinel cells detected in slime sheaths are magnified (boxes, right). Scale bars, 100 μm.

or when other *Dictyostelium* factors that are not bactericidal *per se* but are capable of perturbing the outer membrane structure act in concert with AplD.

There are several examples of SAPLIPs including the saposins themselves that have been found to be glycosylated in their natural form. The vast majority of the potential peptides released from Apl precursors bear a potential N-glycosylation site. This also holds true for AplD. In amoebae, we have previously compared the pore-forming activity toward liposomes of glycosylated and deglycosylated naegleriapores and could not detect a substantial negative effect upon glycan removal (Herbst et al., 2002). However, we cannot exclude that a natural AplD, glycosylated specifically by *D. discoideum,* might have a different activity spectrum against natural targets than the recombinant unglycosylated version. A single glycosylation motif may determine a particular oligomeric structure, e.g., dimerization, to generate a more active protein, it may mediate an interaction with a partner molecule that helps to overcome the outer membrane of Gram-negative bacteria such as *Klebsiella*, or it may simply facilitate binding to bacterial targets, e.g., by shielding the negative charge of particular regions of the protein.

Apart from Apls, there are two other proteins that harbor a SAPLIP domain, i.e., acyloxyacyl hydrolase (AOAH) and countin (Ctn). The enzyme AOAH deacylates lipopolysaccharides in vertebrates, but has not been characterized in amoebae so far (Munford et al., 2009). Countin is a well-studied major component of a protein complex called counting factor, known to play a crucial role in aggregate size determination during development (Brock and Gomer, 1999). When recombinant countin was monitored for pore-forming activity in a liposome-depolarization assay, it exhibited only marginal activity (Gao et al., 2002). In our study, we found that *aplD*$^{-}$ amoebae showed mild defects at early development, such as stream breaks and developmental delay, but finally were able to form slugs and fruiting bodies, although they were smaller than from wild-type Ax2 cells.

We found that *aplD*$^{-}$ amoebae are specifically impaired for growth on one virulent strain of *K. pneumoniae*. Although *apl*D is poorly transcribed in the amoebic stage under axenic growth conditions, it appears as if its gene product is nevertheless instrumental to allow growth in the presence of some *K. pneumoniae* strains. The plethora of *Klebsiella* bacteria present over a longer period in the growth assay, different from the short exposure to *K. pneumoniae* in a killing assay, may change gene expression of several genes including *apl*D. More impressively, we found that *aplD*$^{-}$ slugs are immune-compromised specifically for *K. pneumoniae*. During that multicellular stage, we observed a dramatic increase of *aplD* transcript abundance. Notably, complementation of *aplD* in *aplD*$^{-}$ rescued the capacity of slugs to effectively capture and slough off *K. pneumoniae* in their slime sheath in a way similar to wild-type Ax2.

With respect to the evolution of innate immunity, the antimicrobial capacities of *D. discoideum* are still a relatively unexplored area of research. On the one hand, the amoeba is an interesting model because it resembles in its unicellular stage mammalian macrophages in several aspects (Bozzaro et al., 2008; Cosson and Soldati, 2008; Dunn et al., 2018). On the other hand, the developmental cycle of the social amoeba represents an intriguing example in biology of appearance of multicellularity before the advent of true metazoans. In particular, the slug, which is composed of about 100,000 prespore and prestalk cells, hosts about 1% of Sentinel cells. These phagocytic cells reminiscent of patrolling neutrophils and tissue macrophages of animals, represent an extraordinarily appealing model system for comparative immunologists, as they defend the slug against infection using bactericidal phagocytosis and DNA extracellular traps (Chen et al., 2007; Zhang et al., 2016). Here, we reveal the involvement of an amoebic SAPLIP in the struggle of the slug stage against virulent bacteria, as an early example of a molecular defense implemented at the transition from unicellular to multicellular organisms.

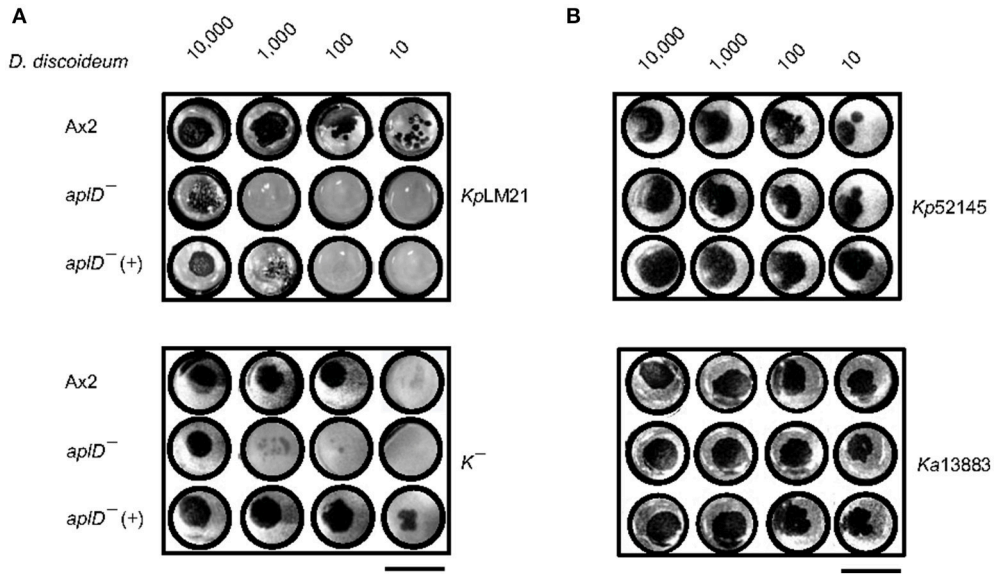

FIGURE 7 | *AplD*$^{-}$(+) strain growth on *K. pneumoniae.* Growth abilities of *aplD*$^{-}$(+) cells were tested on *K. pneumoniae Kp*LM21 and *K*$^{-}$ **(A)** and on *K. pneumoniae Kp52145* and *Ka* 13883 **(B)**. Growth abilities of Ax2 and *aplD*$^{-}$ cells are also represented for comparison. Scale bar, 1.5 cm.

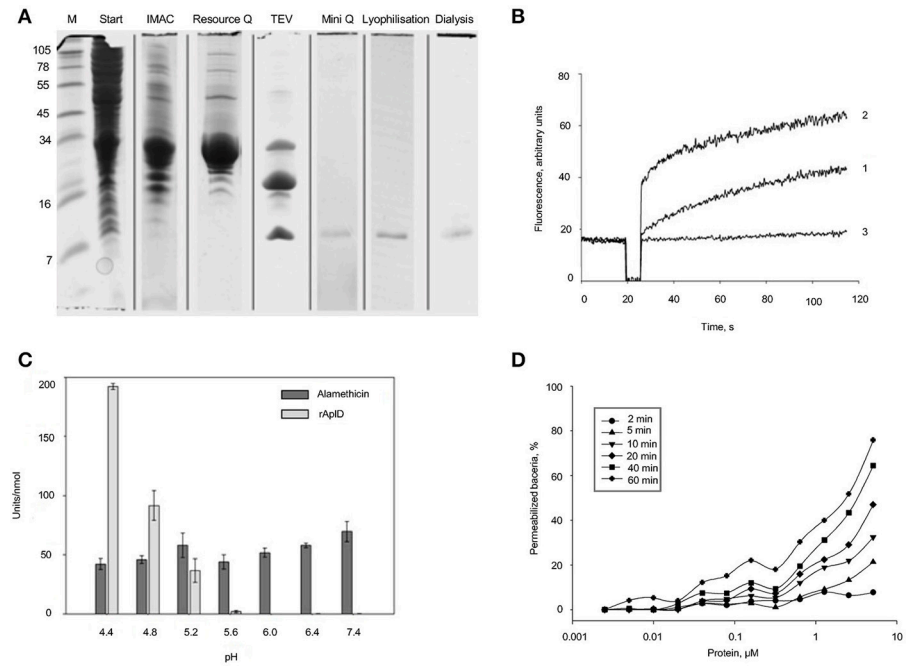

FIGURE 8 | Purification and functional *in-vitro* analysis of recombinant AplD. **(A)** Purification steps of AplD after recombinant synthesis evidenced by SDS PAGE and Coomassie staining of the gel: Extracts of *E. coli* C43 transformed with *aplD* in pET-32a (+) in TBS, pH 7.0 (start), enrichment with IMAC, further purification with anion-exchange chromatography (Resource Q), proteolytic cleavage with TEV, and final purification via a Mini Q column. Purity of AplD after lyophilisation and dialysis is also shown at the right. All samples were reduced and alkylated before separation. At the very left, marker proteins (M) were separated and the molecular masses of these are depicted in kDa. **(B)** Time course of pore formation induced by AplD. The dissipation of a valinomycin-induced diffusion potential in vesicles of asolectin after addition of AplD (80 pmol) (trace 1), control peptide alamethicin (100 pmol) (trace 2), and the peptide solvent (trace 3) were recorded at pH 5.2. Pore-forming activity is reflected by the increase of fluorescence as a function of time. **(C)** pH dependence of pore-forming activity of AplD. Activity of AplD in comparison with that of alamethicin was measured in six independent experiments in Tris-maleate buffer (50 mM Tris-maleate/50 mM sodium sulfate/0.5 mM EDTA/0.02 % sodium azide) adjusted to various pH. Mean and standard deviation are shown. **(D)** Kinetics of membrane permeabilization by AplD. Membrane permeabilization of viable *B. megaterium* was measured as an increase in fluorescence of the DNA intercalating dye SYTOX Green at pH 5.2 induced by AplD and monitored after different time points at various concentrations.

AUTHOR CONTRIBUTIONS

Conceived the study: ML. Designed the experiments: RD, PC, TS, and ML. Performed the experiments: RD and MB. Analyzed the data: RD, MB, PC, TS, and ML. Wrote the paper: RD, PC, TS, and ML.

ACKNOWLEDGMENTS

This study was supported by the German Research Foundation (DFG); CRC 1182 Function and Origin of Metaorganisms (project A1). TS is a member of iGE3 (http://www.ige3.unige.ch); is supported by an RTD grant from SystemsX.ch, and by multiple grants from the Swiss National Science Foundation. The authors thank the Dicty stock center for providing the plasmids/strains used in this study. RD is supported by DST, INDIA. RD thanks Baskar Ramamurthy for providing laboratory space to conduct the rescue experiments. The authors thank Heidrun Lieβegang for technical assistance in the activity assays with the recombinant protein, Judith Bossen for performing Southern hybridization, Christoph Gelhaus for mass spectrometry measurements and Rosa Herbst for creating **Figure 1**.

SUPPLEMENTARY MATERIAL

The Supplementary Material for this article can be found online at: https://www.frontiersin.org/articles/10.3389/fcimb.2018.00073/full#supplementary-material

REFERENCES

Alibaud, L., Köhler, T., Coudray, A., Prigent-Combaret, C., Bergeret, E., Perrin, J., et al. (2008). *Pseudomonas aeruginosa* virulence genes identified in a *Dictyostelium* host model. *Cell. Microbiol.* 10, 729–740. doi: 10.1111/j.1462-5822.2007.01080.x

Andersson, M., Gunne, H., Agerberth, B., Boman, A., Bergman, T., Sillard, R., et al. (1995). NK-lysin, a novel effector peptide of cytotoxic T and NK cells. Structure and cDNA cloning of porcine form, induction by interleukin 2, antibacterial and antitumour activity. *EMBO J.* 14, 1615–1625.

Balestrino, D., Haagensen, J. A. J., Rich, C., and Forestier, C. (2005). Characterization of type 2 quorum sensing in *Klebsiella pneumoniae* and relationship with biofilm formation. *J. Bacteriol.* 187, 2870–2880. doi: 10.1128/JB.187.8.2870-2880.2005

Benghezal, M., Adam, E., Lucas, A., Burn, C., Orchard, M. G., Deuschel, C., et al. (2007). Inhibitors of bacterial virulence identified in a surrogate host model. *Cell. Microbiol.* 9, 1336–1342. doi: 10.1111/j.1462-5822.2006.00877.x

Benghezal, M., Fauvarque, M. O., Tournebize, R., Froquet, R., Marchetti, A., Bergeret, E., et al. (2006). Specific host genes required for the killing of *Klebsiella* bacteria by phagocytes. *Cell. Microbiol.* 8,139–148. doi: 10.1111/j.1462-5822.2005.00607.x

Bozzaro, S., Bucci, C., and Steinert, M. (2008). Phagocytosis and host-pathogen interactions in *Dictyostelium* with a look at macrophages. *Int. Rev. Cell Mol. Biol.* 271, 253–300. doi: 10.1016/S1937-6448(08)01206-9

Brinkmann, V., Reichard, U., Goosmann, C., Fauler, B., Uhlemann, Y., Weiss, D. S., et al. (2004). Neutrophil extracellular traps kill bacteria. *Science* 303, 1532–1535. doi: 10.1126/science.1092385

Brock, D. A. and Gomer, R. H. (1999). A cell-counting factor regulating structure size in *Dictyostelium*. *Genes Dev.* 13, 1960–1969.

Bruhn, H. (2005). A short guided tour through functional and structural features of saposin-like proteins. *Biochem. J.* 389, 249–257. doi: 10.1042/BJ20050051

Charette, S. J., and Cosson, P. (2004). Preparation of genomic DNA from *Dictyostelium discoideum* for PCR analysis. *BioTechniques* 36, 574–575.

Chen, G., Zhuchenko, O., and Kuspa, A. (2007). Immune-like phagocyte activity in the social amoeba. *Science* 317, 678–681. doi: 10.1126/science.1143991

Cosson, P., and Soldati, T. (2008). Eat, kill or die: when amoeba meets bacteria. *Curr. Opin. Microbiol.* 11, 271–276. doi: 10.1016/j.mib.2008.05.005

Cosson, P., Zulianello, L., Join-lambert, O., Faurisson, F., Gebbie, L., Benghezal, M., et al. (2002). *Pseudomonas aeruginosa* virulence analyzed in a *Dictyostelium discoideum* host system. *J. Bacteriol.* 184, 3027–3033. doi: 10.1128/JB.184.11.3027-3033.2002

Dubin, M., and Nellen, W. (2010). A versatile set of tagged expression vectors to monitor protein localisation and function in *Dictyostelium*. *Gene* 465, 1–8. doi: 10.1016/j.gene.2010.06.010

Dunn, J. D., Bosmani, C., Barisch, C., Raykov, L., Lefrançois, L. H., Cardenal-Muñoz, E., et al. (2018). Eat prey, live: *Dictyostelium discoideum* as a model for cell-autonomous defenses. *Front. Immunol.* 8:1906. doi: 10.3389/fimmu.2017.01906

Eichinger, L., and Noegel, A. A. (2005). Comparative genomics of *Dictyostelium discoideum* and *Entamoeba histolytica*. *Curr. Opin. Microbiol.* 8, 606–611. doi: 10.1016/j.mib.2005.08.009

Faix, J., Kreppel, L., Shaulsky, G., Schleicher, M., and Kimmel, A. R. (2004). A rapid and efficient method to generate multiple gene disruptions in *Dictyostelium discoideum* using a single selectable marker and Cre-loxP system. *Nucleic Acids Res.* 32:e143. doi: 10.1093/nar/gnh136

Farbrother, P., Wagner, C., Na, J., Tunggal, B., Morio, T., Urushihara, H., et al. (2006). *Dictyostelium* transcriptional host cell response upon infection with *Legionella*. *Cell. Microbiol.* 8, 438–456. doi: 10.1111/j.1462-5822.2005.00633.x

Favre-Bonté, S., Licht, T. R., Forestier, C., and Krogfelt, K. A. (1999). *Klebsiella pneumoniae* capsule expression is necessary for colonization of large intestines of streptomycin-treated mice. *Infect. Immun.* 67, 6152–6156.

Froquet, R., Lelong, E., Marchetti, A., and Cosson, P. (2009). *Dictyostelium discoideum* a model host to measure bacterial virulence. *Nat. Protoc.* 4, 25–30. doi: 10.1038/nprot.2008.212

Gao, T., Ehrenman, K., Tang, L., Leippe, M., Brock, D. A., and Gomer, R. H. (2002). Cells respond to and bind countin, a component of a multisubunit cell number counting factor. *J. Biol. Chem.* 277, 32596–32605. doi: 10.1074/jbc.M203075200

Hagedorn, M., and Soldati, T. (2007). Flotillin and RacH modulate the intracellular immunity of *Dictyostelium* to *Mycobacterium marinum* infection. *Cell Microbiol.* 9, 2716–2733. doi: 10.1111/j.1462-5822.2007.00993.x

Hagedorn, M., Rohde, K. H., Russell, D. G., and Soldati, T. (2009). Infection by tubercular mycobacteria is spread by nonlytic ejection from their amoeba hosts. *Science* 323, 1729–1733. doi: 10.1126/science.1169381

Hecht, O., Van Nuland, N. A., Schleinkofer, K., Dingley, A. J., Bruhn, H., Leippe, M., et al. (2004). Solution structure of the pore-forming protein of *Entamoeba histolytica*. *J. Biol. Chem.* 279, 17834–17841. doi: 10.1074/jbc.M312978200

Herbst, R., Marciano-Cabral, F., and Leippe, M. (2004). Antimicrobial and pore-forming peptides of free-living and potentially highly pathogenic *Naegleria fowleri* are released from the same precursor molecule. *J. Biol. Chem.* 279, 25955–25958. doi: 10.1074/jbc.M401965200

Herbst, R., Ott, C., Jacobs, T., Marti, T., Marciano-Cabral, F., and Leippe, M. (2002). Pore-forming polypeptides of the pathogenic protozoon *Naegleria fowleri*. *J. Biol. Chem.* 277, 22353–22360. doi: 10.1074/jbc.M201475200

Koller, B., Schramm, C., Siebert, S., Triebel, J., Deland, E., Pfefferkorn, A. M., et al. (2016). *Dictyostelium discoideum* as a novel host system to study the interaction between phagocytes and yeasts. *Front. Microbiol.* 7:1665. doi: 10.3389/fmicb.2016.01665

Kolter, T., Winau, F., Schaible, U. E., Leippe, M., and Sandhoff, K. (2005). Lipid-binding proteins in membrane digestion, antigen presentation, and antimicrobial defense. *J. Biol. Chem.* 280, 41125–41128. doi: 10.1074/jbc.R500015200

Lee, A. K., and Falkow, S. (1998). Constitutive and inducible green fluorescent protein expression in *Bartonella henselae*. *Infect. Immun.* 66, 3964–3967.

Leippe, M. (1999). Antimicrobial and cytolytic polypeptides of amoeboid protozoa-effector molecules of primitive phagocytes. *Dev. Comp. Immunol.* 23, 267–279. doi: 10.1016/S0145-305X(99)00010-5

Leippe, M. (2014). Pore-forming toxins from pathogenic amoebae. *Appl. Microbiol. Biotechnol.* 98, 4347–4353. doi: 10.1007/s00253-014-5673-z

Leippe, M., Ebel, S., Schoenberger, O. L., Horstmann, R. D., and Müller-Eberhard, H. J. (1991). Pore-forming peptide of pathogenic *Entamoeba histolytica*. *Proc. Natl. Acad. Sci. U.S.A.* 88, 7659–7663. doi: 10.1073/pnas.88.17.7659

Liepinsh, E., Andersson, M., Ruysschaert, J. M., and Otting, G. (1997). Saposin fold revealed by the NMR structure of NK-lysin. *Nat. Struct. Biol.* 4, 793–795. doi: 10.1038/nsb1097-793

Michalek, M., and Leippe, M. (2015). Mechanistic insights into the lipid interaction of an ancient saposin-like protein. *Biochemistry* 54, 1778–1786. doi: 10.1021/acs.biochem.5b00094

Müller, I., Subert, N., Otto, H., Herbst, R., Rühling, H., Maniak, M., et al. (2005). A *Dictyostelium* mutant with reduced lysozyme levels compensates by increased phagocytic activity. *J. Biol. Chem.* 280, 10435–10443. doi: 10.1074/jbc.M411445200

Munford, R., Lu, M., and Varley, A. (2009). Chapter 2: Kill the bacteria...and also their messengers? *Adv. Immunol.* 103, 29–48. doi: 10.1016/S0065-2776(09)03002-8

Munford, R. S., Sheppard, P. O., and O'Hara, P. J. (1995). Saposin-like proteins (SAPLIP) carry out diverse functions on a common backbone structure. *J. Lipid Res.* 36, 1653–1663.

Nassif, X., Fournier, J. M., Arondel, J., and Sansonetti, P. J. (1989). Mucoid phenotype of *Klebsiella pneumoniae* is a plasmid-encoded virulence factor. *Infect. Immun.* 57, 546–552.

O'Brien, J. S., and Kishimoto, Y. (1991). Saposin proteins: structure, function, and role in human lysosomal storage disorders. *FASEB J.* 5, 301–308. doi: 10.1096/fasebj.5.3.2001789

Parkinson, K., Bolourani, P., Traynor, D., Aldren, N. L., Kay, R. R., Weeks, G., et al. (2009). Regulation of Rap1 activity is required for differential adhesion, cell-type patterning and morphogenesis in *Dictyostelium*. *J. Cell Sci.* 122, 335–344. doi: 10.1242/jcs.036822

Peña, S. V., Hanson, D. A., Carr, B. A., Goralski, T. J., and Krensky, A. M. (1997). Processing, subcellular localization, and function 519 (granulysin), a human late T cell activation molecule with homology to small, lytic, granule proteins. *J. Immunol.* 158, 2680–2688.

Pukatzki, S., Kessin, R. H., and Mekalanos, J. J. (2002). The human pathogen *Pseudomonas aeruginosa* utilizes conserved virulence pathways to infect the social amoeba *Dictyostelium discoideum*. *Proc. Natl. Acad. Sci. U.S.A.* 99, 3159–3164. doi: 10.1073/pnas.052704399

Robb, C. T., Dyrynda, E. A., Gray, R. D., Rossi, A. G., and Smith, V. J., (2014). Invertebrate extracellular phagocyte traps show that chromatin is an ancient defence weapon. *Nat. Commun.* 5:4627. doi: 10.1038/ncomms5627

Roeder, T., Stanisak, M., Gelhaus, C., Bruchhaus, I., Grötzinger, J., and Leippe, M. (2010). Caenopores are antimicrobial peptides in the nematode *Caenorhabditis elegans* instrumental in nutrition and immunity. *Dev. Comp. Immunol.* 34, 203–209. doi: 10.1016/j.dci.2009.09.010

Schägger, H., and von Jagow, G. (1987). Tricine-sodium dodecyl sulfate-polyacrylamide gel electrophoresis for the separation of proteins in the range from 1 to 100 kDa. *Anal. Biochem.* 166, 368–379 doi: 10.1016/0003-2697(87)90587-2

Shevchuk, O., Pägelow, D., Rasch, J., Döhrmann, S., Günther, G., Hoppe, J., et al. (2014). Polyketide synthase (PKS) reduces fusion of *Legionella pneumophila*-containing vacuoles with lysosomes and contributes to bacterial competitiveness during infection. *Int. J. Med. Microbiol.* 304, 1169–1181. doi: 10.1016/j.ijmm.2014.08.010

Sillo, A., Bloomfield, G., Balest, A., Balbo, A., Pergolizzi, B., Peracino, B., et al. (2008). Genome-wide transcriptional changes induced by phagocytosis or growth on bacteria in *Dictyostelium*. *BMC Genomics* 9:291. doi: 10.1186/1471-2164-9-291

Zhang, X., and Soldati, T. (2016). Of amoebae and men: extracellular DNA traps as an ancient cell-intrinsic defense mechanism. *Front. Immunol.* 7:269. doi: 10.3389/fimmu.2016.00269

Zhang, X., Zhuchenko, O., Kuspa, A., and Soldati, T. (2016). Social amoebae trap and kill bacteria by casting DNA nets. *Nat. Commun.* 7:10938. doi: 10.1038/ncomms10938

Conflict of Interest Statement: The authors declare that the research was conducted in the absence of any commercial or financial relationships that could be construed as a potential conflict of interest.

Advantages of publishing in Frontiers

OPEN ACCESS
Articles are free to read for greatest visibility and readership

FAST PUBLICATION
Around 90 days from submission to decision

HIGH QUALITY PEER-REVIEW
Rigorous, collaborative, and constructive peer-review

TRANSPARENT PEER-REVIEW
Editors and reviewers acknowledged by name on published articles

Frontiers
Avenue du Tribunal-Fédéral 34
1005 Lausanne | Switzerland

Visit us: www.frontiersin.org
Contact us: info@frontiersin.org | +41 21 510 17 00

REPRODUCIBILITY OF RESEARCH
Support open data and methods to enhance research reproducibility

DIGITAL PUBLISHING
Articles designed for optimal readership across devices

FOLLOW US
@frontiersin

IMPACT METRICS
Advanced article metrics track visibility across digital media

EXTENSIVE PROMOTION
Marketing and promotion of impactful research

LOOP RESEARCH NETWORK
Our network increases your article's readership